ELEMENTARY AND COMPOSITE PARTICLES

by

ALAN HALE BOND

A thesis presented for the degree of
Doctor of Philosophy in the
University of London

July 1966

Department of Physics,
Imperial College of
Science and Technology,
LONDON.

ABSTRACT

In this thesis, we study ways of approximating the Mandelstam representation, to give dynamical schemes for the evaluation of the scattering amplitudes. The study originated in an attempt to clarify the idea of a bootstrap calculation. By the use of the Mandelstam representation and Unitarity, one hopes to be able to calculate the $\pi\pi$ scattering amplitude at least at low energies, and one hopes that a solution will exist which agrees closely with experimental findings.

We have used partial wave dispersion relations and partial wave series throughout and have made no use of Regge poles.

In the first chapter, we give a discussion of dispersion theory, a survey of bootstrap calculations and a discussion of the distinction between elementary and composite particles.

In chapter two, we investigate the use of fixed s dispersion relations and their projection into the s channel. We give an attitude to bootstrap calculations and try to develop concepts and ways of thinking about approximate calculations in dispersion theory. We show how to locate arbitrary parameters in approximate calculations.

In chapters three, four and five, we consider the methods of Balazs and Zachariasen and the variational method of Hamilton. We systematically study them numerically and display their faults. We attempt to remove the faults by defining several modified methods.

In chapter six, we look at the inverse amplitude approach. We define new inverse amplitude models, which are interesting but not useful unless some way can be found of estimating the threshold behaviour accurately.

In chapter seven, we consider three ideas relating to the solution of M. R. + U, but do no numerical work.

1. The projection of the fixed s dispersion relation into the t channel, to give an expression for $B_1(\nu)$ in the low energy physical region, in terms of physical region amplitudes in the crossed channel, and without using unitarity.

2. "Consistency checks", a consistency constraint on the simultaneous continuation from the t and u channels to the same region.

3. The transformation of variables, from (s, t) to curvilinear coordinates, enabling a family of single dispersion relations to be written, covering the entire s-, t- and u- physical regions, but avoiding the double spectral regions. This leads to the idea of a physical region dynamical scheme, which is briefly discussed.

CONTENTS PAGE

NOTATION

Note the very free use of $\sim$ to mean "goes like", "corresponds to", "is in some relation to".

0	of the order of
$\|\ \|$	modulus, absolute magnitude
$\Rightarrow$	implies $\quad\rightarrow$ goes to
$\{\ \}$	the set
w.r.t.	with respect to
$\equiv$	equivalent to or identical with
$\in$	is a member of, belongs to, is contained in
$[a,b]$	the closed interval a, b
(a, b)	the open interval a, b
s t u	Mandelstam variables energy squared in s, t, u channels
ν, cos θ	s channel c.o.m. momentum squared and c.o.m., angular variable.
ν', cos θ'	t " " "
ν'', cos θ''	u " " "
P_l	Legendre function of 1st kind
Q_l	" " 2nd kind
p.s.	possibly subtracted s.c. self consistent
Re, Im	real or imaginary part of
$C(\nu)$	$C(\nu)$ function introduced in Chapter 2
BW	Breit Wigner formula
λ	"pi-pi coupling constant" $= A(4/3,\ 4/3,\ 4/3)$
$A(s, t)$ or $A(s,t,..)$ or $F(s,t,u)$ or $F(s,z)$	amplitude
$A_t(s,t)$	absorptive part in t channel decomposition
$A_l(\nu)$, $A_l(s)$, $A_l(t)$	partial wave amplitude
$F(\nu)$	usually refers to trial function
F_j	jth symmetry point
$\{\nu_{Fj}\}$, the ν_{Fj}	the set of symmetry points
$\rho(s, t)$, $\rho_{st}(s,t)$	double spectral functions
Λ, co	cut off
$I(a,b)$, $K(a,b)$	kernel function for N/D

$$B_l(\nu) :\equiv + \int_{-\infty}^{-1} \frac{\mathrm{Im}A(\nu')\,d\nu'}{\nu' - \nu}\ \text{p.s.}\ ;\quad B^{-1}(\nu):\ (\not\equiv B_l(\nu)^{-1}) \equiv \int_{-\infty}^{-1} \frac{\mathrm{Im}A^{-1}(\nu')\,d\nu'}{(\nu' - \nu)}\ \text{p.s.}$$

For numbering, there are 3 types of object, the reference, the figure and the table. These are numbered locally within a chapter or preceded by a chapter number. An index of figures and tables is given at the end of the thesis.

CHAPTER 1

"BASIC THEORETICAL INTRODUCTION"

"Let thy tongue tang arguments of state; put
thyself into the trick of singularity."

Shakespeare. Twelfth Night.
(Advice to Malvolio).

I. INTRODUCTION, KINEMATICS AND SYMMETRIES

1. INTRODUCTION

In attempting to describe the existence and behaviour of the experimentally observed elementary particles, we first distinguish strongly and weakly interacting particles, then spacial and then electromagnetic properties and finally classify them (1) according to assignment of quantum numbers. The most tangible evidence for the existence of these very unstable particles and their interactions is probably from bubble chamber photographs where the paths of particles are made visible by an accompaniment of small bubbles. To set up a mathematical formalism, we invoke the basic ideas of quantum mechanics, notably that the states of a physical system obey a superposition principle and are rays ψ in a Hilbert space, and that acts of measurement correspond to projections in the space. We then introduce the notion of invariance under a symmetry operation (2), (3) and introduce relativistic invariance by requiring that the inhomogeneous Lorentz group be a symmetry. This leads to the concepts of momentum, mass, parity, angular momentum, and allows the existence of states in irreducible representations which are eigenstates of these operators.

These single particle states are elementary in the sense that any decomposition will not be Lorentz invariant. There will be states formed by taking the direct produce of these, corresponding to 2, 3 etc. particle states. When we consider interacting particles, new single particle "bound states" can occur; which will be unstable if $m_3 > m_1 + m_2$, and which have no analogue in the non-interacting system. One expects these to be calculable from a dynamical law. We have time reversal and charge conjugation symmetries. We have also super-selection rules (4), which are that every physically realizable state must be an eigenstate of baryon number, charge and have well defined statistics. From the existence of multiplets of particles with very closely the same Lorentz properties, the differences explicable as electromagnetic effects, we are lead to internal symmetries, isotopic spin $SU(2)$, which when combined with strangeness gives $SU(3)$. Thus particles form degenerate multiplets, within which members are characterised by two quantum numbers I_3 and Y. We thus have the symmetry scheme $\mathcal{L} \otimes SU(3)$ which explains well many observed features and predicts which processes are allowed. The actual amplitude of an allowed process can only be decided by the detailed mechanism or physical law, that is "dynamics." To describe an interaction between two particles, we attempt to calculate the S matrix, where

$$(\varphi_{out}, \Psi_{in}) = (\varphi_{in}, S\Psi_{in})$$

The unitarity of S follows from "asymptotic completeness" (4) and can be written

$$S^+ S = I$$

or decomposing

$$S = 1 + i(2\pi)^4 \delta(P_i - P_f) \cdot T$$

$$\mathrm{Im}\, T_{i \to f} = \underbrace{k}_{\text{kinematic factor}} \cdot \underbrace{\sum_I T_{i \to I} \cdot T_{I \to f}}_{\text{intermediate states}}$$

We work with the invariant amplitude

$$A = \langle T \rangle \cdot E$$

which in an angular momentum decomposition in the c. o. m. system, obeys unitarity condition

$$\mathrm{Im}\, A_\ell^{-1} = -|\vec{p}| / E$$

A will be a function of the independent scalars in the problem (5).

In this thesis, we shall consider only the 2π system, being the simplest, and hopefully most tractable, strongly interacting system.

2. THE Pi MESON

The pion is an S.I.P. It has isotopic spin 1 and three charge states $\pi^+ \pi^- \pi^0$. It has zero strangeness.

$$m_{\pi^\pm} = 139.58 \pm .05 \text{ Mev} = 273.25 \pm 0.12\, m_e$$

$$m_{\pi^0} = 134.97 \pm .05 \text{ Mev} = 264.27 \pm 0.31\, m_e$$

where $\hbar = c = 1$ and unit of mass is Mev. Hereafter we assume mass difference due to e/n effects and take

$$m_{\pi^\pm} = m_{\pi^0} = 1$$

to define units with $\hbar = c = 1$

$$C\,|\pi^+\rangle = |\pi^-\rangle$$
$$C\,|\pi^0\rangle = |\pi^0\rangle$$

No magnetic moment.

They have negative parity and zero spin, i.e. are pseudoscalar. G-parity is (-1) i.e. polar vector in isospace. It is unstable

$$\left.\begin{array}{l}\pi^+ \to \mu_+ + \nu_\mu \\ \pi^- \to \mu_- + \bar{\nu}_\mu\end{array}\right\} \quad 2.5 \times 10^{-8} \text{ secs. weak}$$

$$\pi^0 \to 2\gamma \quad \Big\} \quad 2.2 \times 10^{-16} \text{ secs.} \quad \text{e/n}$$

but stable under strong interactions. If we adopt the isispin formalism SU(2) we have a [3] space with $|\pi^+\rangle, |\pi^-\rangle, |\pi^0\rangle$ and an isotopic spin

operator $\vec{I}$, with z- component, say I_3.

Rotations in isospace correspond to operators $e^{i\vec{I}\cdot\vec{\theta}}$

It is normally more convenient to take the linear combinations

$$|\pi_1\rangle = \frac{1}{\sqrt{2}}\left(|\pi^+\rangle + |\pi^-\rangle\right)$$

$$|\pi_2\rangle = \frac{1}{\sqrt{2}}\left(|\pi^+\rangle - |\pi^-\rangle\right)$$

$$|\pi_3\rangle = |\pi^0\rangle$$

which satisfy

$$\langle \pi^i | \pi^j \rangle = \delta_{ij}$$

$$\langle \pi^i | I_j | \pi^k \rangle = i\,\varepsilon_{ijk}.$$

If we use an SU(3) scheme, then the pions are part of an [8] rep. of pseudo-scalar mesons

$\underbrace{\pi^+ \quad \pi^0 \quad \pi^-}_{I=1 \quad Y=0}$ $\underbrace{K^+ \quad K^0}_{I=\frac{1}{2} \quad Y=1}$ $\underbrace{\bar{K}^0 \quad K^-}_{I=\frac{1}{2} \quad Y=-1}$ $\underbrace{\eta}_{I=0 \quad Y=0}$

again generators $\left(A^{\mu}_{\nu}\right)_{ij}$ can be written down, satisfying

$$\left[A^{\mu}_{\nu}, A^{\lambda}_{\delta}\right]_- = \delta^{\lambda}_{\nu} A^{\mu}_{\rho} - \delta^{\mu}_{\rho} A^{\lambda}_{\mu}$$

which determines them uniquely. There are two independent diagonal operators corresponding to the conserved quantities I_3 and Y.

3. KINEMATICS OF THE TWO PION SYSTEM

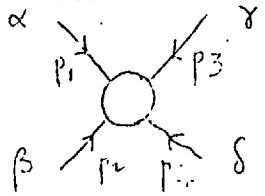

$\alpha, \beta, \gamma, \delta$ distinguish the charge state 1, 2, 3
time-like metric $p_i^2 = n_i^2 = 1$ all i.

define scalar variables $s = (p_1 + p_2)^2$

(Mandelstam variables) $t = (p_1 + p_3)^2$

$u = (p_1 + p_4)^2$

there are only two independent scalar variables

$$s + t + u = 4$$

Taking the p_1 to have different signs gives 3 different "channels." The s channel (p_3, p_4 out) describes the reaction

$$\pi(\alpha, p_1) + \pi(\beta, p_2) \longrightarrow \pi(\gamma, -p_3) + \pi(\delta, -p_4)$$

if we define

$$p = (\vec{q}, E)$$

then in the centre of mass system with axes along the incident direction

$$p_1 = (q, E) = (0, 0, q, E)$$

$$p_2 = (q, E) = (0, 0, -q, E)$$

$$-p_3 = (q\sin\theta\cos\varphi, q\sin\theta\sin\varphi, q\cos\varphi, E) = (\vec{q}', E)$$

$$-p_4 = (-q\sin\theta\cos\varphi, -q\sin\theta\sin\varphi, -q\cos\varphi, E) = (-\vec{q}', E)$$

$$E^2 = q^2 + 1$$

and defining $\nu = q^2$

$$s = 4(\nu+1) = (2E)^2$$

$$t = -2\nu(1-\cos\theta) = (0, \vec{q}-\vec{q}')^2$$

hence physical significance and nomenclature

$$u = -2\nu(1+\cos\theta)$$

The t channel has (p_2, p_4 out) and ν', $\cos\theta'$ as can. variables.

$$s = -2\nu'(1+\cos\theta')$$

$$t = 4(\nu'+1)$$

$$u = -2\nu'(1-\cos\theta')$$

The u channel has (p_2, p_3 out) and ν'', $\cos\theta''$ hence

$$s = -2\nu''(1-\cos\theta'')$$

$$t = -2\nu''(1+\cos\theta'')$$

$$u = 4(\nu''+1)$$

The physical region for these channels is defined by

$\nu > 0$ $\qquad\qquad$ $\cos\theta$ real in $[-1, +1]$

hence in s channel $\quad s \geq 4$

and $\quad -s-4 \leq t \leq 0 \quad$ i.e $\quad u \leq 0$, $t \leq 0$

t channel	$t \geq 4$	$s \leq 0$	$u \leq 0$
u channel	$u \geq 4$	$s \leq 0$	$t \leq 0$

This is shown in Fig. 1. We also wish to record have some useful relations between these variables:

$$\nu' = -\frac{\nu}{2}(1-\cos\theta) - 1$$

$$\cos\theta' = \frac{\nu/2(1+\cos\theta) + (\nu+1)}{-\nu/2(1+\cos\theta) + (\nu+1)}$$

$$\cos\theta' = 1 + 2\left(\frac{\nu+1}{\nu'}\right)$$

$$\cos\theta = 1 + 2\left(\frac{\nu'+1}{\nu}\right)$$

We have only two independent scalar invariants, which the physics depends on; we shall take s and t.

Isospin decomposition

Systen of two pions with I = 1 forms representation $[1]\otimes[1]$ which decomposes into $[2]\times[1]\times[0]$ i.e. we have states with I = 2, 1, 0 and so we only have three scalar amplitudes $\{A^I(s, t)\}$ to describe the scattering, being reduced from the nine possibilities, $\pi_{\frac{+}{0}} + \pi_{\frac{+}{0}}$, by the isospin symmetry.

The scalar amplitudes can only be functions of scalar invariant quantities of which there are two independent, say (s, t). We are thus trying to describe the process $\pi+\pi\rightarrow\pi+\pi$ by giving its transition amplitudes from initial to final states. We take the independent amplitudes

$$\text{out}\langle \pi\pi\, I \mid \pi\pi\, I\rangle_{\text{in}} = A^I(s,t)$$

in corresponding eigenstates of I.

The differential cross section for scattering in pure isospin state in the barycentric system is

$$\frac{d\sigma^I}{d\Omega} = \frac{4}{s}\,|A(s,t)|^2$$

Partial wave decomposition

Since pions spinless only orbital angular momentum and we can decompose into angular momentum eigenchannels

$$A^I(\nu, \cos\theta) = \sum_{l=0}^{\infty}(2l+1)\cdot A_l^I(\nu)\cdot P_l(\cos\theta)$$

usual P_l's and normalisation, $A_l^I(\nu)$ is partial wave amplitude and is a function of one variable only. A knowledge of $\{A_l^I(\nu)\}$ gives the entire description of the $\pi\pi$ system. This is spin zero case of helicity formation decomposition since $d^l_{00}(\theta) = P_l(\cos\theta)$

$$A_l^I(\nu) = \frac{1}{2}\int_{-1}^{+1} d(\cos\theta)\cdot A^I(\nu, \cos\theta)\cdot P_l(\cos\theta)$$

unitarity implies

$$S_l^I(\nu) = e^{2i\delta_l^I(\nu)}.$$

so $\mathcal{A}_\ell^I(\nu) = \sqrt{\frac{\nu+1}{\nu}} \cdot e^{i\delta_\ell^I(\nu)} \sin\delta_\ell^I(\nu)$; $\mathrm{Im}\, A_\ell^{I\,-1}(\nu) = -\sqrt{\frac{\nu}{\nu+1}}$.

Finally remark that Bose statistics require even symmetry of the total state under exchange of the pions, so spacial symmetry x isosyn. = even

$$(-1)^{\ell + I} = 1$$
$$\ell + I = \text{even}$$

So first few possible states (ℓ , I) are (0,0), (0,2), (1,1), (2,0), (2,2), (3,1) called S_0, S_2, P_1, D_0, D_2, F_1.

In most experiments, phenomenological formula based on a few low partial waves fit well.

II. DYNAMICS, THE MANDELSTAM REPRESENTATION

1. ORIGINS

We use the dynamical theory put forward by Mandelstam (7) in 1958 and called "Dispersion Theory" or "The Mandelstam Representation". The study of field theoretic models had lead Chew and Goldberger to the study of dispersion relations as a means of solving the model problem and as a vehicle for generalisation of the model. The relationship of dispersion relations to causality in potential theory was investigated by Toll and van Kampen (8) A microscopic causality principle in relativistic local field theory was made.

$$[\varphi_1(x_1) , \varphi_2(x_2)]_- = 0 \qquad (x_1 - x_2) \quad \text{space like}$$

This is not at all self evident and is a very powerful and deep requirement. Local operators have only been experimentally justified down to 10^{-13}an. Some dispersion theorists argue the impossibility of measurement of position very accurately, due to the attendant emission of soft photons. Using microscopic causality, some dispersion relations have been proved in LSZ field theory and some connections with Wightman field theory established (9).

2. MANDELSTAM'S CONJECTURE

Mandelstam made the big conceptual step in combining the idea of single dispersion relations at fixed momentum transfer or angle and fixed

energy dispersion relations, with a generalisation of the substitution law. He conjectured that there would be one amplitude $A(s, t)$ which described all the crossed processes and time reversed processes

$$\begin{aligned} A + B &\rightarrow C + D \quad ; \quad \bar{C} + \bar{D} \rightarrow \bar{A} + \bar{B} \\ A + \bar{C} &\rightarrow \bar{B} + \bar{D} \quad ; \quad B + \bar{D} \rightarrow \bar{A} + C \\ A + \bar{D} &\rightarrow C + \bar{B} \quad = \quad \bar{C} + B \rightarrow \bar{D} + \bar{A} \end{aligned}$$

which have different physical regions which are, for stable particles, always disjoint. By the same amplitude we mean that there is a connected region, including all the physical regions in which $A(s, t)$ is analytic in s and t. He specified the analytic properties by a generalisation of the two types of single dispersion relation into a double dispersion relation

$$A(s,t) = \frac{1}{\pi^2} \iint_R \frac{\rho_{st}(s',t')\,ds'dt'}{(s'-s)(t'-t)} + \text{cyclic in } (s,t,u)$$

The support of ρ_{st} etc. to be the same as in perturbation theory. The asymptotic behaviour to be like a polynomial in s and to so the equation might have to be substracted N times. Thus for the $\pi\pi$ system, the support of ρ_{st} is

$$st - 4(4s \pm t) = 0$$
$$st - 4(4t + s) = 0$$

and cyclic for others.

The physical region for the s channel is clearly

$\cos\theta$ real and in $[-1, +1]$

ν real and in $[0, \infty]$

transforming this region to s and t variables (note one has to check that boundary of s and t region corresponds to boundary of ν, $\cos\theta$ region and is not a turning point) we obtain the regions shown in Fig. 1.

Thus, from this, one can regain the single dispersion relations in s, t or u, e.g. for fixed s

$$A(s,t) = \frac{1}{\pi} \int dt' \frac{A_2(s,t')}{t'-t} + \frac{1}{\pi} \int \frac{A_3(s,t')}{t'-t}$$

where A_2 and A_3 are called the absorptive parts, since, for s, t' in the t

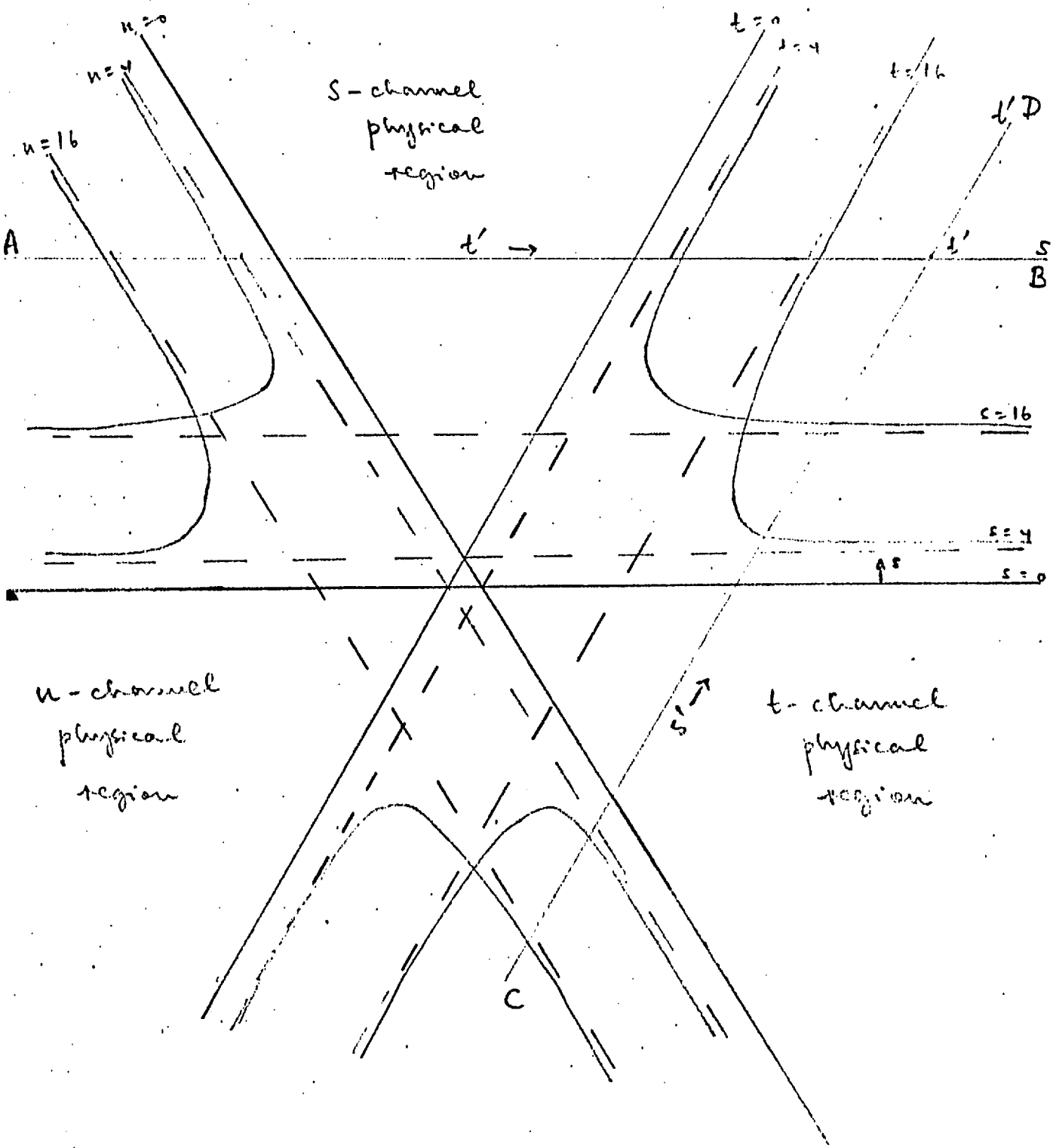

Figure 1-1. Mandelstam diagram

physical region $A_2, (s, t') = \mathrm{Im}A(s, t')$ However, this holds for all s and to and, in some regions, $A_2(s, t')$ will have an imaginary part. In fact,

$$A_2(s,t') = \frac{1}{\pi}\int ds' \frac{\rho_{23}(s',t')}{s'-s} + \frac{1}{\pi}\int \frac{\rho_{12}(s',t')}{s'-s}$$

1st equation is integral along a line like A B, in Fig. 1, 2nd over line like C D from which the integration limits can be deduced. We may also use the notations $\rho_{23} = \rho_{tu} = A_{23} = A_{tu}$ etc. The analytic properties of the ρ are not known, but it was assumed they would be smooth. He also wrote down the unitary condition in the elastic case

$$A_1(s, t(z_1)) = \frac{q}{32\pi^2 W}\int_{-1}^{+1} dz_1 \int_0^{2\pi} A^*\{s, t(z_2)\} \cdot A\{s, t(z_2)\}$$

z_1 = cos (initial $\hat{}$ final)

z_2 = cos (initial $\hat{}$ intermediate)

z_{12} = cos (intermediate $\hat{}$ final) = $z_1, z_2 - \sqrt{(1 - z_1^2)(1 - z_2^2)}\cos\varphi$

= azimuthal (initial intermediate)

Mandelstam proposed an iterative procedure using his representation and unitarity, and that they would form a complete dynamical basis for a theory, although he did not attempt a uniqueness proof (but see section V). [illegible] the desired [illegible] solution

[illegible]

[illegible]

[illegible]

[illegible]

[illegible]

When there are several invariant amplitudes, e.g. different I spins, there will be a Mandelstam representation for each one, with separate double spectral functions. Thus, in the $\pi\pi$ case, we have three amplitudes, $A^I(s,t,u) = \frac{1}{\pi^2}\iint \frac{\rho_{st}^I(s',t')\,ds'dt'}{(s'-s)(t'-t)} + \text{cyclic}$. For other processes there will be stable particles exchanged, i.e. pole terms as well.

B G K T (10) showed MR was true in potential theory, with nonrelativistic variables, except there was only one double spectral region, two if there was an exchange potential. They also showed that the solution by iteration was unique and the theory based on Mandelstam rep + unitarity (MR + U) was equivalent to the Schrodinger equation.

Bros. etal (11) have shown, in LSZ, the crossing analyticity of 2 particle scattering amplitudes, for stable particles with +ve masses. They showed that $\exists$ an open (complex) neighbourhood in all variables of all physical points except the expected s, t, in outs. Also that these physical regions are connected. This also applies in other axiomatic schemes (9).

3. CHEW'S PHILOSOPHY

The Axiomatic Approach, Bootstraps

We have a theory independent of the theories from which it sprang. We also have a philosophy. For every two particles $\longrightarrow$ two particle process is conjectured to obey M R + U. Every higher process is conjectured to obey some (unstated) generalisation. Unitarity in s channel, say, connects a process to all processes with same quantum numbers in the s channel; in the t, u channels to all processes with same q. n.as in the t, u channels. Crossing connects a process to its crossed processes e.g.

$\pi N \to \pi N$	connected by crossing to $\pi\pi \to N\bar{N}$
$\pi N \to \pi N$	connects s channel with $\pi N \to \pi N^*$
$\pi K \to N\bar{N}$	connects in u channel with $\pi\pi \to \Lambda\bar{\Lambda}$

Thus every process affects every other. On the other hand, the requirements of analyticity and unitarity are very powerful. Further, there are many self-consistency conditions to be satisfied, for example an analytic continuation from s channel in πN to t channel should produce the same amplitudes, as this channel is also πN. This leads to the Bootstrap conjecture of Chew, that these equations will be sufficient to determine all the amplitudes for all processes, in terms of a small number of parameters.

To be able to attempt to write down representations for higher processes, and to be able to handle other singularities which may be forced by the equations but not explicitly displayed, Chew has expressed the idea of maximal analyticity, that is, the amplitudes are as analytic as they can be, consistently with unitarity. Presumably this means that, if we have two solutions which differ by an isolated singularity, then we take the one without this singularity. The idea is that strong interactions are as strong as an interaction can be.

As we shall probably not be able to solve over 200 coupled non-linear integral equations simultaneously, then we hope that we can solve a subset of these and that the bootstrap idea holds in the subset, see sec.(I-IV-3).

We note that the $\pi - \pi$ system, which will be studied in this thesis as a prorotype bootstrap problem, is ideally suited for this purpose. For the pions are spinless, also crossing relates it to itself only. Unitarity relates it to itself, right up to the threshold for 4π, so we might reasonably expect elastic unitarity to be a reasonable approximation. Also it has no pole terms. The 4π contribution is usually taken to be dominated by the two body coagulations $K\bar{K}$ and $\pi\omega$.

Subsequently to Chew's idea, work has also been done on completely isolating dispersion theory from field theory and placing it on its own axiomatic basis. Such workers as Stapp and Olive have tried to deduce

concepts like time reversal and pole terms, purely from maximal analyticity ideas.

Some extreme Smatricists have tried to abandon the notion of Hilbert space altogether, however J. R. Taylor (26) showed that attempts (27) to construct a superposition principle sufficient for the needs of Smatrix theory.

ref. H. Stapp. Matscience Report 26

lead to assumptions sufficient for the construction of a Hilbert space of asymptotic states and a unitary S operator which maps this space onto itself. References to the more axiomatic Smatrix theory are (28).

Uniqueness, Constraints on the scattering amplitude and rigorous results

We leave results on asymptotic behaviour until section IV. Froissart (19) showed that if there are a finite number of subtractions

$$A(s,t,u) = \frac{s^N t^N}{\pi^2}\iint \frac{\rho_u(s',t')\,ds'dt'}{(s'-s)(t'-t)\,s'^N t'^N} + \text{cyclic}$$
$$+ \sum_{p=0}^{M<N} t^p \frac{s^M}{\pi}\int \frac{\rho_{p,s}(s')\,ds'}{(s'-s)\,s'^M} + \text{cyclic}$$
$$+ \sum_{p,q=0}^{L} t^p s^q \rho_{pq}$$
$$+ \text{pole terms}$$

then, if the double spectral functions $\rho_u(s',t')$ are given, the subtraction terms are not arbitrary. Indeed the arbitrariness lies almost in the six one dimensional integrals and one constant

$$C + \frac{s}{\pi}\int \frac{\rho_{0,s}(s')\,ds'}{(s'-s)s'} + \frac{t}{\pi}\int \frac{\rho_{1,s}(s')\,ds'}{s'-s} + \text{cyclic}$$

He obtained this result using a weak high energy unitarity condition. Martin (20) also used the existence of purely elastic regions in one or two channels. He showed that

(a) If in one channel, say s, there is a purely elastic region $[s_0, s_1]$, then a knowledge of $\rho_u(s,t)$ and $\rho_t(u,s)$ for s in $[s_0, s_1]$ is sufficient to determine completely the three double spectral functions, and the pole terms in the u and t channels.

(b) If, in addition, there is a purely elastic region in a second channel, say u, then the same information completely determines the whole amplitude. Hence the subtraction terms do not contain any new information.

The application of crossing symmetry should yield an even stronger result for, in neutral $\pi\pi$ scattering for example, a knowledge of $\rho_u(s,t)$ in the elastic s strip determines $\rho_s(t,u)$ in a way which, a priori, does not guarantee the crossing symmetry relation between them. This can be further extended (21); in the $\pi\pi$ pseudoscalar case the amount of input information to determine the amplitude is reduced to a knowledge of $\rho(s,t)$ in an arbitrarily small region of s and t in the elastic regions with an arbitrarily small boundary with the boundary curve of the double spectral function. Further, Martin (21) has recently shown that, starting from the analyticity region provable from axiomatic local field theory and using unitarity, the region of analyticity can be extended to $(|t| \leq R)$ (x) (s in cut plane $s = (M_A + M_B)^2 + \lambda$, $s = (M_A - M_B)^2 - \nu - t$; $\lambda, \nu \geq 0$) R is a fixed number = 4 for $\pi\pi$ case. This domain can be extended by analytic completion and by repeated use of the unitarity condition.

Mandelstam (22) has also obtained a domain partly inside and partly outside this domain. As a consequence of Martin's work, the D waves and higher waves for $\pi^+\pi^0 \rightarrow \pi^0\pi^0$ have positive scattering lengths. This is true for the I = o partial waves of $\pi\pi \rightarrow \pi\pi$. See also '23). Also $A(s,t,u)$, for $\pi^0\pi^0 \rightarrow \pi^0\pi^0$, is bounded numerically for s, t, u < 4. In fact,

$$-4 < \lambda < 25$$

In the physical region, one has absolute limits on averages of the amplitude or of the cross-section. Hence, from field theory, if we assume no $\pi\pi$ bound states exist, we have a limitation on the strength of the $\pi\pi$ interaction, see also references (24). The generalised field theory of J. G. Taylor (25) is an example of a model satisfying the S-matrix postulates.

4. CROSSING MATRICES, ABSORPTIVE PARTS, LEHMANN ELLIPSES, PARTIAL WAVE ANALYTICS

Having decomposed into isospin states in one channel, say S

$$A(s,t,u) = \sum_{I=0}^{2} A_s^{\,I}(s,t,u).\Lambda^I$$

we can relate the amplitudes $A_s^{\,I}$ to those obtained by decomposing in a crossed channel say $A_t^{\,I}$, which will be simply linear combinations, from the superposition of states,

$$A_s^{\,I}(s,t,u) = \sum_{I'=0}^{2} \beta_{II'}\, A_t^{\,I'}(s,t,u)$$

We can obtain the crossing matrix $\beta_{II'}$, by evaluating the recoupling coefficients which relate the different coupling schemes in the combination of I spin

$$\langle (j_1 j_2) j_{12} (j_3 j_4) j_{34}) j \mid (j_1 j_3) j_{13} (j_2 j_4) j_{24} j \rangle$$

so $\beta_{II'} = \langle ((1\ 1)\,I\ (1\ 1)\,I)\,0 \mid ((1\ 1)\,I')\,(1\ 1)\,I')\,0 \rangle$

$$= [(I)(I)(I')(I')]^{1/2} \cdot \begin{Bmatrix} 1 & 1 & I \\ 1 & 1 & I \\ I' & I' & 0 \end{Bmatrix}$$

$$= \frac{(I)(I)(-1)^{I+J'+2}}{[(I)(I')]^{1/2}} \cdot \begin{Bmatrix} 1 & 1 & I \\ 1 & 1 & J' \end{Bmatrix}$$

where $(I) = 2I + 1$

Hence

$$\beta = \begin{bmatrix} 1/3 & 1 & 5/3 \\ 1/3 & 1/2 & -5/6 \\ 1/3 & -1/2 & 1/6 \end{bmatrix}$$

the significance of β_{II} is that the elements of the I^{th} row are factors for projection of different states I' into the I state and the elements of the I'^{th} column are factors for projection of the I'^{th} state into different I states. Thus for P wave

$$P \longrightarrow \begin{matrix} I = \\ \\ \\ \downarrow I = \\ P \end{matrix} \begin{matrix} 0 \\ 1 \\ 2 \\ 0 \\ \end{matrix} \begin{bmatrix} & 1 & \\ & \frac{1}{2} & \\ & \frac{1}{2} & \end{bmatrix} \qquad \begin{matrix} & 1 & 2 \\ \hline \frac{1}{3} & \frac{1}{2} & -5/6 \end{matrix}$$

Elements of 1st column are same, so I = 0 when projected into any state has same factor.

A further crossing condition but deriving from the identity of the

crossed $\pi\pi$ process to the direct one is the "self-consistency" statement

$$A_s^I(\nu, \cos\theta) = A_t^{I'}(\nu', \cos\theta') = A_u^I(\nu'', \cos\theta'')$$

We can decompose the Mandelstam representation in the following way, to obtain a fixed S, say, dispersion relation

$$A(s,t,u) = \frac{1}{\pi}\int_u^\infty \frac{A_t(s,t')\,dt'}{t'-t} + \frac{1}{\pi}\int_4^\infty \frac{A_u(s,u')\,du'}{u'-u}$$

where $A_t(s,t') = \frac{1}{\pi}\int_4^\infty \frac{\rho_{st}(s',t')\,ds'}{s'-s} + \frac{1}{\pi}\int_4^\infty \frac{\rho_{tu}(s',t')\,ds'}{s'-s}$

and $A_u(s,u') = \frac{1}{\pi}\int_4^\infty \frac{\rho_{su}(s,u')\,du'}{u'-u} + \frac{1}{\pi}\int_4^\infty \frac{\rho_{tu}(s',u')\,du'}{u'-u}$

since $\frac{1}{(t'-t)(u'-u)} = \left[\frac{1}{t'-t} + \frac{1}{u'-u}\right]\cdot\frac{1}{[t'+u'-t-u]}$

the lower limits on the integrals are of course the boundaries of the double spectral region. We also note that, since $A_t(s, t, u)$ is analytic in this region, it can be expanded in a power series, or better in a Legendre series and that this is just the partial wave expansion

$$A_t(s,t,u) = \sum_{\ell=0}^{\infty}(2\ell+1)\,\mathrm{Im}A_\ell(s)\cdot P_\ell\left[1 + \frac{2t}{s-4}\right]$$

This expansion will converge in an ellipse which has foci $Z = \pm 1$ where $Z = 1 + \frac{2t}{s-4}$ i.e. $t = 0$ and $t = 4 - S$, the boundaries of the physical region, and which just touches the first singularity. The information that the series is destined to diverge at a certain point is contained in the coefficients $\mathrm{Im}A_\ell(S)$. Now, $\sum_n C_n P_n(Z)$ converges in an ellipse semi axes

$$\frac{1}{2}\left(\rho + \frac{1}{\rho}\right), \quad \frac{1}{2}\left(\rho - \frac{1}{\rho}\right)$$

where ρ is radius of convergence of $\sum C_n z^n$

so, $\rho = \lim_{n\to\infty}\left[|C_n|^{1/n}\right]$

we have the single dispersion relation

$$A(s,t,u) = \frac{1}{\pi}\int_4^\infty \frac{\mathrm{Im}A(s,t')\,dt'}{t'-t} + \frac{1}{\pi}\int_4^\infty \frac{\mathrm{Im}A(s,u')\,du'}{u'-u}.$$

Now, the partial wave series diverges in most regions, however we can still define the partial wave amplitude, use it to calculate with, and finally sum it only in the physical region

$$A_\ell(s) = \frac{1}{2}\int_{-1}^{+1} P_\ell(\cos\theta)\cdot A(s,t,u)\,d(\cos\theta)$$

Partial wave amplitudes are easier to work with because of the simple form of

the unitary condition. However crossing relations are slightly more complicated. From experiment, one expects that in the physical region the amplitude will be well approximated by a few partial waves, however this may not be true away from this region.

If we insert the Mandelstam representation we obtain the analytic properties of the $\{A_\ell(s)\}$, which are simply analytic in the s plane with cuts $[0,\infty]$, $[-1, -\infty]$.

The right hand cut is the physical cut or rescattering cut and the left hand cut is the unphysical or force cut. The exchange of particles mass in or the interaction with Yukawa potential range $1/_m$, lead to force singularities near $s = -m^2$. Short range forces occur on the far left and for low physical energies one expects them to be unimportant. This leads to the "nearest singularity" doctrine, which has been used extensively.

THE SIGNIFICANCE OF THE LEFT HAND CUT

For physical intuition, one might turn to potential theory. General analytic properties have been the subject of much study. A review article due to Newton (12) covers square well, zero range, repulsive core and exponential potentials. A review by Bargmann (13) reviews soluble potential models. Yukawa potentials for s- waves are treated by (14) Martin, Jost, Regge and

Martin, R. E. Peierls

Jost,

[illegible],

and R. E. Peierls

and for $\ell \neq 0$ by (15) Martin

[illegible]

Finite range potentials have left hand poles only e.g. range d, strength vo, has $S_0(k) = e^{-2ikd} \cdot \left[\frac{\cos k_0 d + (ik/k_0)\cdot \sin k_0 d}{\cos k_0 d - (ik/k_0)\cdot \sin k_0 d}\right]$ $k_0^2 = k^2 + |v_0|$ and an essentially singularity at $|k| = \infty$.

Infinite range potentials have left hand cuts, except the exponential potential which has poles only. Oscillating potentials can give extra poles ("redundant" poles). The potential corresponding to a single pole is the Eckart potential, see Bargmann.

Jin and Martin, assuming a finite number of subtractions in MR + U, have shown that the left hand discontinuity must change sign at least ℓ times. In general, there is no easy way to extract the discontinuity on the left hand cut, given the potential. The best one can do is give an iteration procedure for gradually extracting more and further left hand cut; the Born iteration procedure.

THE BORN ITERATION PROCEDURE

The Born term in potential scattering is (16)

$$f_B(t) = -\int_0^\infty d\mu \frac{\sigma(\mu)}{\mu^2 + t}$$

this occurs as a separate term in the potential theory Mandelstam representation.

$$f(s,t) = f_B(t) + \int_0^\infty \int_0^\infty \frac{ds'dt'}{\pi^2} \cdot \frac{\rho(s',t')}{(s'-s-i\eta)(t'-t)}$$

and as the inhomogeneous term in the integral equation

$$f(s,t) = f_B(t) - \int \frac{d^3\vec{k}'}{(2\pi)^3} \cdot \frac{\hat{V}(\vec{k_f} - \vec{k_i}) \cdot f(s',t')}{k'^2 - k^2 - i\varepsilon} .$$

$\tilde{V}$ is the Fourier transf. of potential.

Fredholm solution This has

$$f(\vec{k_f}, \vec{k_i}) = f_B(\vec{k_f}, \vec{k_i}) + \int \frac{d\vec{p}}{(2\pi)^3} \cdot \frac{N(\vec{k_f}, \vec{p}, k)}{D(k)} \cdot f_B(\vec{p} - \vec{k_i})$$

N and D have uniformly convergent series expansion. This generates the Fredholm series, each term of which is analytic in the desired cut plant.

The Born term has partial wave projection

$$\int_{\mu^2}^\infty d\mu\, \sigma(\mu) \cdot \frac{1}{2s} \cdot Q_\ell\left[1 + \mu^2/2s\right]$$

or for a simple potential $b_\ell^1(\nu) = g^2/2\nu \cdot Q_\ell\left[1 + \mu^2/2\nu\right]$

which only has a left hand cut.

The second Born term has partial wave projection which cannot be done explicitly, however it has cuts on

right and left, and all higher Born terms also have a right hand cut

e.g. $\mathrm{Im}\, b_\ell^{2}(\nu) = \frac{q^4}{4\nu^{3/2}} \cdot \left[Q_\ell\left(1+\mu^2/2\nu\right)\right]^2 \qquad \nu \geq 0$

Indeed, eventually the right hand cut will satisfy unitarity. Thus, the Born approximation is not unitary, but the usual procedure is to take the left hand cut from the Born approximation and unitarise by N/D.

Note that the Born series is a power series in g^2. It is to be remarked that a pole in t although occurring in the singularities of a Yukawa potential, is not the whole contribution, but the first Born term. In addition, the Yukawa potential has other branch points at

$k^2 = -\frac{\mu^2}{4}, \; -\mu^2, \; -9\frac{\mu^2}{4}, \; \ldots \; -\frac{1}{4}(n\mu)^2$ nth Born term.

Thus single particle exchange, in the relativistic case, corresponds to the first Born term of a Yukawa potential.

One can project out right and left cuts from the non-relativistic Mandelstam representation. The additional cuts apart from the 1st Born term are contained in the double spectral term

$$\int_0^\infty \frac{ds'}{\pi} \int_{4m^2}^\infty \frac{dt'}{\pi} \cdot \frac{\rho(s',t')}{s'-s-i\varepsilon} \cdot \frac{1}{2s} \cdot Q_\ell\left[1+\frac{t'}{2s}\right]$$

giving left hand cut

$$\mathrm{Im}\,(f_\ell - f_{\ell B}) = \int_0^\infty \frac{ds'}{\pi} \int_{4m^2}^\infty \frac{dt'}{\pi} \cdot \frac{\pi}{4s} \cdot \frac{\rho(s',t')}{s'-s} \cdot P_\ell\left[1+\frac{t'}{2s}\right] \cdot \theta\left(-s-\frac{t'}{4}\right)$$

and right hand cut

$$\mathrm{Im}\, f_\ell(s) = \int_{4m^2}^\infty \frac{dt'}{\pi} \cdot \rho(s',t') \cdot \frac{1}{2s} \cdot Q_\ell\left[1+\frac{t'}{2s}\right] \qquad \begin{matrix} -\infty < s < -m^2 \\ s > 0 \end{matrix}$$

THE BORN APPROXIMATION

The Born approximation is valid at high enough energies in potential scattering provided (17)

$$f_B(t) \underset{t\to\infty}{\longrightarrow} \text{slower than } e^{-|t|^{\frac{1}{2}}+\varepsilon}$$

The extension to the relativistic case was argued by Noyes and Wong (17). BGKT studied the exponential potential and concluded that the approximation was not necessarily reliable (see also Section 7). In relativistic calculations, because of difficulties of computation, the inclusion of the Born

term has been a popular approximation, since it has an appealing interpretation as a single particle exchange; however recently several authors (18) have indicated despair of this mechanism.

INELASTICITY

When there are several channels open, i.e. two incoming particles, there are various allowed outgoing states containing different types of particle, not necessarily all two-body states. Unitarity reads, from equation above

$$\mathrm{Im}\, A_{11} = |a_{11}|^2 + \sum |a_{1i}|^2$$

can be written $= \mathcal{R} \cdot |a_{11}|^2$

$$\mathcal{R} \geq 1$$

$\mathcal{R} = 1$ below inelastic threshold

It might also be remarked that $R(\nu)$ has cuts starting at $\{\nu_i\}$ the inelastic thresholds. In certain cases these will be below the elastic threshold, e.g. $N\bar{N} \to N\bar{N}$ has a $\pi\pi$ cut, so that $R(\nu)$ function would have a branch cut from $4 m_\pi^2 \to \infty$. We discuss consequences of inelasticity in later sections. Hamilton (30) shows that

$$\text{if } R \underset{\nu \to \infty}{\longrightarrow} \infty \text{ , then } \sigma \underset{\nu \to \infty}{\to} 0\left(\frac{1}{\nu}\right)$$

this is self contradictory, hence R must remain bounded. Roughly speaking, the incident wave strikes an area $\frac{2\pi}{\ell}$, and physically the bound demands that a finite fraction of the waves striking this area will be scattered or absorbed. If completely inelastic then $\beta \to \infty$ $(\delta = \alpha + i\beta)$

and $\mathcal{R}_\infty = 2$

so $\sqrt{\nu} \cdot \mathrm{Re}\, A(\nu) \underset{\nu \to \infty}{\longrightarrow} 0$

$$\mathrm{Im}\, A(\nu) \underset{\nu \to \infty}{\to} \frac{1}{\sqrt{2}} \cdot \sqrt{\nu}$$

.... Experimentally $\frac{\sigma_{el}}{\sigma_{tot}} = 0.16$ 17 Gev πN, $R = 6$

0.24 19 Gev NN, $R = 4$

Models have been given (29) which predict

$$\eta_\ell \to 1$$
$$\ell \to \infty$$
$$\eta_s \to 1$$
$$s \to \infty$$

THRESHOLD BEHAVIOUR

Near threshold we expect that behaviour will be as in Schrödinger equation and this is $\mathrm{Re}\, A_\ell(\nu) \propto \nu^\ell$

hence, from elastic unitarity, $\mathrm{Im}\, A_\ell(\nu) \propto \nu^{2\ell+\frac{1}{2}}$.

This is due to the presence of the centrifugal barrier term $\frac{\ell(\ell+1)}{r^2}$

SUBTRACTIONS

If $f \to$ constant, then apply dispersion relation to $(f(x)-f(x_0))/(x-x_0)$

then $\mathrm{Re}\, f(x) = \mathrm{Re}\, f(x_0) + \left(\frac{x-x_0}{\pi}\right)\int_{-\infty}^{\infty} \frac{\mathrm{Im}\, f(x')\,dx'}{(x'-x_0)(x'-x)} \qquad x \neq x_0$.

principal value taken at both poles.

If $f \to 0\,(X^n)$ and if analytic near X_0 on real axis, then

$$\mathrm{Re}\, f(x) = \mathrm{Re}\, f(x_0) + (x-x_0)\,\mathrm{Re}\, f'(x_0) + \cdots + (n!)^{-1}\,(x-x_0)^n\,\mathrm{Re}\, f^n(x_0) + \frac{(x-x_0)^{n+1}}{\pi}\int_{-\infty}^{+\infty} \frac{\left[\mathrm{Im}\, h(x') - \mathrm{Im}\, h(x_0) - \cdots - (n!)^{-1}(x'-x_0)^n\,\mathrm{Im}\, h^n(x_0)\right]dx'}{(x'-x)(x'-x_0)^{n+1}} \qquad \text{(ii)}$$

where $f(x) - f(x_0) - (x-x_0)f'(x_0) - \cdots - (n!)^{-1}(x-x_0)^n f^n(x_0)$ is over $(x-x_0)^{n+1}$.

The principal value need only be taken at X, for, near X_0

$\lim_{\varepsilon \to 0} \int_{x_0-\varepsilon}^{x_0+\varepsilon} dx' \to 0$ cauchy limit

hence can replace by $\lim_{\substack{\epsilon \to 0 \\ \delta \to 0}} \int_{x_0+\varepsilon}^{x_0+\delta}$ ordinary limit.

THE SECOND SHEET OF THE PARTIAL WAVE AMPLITUDE

Using elastic unitarity, we can continue through the elastic cut to the second sheet. Bumps in observed amplitudes are associated with the occurrence of unstable particles in intermediate states, which can be naturally related

to pairs of poles on the second sheet. In most models, variation of parameters continuously connects resonance poles with stable bound state poles. As the poles retreat into the second sheet, it is not clear at what point they cease to qualify as particles and this will lead to trouble in broken symmetry schemes. Compound structure of a bound state can be associated with second sheet cut structure.

OTHER REPRESENTATIONS

We have not space to discuss important extensions of M.R. by Regge (31) Khuri (32) Chew (33), Jones (34) and Eden (35) and others (36). A summary of requirements and formulations has been given by Eden (35).

III. EXPERIMENTAL INFORMATION ON THE TWO PION SYSTEM

1. General features

Over the whole of strong interaction scattering processes, certain general features emerge. Most of them have not been verified for the $\pi\pi$ system, but we assume they obtain in $\pi\pi$ scattering.

(i) In the low energy region, the cross sections can be well fitted with a few low partial waves, which can often be expressed by an effective range formula. As the energy increases more and higher partial waves are needed - the threshold behaviour of higher waves leads one to expect this to a certain extent.

(ii) Most reactions have resonances each of which occurs in one partial wave only. There is usually only one resonance in any one partial wave. S wave resonances are more rare than those of spin 1 or spin 2.

(iii) At higher energies (37) many channels open and the scattering becomes strongly inelastic. It becomes strongly peaked in the forward direction, with usually a smaller peak in the backward direction. In these "diffraction" peaks the amplitude is almost purely imaginary, corresponding to very strong

absorption. At 15 Gev, there is still 25% real part left in the forward direction. The diffraction peak has form

$$\frac{d\sigma}{d\Omega} \propto e^{-At}$$

(iv) At high energies (10 → 30 Gev.) and large angles, the scattering for several different processes agrees well, over a multiplicative range of 10^9, with the Orear formula (38) $\frac{d\sigma}{d\Omega} = \frac{I}{S} \exp(-aq\sin\theta)$

$\frac{1}{a} \sim 160$ Mev/c for processes $pp \rightarrow pp$
$pp \rightarrow \pi + d$

Deduction of $\pi\pi$ data from other reactions (39).

The main features that emerge are three resonances

S_0	ϵ_0	740 Mev	width	90 Mev
P_1	ρ	765 ± 3 Mev ($\nu_R = 6$)	width	124 Mev.
D_0	f_0	1253 ± 20 Mev ($\nu_R = 19$)	"	$118^{\pm 4}_{\pm 16}$ Mev.

The S_0 has a large scattering length which is the subject of much speculation. The S_2 wave is smaller and less accessible. Following Booth and Abashiarn (39) we list existing methods of deducing the $\pi\pi$ amplitude from other processes.

(i) Final state interaction (40) in pion production experiments

(a) $p + d \rightarrow He^3 + 2\pi$

(b) $\pi + N \rightarrow 2\pi + N$.

(ii) final state interaction in decay processes (41)

$k^+ \rightarrow 3\pi$.

(iii) one pion exchange model in pion (42)

production experiments

$\pi + N \rightarrow 2\pi + N$.

(iv) other models of pion production

(a) static theory of Schnitzer (43)

(b) extraction of charge exchange cross section (44)

(v) threshold anomalies (45)

(vi) π - N scattering (46)

2π circular cut

(vii) N - N scattering (47)

ρ , ω exchange

The S_0 resonance, ϵ_0, is a recent discovery and not yet firmly established (48). Chew has suggested (49) that the S_0 wave has a decreasing phase shift, at 770 Mev, associated with a ghost state of a Regge pole with imaginary mass $m^2 = -1.0$ Gev^2 where the Regge trajectory cuts $J = 0$. This would give $|a_0| \sim 0.6$ and $\delta = \pi/2$ near 0.6 Gev^2. It would also mean a_0 negative, in direct contradiction with the results of Hamilton etal. The results of many analyses lead to the general result that the S_0 scattering length is large $a_0 \sim 1.0$. The S_2 wave is not very well known, but is thought to be $\sim \frac{2}{5} S_0$ wave e.g. $a_2 \sim 0.4$. Some workers (5) believe in the existence of a σ meson in $S_0 \sim 400$ Mev. A recent review is by Rosenfeld (51).

A recent experiment (52) for $\pi^- p \to \pi^0 \pi^0 n$ ~ 2 Gev. pion momentum detects neither ϵ_0 nor σ.

The large S_0 scattering length has been attributed to the presence of a virtual particle. Barut (53), ref. A. O. Barut et al. 126 B73 (62) uses a Regge formulation. D. Atkinson (54) calls it an antibound state due to a pole below threshold on the second sheet. Finally we mention a recent ambitious fit (55) of a one pion exchange model, with form factor and off shell corrections, to

$\pi N \to \pi\pi N$ 1.3 Gev

obtains most of the expected effects including the ϵ_0, but not the σ_0 and gets the ρ width as 170 Mev. ϵ_0 is 740 Mev, width 90 Mev. He obtains curves for D_2 and F_1 waves also

$a_{s2} = -0.33$

$a_{so} = 2 \pm 1.$

f_0 1250 width 140 Mev. [illegible] results are shown in the [illegible]

IV. ASYMPTOTIC BEHAVIOUR AND BOUNDS ON THE AMPLITUDE

(a) Pomeranchuk theorem;

(b) Rigorous bounds;

(c) Asymptotic behaviour of partial wave amplitudes.

THE POMERANCHUK THEOREUM

There have been many proofs (56) of the theorem

$$\sigma_{tot}^{AB} \longrightarrow \sigma_{tot}^{\bar{A}B} \quad \text{energy} \longrightarrow \infty \quad \bar{A}B \longrightarrow \bar{A}B$$

Also if $\sigma_{tot}^{AB} \longrightarrow$ constant, then the difference must decrease as fast as $1/(\log E)^{\frac{1}{2}}$.

Martin (57) showed that the necessary assumptions are

(i) inside the analyticity domain, the forward amplitude is bounded by $C(\varepsilon).\exp[\varepsilon|s|]$, for arbitrarily small ε.

(ii) for s physical $\dfrac{|F(s,o)|}{|s|.|\log s|} \longrightarrow 0$.

(iii) $(\sigma_{AB} - \sigma_{\bar{A}B})$ approaches some limit.

If any of these three assumptions are relaxed counter examples can be found. Eden (58) showed that if

$$\log E \gtrsim \sigma_{tot} \gtrsim (\log E)^{-1+\varepsilon}$$

then assumption (ii) can be replaced by unitarity.

RIGOROUS BOUNDS

There is an extension to the real part: If $\dfrac{|F(s,o)|}{|s||\log s|} \longrightarrow 0$ and if $\left[\dfrac{\mathrm{Re}F(s) + \mathrm{Re}F(-s)}{s}\right] \longrightarrow$ some limit, then this limit = 0. Also to the modulus: If $|F(s,o)|$ is bounded by s^N and if limit $\left|\dfrac{F(s,o)}{F(-s,o)}\right|$ exists, then it is 1. This extends to finite $t < o$ if one assumes that $\mathrm{Im}F(s,t)$ does not oscillate infinitely many times at large energies.

A review of rigorous bounds has been published by Martin (59). The bounds depend upon what assumptions are used, of course. If one assumes analyticity

in S for $0 < t < 1$ then $A(s, t) < Cs^2$ $\quad 0 < t < 4$

$$|A(s, 1)| < 16\pi. \quad s. \quad \log^2 \left(\frac{s}{s_o} \right)$$

$$\frac{\sigma_{el}}{(\sigma_{tot})^2} > \log^{-2} s.$$

If one assumes full M.R. and a polynomial bound, then

$$|A(s, z)| < C \log^{3/2} s \Big/ (1 - z^2)$$

According to Martin, the limit on the strength of interaction comes from the polynomial bound. Jin and Martin (60) showed that in $0 < t < 4$, the number of subtractions needed does not exceed two.

Eden (61) has shown how to determine the phase in the high energy limit, given the behaviour of σ_{tot} and a crossing condition.

PARTIAL WAVE AMPLITUDES

From the elastic unitarity condition

$$\mathrm{Im} A_l^{-1}(\nu) = -\sqrt{\frac{\nu}{\nu + 1}}$$

call $\mathrm{Im}A = I$, $\mathrm{Re}A = R$

then $I = \sqrt{\frac{\nu}{\nu + 1}} \cdot \left[I^2 + R^2 \right]$.

$$I^2 \cdot \sqrt{\frac{\nu}{\nu + 1}} - I + R^2 \sqrt{\frac{\nu}{\nu + 1}} = 0$$

$$I = \frac{1 \pm \sqrt{1 - 4R^2 \nu / \nu + 1}}{2\sqrt{\frac{\nu}{\nu+1}}} = \frac{1}{2}\sqrt{\frac{\nu+1}{\nu}} \cdot \left[1 \pm \sqrt{1 - \frac{4R^2\nu}{\nu + 1}} \right]$$

when $R = 0$, $I = \sqrt{\frac{\nu+1}{\nu}}$.

when $\frac{4R^2\nu}{\nu + 1} > 1$, - I becomes imaginary, which case must be excluded.

We thus obtain the bounds

$I < \sqrt{\frac{\nu+1}{\nu}}$ attained when $R = 0$

$|R| < \frac{1}{2}\sqrt{\frac{\nu+1}{\nu}}$ attained when $I = \frac{1}{2}\sqrt{\frac{\nu+1}{\nu}}$

When inelasticity is included, the results are only changed slightly, for, as discussed, R remains bounded. Thus we obtain the analogous results with $\sqrt{\frac{\nu}{\nu+1}}$ replaced by $R\sqrt{\frac{\nu}{\nu+1}}$

From the Froissart bound, $\mathrm{Im}A_l(\nu) < C.\nu^2. \exp\left[-l(t_o/_K 2)^{\frac{1}{2}} \right]$

hence $\mathrm{Im}A_l(\nu)$ becomes negligible for $l >> L$ where

$$L < 2\left(\frac{s}{t_o}\right)^{\frac{1}{2}} \cdot \log s$$

$\therefore$ $\mathrm{Im}A_l(\nu) \underset{l \to \infty}{\longrightarrow} 0$

but, $\eta_l \underset{l \to \infty}{\longrightarrow} 1$ $\quad$ $\delta_l \underset{l \to \infty}{\longrightarrow} 0$

$\therefore$ $\mathrm{Re}A_l(\nu) \underset{l \to \infty}{\longrightarrow} 0$ and negligible for $l \gg L$.

These bounds for $l \to \infty$ presumably include the fact that for

$$\sum_l (2l+1)\ \mathrm{Im}A_l(\nu)\ P_l(z)$$

to converge, we must have

$$\lim_{l \to \infty} \left| \mathrm{Im}A_l(\nu) \cdot (2l+1)^{-1/l} \right| = \rho$$

where the semi-axes of the ellipse of convergence are

$$\tfrac{1}{2}\left(\rho + \frac{1}{\rho}\right), \quad \tfrac{1}{2}\left(\rho - \frac{1}{\rho}\right)$$

Most theories also agree that $\delta_l(\nu) \underset{\nu \to \infty}{\longrightarrow} n\pi$.

From the Phragmen-Lindelof theorem, if we assume

(a) $A_l(\nu)$ continuous on real axis apart possibly from finite interval

(b) It does not grow exponentially, as $|\nu| \to \infty$ in u.h.p., i.e. polynomially bounded

$$\lim_{|\nu| \to \infty} \frac{\log A_l(\nu)}{|\nu|} = 0$$

(c) Limits $A_l(\nu) \to \pm\infty$ exist, then

$$A_l(+\infty) = A_l(-\infty).$$

Hence we have a limit on the strength of the force discontinuity namely that

$$\mathrm{Im}A_l(\nu) \underset{\nu \to -\infty}{\longrightarrow} \text{const.} = R_l(+\infty)$$

In preparation for considerations in the next chapter, we try to get a clear picture of the partial wave series in the physical region. We have said that we expect there to be dominance of a few partial waves at low energies in the physical region. As $|\cos\theta|$ increases out of the physical region, higher waves come in and accumulate at the boundaries of the double spectral regions.

As the energy increases, more partial waves occur, until we reach the asymptotic region. Here, most of the amplitude is in the forward and backward

diffraction peaks with rapid fall-off at larger angles. Also the total asymptotic behaviour is $A(s, t) \xrightarrow[s \to \infty]{} S$ for $t = o$. It is also, probably, purely inelastic. The partial waves thus must either become pure imaginary or else adjust their phases to cancel out the real parts. ~~They certainly cannot all become pure imaginary as we need the series to converge.~~ The diffraction peak clearly contains many fairly equal partial waves.

Away from the diffraction peak, the constructive interference rapidly becomes destructive, and gives a low value to the sum of the series.

HIGH ENERGY LIMIT OF PARTIAL WAVES

At high energies, the amplitude peaks strongly in the forward direction. For any shape of peak we can estimate the partial wave content of the amplitude at high energy by approximating by a constant amplitude

$= c(\nu) \quad z = [1, z_o(\nu)] \quad , = o \quad z \text{ in } [Z_o(\nu), -1]$

then $A_l(\nu) = \frac{C(\nu)}{2} \int_{zo(\nu)}^{1} P_l(z)\, dz.$

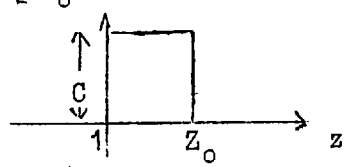

now $P_l(1) = 1$ all l

and low waves will be slowly varying within a narrow peak. Hence

$A_l(\nu) = C(\nu).\, [1 - Z_o(\nu)]\ /_2 \quad \sim$ indep. of l

the same for all waves until sufficiently high l, when oscillations within the peak will cause a reduction in the value of $A_l(\nu)$. If now, we take the peak to vary with ν, such as to retain a fixed width t_o as a function of t, the momentum transfer

$$Z_o(\nu) = 1 + \frac{2t}{s - 4} = 1 + \frac{2to}{4\nu}$$

$$\therefore A_l(\nu) = C(\nu) \cdot -t_o/4\nu \qquad l > L(\nu) \text{ say}$$

hence if $\sigma_{tot} = \frac{\ln A}{s} \xrightarrow[s \to \infty]{}$ constant

so $C(\nu) \propto \nu$.

then $A_l(\nu) \xrightarrow[\nu \to \infty]{}$ constant $\qquad l > L(\nu)$

clearly $L(\nu) \xrightarrow[\nu \to \infty]{} \infty$ and the high waves approach the same constant, but progressively more slowly.

If we try a δ - function peak

$$\delta(t) = \delta(4\nu(z-1)) = \frac{1}{4\nu} \cdot \quad (z-1)$$

we get all waves equal.

The phenomological peak is actually exponential in t, of course. Further the partial waves are found to become purely imaginary in the high energy limit. The value of η depends upon the model, for $\sigma_{tot} \sim C_1 \cdot \log^2 s$ width of peak $\gamma(s) \sim C_2/\log^2 s$.

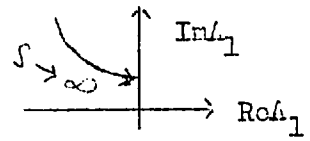

then $A_1 \sim C_1/C_2$

For Regge model $\eta \to 1$.

Experimental asymptotic behaviour and

Theoretical asymptotic bounds

It is important to be clear exactly what problem one is doing. If we are looking at the consequences of M.R. + U, then we can use the rigorously proved bounds, and we are doing a mathematical investigation of a set of equations and even if dispersion theory turns out not to be physical i.e. be a model of the real world, then our results still have a meaning. If we go further and put in experimental asymptotic behaviour, then we are assuming M R + U is physical. The author feels this is particularly relevant when making several different approximations which may lead to quite a different amplitude to the physical one, even if M R + U is true in its exact form. Thus, assuming elastic unitarity may lead to different solutions with different asymptotic behaviour and imposing some experimental constraint in this case might be invalid and lead to distortion.

THE ASYMPTOTIC BEHAVIOUR OF PRINCIPAL VALUE INTEGRALS (63)

To find the asymptotic behaviour of

$$f(\nu) = \frac{P}{\pi}\int_0^{\infty} \frac{\rho(\nu')}{\nu' - \nu} \, d\nu' \qquad (1)$$

given the asymptotic behaviour of $\rho(\nu')$ is fairly simple for ν values outside an angle including the cut, but, within this angle, one has a more complicated situation and a knowledge of the asymptotic bound of $\rho'(\nu')$ is also needed. Then the theorem of Lanz and Prosperi (63) is that, if

(a) (1) exists

(b) $\exists\ \bar{\nu}$ s.t. $|\rho(\nu')| < L/\nu'^{\alpha}$ $\quad \nu' > \bar{\nu}$, $\alpha > 0$

(c) $|\rho(\nu')| \quad g_0(\nu') \qquad \nu' > \bar{\nu}$

where $g_0(\nu')$ is a continuous positive function not smaller than const/$\nu'^{\alpha+1}$ then the following regulations hold

(i) $\alpha < 1$

$$|f(\nu)| < \frac{c_1}{|\nu|^{\alpha}}\left[\log\left(x\, g(x^{+1})\right) + \text{const}\right] \qquad |\nu| > r_1 \quad |\varphi| < \bar{\varphi}$$

$$|f(\nu)| \quad \frac{c_2}{|\nu|^{\alpha}} \qquad |\nu| > r_2 \quad |\varphi| \geq \bar{\varphi}$$

$\alpha = 1$

(ii) $$|f(\nu)| < \frac{c_1'}{|\nu_1'|} \cdot \left[2\log\left(x^2 g(x)\right) + \log x + \text{const}\right] \qquad |\nu| > r_1' \quad |\varphi| < \bar{\varphi}$$

$$|f(\nu)| < \frac{c_2}{|\nu|} \cdot \log|\nu| \qquad |\nu| > r_2' \quad |\varphi| \geq \bar{\varphi}$$

(iii) $\alpha > 1$

$$|f(\nu)| < \frac{c_0}{|\nu|} \qquad |\nu| > r_0$$

and if $\alpha = n + \alpha' \qquad 0 < \alpha \leq 1$

and if $\int_0^{\infty} \rho(\nu') \cdot \nu'^{i} \, d\nu' = 0 \ , \quad i = 0 \ldots \qquad q - 1$

then, for $q = n$

$$f(\nu) \qquad c_1'' \cdot 2\log\left(x^{1+} g(x)\right) + {}_1 \log x + \text{const}$$

$$f(\nu) \qquad c_2'' \cdot 1 + \text{const.} \quad {}_1 \log \frac{x}{z} \qquad 2''$$

for $q < n$

$$|f(\nu)| < c_0'/|\nu| \qquad |z| > \nu_0'$$

where $\nu = x + iy$, $\bar{\varphi}$ fixed in $0, \pi/2$

$c_1 \ldots c_2''$, $\nu_1 \ldots \nu_2''$ $\quad 0$ positive numbers,

Applying these results to $A_1(\ )$ restricts $\frac{d}{d}$ $\mathrm{Im}A_1(\nu)$ and $\mathrm{Im}A_1(\nu)$. If the derivative $\mathrm{Im}A_1'(\nu')$ is bounded by a power of ν' then the right hand integral is bounded by constant.log $|\nu|$. If we assume that $A_1(\nu) \sim c.\nu^{\beta}$ and that $\mathrm{Im}A_1 \underset{\nu \to \infty}{\longrightarrow}$ limit then to satisfy $|A_1(\nu)| < \sqrt{\frac{\nu+1}{\nu}}$ $\beta < N$ we must have $\mathrm{Im}A_1(-\infty) = \mathrm{Im}A_1(+\infty)$, to give cancellation of the logarithms from left and right as $\nu \to +\infty$. Then $A_1(\nu)$ is bounded in every direction of the complex plane.

If, on the other hand, we merely assume $\mathrm{Im}A_1(\nu)$ bounded as $\nu \to -\infty$ and derivative bounded by power of ν then $|A_1(\nu)| \underset{\nu \to \infty}{\longrightarrow}$ const. log $|\nu|$ in all directions. This actually forces

$$|A(s,t)| \underset{\substack{s \to \infty \\ t < 0}}{\longrightarrow} \text{const.} \quad s \quad \log^3 s$$

except small angle near negative real axis

This agrees with the Regge behaviour

$$A(s,t) \underset{s \to \infty}{\longrightarrow} s^{\alpha(t)} \qquad \alpha(0) \leq 1. \qquad (2)$$

Omnès has shown that, assuming (2)

$$|\mathrm{Im}A_1(\nu)| \underset{\nu \to \pm\infty}{\longrightarrow} < \text{const.} \ |\nu|^{\alpha(0)-1}$$

$$\therefore |A_1(\nu)| \underset{\nu \to \infty}{\longrightarrow} \leq \text{const.} \ |\nu|^{\alpha(0)-1} . \log \nu$$

$$\therefore |A(s,t)| \underset{s \to \infty}{\longrightarrow} |s|^{\alpha(0)} . \log^3 s.$$

Another consequence of the theorem is that to justify N/D method, since one needs the Omnès function $D(\nu)$ bounded by $|\nu|^{\beta}$ as $\nu \to \infty$, one merely needs $\delta_1(\nu)$ bounded as $\nu \to \infty$ i.e. $\lim_{\nu \to \infty} \delta_1(\nu)$ need not exist.

V. PARTIAL WAVE DISPERSION RELATIONS

The N/D method

If we define the subproblem, given the left hand cut discontinuity, and given that the amplitude obeys unitarity on the right hand cut, construct the amplitude, then a variety of methods have been suggested. The most popular is

the N/D method (65). One conjectures that $A(\nu)$ can be written in the form

$$A(\nu) = N(\nu)/D(\nu)$$

where $N(\nu)$ only has a left hand cut and $D(\nu)$ only a right hand cut. This separation is certainly possible in potential theory (66)

$$A_l(\nu) = \frac{1}{f_l(-k)} \cdot \left[f_l(k) - f_l(-k) \right] / 2ik$$

and can be carried out in the elastic case since one can explicitly construct the function

$$D_l(\nu) = \exp\left[-\left(\frac{\nu-\nu_0}{\pi}\right) \int_0^\infty \frac{d\nu' \cdot \delta_l(\nu')}{(\nu'-\nu_0)(\nu'-\nu)} \right]$$

Now, $\mathrm{Im}\, N_l(\nu) = \mathrm{Im}\, A_l(\nu) \cdot D_l(\nu)$ $\qquad \nu < -1$

$= 0 \qquad \nu > -1$

$\mathrm{Im}\, D_l(\nu) = -N_l(\nu) \cdot R_l(\nu) \cdot \sqrt{\frac{\nu}{\nu+1}} \qquad \nu > 0$

$= 0 \qquad \nu < 0$

$$\therefore N(\nu) = \frac{1}{\pi} \int_{-\infty}^{-1} d\nu' \cdot \frac{\mathrm{Im}\, N(\nu')}{\nu'-\nu} = \frac{1}{\pi} \int_{-\infty}^{-1} d\nu' \cdot \frac{\mathrm{Im}\, A_l(\nu')}{\nu'-\nu} \cdot D(\nu')$$

and writing $D(\nu)$ in subtracted form

$$D(\nu) = 1 + \left(\frac{\nu-\nu_0}{\pi}\right) \int_0^\infty d\nu' \frac{\mathrm{Im}\, D(\nu')}{(\nu'-\nu)(\nu'-\nu_0)}$$

$$= 1 - \left(\frac{\nu-\nu_0}{\pi}\right) \int_0^\infty d\nu' \sqrt{\frac{\nu'}{\nu'+1}} \cdot \frac{R(\nu')\, N(\nu')}{(\nu'-\nu)(\nu'-\nu_0)}$$

From these N/D equations one can write an integral equation for N or D:-

$$D_l(\nu) = 1 - \left(\frac{\nu-\nu_0}{\pi}\right) \int_{-\infty}^{-1} d\nu' \cdot H_l(\nu,\nu')\, D_l(\nu')$$

where $H_l(\nu,\nu') = -\frac{1}{\pi} \int_0^\infty d\nu'' \cdot R_l(\nu'') \sqrt{\frac{\nu''}{\nu''+1}} \cdot \frac{1}{(\nu''-\nu_0)(\nu''-\nu)(\nu''-\nu')}$

However, the equations are almost certainly non-Fredholm.

Hamilton (67) derives a necessary condition for the equation to be of Fredholm type, $\int_{-\infty}^{-1} d\nu'' \left| \mathrm{Im}\, A(\nu'') \right|^2 < \infty$

which is almost certainly not the case.

The Uretsky form of N/D (68)

is $N(\nu) = B(\nu) + \frac{1}{\pi} \int_0^\infty d\nu' \cdot \sqrt{\frac{\nu'}{\nu'+1}} \cdot \frac{N(\nu')}{\nu'-\nu} \cdot \left[B(\nu') - \left(\frac{\nu-\nu_0}{\nu'-\nu_0}\right) \cdot B(\nu) \right]$

where $B(\nu) = \frac{1}{\pi} \int_{-\infty}^{-1} d\nu' \cdot \sqrt{\frac{\nu'}{\nu'+1}} \cdot \left[\frac{\nu B(\nu) - \nu' B(\nu')}{\nu - \nu'} \right] \cdot N(\nu')$

The equation for D as before. This is a much better form, as one only needs $B(\nu)$ for ν in $[0,\infty]$ and the integral equation for $N(\nu)$ is not singular, however it is non Fredholm. Another form is due to Frye and Warnock (69) and incorporates inelasticity in a natural way

$$\eta(\nu)\cdot N(\nu) = B(\nu) + \frac{1}{\pi}\int_0^\infty d\nu' \sqrt{\frac{\nu'}{\nu'+1}}\cdot\left[\frac{\nu B(\nu) - \nu' B(\nu')}{\nu-\nu'}\right] N(\nu')$$

They give a thorough discussion of this method.

The unsubtracted form of Uretsky N/D is

$$N(\nu) = B(\nu) + \frac{1}{\pi}\int_0^\infty d\nu' \sqrt{\frac{\nu'}{\nu'+1}}\cdot N(\nu')\left[\frac{B(\nu)-B(\nu')}{\nu-\nu'}\right]$$

$$D(\nu) = 1 - \frac{1}{\pi}\int_0^\infty d\nu' \sqrt{\frac{\nu'}{\nu'+1}}\cdot\frac{N(\nu')}{\nu'-\nu}$$

The N/D method has also been extended to complex l.

THE CDD AMBIGUITY (70)

Given the left hand cut and given that unitarity holds on the right, we can write the N/D equations, given in the previous section. If we add poles to $D(\nu)$, then we obtain a different solution A, but it has the same left hand cut and satisfies the same unitarity condition. Thus the problem has an infinite number of solutions and an infinite number of arbitrary parameters. We have not specified the asymptotic behaviour of A we require, but this does not appear to limit the CDD poles.

We do not know how many solutions the integral equation for $N(\nu)$ will have, if any, and if so how many parameters will be involved. Of course, adding a self-consistency or bootstrap requirement will have a big effect and will almost certainly greatly reduce the number of parameters.

One can also introduce other principles to get over the dilemma, the usual one being to say bluntly that there shall be no CDD poles in the acceptable solution. This can be enforced by requiring that Levinson's theorem be satisfied

$$\delta(\infty) - \delta(0) = (n_B - n_{CDD})\pi = n_B\pi$$

Note that at CDD pole the amplitude = 0, so that it does not correspond exactly to a particle. Particles correspond to zeros of D, but the arbitrary parameters of the CDD pole can ensure a zero of D at an arbitrary place with arbitrary gradient. Hence CDD poles are closely related to the existence of incalculable particles. In their treatment of the Zachariasen model, Gell, Mann &

Zachariasen (71) introduced an extra particle by explicitly adding a pole to D, however they took the position of the particle to be the position of the CDD pole. However, in a later treatment (72), the CDD pole parameters r, z are used to introduce an elementary particle g^2, m^2, the conditions

$$D(m^2) = 0$$

$$g^2 = -(s - m^2) \cdot \Gamma(s)\Big|_{s = m^2}$$

being used to eliminate r and z in terms of g^2, m^2. In the treatment by Gell-Mann and Zachariasen, the solution with no CDD pole corresponded to a Lagrangian with bubble interaction only and the solution with a CDD pole corresponded to the addition of graphs containing an extra particle, which appeared in the Lagrangian.

LEVINSON'S THEOREM (73)

We first list the significance of poles and zeros on the physical sheet

pole of A - particle assumed always on real axis, cannot occur on unitarity cut

zero of A - can occur anywhere

pole of D - can occur (CDD pole)

zero of D - particle.
There will be no zeros of D on the physical cut. Resonances correspond to zeros of ReD on the physical cut. CMI prove no zeros of D in complex plane if $N(\nu^1)$ does not change sign, hence provided N has no zero on real axis

pole of N - particle

zero of N - can occur. Probably can only coincide with a zero of D in a single channel calculation, not in all channels simultaneously in a every channel calculation. A coincident zero of N and zero of D is a ghost particle, and affects the assignment of particles ato zeros of D, possibly making Levinson's theorem an inequality rather than equality.

pole of A^{-1} - may correspond to zero of N or pole of D

zero of A^{-1} - particle, can be zero of D or pole of N. Moffat found a condition for no complex zeros of A^{-1}, which was satisfied by his solution.

Another point about A^{-1} is that, for a zero of ReA, we can have either ReA^{-1} = 0 or . For a pole of A, we must have a zero of A^{-1}.

If we have the following problem: "Given discontinuity on the left and that a dispersion relation holds and unitarity holds on the right, determine the amplitude", then the question arises, can we determine the number of bound states and their positions and residues uniquely? In potential theory, Bargman (74) has shown $\exists$ whole classes of potentials which all lead to the same phase shift but differ in bound states.

It is hoped, in relativistic theory, that the bound states will be calculable. This could well arise as a result of crossing symmetry and self consistency demands. In addition, it has been widely proposed that there should be no CDD poles in the correct solution. This is sometimes described as Levinson's theorem being valid. It is certainly an extra constraint on the solution. For, suppose we are given the above-mentioned information, then, in order to determine A we assume it has an N/D decomposition. We do not know how many poles there will be in the N function. We assume there will be n say. We assume no poles in D and calculate D. From the asymptotic phase of D we determine the number of zeros of D. We can also determine their residues and positions. We can carry out this process for n= o, 1, 2 . . We now look at this family of solutions and pick out the one which obeys crossing i.e. that ties up with equations and bound states in other channels. Of course, it may be true that these are arbitrary and incalculable, or they may be determined by crossing.

The theorem follows by using the theorem (75)

$$\frac{1}{2\pi i}\int_C \frac{f'(z)}{f(z)}\,.\,dz = N - P$$

where f(z) is analytic inside and on closed contour C apart from a finite number of polesP and zeros N, and is not zero on the contour. This theorem is applied to the D function, so the left hand side becomes

$$\frac{1}{2\pi i}\int_0^\infty dz\,.\,\frac{d}{dz}\left[\log\left(D(z+i\varepsilon)\,/\,D(z-i\varepsilon)\right)\right]$$

$$= \frac{1}{2\pi i}\int_0^\infty dz\,.\,\frac{d}{dz}\log\left[e^{-2i\delta_\ell(z)}\right] = \frac{1}{\pi}\left[\delta_\ell(0) - \delta_\ell(\infty)\right]$$

Levinson proved that D has no poles in potential theory, so that

$$\frac{1}{\pi}\left[\delta_\ell(0) - \delta_\ell(\infty)\right] = \text{no. of zeros of D}$$

which is Levinson's theorem. Zeros of D correspond to particles. If N happens to have a coincident zero then this will be a ghost particle. This means that strictly the assignment of the number of particles to the number of zeros of D is an inequality.

Chew has remarked (76) that "bound states tend to produce a decrease of phase shifts" which is an interesting way of viewing Levinson's theorem.

Relativistic treatments of Levinson's theorem

Warnock's proof (77) requires that A satisfy a dispersion relation. Inelasticity can occur, and the imaginary part of the phase shift was subject to mild restrictions. The N/D integral equation was assumed to be of Fredholm type with non-vanishing determinant. The theorem is

$$\frac{1}{\pi}\left[\delta(0) - \delta(\infty)\right] = n_c - n.$$

n = no. of bound states. nc = number of CDD poles.

For complete generality of solution, Warnock allowed CDD poles on the real axis below threshold.

Charap (78) on the other hand used LSZ with a scalar hermitian field. His result was

$$\frac{1}{\pi}\left[\delta(0) - \delta(\infty)\right] = nc - p$$

$\delta(\infty)$ meaning the real part of $\delta(\infty)$

nc = no. of poles of D.

p = number of particle poles with $Z_3 = 0$. p is also the number of particle poles in the propagator. Charap obtained his result by considering the integral equation for the vertex function and some of the p poles occur on the second sheet of this function.

Choudhury (79) showed that the Zachariasen model obeys Warnock's form and not Charap's.

Hagen (80) has given a field theoretic proof which agrees with Warnock's and the Zachariasen model, but disagrees with Charap's.

MANY CHANNEL LEVINSON'S THEOREM AND THE EFFECT OF INELASTICITY

When considering the relation between single channel calculations, in which the presence of other channels is represented by an inelasticity function $R(\nu)$ or $\eta(\nu)$ and the full multichannel matrix calculation, the question arises as to whether one will get the same result in each case and also whether the application of Levinson's theorem in a single channel form in each channel is reasonable.

Bander, Coulter and Shaw (81) showed that the two results could be different when the forces in the inelastic channel 2 were sufficient to produce a bound state in that channel. On coupling to channel 1 this would produce a resonance in $A_{11}(\nu)$. However, in this case, putting in the correct inelasticity factor from the multichannel solution into a single channel calculation of channel 1 gives a different function. D Atkinson etal (82) indicated that in order to get the same function, one has to introduce a CDD pole into the single channel calculation. They proposed an alternative form of Levinson's theorem, applying to the eigenamplitudes obtained by diagonalising T above the highest threshold, by a real orthogonal energy independent matrix O. For two channels:

$$\rho_1 t_{11} = \alpha^2 T^{(1)} + \beta^2 T^{(2)}$$
$$\sqrt{\rho_1 \rho_2}\, t_{12} = \alpha\beta\,(T^{(1)} - T^{(2)})$$
$$\rho_2 t_{22} = \beta^2 T^{(1)} + \alpha^2 T^{(2)}$$

Thus, the single channel amplitudes are sums of eigenamplitudes, best represented on argand diagram. The eigenamplitudes obey a unitarity condition

$$\mathrm{Im}\, T^{(i)} = |T^{(i)}|^2 \qquad i = 1, 2 \qquad s \geq s_2$$
$$T^{(i)} = e^{i\delta^{(i)}} \cdot \sin\delta^{(i)}$$

$\delta^{(i)}(s)$, the eigenphase shifts, are real for $s \geq s_2$, however $T^{(i)}(s)$ will have addition branch cuts from α, β and simple assumptions had to be made about these.

Defining $\delta^{(i)}(s_1) = 0$, the Levinson theorem is

$$n_\beta^{(i)} = -\frac{1}{\pi}\delta^{(i)}(\infty)$$

$\sum_{i,\beta} n_\beta^{(i)}$ is the total number of bound states in all channels. Thus the new physical principle is that the eigenamplitudes are more natural physical quantities and compositeness is decided in relation to them. The poles in the eigenamplitudes produce phase changes in them, and this is communicated in a complicated way by vector addition to the single channel amplitudes. Whether or not a resonance in an eigenamplitude produces a resonance in a single channel amplitude depends on the relative sizes of the eigenamplitudes. In the $\pi\pi, K\bar{K}, \eta\eta$ 3 channel case, a simple estimate for the ρ pole is obtained from the $SU(3)$ combinations

$$|\rho\rangle = \sqrt{\tfrac{2}{3}}\,|\pi\pi\rangle + \sqrt{\tfrac{1}{3}}\,|K\bar{K}\rangle$$

Thus, from the crank-shaft rule, if the ρ occurs as a pole of an eigenamplitude it will occur in the single channel $\pi\pi$ calculation and no CDD pole will be necessary.

In a case like this, where a resonance is largely in one channel, then it can be obtained in a single channel calculation in that channel. It cannot be obtained in a single channel calculation in another channel. Thus ρ cannot be bootstrapped in a $K\bar{K}$ calculation. In more complicated cases, e.g.

$$Y_1^* = -\frac{1}{\sqrt{6}}(\bar{K}N) + \frac{1}{\sqrt{6}}(K\Xi) + \frac{1}{\sqrt{6}}(\pi\Sigma) + \frac{1}{2}(\pi\Lambda) - \frac{1}{2}(\Sigma\eta)$$

1385 1434 1812 1331 1253 1342

it is difficult to imagine the resonance occuring in any particular single channel. There is of course no evidence for the truth of this many channel Levinson theorem, and it does depend upon the assumed good behaviour of $\alpha(\nu)$ and $\beta(\nu)$. Squires has remarked that, if quarks exist, then all particles, e.g. ρ may well be best considered as bound states of quark systems, so that all bootstrap calcs. would be thrown into doubt.

Further work has been carried out on many channel calculations and inelasticity by Squires (83) and others (84) (85).

VI. DYNAMICAL CALCULATIONS

The first dispersion theoretic calculation was made by Chew and Low in 1956. After the introduction of the Mandelstam representation in 1958, the first attempts at approximate $\pi\pi$ calculations were done mainly in 1960. There were three main calculations

(i) N/D by Chew and Mandelstam

(ii) Inverse amplitude by Barnsden and Moffat

(iii) The work of Shirkov etal.

The Chew-Mandelstam equations (86)

This wasthe first formulation of the $\pi\pi$ problem for M R + U and the first occurrence of many ideas. They used a partial wave series in the t channel to continue to the near left of the s channel. The partial wave amplitude was projected out and a nearby singularity attitude adopted. The partial wave series was truncated. They assumed asymptotic behaviour

$$\mathrm{Im}\, A_\ell(\nu) \underset{\nu\to\infty}{\longrightarrow} \frac{1}{2} \quad ; \quad \mathrm{Re}\, A_\ell(\nu) \underset{\nu\to\infty}{\longrightarrow} 0$$

corresponding to diffraction scattering. They used N/D method, an expected inelasticity to be significant only above $\nu \times 10$. They introduced the symmetry point $s = t = u = 4/3$, and the constant λ where $A^0 = -5\lambda$, $A^1 = 0$, $A^2 = -2\lambda$ at the symmetry point. They suggested an S dominant calculation remarking that it was usually true for marginally singular integral equations that, if the singular term is less than some critical value, the equation had a unique solution obtainable by standard methods. They expected this to be the case for S dominant solutions, but not with a large P wave. CMN did numerical circular iteration and obtained S dominant solutions for different values of λ.

For large P wave CM introduced the idea of "matching" the crossed channel at symmetry points. They used a two pole unitary form in the direct channel. They justified this procedure by showing it worked quite well for the S wave. They wrote down symmetry point conditions of various orders by differentiation.

They could obtain a P wave resonance for some values of λ, but the validity of this solution was dubious.

The work of Bransden and Moffat (87)

This is discussed in Chapter 6. They used an inverse amplitude approach and a clever iteration procedure. The physical assumptions were the same as CM except that they were using a nearby singularity approach for the inverse amplitude which makes it a different approximation. They obtained the S dominant solutions of CMN and also P wave resonant solutions. Their solutions were very sensitive to λ, but could give a sensible width for the ρ.

The Shirkov Equations (88)

This used a different way of deriving coupled partial wave dispersion relations from the Mandelstam representation. They used a partial wave series and substituted this for real and imaginary parts in a forward dispersion relation and its angular derivatives . They studied a neutral S - P model, which they could solve explicitly and a charged S - P model for which the asymptotic behaviour of the solutions could be deduced analytically and families of solutions identified. Numerical solutions were obtained. These involved many parameters and a resonant P_1 wave could be obtained provided the S_0 wave was large, although not necessarily resonant, but if resonant then S_0 resonance width ~ 10 x width of ρ . Thus the Shirkov equations indicate that the major force producing the ρ is the S_0, whereas C M expected the ρ to produce itself and be self-supporting.

Criticism by Lovelace (89)

proved CM equations with both S and P waves possess no exact solution, with possible exception of solutions oscillating at infinity. The normal iteration procedures for solving will only be asymptotically convergent in the low energy region, convergence being worse the larger the P wave. A cut off is unavoidable. Exact solution has much worse behaviour than any order in expansion in powers

of λ. For finite $\mathrm{Re}\, A_\ell^I(\infty)$, need $\mathrm{Im}\, A_\ell^I(-\infty) = \mathrm{Im}\, A_\ell^I(+\infty)$, which cannot be satisfied unless P wave vanishes in the physical region. Comparison with Shirkov equations by Pivarova (90).

BOOTSTRAP CALCULATIONS

It soon become clear that, in approximate calculations, one did not know how many arbitrary parameters there would be and, therefore, how to apply the constraint of crossing symmetry in a sensible way. This lead to the bootstrap conjecture in which one assumed that there would be no free parameters. This is thus an instruction to apply enough approximate constraints to determine all parameters. This is a dangerous assumption but can be modified, e.g. one can assume there will be one parameter like Bransden & Moffat or one can try to discover numberically how many free parameters there should be (see next chapter). The first bootstrap calculation was performed for $\pi\pi$ by Zachariasen (91).

FEYNMAN'S PRINCIPLE OF INDIFFERENCE (92).

That it was possible that there were several subsets of particles which could be taken as elementary and the rest could then be calculated. Further that it would be impossible to tell which of the subsets was most elementary. F. E. Low has remarked that if one only used renormalisable interactions between known strongly stable particles, then the requirement of indifference gives many more equations between mass and coupling constants than unknowns, so that unless some remarkable identities occurred there would be no solution. Even if one satisfied these there was no guarantee that all scattering amplitudes will be identical for different choices of enementary subset. Salam has given an appealing approach to this principle by including all particles in the Lagrangian and on an equal footing, see section 8. In a practical calculation, the oligarchic tendencies reported by Morgan etal, see section 5, would make things difficult. That is some composite particles

may be incalculable in many channel calculations with certain choices of subset of particles and calculable in others.

The Bootstrap idea

If, take some particles elementary i.e. occurring in basic equations, e.g. Lagrangian or S matrix, and the rest composite, i.e. calculable, derived from the equations, regarded as bound states of elementary particles in iteration, then, have unpleasant task of saying which are elementary and whether this set is unique, for certainly in model field theories (see later) this is meaningless in the form stated. One way out is to say all are composite i.e. all calculable.

One can go further and say that all poles of the S matrix are Regge poles and all naturally occurring particles lie on Regge trajectories. Regge poles were assumed obviously dynamical and calculable. However, see (95) where in massive electrodynamics the elementary spin 1 particle and elementary spin $\frac{1}{2}$ particle occur in Lagrangian and interact through conserved current. The spin $\frac{1}{2}$ particle is then found to lie on a Regge trajectory. Also there is no restriction on its mass or coupling constant.

The spin 1 particle does not lie on a trajectory and thus if one uses Mandelstam's conjecture (96) that one needs all particles to be Regge like, then one may still preserve the idea that if all particles were Regge-like then they could be bootstrapped i.e. all determined from dynamical equations.

It was also taken that elementary particles would be fixed poles in l and would occur as CDD poles. Thus one assumed CDD poles were incalculable.

To keep things straight, we note that CDD poles introduce arbitrary parameters, which can be used to give zeros of D producing extra arbitrary particles. That pole terms $g^2 P_\ell(\cos\theta)/(t-m^2)$ are incalculable from self consistency is far from obvious. Indeed, Dragt and Karplus showed that given the parameters of a pole in the processes $A + A \to A + A$ the parameters of a pole in the process $A + A \to B + B$ could be deduced solely

by the use of M R + U.

Finally we note that the bootstrap hypothesis is unaffected by dynamical details such as whether the Regge representation is true or whether the ρ bootstraps itself.

Bootstrap calculations in dispersion theory

What has come to be meant by a bootstrap calculation is an approximate and usually single channel partial wave calculation based on left hand singularities from single particle exchange terms only and solution by unitarising the amplitude. Zachariasen's method is the most popular as it is simplest. It will be discussed in Chapter 4 in detail, but is based on the ansatz

$$N(\nu) = B(\nu)$$

The Balazs method will be discussed in Chapter 3 and is a modification of Chew & Mandelstam's method.

Zachariasen considered the P_1 wave in $\pi\pi$ in which the ρ meson should occur and for which the main left hand singularities may come from the exchange of a ρ. Thus by demanding self consistency in that the position and residue of the ρ in the crossed channel should be the same as those in the direct channel, he was able to deduce two equations for two unknowns and a hopefully unique answer for the position and width of the ρ, to be compared with experiment. The values were bad - 350 Mev compared with 750 Mev for position and width 4 x too large. However, the fact that values could be obtained at all was encouraging. In this case, the ρ bootstraps itself. Another type conjectured by Chew was the "reciprocal bootstrap", exemplified by N & N*, where it was conjectured the dominant "force" "producing" the N was the exchange of N*

, and " " " " N* " N

One can escalate such considerations to bootstrapping whole families of particles simultaneously. However, at bottom, the basic idea is one of solving M R + U by approximate means and using the obviou requirement of self consistency as an aid.

SURVEY OF CALCULATIONS

Bootstrap calculations using the Zachariasen method

1. A Wazed preprint Reciprocal for Quarks.
2. G. Payne P.L. 15 63 3/65. K^* s.c. with K^π, ρ, f_0 exchange.
3. Zachariasen and Zemach P.R. 128 849 10/12. $\pi\pi, \pi\omega$ coupled.
4. Abers and Zachariasen $\pi N, \pi N^*$ reciprocal bootstrap.
5. Gotsman Ω^-
6. A. Kanazawa and N. Jokuda, P.T.P. 142 4/63.
   K^π, ρ exchange, width of K^* 4 x too large
7. R. Kawamura. P.T.P. 30 2685/63.
8. A. D. Martin and L. J. Vick N.C. 39 904 10/65 K^* in πK unsuccessful.

Bootstrap calculations using the Balazs method

1. S. K. Bose and M. Desarkissian N.C. 30 878 '63 D in NN
   N.C. 30 894 '63 $\pi\Lambda$ scattering
2. J. C. Pati P.R. 134 387 '64 Ξ^* in $\bar{K}\Lambda$
3. G. L. Kane P.R. 135 843 64 Ω^- in $\bar{K}\Xi$
4. S. R. Chaudhury and L. K. Pandit P.R. 135 1027 64 Ω^- in $\bar{K}\Xi$
5. V. Singh and B.M. Udgaonkar P.R. 128 1820 11/62 Nucleon ff.
6. " 130 1177 63 N^* in π N.
7. Balazs P.R. 128 1939 10/62 in
8. M. Swiecki P.L. 19 333 11/65 Y_1^* in N, $\bar{K}$ N coupled.
9. Wong P.R. 138 B246 '65 sinil.

The variational method of Hamilton was used by Oades
ref. G.C. Oades U.C.L. and Sienna '64 for ρ in $\pi\pi$.

Different formulations of partial wave calculations have been developed by

1. Omnès
   R. Omnès N.C. 21 524 8/61
2. Taylor and Truong.
   Taylor and Truong N.C. 25 946 8/62
3. D. Atkinson CERN TH 399 1/64
   Antibound states in S_0, also in S_2 further away.
4. B. R. Desai P.R.L. 6 497 '61.
   $\lambda < -0.15$, $a_0 \lesssim 1.9$
5. R. C. Hwa P.R. 136 1525 12/64
6. A. W. Martin's method
   A.W. Martin P.R. 135 B 967 '64

$$N(\nu) = B(\nu) + \frac{1}{\pi}\int_0^\infty d\nu' \sqrt{\frac{\nu'}{\nu'+1}}\,\frac{N(\nu')}{\nu'-\nu}\left[B(\nu') - \left(\frac{\nu-\nu_0}{\nu'-\nu_0}\right)B(\nu)\right]$$

makes a rational approximation to the kernel

$$\frac{1}{\nu'-\nu}\left[B(\nu') - \left(\frac{\nu-\nu_0}{\nu'-\nu_0}\right)B(\nu)\right] \qquad \text{(regular at } \nu=\nu'\text{)}$$

$$\simeq \frac{P_n(\nu,\nu')}{Q_m(\nu,\nu')}$$

The kernel is now degerate and integral equation reduces to an algebraic one. It essentially makes a cut off in B replacing logarithmic behaviour by constant asymptotically. Tho approximation preserves ν_0 independence.

7. J. Franklin's method.
J. Franklin P.R. 139 B912 8/65

Defines the separation $A(s) = B(s) \cdot G^{-1}(s)$.

More general methods are due to

1. Kanki and Tubis P.R. 136 723 11/64
2. R. Kreps etal. . P.R. 133 1526 '64.

Further models in

R. Kreps P.R. 141 1380 1/66 found to have no physical solutions.

3. Burkhardt and McCauley, N.C. 38 872 '65.

Fixed angle amplitudes can be suitably chosen to resemble partial wave amplitudes in any specified low energy region.

4. Burkhardt CERN TH. 593.
uses fixed angle method to write dispersion relations for the logarithm of the amplitude which thus automatically ensures exponential behaviour at fixed angle.

For Inelastic calculations

1. Froissart's η method.

Advantage of not needing P.V. integrals unlike method of

2. W. Frazer and J. Ball P.R.L. 7 204 '61.

Used to explain cusps in inelastic amplitudes due to inelastic channels opening.

Regge calculations

ref. Zachariasen. Edinburgh '63.

The idea of a Regge bootstrap (97) is to determine a set of Regge trajectories by applying crossing and self consistency. One has to define a continuation of the amplitude to complex l.

WORK WITH THE FULL AMPLITUDE

Work with the full amplitude, i.e. not in partial waves, is a long and

difficult process. Indeed it has only been possible since the advent of good computing facilities. The first one was due to Bransden, Burke, Moffat, Moorhouse and Morgan (98), which tried to perform, for $\pi\pi$ system, the iteration procedure suggested by Mandelstam. From the asymptotic behaviour of the double spectral functions, they identified Regge trajectories. Regge trajectories were extracted and double spectral functions found. However the solution was not self-consistent in needing the f_0 to produce the ρ but not supporting the f_0. A nonrelativistic calculation on the same lines had previously been performed with great success by Burke and Tate (99).

Another method is to use the full amplitude in Regge form to calculate $B_1(\nu)$ and then to solve by Uretsky N/D. This was performed by Collins and Teplitz for the ρ trajectory in $\pi\pi$(100) and, although they obtained a self-consistent trajectory, it did not have a meson on it, but turned down after threshold. A discussion of inadequacies and further proposals have been given by Collins (101).

Many channel calculations

In view of possible competition between channels and large inelastic effects, many channel calculations have been performed. The many channel $N D^{-1}$ is due to Bjørken (102), which is automatically unitary and symmetric. The computation can be greatly simplified using the Zachariasen approximation (103), but this formulation is sensitive to subtraction point and not symmetric. An approximate formulation not suffering from these drawbacks has been given by Shaw (104).

Multi-channel calculations

P. Nath & G. L. Shaw P.R. 137 B711 2/65
also " & C. Iddings P.12 133 B1085 '64
"Uncoupled-phase" method.
H. Pagels P.R. 140 B1599 12/65
Nath & Shaw P.R. 138 B702 5/65
Multichannel effective range N/D

Inelastic calculations

1. Coulter, Scotti and Shaw P.R. 136 B1399 12/64
   NN scattering - effect of inelastic unitarity.
2. Fulco, Shaw & Wong P.R. 137 B1242 3/65
   Effect of closed inelastic channels.
3. Coulter & Shaw P.R. 138 B1273 '65
   ρ with inelasticity. More narrow but still no good.

SYMMETRIES AND BOOTSTRAPS

One can bootstrap multiplets of particles together in a many-channel calculation and one can also do bootstrap calculations assuming that degenerate multiplets will occur. One can further calculate splitting of one multiplet due to the splitting of another. However this is a separate matter from the idea of bootstrapping the symmetry itself.

The statement of the symmetry is equality of masses of particles in multiplets and certain relations between their coupling constants. Thus one can be said to have bootstrapped the symmetry if a calculation involving the correct numbers of particles and having arbitrary masses and coupling constants obey the symmetry requirements. No one has yet done such a calculation but various more limited attempts have been made (105) e.g. Fulco and Wong (105) using a method of Capps, found the effect that a mass splitting of pseudoscalar mesons would have on the masses of the dynamically produced vector mesons. It gave twice the experimental splitting, but the experimental ordering was obtained. A calculation was done by Cutkosky (106) which considered vector mesons bootstrapping themselves with coupling constants Cijk, in which he showed these satisfied

$$C_{ijk}\ C_{lmk} + C_{jlk}\ C_{imk} + C_{lik}\ C_{jmk} = 0$$

making them the structure factors of a lie group and restricting the number of particles to 3, 8 etc. Other workers (107) have tried to extend this idea of deriving a model independent "bootstrap algebra". Quark models have been developed by Dalitz and others (108).

Other references:

R. Capps	P.R.L.	10	312	'63	
R. E. Cutkosky	P.R.	131	1888	'63	
E. Abers, F Zach & C. Zemach.	P.R.	132	1831	'63	
M. Baker & S. Glashow	P.R.	128	2462	'62	
Zach. & Zem.	P.R.	136	B441	4/65	Parity.
J. Franklin	P.R.	138	1202	6/65	
R.C. Hwa & S.H. Patil.	P.R.	138	B933	5/65	
A. W. Martin	P.R.	136	B1515	12/64	Soluble static model and prediction of symmetries.
Martin and Wali	N.C.	31	1324	3/64	Meson-Baryon resonances proof
	P.R.	130	2455	'63	of independence uses symmetrised N/D ref. Martin's thesis.
Y. Miyamoto	P.T.P.	28	967	12/62	
Haw and Patil	P.R.	139	969	'65	
Chan Hong-Mo etal.	CERN	TH. 395			
		N.C.	33	70 '64	
		P.R.L.	11	521 '63	

One should be able to bootstrap broken symmetries as well and hopefully say why broken symmetric solutions occur rather than fully symmetric. Other ideas are to bootstrap parity conservation in strong interactions and also T and C. After all, indispersion theories these are just relations between positions and residues of poles.

BOOTSTRAP METHODOLOGY

There have been several papers on the validity of the bootstrap idea or of bootstrap calculations. Massida and Pignotti (109) claim that S wave bound states occurring in scalar-scalar interaction in a calculation, using N/D, by Chan etal, were accidental solutions. Chew and Low have argued (110) about the reciprocal bootstrap of N and N*. Din has examined the Zachariasen model (see Chapter 4) and concluded it is unreliable. He also examined an exactly soluble model (111) which had a family of solutions, but when solved using the Zachariasen approximation had no solutions. Squires (112) has retorted that Din's exact solution does not satisfy Levinson's theorem and hence has a CDD pole. Huang and Low (113) have also considered bootstraps in soluble models.

VII. FURTHER THEORETICAL RESULTS

VALIDITY OF APPROXIMATION, tested by potential scattering

ref. J.D. Bjórken and A. Goldberg N.C. 16 539 '60
M. Luming P.R. 136 B1120 '64

Bjórken and Goldberg (114) tested various approximations used in dispersion theory in a soluble potential theory namely S wave scattering by an exponential potential. M. Luming (115) considered s, p, d waves for a Yukawa potential. Five approximation schemes were considered by B and G

(i) Fredholm or determinantal expansion i.e. expressing T_0 as the ratio of two power series in λ, each of which converges for all λ.

(ii) An approximation method due to Wilson, of expanding T_0^{-1} in a power series in λ.

(iii) Expansion of $\tan \delta_0$ in powers of λ.

(iv) The Born approximation.

(v) The Chew-Mandelstam approximation. By this B & G mean that one uses nearby singularities in the s plane.

Only methods 1, 2, 5 in 2nd order were in reasonable agreement with exact solution by inspection of effective range plots i.e. $k \cot \delta_0$ vs. S. The existence of bound states was also investigated. The energies of the bound states were only at best in qualitative agreement with the exact values. Method 2 gave a good value in 2nd order. All methods except 1 predicted bound states for repulsive potentials. Method 1 predicted no bound state for any λ. It was remarked that as the exponential potential is smoother than the Yukawa potential the approximations should be worse for the latter.

Luming considered left hand configurations

(a) only 1st Born cuts N/D

(b) 1st and 2nd Born cuts N/D i.e. left hand cut part of the 1st and 2nd Born terms - 2nd Born term minus its right hand cut part, only.

and the solution for unitary amplitude by

1. Uretsky (exact) N/D ImA^{-1}left = ImB
2. Determinantal approximation i.e. N = B.

for a single Yukawa potential. For g^2/μ = 3, 1; l = o, 1, 2.

3. The Born approximation

$$\mathrm{Re}A^{-1} = \nu^{\frac{1}{2}} \cdot \cot\delta_l = \frac{1}{B}$$ note this is a unitary Born approximation.

For N/D 2nd Born reasonable approximation in low energy region

1st Born " near threshold

worse than Born approx. at high energies. Roughly if correct left hand cuts to $-\nu_n$ then correct right hand to $+\nu_n$. The determinantal method was not in good agreement. First order gave a spurious P wave resonance and second order gave spurious zero of N function and no bound states at all. Luming considers a zero of N must appear (as g^2 increases) after a zero of D corresponding to phase shift going through 90° then 180°. The determinantal method is, in fact, in its exact form, a ratio of two power series in g^2. In the S wave first order determinantal again gives too strong attraction. As it could not give uniform results for different l, it was considered unsuitable for Regge continuation. The 2nd Born approximation for l > o was superior than both N/D or determinantal i.e. perturbation theory superior to unitarised form.

Finally Luming remarked that his studies lend support to low energy N/D analyses of N - N scattering etc. where long range forces and two-body unitarity give reasonable solution. On the other hand, they were of little relevance to short range problems like $\pi\pi$.

Marginally singular forces (116)

Define as Im$A(k) \to$ constant. In potential scattering, this $\sim V(r) \underset{r\to 0}{\sim} \frac{1}{r^2}$, for which $\delta_l \to$ const $\neq n\pi$. One parameter ambiguity in solutions (CDD poles with 2 parameters each).

Morgan did not consider a self consistent problem, but only the problem

"given the left hand cut etc." (116). For certain forms of left hand cut all solutions had a resonance in them.

Assume no bound state, spinless equal mass bosons. Write dispersion relation for $f = A(\nu)/\nu$. P wave

$$f(\nu) = \frac{1}{\pi}\int_0^\infty d\nu' \frac{\mathrm{Im} f_R(\nu')}{\nu'-\nu} + \frac{1}{\pi}\int_{-\infty}^{-1} d\nu' \frac{\mathrm{Im} f_L(\nu')}{\nu'-\nu} \tag{2.1}$$

$$\mathrm{Im} f_R(\nu) = \frac{1}{\nu}\sqrt{\frac{\nu}{\nu+1}}\cdot|f(\nu)|^2 \tag{2.2}$$

Assume $|f(\nu)| \underset{\nu\to\infty}{\longrightarrow} O(\nu^{-\varepsilon}) \quad \varepsilon > 0$ (2.3)

Now $\mathrm{Im} f_R(\nu) \underset{\nu\to\infty}{\longrightarrow} O\left(\frac{1}{\nu}\right)$ (2.4)

Assume $\mathrm{Im} f_L(\nu) \underset{\nu\to-\infty}{\longrightarrow} \sim A/\nu$ (2.5)

Define $B(\nu) = \frac{1}{\pi}\int_{-\infty}^{-1} \mathrm{Im} f_L(\nu')\, d\nu'/(\nu'-\nu)$ (2.6)

from (2.5) $B(\nu) \underset{\nu\to\infty}{\sim} \frac{A}{\pi}\log\nu/\nu \quad \therefore \quad f(\nu) \underset{\nu\to\infty}{\to} B(\nu)$ (2.7)

demand $\mathrm{Im} f_R(\nu) \underset{\nu\to\infty}{\to} A/\nu$ (2.8)

$\therefore$ from (2.2) $\sin^2\delta \sim A$ (2.9)

$\therefore \quad 0 \leq A \leq 1$ (2.10)

giving limit strength of force.

As an example, the function $f(\nu) = \sqrt{\frac{-\nu}{\nu+1}}$

has $\mathrm{Im} f(\nu) \longrightarrow 1$ as $\nu \longrightarrow \pm\infty$

and $\mathrm{Re} f(\nu) \longrightarrow 0$ as $\nu \longrightarrow \pm\infty$

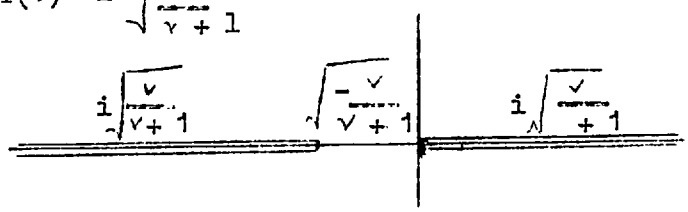

Exact solution of

$$N(\nu) = B(\nu) - \frac{1}{\pi}\int_0^\infty d\nu' \left[\frac{\nu B(\nu) - \nu' B(\nu')}{\nu'-\nu}\right]\cdot\rho(\nu')\cdot N(\nu')$$

$$D(\nu) = 1 - \frac{\nu}{\pi}\int_0^\infty d\nu'\cdot\rho(\nu')\frac{N(\nu')}{\nu'-\nu}.$$

in the case $B(\nu) \propto \frac{A}{\pi}\cdot\log\nu/\nu$

Note we are dealing with $A(\nu)/\nu$

$$N(\nu) = B(\nu) + \int_0^\infty d\nu' K(\nu,\nu')\ N(\nu')$$

$K \in \mathcal{L}^2$, marginally i.e. logarithmic divergence.

Wioner-Hopf suggested by Chew and by Jones (117)

Split $K = AK_1 + K_2$. AK_1 is asymptotic part, K_2 is remainder and is Fredholm.

Using Wiener-Hopf gives explicit construction for resolvent kernel

$$0 = (I - AK_1)^{-1}$$

One then has a Fredholm equation with formal solution

$$N = 0(I - K_2 0)^{-1} . B$$

i.e. $$N = N_o + \lambda K_1 N$$

$$N_o = B + K_2 N$$

Dave Morgan solved by Wiener-Hopf
Dietz and Domokos (118) and Atkinson and Contogouris for $\nu_L = 0$
by Mellin Transform.
Atkinson and Contogouris for $\nu_L \neq 0$ by Mehler transform.

The main result of Morgan's (116) and Atkinson and Contogouris' (119) work is that, for marginally singular forces

$$B(\nu) \sim \frac{\lambda}{\pi} . \log \nu \quad ,$$

there is one parameter family of solutions. The asymptotic part of the solution for single vector meson exchange

$$B(\nu) = \frac{\lambda}{4\pi} . \frac{8\nu + 4 + m^2}{\nu} . Q_1\left[1 + \frac{m^2}{2\nu}\right]$$

asymptotic part is that due to

$$B(\nu) \underset{\sim}{\sim} \frac{\lambda}{4\pi} . \log\left(\nu + \frac{m^2}{4}\right) + 0(1)$$

and $$\rho(\nu) = \frac{\nu}{\sqrt{\nu + 1}} \approx 1 + 0\left(\frac{1}{\nu}\right)$$

$$f(x) = \frac{\log x}{x} + \frac{\lambda}{\pi^2} \int_1^\infty dx' . \frac{\log x'/x}{x' - x} . f(x')$$

This asymptotic equation has a one parameter infinity of solutions

$$f(x) = \frac{\log x}{x} + \lambda \int_1^\infty dx' . R(x, x'; \lambda) . \log x'/x'$$

$$+ A . P_{-so}(2x - 1)$$

$$S_o = \frac{1}{\pi} \text{ arc } \sin\sqrt{\lambda} \qquad o < \text{arc sin} < \pi/2 .$$

$$R(x, x'; \lambda) = \frac{1}{2} \int_C ds . \frac{s \tanh(\pi s)}{[\cosh^2(\pi s) - \lambda]} . P_{-\frac{1}{2}+is}(2x - 1) P_{-\frac{1}{2}+is}(2x' - 1)$$

resolvent kernel

$P_{-so}(2x - 1)$ is the general homogeneous solution and A is arbitrary constant.

The contour C is given.

The one parameter ambiguity has immediate implications for bootstrap calculations. For, suppose one carries out a bootstrap calculation with vector exchange, then given λ, m^2 for the exchanged particle, there are an infinity of solutions for the "output" amplitude. One demands λ in $= \lambda$ out $m^2_{in} = m^2_{out}$ and hopes to determine both λ and m^2 uniquely. However, it would seem that in general only one of these can be determined and the other can be chosen arbitrarily. The arbitrariness will not be complete as one must choose λ, m^2 so as to obtain a resonant output. Having done this, it is reasonable that one can vary the free parameter to obtain λ in $= \lambda$ out, whenever $m^2_{in} = m^2_{out}$, at least for some range of m^2_{in}. In the exact case, these considerations no longer apply although we might still expect a one parameter family of self-consistent solutions. Thus if we take $\mathrm{Im}A_1(v)$ in the crossed channel and have marginally singular asymptotic behaviour then, for each member of a range of functions $\mathrm{Im}A_1(v)$, we will have a one parameter family of output functions. However, for self consistency in the exact case, we need $\mathrm{Im}A_1(v)_{out} = \mathrm{Im}A_1(v)_{in}$, for all v in $[o, \infty]$. Thus it is impossible to tell from the result just how many free parameters there will be. This throws light on the difficulty of using a trial function in such a calculation, for given $\mathrm{Im}A_{in}$ there will be a one parameter family of $\mathrm{Im}A_{out}$ functions, none of which will be equal to $\mathrm{Im}A_{in}$ for any choice of parameters. For certain choices, the difference may be small and one has to assume that one is then close to an analytic self consistent solution; again suppose one now plots contours, then any parametric freedom will be a distorted shadow of the true freedom.

A suitable choice of C, the resolvent kernel, can be made to only have a branch point at $\lambda = 1$, and this will be true of the solution if we take $A = 0$. By this specification we can get a unique solution and it is equivalent to demanding analyticity in λ at the origin or renormalizability of the interaction.

It is also remarked that the Zachariasen method viewed as the first iteration of an iterative method gives approximate solutions regular at $\lambda = 0$, which can only approximate to the regular exact solutions. One might expect good agreement for small λ. When a cut-off is used, this replaces the singular by a Fredholm kernel and replaces the cut in (λ) by a sequence of poles. One expects such a procedure to only be valid for small λ.

A further result obtained by Morgan was that for certain families of left hand cut every solution of each contained a narrow resonance. He hoped that this mechanism might prove useful for explaining the existence of narrow resonances.

The consequences of pure absorption

The analytical consequences of absorption have been considered in some detail by Lyth (120). Do defines "pure absorption" as

$$T_{nn} \rightarrow \delta_{nm} \cdot A \cdot i \qquad 0 < A < 1$$

which corresponds to $S_1(E) \rightarrow c \; ; E \rightarrow \infty \quad c \text{ real} \quad c^2 < 1$

and hence $\left| \text{out}_1 \right\rangle = C \left| \text{in}_1 \right\rangle \qquad c \text{ real} \quad c^2 < 1$

for which there is some experimental evidence (121). However, at highest energies yet studied $\text{Im}A_1$ still shows appreciable variation for some processes. He also defines "complete absorption" as $c = 0$ or $A = \frac{1}{2} \sim$ black disc, for which there is little evidence either way. He considers briefly the possibility of smooth behaviour $\not\rightarrow$ constant, but not oscillating.

If $T(z) \rightarrow i \; \text{Im}T(z)$, then $\text{Im}T(z) \rightarrow 0$ and $R(z) \rightarrow \infty$

if $R(z) = \text{const.} \; z^{\gamma} + o\,(z^{\gamma-\varepsilon})$. $\qquad \gamma > 0$, finite ε

then similar results to pure absorption.

If $R(z) \sim \log z$ (Regge pole theory), then T would decrease but no faster than $z^{-\beta}/R(z)$, and the N/) equations are at least marginally singular.

He considers the amplitude $F = K\,T$

where $\text{Im}T^{-1} = R \geq 1$

$T_{nm}(z) = \delta_{nm} A_i + O(z^{-\alpha})$

and K is the Kinematic factor

$$K(z) \sim z^{-\beta} \qquad \beta > 0$$

$\frac{K(z)}{z^{-\beta}}$ regular at $z = \infty$

i.e. $K(z) = z^{-\beta} \sum_{i=0}^{\infty} k_i . Z^{-i}$

Find solutions more unique with increasing β.

Thus $F(z) = iAK(z) + O(z^{-\beta-\alpha})$

Also assumes $\frac{d}{dz} \operatorname{Im}F(z) = O(Z^m)$

From these asymptotic assumptions and also the assumption of a dispersion relation, Lyth derives asymptotic forms for F_L and F_R the contributions from right and left hand cuts.

(i) $F_L(z) = -A \cot(\pi\beta) . K(z) + \frac{f_1}{z} + \ldots + \frac{f_\alpha}{z^\alpha} + o(z^{\epsilon-\beta-\alpha})$

$F_R(z) = -F_L(z) + o(z^{\epsilon-\beta-\alpha})$

(ii) $F_L(z) = A . \log z \; K(z) + f_1/z + \ldots + \frac{f_\alpha}{z^\alpha} + O(z^{\epsilon-\beta-\alpha})$ $\beta \neq$ integer.

$F_R(z) = -F_L(z) + o(z^{\epsilon-\beta-\alpha})$ $\beta =$ integer

f_i are real negative numbers

$$f_1 = -\frac{1}{\pi} \int_{z_t}^{\infty} dz' . \; z'^{i-1} . \; \operatorname{Im}F(z') \qquad i < \alpha$$

Implications are that the nearest singularity approach which has

$$F_L(z) = \sum_{i=1}^{\infty} f_i / z^i$$

is only consistent with pure absorption if β = integer + $\frac{1}{2}$. Lyth has carried out the calculation in this case for N and N*. (122)

One can deduce the asymptotic behaviour of the discontinuity on the left hand cut with further reasonable assumptions.

A power law $\operatorname{Im}F(z) \underset{z \to -\infty}{\sim} z^{-\gamma}$

must have $\gamma = -\beta$ $\qquad \beta \neq$ integer + $\frac{1}{2}$

$\gamma < -\beta - \alpha$ $\qquad =$ " "

Kinematic factors, with β = integer + $\frac{1}{2}$ have been extensively used in semi-phenomenological calculations, e.g. by Hamilton and co-workers.

Another consequence of pure absorption is that taking a finite number of

channels will not make the deviation from inelastic unitary small at all high energies. For demanding pure absorption and unitarity gives $A = 0$ or 1. The use of R rather than η is simpler in those considerations. We must have R factors, even in a multichannel calculation.

Assuming the phase satisfies

$$\phi(z) = \phi(\infty) + o(z^{-\alpha}) \qquad \text{some } \alpha > 0$$

$$\phi'(z) = 0\,(z^{n}) \qquad \text{some } n$$

one obtains $\frac{\phi(\infty)}{\pi} =$: integer $+ \frac{1}{2}$

This contradicts Levinson's theorem in single channel case.

Lyth suggests $\phi(\infty) = \pm \pi/2$ as a working rule to replace Levinson's theorem.

For β = integer $+ \frac{1}{2}$, th N/D equations are of Fredholm type and have a unique solution. If $\beta \neq$ integer $+ \frac{1}{2}$, we have marginally singular case and one parameter ambiguity. Hence for β = integer $+ \frac{1}{2}$ there is only the CDD ambiguity.

Further assumptions can lead to removal even of the CDD ambiguity in the single channel case i.e. a unique solution giving a rigorous version of a theorem due to Frye and Warnock.

VIII COMPOSITENESS

CONCEPT OF A BOUND STATE

Our conception of a bound state must stem in the first place from non-relativistic quantum mechanics or even classical mechanics. In classical mechanics two particles can coalesce to form another compound particle, or two particles in a central field of force will continually orbit, conserving angular momentum, forming a compound system. In nonrelativistic quantum mechanics two particles can exist separately in stable states, or form scattering states and various types of bound state. The nature of these bound states has a very compelling interpretation as an amalgamation of constituent

particles. Especially in the case of dominant central force in which a good approximation to the state is obtained by a separated wave function, i.e. separated into wave functions describing the individual constituents. Excitations can be described as the result of individual excitation. In the case of nuclear physics with much stronger noncentral, short range forces, this decomposition becomes blurred. The energy states of a nucleus can be described in part by a "shell" model and in part by collective excitations. The binding energies are normally fairly small compared with rest energies, 8 Mev per nucleon of mass, 1000 Mev. Thus when we consider the highly relativistic, very strong interactions of the elementary particles, the naive idea of one particle being a bound state of two or more others may well have no real meaning. For the "constituent idea to be at all useful one would like properties like the following:

a. The composite state vector be separable into the direct produce of constituent vectors;

b. Excitations and other behaviour like scattering of composite particles be interpretable as due to constituents;

c. Formation from and decomposition into constituents should be physically possible.

In regard to c, most elementary particles have several different weak interaction decay modes

$$\text{e.g.}\ \Omega^- \longrightarrow \quad \overset{=}{\Lambda} \quad \overset{-}{K}$$

also one can phenomenologically identify a particle (as a pole term) as an intermediate state in many different strong interaction processes

e.g. $\pi N \longrightarrow N \longrightarrow \pi N$

$\bar{K} N \longrightarrow Y_1^* \longrightarrow \Lambda\pi$

A less confusing picture is then to take each particle as being an object in

its own right and forming scattering states with other particles. When $\bar{K}N \rightarrow Y_1^* \rightarrow \Lambda\pi$, we imagine the incoming particles as interacting so strongly that all individual identities are lost and then the energy being transformed into the final state particles. This sort of idea was proposed some time ago with success in relation to nuclear processes. In a strong interaction, certainly the interaction region is equal in size to the size of each constituent, that is, the wave functions completely overlap. The actual distribution of matter within a particle as measured by form factors is fairly homogeneous with no dense core.

BOUND STATES IN FIELD THEORY

For the description of bound states in field theory, one can use the Bethe-Salpeter equation (123). Also in q.e.d. one can extend the Feyman Dyson formalism to bound electrons by using the Furry picture (124). Formally a bound state can be represented by a field which is presumed calculable from the fields occurring in the Lagrangian i.e. it is a function of the other fields.

In a historic paper, Zimmermann (125)

investigated a causal invariant scalar field theory involving a stable bound state using LSZ formalism. He showed that the bound state can be described by a local and invariant field operator. See also (126).

Haag (126) showed complete "symmetry" between composite field and elementary field and proved corresponding asymptotic conditions. The bound state operators for example obey the microscopic causality condition. The bound state field does not have to be renomalised hence all Z's = 0 for it. However the elementary ones apparently need non-vanishing Z's. This lead Salam (127) to conjecture that one should write down field theories with all particle fields occurring in the Lagrangian but with the renormalisation

constants of the bound state fields equal to zero. This enables one to set up Feynan graphs for the interactions between all particles. One can demand that all particles be composite by demanding that all Z's = 0 for all particles. Using this condition, Salam was able to renormalise a vector field theory which was unrenormalisable in the usual sense. This renormalisation has been pursued further by J. Boyce.

Thus for a theory with the π, N and D, the renormalised Lagrangian could be

$$L = Z_2 N^+ (\not\partial + K) N + Z_3 [(\partial\pi)^2 + \mu^2 \pi^2] + Z_3' [(\partial D)^2 + M_d^2 D^2] + g_\pi Z_1^\pi N^+ N \pi + g_{\pi d} Z^{\pi d} . D^+ . D\pi + g_{NNd} . Z_1^{Nd} D^+ N N + \text{self mass terms.}$$

One would then determine M_d^2, μ^2, K^2 and the g's be calculating expressions for Z_1^π, $Z_1^{\pi d}$, Z_1^{Nd}, δM_d^2, δk^2, $\delta \mu^2$ and then equating to zero. This was done in 4th order perturbation theory with some success by R. Delbourgo. There has been some debate on Salam's suggestion (128) under three categories... First the exact meaning has been looked at, for there has been some suggestion that the order in which the limits $Z \longrightarrow \bullet$ are taken, will alter the result.

Second, the conditions Z = 0 have been looked at in model field theories and are shown to give very sensible effects.

Third, the correspondence of the condition to the Levinson theorem criterion of composteness used in dispersion theory has been investigated.

RESULTS FROM MODEL FIELD THEORIES

Vaughn etal (129) showed that two elementary particle theories

(i) Lee Model $V \rightleftharpoons N + \Theta$

(ii) Crossing symmetric Lee Model $V \rightleftharpoons N + \Theta$ $\quad N \rightleftharpoons V + \Theta$

in which wave function renormalisation constant for the V particle $\longrightarrow$ o, were equivalent to two composite particle theories.

(iii) Separable potential model with fixed N and scalar Θ.

(iv) generalisation of Wentzel's meson pair theory with complex Θ interacting with N through quadratic interaction, in which the V particle occurs as a bound state. However, there was an observable distinction between the elementary and composite theories from high energy phase shifts in N - Θ scattering, using Levinson's theorem. Diu has argued against this (132). They also showed that any model field theory with fixed source and potential interaction with a bound state between source and field could be obtained from an elementary theory with $Z \rightarrow 0$.

Howard and Jouvet (130 (131) showed that a 4 fermi interaction theory and a Yukawa coupling theory with an intermediate particle were equivalent when $Z \rightarrow 0$ for the intermediate particle. By replacing Yukawa interactions by 4 Fermi interactions with Z = 0 one might hope to make the theory more tractable.

Further papers are (132). Low (133) considered three models of Λ K and Λ $\bar{K}$. scattering with N and Ξ poles, with different Lagrangian formulations

(i) N, Λ, K $\quad H_1 = g_1^{\circ} \bar{\psi}_N \psi_\Lambda \varphi_K + h.c.$

Ξ as bound state in $\Lambda \bar{K}$

(ii) Ξ, Λ, K

$H_2 = g_2^{\circ} \bar{\psi}_\Xi \psi_\Lambda \cdot C \varphi_K + h.c.$

N bound state in ΛK

(iii) N, Ξ, Λ, K

$H_3 = H_1 + H_2$

He showed that for suitable choice of renormalised g_1 and g_2 all three models gave the same Λ K and Λ $\bar{K}$ scattering and hence same N and Ξ masses. If this was the case in dispersion theory, then Chew's reciprocal bootstrap was automatically satisfied and had a two parameter infinity of solutions.

Lardner & Woo (134) examined this point furt er. They also noted that when a theory can accommodate additional particles with zero coupling to other

particles, then Levinson's theorem loses its significance, in distinguishing between elementary and composite particles.

Rowe (135) considered three theories of three scalar particles, nucleon φ, pion A, deuteron D.

(i) $g\varphi\bar{\varphi}A$ D as bound state

(ii) $\frac{g}{2}[\varphi\varphi\bar{D} + \bar{\varphi}\bar{\varphi}D]$ π as $\varphi\bar{\varphi}$ bound states.

(iii) $\lambda/_2 \cdot \bar{\varphi}\varphi\bar{\varphi}\varphi$ D and π as " .

These are renormalisable theories, with a finite number of renormalisation constants equivalent to putting in an equivalent number of physical parameters. Thus the number of arbitrary parameters is equal to number of renormalisation constants. In (i) there is only self energy divergence parameters m, μ, (ii) m, M (iii) M and information about $\varphi\bar{\varphi} \rightarrow \varphi\bar{\varphi}$ scattering, either the value at some point or whether a bound state exists. Two in each case, one hopes all other parameters can be fixed in terms of them. In more realistic theories, one has more constants e.g. vertex part divergence constants. The thesis showed that (i) and (ii) are equivalent to (iii) if $Z_3 = 0$. This fixes the coupling constant in terms of the masses. Thus, the criterion of elementarity as appearing in the Lagrangian is meaningless; however one could modify this to appearance in every equivalent Lagrangian.

THE ZACHARIASEN MODEL (136)

This is a useful theory it being easily expressible in dispersion theory or field theory. It has two types of particle A, B spinless bosons, A its own antiparticle, $B \neq \bar{B}$. Zachariasen obtained solutions by dispersion theory and by perturbation field theory, which were identical.

Dowker (137) showed that in the limit $Z_3 \rightarrow 0$, the A particle could be considered as a bound state.

The Levinson theorem is

$$\delta(0) - \delta(\infty) = \pi \quad Z_3 = 0$$
$$= 0 \quad Z_3 > 0$$

In the nonrelativistic limit, the theory with $Z_3 = 0$ goes over to a singular potential theory.

Dowker and also Acharya (138) considered only $\bar{B} \Lambda B$ interactions. It is also possible to include a contact interaction, and this case was considered by Whippman and Gerstein (139). They showed that demanding equivalence of elementary and composite theories without CDD poles fixes the residues and positions of CDD poles, the residues being $\propto Z_3$. With $Z_3 = 0$ the solution was unique and the CDD ambiguity was by-passed. They find that g^2, the coupling to the composite state, has its maximum value for $Z_3 = 0$, which may relate to the idea of maximal strength.

Limitations of model field theories

One must remember that these model field theories are very unrealistic. The Zachariasen model violates space like commutability, although because it obeys a dispersion relation it is causal in some sense. It violates crossing symmetry, but obeys a unitarity condition. Thirring (140), has given a Lagrangian formulation of the Zachariasen model which has a continuous mass distribution of particles and is perfectly local and satisfies all axions except the asymptotic condition, which was a full field theory, the only restriction being to elastic unitarity. It was shown that the field theoretic criterion of $Z_3 = 0$ was equivalent to the dispersion theoretic criterion of the particles occurring as zeros of D in the N/D method.

Zimmermann (144) has recently shown that one can eliminate fields from a Lagrangian to obtain a new equivalent Lagrangian which is not in general local. Demanding $Z_3 = 0$ for the eliminated fields makes the new Lagrangian local. He suggests that one can achieve elementary particle democracy by eliminating fields from the Lagrangian and requiring all the final self-interacting Lagrangians be local.

This ties up with the work of Weinberg (145) to extract bound states and leave the residual interaction weak, and tractable.

THE RELEVANCE OF THIS CHAPTER TO THE WORK IN THE REST OF THE THESIS

In the rest of the thesis, we are going to consider approximate calculations in partial wave formalisms based upon M R + U. The work can be considered as a computational exercise and a study of approximations. The discussion in this chapter is an attempt to gain perspective in the relationship of these approximate calculations to the underlying ideas of dispersion theory, to previous calculations in dispersion theory carried out by other workers, and to other theories of particle interaction.

CHAPTER 2

I. THE FIXED S DISPERSION RELATION

DERIVATION FROM THE MANDELSTAM REPRESENTATION

$$A(s, t, u) = \int_4^\infty ds' \frac{\rho_s(s')}{(s'-s)} + \text{cyclic} + \iint \frac{ds'\, dt'\, \rho_{st}(s', t')}{(s'-s)\,(t'-t)} + \text{cyclic} \qquad \text{(i)}$$

As shown previously, this decomposes into

$$A(s, t, u) = \int \frac{ds'\, \rho_s(s')}{s'-s} + \int \frac{dt'\, A_t(s, t')}{t'-t} + \int \frac{d \cdot A_u(s, u)}{\rho -} . \qquad \text{(ii)}$$

$$A_t(s, t') = \rho_t(t') + \int \frac{ds'\, \rho_{st}(s', t')}{s'-s} + \int \frac{d \cdot \rho}{-} \qquad \text{(iii)}$$

$$A_u(s, u) = \rho_u(\,) + \int \frac{ds'\, \rho_s(s, u)}{s'-s} + \int \frac{dt'\, \rho_{tu}(t', u)}{t'-t} \qquad \text{(iv)}$$

Now the integrals in (ii) lie for $-32 < S < 4$ outside the double spectral regions, and, from (iii) and (iv), A_t and A_u are real in these regions. Hence A_t and A_u are the imaginary parts of $A(s, t, \cdot)$ in these regions.

$$A_t(s, t') = \text{Im}A(s, t')$$

Hence we don't have to worry about ρ_t or ρ_u, they are automatically included.

Applying crossing and, dropping single spectral term for the moment, we obtain $A(s, t, u) = \int_4^\infty dt' \cdot \text{Im}A(s, t') \cdot \left[\frac{1}{t'-t} + \frac{(-1)^I}{t-u}\right]$ (v)

Assuming $A_t(s, t') \longrightarrow$ constant

$$s < 0$$

$$t' \longrightarrow \infty$$

we see that this integral diverges and needs one subtraction only. We actually only need $A_t(s, t') \longrightarrow o(t')$. This is quite a reascnable assumption and is given by a Regge hypothesis

$$A_t^I(s, t') \underset{t' \longrightarrow \infty}{\propto} t'^{\alpha_I(s)}$$

where $\alpha_I(s)$ is the furthest right regge pole in the S channel. From Chew & Frantschi (1) the expected trajectories are

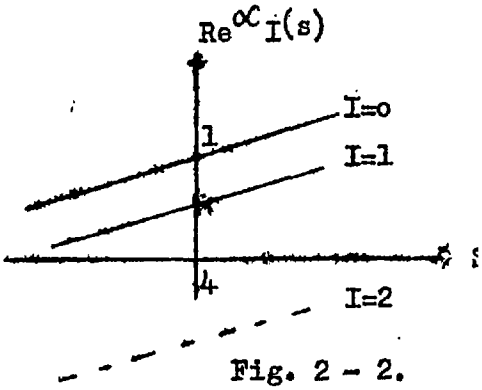

Fig. 2 - 2.

hence for $s < 4$, $\alpha_I(s) < 1$.

$$A(s, t, u) = A(s, t_o, u_o) + \frac{(t - t_o)}{\pi}\int_4^\infty dt' \cdot \frac{\mathrm{Im}A(s, t')}{(t' - t_o)}\left[\frac{1}{t' - t} + \frac{(-1)^I}{t' - u}\right]$$

the term $A(s, t_o\ u_o)$ is independent of t and thus will only contribute to the s wave projection, when projected into partial waves in the s channel.

We now look at the single spectral term, we dropped earlier. It is also independent of t, so the same remarks apply to it.

One may further remark that upon projecting into the s channel in the unsubtracted form, all waves converge except the s wave which requires one subtraction. Thus as the subtracted and unsubtracted forms are identical when both converge we can take the unsubtracted form for projection into s channel

partial waves for ≥ 1. To put it another way, one could project using the subtracted form and then re-insert the subtraction term into the integral.

ASYMPTOTIC BEHAVIOUR, as $t \longrightarrow \infty$, s fixed.

$$A^I(s, t) = \int_4^\infty A_t^I(s, t')\, dt' \left[\frac{1}{t' - t} + \frac{(-1)^I}{t' - u} \right]$$

We use the result (essentially an application of the Phragmen-Lindelof theorem) obtained by Kanazawa and Sugawara and described in G. Barton's book (6). "If $f(z)$ is analytic in a cut plane, with cuts only on the real axis, and if bounded in n.h.p. by a polynominal, and if $f(z) \longrightarrow$ limit along the cuts. $|z| \longrightarrow \infty$ Then this limit is the same in any direction." Applying this result to $A^I(s, t)$ in the t plane, with s fixed, we obtain

$$\lim_{t \longrightarrow +\infty + i\varepsilon} A_t^I(s, t) \text{ —— } \lim_{t \longrightarrow -\infty + i\varepsilon} (-1)^I \cdot A_t^I(s, t)$$

$$\lim_{t \longrightarrow \pm \infty} A_t^I(s, t) = 0, \text{ for I odd.}$$

This certainly applies for s in $[0, 4]$, when the cuts in t do not overlap, and probably applies for all s.

PROJECTION INTO S CHANNEL PARTIAL WAVES

Assuming, at first, no subtractions,

$$A(s, t) = \int_4^\infty \frac{A_t(s, t')\, dt'}{t' - t} \qquad \text{(i)}$$

if $A_t(s, t') \underset{t' \longrightarrow \infty}{\longrightarrow} 0$ (s fixed.) then (i) converges.

$$A_\ell(s) = \frac{1}{2} \int_{-1}^{+1} P_\ell(\cos\theta) \cdot d(\cos\theta) \int_4^\infty \frac{A_t(s, t')dt'}{t' - t}$$

$$\cos\theta \sim s, t \qquad \cos\theta = 1 + \frac{2t}{s - 4}$$

$$\cos\theta = +1 \sim t = 0$$
$$-1 \sim t = -(s - 4)$$

$$d(\cos\theta) = \frac{2dt}{s - 4}$$

$$\frac{1}{s-4}\int_{-(s-4)}^{0} dt.\ P_\ell\left[1+\frac{2t}{s-4}\right]\int_4^\infty \frac{\Delta t(s,t').\,dt'}{t'-t}$$

$$= \int_4^\infty dt'.\ \Delta t(s,t')\ .\ \frac{1}{s-4}\int_{-(s-4)}^{0} \frac{dt\ P_\ell\left[1+\frac{2t}{s-4}\right]}{t'-t}$$

$$= \int_4^\infty dt'.\ \Delta_t(s,t').\ Q_\ell\left[1+\frac{2t'}{s-4}\right] \qquad \text{(ii)}$$

for $\dfrac{1}{(s-4)}\displaystyle\int_{-(s-4)}^{0} \frac{dt\ P_\ell\left[1+\frac{2t}{s-4}\right]}{t'-t}$

$$= \frac{1}{2}\int_{-1}^{+1} \frac{d(\cos\theta)\ P_\ell(\cos\theta)}{\left\{t'+\frac{(s-4)}{2}(1-\cos\theta)\right\}}$$

$$= \frac{1}{2}\int_{-1}^{+1} \frac{dz.\ P_\ell(z)}{\left\{\left[t'+\frac{(s-4)}{2}\right]-\frac{(s-4)}{2}\cos\theta\right\}}$$

$$= \frac{1}{s-4}\int_{-1}^{+1} \frac{dz.\ P_\ell(z)}{\left\{\left[\frac{2t'}{s-4}+1\right]-z\right\}}$$

$$= \frac{2}{(s-4)}\cdot Q_\ell\left[1+\frac{2t'}{s-4}\right]$$

Now, $Q_\ell(x) \underset{x\to\infty}{\longrightarrow} O(x^{-\ell-1})$, all ℓ, $\mathrm{Re}\,\ell > -1$ (iii)

so, if $\Delta_t(s,t') \longrightarrow$ constant, then (ii) converges for $\ell = 1, 2, \ldots$ and diverges logarithmically for $= 0$. The increased convergence on integration with $P_\ell(\cos\theta)$ presumably comes from cancellation. The second term in II(v) involves

$$(-1)^I\ \frac{1}{2}\int_{-1}^{+1} \frac{dz\ P_\ell(z)}{t-\ldots}$$

$$= \frac{(-1)^I}{2}\int_{-1}^{+1} \frac{dz.\ P_\ell(z)}{\left\{t'+\frac{(s-4)}{2}(1+z)\right\}}$$

$$= \frac{(-1)^I}{(s-4)}\int_{-1}^{+1} \frac{dz.\ P_\ell(z)}{\left\{\left[\frac{2t'}{s-4}+1\right]+z\right\}}$$

$$= (-1)^I\ .\ \frac{2}{s-4}\left\{-Q_\ell\left[-\left(1+\frac{2t'}{s-4}\right)\right]\right\}$$

but $(-1)^I = (-1)^\ell$ Bose statistics

and $(-1)^{\ell+1} \cdot Q_\ell(-z) = Q_\ell(z)$

hence we obtain

$$\frac{2}{(s-4)} \cdot Q_\ell\left[1 + \frac{2t'}{(s-4)}\right]$$

identical with the 1st term.

If we now use the subtracted form instead

$$A(s, t, u) = A(s, to, uo) + \frac{1}{\pi}\int_4^\infty \left[\frac{At(s, t')}{t' - t} - \frac{At(s, t')}{t' - to}\right] dt'.$$

projecting into the s channel partial waves, the 1st term gives

$$\tilde{A}_o(s) = \frac{1}{2}\int_{-1}^{+1} P_\ell(z) \cdot A(s, to, uo)$$

$$= A(s, to, uo). \quad \delta_{\ell o}$$

1st term in the integral is the same as before and the subtraction term gives

$$\int_4^\infty dt' \; A(s, t'). \; \frac{1}{2}\int_{-1}^{+1} \frac{dz. \; P_\ell(z)}{\left[t' + \left(\frac{s-4}{z}\right)(1 - z_o)\right]}$$

where .. $t_o = -2\nu(1 - z_o)$.

$$= \frac{2}{s-4}\int_4^\infty \frac{dt' \cdot A(s, t'). \delta_{\ell o}}{\left[\left(\frac{2t'}{s-4} + 1\right) - z_o\right]}$$

the 2nd term in II(v) gives the same, except that it has the alternative factor

$$\frac{(-1)^I \cdot \delta_{\ell o}}{\left[\left(\frac{2t'}{s-4} + 1\right) + z_o\right]}$$

The fact that the subtraction term vanishes for $\ell \neq o$ confirms that no subtraction is necessary. It is because the term is independent of t, which is the angular variable in the s channel.

For $\ell = o$ we have

$$A_o(s) = \tilde{A}_0(s) + \frac{4}{\pi(s-4)}\int_4^\infty dt' \, A_t(s, t')\left\{ Q_o\left[1 + \frac{2t'}{s-4}\right] - \frac{\left(\frac{2t'}{s-4} + 1\right)}{\left[\left(\frac{2t'}{s-4} + 1\right)^2 - z_o^2\right]}\right\}$$

Hence, the s waves cannot be determined using this expression.

If we look at the diagrammatic representation of those formulae, Fig. 1, the two integrals over t' in II(v) are along the line of constant s, AF. The first term is an integral along CF and the second along DA. The integrand must be known at all points, in these intervals, thus we must know $A_t(s, t')$ in unphysical regions, although we note that the major part of the integrals always lies in the physical region for small s, To obtain $A_t(s, t')$ off the physical region we must choose a continuable representation and we shall discuss mainly the use of the partial wave series.

We take

$$A_t^{I'}(\nu', \nu) = \sum_{\ell'=0}^{\infty} (2\ell'+1)\, P_{\ell'}\left[1 + 2\,\frac{(\nu+1)}{\nu'}\right] \cdot \mathrm{Im}A_{\ell'}^{I'}(\nu') .$$

and also change over to new coordinates ν, ν'. As already discussed, for $\nu' > 0$ the series converges in a Lehman ellipse in the ν plane, whose extent depends upon ν' and which touches the double spectral region at points like H and J.

This region is sufficient to give the absorptive part for our integrals. The above series is expressed in terms of I' the isospin in the t channel so we have to take new linear combinations to obtain the absorptive part for isospin eigenchannels in the s channel given by the crossing matrix.

$$A_t^{I}(\nu', \nu) = \sum_{I'=0}^{2} \sum_{\ell'=0}^{\infty} (2\ell'+1) \cdot \beta_{II'} \cdot P_{\ell}\left[1 + 2\,\frac{(\nu+1)}{\nu'}\right] \cdot \mathrm{Im}A_{\ell'}^{I'}(\nu')$$

We can consider the functions

$$C_{\ell\ell'}^{II'}(\nu) = (2\ell'+1)\,\beta_{II'}\,\frac{4}{\pi\nu}\int_0^{\infty} d\nu'\, \mathrm{Im}A_{\ell'}^{I'}(\nu') \cdot P_{\ell'}\left[1 + 2\,\frac{(\nu+1)}{\nu'}\right] \cdot Q_{\ell}\left[1 + 2\,\frac{(\nu'+1)}{\nu}\right]$$

to be the contribution from the ℓ' I' wave in the t channel to the ℓ I wave in the s channel.

$$C_{\ell\ell'}^{I}(\nu) = \sum_{I=0}^{2} C_{\ell\ell'}^{II'}(\nu)$$

$$C_{\ell}^{I}(\ ) = \sum_{\ell'=0}^{\infty} C_{\ell\ell'}^{I}(\nu).$$

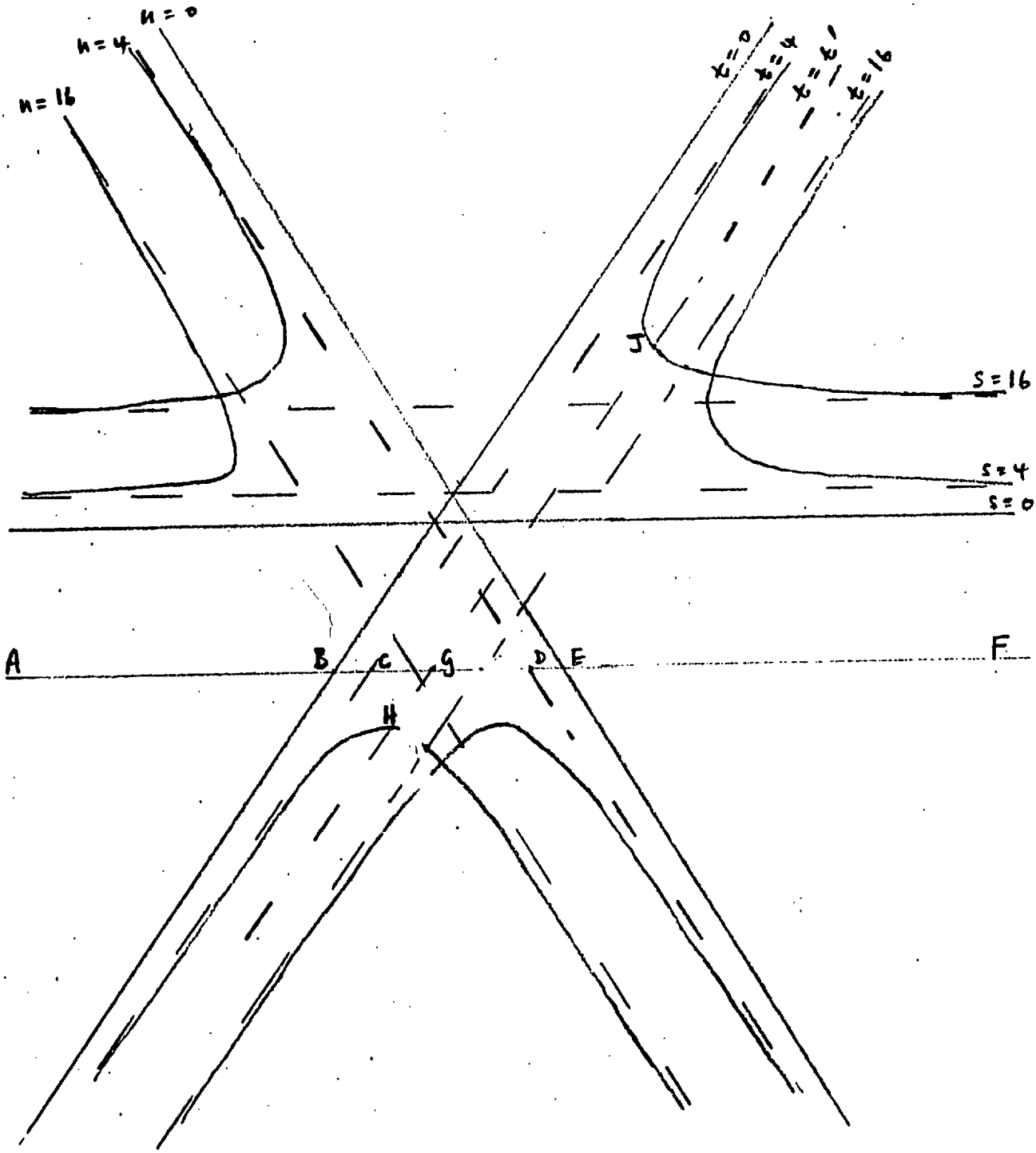

Fig. 2-1. Fixed s dispersion relation on Mandelstam plot

THE EVALUATION OF $C^{\Pi\Pi'}_{\ell\ell'}(\nu)$

$$\int_0^{\Lambda} d\nu'.\ \mathrm{Im}A_{\ell'}(\nu').\ P_{\ell'}\left[1 + 2\left(\frac{\nu+1}{\nu'}\right)\right].\ Q_{\ell}\left[1 + 2\frac{(\nu'+1)}{\nu}\right]$$

First two factors are regular in the interval but $Q_{\ell}\left[1 + 2\left(\frac{\nu'+1}{\nu}\right)\right]$ has a logarithmic singularity at $\nu' = -\nu_{*} - 1$, as can be seen from the general expression

$$Q_{\ell}(x) = P_{\ell}(x).\ Q_0(x) + \sum_{i=1}^{\ell-1} a_i P_i(x)$$

$$Q_0(x) = \frac{1}{2}\log\frac{x+1}{x-1}$$

latter having singularities at $x = \pm 1$, and the fact that the argument of $Q_{\ell'}$ in our integral

$$x = 1 + \frac{2(\nu'+1)}{\nu}$$

$$= x_1 = 1 + \frac{2}{\nu} > -1 \quad \text{when } \nu' = 0.\ \ \nu < -1$$

$$= x_2 = 1 + \frac{2(\Lambda+1)}{\nu} \quad \text{when } \nu' = \Lambda$$

$$< -1 \quad \text{when } \nu' < -1$$

$$\Lambda > -\nu - 1$$

$$x = -1 \quad \text{when } \nu' = -\nu - 1.$$

To do our integral, we can subtract any regular factor of the integrand. We choose

$$\int_0^{\Lambda} d\nu'.\ \left[\mathrm{Im}A(\nu')\ P_{\ell'}\left[1 + 2\left(\frac{\nu+1}{\nu'}\right)\right] - \mathrm{Im}A(-\nu-1).\ P_{\ell'}(-1)\right].\ Q_{\ell}\left[1 + 2\left(\frac{\nu'+1}{\nu}\right)\right]$$

$$+ \mathrm{Im}A(-\nu-1).\ P_{\ell'}(-1).\ \int_0^{\Lambda} d\nu' Q_{\ell}\left[1 + 2\left(\frac{\nu'+1}{\nu}\right)\right].$$

$$I = \int_0^{\Lambda} d\nu' Q_{\ell}\left[1 + 2\left(\frac{\nu'+1}{\nu}\right)\right]$$

put $x = 1 + 2\left(\frac{\nu'+1}{\nu}\right)$; $dx = \frac{2\,d\nu'}{\nu}$; $d\nu' = \frac{\nu}{2}.\ dx$

$\nu' = 0 \sim x = x_1 = 1 + \frac{2}{\nu}$

$\nu' = \Lambda \sim x = x_2 = 1 + 2\left(\frac{\Lambda+1}{\nu}\right)$

$$I_{\ell} = \frac{\nu}{2}\int_{x_1}^{x_2} dx.\ Q_{\ell}(x)$$

pathological when $\nu = 0, -1$ or $-\Lambda - 1$.

The evaluation of

$$\tilde{I}_\ell(x) = \int^x dz\, Q_\ell(z)$$ is found in an Appendix, they are found to be

$$\tilde{I}_0(x) = \frac{x}{2} \log \frac{x+1}{x-1} + \frac{1}{2} \log (x^2 - 1)$$

$$\tilde{I}_1(x) = \frac{1}{4}(x^2 - 1) \log. \frac{x+1}{x-1} - \frac{x}{2}$$

$$\tilde{I}_2(x) = \frac{x}{4}(x^2 - 1) \log. \frac{x+1}{x-1} - \frac{(x^2 - 1)}{2}$$

$$\tilde{I}_3(x) = \frac{(5x - 6x^2 + 1)}{16} \log. \frac{x+1}{x-1} - \frac{5x^3}{8} + \frac{13x}{24} .$$

We now look at the factor $Q_0\left[1 + 2\frac{(\nu'+1)}{\nu}\right]$, the singular factor of

$$Q_\ell\left[1 + 2\frac{(\nu'+1)}{\nu}\right]$$

$$Q_0(x) = \frac{1}{2} \log \frac{x+1}{x-1} = \log. \frac{\nu + \nu' + 1}{\nu' + 1}$$

suppose $y = \frac{\nu + \nu' + 1}{\nu' + 1}$

then $(y - 1).(\nu' + 1) = \nu$

a hyperbola

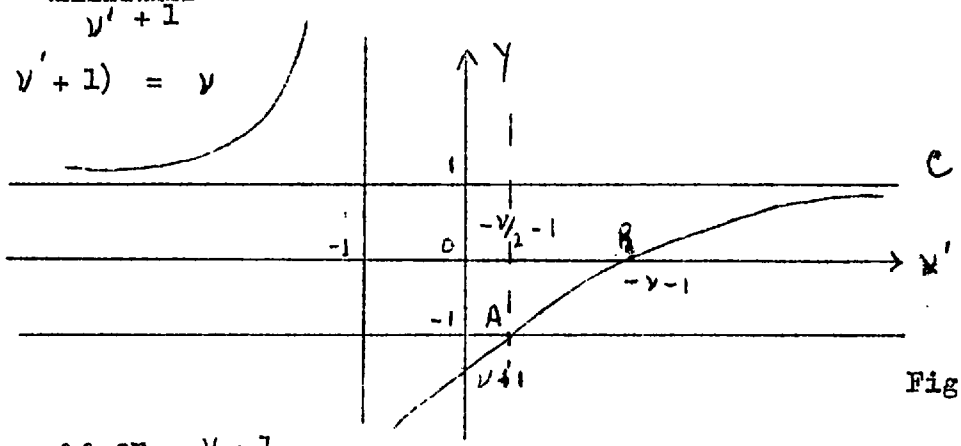

Fig.2-3(a)

$y = 0$ when $\nu' = -\infty$ or $-\nu - 1$.

$y = -1$ when $\nu' = -\frac{\nu}{2} - 1 \quad < 0$ when $-\nu < 2$

$= 0$ when $y = \nu + 1$

$\nu + 1 > -\frac{\nu}{2} - 1$ when $\frac{3\nu}{2} > -2$ i.e. $\nu > -\frac{4}{3}$.

Near the singularity the integrand is behaving like $x \log |x|$ which looks like

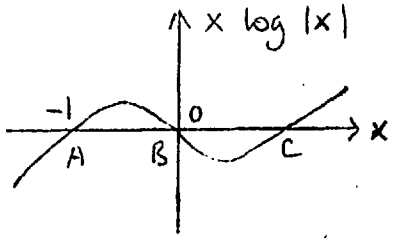

Fig. 2 - 3(b)

thus the singular region is defined by the points x = -1, 0, + 1. In our case the argument

$$y = 0 \quad \text{when} \quad \nu' = -\nu - 1$$
$$= +1 \quad \text{when} \quad \nu' = \infty$$
$$= -1 \quad \text{when} \quad \nu' = -\frac{\nu}{2} - 1$$

to effectively numerically integrate one must have sufficient points within this interval, although one usually varies the step length until the desired accuracy is obtained. One also has to be careful in computation because near the singular point one factor $\longrightarrow$ 0 the other $\longrightarrow \infty$. This is likely to cause overflow or rounding, further any attempt to approximate in this singular region needs careful assessment as one may introduce "large" corrections. An easier subtraction may well be as follows, explicitly bringing out the logarithmic factor from Q_ℓ.

$$\int_0^{\Lambda} d\nu' \cdot \mathrm{Im}\, A_\ell(\nu') \cdot P_\ell\left[1 + 2\left(\frac{\nu+1}{\nu'}\right)\right] \cdot Q_\ell\left[1 + 2\left(\frac{\nu'+1}{\nu}\right)\right]$$
$$= \int_0^{\Lambda} d\nu' \cdot \mathrm{Im}\, A_\ell(\nu') \cdot P_{\ell'}\left[1 + 2\left(\frac{\nu+1}{\nu'}\right)\right] \cdot \left\{ P_\ell\left[1 + 2\left(\frac{\nu'+1}{\nu}\right)\right] \cdot Q_0\left[1 + 2\left(\frac{\nu'+1}{\nu}\right)\right] + \sum_{n=0}^{\ell-1} a_n P_n\left[1 + 2\left(\frac{\nu'+1}{\nu}\right)\right] \right\}$$

and subtracting the singular term:

$$\mathrm{Im}\, A_\ell(-\nu-1) \cdot P_{\ell'}(-1) \cdot P_\ell(-1) \cdot \int_0^{\Lambda} d\nu' \cdot Q_0\left[1 + 2\left(\frac{\nu'+1}{\nu}\right)\right]$$

involving the evaluation of $I_0(x)$ only but the numerical integration of a more complicated algebraic expression.

ANALYTIC PROPERTIES AND ASYMPTOTIC BEHAVIOUR

As a function of ν, $\mathrm{Im}A_{\ell'}(\nu')$ is constant and $P_{\ell'}\left[1 + 2\left(\frac{\nu+1}{\nu'}\right)\right]$ is analytic and has asymptotic behaviour $O(\nu^{\ell'})$.

Now, $Q_\ell(x)$ is cut $[-1, +1]$ with discontinuity $\frac{1}{2}P_\ell(x)$ as is shown by the general expression

$$Q_\ell(x) = \frac{P_\ell(x)}{2} \cdot \log\frac{x+1}{x-1} + R_\ell(x)$$

$R_l(x)$ is a polynominal of degree $\ell - 1$.

hence, $Q_\ell\left[1 + 2\left(\frac{\nu'+1}{\nu}\right)\right]$ is cut ν $[-\nu'-1, -\infty]$ and the whole integral from -1 to $-\infty$, with discontinuity

$$\mathrm{Im}C^{II}_{\ell\ell'}(\nu) = (2\ell'+1)\cdot\beta_{II'}\cdot\frac{2}{\nu}\int_0^{\infty} d\nu'\cdot \mathrm{Im}A^{I}_{\ell'}(\nu')\cdot P_{\ell'}\left[1 + 2\left(\frac{\nu+1}{\nu'}\right)\right] P_\ell\left[1 + 2\left(\frac{\nu'+1}{\nu}\right)\right].$$

There are no other singularities, however, the partial wave series cannot be used to continue

$C^{I}_{\ell}(\nu)$ to the physical region of the s channel

$\nu > 0$ as it accumulates and diverges at

$\nu = 0$ It also diverges at $\nu = -9$.

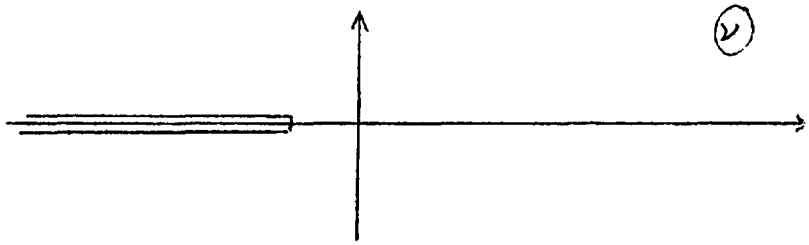

Fig. 2 - 4. Analytic properties of a finite sum of partial waves.

TO OBTAIN THE ASYMPTOTIC BEHAVIOUR

Now, $Q_\ell(x) \underset{x\to\infty}{\longrightarrow} x^{-\ell-1}$

$P_{\ell'}(x) \underset{x\to\infty}{\longrightarrow} x^{\ell'}$

$P_{\ell'}(x) \underset{x\to 1}{\longrightarrow} (-1)^{\ell'}$

$$Q_\ell(x) = \frac{P_\ell(x)}{2}\cdot\log\frac{x+1}{x-1} + R_\ell(x).$$

$\therefore$ as $x \to +1$ $\quad Q_\ell(x) \longrightarrow (-1)\cdot\log(x-1)$

-1 $\quad$ " $\longrightarrow$ " $\cdot\log(x+1)$

Hence

$$\mathrm{ReC}_{\ell\ell'}(\nu) \underset{\nu \to \pm\infty}{\longrightarrow} \frac{1}{\nu} \cdot \nu^{\ell'} \cdot \log \nu$$

$$\mathrm{ImC}_{\ell\ell'}(\nu) = \frac{4}{\pi\nu}\int_0^{-\nu-1} (2\ell'+1)\,\beta_{II'}\,\mathrm{Im}A_{\ell'}(\nu')\,P_{\ell'}\left[1+2\left(\frac{\nu+1}{\nu'}\right)\right] P_{\ell}\left[1+2\left(\frac{\nu'+1}{\nu}\right)\right]$$

$$\mathrm{ImC}_{\ell\ell'}(\nu) \underset{\nu\to-\infty}{\longrightarrow} \frac{1}{\nu} \cdot \nu^{\ell'} \cdot \nu \leftarrow \text{for length of range of integration}$$

Hence $\dfrac{\mathrm{ImC}_{\ell\ell'}}{\mathrm{ReC}_{\ell\ell'}} \longrightarrow \dfrac{\pi}{\log\nu}$

hence $\mathrm{ImC}_{\ell\ell'}^{-1} = \dfrac{-\mathrm{ImC}_{\ell\ell'}}{\mathrm{Re}^2+\mathrm{Im}^2} \longrightarrow \dfrac{1}{\mathrm{Im}} \longrightarrow \nu^{-\ell'}$

$$\mathrm{ReC}_{\ell\ell'}^{-1} = \frac{\mathrm{ReC}_{\ell\ell'}}{\mathrm{Re}^2+\mathrm{Im}^2} = \frac{\nu^{\ell'-1}\log\nu}{\nu^{2\ell}} = \nu^{-\ell'-1}\cdot\log\nu$$

We can also obtain the Left hand cut "threshold" behaviour.

For the Imaginary part,

$$\mathrm{Im}A_{\ell}(\nu) = \int_0^{-\nu-1} d\nu' \cdot \mathrm{Im}A_{\ell'}(\nu') \cdot P_{\ell'}\left[1+2\frac{(\nu+1)}{\nu'}\right] \cdot P_{\ell}\left[1+2\left(\frac{\nu'+1}{\nu}\right)\right]$$

we wish to obtain the lowest power of $(\nu+1)$ in the expansion about the point $= -1$; (from the left only ,as it has singularity there). Take

$$\mathrm{Im}A_{\ell}(\nu') \sim \nu'^{2\ell'+\frac{1}{2}}$$ since contributes only in $[0, -\nu-1]$ and near $\nu = -1$ has contributions only from threshold of right hand cut. $P_{\ell'}\left[1+2\frac{(\nu+1)}{\nu'}\right]$ gives power series in $\frac{\nu+1}{\nu'}$ starting with 1, contains all powers

$P_{\ell}\left[1+2\left(\frac{\nu'+1}{\nu}\right)\right]$ powers of $\frac{\nu'+1}{\nu}$ or better $\frac{\nu'}{\nu}$

to obtain lowest power in $(\nu+1)$ we want lowest in ν' and $(\nu+1)$. The factor $P_{\ell'}$ is homogeneous

$$1 + a\left(\frac{\nu+1}{\nu'}\right) + b\left(\frac{\nu+1}{\nu'}\right)^2$$

gives $\sim \nu' + a(\nu+1)\cdot\log\nu' - b\left(\frac{\nu+1}{\nu'}\right)^2 \cdot$

$$\sim (\nu+1) + a(\nu+1)\log(\nu+1) - b(\nu+1).$$

The factor P_{ℓ} has lowest power 1, hence lowest power from terms

$$\nu'^{2\ell'+\frac{1}{2}} \cdot [1]$$

since $\frac{1}{\nu'}$ term from $P_{\ell'}$ now joins the rest in being homogeneous when

integrated.

Hence the term is

$$\sim \quad \nu^{2\ell' + 3/2}$$

$$\mathrm{Im} A_\ell(\nu) \quad \sim \quad (\nu + 1)$$

Note independent of the direct channel ℓ. For a number of waves $\{\ell_i'\}$ in crossed channel

$$\sim \quad (\nu + 1)^{2\ell'_{min} + 3/2}$$

FIXED DISPERSION RELATION WITH S COMPLEX

$$A_t(s, t') = \rho_t(t') + \int \frac{ds' \cdot \rho_{st}(s', t')}{s' - s}$$

or something like this

hence for fixed real t'

$A_t(s, t')$

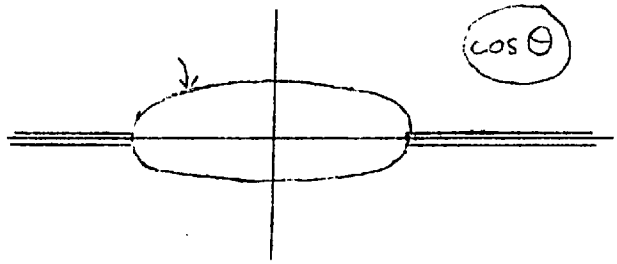

Lehman ellipse

Fig. 2-5(a)

hence $A_t(s, t')$ is analytic in cut plane (which includes Lehman ellipse). However $A_t(s, t')$ is complex, in general, off the real axis, and real analytic

$$A_t(s, t') = A^*_t(s^*, t')$$

Then $$A_\ell(s) = \int_4^\infty dt' \cdot A_t(s, t') \cdot Q_\ell\left[1 + \frac{2t'}{s-4}\right]$$

but Q_ℓ is also real analytic
hence $A_\ell(s)$, obtained by this formula, is real analytic.

Thus, we can use this formula for all s in the cut plane.

We can only put in the partial wave expansion in the Lehman Ellipse, however this does give a neighbourhood of the real S axis, and its extent can be calculated from the boundary of Lehman ellipse.

$$\cos\theta' = 1 + \frac{2s}{t' - 4} \cdot \qquad ; \qquad s = -2\ (1 - \cos\theta')$$

standard result

diagram in s plane ~

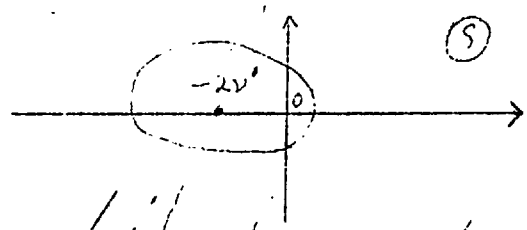

$\cos\theta' = 0 \sim S = -2\nu'$

Fig. 1-5(b)

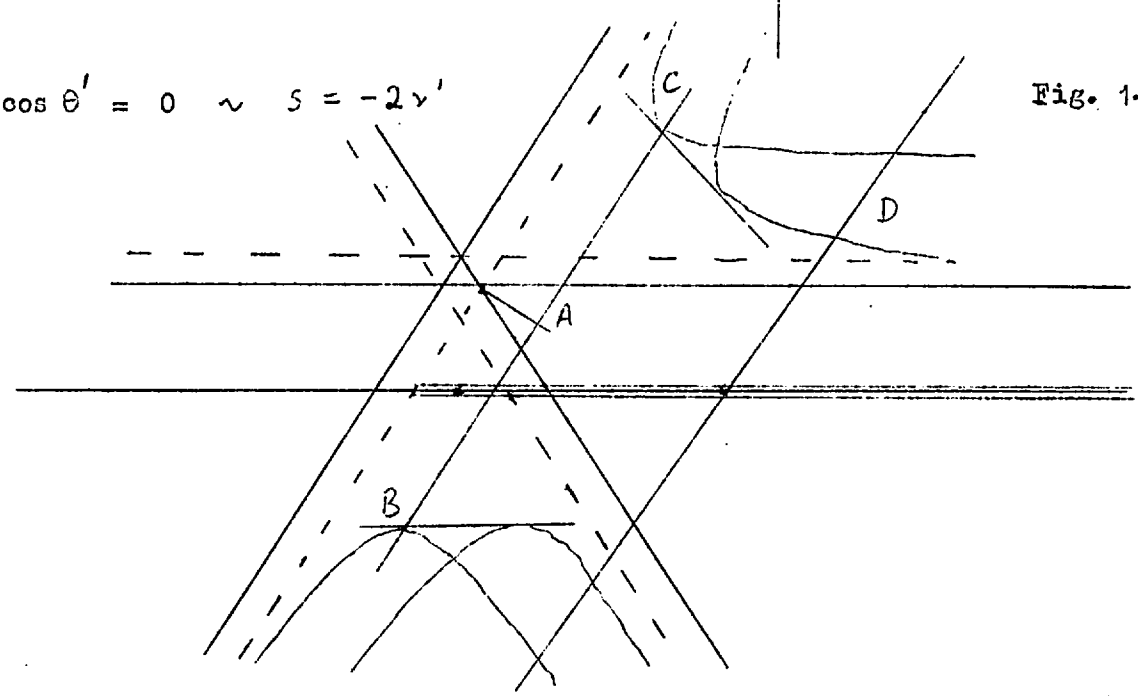

Fig. 2 - 6(a)

We can see from the diagram that the region of convergence of the integral of the sum is the smallest Lehmon ellipse over the integral which obtains at $\nu = -9$.

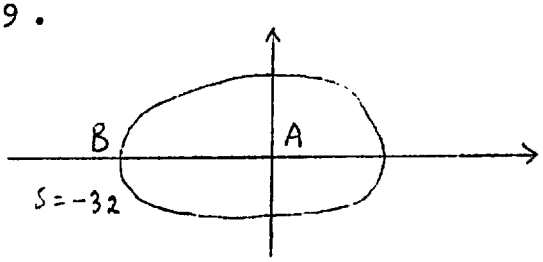

for left hand limit

Fig. 2 - 6(b)

and the asymptotic ellipse for right hand limit which touches the imaginary axis.

So, in the ν plane, it is an ellipse.

However, this is cut away by the nearer region near D.

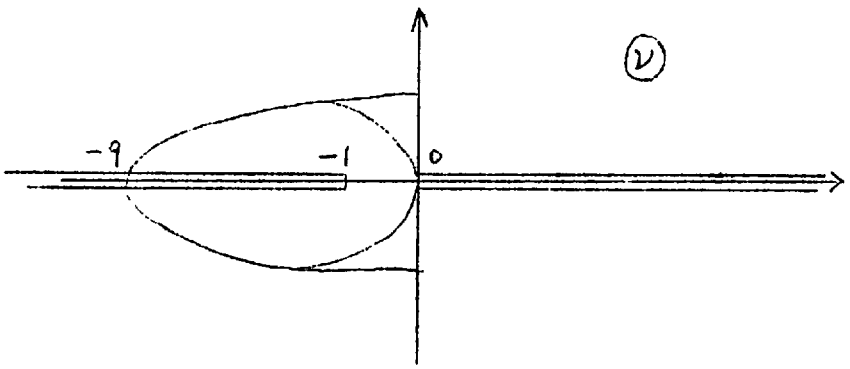

Fig. 2 - 6(c)

IMAGINARY PARTS OF PARTIAL WAVE AMPLITUDES

$$A_\ell(\nu) = \frac{4}{\pi\nu}\int_0^\infty d\nu' \cdot Q_\ell\left[1 + 2\left(\frac{\nu'+1}{\nu}\right)\right] \cdot A_t(\nu', \nu)$$

For ν in $[0, -9]$, A_t is real and Q_ℓ is cut $[-1, -\infty]$

$$\therefore \quad \mathrm{Im}A_\ell(\nu) = \frac{2}{\nu}\int_0^{\nu-1} d\nu' P_\ell\left[1 + 2\left(\frac{\nu'+1}{\nu}\right) \cdot A_t(\nu', \nu)\right.$$

$-9 < \nu < -1$

For ν in $[0, \infty]$, Q_ℓ is real, A_t is cut with discontinuity ρst, the double spectral function

$$A_t(\nu', \nu) = \frac{1}{\pi}\int_a^\infty \frac{ds'\,\rho st(s', t)}{s' - s} + \frac{1}{\pi}\int_{-\infty}^b ds'\,\rho tu\frac{(s', t)}{s' - s}$$

$$\therefore \quad \mathrm{Im}A_\ell(\nu) = \frac{4}{\pi\nu}\int_0^\infty d\nu' \cdot Q_\ell\left[1 + 2\left(\frac{\nu'+1}{\nu}\right)\right] \cdot \rho\, st(s, t')$$

$0 < \nu < \infty$

For $\nu < -9$ both Q_ℓ and A_t are cut

above the cut, we have

$$(Q + iP)\ (A_t + i\rho) = (QA_t - P\rho) + i\,(PA_t + \rho Q)$$

below the cut

$$(Q - iP)\ (A_t - i\rho) = (QA_t - P\rho) - i\,(PA_t + \rho Q)$$

$$\therefore \quad \mathrm{Im}A_\ell(\nu) = \frac{4}{\pi\nu}\int_0^\infty d\nu' \left\{Q_\ell\left[1 + 2\left(\frac{\nu'+1}{\nu}\right)\right] \cdot \rho_{tu}(\nu', \nu)\right.$$

$-\infty < \nu < -9$

$$\left. + \frac{\pi}{2} P_\ell\left[1 + 2\left(\frac{\nu'+1}{\nu}\right)\right] \cdot \mathrm{Re}A_t(\nu', \nu)\right\}$$

The amplitude is real for ν in $[0, -1]$.

SHIRKOV'S CRITERION FOR THE RELIABILITY OF CONTINUATION OF THE PARTIAL WAVE SERIES

The absorptive part obeys a dispersion relation of the form

$$A_t^I(\nu, \cos\theta) = \frac{1}{\pi}\int_{\cos\theta_0(\nu)}^\infty d(\cos\theta') \cdot \left[\frac{\rho_1^I(\cos\theta', \nu)}{\cos\theta' - \cos\theta} + \frac{\rho_2^I(\cos\theta', \nu)}{\cos\theta' + \cos\theta}\right]$$

and we are making an approximate continuation using a partial wave expansion

$$A_t^I(\nu, \cos\theta) = \sum_{\ell'=0}^{L} (2\ell+1) \cdot \mathrm{Im}A_{\ell'}(\nu) \cdot P_{\ell'}(\cos\theta)$$

Shirkov etal. (2) (3) proposed a way of estimating the error involved by observing that it was the same as the error in cating the Heine development

$$\frac{1}{\cos\theta' - \cos\theta} = \sum_{\ell'=0}^{\infty} (2\ell'+1) \cdot Q_{\ell'}(\cos\theta')\, P_{\ell'}(\cos\theta)$$

For inserting the development into the dispersion relation enables one to factor out the P_{ℓ}'s since the spectral function is independent of cos θ Alternatively, project the dispersion relation into partial waves by integrating.

Taking $\nu = 3$, the inelastic threshold, and $\theta' = \theta_0$ the edge of the double spectral region, then for an S & P wave truncation, the error was

for $\theta = 0$	2 - 4%	adequate
for $\theta = \pi/2$	300%	inadequate

Of course, this gives the estimated error for a double spectral function massed at the end of the cut. Presumably the error will be less for those spectral functions which give dominant S and P waves, in the physical region.

On the diagram one can see the locations of the points ($\nu = 3$, $\theta = 0$) and ($\nu = 3$, $\theta = \frac{\pi}{2}$).

Diagram for Shirkov Criterion

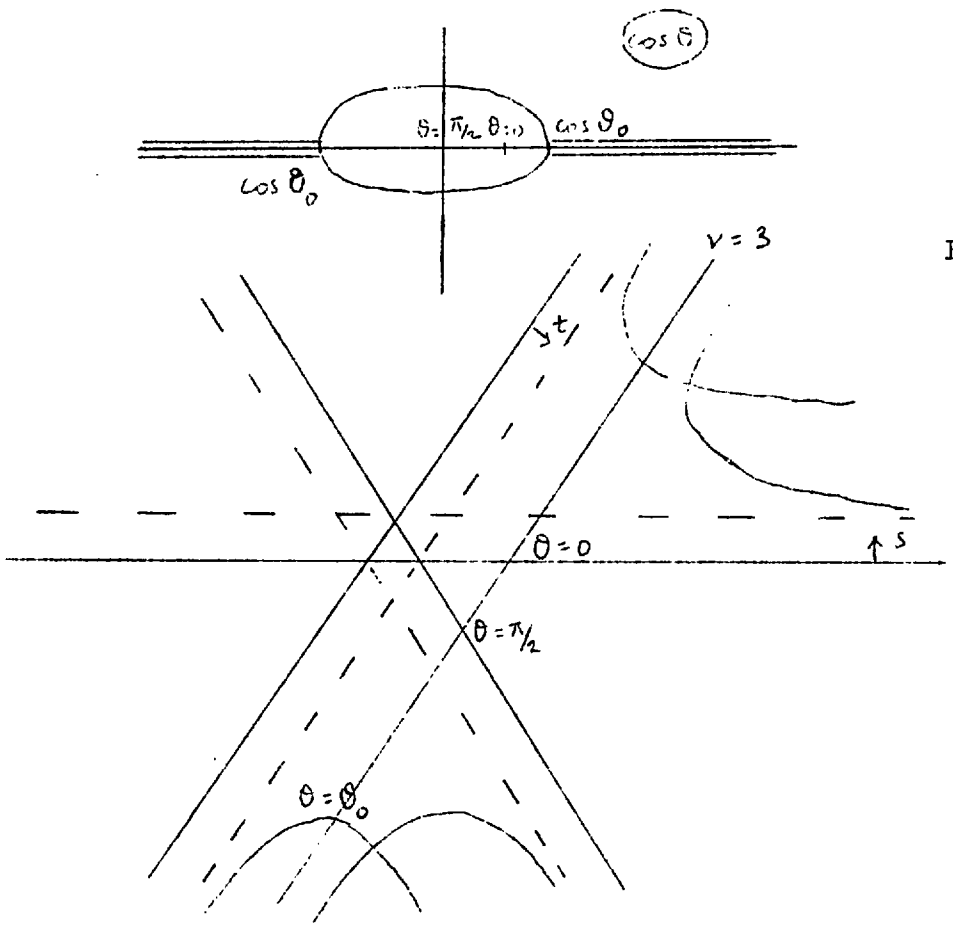

Fig. 2 - 7(a)

Fig. 2 - 7(b)

CONVERGENCE OF THE REAL PART SERIES

The real part can also be expanded in a partial wave series in the physical region

$$A(s, t') = \sum_{\ell=0}^{\infty} (2\ell + 1) \cdot A_\ell(t') \cdot P_\ell\left[1 + \frac{2s}{t' - 4}\right]$$

but this series converges in a smaller region than the series from the imaginary part.

From M. R. , $A(s, t')$, as s varies with t fixed in $[4, \infty]$, will be cut for s in $[4, \infty]$ and for u in $[4, \infty]$. Hence the series converges only in the region $s = -t$ to $s = 4$.

These considerations are made transparent by a Mandelstam diagram

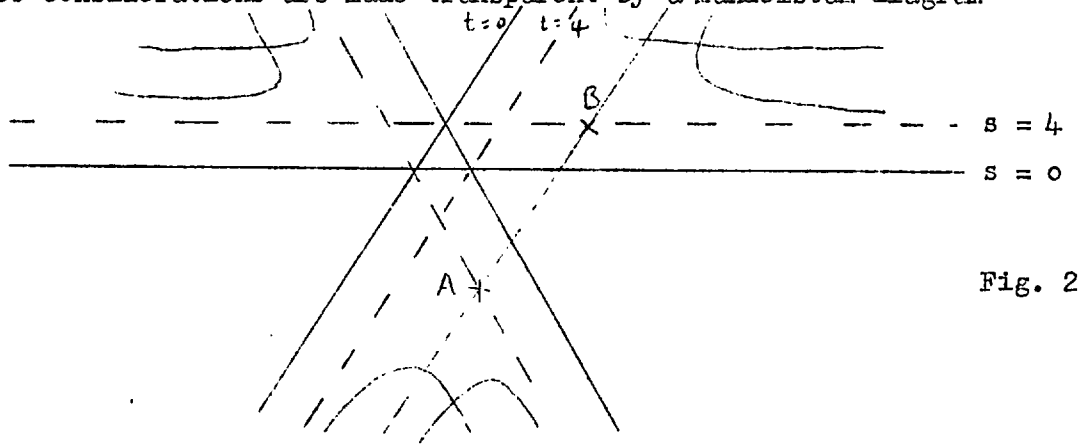

Fig. 2 - 8

The series diverges at A and B i.e. as soon as it "gets level" with the double spectral region or as soon as it is level with the threshold in the s or . U channel.

RESULTS OF CALCULATING $C_{\ell\ell'}^{II'}(\nu)$

Table 1 gives the values obtained by numerical integration of the real and imaginary parts of $C(\nu)$ for the first six waves, i.e. up to F_1. We give a breakdown of the effects of different waves in the crossed channel and the total $C(\nu)$. We used experimental values discussed later in this chapter and had S_0, S_2, P_1, D_0 in the crossed channel. Figures 9 are graphs to total and breakdown values of $C(\nu)$. $C(\nu)$ is displayed in detail because it is basic to most of the thesis. The behaviour of $C^{-1}(\nu)$ is discussed in Chapter 6.

Fig 2-9-P$_1$-1
Total → P$_1$

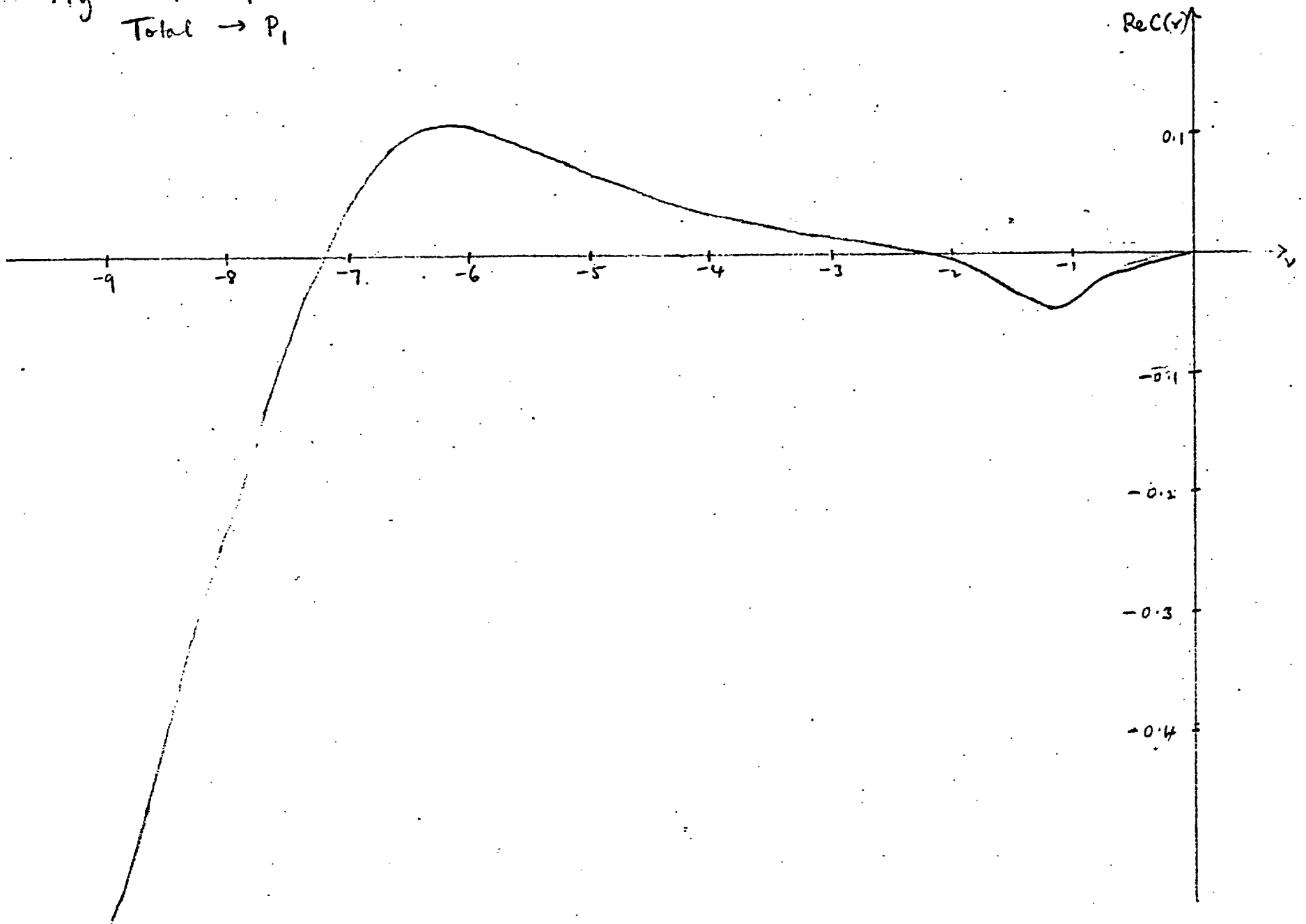

Fig 2-9-P1-2
Breakdown

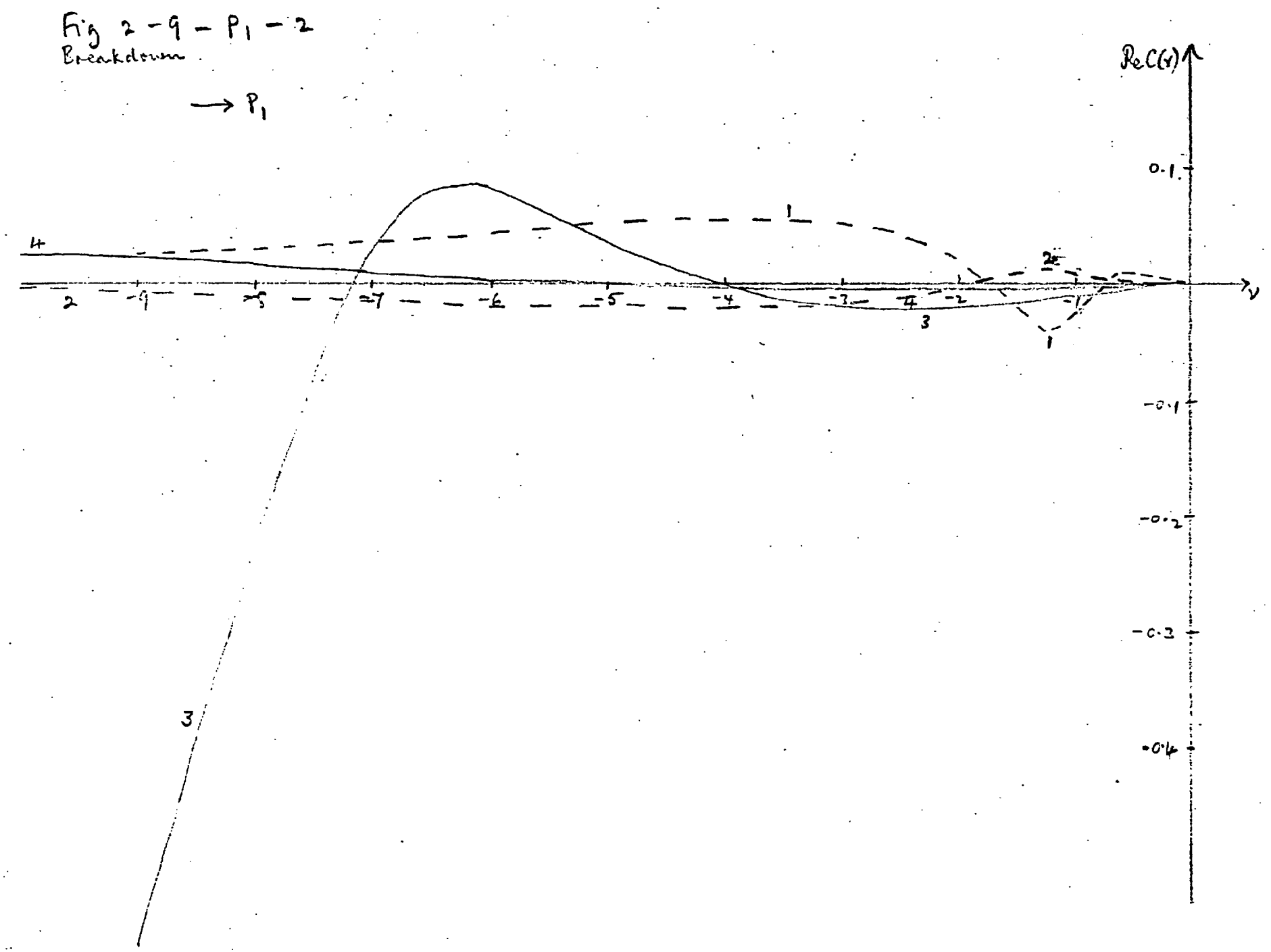

Fig 2-9-P_1-3

1 Total

$\longrightarrow P_1$

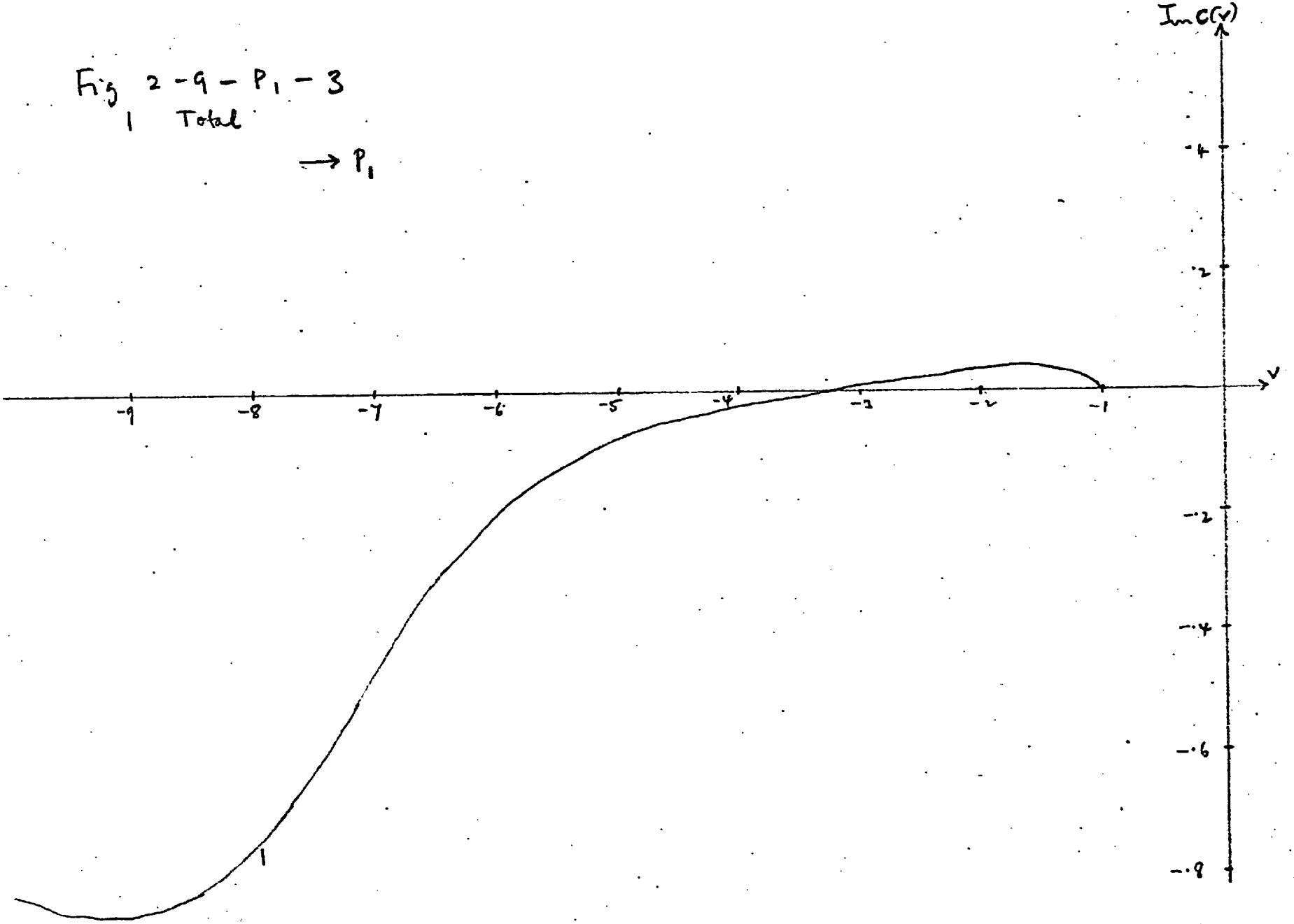

Fig 2-9-P1-4
Breakdown.

3 $P_1 \longrightarrow P_1$

4 D_0 negligible.

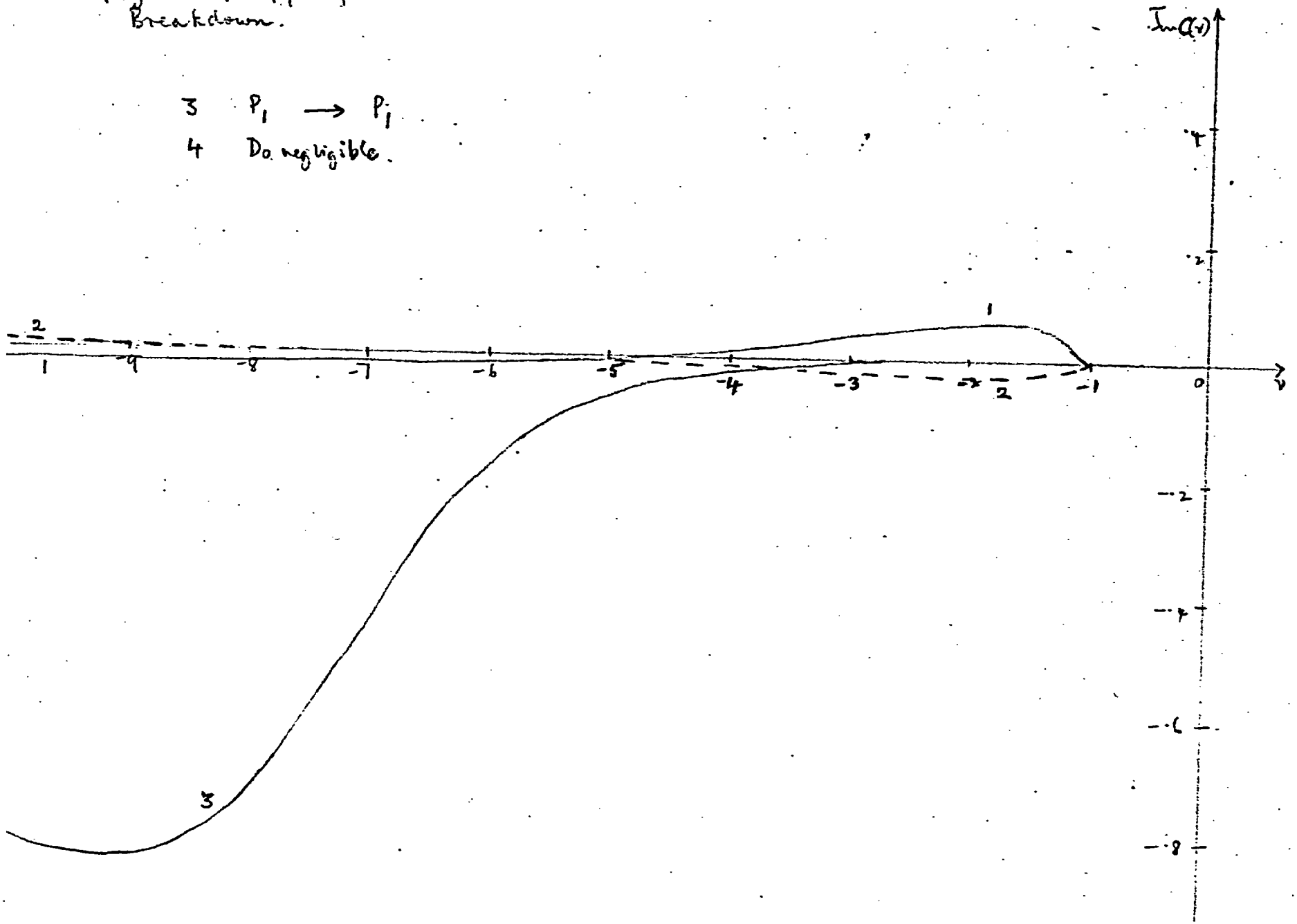

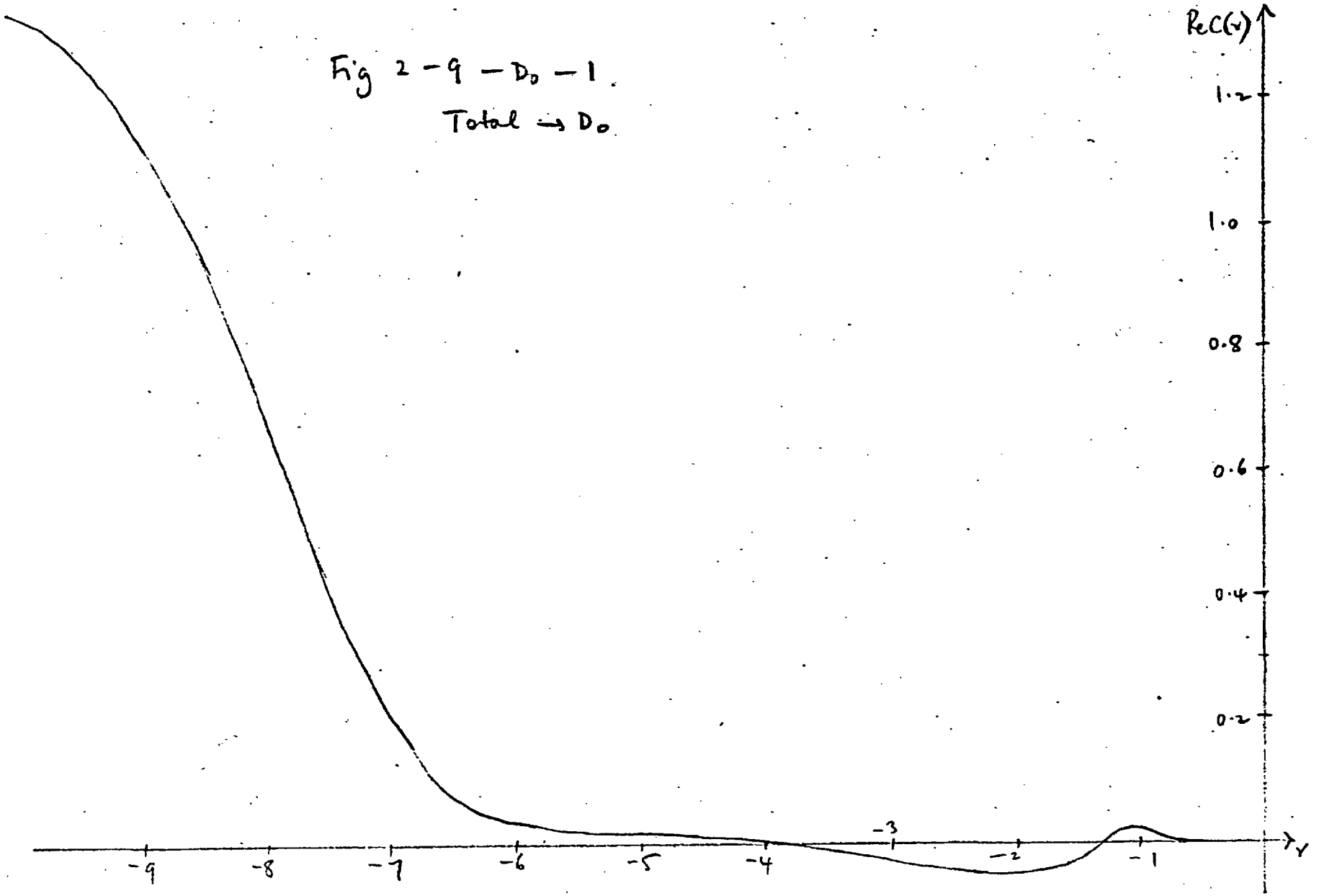
Fig 2-9-D₀-1.
Total → D₀
ReC(ν)
1.2
1.0
0.8
0.6
0.4
0.2
-9
-8
-7
-6
-5
-4
-3
-2
-1
ν

Fig 2-9 – $D_0 - 2$

Breakdown $\rightarrow D_0$

$D_0 \rightarrow D_0$ negligible.

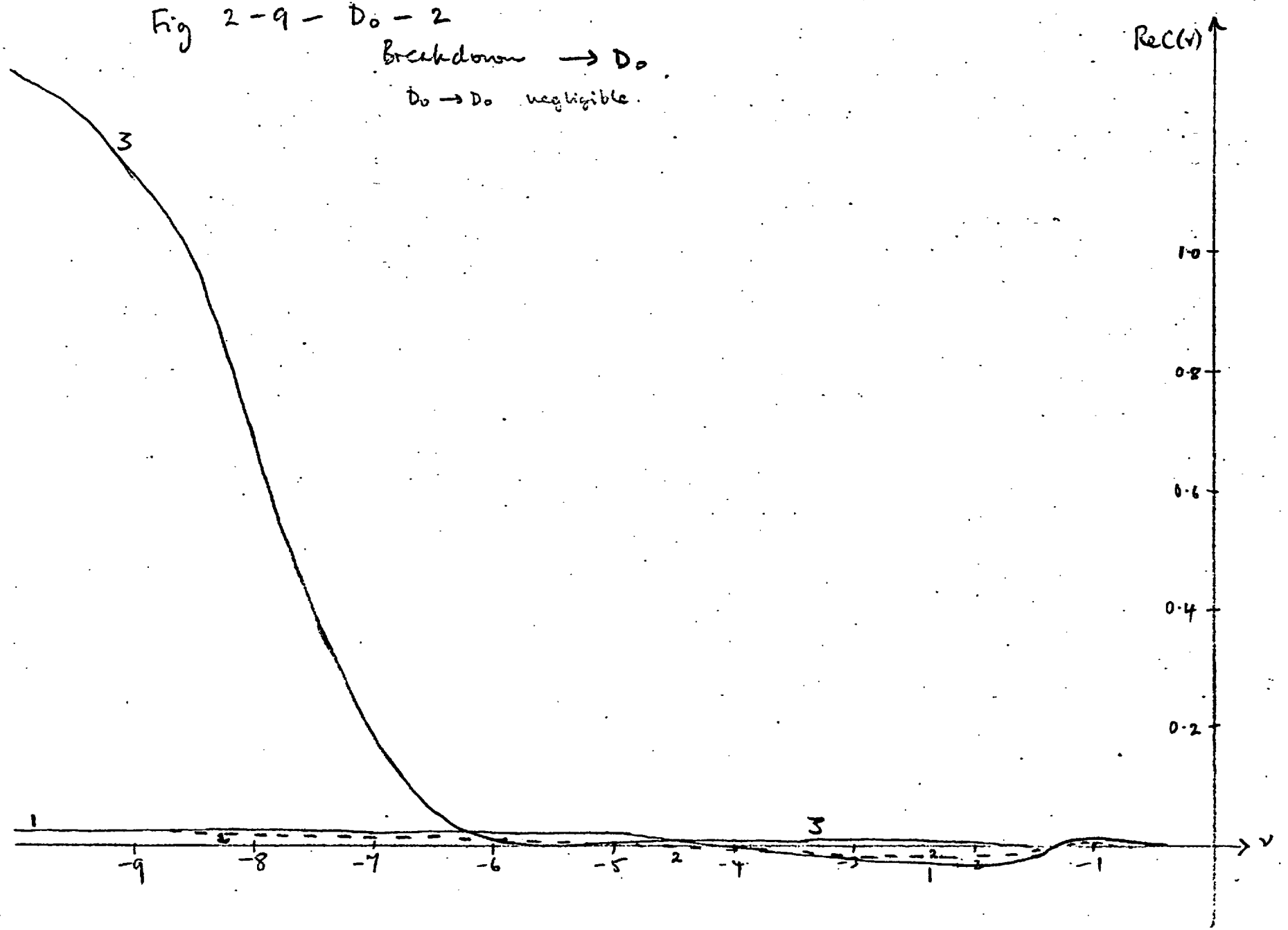

Fig 2-9-D_0-3
Total → D_0

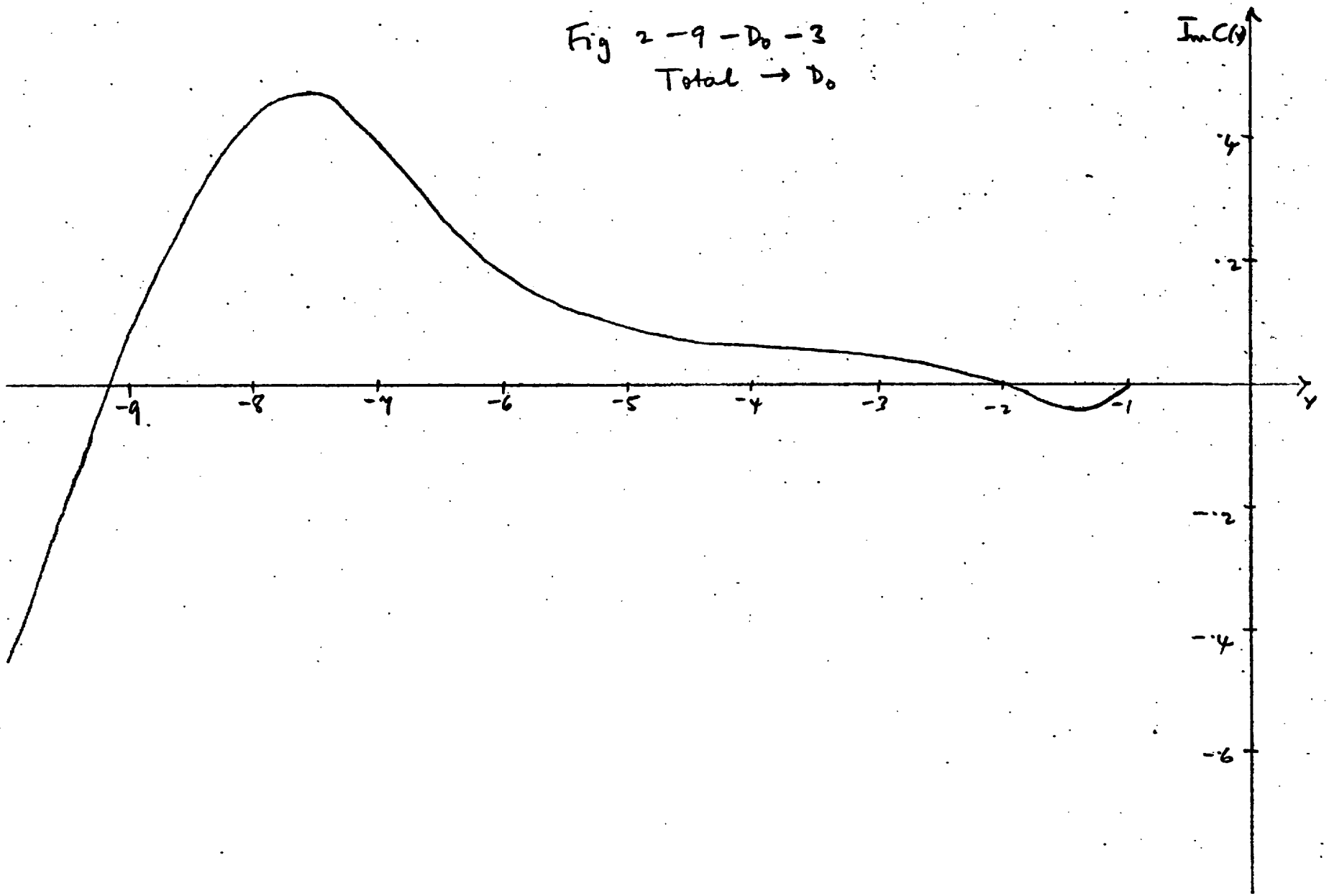

Fig 2-9 - D_0 - 4

Breakdown $\rightarrow D_0$

$D_0 \rightarrow D_0$ negligible

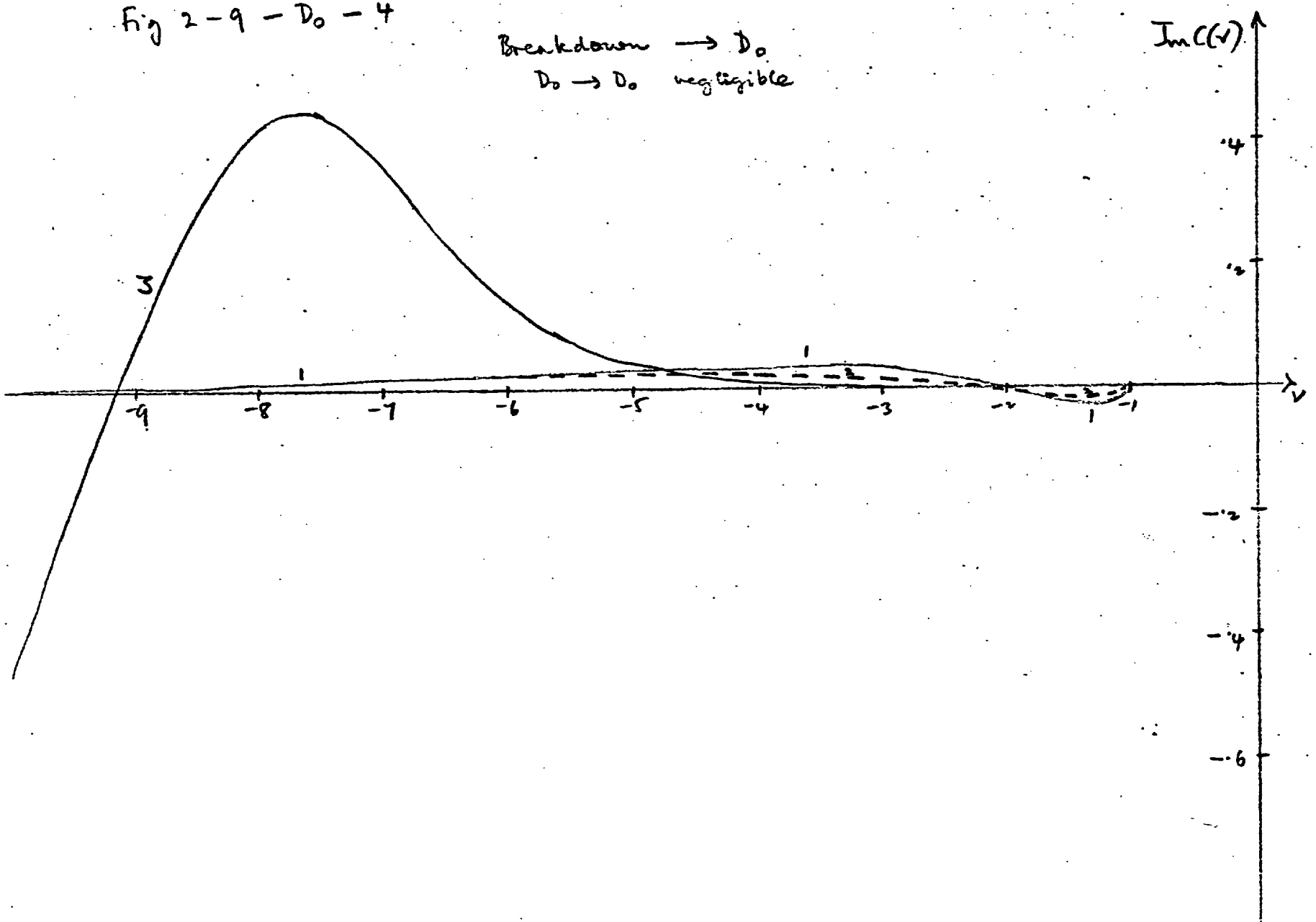

Total → D_2 Fig 2-9-D_2-1.

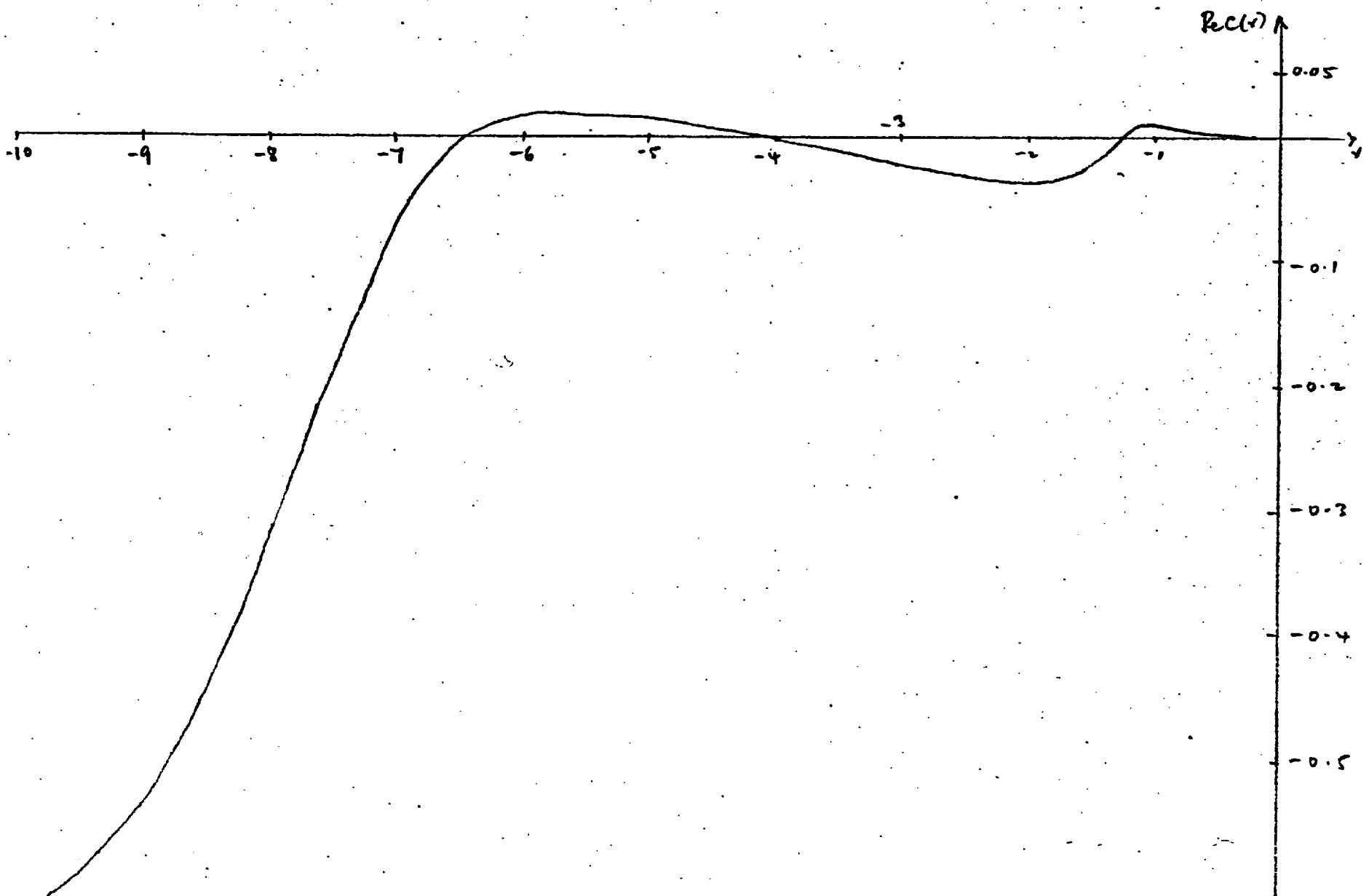

Fig 2-9-D_2-2

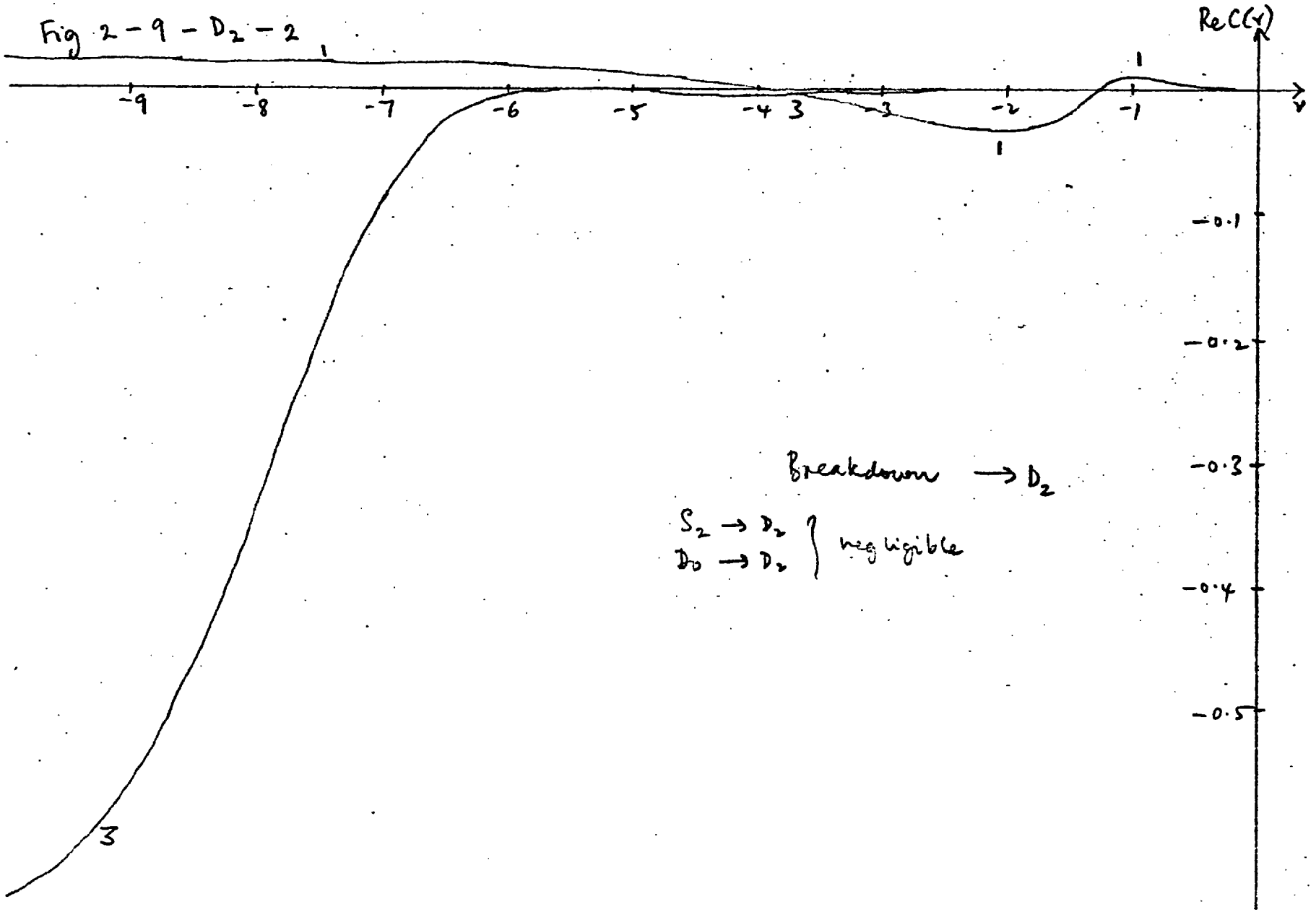
Re C(γ)
-9
-8
-7
-6
-5
-4
-3
-2
-1
γ
1
1
1
3
-0.1
-0.2
-0.3
-0.4
-0.5
Breakdown → D_2
$S_2 \rightarrow D_2$
$D_0 \rightarrow D_2$
negligible

Fig 2-9 – D_2 – 3

Total → D_2

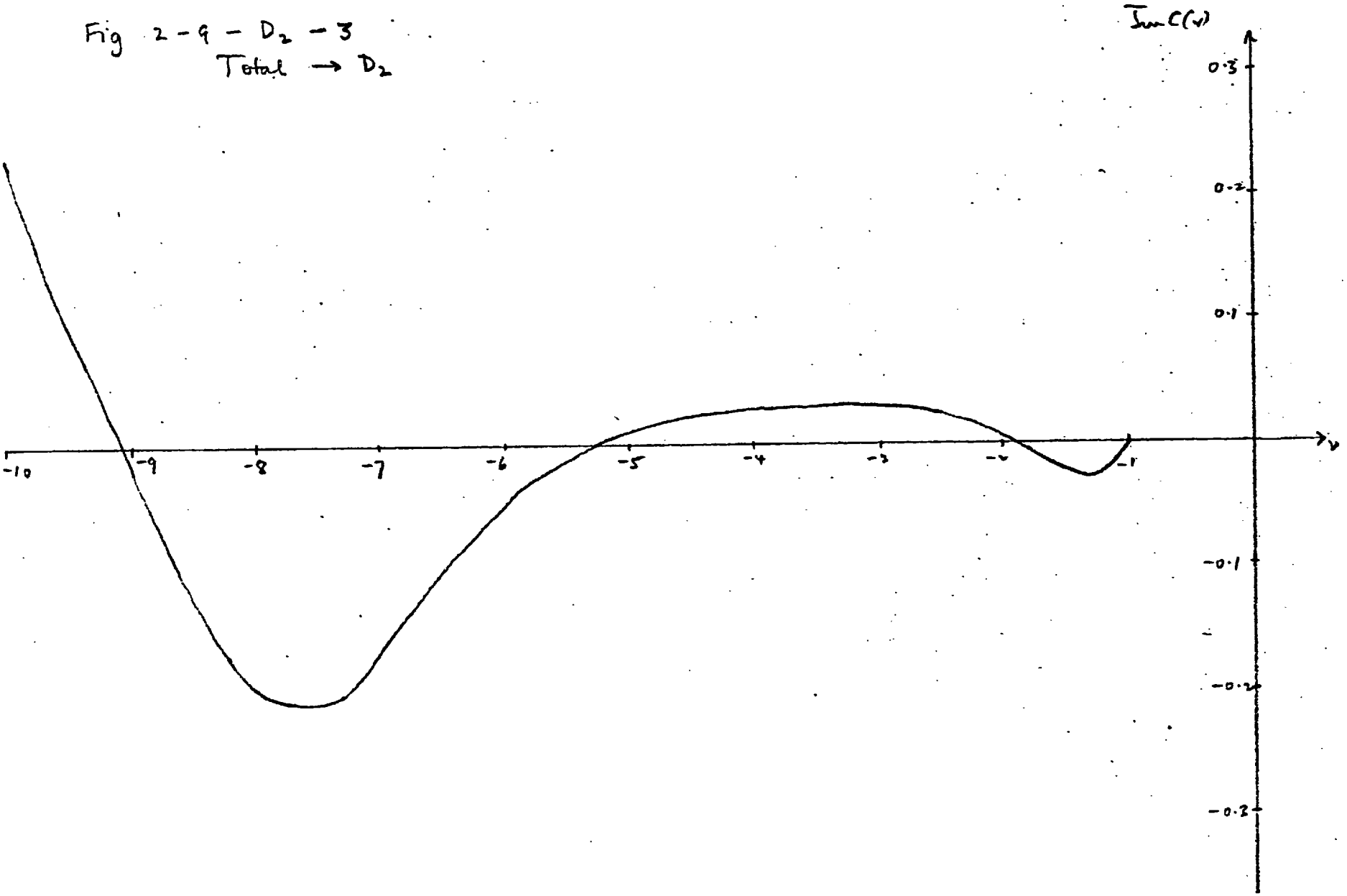

Fig. 2-9 - D_2 - 4

Breakdown $\longrightarrow D_2$

$S_2 \rightarrow D_2$

$D_0 \rightarrow D_2$ negligible.

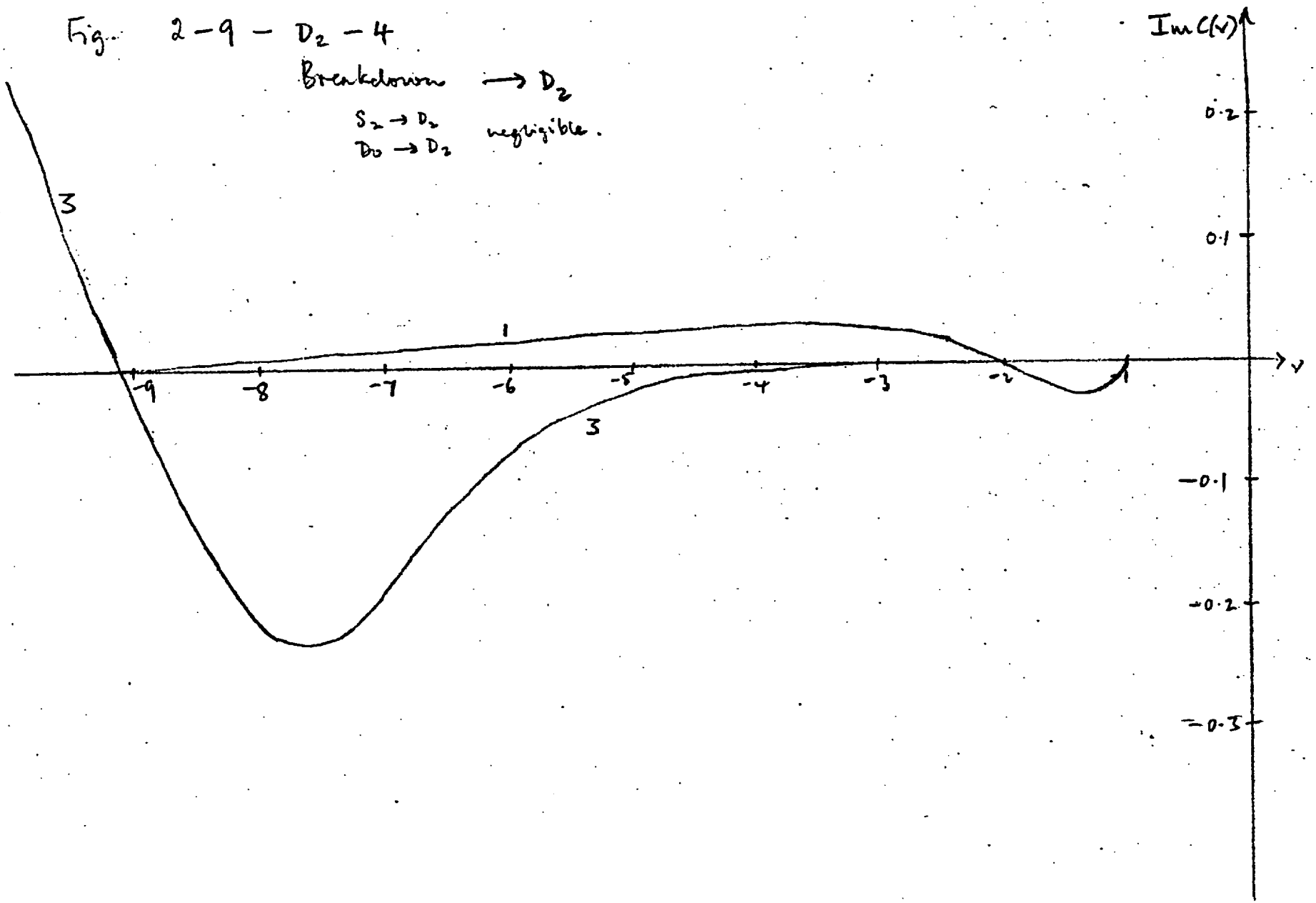

FIG - 2-9 - F_1 - 1
Total → F_1

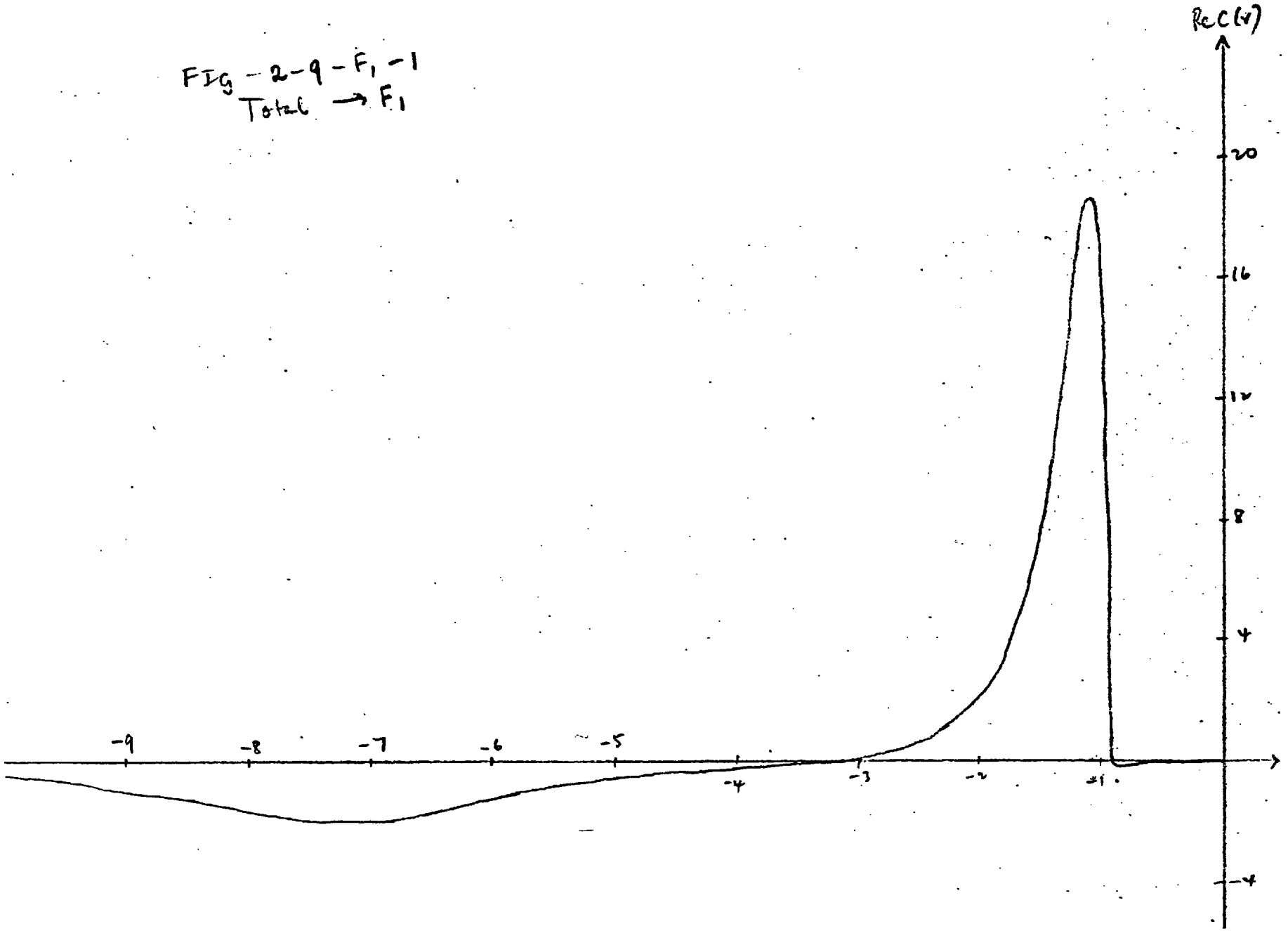

Fig 2-9 - F_1 - 2.
Breakdown → F_1
Do negligible.

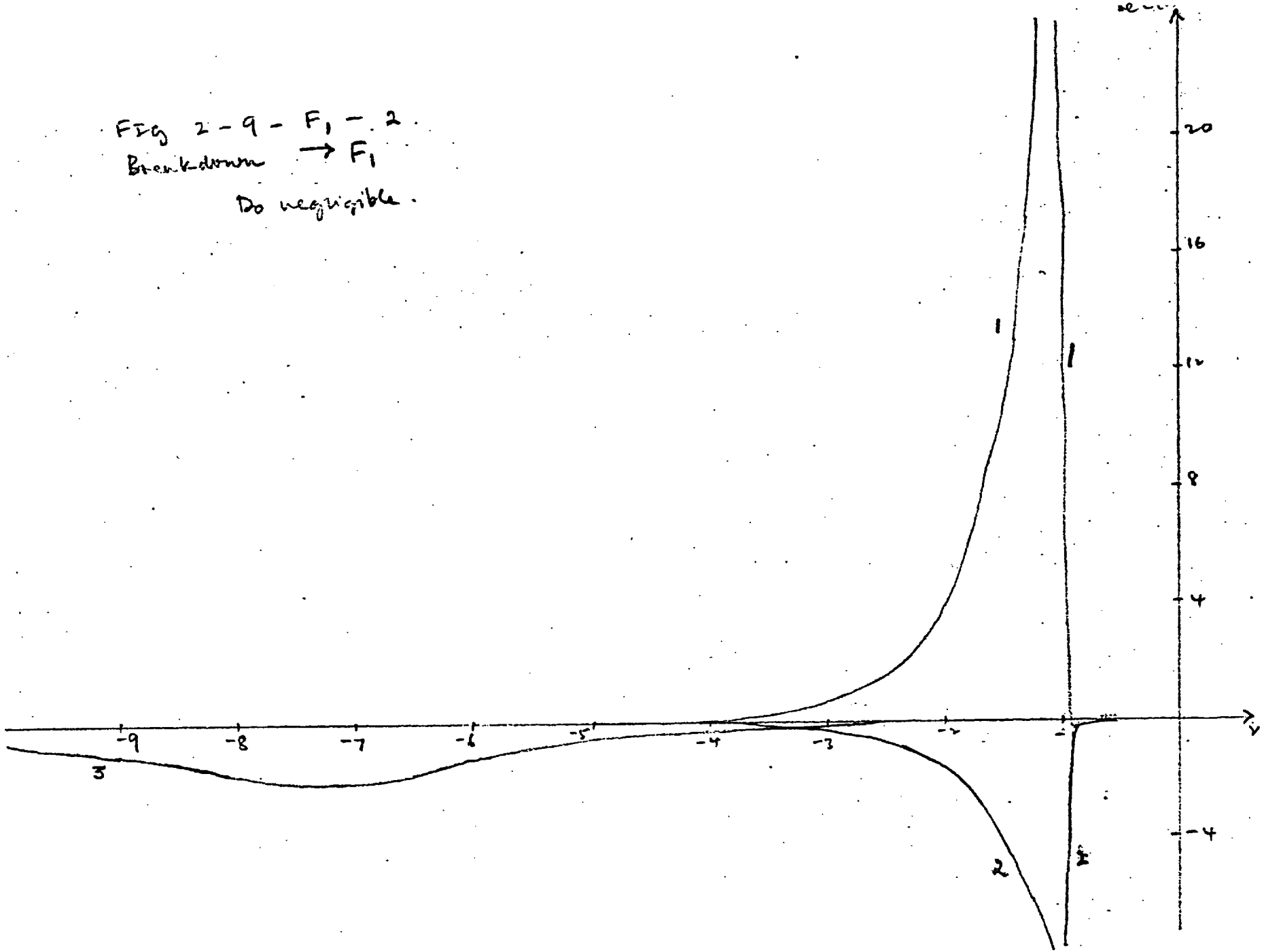

Fig 2-9-F_1-3.
Total → F_1

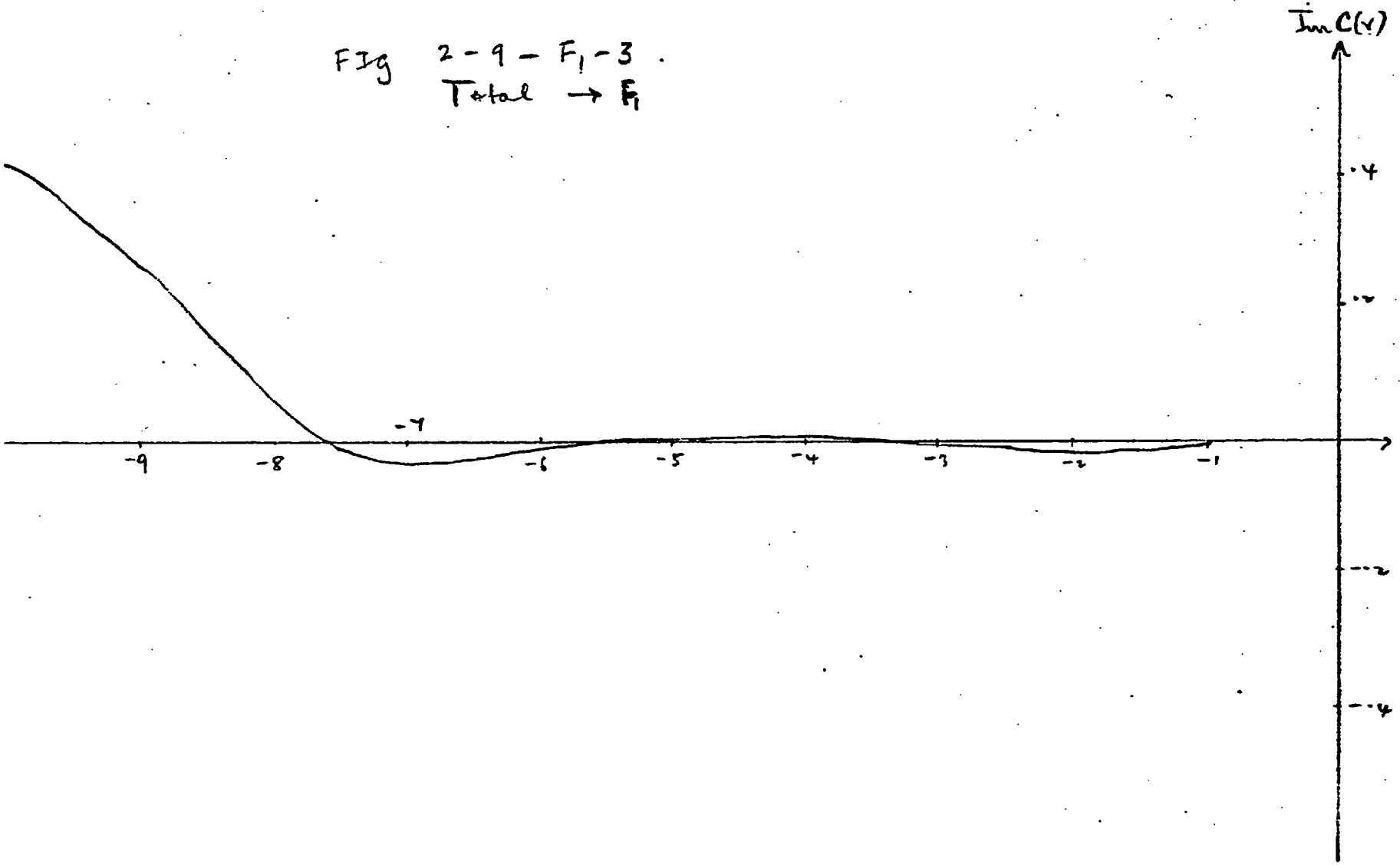

Fig. 2-9 - F_1 - 4

Breakdown $\longrightarrow F_1$

$S_2 \rightarrow F_1$

$D_0 \rightarrow F_1$ negligible

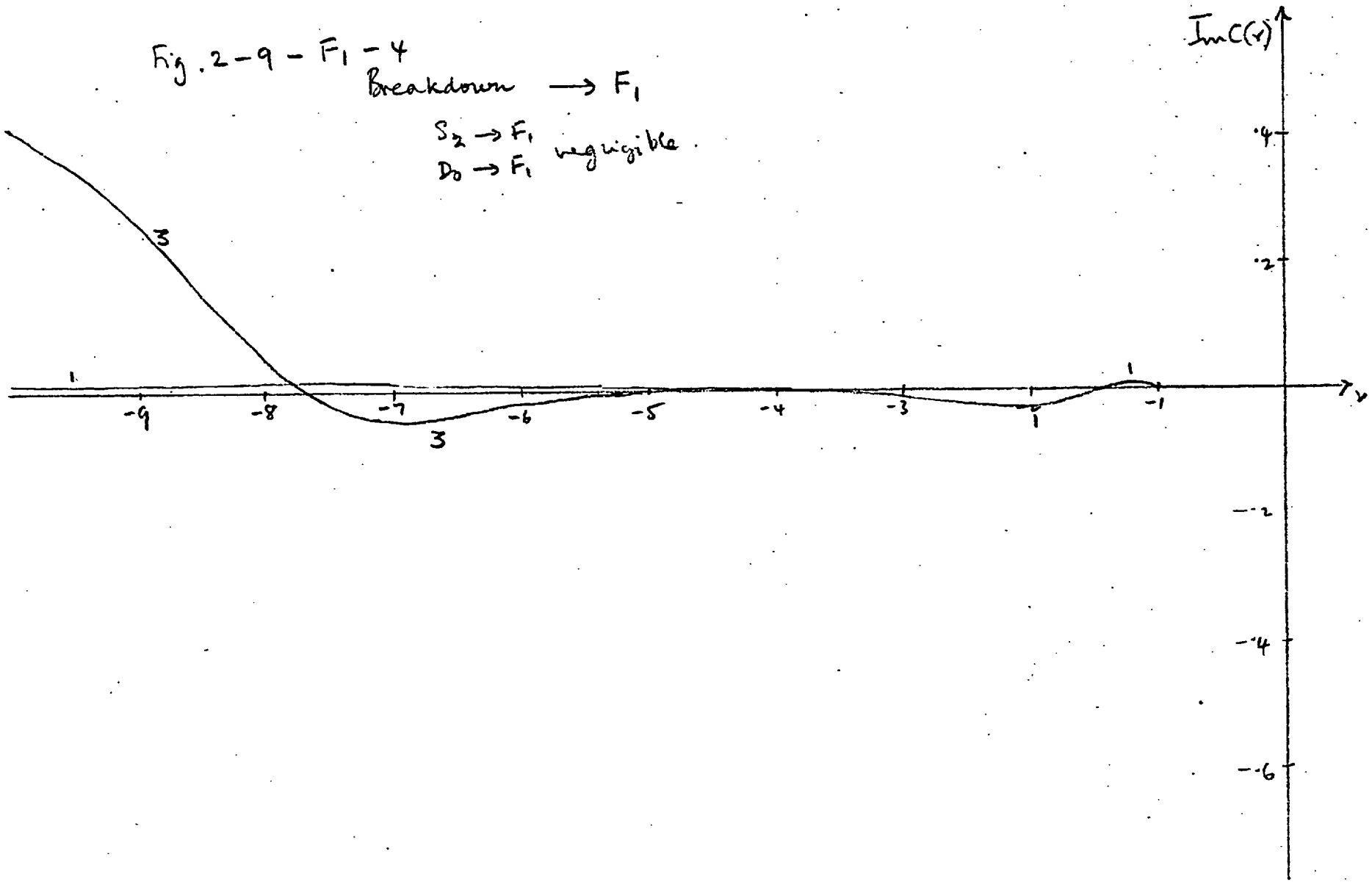

Table 2-1-a. Total and Breakdown of $Re\,C(\nu) \to P_1$

ALL	S_0	S_2	P_1	D_0	ν
-1.130	0.016	-0.001	-1.145	0.034	-11.000
-0.990	0.016	-0.003	-1.004	0.031	-10.500
-0.850	0.019	-0.005	-0.864	0.028	-10.000
-0.700	0.021	-0.007	-0.715	0.024	-9.500
-0.542	0.024	-0.008	-0.558	0.021	-9.000
-0.376	0.027	-0.010	-0.393	0.018	-8.500
-0.211	0.030	-0.012	-0.230	0.015	-8.000
-0.063	0.034	-0.013	-0.084	0.012	-7.500
0.046	0.037	-0.015	0.024	0.009	-7.000
0.102	0.041	-0.016	0.078	0.006	-6.500
0.109	0.044	-0.018	0.083	0.004	-6.000
0.092	0.048	-0.019	0.063	0.002	-5.500
0.069	0.051	-0.020	0.038	-0.000	-5.000
0.049	0.054	-0.020	-0.016	-0.002	-4.500
0.034	0.056	-0.020	-0.002	-0.003	-4.000
0.024	0.056	-0.019	-0.014	-0.004	-3.500
0.016	0.053	-0.016	-0.021	-0.005	-3.000
0.008	0.042	-0.011	-0.024	-0.005	-2.500
-0.005	0.020	-0.002	-0.024	-0.005	-2.000
-0.012	0.008	0.003	-0.023	-0.005	-1.800
-0.023	0.009	0.008	-0.022	-0.004	-1.600
-0.035	0.027	0.012	-0.020	-0.004	-1.400
-0.045	0.041	0.014	-0.018	-0.004	-1.200
-0.037	0.031	0.010	-0.015	-0.003	-1.000
-0.023	0.015	0.005	-0.013	-0.003	-0.800
-0.016	0.009	0.003	-0.010	-0.002	-0.600
-0.010	0.005	0.002	-0.007	-0.001	-0.400
-0.005	0.002	0.001	-0.003	-0.001	-0.200

$S_0 \to P_1$ Re; $S_2 \to P_1$ Re; $P_1 \to P_1$ Re; $D_0 \to P_1$ Re; $P_{S_2} \to P_1$ Re

ALL	S_0	S_2	P_1	D_0	ν
-0.733	-0.020	0.008	-0.722	0.004	-11.000
-0.791	-0.021	0.008	-0.778	0.003	-10.500
-0.836	-0.022	0.008	-0.822	0.002	-10.000
-0.864	-0.022	0.008	-0.849	0.002	-9.500
-0.867	-0.022	0.007	-0.852	0.001	-9.000
-0.835	-0.022	0.007	-0.821	0.001	-8.500
-0.758	-0.021	0.006	-0.743	0.001	-8.000
-0.628	-0.020	0.005	-0.614	0.000	-7.500
-0.465	-0.018	0.004	-0.451	0.000	-7.000
-0.310	-0.016	0.003	-0.297	0.000	-6.500
-0.195	-0.013	0.001	-0.184	0.000	-6.000
-0.120	-0.009	-0.001	-0.110	0.000	-5.500
-0.073	-0.004	-0.003	-0.066	0.000	-5.000
-0.042	0.003	-0.006	-0.039	0.000	-4.500
-0.021	0.011	-0.010	-0.022	0.000	-4.000
-0.004	0.022	-0.014	-0.012	0.000	-3.500
0.011	0.035	-0.018	-0.006	0.000	-3.000
0.025	0.050	-0.022	-0.003	0.000	-2.500
0.039	0.063	-0.023	-0.001	0.000	-2.000
0.042	0.065	-0.023	-0.000	0.000	-1.800
0.043	0.063	-0.020	-0.000	0.000	-1.600
0.038	0.054	-0.015	-0.000	0.000	-1.400
0.024	0.032	-0.008	-0.000	0.000	-1.200
0.000	0.000	0.000	0.000	0.000	-1.000
0.000	0.000	0.000	0.000	0.000	-0.800
0.000	0.000	0.000	0.000	0.000	-0.600
0.000	0.000	0.000	0.000	0.000	-0.400
0.000	0.000	0.000	0.000	0.000	-0.200

$S_0 \to P_1$ Im; $S_2 \to P_1$ Im; $P_1 \to P_1$ Im; $D_0 \to P_1$ Im; $P_{S_2} \to P_1$ Im

Total & Breakdown of $Im\,C(\nu) \to P_1$

Total + Breakdown $Re\,C(\nu) \rightarrow P_0$

ALL S_0	S_2	P_1	D_0	ν
0.025	0.024	0.747	-0.007	-11.000
0.026	0.023	0.920	-0.006	-10.500
0.026	0.022	1.083	-0.005	-10.000
0.025	0.021	1.223	-0.004	-9.500
0.025	0.020	1.298	-0.003	-9.000
0.025	0.019	1.309	-0.002	-8.500
0.024	0.018	1.298	-0.002	-8.000
0.024	0.017	1.239	-0.001	-7.500
0.023	0.015	1.120	-0.001	-7.000
0.021	0.013	0.927	-0.001	-6.500
0.019	0.011	0.673	-0.000	-6.000
0.017	0.008	0.397	-0.000	-5.500
0.013	0.004	0.175	-0.000	-5.000
0.008	0.000	0.051	0.000	-4.500
0.001	0.006	0.008	0.000	-4.000
0.007	0.011	-0.000	0.000	-3.500
0.017	0.017	0.002	0.000	-3.000
0.027	0.021	0.005	0.000	-2.500
0.033	0.020	0.007	0.000	-2.000
0.031	0.017	0.007	0.000	-1.800
0.024	0.012	0.007	0.000	-1.600
0.012	0.003	0.005	0.000	-1.400
0.007	0.006	0.003	0.000	-1.200
0.010	0.006	0.003	0.000	-1.000
0.003	0.002	0.002	0.000	-0.800
0.001	0.001	0.002	0.000	-0.600
0.000	0.000	0.001	-0.000	-0.400
0.000	0.000	0.000	0.000	-0.200

($S_0 \rightarrow D_0$ Re; $S_2 \rightarrow D_0$ Re; $P_1 \rightarrow D_0$ Re; $D_0 \rightarrow D_0$ Re)

Total and Breakdown $Im\,C(\nu) \rightarrow P_3$

ALL S_0	S_2	P_1	D_0	ν
-0.002	0.004	-1.705	-0.001	-11.000
0.000	0.005	-1.553	-0.001	-10.500
0.002	0.007	-1.377	-0.000	-10.000
0.004	0.008	-1.177	-0.000	-9.500
0.006	0.010	-0.955	-0.000	-9.000
0.008	0.011	-0.711	-0.000	-8.500
0.011	0.013	-0.452	-0.000	-8.000
0.013	0.015	-0.186	-0.000	-7.500
0.016	0.017	0.068	-0.000	-7.000
0.019	0.019	0.284	-0.000	-6.500
0.022	0.021	0.423	-0.000	-6.000
0.025	0.022	0.448	-0.000	-5.500
0.028	0.023	0.366	-0.000	-5.000
0.030	0.024	0.242	-0.000	-4.500
0.032	0.023	0.140	-0.000	-4.000
0.032	0.021	0.076	-0.000	-3.500
0.029	0.016	-0.041	-0.000	-3.000
0.020	0.008	0.022	-0.000	-2.500
0.002	-0.005	0.011	-0.000	-2.000
-0.008	-0.010	0.006	-0.000	-1.800
-0.018	-0.014	0.003	-0.000	-1.600
-0.026	-0.016	0.002	-0.000	-1.400
-0.023	-0.012	0.001	-0.000	-1.200
0.000	0.000	0.000	0.000	-1.000
0.000	0.000	0.000	0.000	-0.800
0.000	0.000	0.000	0.000	-0.600
0.000	0.000	0.000	0.000	-0.400
0.000	0.000	0.000	0.000	-0.200

($S_0 \rightarrow D_0$ Im; $S_2 \rightarrow D_0$ Im; $P_1 \rightarrow D_0$ Im; $D_0 \rightarrow D_0$ Im)

Table 7 – 1 – 6 $C(\nu)$ for D_0 wave.

Total and Breakdown Re $C(\nu) \rightarrow D_2$

ALL	S_0	S_1	P_1	D_0	ν
-0.629	0.025	0.002	-0.649	-0.007	-11.000
-0.632	0.026	0.002	-0.654	-0.006	-10.500
-0.626	0.026	0.002	-0.649	-0.005	-10.000
-0.596	0.025	0.002	-0.619	-0.004	-9.500
-0.536	0.025	0.002	-0.560	-0.003	-9.000
-0.439	0.025	0.002	-0.463	-0.002	-8.500
-0.312	0.024	0.002	-0.336	-0.002	-8.000
-0.175	0.024	0.002	-0.199	-0.001	-7.500
-0.064	0.023	0.002	-0.088	-0.001	-7.000
-0.003	0.021	0.001	-0.025	-0.001	-6.500
0.016	0.019	0.001	-0.004	-0.000	-6.000
0.018	0.017	0.001	0.000	-0.000	-5.500
0.012	0.013	0.000	-0.001	-0.000	-5.000
0.005	0.008	0.000	-0.003	0.000	-4.500
-0.003	0.001	0.001	-0.004	0.000	-4.000
-0.012	0.007	0.001	-0.004	0.000	-3.500
-0.022	0.017	0.002	-0.003	0.000	-3.000
-0.032	0.027	0.002	-0.002	0.000	-2.500
-0.036	0.033	0.002	-0.002	0.000	-2.000
-0.035	0.031	0.002	-0.001	0.000	-1.800
-0.027	0.024	0.001	-0.001	0.000	-1.600
-0.013	0.012	0.000	-0.001	0.000	-1.400
0.007	0.007	0.001	-0.001	0.000	-1.200
0.010	0.010	0.001	-0.000	0.000	-1.000
0.003	0.003	0.000	-0.000	0.000	-0.800
0.001	0.001	0.000	-0.000	0.000	-0.600
0.000	0.000	0.000	-0.000	-0.000	-0.400
0.000	0.000	0.000	-0.000	0.000	-0.200

Total and Breakdown Im $C(\nu) \rightarrow D_2$

ALL	S_0	S_1	P_1	D_0	ν
0.475	-0.002	0.000	0.478	-0.001	-11.000
0.356	0.000	0.001	0.356	-0.001	-10.500
0.229	0.002	0.001	0.226	-0.000	-10.000
0.098	0.004	0.001	0.093	-0.000	-9.500
-0.027	0.006	0.001	-0.034	-0.000	-9.000
-0.133	0.008	0.001	-0.142	-0.000	-8.500
-0.199	0.011	0.001	-0.211	-0.000	-8.000
-0.210	0.013	0.001	-0.224	-0.000	-7.500
-0.166	0.016	0.002	-0.183	-0.000	-7.000
-0.100	0.019	0.002	-0.121	-0.000	-6.500
-0.046	0.022	0.002	-0.070	-0.000	-6.000
-0.011	0.025	0.002	-0.038	-0.000	-5.500
0.010	0.028	0.002	-0.020	-0.000	-5.000
0.022	0.030	0.002	-0.011	-0.000	-4.500
0.029	0.032	0.002	-0.006	-0.000	-4.000
0.031	0.032	0.002	-0.003	-0.000	-3.500
0.029	0.029	0.002	-0.002	-0.000	-3.000
0.020	0.020	0.001	-0.001	-0.000	-2.500
0.001	0.002	-0.000	-0.000	-0.000	-2.000
-0.009	-0.008	-0.001	-0.000	-0.000	-1.800
-0.020	-0.018	-0.001	-0.000	-0.000	-1.600
-0.028	-0.026	-0.002	-0.000	-0.000	-1.400
-0.024	-0.023	-0.001	-0.000	-0.000	-1.200
0.000	0.000	0.000	0.000	0.000	-1.000
0.000	0.000	0.000	0.000	0.000	-0.800
0.000	0.000	0.000	0.000	0.000	-0.600
0.000	0.000	0.000	0.000	0.000	-0.400
0.000	0.000	0.000	0.000	0.000	-0.200

Table 2-1-c $C(\nu)$ for D_2 wave.

Total and Breakdown Re $C(\gamma) \rightarrow F_1$

All	S_0	S_2	P_1	D_0	γ
-0.146	0.035	-0.009	-0.181	0.009	-11.000
-0.320	0.027	-0.008	-0.346	0.007	-10.500
-0.524	0.023	-0.007	-0.545	0.005	-10.000
-0.757	0.021	-0.007	-0.775	0.004	-9.500
-1.028	0.020	-0.007	-1.043	0.003	-9.000
-1.342	0.019	-0.007	-1.356	0.002	-8.500
-1.695	0.018	-0.007	-1.707	0.002	-8.000
-1.994	0.018	-0.008	-2.006	0.001	-7.500
-2.017	0.019	-0.009	-2.028	0.001	-7.000
-1.673	0.022	-0.011	-1.683	0.001	-6.500
-1.205	0.026	-0.015	-1.217	0.001	-6.000
-0.826	0.035	-0.022	-0.840	0.000	-5.500
-0.565	0.053	-0.034	-0.585	0.000	-5.000
-0.387	0.087	-0.055	-0.420	0.000	-4.500
-0.250	0.154	-0.094	-0.311	0.000	-4.000
-0.109	0.298	-0.171	-0.236	0.000	-3.500
0.110	0.626	-0.335	-0.181	0.000	-3.000
0.610	1.453	-0.709	-0.135	0.000	-2.500
2.093	3.826	-1.643	-0.089	0.000	-2.000
3.456	5.886	-2.361	-0.069	-0.000	-1.800
5.833	9.309	-3.428	-0.048	-0.000	-1.600
10.099	15.078	-4.952	-0.026	-0.000	-1.400
17.266	23.927	-6.654	-0.008	-0.000	-1.200
-0.003	-0.004	0.001	-0.000	-0.000	-1.000
-0.000	-0.001	0.000	-0.000	0.000	-0.800
0.000	-0.000	0.000	0.000	0.000	-0.600
0.001	-0.000	0.000	0.000	0.001	-0.400
-0.004	0.000	-0.000	-0.001	-0.004	-0.200

PDS $\rightarrow F_1$ Re; $S_0 \rightarrow F_1$ Re; $S_2 \rightarrow F_1$ Re; $P_1 \rightarrow F_1$ Re; $D_0 \rightarrow F_1$ Re

Total and Brea. down Im $C(\gamma) \rightarrow F_1$

ALL	S_0	S_2	P_1	D_0	γ
0.460	0.013	-0.006	0.453	-0.000	-11.000
0.453	0.014	-0.006	0.445	-0.000	-10.500
0.419	0.014	-0.006	0.411	-0.000	-10.000
0.356	0.015	-0.007	0.348	-0.000	-9.500
0.267	0.016	-0.007	0.258	-0.000	-9.000
0.162	0.017	-0.007	0.152	-0.000	-8.500
0.060	0.017	-0.007	0.050	-0.000	-8.000
-0.010	0.018	-0.007	-0.021	-0.000	-7.500
-0.032	0.018	-0.007	-0.044	-0.000	-7.000
-0.022	0.018	-0.006	-0.034	-0.000	-6.500
-0.006	0.018	-0.006	-0.018	-0.000	-6.000
0.004	0.017	-0.005	-0.008	-0.000	-5.500
0.008	0.015	-0.004	-0.003	-0.000	-5.000
0.009	0.012	-0.002	-0.001	-0.000	-4.500
0.007	0.007	-0.000	0.000	-0.000	-4.000
0.003	0.001	0.002	0.000	-0.000	-3.500
-0.003	-0.007	0.004	0.000	-0.000	-3.000
-0.010	-0.016	0.006	0.000	-0.000	-2.500
-0.014	-0.019	0.005	-0.000	-0.000	-2.000
-0.013	-0.016	0.004	-0.000	0.000	-1.800
-0.008	-0.009	0.001	-0.000	0.000	-1.600
0.001	0.003	-0.002	-0.000	0.000	-1.400
0.009	0.012	-0.003	-0.000	0.000	-1.200
0.000	0.000	0.000	0.000	0.000	-1.000
0.000	0.000	0.000	0.000	0.000	-0.800
0.000	0.000	0.000	0.000	0.000	-0.600
0.000	0.000	0.000	0.000	0.000	-0.400
0.000	0.000	0.000	0.000	0.000	-0.200

PDS $\rightarrow F_1$ Im; $S_0 \rightarrow F_1$ Im; $S_2 \rightarrow F_1$ Im; $P_1 \rightarrow F_1$ Im; $D_0 \rightarrow F_1$ Im

Table 2-1-d. $C(\gamma)$ for F_1 meson.

It is difficult to give any conclusive statement about the rate of convergence of $C(\nu)$ as more waves are added in the crossed channel. We note that the effect of the D_0 wave is small on the near left, say in $[-5, 0]$, but this may be due to the particular experimental values for the D_0 wave. We do not know if the values of other waves like F_1 will be large. In Figs. 10, we give graphs of contributions to $C(\nu)$ if resonances were present in various waves. To do this we used a Breit Wigner form with correct threshold behaviour in each wave, and took position and width the same as the ρ. The result is to give a bump in $C(\nu)$ near $-\nu_\rho - 1$ with more rapid fall-off towards the right for higher ℓ' waves.

We conclude that if the experimental values used give a good representation of the amplitude in the low energy physical region of the crossed channel up to say $\nu = 7$, then we obtain a reasonably reliable value of $C(\nu)$ out to $= -7$. To get a reliable value out to -8, we might well need a great deal more information.

The accuracy of numerical integration was checked to 10^{-4} by using a variable accuracy routine Q4021. Setting the accuracy to 10^{-4} gave values identical to those used in the fixed accuracy routine. Only 4 significant figs. were checked. Use of a variable accuracy routine takes at least twice as long as a fixed accuracy one. The routine doubles the number of integration points until successive evaluations give answers agreeing to the desired accuracy. Hence it saves a lot of time to first of all find out how many points will give the desired accuracy and then to stick to this number. Further, when the integrand is a function of another variable and when we want the value of integral over a range of values of this variable, it is most important to store the values of the integrand at the integration points and to store the values of the kernel; this saves time by a factor of 20 or so. Such a procedure is more difficult using a variable accuracy integration routine.

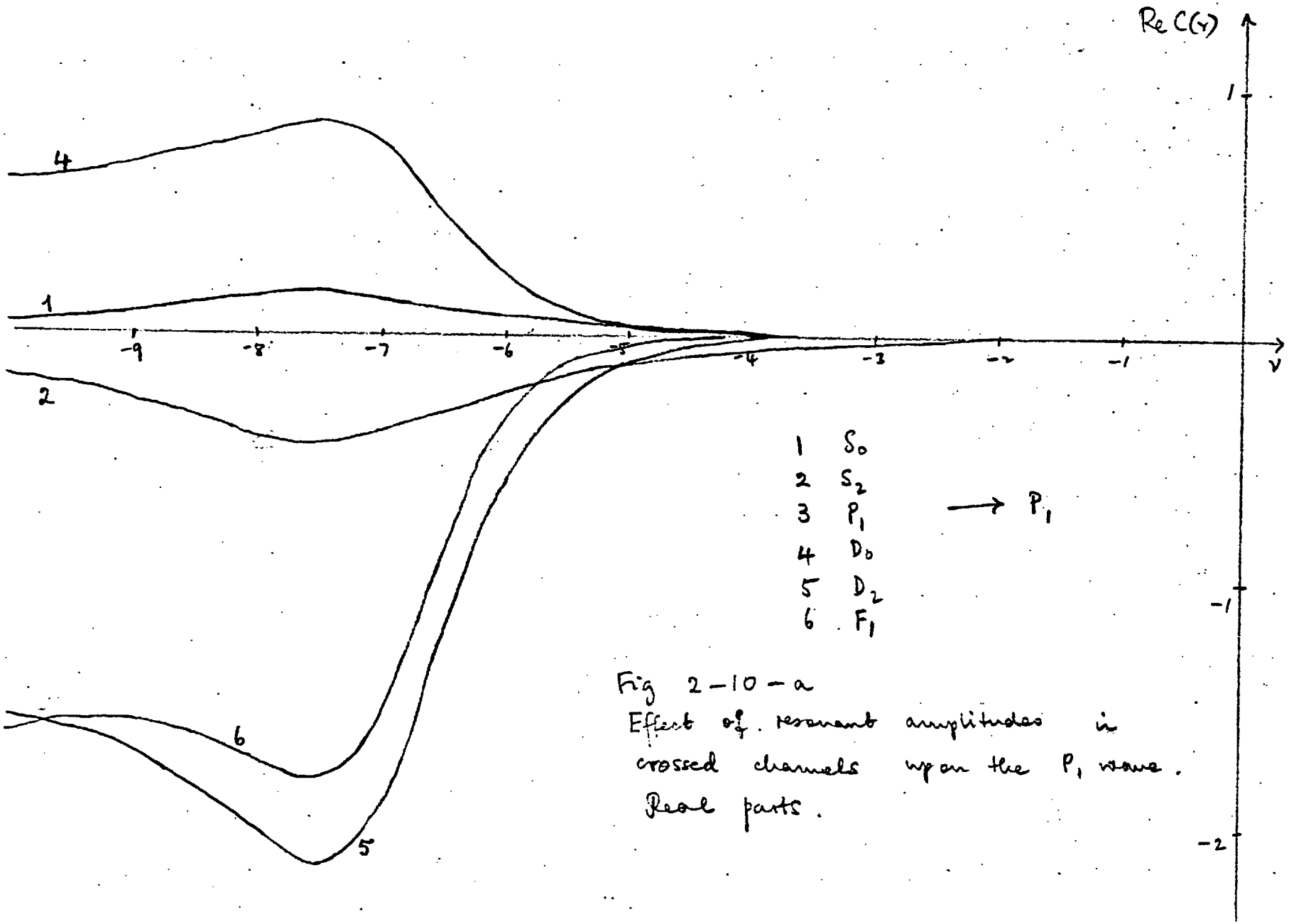

1 S_0
2 S_2
3 P_1 → P_1
4 D_0
5 D_2
6 F_1

Fig 2-10-a
Effect of resonant amplitudes in crossed channels upon the P_1 wave.
Real parts.

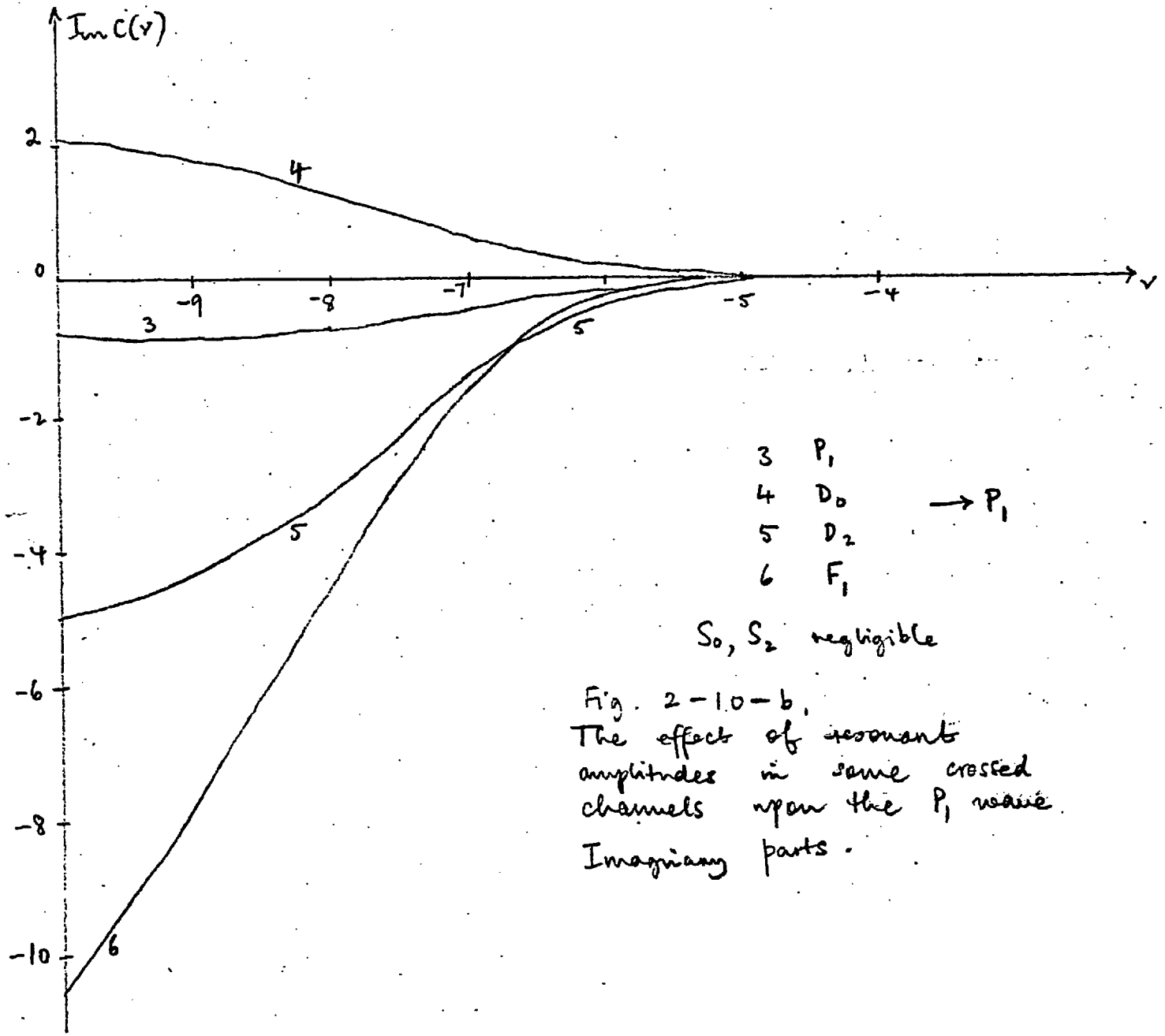

3 P_1
4 D_0 → P_1
5 D_2
6 F_1

S_0, S_2 negligible

Fig. 2-10-b.
The effect of resonant amplitudes in some crossed channels upon the P_1 wave Imaginary parts.

THE δ FUNCTION APPROXIMATION

If $\mathrm{Im}A_{\ell'}(\nu')$ is dominated by a sharp resonance, then one can make the approximation

$$\mathrm{Im}A_{\ell}(\nu') = \pi . \Gamma_{\ell} \delta(\nu' - \nu_R)$$

where Γ_{ℓ} is the half-width. This is shown in the Breit Wigner case in Section III.

Fig. 11 compares the $C(\nu)$ function evaluated by numerical integration with the $C(\nu)$ function obtained by approximating with a δ function. In the latter case, the cut starts at $-\nu_R - 1$, the discontinuity having a finite value at the end of the cut and the real part having an infinity. We can regard the more exact $C(\nu)$ as a smoothed out version of this. It does emphasise the correspondence between structure at ν', in the crossed channel, and at $-\nu' - 1$, in the direct channel.

CONTRIBUTIONS FROM THE HIGH t REGION

In truncating the partial wave expansion, we have neglected higher waves, which are important in the diffraction peak at high t. Also, making a δ function approximation to $\mathrm{Im}A$ has the effect of neglecting high t contributions.

Two ways of accounting for these contributions have been suggested by Singh and Udgaonkar (5) and Balazs (BV) (4).

Singh and Udgaonkar found that these contributions were important in the πN problem and Balazs found that a calculation putting in estimates for both inelasticity and high t contributions, moved the self consistent value, found by his bootstrap method, for the ρ, from 585 Mev to 712 Mev. The present author does not consider either of these calculations to be very reliable, but his numerical studies of the $C(\nu)$ integral bring him to the following attitude.

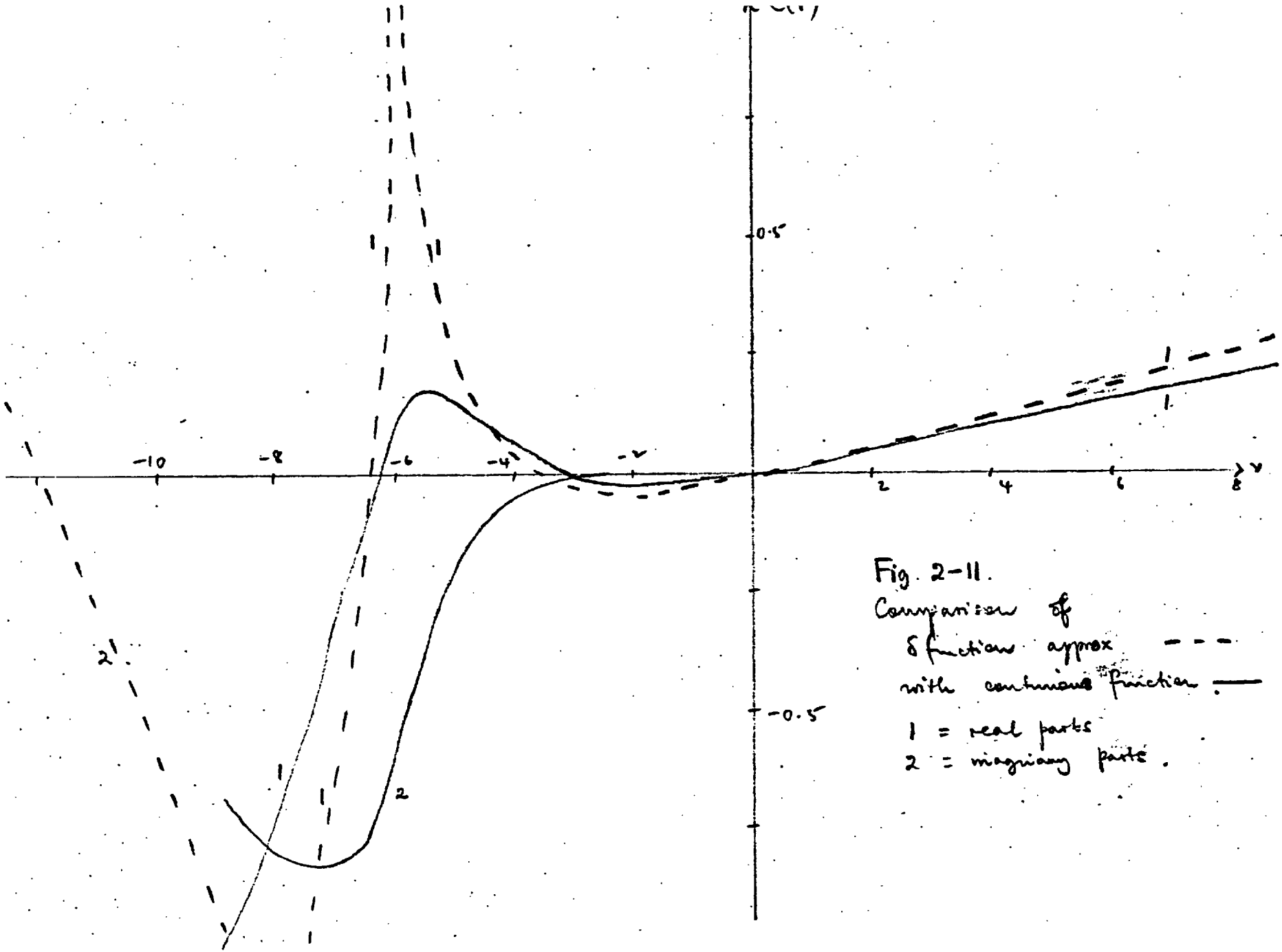

Fig. 2-11.
Comparison of
δ function approx - - -
with continuous function ——
1 = real parts
2 = imaginary parts.

Since the integral converges (for $\ell \geq 1$) the very high energy region can only make a small contribution and so truncating the partial wave series will not make much difference. The author has evaluated the integrals numerically, for a small number of partial waves and found only a small change on removing a cut-off from $\nu' = 10$ to $\nu' = 30$. Now, as we approach the diffraction peak, i.e. $\nu \longrightarrow -1$, the integral gets less convergent until it only just (logarithmically) converges. So the very high region starts higher, and one may get contributions from higher waves in the intermediate region. In this case, one may well get contributions from high t, but we expect this only in the near left region of the s channel say ν in $[0, -2]$.

ESTIMATION OF THE CONTRIBUTION TO $C(\nu)$ FROM THE HIGH t' REGION

As we wish to include a small number of waves at low t', and the diffraction peak at high t', which involves many partial waves, one simple suggestion is to use a truncated partial wave series for $A_t(s, t')$ in the low t' part of the integral for $C(\nu)$, $A_t(s, t') = \sum_{\ell'=0}^{L} A_{\ell'}(t') P_{\ell'}(\cos\theta')$, and use an explicit diffraction peak for $A_t(s, t')$ at high t'. $A_t(s, t') =$ exp. law (s, t'), $t' > T$. As there are no experimental values for the diffraction peak, we could take the width arbitrarily as 1 Bev. We did not carry out this calculation.

REGGEIZED PROJECTION

Projection into physical and partial waves

For a single Regge pole

$$A(s,t') = \frac{(2\alpha_i(t') + 1) \cdot \gamma_i(t')}{\sin[\pi \alpha_i(t')]} \cdot P_{\alpha_i(t')}\left[1 + \frac{2s}{t'-4}\right] \qquad (1)$$

contains both real and imaginary parts. For real fixed t', it is cut in s from $s = 4 \longrightarrow \infty$
$s = 4 - t' \longrightarrow -\infty$
and as $s \longrightarrow \infty$ $\quad A(s, t') \longrightarrow s^{\alpha(t')}$

If we project into a partial wave in the t channel

$$A_\ell(t') \sim \gamma_i(t') / (\ell - \alpha_i(t'))$$

If project into s channel, get

$$A_\ell(s) = \frac{4}{\pi\nu}\int_4^\infty dt'.\ P_\ell\left[1+\frac{2t'}{s-4}\right]\cdot\frac{[2\alpha_i(t')+1]}{\sin[\pi\alpha_i(t')]}\cdot\gamma_i(t')\cdot P_{\alpha_i(t')}\left[1+\frac{2s}{t'-4}\right]$$

and for real and imaginary parts, need to disentangle from A.

For asymptotic behaviour

$$A_\ell(s)\underset{s\to\infty}{\longrightarrow}\frac{4}{\pi\nu}\int_4^\infty dt'.\ P_\ell\left[1+\frac{2t'}{s-4}\right]\cdot\frac{[2\alpha_i(t')+1]}{\sin[\pi\alpha_i(t')]}\cdot\gamma_i(t')\cdot\left[1+\frac{2s}{t'-4}\right]^{\alpha_i(t')}$$

If one now wants to continue to unphysical ℓ., Gribor's suggestion of

$$\mathcal{A}_\alpha(s) = \frac{4}{\pi\nu}\int_4^\infty dt'.\ Q_\alpha\left[1+\frac{2t'}{s-4}\right]\cdot A_t(\nu',\nu).$$

is used, and this gives an alternative form, since $A_t(\nu',\nu)$ will be the imaginary part of (1).

II. AN ATTITUDE TO BOOTSTRAP CALCULATIONS

In Chapter 1 we discussed the concepts of elementarity and compositeness. We want, in this section, to discuss bootstrap calculations in dispersion theory, in which mathematical description of scattering processes involving elementary and composite systems is attemptod.

We want to discuss some principles of practical bootstrap calculations, insofar as they have emerged in our work.

Dispersion theory is often called a model independent theory. Also its microscopic interpretation is unclear. The effect of elementarity and compositeness upon the description by dispersion theory is found in the number of arbitrary parameters assumed, which affects both the formulation of the specific equations for the system considered and the procedure for approximate calculation.

The number of arbitrary parameters is directly related to the number of elementary particles. If there are arbitrary parameters in the theory then

they can be determined by experiment. However, a perfectly good mathematical solution of the equations exists for a range of values of the parameters, just as quantum electrodynamics has solutions for a range of values of e , the charge on the electron.

One does not know how many arbitrary parameters there will be. However, having written down the equations to be solved, the number of solutions is fixed and cannot be made the subject of a further assumption. If there is inelasticity then one had better take this as given. Thus either there are no solutions, 1 solution, 2, . . .,27,etc., an infinite number parametrised by 1 parameter, 2 . . . It has even been suggested that there will be an infinite number of parameters (arising from asymptotic exponential behaviour and the infinite number of subtractions required), by C. Lovelace (7). Field theory suggests that, in the $K\pi$ case, there will be one parameter, corresponding to the λ in the $\lambda \varphi^n$ interaction. This assumption was common in the literature in 1960, but now several dispersion theorists conjecture there will be no parameters and, further, that there will be 1 solution only. In the whole of strong interactions i.e. the infinite number of coupled integral equations, field theory possibly suggests three parameters at least; again, dispersion theorists have suggested one solution only.

Discussions on the number of arbitrary parameters have been given by Taylor and Truong and by Capps.

We wish to argue here that, not only is the number of parameters determined by the exact equations, it is also possible to discover the existence of these parameters and identify them in approximate calculations. This attitude has arisen as a result of education by Dr. R. F. Streater. We must first however discuss our numerical philosophy and the implications of making numerical approximations.

NUMERICAL PHILOSOPHY

The value of a function is very rarely given in closed form, but usually in a series which has a calculable maximum error. One takes sufficient terms to ensure the desired accuracy. In a chain of calculations, one must take sufficient accuracy at each stage to ensure the desired accuracy at the final stage. In a long calculation on a computer, the arithmetic and storage is carried out to 38 significant figures, however the final answer is usually only reliable to 10 significant figures. This rounding accuracy is very much better than other sources of inaccuracy. An integral usually has to be evaluated numerically and may only be accurate to 4 significant figures and it is important to check the errors on such steps

In the numerical solution of very difficult sets of equations such as M. R. + U, one is faced with the task of representing the analytic expressions in a numerical form, which usually means replacing integrals by sums and operators by matrices. One may choose an iterative method, not using a trial function but using values on a set of points, or one may decide to use a trial function as a basic part of the calculation, so one has gone further and assumed that the values on the sets of points can be replaced by a knowledge of some small number of parameters and a suitable parametric function. Parametrisation is discussed later in this chapter. To determine whether two functions are equal in a region, one can use a χ^2 test or some other criterion like max $|f_1 - f_2|$ over the interval. To demand an equation be satisfied can also be achieved in this way. In demanding two functions be equal, one should find that increasing the number of sampling points causes the fit to settle down to a steady value. The density of points at which this occurs depends upon the smoothness of the curves. When this has been achieved there is no reason to take any more sampling points, in fact to take more would be bad since it would increase computing time. We would thus have

"saturated" the constraint. A similar effect should occur with the number of parameters. When the number is too low so that the parametric functions are not sufficiently "flexible", then either no solutions or spurious effects will occur. On increasing the number of parameters one should reach a point at which adding one more parameter makes very little difference to the values obtained. Too many parameters are a bad thing, since, not only do they increase computing time and space, they can lead to spurious effects.

To decide whether two differently parametrised functions are sufficiently equal in value, as to be taken as representing the state of exact equality in the analytic solution is difficult. Too stringent a criterion can lead to no solutions being accepted. Largely by subjective means, one has to arrive at values in the χ^2 which will be acceptable for the fit of two functions together, or an equation to be satisfied. Also one must derive from this an idea of a "significant" change in the function as the parameters vary.

It is a fundamental tenet of numerical work that the approximate numerical forms and conditions can be made close enough as to give solutions which are close to the exact solutions. To test whether we may be close to the exact solution, we make sure our parametrisation is sufficiently flexible and that our constraints are saturated, so that our solution has settled down. There is then reason to suppose that our solution is close to the exact solution, a condition one might term "meaningful". If this is not the case, then our solution may be far from the exact solution, it may even be unrelated and its origin due to an overlooked effect.

ILL-DETERMINED PARAMETERS

In an approximate calculation, the existence of free parameters will be revealed by the occurrence of ill-determined parameters. What interpretation must one put on finding that a self-consistent solution (within pre-

arranged numerical smallness criterion) exists for a range of values of one of the parameters (or in general some function of the parameters chosen for the calculation i.e. some [l] connected region in [n] parameter space)? We will sometimes find a very flat minimum, but, because of approximations, never an exactly flat curve. The parameter along the curve is thus "ill-determined". A more easily detected effect will be that this parameter, determined as the minimum point of the shallow valley, will be very sensitive to the approximation procedure, for the latter determines the slight slope of the valley.

Two cases can arise, either

(i) The solution varies very little as the parameter varies; or

(ii) The solution varies significantly.

Case (i) will be called "extra", (ii) "arbitrary". One again needs some numerical criterion for the concept "significant". Case (i) will arise when the parameter, call it ϵ, is an extra trimming parameter relating to the detailed form of the solution, but ill-determined because the constraints cannot fix it well, the approximation is just too rough to allow its determination. One might think of some parameter in a weakly coupled channel. Case (ii) will arise when the parameter, call it λ, is a truly mathematically arbitrary parameter so that a solution exists for a range of λ and the solutions from a family labelled by λ. For example, if one solves the Schrodinger Equation with potential $\frac{e^{-\mu r}}{r}$, then μ is truly arbitrary. A solution exists for a range of μ and the solutions for different μ are different. If one did a numerical approximation and tried to include as a parameter it would be ill-determined. Similarly if λ is an arbitrary parameter for the $\pi\pi$ system then a solution will exist for a range of λ. λ cannot be determined mathematically; it is a universal constant and must be determined experimentally. As we increase the accuracy of the approximation, we expect the shallow valley to become flatter, but eventually we will

have "saturated" the constraints. One can then meaningfully go ahead and locate "extra" and "arbitrary" parameters and produce a family of solutions labelled by the arbitrary parameters and can discard the extra parameters.

Of course, if one finds that one of the a priori important parameters is "extra", one concludes that one is doing a bad calculation.

To locate the ill-determined parameters, a good method is to obtain a plot of χ^2 in [n] space. Then if $\chi^2 = 0$ on a surface

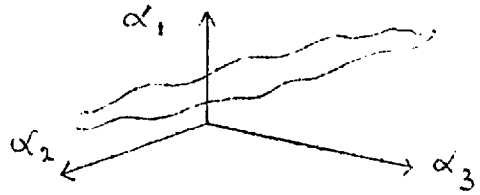

Then a self consistent solution is obtained for all $\{\alpha_i\}$ s.t.

$$f(\{\alpha_i\}) = 0$$

Let us now take new parameters $\{\beta_i\}$ s.t. β_1 and β_2, for a particular set $\{\beta_3, \ldots\}$, are coordinates in the surface. Then β_1 and β_2 are the ill-determined parameters and $\{\beta_3, \ldots\}$ are determined. So, in general,

$$\beta_1 = \beta_1(\{\alpha_i\})$$
$$\beta_2 = \beta_2(\{\alpha_i\})$$

we can test whether they are arbitrary or free by looking at the solution, i.e. functions at different points on the surface. Of course, we may have to take further coords.

$$\gamma_1 = \gamma_1(\beta_1, \beta_2)$$
$$\gamma_2 = \gamma_2(\beta_1, \beta_2)$$

if one is arbitrary and the other free. We may want to do this anyway, since we may feel that the family of solutions, at constant γ_2, are, in some sense, similar, i.e. we may want to take a "natural" parametrisation.

One ill-determined parameter defines a line in [n] space i.e. [1] manifold.

The next thing to observe is that we may not be acknowledging the

existence of an arbitrary parameter and for example neglecting an influential term. In this case even if we find that all the parameters we have taken are well-determined we may be in error in declaring that there are no arbitrary parameters. Our calculation may be only finding the particular member of the family with that unconsciously assumed value of label. This may still be valuable however. To eliminate this effect we must examine the neglected terms , make sure they are small and that varying them does not vary the self-consistent solution significantly.

APPROXIMATION THEORY

Walsh (8) gives an account of the approximation of functions in the complex domain. The possibility of approximation of any analytic function by a polynomial or rational function is discussed and the existence of best approximations proved. The criteria of minimal $\left(\underset{z \in R}{\text{maximum}} \left| f_{app}(z) - f_{exact}(z) \right|\right)$,

of $\text{min.} \left(\int_R dS \left| \Delta f(z) \right|^p \right), \quad p > 0$

of $\text{min.}\left(\underset{z \in C}{\text{max.}} \left| \Delta f(z) \right|\right)$ (using max. modulus theorem),

and of $\text{min.} \left(\int_C |dz| \left| \Delta f(z) \right|^p \right) \quad p > 0$

lead to similar results. However, no idea of how good an approximation to n terms is going to be, or how to choose a method of approximation are given. Some useful ideas are given. In making a rational function approximation, one can choose the poles arbitrarily and then obtain a best approximation, given their positions. The region of analyticity used is related to which set of polynomials one might naturally choose for approximation purposes.

This is in contrast to the work of Baker and others on Padé approximants, who makes intuitive guesses as to regions of convergence and best ways of approximating. No other sets of functions for approximation are ever treated, other than polynomials and rational functions.

PADÉ APPROXIMANTS

The Padé approximant method (9) is a most promising way of obtaining a good rational function approximation for which the asymptotic behaviour can be specified. The approximation puts poles over the singularities of the given function and, because of its invariance under conformal transformations, probably converges in most of the analytically connected regions of the function. Baker has proved a few results and conjectured others, see also Chisholm (10) who is attempting rigorous proof of convergence of the approximation in the domain of meromorphy.

A truncated Padé approximation will have poles near and round the singularities of the exact function, but also it will sometimes have isolated "spurious poles" unrelated to the exact singularities. These spurious poles eventually disappear and are always accompanied by a nearby zero. Chisholm has conjectured that the total number of poles of the approximant, in a region of meromorphy, remains finite as $N \longrightarrow \infty$.

The convergence of the certain series of Padé approximation in the case of functions with a series of Stieltjes has been known by Baker and applied to fixed s dispersion relations, since the absorptive part is always positive. Two convergent sequences of Padé approximants to $\sim A(s, t)$ were found which were bounded by the exact function above and below respectively

$$[N, N-1] \leq A(s, t) \leq [N, N] .$$

Other applications to scattering problems have been made by other authors (11) but usually to non relativistic problems.

THE APPROXIMATION OF CUTS BY SEQUENCE OF POLES

Thus, the work of Walsh shows the possibility of approximation and the Padé method gives a way of obtaining the approximate function, given a power series for the exact function, about some point. To obtain a unitary function, it is better to approximate only the left hand cut by poles and this can be

done by a pole approximation to the N function. In practice, one does not have an accurate enough power series to use the Padé method. Balazs used an auxiliary method to determine the positions of the poles and got the residues from the power series. Other authors have determined the positions and residues by overall crossing and self consistency requirements.

Bander (12) has described an N/D pole method which iterates, adding an extra pole to the left hand cut each time.

Pole approximations to the right hand cut, when inelasticity is present, have been used by Gammel and McDonald (loc. cit.) in low energy n - d scattering and by Bransden, Moorhouse and O'Donnell in their inverse amplitude parametrisations for phase shift analysis of high energy π - N scattering.

ANALYTICAL CONTINUATION USING NUMERICAL METHODS

The problem of numerical continuation is fraught with difficulties. We have the phenomenon of over convergence of subsets of power series, also the theorem that an analytic function whose values are given on a finite set of points can be made to have any value whatsoever at any other given point.

If one tries to continue using power series one is up against the "re-arrangement problem." For suppose one has a power series about the origin and one tries to continue by expanding about another point and using values from a truncated version of the first series. Then one is merely rearranging the series and the values of the two series are equal everywhere and will diverge together on the same boundary. Lewis (13) has developed a way of getting round this problem using suitably chosen subseries and gives numerical tests of his work. The Padé approximant is probably the best method of continuation and gives convergent series of rational functions.

Another way is to conformally map the region until the two points it is desired to continue between lie within a circle within which a power series can be used. Viewed in the original plane this is a rigorously convergent procedure

of expansion in terms of nonrational functions. In practice, one truncates the series and then has the problem of estimating the error involved.

MATCHING

In order to demand two functions be equal in a region, sometimes matching criteria are used, that is the two functions are demanded equal on a (finite) set of points. Sometimes their derivatives are used as well. This was used by Chew-Mandelstam and by Balazs and is certainly a source of error in their calculations as will be seen in Chapter 3.

Balachandran (14) has considered the effect of constraints on the partial wave amplitude in the form of specification of its values on a finite set of points. He derived a class of inequalities which are necessary conditions for the existence of such an amplitude. Further work (15) uses the method of moments. However, matching is another name for interpolation and is quite respectable if used properly. The excellent book of Walsh (8) gives a rigorous presentation. The present author would like to paraphrase Theorem 2. of Chapter 9. "The rational function, with preassigned poles at $\{\alpha_n\}$, which is the best approximation, to a function $f(z)$, analytic within and on the unit circle C, in the sense of least squares on C, is obtained uniquely by interpolation to f(z) in the points $\{0, \{1/\bar{\alpha}_n\}\}$."

REMARKS ON PROCEDURE FOR JUSTIFICATION OF AN APPROXIMATION

(a) look at as many types of consequence as possible, forward and backward in the calculation;

(b) get perspective amongst other approximations by looking at them and their consequences;

(c) look at effect of increasing accuracy of the approximation compared to estimates of accuracy;

(d) where successive approximations vary accuracies independently and note relative effects, vary dependently and note interaction.

BOOTSTRAP CALCULATIONS

We approach the problem of the solution of M R + U as one of continuation from the t channel to the s channel consistent with the singularity structure implied by M.R. and subject to a unitarity condition. One first chooses a way of obtaining a set of coupled integral equations for the partial wave amplitudes from the Mandelstam representation. The methods of

(i) Chew and Mandelstam

(ii) Shirkov

each introduce a different type of approximation with different physical content. The exact forms are intractable and one then chooses a way of obtaining a unitary amplitude satisfying the equations as well as possible. One large class of methods can be described as follows:-

1. Choose certain partial waves and neglect the others as a first assumption.
2. Choose trial functions and starting values of parameters for amplitudes in crossed channel $\{A_{\ell'}(\nu')\}$. If possible, automatically unitary.
3. By crossing or an intersecting dispersion relation obtain information about left hand side of s channel (this only uses $\mathrm{Im}A_{\ell'}(\nu')$).
4. By some technique, continue (or extrapolate) to right hand side, consistent with unitarity.
5. Compare in some way the "output" function obtained with the input, quantified by the evaluation of a discrepancy function χ^2.
6. Vary parameters to obtain minimal χ^2, giving self consistency in an approximate sense.

A reasonable assumption for selection of channels is to assume resonant channels will be most important, just simply because $\mathrm{Im}A_{\ell'}(\nu')$ is so much larger and affects the dispersion relation more. This may not be a correct assumption due to the subtleties of the influence of left on right.

Different ℓ' will have different kinematic factors, $\nu'^{\ell'}$, which will tend to push the large part of the reflected amplitude out to the further left for higher ℓ'. The steep rise of the s waves on the near left may make them important even though this effect does not depend upon the existence of

resonances in the s wave. This is found using inverse amplitude methods. One can check finally the assumption by taking the self consistent amplitudes and working out the values of the neglected amplitudes i.e. take the chosen ones in the crossed channel, go through the continuation to the direct channels, for the neglected channels. If any of these is large, then one will have discovered an inconsistency. One can do a further test by putting a large neglected channel together with the chosen ones in the crossed channel and again calculating all channels. If there is a significant change, then one had better repeat with this channel included.

THE IDEA OF AUTOMATIC BOOTSTRAP CONSTRAINT

In the variational method, discussed in Chapter 5, the input and output amplitudes are automatically always equal and the parameters are determined by demanding unitarity be satisfied. Of course, we don't gain anything by this, we merely move the uncertainty to another part of the calculation.

INTUITIVE APPROACH TO SINGULARITIES AND ANALYTICITY

In trying to develop intuition in dispersion theory, we run up certain difficult ideas such as the fact that the values of an analytic function everywhere in a connected analytic region is determined by its values on any finite region (in fact on any set with a limit point in a region of analyticity). We should however like to develop some idea of the behaviour of a function due to its singularities, in view of such ideas as force cuts. A simple pole has an easily graspable effect and higher order poles have similar effects.

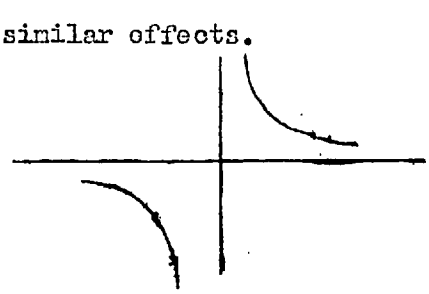

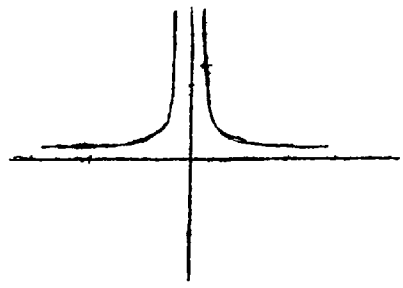

Two common types of branch cut are the surd branch cut exeemplified by $\sqrt{z}$ and the logarithmic branch cut as in log z. At the surd branch point the value is finite for positive powers and there is a discontinuous derivative of some order and as the power increases the curve gets more smooth. $\sqrt{z}$ has a first order cusp at z = o. log z has an infinity at its branch point and a finite imaginary part up to the branch point.

The relation between the real and imaginary parts for a function satisfying a dispersion relation is fairly predictable. A bump in the imaginary part will cause the real part to tend to change sign giving the normal resonance form; and vice versa. The effect of a singularity dies away

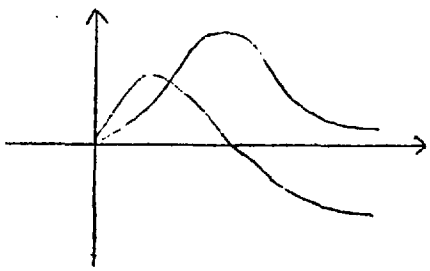

as we get further away due to the damping effect of the cauchy denominator. However if there are significant singularities out to infinity, such as for marginally singular forces where the singularity strength remains constant to infinity and the real part goes logarithmically in all directions, the nearby singularity idea can be invalid. In this case, the distant singularities dominate and there is not the same falling off in effect as we retreat from the cut, indeed in the marginally singular case discussed, the function increases as we retreat from the cut.

Asymptotic behaviour and its importance are difficult to grasp Indeed, in applying intuition, we are trying to establish local "causal" relations between singularities and behaviour of the value of the function, in situations where large scale and overall factors like asymptotic behaviour can be the real key to understanding.

Cancellation by oscillation is another effect. If we want a fast polynomial fall-off at the edge of a cut, the discontinuity must change sign the same number of times as the value of the power of fall-off. For

exponential fall-off we need a periodic function.

The effect of unitarity usually seems to be to turn the function towards the real axis. Thus given a rising $B(\nu)$, solving by unitarity will give an $A(\nu)$, which turns towards the axis compared to $B(\nu)$, see Figs. in Chapter 3.

The effect of the rescattering cut in a resonant situation will be large, on the physical cut, compared to the contribution from the force cut. Thus, as found in Chapter 5, and as discussed in Chapter 7, this makes it difficult to determine the left hand singularities, given the real and imaginary parts on the right hand cut.

When we consider the inverse amplitude as in Chapter 6, our intuition gets a jolt. For, regions that were important are no longer and asymptotic behaviour that was important is not, and vice versa.

CLASSIFICATION OF METHODS

(1) Given the left hand imaginary part we can either use:

(a) N/D which is usually singular	(Ch. 3)
(b) The variational method	(Oades and Ch.5)
(c) Bransden & Moffat iteration procedure for inverse amplitude	(Bransden & Moffat)

(2) Given real part on left:

Balazs	(Balazs and Ch.3)

(3) Given real and imaginary parts on left:

(a) N/D in constraint on left, e.g. generalised Balazs	(Ch. 5)
(b) Variational method and constraint on left	(Ch. 5)
(c) My inverse amplitude method	(Ch. 6)

(4) Given the force function $B(\nu)$:

(a) Uretsky or F W. – N/D, no solution for some types of $B(\nu)$	(Morgan etal discussed in Ch. 1)
(b) Variational method	(Ch. 5)

(c) Zachariasen method N = B (Zachariasen and Ch. 4)

(5) Given inverse amplitude force function $B^{-1}(\nu)$:

My inverse amplitude method (Ch. 6)

To obtain the left hand information, one either uses:

(1) continuation of absorptive part by partial wave series,

(2) (3) (4) (5) either from fixed s dispersal or the δ function form of this, from a pole term in field theory,

or use

Regge formula or modified Regge representations.

METHODS GIVEN THE IMAGINARY PART ON THE NEAR LEFT

One must assume that nearby singularities dominate the amplitude. One either cuts off the far left contribution or one can represent the far left by a pole form and hopefully determine the extra pole parameters by either criteria e.g. self-consistency or unitarity. To obtain a unitarity amplitude one can use N/D which is of Fredholm type, since one has cut off and has a unique solution apart from CDD poles, See Chapter 3. Or one can use the variational method following Oades, See Ch. 5. Or one can use Moffat's iteration procedure in an inverse amplitude formulation, See Chapter 6.

GIVEN THE REAL PART ON THE NEAR LEFT

One can use the Balazs method of choosing a parametrisation and determining the parameters by the requirement of correct real part on the left and self-consistency.

GIVEN REAL AND IMAGINARY PARTS ON THE NEAR LEFT

One has the previous methods with an additional crossing constraint, See Chapters 3, 5. Also a different inverse amplitude method, See Chapter 6.

GIVEN THE "FORCE FUNCTION" $B(\nu)$

One can use the Zachariasen (determinantal) method (Chapter 4). Or a variational method. However, as discussed in Chapter 1, the Uretsky N/D

formulation can be solved exactly for reasonable asymptotic behaviours.

The asymptotic part of the solution in the logarithmic (marginally singular) case have been expressed by Atkinson and Contogouris and the rest of the solution obeys a Fredholm equation.

GIVEN THE INVERSE AMPLITUDE FORCE FUNCTION $B^{-1}(\nu)$

One can then write down the solution

$$A^{-1}(\nu) = \frac{(\nu-\nu_0)}{\pi} \cdot I(\nu,\nu_0) + [B^{-1}(\nu) - B^{-1}(\nu_0)] + A^{-1}(\nu_0)$$

where I, the right hand cut contribution, is known in closed form in the elastic case.

THE USE OF THE REAL PART ON THE LEFT

How the real part on left helps to estimate the far left

$$\mathrm{Re}\, A(\nu) = \int_{-\infty}^{-1} \frac{\mathrm{Im}A(\nu')}{\nu'-\nu} d\nu' + \int_{0}^{\infty} \frac{\mathrm{Im}A(\nu')}{\nu'-\nu} d\nu' \qquad \text{(i)}$$

possibly subtracted

From data we obtain estimates for $\mathrm{Im}A(\nu')$ in $[0,\infty]$ and using crossing we obtain estimates for $\mathrm{Im}A(\nu')$ in $[-1,-9]$ and for $\mathrm{Re}A(\nu)$ in $[0,-9]$ then we want to estimate the far left force function

$$B'(\nu) = \int_{-\infty}^{-9} \frac{\mathrm{Im}A(\nu')}{\nu'-\nu} d\nu' \qquad \text{(ii)}$$

we have an estimate for $B'(\nu)$ in $[0,-9]$ using the real part for

$$\mathrm{Re}\, A(\nu) - \int_{-9}^{-1} \frac{\mathrm{Im}A(\nu')}{\nu'-\nu} d\nu' - \int_{0}^{\infty} \frac{\mathrm{Im}A(\nu')}{\nu'-\nu} d\nu' = B'(\nu) \qquad \text{(iii)}$$

$\nu \in [0,-9]$

and if we also assume the analytic properties implied by (ii) we can try to estimate the value of $B'(\nu)$ in $[0,\infty]$. More realistically, we should only estimate a finite part of the right hand cut up to cut off Λ, and include the rest in $B'(\nu)$ so

$$B'(\nu) = \int_{-\infty}^{-9} \frac{\mathrm{Im}A(\nu')}{\nu'-\nu} d\nu' + \int_{\Lambda}^{\infty} \frac{\mathrm{Im}A(\nu')}{\nu'-\nu} d\nu' \qquad \text{(iv)}$$

$$\mathrm{Re}\, A(\nu) - \int_{-9}^{-1} - \int_{0}^{\Lambda} = B'(\nu) \qquad \text{(v)}$$

A reasonable estimate for $B'(\nu)$ would be a pole form (vi)

$$B'(\nu) = \sum_{i=1}^{n} \frac{F_i}{\nu-\nu_i}$$

where the ν_i are in $[-9, -\infty]$, $[\Lambda, \infty]$.

We only wish to know $B'(\nu)$ in the near region from a practical point of view.

This procedure is carried out in the Balazs method, which obtains the F^i by demanding (V) be exactly true at n points in $[-1, -9]$ and using the F^i uniquely obtained to substitute in (vi) as an estimate for $B'(\nu)$ in $[0,10]$. To get an idea of $B'(\nu)$, we can take $\mathrm{Re}A(\nu) = \mathrm{Re}C(\nu)$, $\mathrm{Im}A(\nu) = \mathrm{Im}C$ in $[-1,-9]$.

so $$B'(\nu) = \mathrm{Re}\, C(\nu) - \int_0^{\Lambda} \frac{\mathrm{Im}\, A(\nu')\, d\nu'}{\nu' - \nu}$$

This form has wrong analytic structure of course.

UNFEASIBLE METHODS USING THE REAL PART

1. Analytic continuation using unitary functions

Obtain $A_\ell(\nu)$ ν in $[0, -9]$

Introduce sequence of unitary functions $\mathcal{F}_\ell^n(\nu)$ and interpolate

$$\mathcal{F}_\ell^n(\nu_i) = A_\ell(\nu_i) \qquad i = 1, \cdots n.$$

on a set of points

Let $n \to \infty$ and let the set $\{\nu_i\}$ have a limit point interior to the region of analyticity. Then if $\mathcal{F}_\ell^n(\nu) \xrightarrow[\lim n \to \infty]{} \mathcal{F}_\ell(\nu)$ uniformly in a region of ν, it is the continuation of $A_\ell(\nu)$.

2. Conformal mapping method

Map the cut ν plane onto the unit circle and use a power series in the new variable to continue to the right hand side.

3. Padé approximants

Again, in principle one can expand in a power series about some point on the left, and use a Padé approximant series which will probably converge in a large connected region.

These methods are unfeasible in practice because one only has a small number of terms at one's disposal which leads to very large inaccuracies. Note that there is an exact continuation of a truncated series for $C(\nu)$, namely

$C(\nu)$ itself which has no right hand cut!

ZEROS

A further remark can be made about zeros. The $C_\ell(\nu)$ function has usually one or two zeros on the left in the δ function case. In the inverse amplitude formulation, these may lead to dominating singularities.

None of the ideas previously expressed is feasible as one does not have a good enough idea of $\{\mathrm{Im}A_\ell(t)\}$ to make the continuations meaningful. The only mathematically reasonable dynamical scheme is to neglect all structure outside the known region, perhaps assume ImA constant or cut off (which may have similar effects). One can try subtracting a few times as well to damp down effect of high energies, but one needs accurate subtraction constants.

One could possibly do an S - P calculation assuming that the fo had small effect and parametrising the high energy P wave. Of course, two schemes, truncated by the same amount, do not yield the same accuracy and cannot be expected to agree hence cannot be used to check exactly Chew-Mandelstam. Nevertheless, one expects some sort of order of magnitude check.

ASYMPTOTIC ASSUMPTION

Because of the importance of asymptotic behaviour upon existence of solutions, threshold behaviour etc., it is important to specify the asymptotic behaviour, that is being assumed, in an approximate calculation. Thus one is searching for the existence of solutions of a specified type. One does not know what asymptotic behaviour the exact solution has or what asymptotic behaviours are allowed, i.e. for which solutions exist. Ideally, as equations, one should solve the asymptotic equation and determine the allowed types of asymptotic behaviour. Then one should look for solutions of this type of the full equations, or solve the "remainder" equation using the asymptotic solution. If one has no lead whatsoever, then presumably one should try a range of different behaviours, and see what happens.

A reasonable assumption for the far left is the marginally singular case $\mathrm{Im}A_\ell(\nu) \longrightarrow$ constant $\nu \longrightarrow -\infty$ treated by Morgan and others, see Chapter 1. The pure absorption assumption of Lyth (Chapter 1) also leads to restrictions on asymptotic behaviour which one can incorporate.

There are also results from the diffraction peak and M.R.+U. as a guide.

INELASTICITY ASSUMPTION

Again, one can choose to look for elastic solutions, assuming this is a valid sub-problem or one can put in an inelasticity function numerically. One has to assume an asymptotic behaviour of the inelasticity function (see Chapter 1). There is also Lyth's pure absorption assumption which helps to tie down the form of the solution.

SELF-CONSISTENCY CONDITIONS AND THEIR ATTAINMENT

To compare the output with the input functions, the first thing that comes to mind is a χ^2 test, that is evaluate

$$\chi^2 = \sum_i \left[A_{out}(\nu_i) - A_{in}(\nu_i) \right]^2$$

over a set of sample points $\{\nu_i\}$.

Now the input and output functions are usually not members of the same family of parametrised trial functions, the parameters being the ones we are varying. If they are, then things are much simpler, and less treacherous. If they are not then we are left with a lot of arbitrariness.

(1) Choice of ν_i:

there is no need for them to be equally spaced. What interval do we place them in, finite or infinite, what distribution?

(2) Weights, W^i:

More generally, we should take

$$\chi^2 = \sum_i \omega_i \cdot \left[A_{out}(\nu_i) - A_{in}(\nu_i) \right]^2$$

whether the effects can be simulated by choice of $\{\nu_i\}$, as can be done to a certain extent in numerical integration, is not clear. At least, the bias

is more transparent using W^i. One might well expect different W^i e.g.

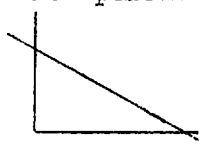
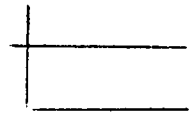
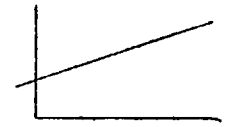

to give different self consistent values.

Choosing 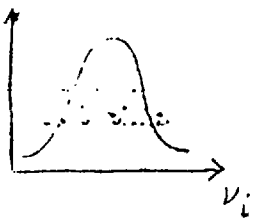 might be expected to play havoc, however how does one know that this is not effectively being perpetrated by taking 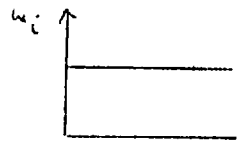 with certain types of parametrisation?

(3) Which function to be used:

One can use ReA or ImA or some function or both. If one has automatic unitarity for A_{in} and A_{out} then only one might be necessary, although different choices could lead to different effects.

(4) Dynamical weighting

Some people might make the obvious assumption as the % deviation

$$\chi^2 = \sum_i \omega_i \cdot 4 \left(\frac{A_{out}(\nu_i) - A_{in}(\nu_i)}{A_{out}(\nu_i) + A_{in}(\nu_i)} \right)^2$$

This gives a weight function which is not fixed like the W^i but moves as the parameters move. More generally

$$\chi^2 = \sum_i \omega_i \cdot \left[\frac{(A_{out}(\nu_i) - A_{in}(\nu_i))^{p_1}}{(A_{out}(\nu_i) + A_{in}(\nu_i))^{p_2}} \right]^2$$

Now, the % deviation function is, in the author's opinion, a bad one to take for the following reason. One is seeking to demand similarity of large scale features of the input and output functions. For example one would be fairly happy with

i.e. the bumps in the same place. Thus one would like most attention to be placed on the bumps and little on the smaller parts. The % weighting makes the effect of the large parts small and of small parts as important as the large parts and is thus a bad thing. Better would be to take $p_1 = 1$, $p_2 = -1$.

(5) Functional weighting:

One can take this dynamic weighting one step further by taking

$$\tilde{\chi}^2 = F(\chi^2)$$

e.g. $\tilde{\chi}^2 = \log \chi^2$ etc.

(6) Dynamical variation of sampling region:

To obviate one's choice of parameters fixing the solution one ought to make the sample region capable of varying with the parameters. Thus if a resonant amplitude is trying to move to high energy, a low sample region can hold it back.

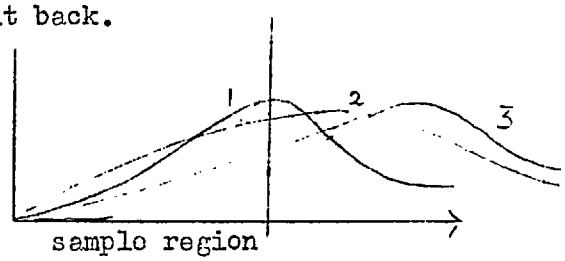

This idea can be extended to other parts of the calculation. For example, the symmetry points and normalisation point can be made functions of the parameters. Indeed this very thing is done in the Zachariasen calculation where

$$\nu_o = -\nu_R - 1.$$

In order to determine those values of the parameters for which the amplitude most nearly satisfy the desired conditions, we could use a graphical method of drawing curves, in the parameter space, which are the self consistency equations, and finding their intersection. As this method is not easy to use for several parameters, we used the method of searching the parameter space by iteration methods **until** a χ^2 criterion was satisfied. We used standard iteration programme which are quite general. Given χ^2 as a function of the parameters, such a programme will vary the parameters, testing χ^2 at each step, and optimising its search as a result, until it finds a minimum. The numerical analytic methods used are sophisticated and are described in computer literature. We mainly used a programme called VA02 A written by

M. Powell of AERE which is designed for functions which are a sum of squares, whose minimum value is close to zero.

THE NUMERICAL VALUE OF χ^2 FOR SELF CONSISTENCY

Of course, we want consistency between the various approximations and criteria used in the calculation. In his variational method, Hamilton found that 0.1% self consistency was necessary before he considered the result to be a solution (see Chapter 5). In the author's opinion, this merely shows that one is solving near identities, for the dispersion relation and the many approximations used could not be relied upon to such a high accuracy, 5% at the very most. In general, as explained previously, the value of χ^2 which determines self consistency must be found by experience, bearing in mind the principles we have been describing.

REASONS FOR NOT EXPLICITLY INCLUDING REGGE POLES

Regge poles were not used, for two main reasons. First the hypothesis may not be true. The lack of shrinking of the diffraction peak means that nearly all the phenomenological support for Regge poles has disappeared. One is driven to putting the shape of the diffraction peak into $\beta(s)$ and to the conclusion that many Regge poles contribute significantly. The only remaining success is in charge exchange scattering, analised by Barita and Phillips .

On the theoretical side, the hypothesis is highly desirable as a simple way of describing desired asymptotic behaviour of the amplitude and double spectral functions. It can give dominance of strips, low energy resonances, forward peaking at high energies all very naturally. However it is still not clear that there are no Regge cuts in the j plane in the relativistic case, in particular the Gribor-Pomerarchuk branch point at $j = -1$. Second, to carry out a calculation using Regge poles is a much more complicated business than for partial wave series. It involves a lot of programming and a lot of

execution time. A survey of different methods would be impossible. Further, it probably would not be so easy to see what was going on in the calculation. Thus two main aims of our work, to survey methods and to understand the mechanism of dynamical calculations, would not be possible.

III. PARAMETRISATION

In order to carry out self consistent calculations especially by iterative procedures one must often use a trial function with a small number of parameters, which can be adjusted to give the best approximation to self-consistency. It is then assumed that the function obtained will be close to the true analytic solution. To check this one should find that on making the parametrisation more flexible it gives a better fit and also that, on using a different parametric form, the best fit has similar features. Desirable features are thus flexibility with as few as possible parameters to limit computing time. It is possible to have too much flexibility of course. One usually would like the function representing a partial wave amplitude to automatically obey unitarity on the right. One would also like the function to have similar analytic properties to the expected solution, in our case cuts $[-1, -\infty]$, $[0, \infty]$. This is because the process of approximating functions, with similar analytic properties by fitting over a region, very often leads to the singularities moving to coincide as well as possible. In other cases, the expected cut structure may be different and thus different parametrisations more suitable. For example, in the π N case with $\pi\pi$ singularities in the complex plane the Layson form (16) has been used, which is a modified Breit-Wigner form and puts poles in roughly the right region. As we often look for resonant solutions, the function must be able to assume resonant form, however it must be able to assume non-resonant form. Thus the use of a Breit-Wigner formula, cannot lead to non-resonant solutions and is not sufficiently flexible.

We use a parametric form usually only in a closely specified region and do not use it for continuation.

The most general unitary form may be written

$$A(\nu) = \frac{1}{\mathrm{Re}\,A^{-1}(\nu) - i\,R(\nu)\cdot\sqrt{\frac{\nu}{\nu+1}}}$$

If one wants correct threshold behaviour one can write

$$A(\nu) = \frac{\nu^{\ell}}{\nu^{\ell}\,\mathrm{Re}\,A^{-1}(\nu) - i\,R(\nu)\cdot\nu^{\ell}\sqrt{\frac{\nu}{\nu+1}}}$$

One would also like any poles to occur on the second sheet only, although this is hard to arrange.

There is also asymptotic behaviour to consider. We shall consider 3 types of parametrisation for the amplitude

(i) extensions of the Breit Wigner formula starting from the standard form

$$A(\nu) = \frac{\Gamma\nu^{\ell}}{(\nu_R - \nu) - i\,\Gamma\nu^{\ell}\cdot\sqrt{\frac{\nu}{\nu+1}}}$$

This is the form used by Balazs (17). Various forms of B-W formulae are discussed in Oades' thesis (18)

(ii) N/D pole forms

$$A(\nu) = \frac{A_0 + (\nu-\nu_0)\sum_{i=1}^{n} F^i/(\nu-\nu_i)}{1 - \left(\frac{\nu-\nu_0}{\pi}\right)\cdot\sum_{i=1}^{n} F^i\cdot K(\nu,\nu_i)}$$

(iii) A form obtained by having a pole in the inverse amplitude.

We shall also consider parametrisations for R(ν) the inelasticity function.

We shall find fits to experimental data using some of the forms, for later use.

1. BREIT WIGNER FORMULAE

(a) Standard form

$$F(\nu) = \frac{\Gamma\nu^{\ell}}{(\nu_R - \nu) - i\,\Gamma\nu^{\ell}\cdot\sqrt{\frac{\nu}{\nu+1}}}$$

Analytic properties

We define $\sqrt{z} = +r^{1/2} e^{i\theta/2}$ $z + i\varepsilon$ 1st sheet pos. real axis

$+ir^{1/2} e^{i\theta/2}$ 1st sheet neg. real axis

$-r^{1/2} e^{i\theta/2}$ $z + i$ 2nd sheet pos. real axis

$-ir^{1/2} e^{i\theta/2}$ 2nd sheet neg. real axis

and we note that

$\frac{\nu}{\nu+1} > 0$ for $\nu > 0$ $\nu < -1$

< 0 ν in $[-1, 0]$

also that

$$\frac{\nu + i\varepsilon}{\nu + 1 + i\varepsilon} = \frac{\nu(\nu+1) + i\varepsilon + \varepsilon^2}{(\nu+1)^2 + \varepsilon^2} = \frac{\nu}{\nu+1} + i\varepsilon' + \theta(\varepsilon^2)$$

so that just above the cuts in the (ν) plane corresponds to just above the cut in the ($\frac{\nu}{\nu+1}$) plane.

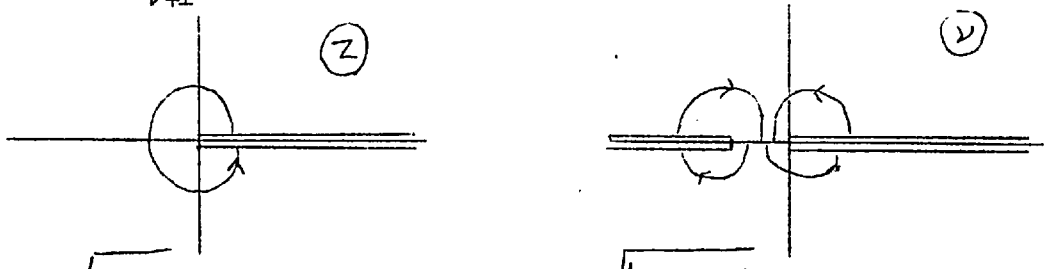

hence $\sqrt{\frac{\nu}{\nu+1}}$ at $\nu \mp i\varepsilon$ $= +\sqrt{\left|\frac{\nu}{\nu+1}\right|}$ 1st sheet on cut

$+i$ " 1st sheet off cut

$-$ " 2nd sheet on cut

$-$ " 2nd sheet off cut

so $\mathrm{Re}\, F(\nu) = \dfrac{\Gamma \nu^\ell (\nu_R - \nu)}{(\nu_R - \nu)^2 + \Gamma^2 \nu^{2\ell} \cdot \left[\frac{\nu}{\nu+1}\right]}$ both sheets $\nu > 0$ $\nu < -1$

$$\mathrm{Im}\, F(\nu + i\varepsilon) = \frac{\mp \Gamma^2 \nu^{2\ell} \sqrt{\frac{\nu}{\nu+1}}}{(\nu_R - \nu)^2 + \Gamma^2 \nu^{2\ell} \cdot \left[\frac{\nu}{\nu+1}\right]} \qquad \nu > 0 \quad \nu < -1$$

$$\mathrm{Re}\, F(\nu) = \frac{\Gamma \nu^\ell}{(\nu_R - \nu) \pm \Gamma \nu^\ell \sqrt{\left|\frac{\nu}{\nu+1}\right|}} \qquad \nu \text{ in } [0, -1].$$

Near $\nu = 0$.

$0+$ $\mathrm{Re}\, F(\nu) = \dfrac{(\nu_R - \nu) \cdot \nu^\ell \cdot \Gamma}{(\nu_R - \nu)^2 + \nu^{2\ell} \cdot \Gamma^2 \cdot \left[\frac{\nu}{\nu+1}\right]} \approx \dfrac{\Gamma \nu^\ell}{\nu_R}$

$0-$ $\mathrm{Re}\, F(\nu) = \dfrac{\Gamma \nu^\ell}{(\nu_R - \nu) \pm \Gamma \nu^\ell \sqrt{\frac{-\nu}{\nu+1}}} \approx \dfrac{\Gamma \nu^\ell}{\nu_R}$

$0+$ $\mathrm{Im}\, F(\nu) = \dfrac{\mp \Gamma^2 \nu^{2\ell} \sqrt{\frac{\nu}{\nu+1}}}{(\nu_R - \nu)^2 + \nu^{2\ell} \cdot \Gamma^2 \Gamma[\nu/(\nu+1)]} \approx \dfrac{\Gamma^2}{\nu_R^2} \cdot \nu^{2\ell + \frac{1}{2}}$

Fig 2-12.
Breit-Wigner Formula.

1 Real part 1st sheet
2 " 2nd sheet.
3 " both sheets.
4 Imaginary part.

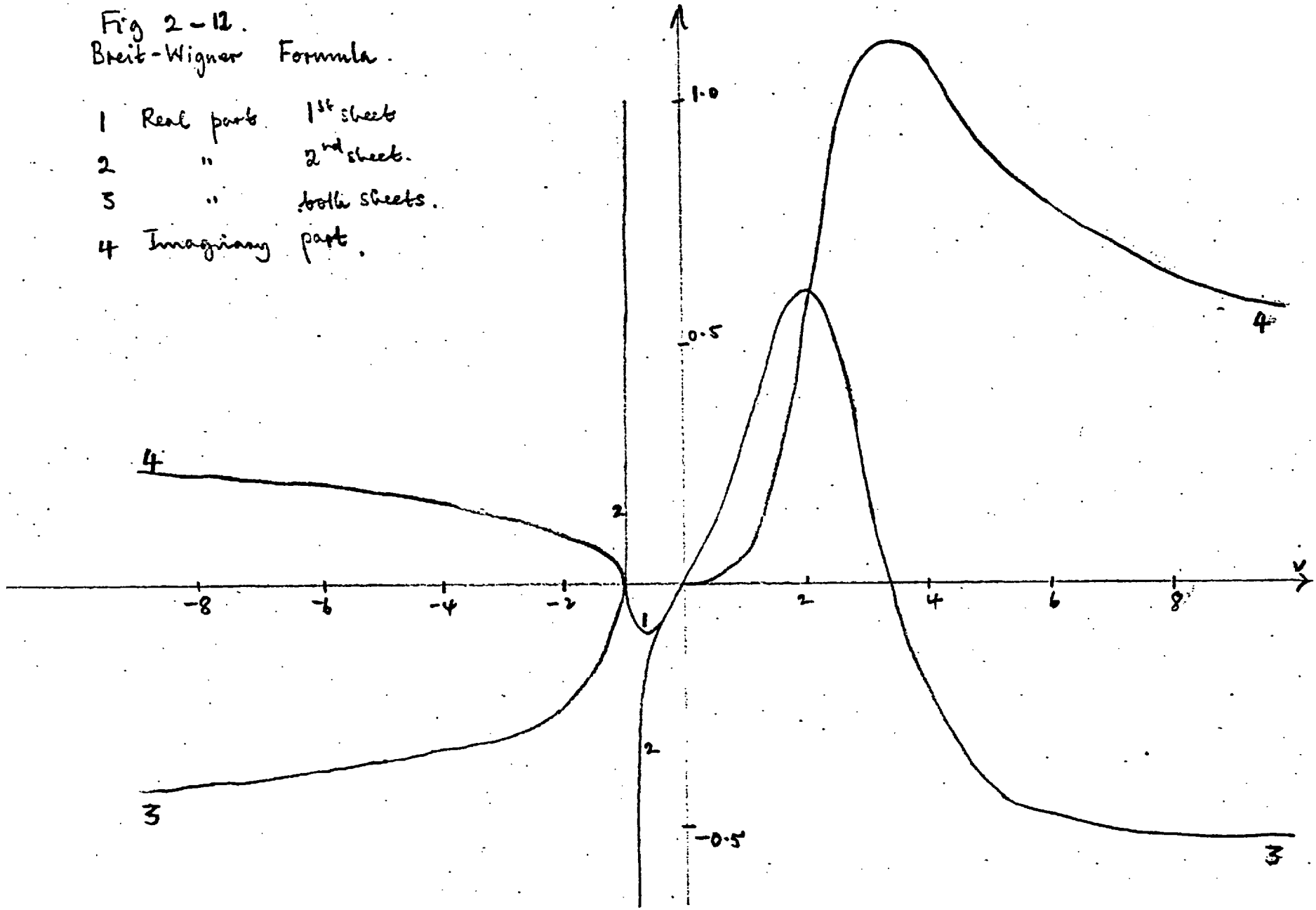

Near $\nu = -1$

$$-1_- \quad \mathrm{Re}\, F(\nu) = \frac{(\nu_R - \nu)\cdot \nu^\ell \Gamma}{(\nu_R-\nu)^2 + \nu^{2\ell}\cdot \Gamma^2 \left[\frac{\nu}{\nu+1}\right]}$$

$$\approx \frac{(\nu+1)(\nu_R-\nu)\nu^\ell \Gamma}{\nu^{2\ell}\Gamma^2 \nu} \approx \frac{(\nu+1)(\nu_R+1)}{(-1)^{\ell+1}\cdot \Gamma}$$

$$-1_+ \quad \mathrm{Re}\, F(\nu) = \frac{\Gamma \nu^\ell}{(\nu_R-\nu) \pm \Gamma \nu^\ell \sqrt{-\nu/(\nu+1)}} \approx \pm \sqrt{|\nu+1|}$$

$$-1_- \quad \mathrm{Im}\, F(\nu) = \mp \sqrt{|\nu+1|}$$

$$-1_+ \quad \mathrm{Im}\, F(\nu) = 0$$

$$-1_- \quad \mathrm{Re}\, F'(\nu) = (\nu_R+1)/(-1)^{\ell+1}\cdot \Gamma$$

$$-1_+ \quad \mathrm{Re}\, F'(\nu) = \pm \frac{1}{2}\frac{1}{\sqrt{\nu+1}}$$

SECOND SHEET POLES

The denominator has 3 roots, corresponding to 3 poles, all on the 2nd sheet. This can be suggested as follows:-

$$D(\nu) = \nu_R - \nu \mp i\Gamma \nu^\ell \sqrt{\frac{\nu}{\nu+1}}$$

if Γ is small vanishes near

$$\nu = \nu_R + i\varepsilon$$

where $\varepsilon = \mp i \Gamma \nu_R^\ell \sqrt{\nu_R/(\nu_R+1)}$

now

$$D^{I}(\nu+i\varepsilon) = \nu_R - \nu - i\Gamma \nu^\ell \sqrt{\frac{\nu}{\nu+1}} + O(\varepsilon)$$

$$D^{I}(\nu\cdot e^{2\pi i} - i\varepsilon) = \nu_R - \nu + i\Gamma \nu^\ell \sqrt{\frac{\nu}{\nu+1}} + O(\varepsilon)$$

$$D^{II}(\nu+i\varepsilon) = \nu_R - \nu + i\Gamma \nu^\ell \sqrt{\frac{\nu}{\nu+1}} + O(\varepsilon)$$

$$D^{II}(\nu\cdot e^{2\pi i} - i\varepsilon) = \nu_R - \nu - i\Gamma \nu^\ell \sqrt{\frac{\nu}{\nu+1}} + O(\varepsilon)$$

at the point	$\nu_R + i\varepsilon$	D^{II} o vanishes but not D^{I}
	$\nu_R - i\varepsilon$	D^{II} " "

The third zero lies on the real axis in $[0, -1]$ near $= -1$ as can be seen by writing

$$(\nu+1)\cdot(\nu_R-\nu)^2 = -\Gamma^2 \cdot \nu^{2\ell}$$

putting $\Gamma = 0$ gives $\nu = \nu_R$ twice
or -1

One can develop an expression for the position of this pole by the iterative procedure

$$\nu = -1 - \Gamma^2 \nu^{2\ell} / (\nu_R - \nu)^2$$

$$\nu_1 = -1 - \Gamma^2 \nu^{2\ell} / (\nu_R + 1)^2$$

$$\nu_{i+1} = -1 - \Gamma^2 \nu_i^{2\ell} / (\nu_R - \nu_i)^2 \quad , \quad \text{to convergence.}$$

This pole is usually weak and close to -1.

Putting it at $-1 + x$

$$\nu_R = -1 + x \pm \sqrt{\frac{\Gamma^2 (-1+x)^{2\ell}}{x}}$$

as $x \to 0$ $\quad \nu_R \to \frac{1}{\sqrt{x}} \to \infty$

$\to 1$ $\quad \nu_R \to \sqrt{(-1+x)^{2\ell}} \to 0$

$$\Gamma^2 = \frac{-x}{(-1+x)^{2\ell}} \cdot (\nu_R + 1 - x)^2$$

as $x \to 0$ $\quad \Gamma^2 \to 0$

$x \to 1$ $\quad \Gamma^2 \to \infty$

Thus for large ν_R or small Γ, the pole is near -1, and for small ν_R or large Γ, near the origin.

Iterative procedure will also give the exact positions of the other two poles, when $\ell > 1$ there will be $(2\ell + 1)$ poles on the second sheet. For the s wave 3 poles, P wave 3. Thus one is solving progressively higher order polynomials.

Width

The width of a Breit-Wigner curve is not Γ, but $2.\Gamma \nu_R^{\ell}$.

The centre of the resonance is when the phase shift is $\pi/2$ and this occurs at $\nu = \nu_R$. To find the width, we find at what position the $|\text{amplitude}|^2$ has half the resonant value.

$$\text{Im } F(\nu) = \frac{\Gamma^2 . \nu^{2\ell} \sqrt{\frac{\nu}{\nu+1}}}{(\nu_R - \nu)^2 + \Gamma^2 \nu^{2\ell} . \left[\frac{\nu}{\nu+1}\right]}$$

$$\mathrm{Im}\, F(\nu_R) = \sqrt{\frac{\nu_R+1}{\nu_R}}$$

take half height to be at $\nu_R + W$, neglect the change in $\sqrt{\frac{\nu}{\nu+1}}$ which cancels

$$\frac{1}{\sqrt{2}} = \frac{\Gamma^2 (\nu_R + W)^{2\ell}}{W^2 + \Gamma^2 (\nu_R + W)^{2\ell} \cdot [(\nu_R + W)/(\nu_R + W + 1)]}$$

thus, to a good approximation

$$W^2 = (\sqrt{2} - 1) \cdot \Gamma^2 \cdot \nu_R^{2\ell}$$

$$W = \Gamma \nu_R^{\ell} \cdot 0.645 \text{ or if } \nu_R \text{ is small } \Gamma \cdot \nu_R^{\ell} \sqrt{\frac{\nu_R}{\nu_R + 1}}$$

so the full width is $1.3\ \Gamma \nu_R^{\ell}$.

This is supported by numerical results obtained by the author.

For $\nu_R = 5.768$, $\Gamma \nu_R^{\ell} = 4.970$

$\mathrm{Im}\, F(\nu_R) = 1.09$

ν when $\mathrm{Im}\, F(\nu) = \frac{1}{2}\, \mathrm{Im}\, F(\nu_R) = 0.505$ is 3.1

giving $W = 5.32$

compared to $(1.3) \cdot \Gamma \nu_R^{\ell} = 6.4$

The suthor has also worked out the correct expression keeping in all terms and has obtained, for small Γ

$$W = \frac{\Gamma \nu_R^{\ell}}{\sqrt{2}} = 0.707 \cdot \Gamma \nu_R^{\ell}$$

which holds provided

$$\Gamma \nu_R^{\ell} \cdot \frac{2\ell}{\nu_R} \ll 1$$

i.e. $$W \ll \frac{\nu_R}{2\sqrt{2}\,\ell}$$

For the ρ, $\ell = 1$, $\nu_R \sim 6$, $W \sim 1$.

$$\frac{\nu_R}{2\sqrt{2}\,\ell} \sim 2$$

for the f_o, $\ell = 2$, $\nu_R \sim 20$, $W \sim 1$

$$\frac{\nu_R}{2\sqrt{2}\,\ell} \sim 3$$

which conditions are just about valid. A graph of the Breit Wigner formula, its real and imaginary parts just above the real axis on sheets 1 and 2 is given in Fig. 12.

δ function reduction

Using the standard formula

$$\delta(x) = \lim_{\varepsilon \to 0} \frac{1}{\pi} \frac{\varepsilon}{x^2 + \varepsilon^2}$$

$$\mathrm{Im}F(\nu) = \frac{\Gamma^2 \nu^{2\ell} \sqrt{\frac{\nu}{\nu+1}}}{(\nu - \nu_R)^2 + \Gamma^2 \nu^{2\ell} \cdot [\nu/(\nu+1)]}$$

$$= \pi \Gamma \nu^{\ell} \sqrt{\frac{\nu}{\nu+1}} \cdot \left[\frac{1}{\pi} \cdot \frac{\Gamma \nu^{\ell} \sqrt{\frac{\nu}{\nu+1}}}{(\nu - \nu_R)^2 + \Gamma^2 \nu^{2\ell} \left[\frac{\nu}{\nu+1}\right]} \right]$$

$$\Gamma \longrightarrow \text{small} \quad \pi \Gamma \nu_R^{\ell} \cdot \sqrt{\frac{\nu_R}{\nu_R+1}} \cdot \delta(\nu - \nu_R)$$

$$= \pi . W . \delta(\nu - \nu_R)$$

(b) Polynomial generalisation

$$F(\nu) = \frac{\nu^{\ell}}{\left(\sum_{i=0}^{n} a_i \nu^i\right) - i \nu^{\ell} \sqrt{\frac{\nu}{\nu+1}}}$$

$a_0 \neq 0$ is related to the scattering length

$$a = \lim_{\nu \to 0} \left[\nu^{\ell} \sqrt{\frac{\nu}{\nu+1}} \cdot \tan\delta(\nu) \right]$$

$$\tan\delta(\nu) = \sqrt{\frac{\nu}{\nu+1}} \Big/ P(\nu)$$

$$a = \frac{1}{a_0}$$

In the case n = 2, P(ν) is quadratic, and one can see how this allows a general non-resonant bump, for with $P(\nu) = \nu - \nu_R$, it is inevitable that $\mathrm{Re}A^{-1}(\nu) = 0$ on the real axis at $\nu = \nu_R$. However, when $P(\nu) = a + b\nu + c\nu^2$, it can either cut the axis or turn back just near the axis giving either a resonance or a bump.

Exactly analogous forms to case (a) hold for the value of F(ν) on the two sheets. One is not sure where the poles will be and one hopes they are all on the second sheet.

Asymptotic behaviour

$$\text{as } \nu \longrightarrow \pm\infty \quad \sqrt{\frac{\nu}{\nu+1}} \longrightarrow 1.$$

$$\mathrm{Im}F(\nu) \longrightarrow \frac{\nu^{2\ell}}{P(\nu)^2 + \nu^{2\ell}}$$

thus if $n < \ell$, $\nu^{2\ell}$ dominates the denominator and

$$\mathrm{Im}\,F(\nu) \to 1$$

$$n = \ell \qquad \mathrm{Im}\,F(\nu) \longrightarrow \frac{\nu^{2\ell}}{a_\ell^2\,\nu^{2\ell} + \nu^{2\ell}} \longrightarrow \frac{1}{a_\ell^2 + 1}$$

$$n > \ell \qquad \mathrm{Im}\,F(\nu) \longrightarrow \frac{1}{a_n^2 \cdot \nu^{2n-2\ell}} \longrightarrow O\left(\frac{1}{\nu^{2n-2\ell}}\right)$$

this asymptotic behaviour will emerge when

$$a_n^2 \cdot \nu^{2n-2\ell} \sim 2\,a_n \cdot a_{n-1} \cdot \nu^{2n-2\ell-1}$$

$$\text{i.e. } \nu \gtrsim 2a_{n-1}/a_n \qquad \text{is asymptotic region.}$$

Left hand cut

$$\mathrm{Im}\,F^{-1}(\nu) = \mp i\sqrt{\frac{\nu}{\nu+1}} \qquad \nu < -1$$

i.e. it satisfies a unitarity condition on the left as well as the right; this is because we have removed the left hand singularities located in $\mathrm{Re}A^{-1}(\nu)$.

The threshold behaviour on the left is the similar to case (a)

$$\mathrm{Re}\,F(\nu) = \frac{P(\nu)\cdot\nu^{\ell}(\nu+1)}{\nu^{2\ell}\cdot\nu} = \frac{O(\nu+1)}{(-1)^{\ell}}$$

$$\mathrm{I}\cdot F(\nu) = \pm\sqrt{|\nu+1|}$$

(c) Rational function generalisation

$$F(\nu) = \frac{\nu^{\ell}}{P(\nu)/Q(\nu) - i\,\nu^{\ell}\sqrt{\nu/(\nu+1)}}$$

$$P(\nu) = \sum_{i=0}^{n} a_i\,\nu^i$$

$$Q(\nu) = 1 + \sum_{j=1}^{m} b_j\,\nu^j$$

This allows us to get the asymptotic behaviour under control, but introduces more singularities over which we have little control. Zeros of $Q(\nu)$ are poles of $A^{-1}(\nu)$. Zeros of $P(\nu)$ correspond to poles of $A(\nu)$ and should be on left hand cut or second sheet.

Asymptotic behaviour is now

$$P/Q \longrightarrow O(\nu^{n-m})$$

1. $\ell + m - n < 0$

$$\mathrm{Re}\,F(\nu) \to O(\nu^{\ell+m-n}) \to 0$$

$$\mathrm{Im}\,F(\nu) \to O(\nu^{2(\ell+m-n)}) \to 0$$

2. $l + m - n > 0$

$\mathrm{Re}\, F(\nu) \longrightarrow 0$

$\mathrm{Im}\, F(\nu) \longrightarrow 1$

3. $l + m - n = 0$

$$\mathrm{Re}\, F(\nu) \longrightarrow \frac{a^n / b^m}{\left[\left(a^n / b^m \right)^2 + 1 \right]} = \text{constant}$$

$$\mathrm{Im}\, F(\nu) \longrightarrow \frac{1}{\left[\left(a^n / b^m \right)^2 + 1 \right]} = \text{constant.}$$

For m = n

$l > 0$ $\quad \mathrm{Im}\, F \longrightarrow 1$, $\mathrm{Re}\, F \longrightarrow 0$

$\mathrm{Im}\, F \longrightarrow 1$, $\mathrm{Re}\, F \longrightarrow 0$ when $l > n - m$ or $m > n - l$

$\mathrm{Im}\, F \longrightarrow 0$, $\mathrm{Re}\, F \longrightarrow 0$ when $l < n - m$, $m < n - l$

2. N/D Pole formulae

$$F(\nu) = N(\nu) / D(\nu)$$

$$N(\nu) = (\nu - \nu_0) \sum_{i=1}^{n} F^i / (\nu - \nu_i) + A(\nu_0) = (\nu - \nu_0) \sum_{i=0}^{n} F^i / (\nu - \nu_i)$$

$$D(\nu) = 1 - \left(\frac{\nu - \nu_0}{\pi} \right) \cdot \int_0^\infty d\nu' \sqrt{\nu' / \nu' + 1} \cdot \frac{N(\nu')}{(\nu' - \nu_0)(\nu' - \nu)}$$

$$= 1 - \left(\frac{\nu - \nu_0}{\pi} \right) \cdot \sum_{i=0}^{n} F^i \cdot I(\nu_i, \nu)$$

where $F^0 = A(\nu_0)$.

$$I(\nu_i, \nu) = \int_0^\infty d\nu' \cdot \sqrt{\frac{\nu'}{\nu' + 1}} \cdot \frac{1}{(\nu' - \nu)(\nu' - \nu_i)} = I(\nu, \nu_i)$$

the evaluation of this integral and its analytic properties are discussed in an Appendix.

The result is

$$I(\nu, \nu_i) = \frac{2}{\nu_i - \nu} \cdot \left[\sqrt{\frac{\nu}{\nu + 1}} \log \left[\sqrt{\nu} + \sqrt{\nu + 1} \right] - \sqrt{\frac{\nu_i}{\nu_i + 1}} \cdot \log \left[\sqrt{\nu_i} + \sqrt{\nu_i + 1} \right] \right]$$

This parametric form can represent resonant or non-resonant amplitudes. It has the correct cut structure on the physical sheet, however the cut connects this to an infinite number of sheets because of logarithmic behaviour. In the above form it does not have automatically correct threshold behaviour, however some calculations will constrain the F^i to give it. We can take the ν_i to be free parameters, or, following Balazs (see Chapter 3), we can take them fixed at optimum values, determined in an auxiliary calculation.

$$A^{-1}(\nu) = D(\nu) / N(\nu)$$

has zeros on the left at ν_i and poles at the zeros of $N(\nu)$, one is not sure that these will all be on the real axis. In any case, we have more control over singularities and the only ones we need worry about are zeros of $D(\nu)$. Figure 13 gives graphs of ReA and ImA and the contribution from the left hand cut for a resonant amplitude using N/D parametrisation. The N and D functions can be seen in Figures 3 - 2.

Asymptotic Behaviour

$$\mathrm{Im}A = \sqrt{\frac{\nu}{\nu+1}} \cdot |A|^2 = \sqrt{\frac{\nu}{\nu+1}} \cdot \frac{\mathrm{Re}N^2}{\mathrm{Re}D^2 + \mathrm{Im}D^2}$$

$$\mathrm{Im}D = -\sqrt{\frac{\nu}{\nu+1}} \cdot \mathrm{Re}N$$

$$\therefore \quad \mathrm{Im}A = \sqrt{\frac{\nu}{\nu+1}} \cdot \frac{1}{\left\{ \left(\frac{\mathrm{Re}D}{\mathrm{Re}N}\right)^2 + \left[\frac{\nu}{\nu+1}\right] \right\}}$$

$$N(\nu) = (\nu - \nu_0) \sum_i F^i/(\nu - \nu_i) \longrightarrow \sum_i F_i$$

$$D(\nu) = 1 - \left(\frac{\nu - \nu_0}{\pi}\right) \sum_i F^i \, I(\nu, \nu_i)$$

$$I(\nu_i, \nu) = \frac{2}{(\nu_i - \nu)} \cdot \left[\sqrt{\frac{\nu}{\nu+1}} \cdot \log\left[\sqrt{\nu} + \sqrt{\nu+1}\right] - \sqrt{\frac{\nu_i}{\nu_i+1}} \cdot \log\left[\sqrt{\nu_i} + \sqrt{\nu_i+1}\right] \right]$$

$$\nu \to \infty \quad \frac{2}{-\nu} \log(2\sqrt{\nu})$$

$$\longrightarrow \frac{\log \nu}{-\nu}$$

$$\mathrm{Re}D(\nu) \to 1 - \left(\frac{\nu - \nu_0}{\pi}\right) \cdot \sum_i F^i \cdot \log\nu / \nu$$

$$\longrightarrow \frac{1}{\pi} \log\nu \sum F^i$$

indep. ν_i (although these affect where asymptotic region starts)

$$\mathrm{Im}A \longrightarrow \sqrt{\frac{\nu}{\nu+1}} \Big/ \left\{ \left(\frac{1}{\pi} \log\nu\right)^2 + \left[\frac{\nu}{\nu+1}\right] \right\}$$

$$\longrightarrow \sqrt{\nu} \cdot \pi^2 \cdot (\log \ldots)^{-2} \longrightarrow 0$$

indep ν_i, F^i, n, ℓ.

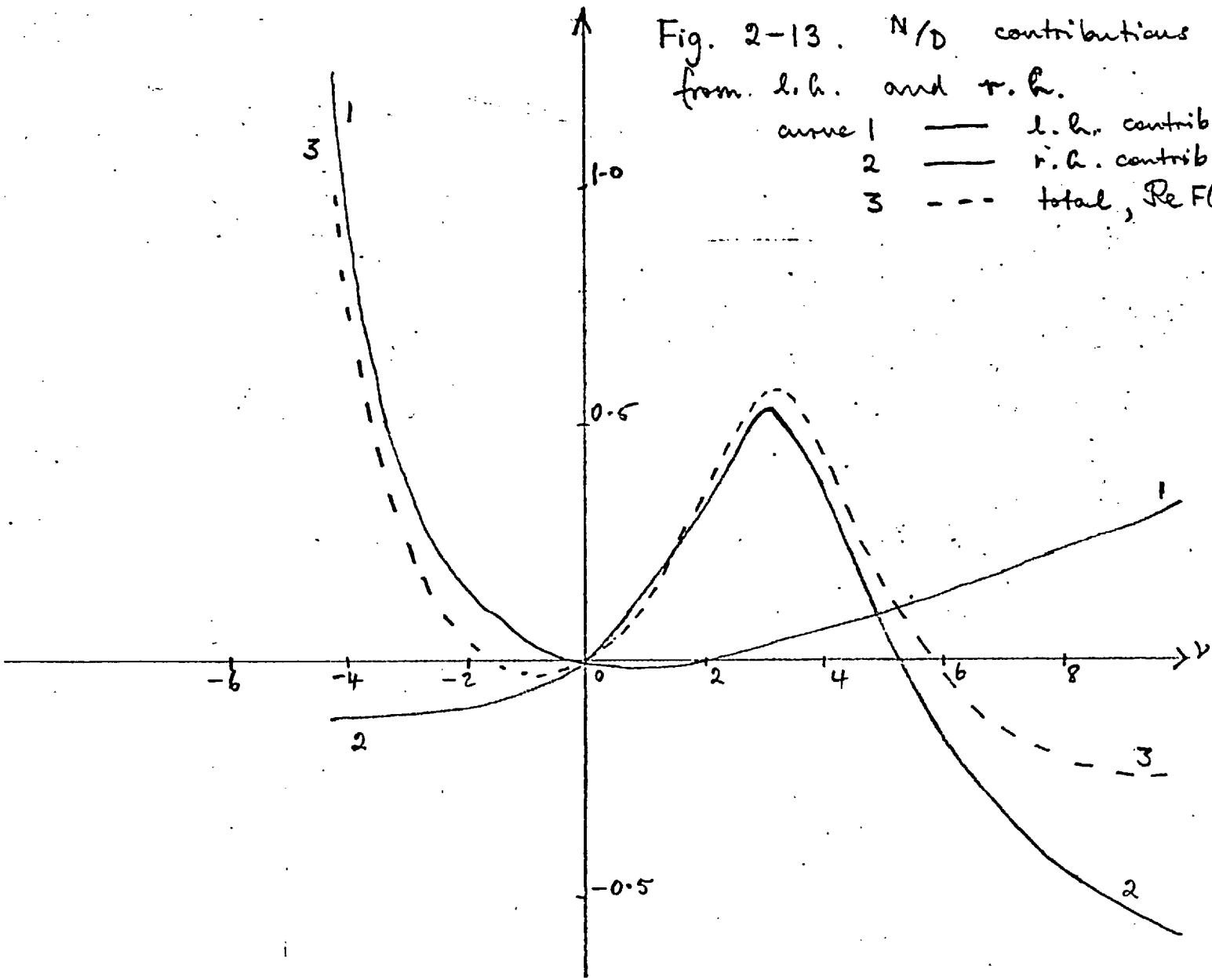

Fig. 2-13. N/D contributions from l.h. and r.h.

curve 1 —— l.h. contrib.
2 —— r.h. contrib
3 - - - total, $\mathrm{Re}\, F(\nu)$.

$$\underset{\nu\to\pm\infty}{\mathrm{Re}} = \frac{\text{N.D.}}{|D|^2} \longrightarrow \frac{\sum F^i}{\frac{1}{\pi}\log\nu \sum F^i} \longrightarrow \frac{\pi}{\log\nu} \longrightarrow 0$$

$$\delta \underset{\nu\to\infty}{\longrightarrow} n\pi \,. \qquad \underline{\text{purely real}}$$

<u>Possible analogy of B - W to N/D</u>

if $\mathrm{Re}D = X$

$\mathrm{Re}N = Y$

then $\mathrm{Im}A = \dfrac{\mathrm{Re}N \cdot -\mathrm{Im}D}{\mathrm{Re}D^2 + \mathrm{Im}D^2}$

but $\mathrm{Im}D = -\sqrt{\frac{\nu}{\nu+1}} \cdot \mathrm{Re}N$

$\therefore \mathrm{Im}A = \dfrac{\sqrt{\frac{\nu}{\nu+1}} \cdot \mathrm{Re}N^2}{[\mathrm{Re}D^2 + [\nu/(\nu+1)] \cdot \mathrm{Re}N^2]}$

$$= \frac{\sqrt{\frac{\nu}{\nu+1}} \cdot X^2}{\left\{ Y^2 + X^2 \cdot \left[\frac{\nu}{\nu+1}\right]\right.}$$

if $\Gamma_\nu{}^\ell = X$

$\nu_R - \nu = Y$

then $\mathrm{Im}A = \dfrac{\Gamma^2 \nu^{2\ell} \sqrt{\frac{\nu}{\nu+1}}}{(\nu_R-\nu)^2 + \left[\frac{\nu}{\nu+1}\right] \cdot \Gamma^2 \nu^{2\ell}}$

$$= \frac{\sqrt{\frac{\nu}{\nu+1}} \cdot X^2}{\left\{ Y^2 + X^2 \left[\frac{\nu}{\nu+1}\right]\right\}}$$

thus $\Gamma_\nu{}^\ell$ analogous to ReN( )

$\nu_R - \nu$ " " ReD

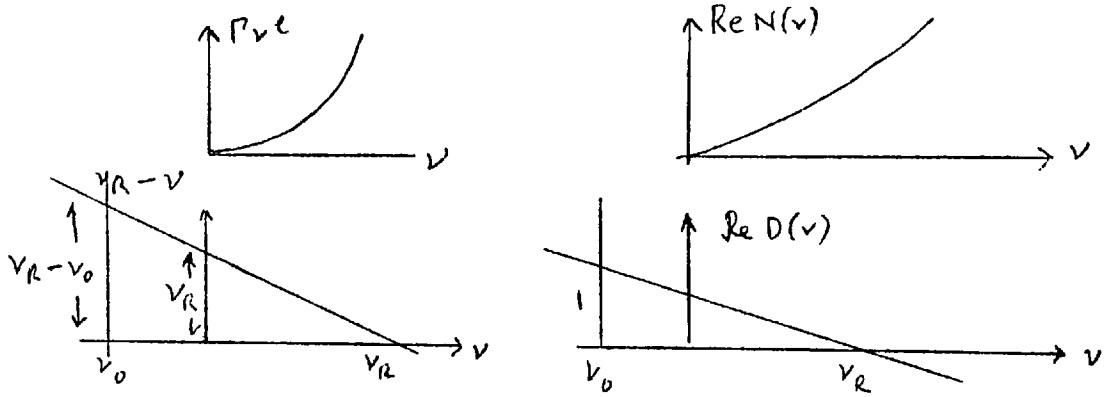

3. Inverse Amplitude parametrisation

Based on Model 2 of inverse amplitude

$$A^{-1} = \frac{(\nu-\nu_0)}{\pi}.I(\nu,\nu_0) + \sum\left(\frac{\nu-\nu_0}{\nu_i-\nu_0}\right)\frac{F_i}{(\nu-\nu_i)} + A^{-1}(\nu_0) + \left(\frac{\nu-\nu_0}{-\nu_0}\right)\sum_{n=1}^{\ell}\frac{a_n}{\nu^n}$$

$$\text{Re}A \text{ r.h. side} = \frac{\left\{\mathcal{R}e\,K(\nu,\nu_0) + \sum\left(\frac{\nu-\nu_0}{\nu_i-\nu_0}\right)\frac{F_i}{(\nu-\nu_i)} + A^{-1}(\nu_0) + \left(\frac{\nu-\nu_0}{-\nu_0}\right)\sum_{n=1}^{\ell}\frac{a_n}{\nu^n}\right\}}{|A^{-1}|^2}$$

$$\text{Im}A \text{ r.h. side} = \frac{\mathcal{R}(\nu).\sqrt{\frac{\nu}{\nu+1}}}{|A^{-1}|^2}$$

$$\text{Im}A \text{ l.h. side} = \pi.\sum_i F_i\,\delta(\nu-\nu_i)$$

$$\text{Re}A \text{ l.h. side} = \frac{1}{\left[K(\nu,\nu_0) + \sum\left(\frac{\nu-\nu_0}{\nu_i-\nu_0}\right)\frac{F_i}{(\nu-\nu_i)} + A^{-1}(\nu_0) + \left(\frac{\nu-\nu_0}{-\nu_0}\right)\sum_{n=1}^{\ell}\frac{a_n}{\nu^n}\right]}$$

$\nu \neq \nu_i$

Thus, for a single pole, which may be quite realistic, with elastic unitarity, we have a $(3+\ell)$ parameter formula

$$A^{-1} = K(\nu,\nu_0) + \left(\frac{\nu-\nu_0}{\nu_\rho-\nu_0}\right).\frac{g_\rho}{\nu-\nu_\rho} + A_0 + \left(\frac{\nu-\nu_0}{-\nu_0}\right).\sum_{n=1}^{\ell}\frac{a_n}{\nu^n}.$$

so, S - wave $\sim$ 3 parameters

P - wave $\sim$ 4 parameters

hence for $S_0 + S_2 + P_1 + D_0$ need 15

for $(S_0 + S_2) + P_1 + D_0$ need 9 parameters

S.C. in Model 2 when input parameters = output parameters

$$\left(\begin{array}{l} g_\rho' = g_\rho \\ \nu_\rho' = \nu_\rho \\ A_0' = A_0 \\ \{a_n'\} = \{a_n\} \end{array}\right)^2$$

This enables the scattering lengths a_n to be varied independently of the rest of the parameters. Fig. 14 displays A and A^{-1}. If one used B W then,

$$A(\nu) \underset{\nu\to 0}{\longrightarrow} \frac{\Gamma\nu^\ell}{-\nu_R} \qquad \text{or more generally} \qquad \frac{\nu^\ell}{a_1}$$

Fig. 2-14.

A^{-1} parametrisation.

curve 1 Re A
2 r.h. cut
3 l.h. pole
4 threshold pole

contributions to A^{-1}.

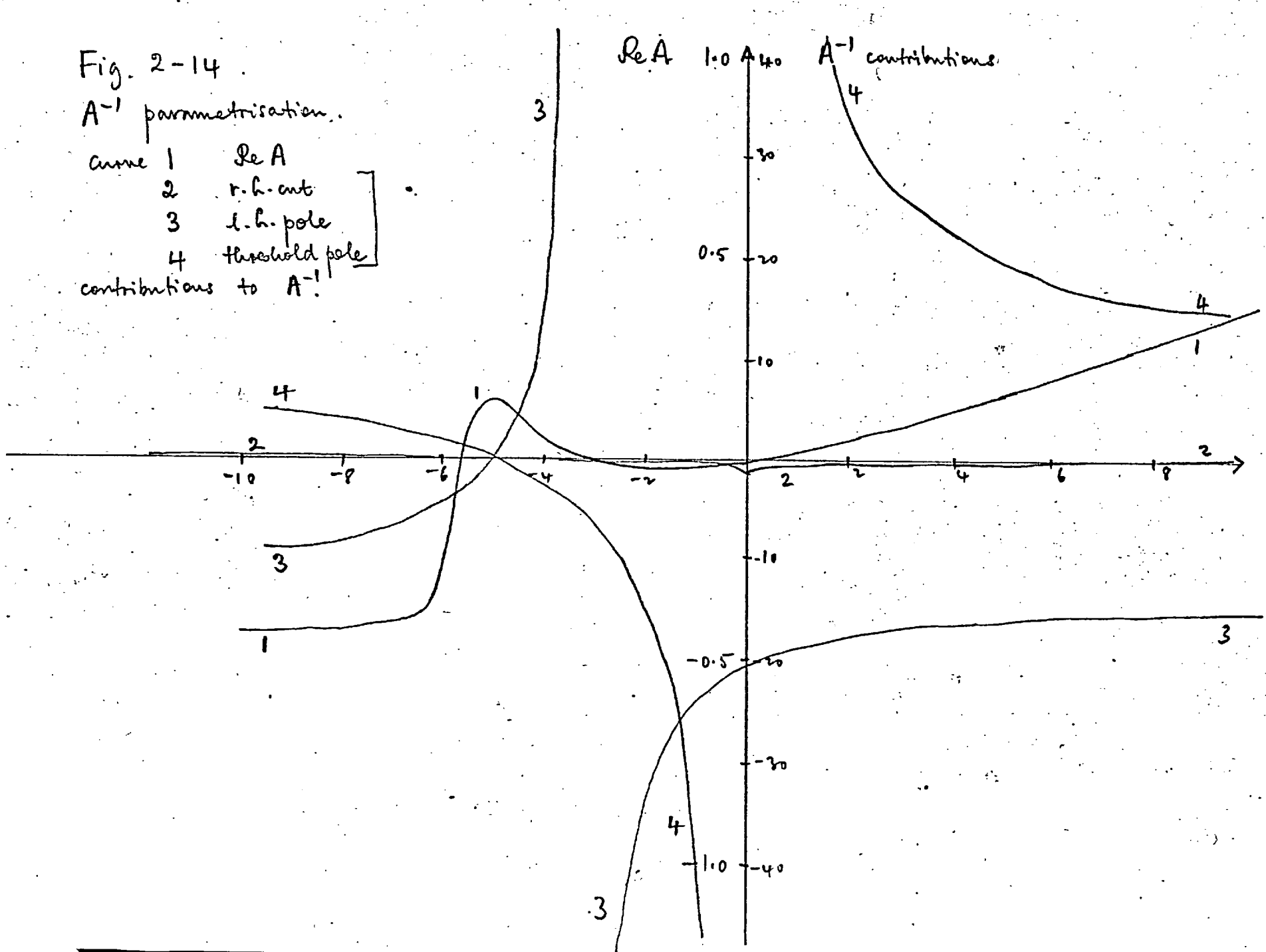

so the scattering length would be determined by position and width of resonance

$$a_1 = -\nu_R / \Gamma \qquad *$$

In practice however $\nu_R = 6.0$, $\Gamma = 0.4$ } "a_1" $= -9.0$

but $a_1 = -30.0$ from expt

so if the calculation depends upon a_1 at all strongly it will be drastically upset by using an unsuitable parametrisation. This is really just the same as the rational function generalisation of the Breit-Wigner formula, except that we now directly parametrise the threshold pole and the left hand singularities of the inverse amplitude.

In the multi-channel case (19), the real part of inverse amplitude goes over to the inverse K matrix and is much used for multichannel effective range formula etc. obtained by expanding K^{-1} in powers of ν.

$$S = (1 + iK)^{-1} \cdot (1 - iK).$$

$$T^{-1} = K^{-1} + ik.$$

K is symmetric by time reversal, hermitian by unitarity, hence real.

Effective range formulae by

$$K^{-1} = \frac{1}{a_0} + r_0 k^2$$

$\therefore$ since $T^{-1} = k \cot\delta - ik$, we have

$$k \cot\delta = \frac{1}{a_0} + r_0 k^2 + \ldots$$

Given the functions

$$f_1(\nu) = \sqrt{\frac{\nu}{\nu+1}} \quad \text{and} \quad f_2(\nu) = \frac{(\nu - \nu_0)}{\pi} \bar{I}(\nu, \nu_0)$$

both with a right hand cut with discontinuity $-\sqrt{\frac{\nu}{\nu+1}}$, we can construct parametrisations by parametrising $A^{-1} + f(\nu)$, which will have no right hand cut. Using a power series in ν gives Breit Wigner formulae. Assuming poles on the left and threshold behaviour gives the inverse amplitude parametrisation. Using $f_1(\nu)$ gives a left hand cut as well. So we have

$$1 \Big/ \left[\frac{P(\nu)}{Q(\nu)} + f(\nu) \right]$$

The N/D pole form is a further extension using $f_2(\nu)$.

The simple case

$$\frac{1}{\frac{P(\nu)}{Q(\nu)} + \left(\frac{\nu-\nu_0}{\pi}\right).I(\nu,\nu_0)}$$

does not correspond to any of the parametrisations previously discussed.

VALUES OF PARAMETERS

In order to be able to use experimental curves for $A_\ell(\nu)$, we fitted the curves, obtained by other workers using different parametrisations, to the parametric forms discussed. This was done by an auxiliary programme which varied the parameters to find a least squares fit, between the curves. The two parameters in the simple resonance formulae could be determined from the position and width.

For the ρ and the fo described by a simple Breit Wigner, taking the ρ as 763 Mev full width 124 Mev the correspondences are

$$\left.\begin{array}{ll} 701 \text{ Mev} & \sim 5.29\, m_\pi{}^2 \\ 763 \text{ Mev} & \sim 6.4\, m_\pi{}^2 \\ 825 \text{ Mev} & \sim 7.68\, m_\pi{}^2 \end{array}\right\} \begin{array}{l} 1.13 \\ 1.26 \end{array} \Big) \; 1.2$$

$$\therefore \quad \nu_R = 6.4 \; ; \; \Gamma\nu_R = 0.92 \; ; \; \Gamma = 0.144$$

or in terms of a_i in type 2 Breit Wigner

$$a_1 = 24.3; \qquad a_2 = -3.78$$

For the fo 1253 Mev width 118 Mev.

$$\left.\begin{array}{ll} 1194 & \sim 17.15 \\ 1253 & \sim 19.00 \\ 1312 & \sim 20.90 \end{array}\right\} \begin{array}{l} 1.85 \\ 1.90 \end{array} \Big) \; 1.88$$

$$\therefore \quad \nu_R = 19.00, \quad \Gamma\nu_R{}^2 = 1.44, \quad \Gamma = 0.00040$$

or $\quad a_1 = 2585.0; \quad a_2 = -136.0$

The ρ and fo amplitudes are given in Table 2.

For S-waves, three different sets of data with different scattering lengths a, were fitted

(1) $a = 0.67$ $\quad \delta$ rising to 20°
(2) $a = 1.2$ $\quad$ " 28°
(3) $a = 0.35$ $\quad$ " 12°

Fig. 15. S-wave curves.

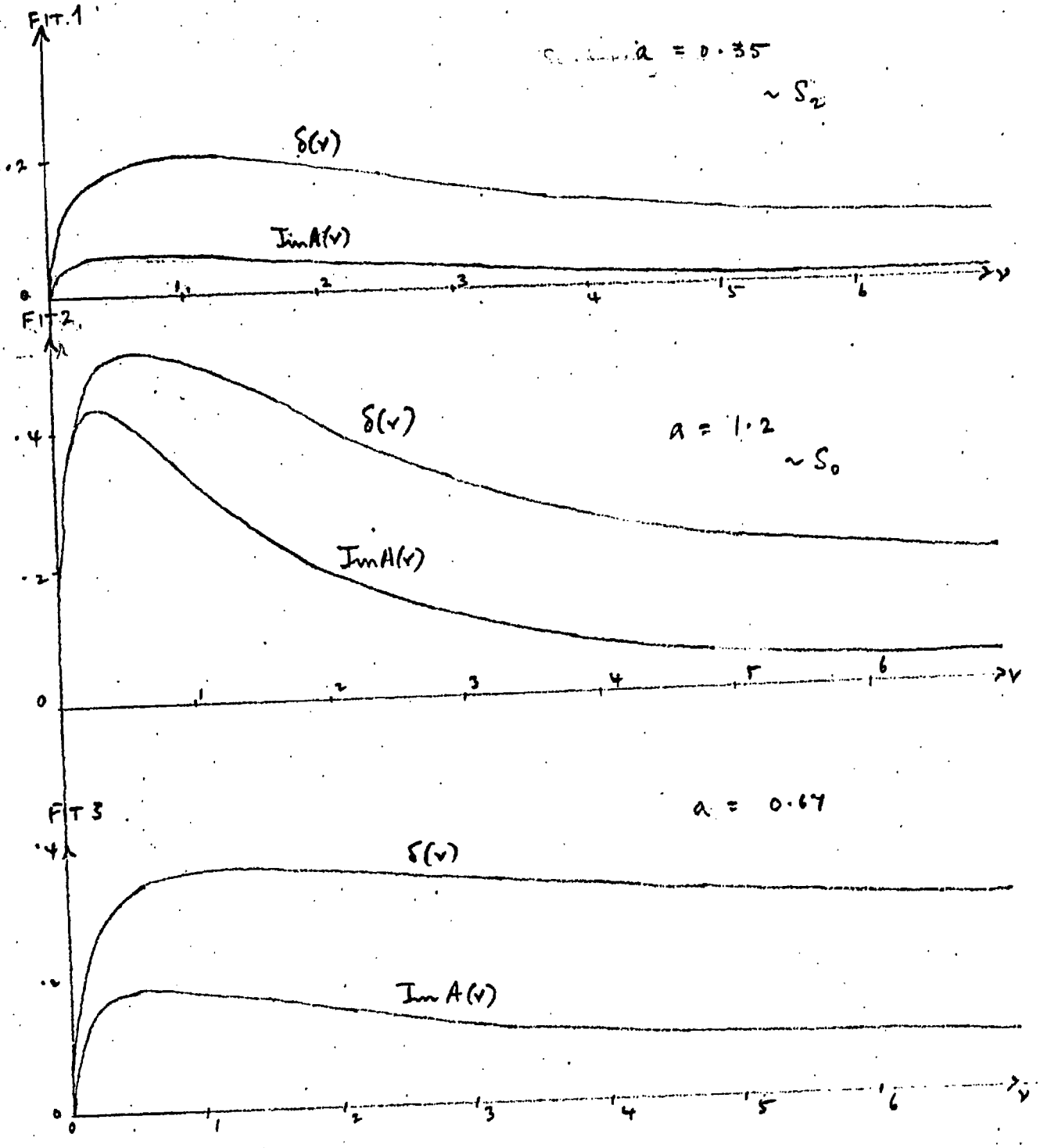

Table 2-2-a Experimental Values - P_1 and D_0 waves.

P_1 wave		D_0 wave		
Re A(ν)	Im A(ν)	Re A(ν)	Im A(ν)	ν
0.004	0.000	0.000	0.000	0.100
0.008	0.000	0.000	0.000	0.200
0.018	0.000	0.000	0.000	0.400
0.027	0.000	0.000	0.000	0.600
0.038	0.001	0.000	0.000	0.800
0.049	0.002	0.000	0.000	1.000
0.061	0.003	0.001	0.000	1.200
0.073	0.004	0.001	0.000	1.400
0.087	0.006	0.001	0.000	1.600
0.102	0.008	0.001	0.000	1.800
0.118	0.012	0.002	0.000	2.000
0.165	0.023	0.003	0.000	2.500
0.223	0.045	0.004	0.000	3.000
0.293	0.082	0.006	0.000	3.500
0.378	0.147	0.008	0.000	4.000
0.471	0.263	0.010	0.000	4.500
0.540	0.456	0.013	0.000	5.000
0.509	0.734	0.016	0.000	5.500
0.290	0.995	0.020	0.000	6.000
-0.048	1.072	0.025	0.001	6.500
-0.318	0.964	0.030	0.001	7.000
-0.460	0.800	0.036	0.001	7.500
-0.516	0.655	0.043	0.002	8.000
-0.528	0.543	0.050	0.002	8.500
-0.523	0.459	0.059	0.003	9.000
-0.510	0.397	0.069	0.005	9.500
-0.494	0.349	0.081	0.006	10.000
-0.479	0.312	0.095	0.009	10.500
-0.464	0.283	0.110	0.012	11.000
-0.451	0.259	0.128	0.016	11.500
-0.438	0.240	0.148	0.021	12.000
-0.427	0.224	0.172	0.029	12.500
-0.417	0.210	0.199	0.040	13.000
-0.408	0.199	0.231	0.054	13.500
-0.400	0.189	0.267	0.074	14.000
-0.392	0.180	0.309	0.103	14.500
-0.386	0.173	0.356	0.142	15.000

BW P_1 expt Re

BW P_1 expt Im

Re BW D_0 expt

Im BW D_0 expt

parameters	a_1	a_2	ν_R	$\Gamma_{\nu_R}^{\ell}$
P_1 wave:	24.3,	-3.78	6.4	0.92
D_0 wave:	2585.0,	-136.0	19.00	7.44

Table 2-2-b Experimental Values - S waves.

FIT 1		FIT 2			FIT 3		
Im A(ν)	δ(ν)	Im A(ν)	δ(ν)	ν	Im A(ν)	δ(ν)	ν
0.012	0.035	0.144	0.120	0.010	0.045	0.067	0.010
0.036	0.104	0.364	0.338	0.100	0.124	0.195	0.100
0.047	0.138	0.419	0.426	0.200	0.154	0.253	0.200
0.052	0.159	0.430	0.472	0.300	0.167	0.287	0.300
0.056	0.174	0.425	0.497	0.400	0.173	0.309	0.400
0.058	0.183	0.413	0.510	0.500	0.175	0.324	0.500
0.056	0.200	0.325	0.500	1.000	0.166	0.350	1.000
0.048	0.194	0.246	0.452	1.500	0.151	0.349	1.500
0.039	0.180	0.186	0.400	2.000	0.138	0.342	2.000
0.032	0.165	0.142	0.354	2.500	0.126	0.333	2.500
0.026	0.151	0.111	0.316	3.000	0.118	0.325	3.000
0.021	0.138	0.089	0.285	3.500	0.110	0.317	3.500
0.018	0.127	0.074	0.260	4.000	0.105	0.311	4.000
0.015	0.119	0.062	0.240	4.500	0.100	0.305	4.500
0.013	0.110	0.054	0.224	5.000	0.096	0.300	5.000
0.012	0.103	0.048	0.212	5.500	0.092	0.295	5.500
0.010	0.098	0.044	0.204	6.000	0.089	0.291	6.000
0.010	0.094	0.042	0.199	6.500	0.086	0.287	6.500
0.009	0.092	0.041	0.195	7.000	0.083	0.283	7.000
0.009	0.090	0.041	0.197	7.500	0.080	0.278	7.500
0.008	0.089	0.043	0.202	8.000			
0.008	0.090	0.047	0.212	8.500			
0.009	0.091	0.054	0.228	9.000			
0.009	0.095	0.067	0.255	9.500			
0.010	0.100	0.092	0.300	10.000			
0.012	0.109	0.146	0.383	10.500			
0.015	0.122	0.302	0.568	11.000			
0.021	0.144	0.840	1.115	11.500			
0.034	0.183	0.657	0.918	12.000			
0.074	0.269	0.177	0.425	12.500			

S2 2.837.

S0 0.822

S1 1.478

Parameters						
FIT	1	~	2.837	0.434	0.239	-0.022
	2	~	0.822	0.363	0.123	-0.014
	3	~	1.478	0.516	-0.059	0.003

The results of the fit for a four parameter polynomial BW formula were, for

a_1 :

(1) 1.478, 0.516, -0.059, 0.003

(2) 0.822, 0.363, 0.123, -0.014

(3) 2.837, 0.434, 0.239, -0.022

shown in Figure 15 and Tables 2.

The S waves only had a small effect in most calculations and the curves deduced from these parameters were only used to give a general idea of the effect of S waves. In the inverse amplitude calculations, the S waves had a large effect and all 3 fits were used at times. Usually S_0 used fit 2 and S_2 fit 3. A few searches were tried using the N/D parametrisation but no convincing fits were found. To find promising starting values in parametric searches, a technique of "parametric matching" was used. This simply means taking only the many data points as there are parameters and inverting the linear equations usually obtained (if we use $\tan\delta(\nu_i)$ as data values) to get unique values for the parameters which gives a curve going exactly through the small number of data points and perhaps not fitting very well elsewhere. Starting from these values, the parameters can now be varied by a minimising routine to give a least squares fit.

INELASTICITY

We used mainly the parametrisation due to Oades

$$R(\nu) = 1 + \sqrt{\frac{\nu-3}{\nu}} \cdot \left[1 - \frac{a}{\nu+b}\right] \cdot \theta(\nu-3)$$

which has a square root behaviour at the inelastic threshold and $\to 2$. His $\nu \to \infty$ values of a and b were: a = 75.0, b = 100.0. With these values, the factor

$$f_1 = 1 - \frac{a}{\nu+b} = \frac{\nu+b-a}{\nu+b} = \frac{\nu+25}{\nu+100}$$

for $\nu = 10$, $f_1 = \frac{35}{110} \sim \frac{1}{3}$; $\nu = 100 \sim \frac{1}{2}$

$\nu = 20$, $f_1 \sim \frac{1}{3}$; $\nu = 1000 \sim 1$.

The factor $f_2 = \sqrt{\frac{\nu-3}{\nu}}$, for $\nu = 6$ $f_2 \simeq .7$

$\nu = 12$ $f_2 \simeq .9$

Thus the factor f_1 hardly varies in the near region.

The analytic properties of the parametrisation are unimportant, as we only use the values of the function in the regions where they were fitted. It is a convenient way of expressing data.

A simpler form without the finite limit 2 at infinity is

$$R(\nu) = 1 + \theta(\nu-3)\cdot a\cdot(\nu-3)$$

or if one is going to integrate it with $\sqrt{\frac{\nu}{\nu+1}}$, one might take

$$R(\nu) = 1 + \theta(\nu-3)\cdot a(\nu-3)\cdot\sqrt{\frac{\nu+1}{\nu}}$$

An extended form of the Oades parametrisation is

$$R(\nu) = 1 + \theta(\nu-c)\cdot\sqrt{\frac{\nu-c}{\nu}}\cdot\left[1 - \sum_{i=1}^{n}\frac{a_i}{\nu+b_i}\right]$$

The evaluation of the inelastic kernel function

$$\int_0^\infty \sqrt{\frac{\nu'}{\nu'+1}}\cdot\frac{R(\nu')\,d\nu'}{(\nu'-\nu)(\nu'-\nu_0)}$$

, for this parametrisation, is shown in the appendix.

Inelasticity can be incorporated in the other parametrisations by replacing

$$\sqrt{\frac{\nu}{\nu+1}} \rightarrow R(\nu)\cdot\sqrt{\frac{\nu}{\nu+1}}$$

The effect of inelasticity upon a resonant amplitude and upon the $C(\nu)$ function is shown in Figs. 16 and 17.

When inelasticity is present, especially rapidly varying inelasticity, there is some arbitrariness in the definition of resonant behaviour and in the position of the resonance. This is particularly important in phenomenological analyses of data and especially in phase shift analysis. In this case one uses an argand diagram ReA vs. Im$A(2\theta)$. A constant inelasticity Breit Wigner formula gives a circle. An inelastic resonance is identified by a closed loop and the position of the resonance is arbitrarily taken as at the top of the loop.

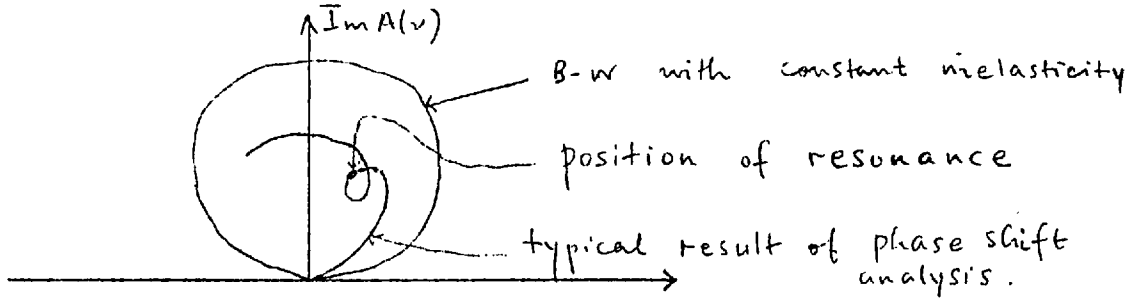

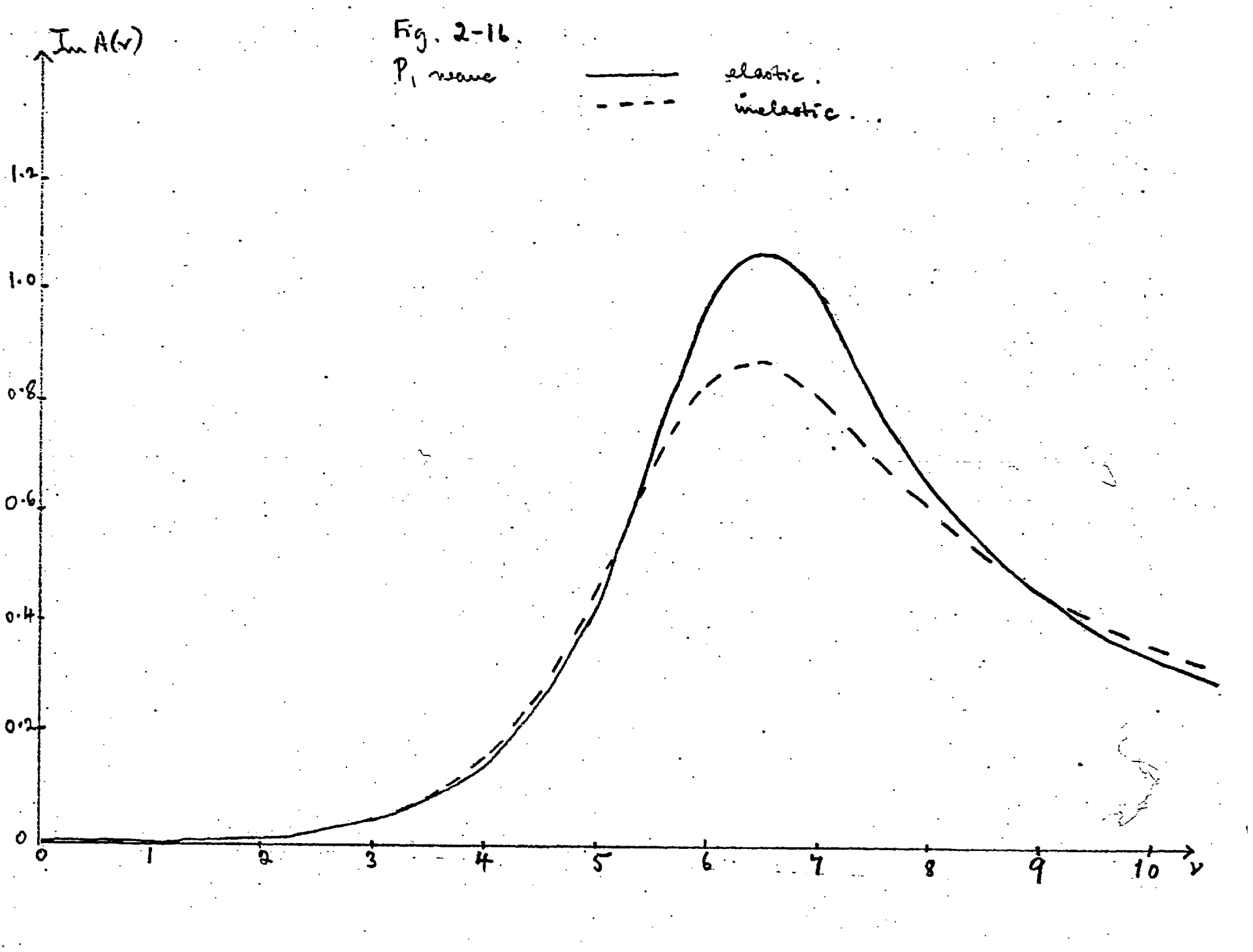
Im A(ν)
Fig. 2-16.
P, wave
elastic.
inelastic..
1.2
1.0
0.8
0.6
0.4
0.2
0
0
1
2
3
4
5
6
7
8
9
10
ν

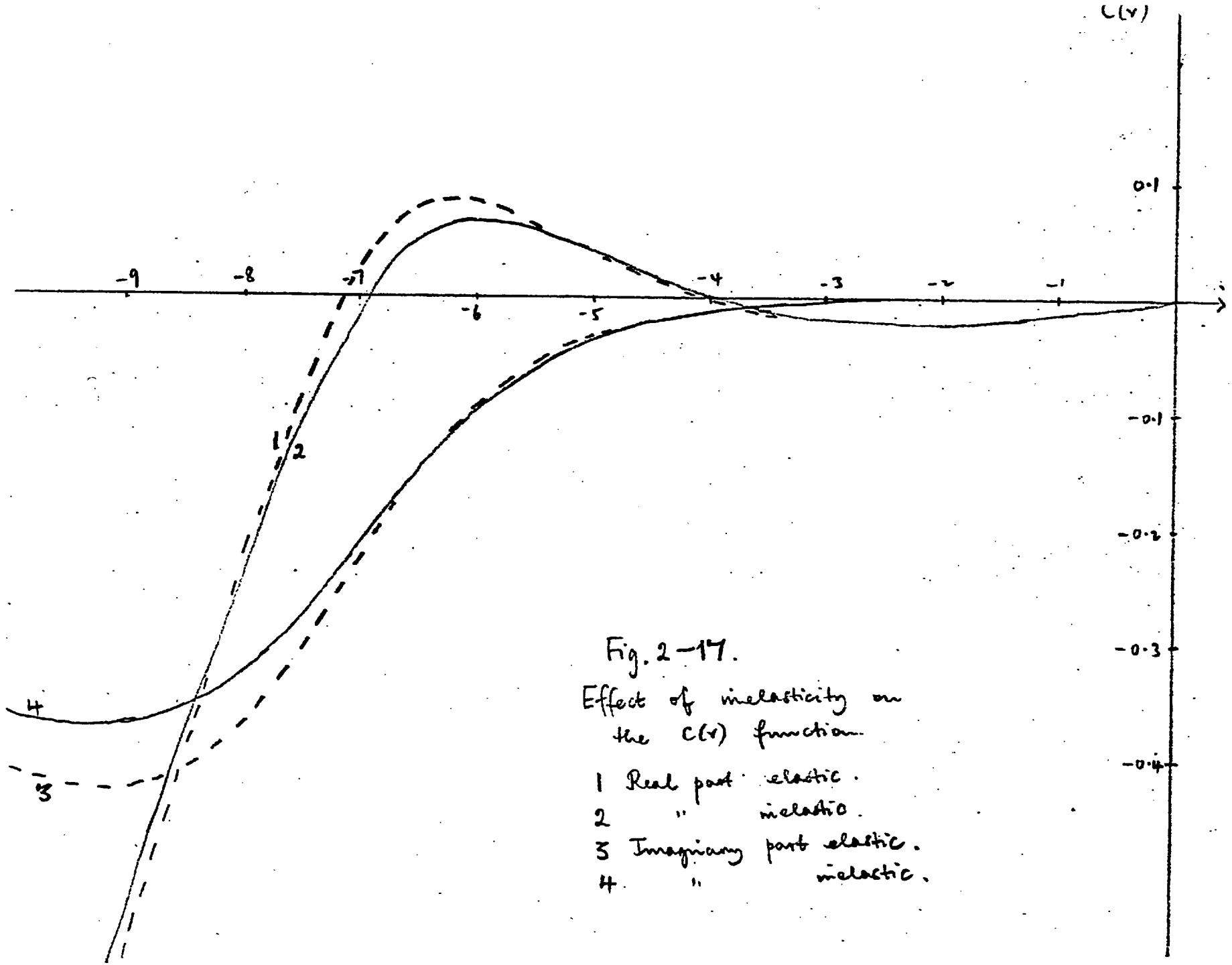

Fig. 2-17.

Effect of inelasticity on the C(r) function

1 Real part elastic.
2 " inelastic.
3 Imaginary part elastic.
4 " inelastic.

CHAPTER 3

THE BALAZS METHOD

I. THE ORIGINAL METHOD AS USED BY BALAZS

1. Statement of the method

Using a fixed s dispersion relation, in the δ function approximation discussed in Chapter 2, one obtains an estimate for the real part of the amplitude on the near left.

$$A_\ell(\nu) \sim C_\ell(\nu) = \frac{4}{\pi\nu} \sum_{\ell'=L1}^{L2} (2\ell'+1) \sum_{I'=0}^{2} \beta_{II'} \cdot \pi \Gamma_{\nu_R}^{\ell'} \cdot P_{\ell'}\left[1 + 2\left(\frac{\nu+1}{\nu_R}\right)\right] Q_\ell\left[1 + 2\left(\frac{\nu_2+1}{\nu}\right)\right]$$

where we have chosen to consider a finite set of partial waves in the crossed (t) channel with angular momenta $\ell' = L1, L2$, in each of which there is a resonance, and we are neglecting all the other partial waves. Thus, for any particular partial wave we have this estimate for the amplitude for ν in $\approx [-\infty, 0]$, in a form which has only a left hand cut. We wish to obtain a form for $A_\ell(\nu)$ approximately equal to this on the left, but having a right hand cut and obeying unitarity. Note that $C_\ell(\nu)$ is an estimate for the whole of $A_\ell(\nu)$, not just the contribution from the left hand cut.

In order to continue to the right hand side, i.e. s channel physical region, we match to an N/D pole form, which has a right hand cut and satisfies unitarity.

$$N(\nu) = A(\nu_0) + (\nu - \nu_0) \cdot \sum_{i=1}^{u} \frac{F^i}{\nu - \nu_i}$$

$$D(\nu) = 1 - \left(\frac{\nu - \nu_0}{\pi}\right) \sum_{i=0}^{u} F^i \cdot I(\nu, \nu_i)$$

where $I(\nu, \nu_i)$ is the kernel function discussed in Chapter 2.

$$I(a,b) = \int_0^\infty dv' \cdot R(v') \cdot \sqrt{\frac{v'}{v'+1}} \cdot \frac{1}{(v'-a)(v'-b)}$$

We take $R(v') = 1$, all v' in $[0, \infty]$.

The positions of the poles on the left, $\{v_i\}$ are not regarded as variable parameters but are held fixed at values determined, in an auxiliary calculation (see next section), as the best positions in some sense. In order to determine $A_\ell(v) = \frac{N_\ell(v)}{D_\ell(v)}$ everywhere, we need to find $A(v_0)$ and $\{F_i\}$, and this we do by the already mentioned matching process. We match N/D to C (v) at a finite set of "symmetry points" on the left, i.e. we equate

$$C(v_{Fj}) = \frac{N(v_{Fj})}{D(v_{Fj})} \quad , \quad j = 1 \qquad n+1.$$

which gives linear algebraic equations for the $\{F_i\}$. The $\{v_{Fj}\}$ are supposed arbitrary but must lie in the region where C (v) is known viz [9-9]. We must avoid the singularity of C (v) at $v = -v_R - 1$, and as the behaviour of C (v) in $[0, -v_R - 1]$ is thought to be more relevant to the right hand side than that in $[-v_R - 1, -9]$, we take the $\{v_{Fj}\}$ in $[-v_R - 1, 0]$, but not too close to the singularity.

Putting $$N(v) = (v - v_0) \cdot \sum_{i=0}^{n} \frac{F^i}{v - v_i}$$

where $F^0 = A(v_0)$

the matching equations are

$$\frac{(v_{Fj} - v_0) \cdot \sum_{i=0}^{n} F^i / (v_{Fj} - v_i)}{\left[1 - \left(\frac{v_{Fj} - v_0}{\pi}\right) \sum_{i=0}^{n} F^i, I(v_i, v_{Fj})\right]} = C(v_{Fj}) \; ; \; j = 0 \cdots n$$

i.e. $$\sum_{i=0}^{n} E^{ji} F^i = C^j .$$

where $$C^j = C(v_{Fj})$$

$$E^{ji} = (v_{Fj} - v_0) \cdot \left[\frac{1}{v_{Fj} - v_i} + \frac{C^j, I(v_i, v_{Fj})}{\pi}\right]$$

The $\mathrm{Im}\, A_\ell^I(v)$, $= -\sqrt{\frac{v}{v+1}} \cdot \left|\frac{N}{D}\right|^2$, function in the s channel physical region constitutes the output to be compared with the $\mathrm{Im}\, A_\ell^{I'}(v')$ input from the t channel, and one demands rough self consistency by

$$v_{R\,out} = v_{R\,in}$$

$$\Gamma^{l}_{v_{R}\,out} = \Gamma_{in}\, v_{R\,in}^{l}$$

where $R^{l}_{out} = N_{in}(R_{in}). \quad (R_{in} - o)$

This definition of $(\Gamma^{l}_{v_R})_{out}$ is more convenient than and very close to

$$(\Gamma^{l}_{v_R})_{out} = -N_{out}(v_{R\,in}) \,/\, Re\, D'_{out}(v_{R\,in})$$

and is obtained from this by the linear approximation for D

$$Re\, D'(v) = -1 \,/\, (v_{R\,in} - v_0)$$

which is justified a posteriori.

The first condition is specified by

$$Re\, D_{out}(v_{R\,in}) = 0 .$$

The Balazs method was initiated in BI(1) and BII(1), BI explaining the kernel approximation and BII carrying out the calculation for the $I = 1 \;\; J = 1 \;\; \pi\pi$ state, obtaining self-consistent values $v_R = 3.4, \Gamma_{v_R} = 2.6$ i.e. $v_R \sim 585$ Mev, full width ~ 150 Mev. BIII(1) extended the calculation to $I = o \;\; J = 2$ and $I = 1 \;\; J = 1$ coupled and also did a calculation for $I = o$, 2 s waves. The method has been used by various other authors (3) (4).

2. The Kernel approximation

The significance of the Balazs method is in the pole approximation which finds optimum positions for the poles depending only upon the kernel in

$$N(v) = A(v_0) + \left(\frac{v - v_0}{\pi}\right) \int_{-\infty}^{-1} \frac{Im\, A(v')\, D(v')\, dv'}{(v' - v)(v' - v_0)}$$

The kernel is approximated by a pole form which simultaneously expresses it as a sum of degenerate kernels and gives $N(v)$ a form which is easily integrable to give $D(v)$. Writing $x = -1/v'$ we approximate

$$K_{exact}(x,v) = \frac{1}{1 + xv} \approx \sum_{i=1}^{n} \frac{G_i(x)}{1 + x_i} = K_{app}(x,v)$$

where the $\{ G_i(x) \}$ are Lagrange interpolatory rational functions having values unity at $\{ x_i \}$. One varies $\{ x_i \}$ to give the best agreement for ν fixed at some point in the range over which the approximation is to be used. One also chooses a cut off ν_L for generality, taking the integral from ν_L to $-\infty$.

There is some freedom of interpretation of the requirement if best fit, and we minimised over a set of points in the range $[0, \nu_L]$. The distribution of points was determined by a power law

$$\nu^j = \nu_L \cdot \left(\frac{j}{m}\right)^p \qquad j = 1, m$$

m being the number of points, usually kept at value 20, and p an index, which could be varied. The results of a typical fit are shown in Fig. 1. Values of the pole positions and an indication of dependence on ν_L, ν and p are shown in Table 1, also the change in CHI^2 during optimisation. The solution 6 (1) has a pole on the right hand side and may be permissible, if we take the N function to include the inelastic cut as well as the left hand cut, as explained in BII. The effects on the Balazs calculation will be seen later. Note that the difference in CHI^2 produced by optimisation is only of the same order as that from increasing n by 1.

We wish to make three points about the kernel approximation;

i. It is valid if and only if the dispersion integral converges.

For the exact integral

$$I_1(\nu) = \int_{-\infty}^{\nu_L} \frac{f(\nu')d\nu'}{\nu' - \nu} = \int_{-\infty}^{\nu_L} f(\nu') \cdot \frac{K_{exact}(\nu', \nu)}{\nu'} \cdot d\nu'$$

is replaced by

$$I_1'(\nu) = \int_{-\infty}^{\nu_L} d\nu' \cdot \frac{K_{app}(\nu', \nu)}{\nu'} = C_1 \cdot \frac{I_2(\nu_2)}{\nu_1 - \nu} + \frac{C_2 \cdot I_2(\nu_1)}{\nu_2 - \nu}$$

where

$$I_2(a) = \int_{-\infty}^{\nu_L} \frac{f(\nu') \cdot (\nu' - a)}{\nu'^2} d\nu'$$

for a two pole approx., and

$$C_1 = \frac{\nu_1}{\nu_2} \cdot \frac{1}{x_1 - x_2} \; ; \quad C_2 = \frac{\nu_2}{\nu_1} \cdot \frac{1}{x_2 - x_1}$$

TABLE 3 -1 Belazs Pole Positions

(1) Basic Result:

$n = 2$, $\nu = 0.5$, $\nu_L = -5$, $P = 1$.

$\nu_i = -6.0, -25.0$.

(2) Variation with ν_L:

$\nu_L = -10$	$\nu_i = -12.3, -42.2$
" -2	" $-2.48, -8.696$
" -1	" $-1.25, -4.46$.

(3) Variation with p:

$p = 0.5$	$\nu_i = -5.78, -12.3$
" 2.0	" $-6.45, -39.8$

(4) Variation with ν:

$\nu = 1.0$	$\nu_i = -6.135, -22.5$
3.0	$-6.25, -22.6$
5.0	$-6.29, -23.4$

(5) Variation with n:

$n = 3$	$\nu_i = -5.49, -9.62, -36.1.$
4 "	$-5.316, -7.194, -13.44, -50.8.$
5 "	$-5.13, -6.33, -9.62, -19.3, -64.5.$
6(1) "	$-5.07, -7.87, -8.13, -11.55, -47.6, +14.6.$
6(2) "	$-5.29, -6.94, -9.52, -13.89, -14.28, -19.23.$

(6) Chi-squared optimisation:

n	initial χ^2	final χ^2
3	$.9 \times 10^{-8}$	$.3 \times 10^{-8}$
4	$.8 \times 10^{-11}$	$.1 \times 10^{-11}$
5	$.5 \times 10^{14}$	$.8 \times 10^{-15}$
6(1)	$.3 \times 10^{-14}$	$.2 \times 10^{-16}$
6(2)	$.3 \times 10^{-15}$	$.3 \times 10^{-17}$

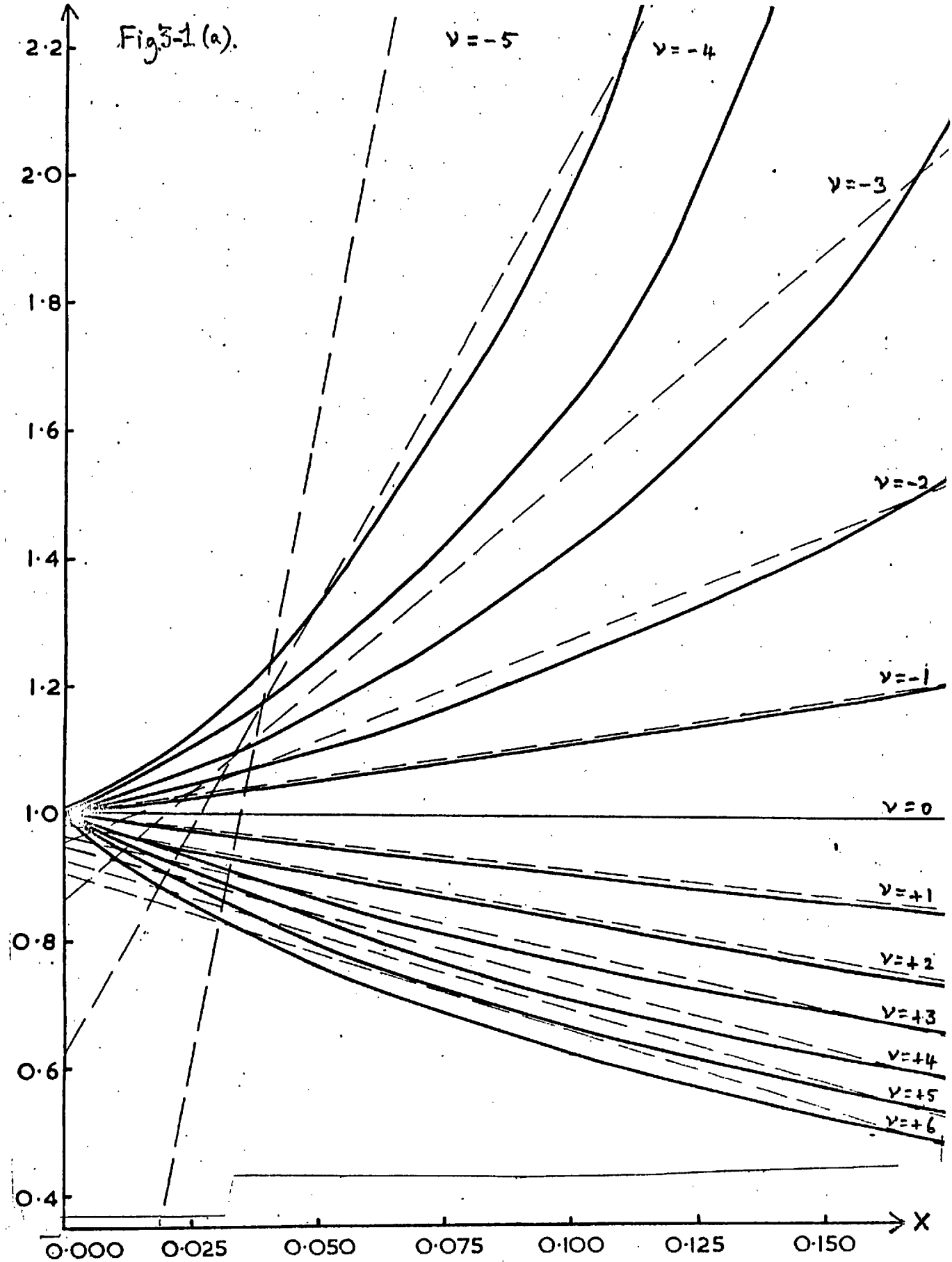
Fig3-1 (a).
ν = -5
ν = -4
ν = -3
ν = -2
ν = -1
ν = 0
ν = +1
ν = +2
ν = +3
ν = +4
ν = +5
ν = +6
2·2
2·0
1·8
1·6
1·4
1·2
1·0
0·8
0·6
0·4
X
0·000
0·025
0·050
0·075
0·100
0·125
0·150

Fig. 3-1(b).

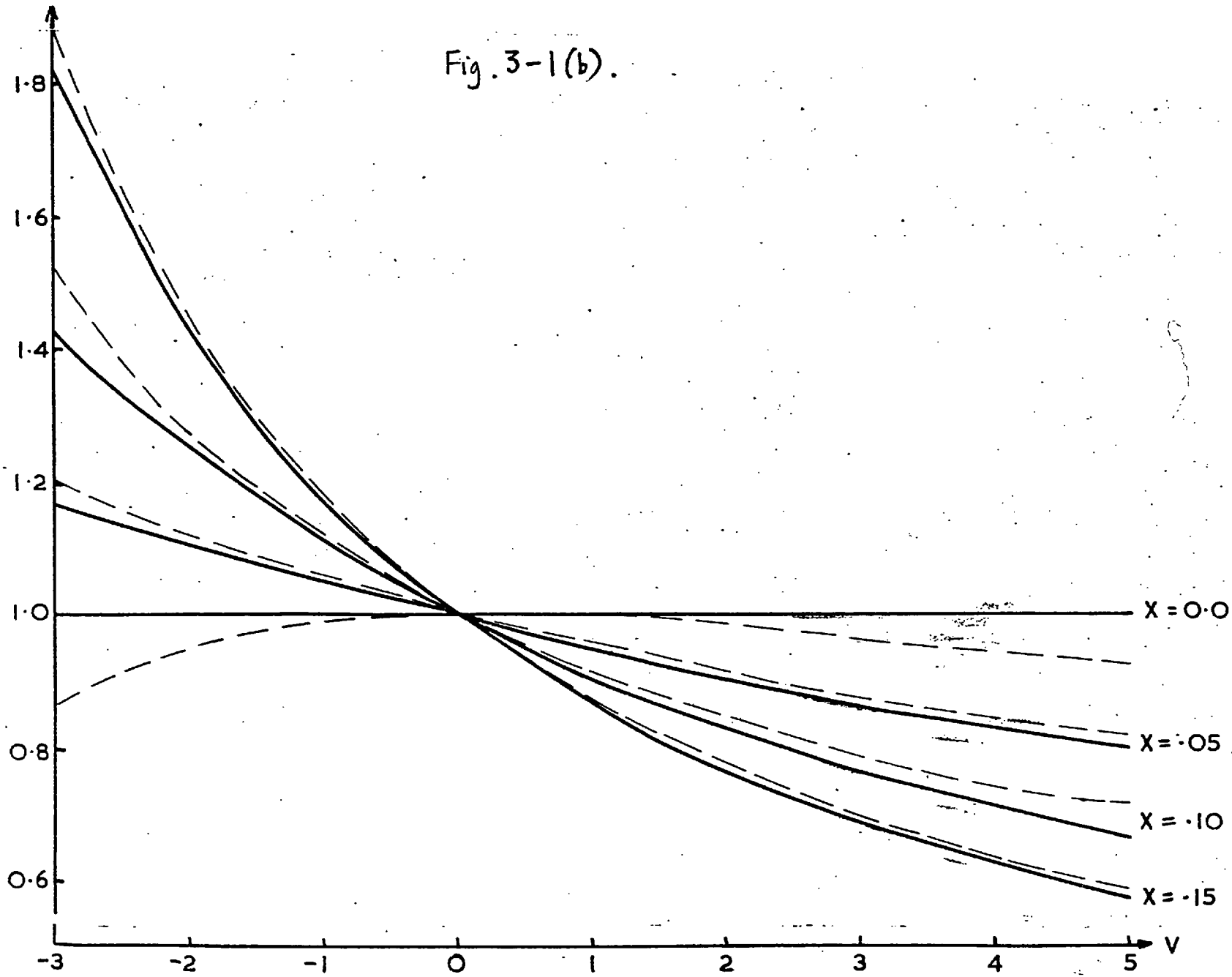

Now the conditions for convergence of $I_1(\nu)$ and $I_2(a)$ are identical, and in practice reduce to

either (a) $f(\nu') \to 0$
$\nu' \to \infty$

or (b) $f(\nu') = \sin(u\nu') \cdot g(\nu')$, u real > 0

$\frac{g(\nu')}{\nu'} \to 0$ steadily.
$\nu' \to \infty$

for all finite ν, a.

(ii). The asymptotic behaviour of the approximated integral is not necessarily $O\left(\frac{1}{\nu}\right)$.

For what the kernel approximation asserts is that

$$\int \frac{f(\nu')\,d\nu'}{\nu'-\nu} \simeq \sum_i \frac{F^i}{\nu_i-\nu}$$

in a small range of ν, where ν is sufficiently far from the cut. It does not attempt to be valid on the cut as $\nu \to -\infty$, $\nu_i \to -\infty$ (i) and (ii) indicate that it is not a usual pole approximation and not equivalent to a cut off.

iii. It is still a good approximation for oscillating functions, i.e. conditionally convergent integrands. For, from (i) it still converges and, in BI, Balazs gives an estimate for the % error for an oscillating function. Now when the oscillations exactly cancel the exact integral has a zero, so the % error is infinite; however this is merely due to the fact that the approximate integral has a zero slightly displaced. Numerical estimates of Balazs expression from BI for the % error, using the kernel approx. of Fig.1.

$$E = \left[\frac{\Delta D_1'}{D_1} - \frac{\Delta D_2'}{D_2}\right] \Big/ \left[\frac{D_1}{D_1} - \frac{D_2}{D_2}\right] \quad \times 100\%$$

If we take the oscillations to exactly cancel at $\nu = -2$, $E = \infty$, then when

ν =	-1	E = 0.4%
	+1	0.04%
	+5	0.3%
		0% always.

Note from Figs. 2 the % error is zero for = 0 and 5% as $\nu \to -\infty$.

The assertion is not that any kernel approximation within 5% of the exact is accurate for oscillating functions, for this is clearly untrue, but that this particular approximation is. We have made it plausible that the $N(\nu)$ function can be well approximated by the pole form in a certain finite range. For example, a two pole fit is accurate to 10%, for ν in $[-3, 6]$, for all ν' in $[VL, -\infty]$, and a six pole fit is accurate to 1%, for ν in $[-3,15]$. However, to form the $D(\nu)$ function we need an estimate for $N(\nu)$ for the entire range $[0,\infty]$. (8).

To see how the approximation varies in this range, we did two studies. First, we found the optimum ν_i for n = 2, for a series of values of ν in the range. The results are shown in Table 1(4) and show that the optimum ν_i change slowly and monotonically from $\nu = 1.0$, $\nu_i = 6.17$, 21.6, to $\nu = 100.0$, $\nu_i = 6.80$, 37.6, but that the value of χ^2 at the optimum value changes rapidly, starting at 10^{-5}, rising to 10^{-1} at $\nu = 50$, and then decreasing to 10^{-3}, for $\nu = 10^3$. Second, we evaluated K exact - K approx. for a series of values of ν, the ν_i being the optimum values for $\nu = 0.5$. K exact - K approx. was roughly constant for ν' in $[VL, -\infty]$, except that, for large negative ν', it rose by a factor of 10 or so. The values for typical ν' are plotted versus ν in fig. 1(C). We see the following, (A) the "asymptotic" value of K exact- K approx. is roughly the same for all n. and is 10^{-4}, so the % error = 10%.

(B) The error rises from very low values for $\nu < 10$ to 10^{-3} or so for $\nu = 50$, for n = 2, K exact- K approx. = 10^{-2} and the % error $< 10\%$.

(C) As n increases the error gets very small for ν in $[0,100]$.

Now, because we are evaluating $D(\nu)$, the very high values in the integral will be damped by the Cauchy denominators. Also for large negative ν', the error rises by a factor of 10 for all ν, however the contributions from this region are damped by the $(\nu' - \nu_0)$ denominator in the $N(\nu)$ integral.

Thus, our conclusion is that, for a sufficient number of poles, one can achieve sufficiently accurate values of $N(\nu)$, to achieve an accurate value of $D(\nu)$, provided one has accurate values of F^i.

We should finally like to compare the pole positions obtained by the

Fig 3-1(c).

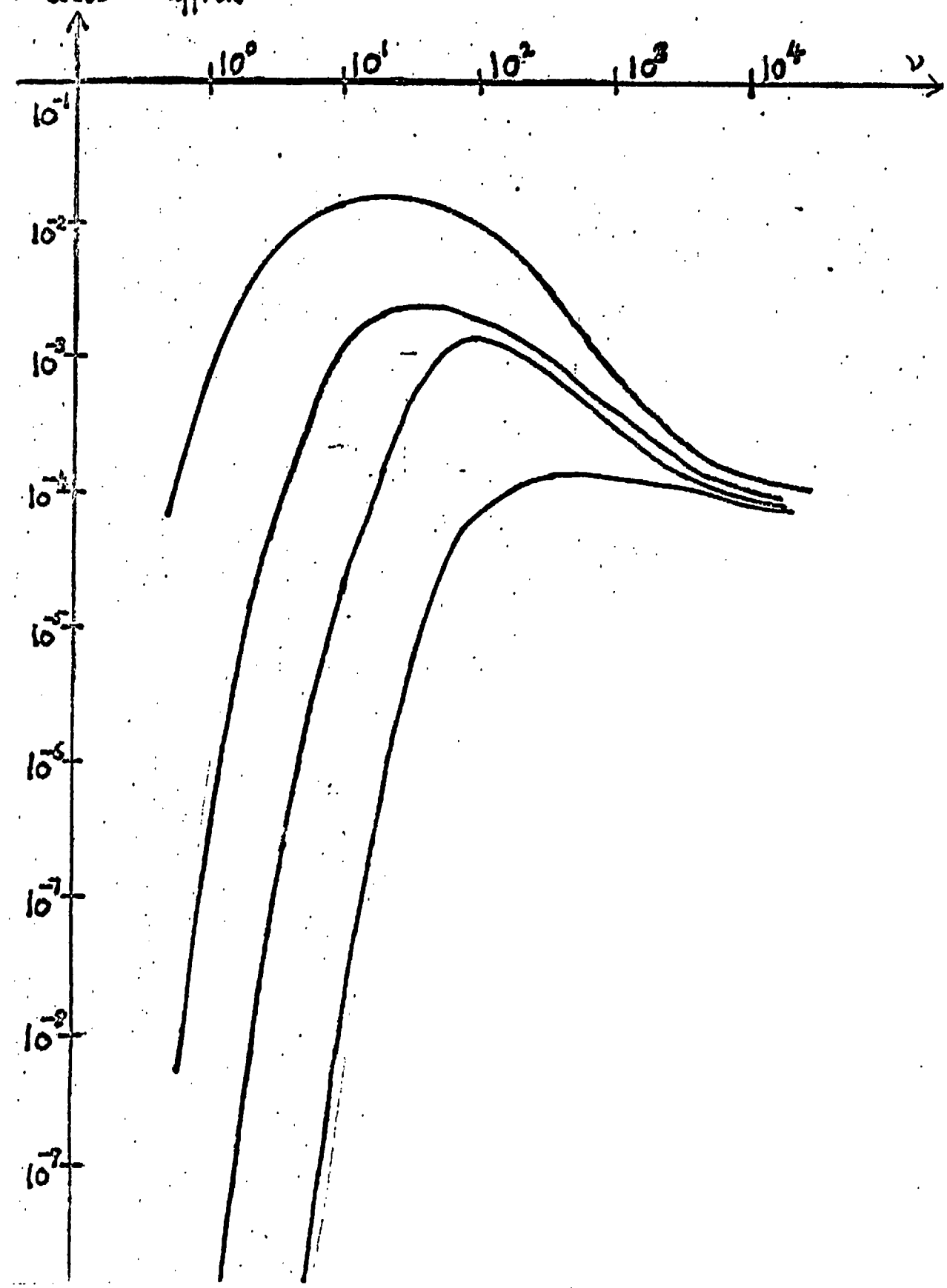
$(K_{exact} - K_{approx})$
10^0
10^1
10^2
10^3
10^4
ν
10^{-1}
10^{-2}
10^{-3}
10^{-4}
10^{-5}
10^{-6}
10^{-7}
10^{-8}
10^{-9}

Balazs optimisation prooedure with those obtained by using a numerical integration formula. If we wish to integrate

$$\int_{-\infty}^{-\nu_L} dx.\ f(x)$$

then we can first transform to a finite range by

$$z = \frac{x - \nu_L}{x}$$

then z decreases from 0 to -1 as

x decreases from $-\nu_L$ to $-\infty$

further

$$x = \frac{\nu_L}{1 - z}$$

so $$dx = \nu_L \cdot \frac{dz}{(1-z)^2}$$

and we have

$$\int_{-1}^{o} dz.\ \frac{\nu_L}{(1 - z)^2} \cdot f\left[x\ (z) \right].$$

if we do this integration numerically, we take n integration points z^i and weights w^i and take the value of the integral as

$$\sum_{i-1}^{n} w^i.\ \frac{\nu_L}{(1 - z_i')^2} \quad f\left[x\ (z_i) \right]$$

Thus for a dispersion integral

$$f(x) = \frac{h(x)}{(x-\nu)(x-\nu_o)}, \quad \text{say}$$

$$\int_{-\infty}^{-\nu_L} \frac{h(x)\,dx}{(x-\nu)(x-\nu_o)} \approx \sum_{i=1}^{n} w^i \cdot \frac{\nu_L}{(1-z_i)^2} \cdot \frac{h[x(z_i)]}{[x(z_i)-\nu]\cdot[x(z_i)-\nu_o]}$$

a pole approximation with poles at

$$x(z_i) = \frac{\nu_L}{1-z_i}$$

This is equivalent to approximation of the integrand

$\frac{f[x(z)]}{(1-z)^2}$ by polynomials $g^n(z)$

so $\frac{f(x)}{(1-z)^2}$ is approximated by $g^n\left(\frac{x-\nu_L}{x}\right)$

so f(x) is approximated by $\frac{1}{x^2} \cdot g^n\left(\frac{x-\nu_L}{x}\right)$

For Gaussian integration, the $g^n(z)$ are Legendre functions $P_n(z)$ and z^i are its roots. Hence f(x) is approximated by poles of various orders at the origin.

If we put in gaussian points z^i and calculate the corresponding $x(z_i)$, the pole positions on the left hand cut, we obtain the results shown in Table 2. If one takes equally spaced points, omitting the end points, then

$$z^i = \frac{i}{n+1} \qquad i = 1 - - n$$

$$i = \frac{L}{1 - \frac{i}{n+1}} = \frac{(n+1)\cdot\nu_L}{n+1-1}$$

reordering,

$$\nu_j = \frac{(n+1)\cdot\nu_L}{j} \quad ; \quad j = 1 - - n,$$

a harmonic series. The pole distributions are shown in Table 2.

The positions for Gaussian integration are remarkably similar to the Balazs positions and agree much better than those from equal spacing integration.

TABLE 3 - 2

Gaussian Integration Pole Positions:

For $\nu'_L = 5$

n = 2		- 6,	-30			
3		- 5.6	-10.0	-50.0		
4		- 5.4	- 7.5	-15.0	-70.0	
5	-5.15	- 6.0	- 8.05	-13.1	-29.4	-143.0

Evenly spaced Integration Pole Positions:

For $\nu'_L = 5$

n = 2	- 7.5,	-15.0		
3	- 6.5,	--10.0,	-20.0	
4	- 6.25	- 8.33,	-12.5,	-25.0.

Balens Pole Positions:

For $\nu'_L = 5$

n = 2	- 6,	-25			
3	- 5.49	- 9.62	-36.1		
4	- 5.32	- 7.19	-13.44	-50.8	
5	- 5.13	- 6.33	- 9.62	-19.3	-64.5

Now, gaussian points can be generated by a best fit procedure (6) and one wonders whether there is any connection between this and the Balazs optimisation procedure.

Note that there is a simple connection between the pole positions for different ν_L viz.

$$x^i \propto \nu_L$$

If we look at the ν_L variation of the Balazs poles, shown in Table 1 (a), we see a similar behaviour.

Of course, in this treatment, there is no dependence on ν. However, one can see that, for ν near the cut, some modification of the ν^i to fit best might be necessary. Further the Balazs poles become very insensitive to ν, when it is reasonably far from the cut.

Since the integral is

$$\frac{\nu_L}{\nu\nu_0} \int_{-1}^{0} \frac{h[x(z)]}{(a-z)\,(a_0-z)\,(1+z)^2}$$

$$a = \frac{\nu_L}{\nu} - 1\,; \quad a_0 = \frac{\nu_L}{\nu_0} - 1; \quad a,\ a_0 \text{ real} > 0$$

then, presumably, the best positions are given by the roots of polynomials

$gn(z_i) = 0$

where $gn(z)$ are defined by the weight function

$$w(z) = \frac{1}{(a-z)\,(a_0-z)\,(1+z)^2}$$

and interval $[0, -1]$.

Now there is an essential difference between the numerical integration procedure and the Balazs procedure, namely that the Balazs F^i are determined by matching the approximate form to the exact integral, but the numerical integration procedure uses the f $x(z_i)$ to get them. The numerical integration procedure is only valid for integrands which can be approximated by polynomials whereas the Balazs procedure is valid for a

much wider range of integrands.

The similarity between the two lies in the fact that if we tried to approximate a well behaved integral by the Balazs procedure, then we should get the same answer as by numerical integration, hence the pole positions are the same.

3. The P_1 Channel

The N/D form is matched to the $C(\nu)$ function at (n+1) symmetry points to give F_i and $A(\nu_o)$. The properties of the pole form and the mechanism of the process are shown in Fig. 2. Note the near linearity of Re $D(\nu)$ although of course $D \underset{\nu \to \infty}{\longrightarrow}$ constant, justifying the self-consistency conditions used by Balazs and supporting the linear approximation of Pati and also Kane (3). Note that $C(\nu)$ has a logarithmic singularity at $-\nu_R - 1$ but that N/D has a pole at -6.

Symmetry points close together are equivalent to matching derivatives. Because of the sensitivity to symmetry points, it was found clearest to adopt two classes of distribution:

1. "derivative" i.e.1. at the origin to give ν^{-1} behaviour, and (n-1) clustered round one point, usually $\nu = -2$;
2. "distributed" i.e. spread out in $[0, -2.5]$

We did static studies, i.e. fix t channel, match and find s channel, and dynamic studies, i.e. self consistent values of $\nu_R, \Gamma\nu_R^{-1}$. The result of a static study is thus a tabulation of functions $N(\nu)$ and $D(\nu)$ and we shall in general display the function Re $A(\nu)$ derived from them. The result of a dynamic study is whether a self-consistent acceptable solution was obtained and, if so, the self-consistent values of ν_R and $\Gamma\nu_R^{-1}$.

We obtained self consistency by minimising the function

Fig. 3-2.

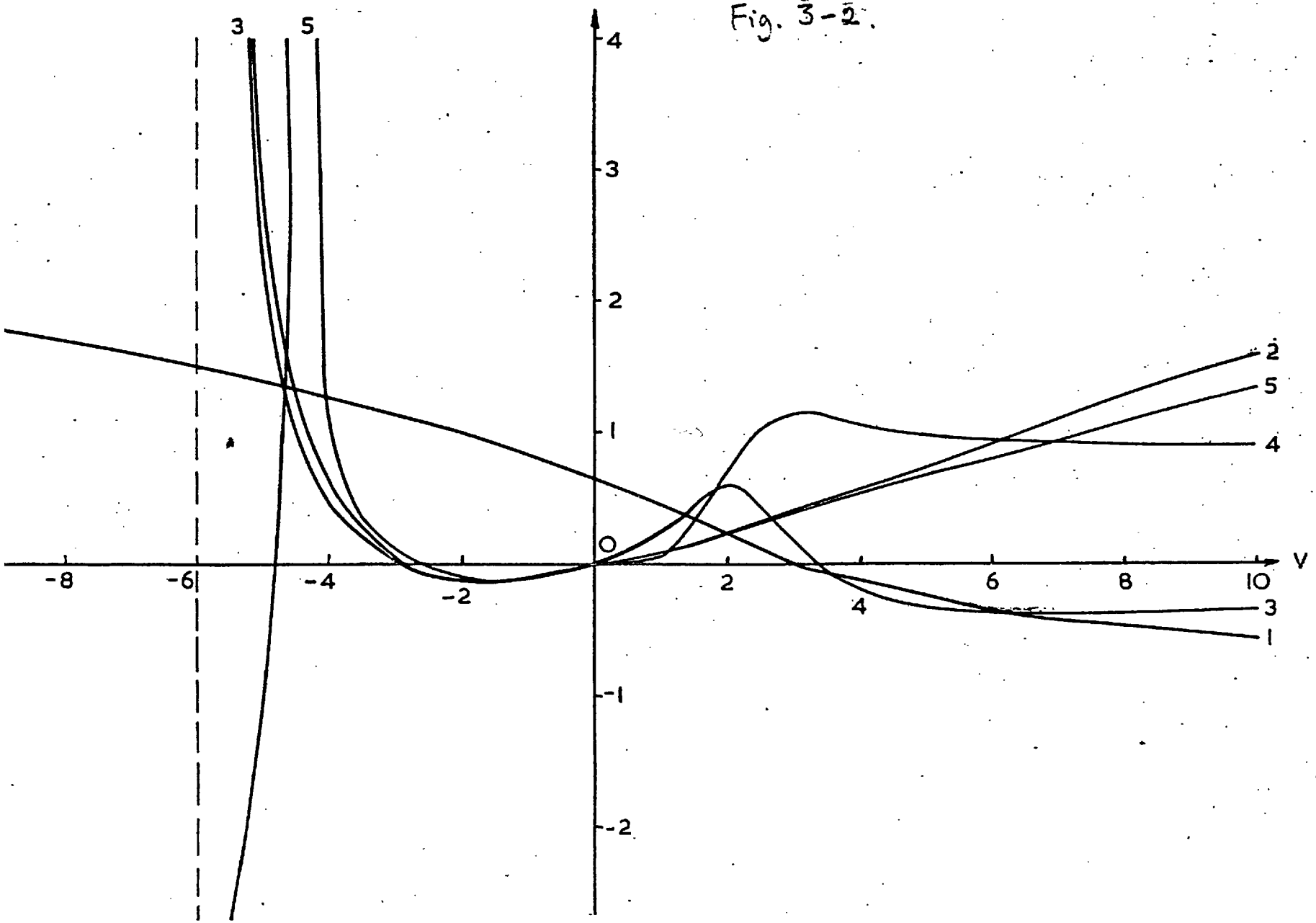

$$F = \left[\mathrm{Re}\, D_{out}(\nu_{R\,in})\right]^2 + \left[\Gamma_{in}\nu_{R\,in}^{1} - N_{out}(\nu_{R\,in}) \cdot (\nu_{R\,in} - \nu_o)\right]^2$$

Figure 3 is a contour plot of it. We see a long shallow valley roughly along the line

$$\Gamma\nu_R = \nu_R.$$

Instead of finding the absolute minimum and taking those values of $(\Gamma\nu_R, \nu_R)$ as the solution, one ought to deduce that only Γ is fixed by the minimisation process to be ≈ 1 and that ν_R is a free parameter.

Looking first at the I = I, J = 1 channel, the static results for variation of $\{\nu_{Fi}\}$ and n are shown in Figs. 4. The variation of ν_o from -3 to 0 produced no detectable change in Re $A(\nu)$ to 1% over the entire range $[-9, +10]$. The dynamic studies show a similar insensitivity to ν_o. The dynamic results are shown in Table 3. It has been pointed out to the author that the extreme insensitivity of the static studies to variation of ν_o is probably a rigorous result derivable from existing theorems. In fact, it does follow easily, but not obviously, and a proof is given below.

The small ν_o dependence of the dynamic studies is due to the ν_o dependence of the self-consistency criterion given by equation (11). Here we prove that a once subtracted N/D pole form, with given left hand pole positions ν_i, whose n + 1 parameters are determined by matching to values C_j at points ν_{Fj}, is independent of the choice of subtraction point. For, given A = N/D

$$N(\nu) = A_o + (\nu - \nu) \sum \frac{F_i}{\nu - \nu_i}$$

$$D(\nu) = 1 - \frac{\nu - \nu_o}{} \int^{x} R(\nu) \cdot d\nu' \sqrt{\frac{\nu'}{\nu'+1}} \cdot \frac{N(\nu)}{(\nu - \nu)(\nu - \nu_o)},$$

one can construct an N', D' with the same form such that $A' = N'/D' = A$, with different subtraction point ν_o'. This can be verified by direct manipulation; N' & D' differ from N & D by a factor $D(\nu_o')$.

TABLE 3 - 3 - a

Dynamic Studies

Self-consistent values of ($\nu_R, \Gamma\nu_R$):

(i) Variation w.r.t. ν_{Fi}:

			ν_R	$\Gamma\nu_R$
-2.1	-1.9	0.0	3.308	2.525
-2.1	-1.9	-0.1	3.436	2.721
-1.5	-1.0	0.0	1.88	1.193
-2.5	-2.3	0.0	3.82	3.129
-2.1	-1.0	0.0	2.568	1.760
-2.8	-2.2	-1.6	5.02	4.71

(ii) Variation with ν_o:

ν_o		
-3	3.465	2.849
-2	3.308	2.525
-1	3.22	2.35
-0.001	3.23	2.37

(iii) Variation with n:

n		
2	3.4	2.6
4	2.08	0.15
3	no solution	
5		
7		
1		
6(1)		
6(2)		

Table 3-3-b.

RED	IMD	REN	IMA	REA	REC	IMC	ν
1.771	0.	-5.351	0.	-3.022	-6.631	0.675	-9.000
1.726	0.	-5.507	0.	-3.190	-6.469	-0.499	-8.500
1.681	0.	-5.840	0.	-3.475	-6.237	-1.750	-8.000
1.634	0.	-6.518	0.	-3.990	-5.917	-3.076	-7.500
1.585	0.	-8.058	0.	-5.083	-5.480	-4.475	-7.000
1.536	0.	-13.027	0.	-8.482	-4.889	-5.932	-6.500
1.485	0.	+++++++	0.	+++++++	-4.084	-7.421	-6.000
1.432	0.	7.854	0.	5.484	-2.961	-8.888	-5.500
1.378	0.	2.874	0.	2.086	-1.282	-10.229	-5.000
1.321	0.	1.316	0.	0.996	2.254	-11.246	-4.500
1.263	0.	0.611	0.	0.484	1.489	0.	-4.000
1.202	0.	0.245	0.	0.204	0.471	0.	-3.500
1.138	0.	0.047	0.	0.042	0.113	0.	-3.000
1.071	0.	-0.055	0.	-0.052	-0.040	0.	-2.500
1.000	0.	-0.100	0.	-0.100	-0.100	0.	-2.000
0.970	0.	-0.106	0.	-0.109	-0.109	0.	-1.800
0.940	0.	-0.108	0.	-0.114	-0.111	0.	-1.600
0.908	0.	-0.104	0.	-0.115	-0.108	0.	-1.400
0.876	0.	-0.098	0.	-0.111	-0.101	0.	-1.200
0.842	0.	-0.087	0.	-0.104	-0.090	0.	-1.000
0.807	0.	-0.074	0.	-0.092	-0.076	0.	-0.800
0.770	0.	-0.059	0.	-0.076	-0.060	0.	-0.600
0.732	0.	-0.041	0.	-0.056	-0.042	0.	-0.400
0.690	0.	-0.021	0.	-0.031	-0.022	0.	-0.200
0.643	0.	0.	0.	0.	+++++++	0.	0.000
0.589	-0.009	0.023	0.001	0.039	0.023	0.	0.200
0.539	-0.025	0.047	0.004	0.087	0.047	0.	0.400
0.491	-0.044	0.072	0.013	0.146	0.072	0.	0.600
0.445	-0.066	0.099	0.032	0.217	0.097	0.	0.800
0.402	-0.089	0.126	0.066	0.299	0.124	0.	1.000
0.360	-0.114	0.154	0.123	0.390	0.151	0.	1.200
0.320	-0.140	0.183	0.210	0.481	0.178	0.	1.400
0.281	-0.167	0.213	0.333	0.560	0.206	0.	1.600
0.243	-0.195	0.243	0.487	0.608	0.234	0.	1.800
0.207	-0.223	0.273	0.658	0.611	0.262	0.	2.000
0.122	-0.297	0.352	1.012	0.416	0.335	0.	2.500
0.044	-0.374	0.432	1.139	0.133	0.407	0.	3.000
-0.028	-0.453	0.514	1.130	-0.070	0.481	0.	3.500
-0.095	-0.533	0.596	1.084	-0.192	0.554	0.	4.000
-0.156	-0.615	0.679	1.039	-0.264	0.627	0.	4.500
-0.212	-0.696	0.763	1.002	-0.306	0.700	0.	5.000
-0.265	-0.779	0.846	0.974	-0.331	0.772	0.	5.500
-0.313	-0.861	0.930	0.954	-0.347	0.844	0.	6.000
-0.357	-0.943	1.013	0.939	-0.356	0.915	0.	6.500
-0.398	-1.024	1.095	0.929	-0.361	0.985	0.	7.000
-0.436	-1.106	1.177	0.921	-0.363	1.054	0.	7.500
-0.471	-1.187	1.259	0.916	-0.364	1.123	0.	8.000
-0.503	-1.267	1.339	0.913	-0.363	1.190	0.	8.500
-0.532	-1.347	1.419	0.912	-0.360	1.257	0.	9.000
-0.559	-1.425	1.499	0.911	-0.357	1.323	0.	9.500
-0.584	-1.504	1.577	0.911	-0.354	1.388	0.	10.000

Standard tabulation. $n = 2$. $\gamma_{Fj} = -2.1, -1.9, 0.0$

$\gamma_R = 3.35$, $\Gamma\gamma_R = 2.65$. $\gamma_i = -2.0, -6.0, -50.0$.

TABLE 3 - 3 - C

Matching equation :: for $a_i = 4.260 \quad - 1.27$

$E \cdot F = A$ $\qquad \nu_j = -2.1, \quad - 1.9, \quad 0.0$

$\nu_i = - 2.0, - 6.0, -50.0$

$$\begin{bmatrix} 1.00109 & - 0.02499 & - 0.00191 \\ 0.99871 & 0.02363 & 0.00188 \\ 1.000 & 0.33333 & 0.04000 \end{bmatrix} \begin{bmatrix} - 0.09985 \\ - 1.28460 \\ 13.20127 \end{bmatrix} = \begin{bmatrix} - 0.09312 \\ - 0.10529 \\ 0.0 \end{bmatrix}$$

FIG. 3-3.

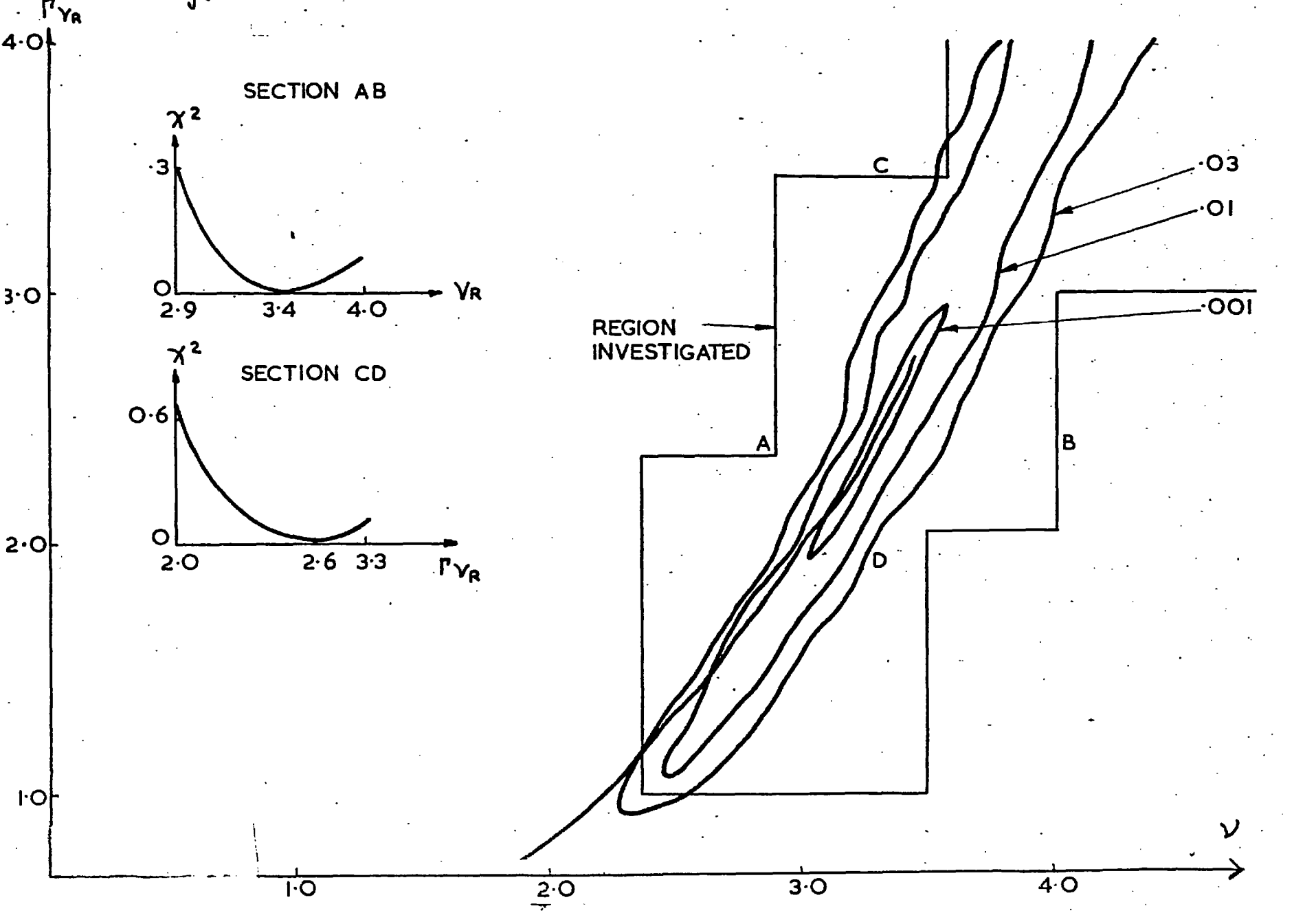
Γ_{V_R}
4·0
3·0
2·0
1·0
SECTION AB
χ^2
·3
O
2·9
3·4
4·0
V_R
χ^2
SECTION CD
0·6
O
2·0
2·6
3·3
Γ_{V_R}
C
·03
·01
·001
REGION
INVESTIGATED
A
B
D
1·0
2·0
3·0
4·0
ν

Fig 3-4(a). Static study. Derivative matching $n = 1, 2, 3, 4, 5, 6, 7$.

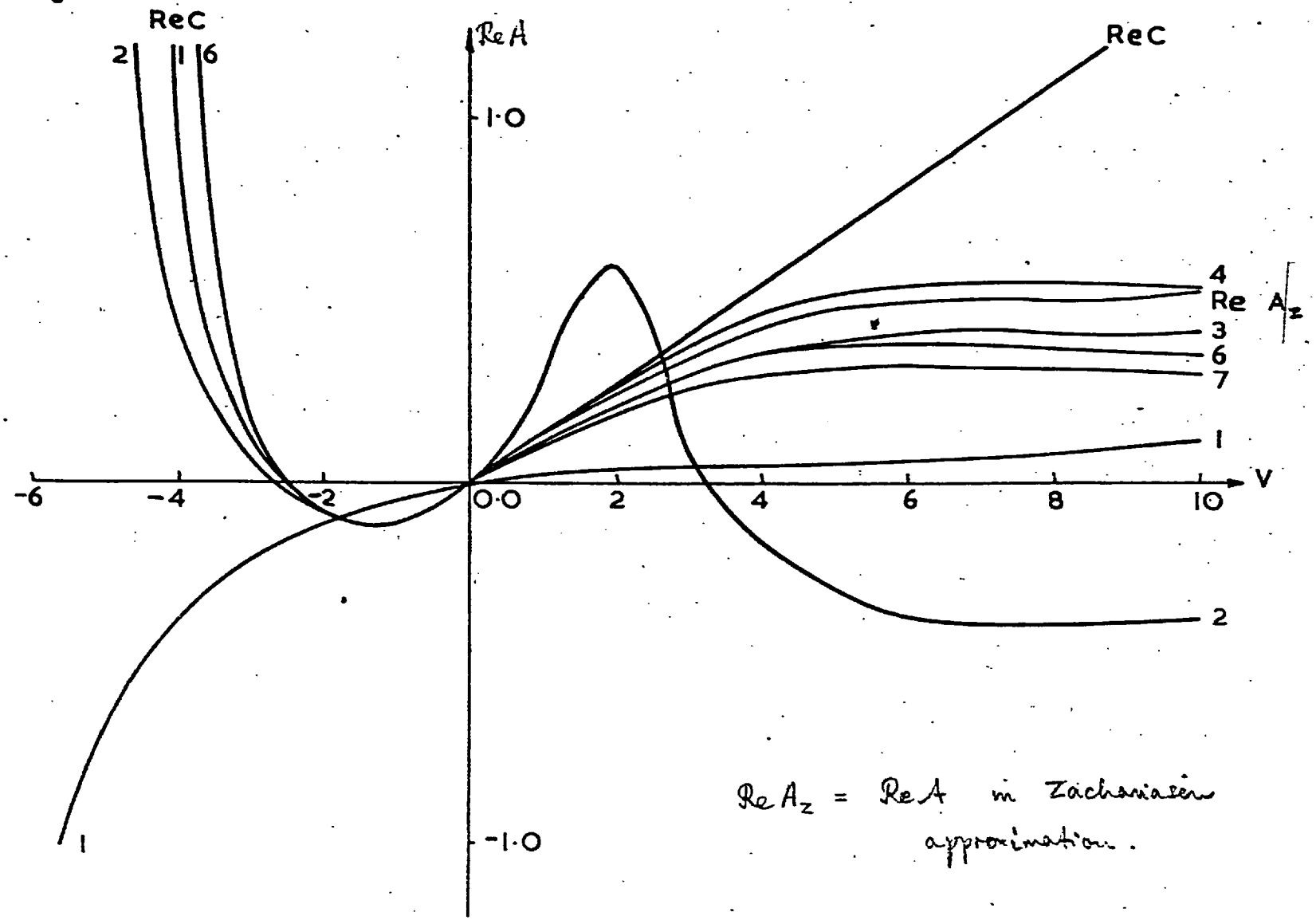

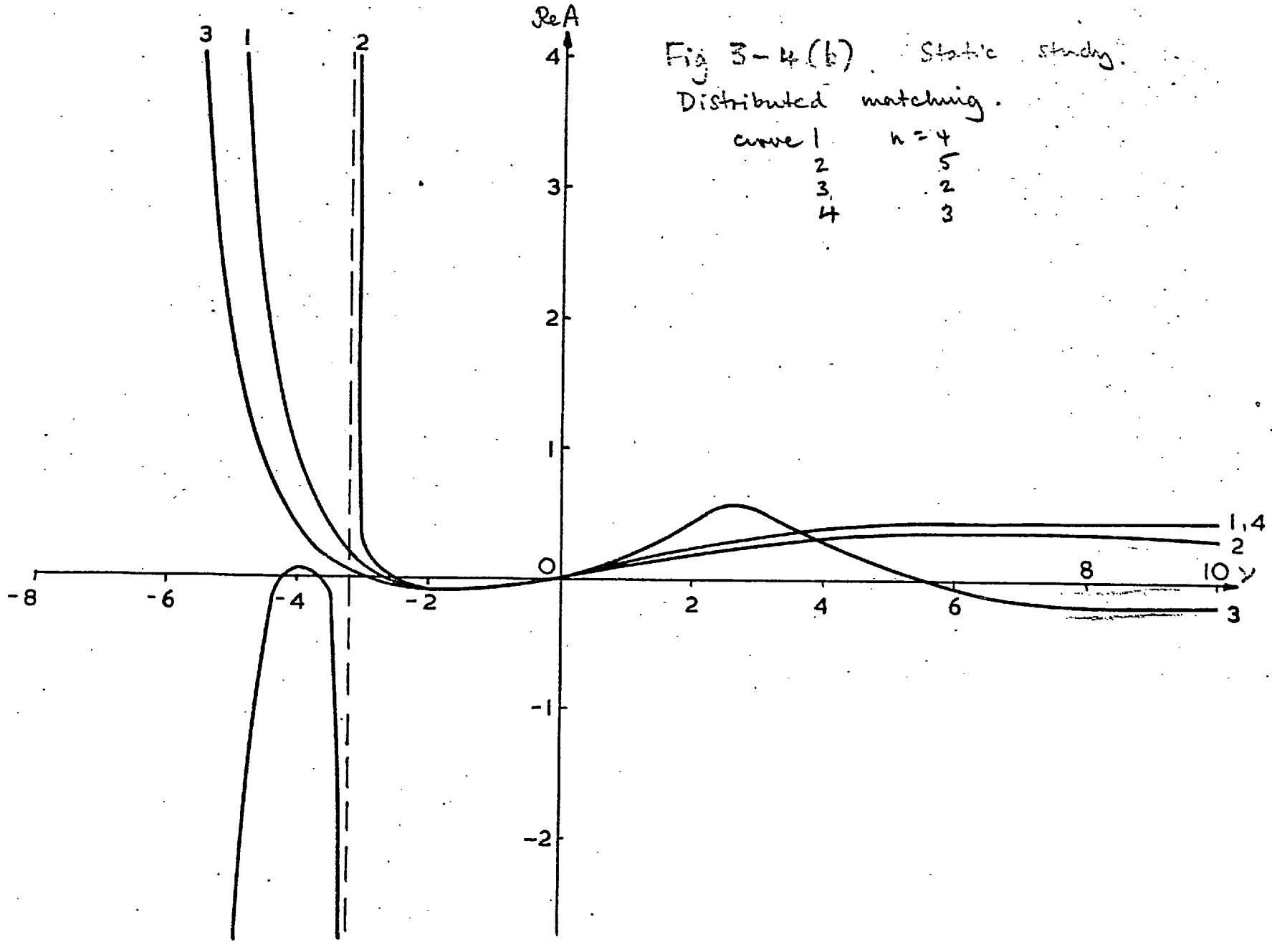

Fig 3-4(b) Static study.
Distributed matching.

curve	n =
1	4
2	5
3	2
4	3

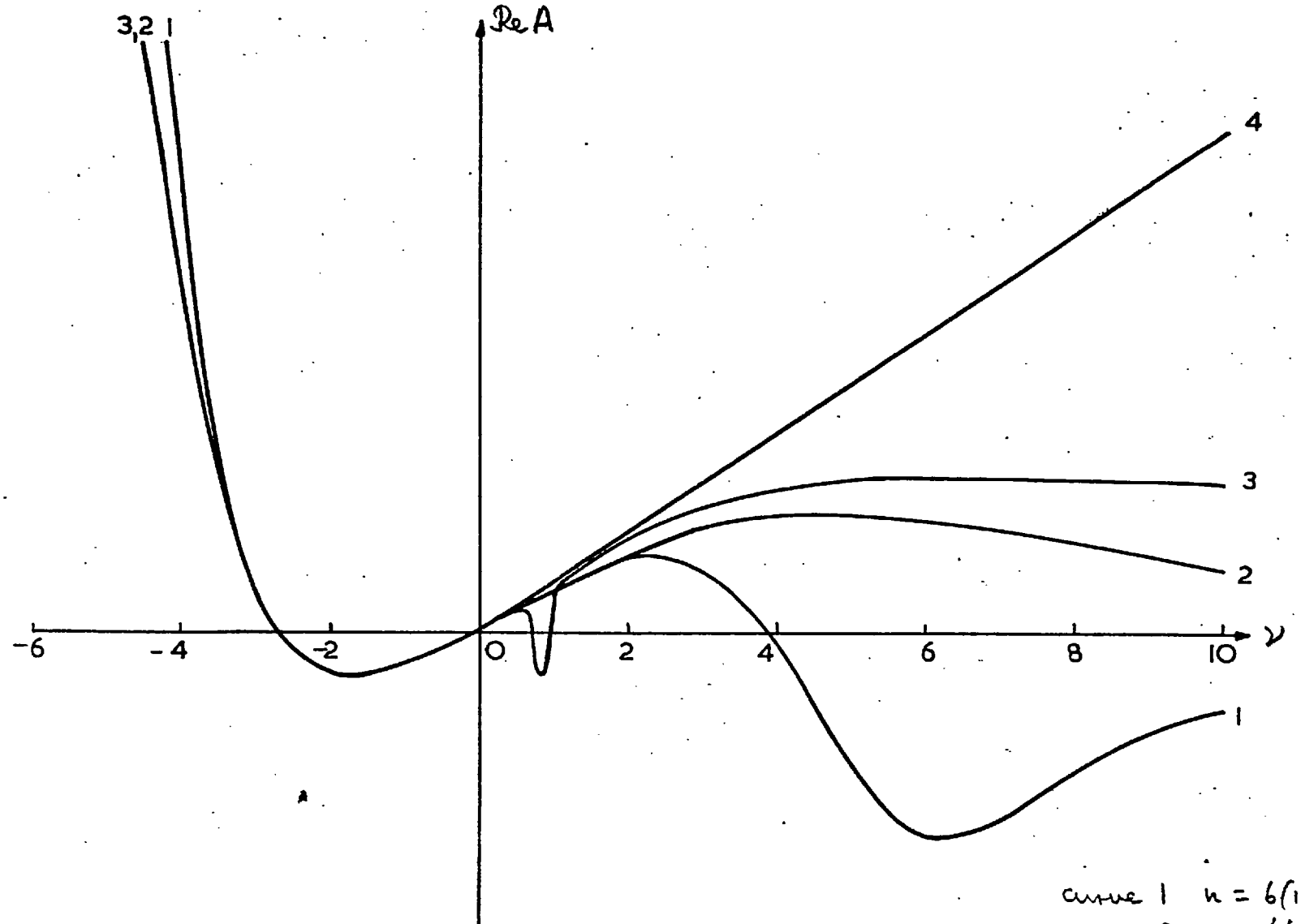

curve 1 $n = 6(1)$
2 $6(2)$
3 4
4 $Re\, C(\nu)$

Fig 3-4(c). Static study. Distributed matching.

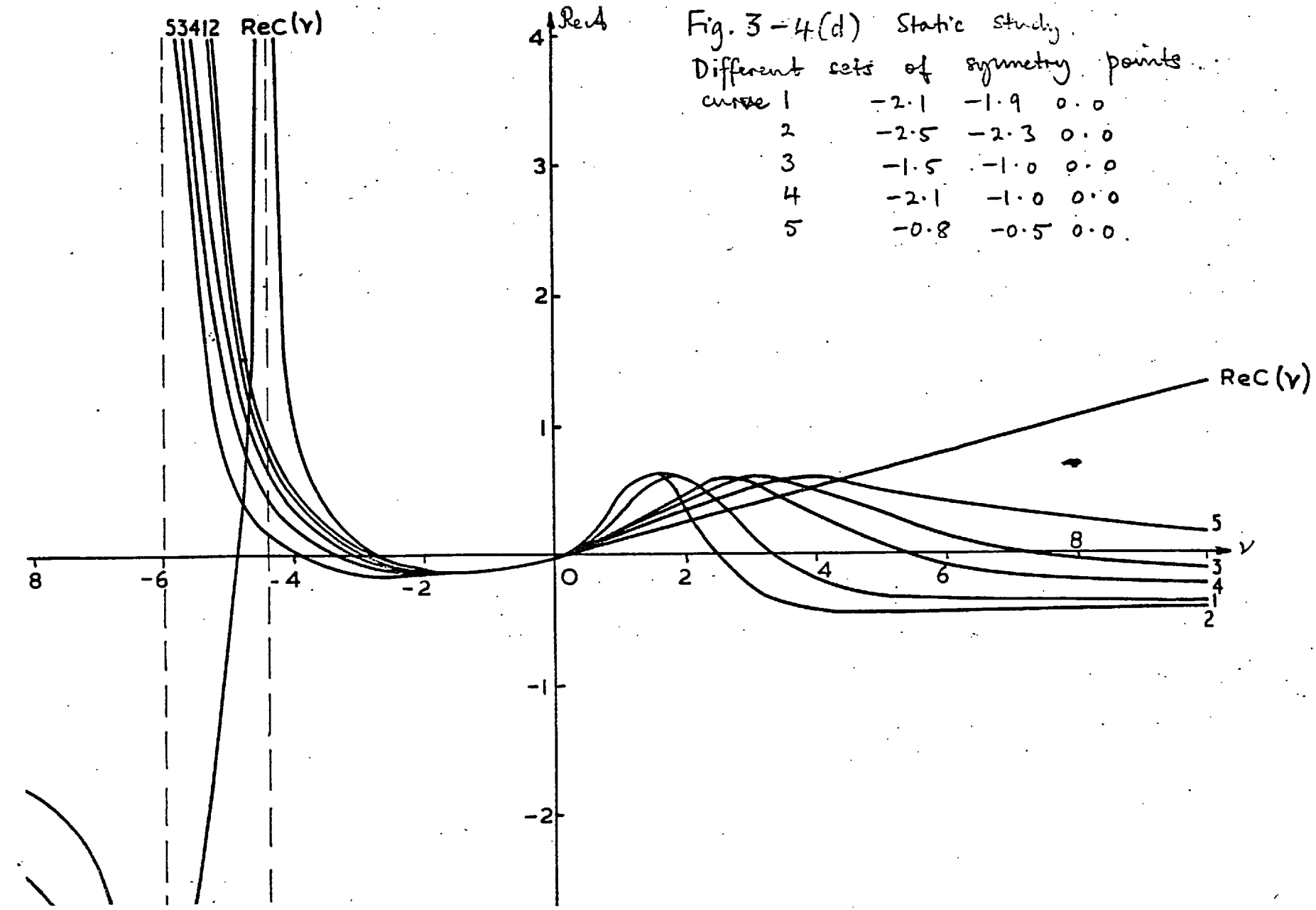

Fig. 3-4(d) Static study.

Different sets of symmetry points...

curve			
1	-2.1	-1.9	0.0
2	-2.5	-2.3	0.0
3	-1.5	-1.0	0.0
4	-2.1	-1.0	0.0
5	-0.8	-0.5	0.0

Then, if A obeys the conditions

$$A(\nu_{Fj}) = C_j \qquad j = 1 \ldots n+1.$$

these will be linear equations for $A_o, \{F_i\}$ and will uniquely determine them, and hence $A(\nu)$ at all points.

Hence $A = A'$ at all points, in particular

$$A'(\nu_{Fj}) = C_j \qquad j = 1 \ldots n+1.$$

Thus, we can explicitly construct an identical N/D amplitude with different subtraction point and obeying the same matching conditions. This proves the desired result.

Sensitivity to $\{\nu_{Fi}\}$ is very marked and makes predictions by the Balazs method so unreliable as to be meaningless. The significance of the $\{\nu_{Fi}\}$ -2.8, -2.2, -1.6 is that these are the positions used by Kani and Tubis (4) in a Balazs $\pi\pi$ calculation using a different crossing continuation. Their result was (3,2, 3.0).

The pole positions were also varied to find what effect they would have. The results are shown in Table 4. This enabled the cut off ν_L in the kernel approximation to be varied and the effect seen. From Table 4, the values of $(\nu_R, \Gamma\nu_R)$ are fairly sensitive to the pole positions but not as much as to the symmetry point positions. For the last two entries, the symmetry points had also to be moved in, in proportion, to satisfy the condition that $\{\nu_{Fi}\}$ not too close to ν_L or $-\nu_R - 1$.

Possibly more striking than the $\{\nu_{Fi}\}$ dependence is the n dependence where the position and width change drastically and the solution even disappears for some n. In Fig. 4(b) the first six pole fit has Re $A(\nu) = 0$ when $\nu \sim 4$, due to a zero of Re N, so phase shift is zero, indicating that 6 (1) pole positions do not belong to the same approximation as the others. The seven pole fit has Re $A(\nu) = 0$ at two points, the first being due to a zero of Re N and the second to a zero of Re D, which are very close together for both derivative and distributed matching and are presumably striving to cancel each other out.

TABLE 3 - 4

Self-consistent values

Variation with $\{\nu_{1j}\}$, the pole positions,

$\{\nu_{1j}\}$		$\sim \nu_L$	ν_R	$\Gamma\nu_R$
- 6.0	-50.0		3.33	2.525
- 6.0	-25.0	- 5	3.06	2.788
-10.0	-50.0		4.17	3.00
- 6.25	-100.0		3.55	2.29
-12.3	-42.2	-10	4.41	3.22
- 1.25	- 4.46	- 1	0.08	0.3
- 2.480	- 8.696	- 2	0.93	1.17

TABLE 3 - 5

Single Channel Searches - Values of (ν_R, $\Gamma\nu_R$)

n	2	2	3	3	4	4
ν_{F_i}	distributed	derivative	distributed	derivative	distributed	derivative
S_0	-	2.048, 2.166	-	-	-	-
S_2	-	1.80, 1.79	-	-	-	-
P_1	2.57, 1.76	3.4, 2.6	-	-	1.86, 0.06	2.6, 0.26
D_0	-	-	-	-	2.0 0.1	-
D_2	-	-	-	-	1.7, 0.06	-
F_1			-	-	-	-

- indicates search done but no solution found.

FIG. 5-5. S-wave self consistent solution.

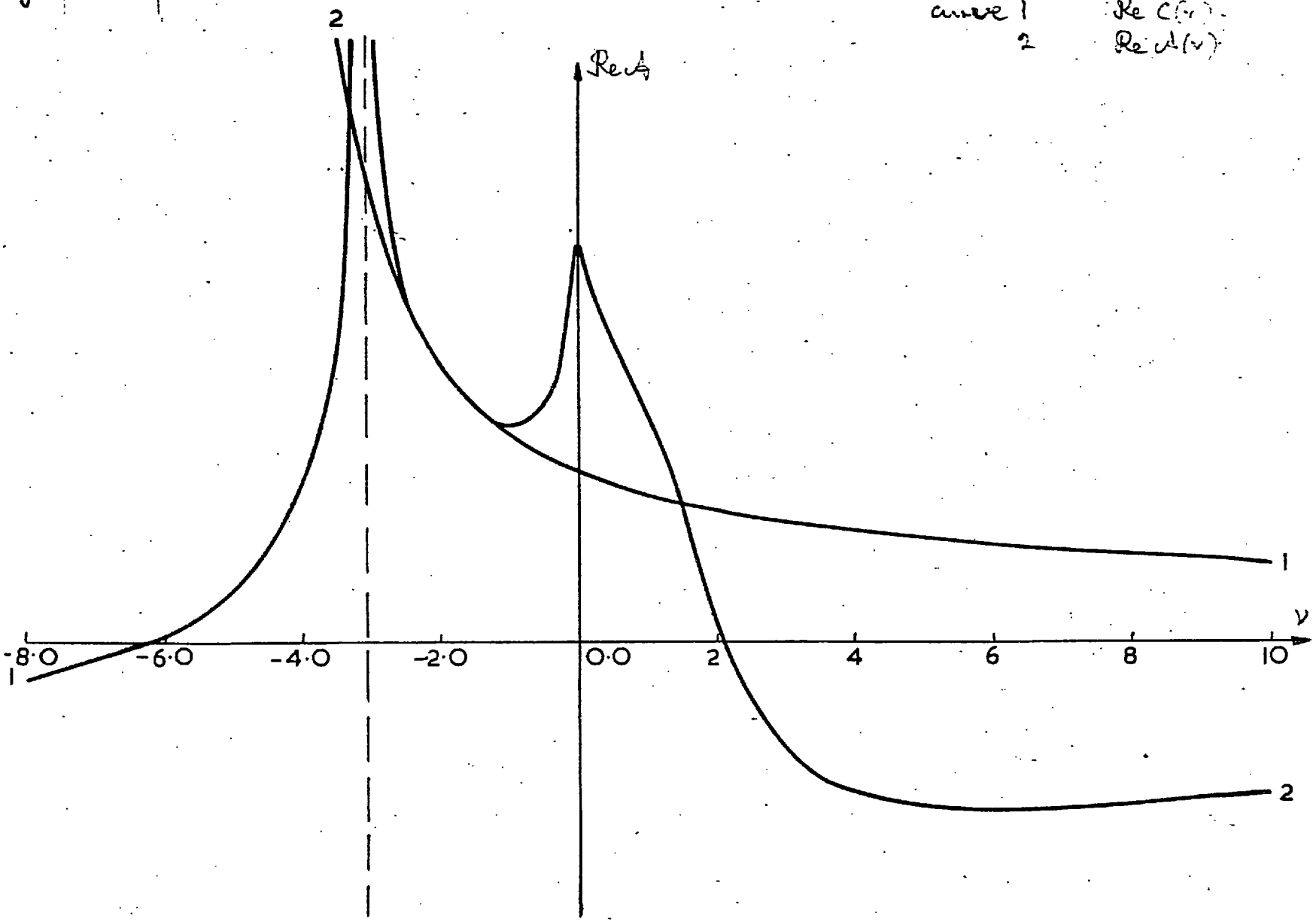

for in the cases $S_o - S_2$, 2 pole; $S_o - P$, 2 pole; $D_o - D_2$, 4 pole; . $P_1 - D_o - D_2$, 4 pole; $S_o - S_2 - P$, 2 pole. Only one search was done, i.e. minimisation of discrepancy from given initial values and the only solutions found were for the case found by Balazs in BIII viz. $P_1 - D_o$, 3 pole. However, the sensitivity of the calculation to the parameters and the pathology of the discrepancy function lead one to believe that the search is a difficult one. We even found a possible multiple solution i.e. two sets of values both satisfying the self-consistency conditions. See Table 6. A pictorial breakdown of the $P_1 - D_o$ calculation is shown in Figs. 6. Note the smallness of the $D_o \rightarrow D_o$ and $D_o \rightarrow P_1$ interaction, so that the D_o wave comes mainly to P_1 exchange modified by D_o exchange and the P_1 by self-stability modified numerically by D_o exchange. The effect of the D_o upon the P_1 channel for different n is shown in Fig. 7 and P_1 upon D_o for different n in Fig. 8(c). Again we see the accidental nature of the solutions in the $P_1 - D_o$ case, where only n = 3 can give a D_o resonance as seen from Fig. 8(c). Hence only n = 3 can give $P_1 - D_o$ self-consistent values. One expects, on intuitive grounds, that the self-consistency will become better resolved i.e. there will be sharper minima for a larger number of component systems but that, due to complication, solutions will be harder to find.

An attempt was made to find the effect of the ρ upon other channels by taking the ρ pole only to give the left-hand side and then solving by matching. The results are shown in Figs. 8.

6. Conclusions

Clearly, the method as used by Balazs is very sensitive to $\{\nu_{Fi}\}$ and to n and is thus unreliable for making predictions about the $\pi\pi$ system.

The kernel approximation seems reasonable where ν is sufficiently far from the cut. It is not obviously equivalent to a cut off. The pole positions are close to those obtained by a Gaussian integration procedure.

Fig 3-6(a) The P_1-D_0 calculation. Reflections into the P wave.

curve 1	Re A	P+D → P
2	Re C	P+D → P
3	Re A	D → P
4	Re C	D → P
5	Re A	P → P
6	Re C	P → P

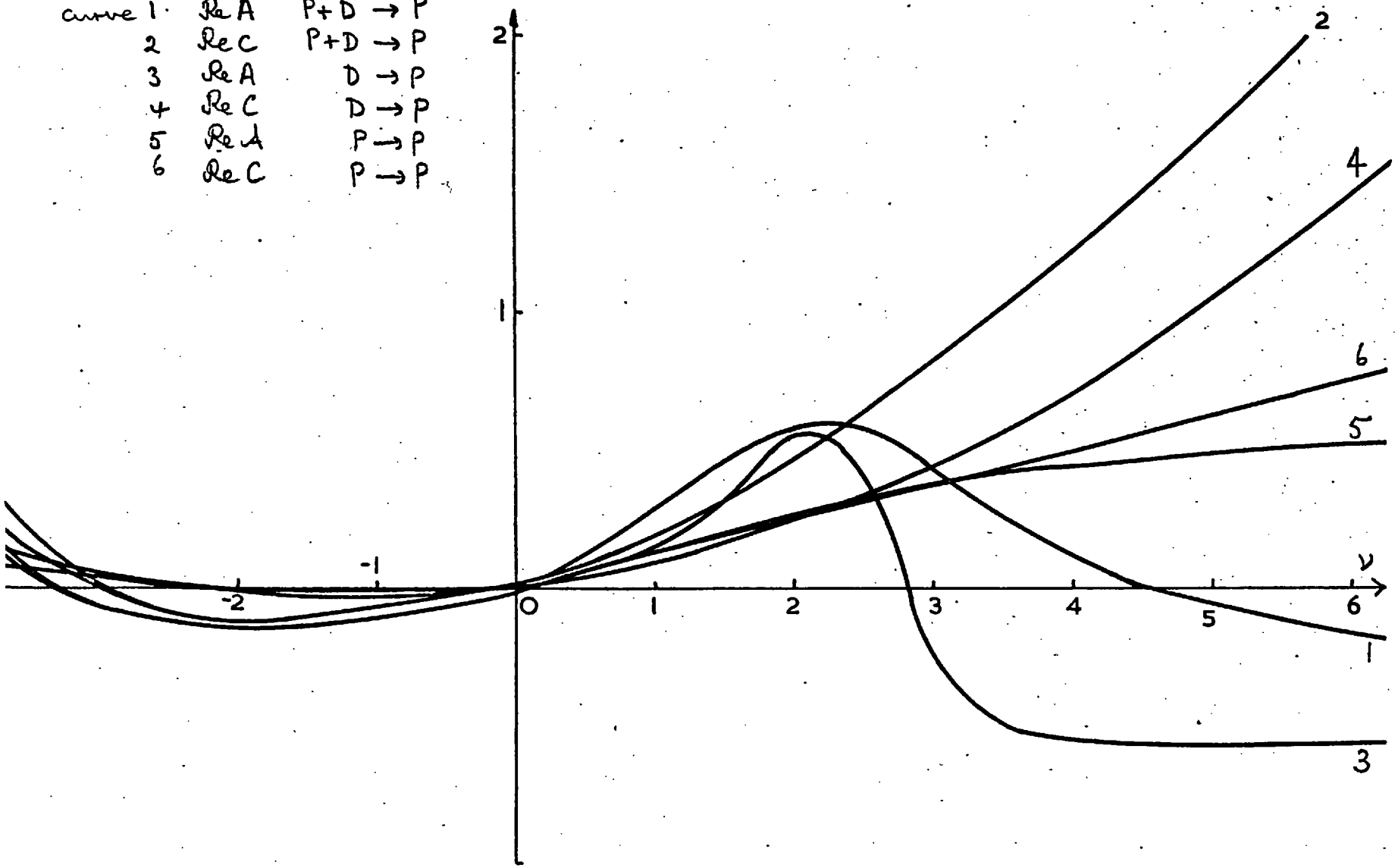

Fig 3-6(b) The P_1-D_0 calculation. Reflections into the Dwave.

curve		
1	Re A	P + D → D
2	Re C	P + D → D
3	Re A	D → D
4	Re C	D → D
5	Re A	P → D
6	Re C	P → D

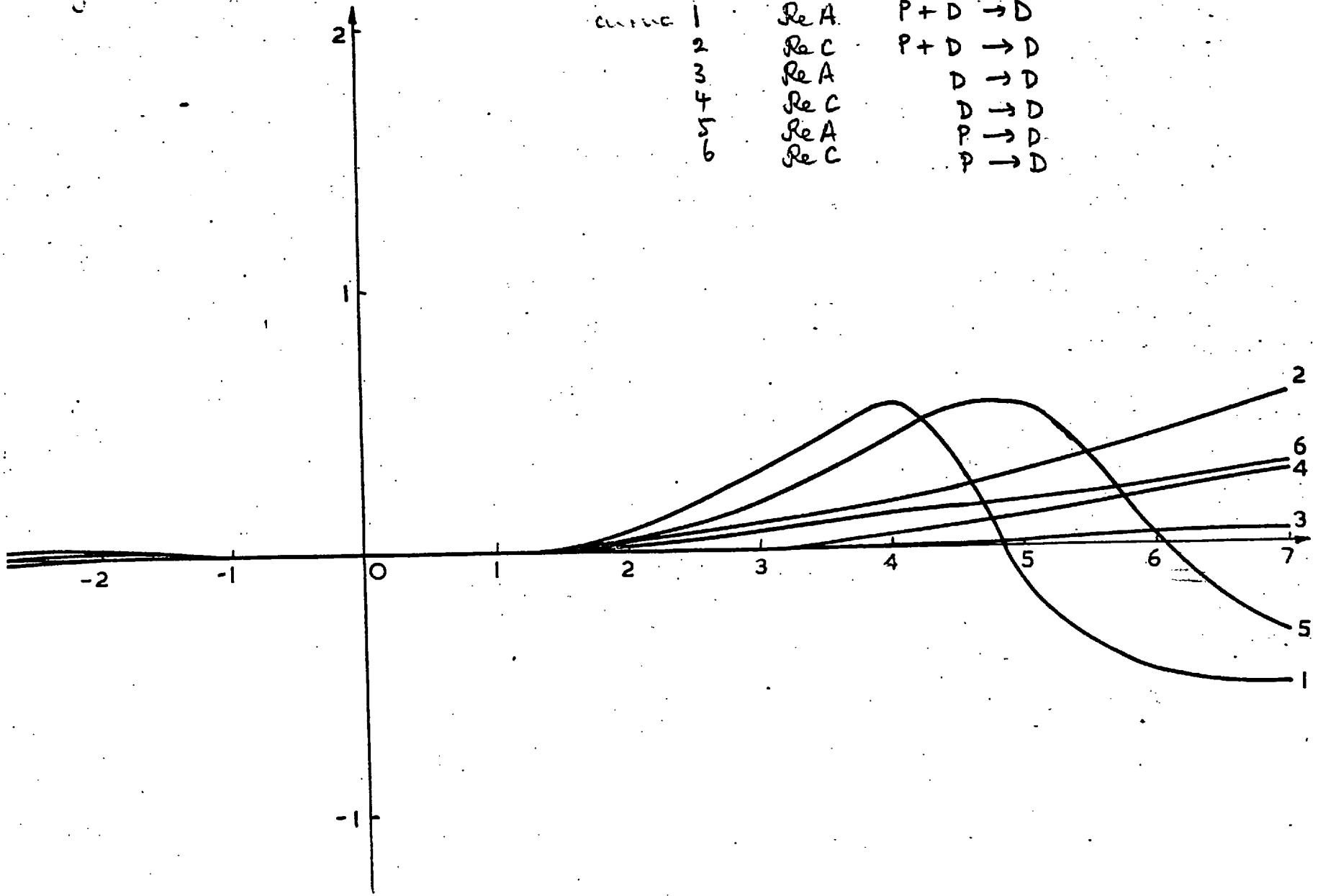

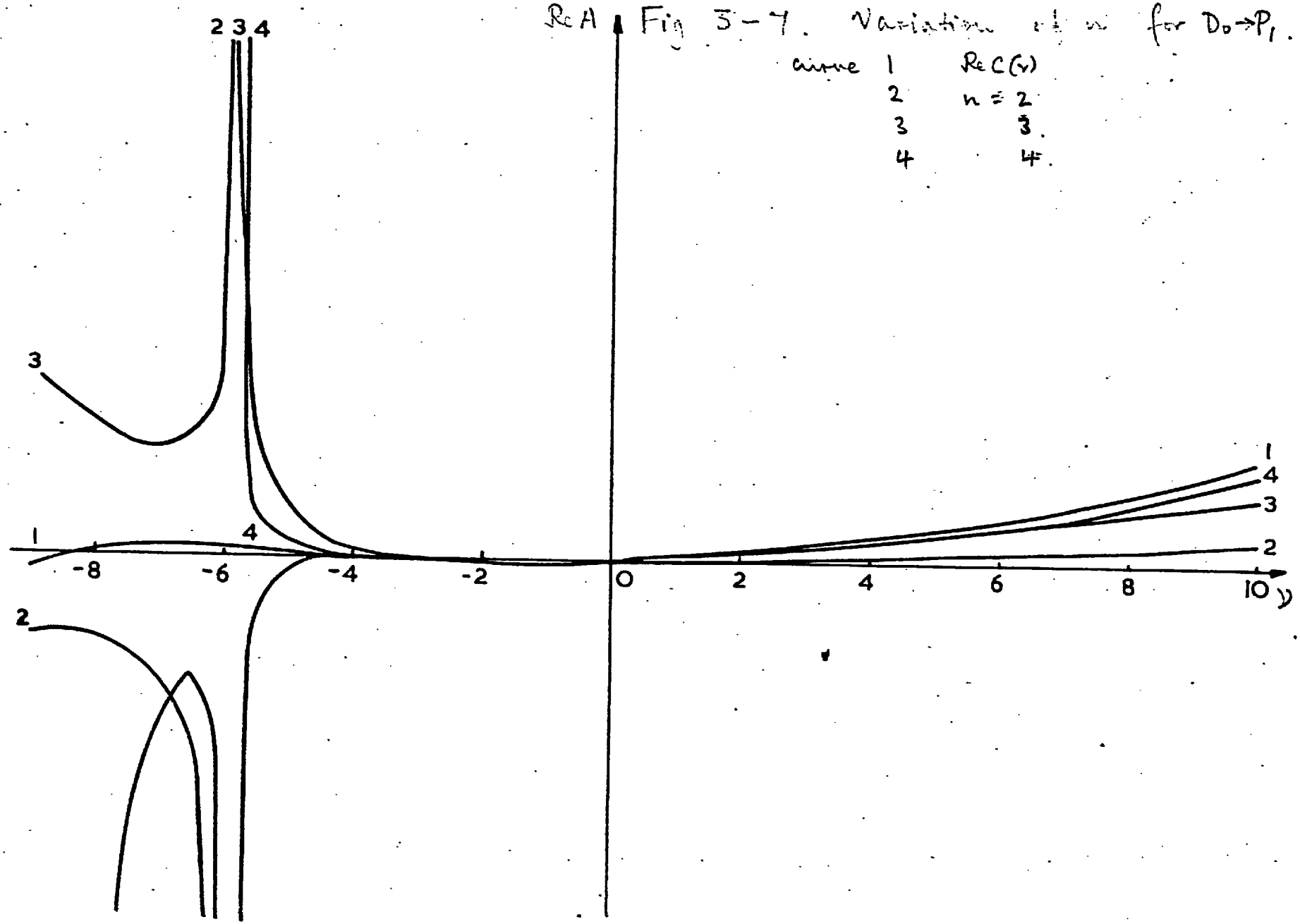

Fig 5-7. Variation of A with ν for $D_0 \to P_1$.

curve	Re C(ν)
1	
2	n = 2
3	3
4	4

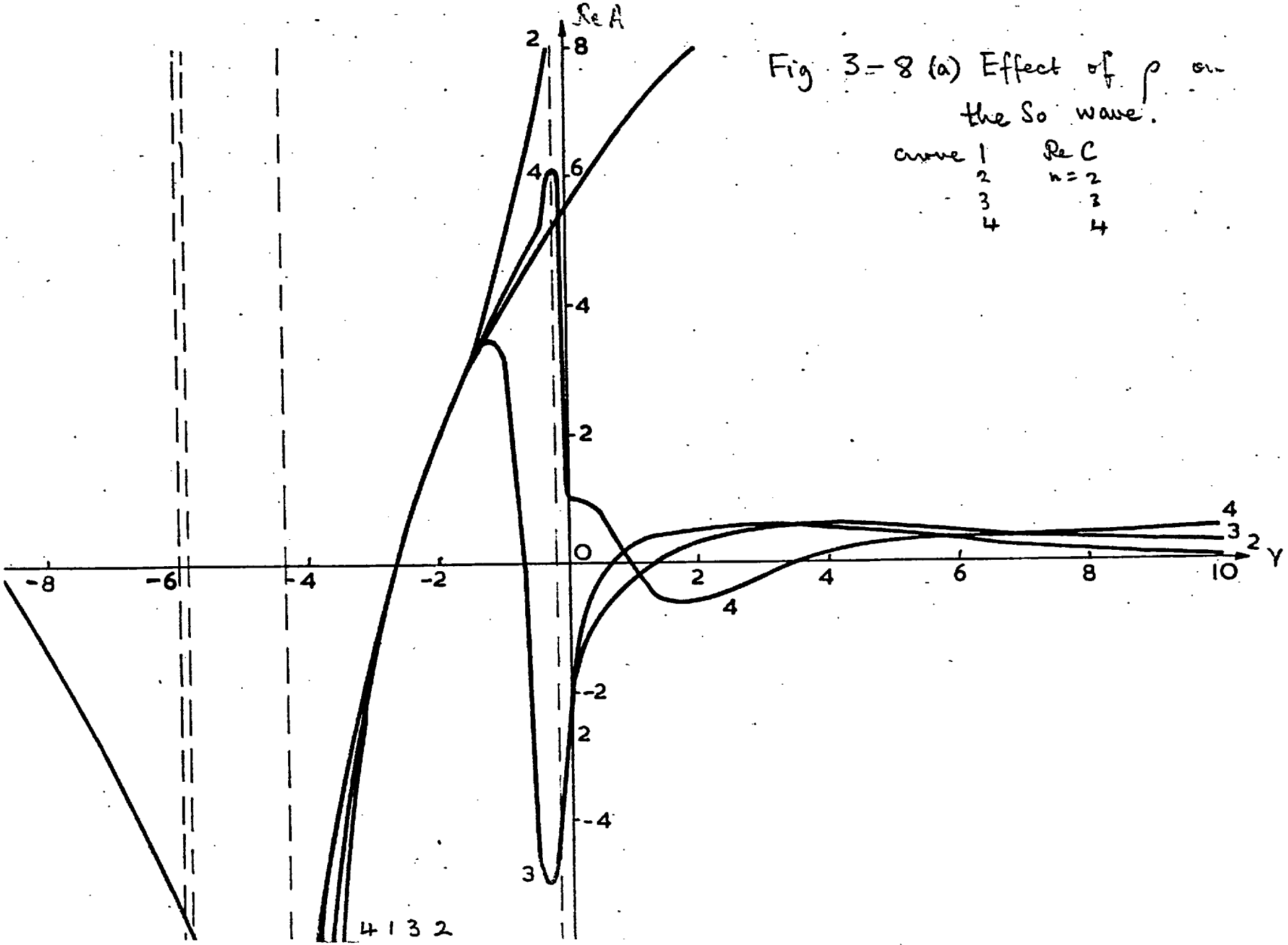

Fig 3-8 (a) Effect of ρ on the So wave.

curve	Re C
1	
2	n = 2
3	3
4	4

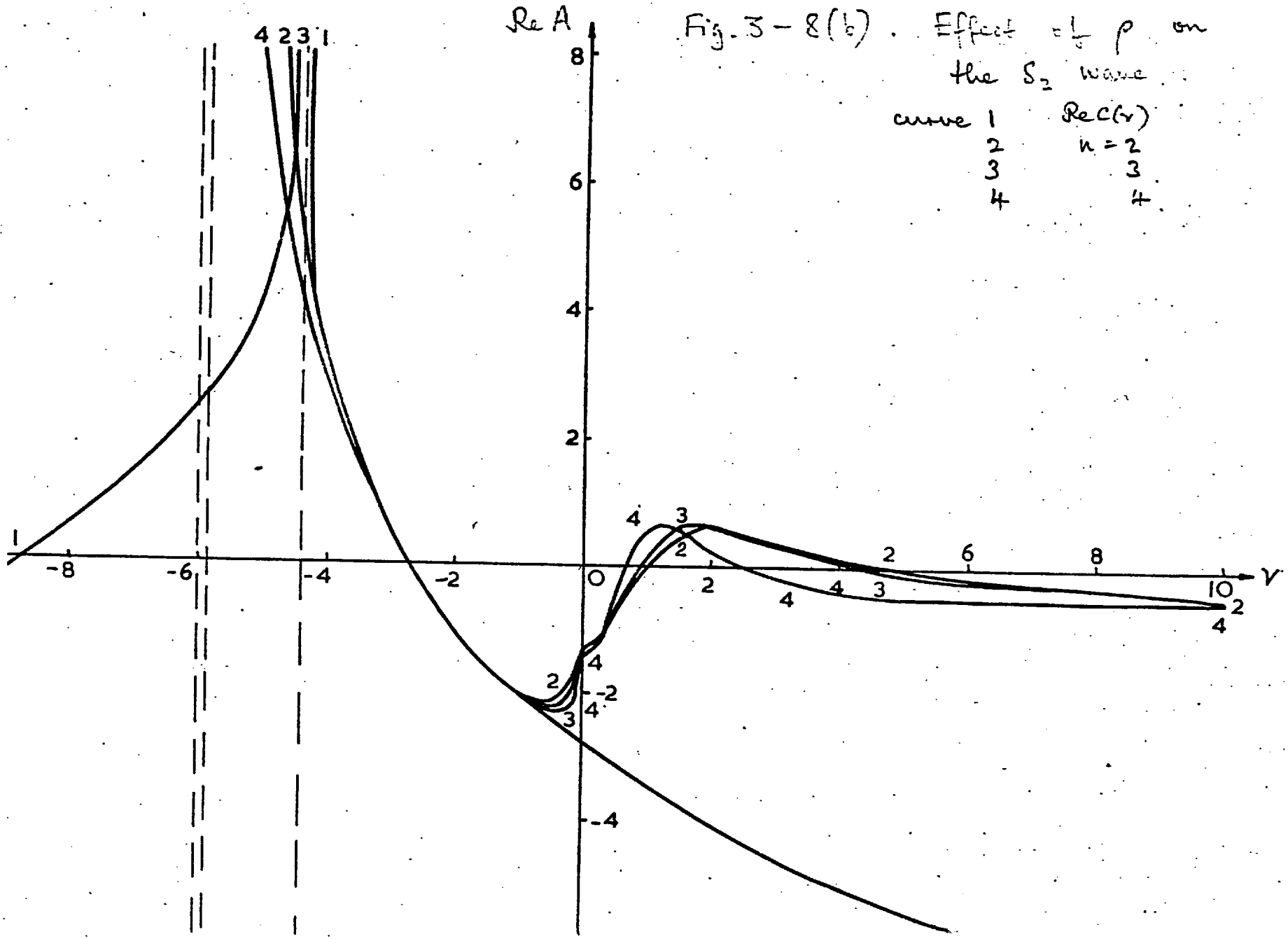

Fig. 3-8(b). Effect of ρ on the S_2 wave

curve	Re C(ν)
1	n = 2
2	3
3	4
4	

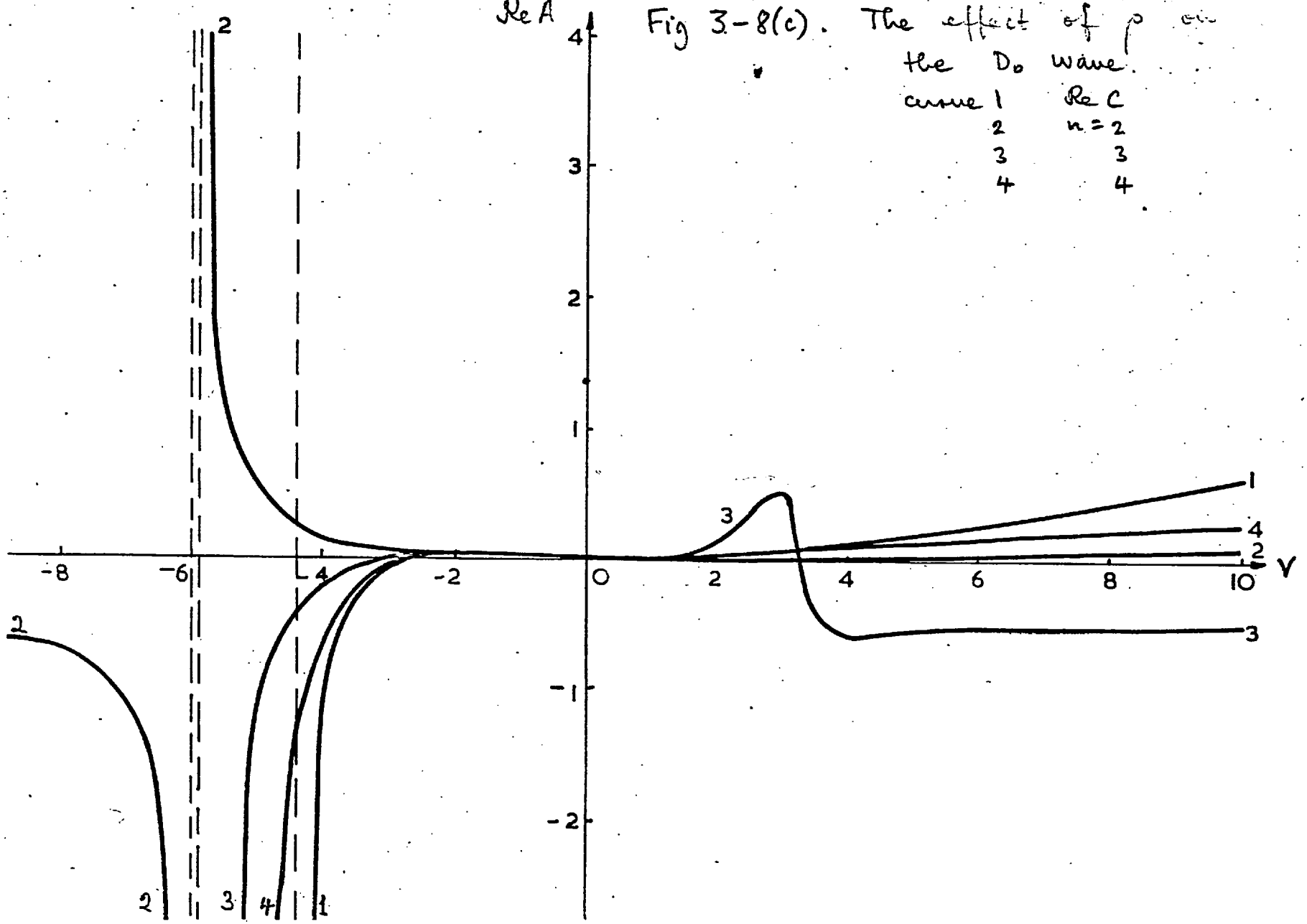

Fig 3-8(c). The effect of ρ on the D_0 wave.

curve	Re C
1	$n=2$
2	3
3	4
4	

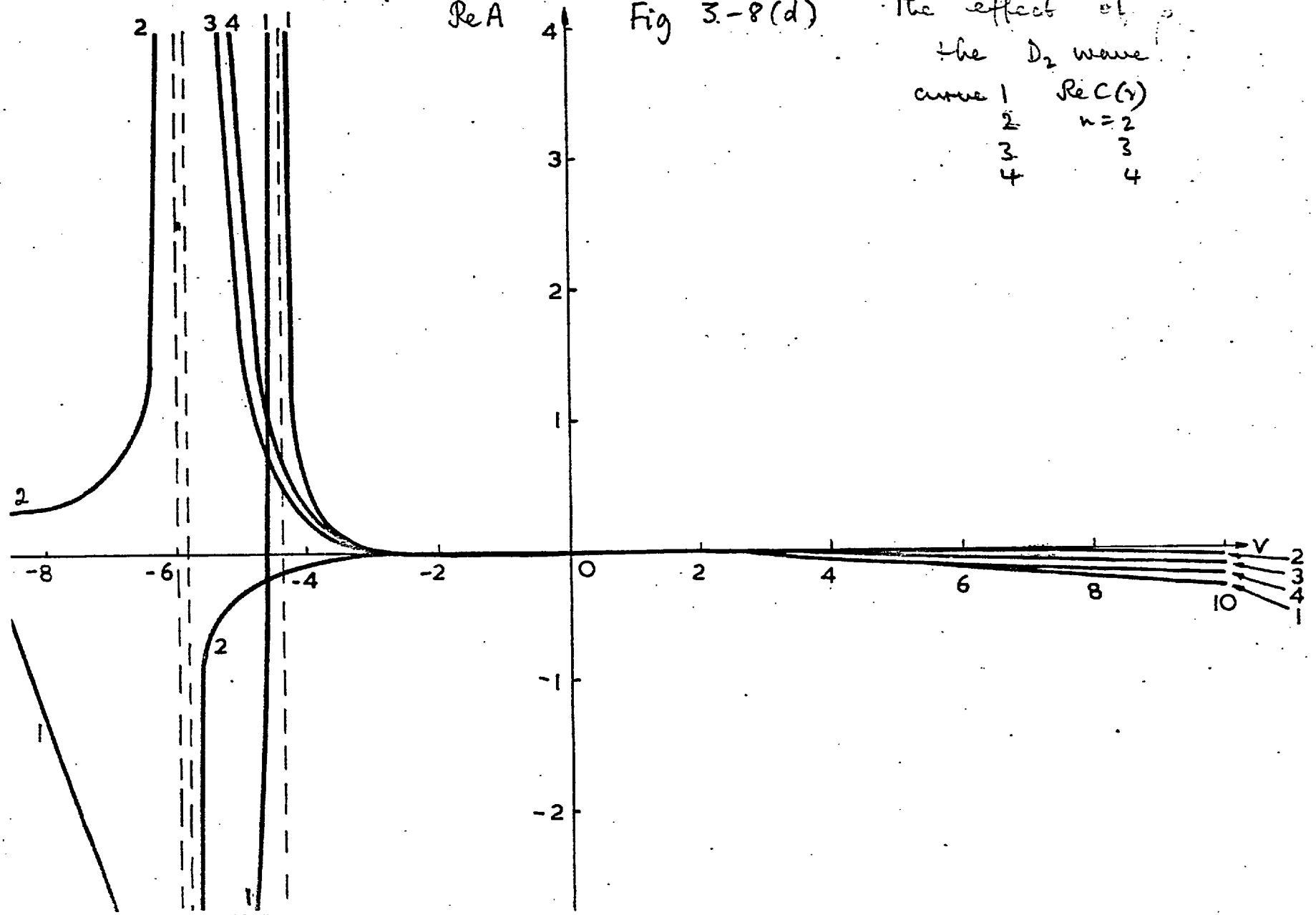

Fig 3.-8(d) The effect of the D_2 wave

curve 1 ReC(ν)
2 n=2
3 3
4 4

TABLE 3 - 6

P_1 - D_o Self-consistent Values

(1) For different $\{\nu_{Fi}\}$.

$\{\nu_{Fi}\}$				P_1 ν_R	P_1 $\Gamma\nu_R$	D_o ν_R	D_o $\Gamma\nu_R^2$
-2.1	-2.05	-1.0	0.0	4.53	4.26	4.817	1.378
-2.1	-2.05	-0.5	0.0	4.26	4.08	3.74	0.84
-2.1	-2.05	-0.2	0.0	4.02	3.82	3.09	0.58
-2.1	-2.05	-0.05	0.0	4.39	4.37	3.40	0.75
-2.1	-2.05	-1.5	0.0	4.74	4.33	5.90	2.007
-2.1	-2.05	-1.95	0.0	4.89	4.37	6.90	2.667

(2) With derivative configuration Γ_{Fi}

P_1 $\quad \nu_R = 5.76 \quad \Gamma\nu_R = 5.0$

D_o $\quad \nu_R = 9.37 \quad \Gamma\nu_R^2 = 4.58$

which is near Balazs' result.

(3) Possible multiple solution

with $\{\nu_{Fi}\}$ = -2.05 -1.95 -0.05 0.0

in both P_1 and D_o waves.

Solution 1

P_1 $\quad \nu_R = 6.663 \quad \Gamma\nu_R = 6.548$

D_o $\quad$ " $\quad 6.691 \quad \Gamma\nu_R^2 = 2.766$

Solution 2

P_1 $\quad \nu_R = 4.378 \quad \Gamma\nu_R = 4.372$

D_o $\quad$ " $\quad 3.228 \quad \Gamma\nu_R^2 = 0.693$

both appeared to satisfy the self-consistency requirements.

The determination of the $\{F^i\}$ by matching points $\{\nu_{fj}\}$ is justified, provided we have a reasonable estimate of the value of the integral and provided the $\{\nu_{Fj}\}$ are sufficiently far from the $\{\nu_i\}$. Herein almost certainly lies the source of instability and is strongly indicated by the sensitivity of $\{F^i\}$ to $\{\nu_{Fj}\}$. In short, $-\nu_R - 1$ is too close to $\{\nu_{Fj}\}$ and $\{\nu_{Fj}\}$ are too close to $\{\nu_i\}$.

As one must take $\nu_{Fj} < 0$ and $\nu_L << \nu_{Fj}$ one must have a special treatment of the near left, if only in specifically neglecting it, and use the approximation only for the far left.

Other authors have, almost without exception, used the kernel approximation only as a part of a more detailed treatment of the unphysical cuts. The method is insensitive to variation of the normalisation point ν_o. The uncertainty of interpretation of the width can lead to comparable uncertainties in both position and width of the self-consistent solution.

7. Other analyses of the original Balazs method

M. L. Mehta and P. K. Srivastava (2) examined the bootstrap for two poles only. They reported insensitivity to ν_o. They also reported sensitivity to ν_F, where value and gradient were matched at one point ν_F, concluding that no solution exists for $\nu_F < -1.5$. The present author finds this difficult to understand as Balazs's own solution had $\nu_F = -2$, also Table 3 shows values for $\nu_F \approx -2.4$ Thus the present author agrees with Balazs and disagrees with Mehta and Srivastava, and concludes that the latter made a numerical error. They displayed their results by plotting curves of ν_R against ν_F, where Γ_{in} is fixed and $D(\nu_R) = 0$. This gave a family of curves, one for each value of Γ_{in}, with a curve $\Gamma_{in} = \Gamma_{out}$ cutting them and asymptotic to $\nu_F = -1.5$ They also fixed Γ_{in}, found ν_R and Γ_{out} and plotted $\frac{\Gamma_{out} - \Gamma_{in}}{\Gamma_{out} + \Gamma_{in}}$. 200% against ν_F, there being a curve for each value of Γ_{in}. They also looked at the Dersarkissian calculation

(3) of deuteron parameters and disagreed with their numbers. Golowich (4) studied the Balazs method in connection with a treatment of meson Baryon scattering = $\bar{K}, I = 0$ and also $\pi N, I = 3/2$. He concluded that the position of poles was unimportant but the matching process was important and that the method could not be used unambiguously. He modified the method and got good results by virtue of the representation of short range effects. He used two poles only.

II. IMPROVEMENTS TO THE BALAZS METHOD

In an attempt to remove the difficulties and sources of error of the Balazs method, various improvements were tried. These can be loosely categorised as

i. Replacing δ function approximation in the $C(\nu)$ function by the exact integral;

ii. Improving the matching procedure to a larger number of points, to real and imaginary parts and to replacement by a fitting procedure rather than matching.

Some experimentation was also carried out in looking at different self-consistency conditions.

1. Taking a smooth $C(\nu)$ function

Since the δ function approximation to the $C(\nu)$ function had a singularity at $-\nu_R - 1$, it was thought that the replacing of it by the more exact smooth version would remove some of the instability. This would also allow one to put the symmetry points over a larger region, hopefully giving greater stability and in the vicinity of $-\nu_R - 1$.

We see from Table 7 that the change from δ function form to smooth form made a small change to the better, the self-consistent value having larger ν_R and smaller $\Gamma\nu_R$. However, the sensitivity to choice of $\{\nu_{Fi}\}$

TABLE 3 - 7

Dynamic studies - real part matching - continuous $C(\nu)$

1. Standard result:

$n = 2 \quad \nu_{Fj} = -2.46, -1.35, 0.0$

$\nu_R = 3.77, \quad \Gamma\nu_R = 1.98$

2. Variation of ν_{Fj}. $n = 2$:

ν_{Fj} in	ν_R	$\Gamma\nu_R$
$[-3.5, 0]$	1.88	2.49
$[-2.5, 0]$	none found	
$[-1.6, 0]$	none found	
$[-1.8, 0]$	1.64	0.95
$[-1.2, 0]$	0.86	0.45

3. Other searches:

$n = 4 \quad \nu_{Fj}$ in $[-3.5, 0] \quad \nu_R = 3.69, \Gamma\nu_R = 5.0$

$n = 5 \quad [\ \text{"}\ ]$ none found.

remained. The effect of taking more poles and hence more symmetry points and a better fit to the real part on the left is tabulated in Table 8. The output A (ν) function is still very sensitive to movement of the symmetry points, giving a good fit in the region of the symmetry points but becoming very badly behaved, further left. Keeping the symmetry point region fixed and varying the number of poles causes some change but seems to settle down as n gets large. However, it settles down to an amplitude with a zero on the physical cut. ReA is tabulated for n = 9 in Table 9 and shown for n = 8 in Fig. 9.

2. Improvement and Generalisation of the Matching Procedure

To get a more realistic behaviour of the trial N/D form on the left, the author augmented the matching equations by including the imaginary part on the near left. Although the near left discontinuity only has a small effect (and of wrong sign) on the physical region, it can and does sometimes have a large effect in the near left region itself. We first attempted to use the near imaginary part only by taking an N/D pole form with several poles on the near left ($[-1, -9]$) and demanding that the imaginary part were equal to Im C. This is the same as numerically integrating the near cut, which replaces the cut by poles. The output amplitude was small and negative in the physical region. We now added "far poles," to represent the far cut, the positions being obtained by the Balazs prescription with $\nu_L = -9$, the limit of the near region. The residues obtained by matching real parts on the near left. This leads to complicated matching equations since the near left hand cut contributes and the near and far poles are coupled together and have to be solved together in one big linear equation set. Three approaches described were called "real part" - "imaginary part" and "complex" - matching.

Finally, it is possible to include extra poles which enter into the

TABLE 3 - 8

Static studies: real part matching: input $-\nu_R = 3.4$, $\Gamma\nu_R = 2.6$

(a) continuous $C(\nu)$

n	matching region	comments
2	[-0.8, 0]	output resonance at 8.75
2	[-2.5, 0]	" 1.5
3	[-4, 0]	ReA negative
4	"	ReA rises to 0.5 then falls
5	"	zero of ReN at 0.8
6	"	" 2.0
7	"	" 3.0
8	"	" 1.5 zero of ReD at 9.8
9	[-4,0]	" 1.7
9	[-8,0]	" 7.3

(b) δ function approximation in $C(\nu)$

3	[-4, 0]	ReA negative, zero of ReD - 3.0
9	[-8, 0]	ReA rises to 0.3 then falls.

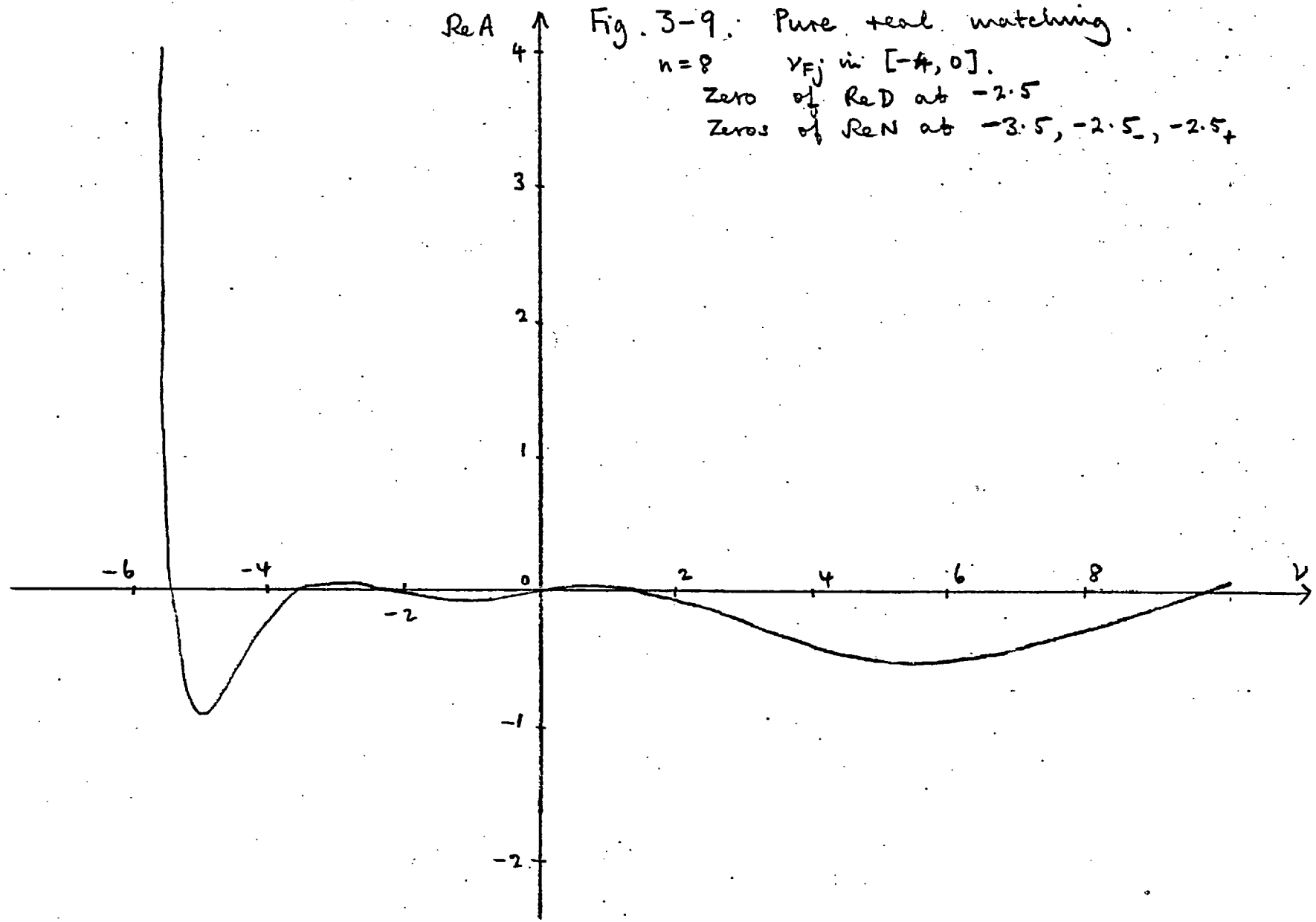

Fig. 3-9. Pure real matching.
$n = 8$ ν_{Fj} in $[-4, 0]$.
Zero of ReD at -2.5
Zeros of ReN at $-3.5, -2.5_-, -2.5_+$

Table 3-9.

RED	IMD	REN	IMN	REA	IMA	REC	IMC	Y
2.732	0.0000	999.199	0.0004	025.511	0.000	-3.229	0.261	-10.000
2.394	0.0004	391.857	0.0001	834.594	0.000	-3.092	0.068	-9.500
2.078	0.000	-858.287	0.000	-413.130	0.000	-2.942	-0.125	-9.000
1.784	0.000	-21.222	0.000	-11.897	0.000	-2.773	-0.316	-8.500
1.513	0.000	-3.902	0.000	-2.578	0.000	-2.578	-0.503	-8.000
1.267	0.000	-2.835	0.000	-2.238	0.000	-2.384	-0.681	-7.500
1.046	0.000	-2.220	0.000	-2.123	0.000	-2.123	-0.844	-7.000
0.850	0.000	-1.583	0.000	-1.863	0.000	-1.836	-0.985	-6.500
0.680	0.000	-1.042	0.000	-1.533	0.000	-1.533	-1.092	-6.000
0.537	0.000	-0.633	0.000	-1.179	0.000	-1.202	-1.149	-5.500
0.422	0.000	-0.346	0.000	-0.820	0.000	-0.820	-1.136	-5.000
0.336	0.000	-0.160	0.000	-0.476	0.000	-0.479	-1.032	-4.500
0.280	0.000	-0.051	0.000	-0.184	0.000	-0.184	-0.825	-4.000
0.254	0.000	0.001	0.000	0.002	0.000	0.017	-0.549	-3.500
0.260	0.000	0.014	0.000	0.055	0.000	0.055	-0.288	-3.000
0.299	0.000	0.006	0.000	0.020	0.000	0.020	-0.116	-2.500
0.371	0.000	-0.012	0.000	-0.031	0.000	-0.030	-0.033	-2.000
0.410	0.000	-0.019	0.000	-0.046	0.000	-0.044	-0.016	-1.800
0.454	0.000	-0.025	0.000	-0.055	0.000	-0.054	-0.007	-1.600
0.504	0.000	-0.030	0.000	-0.059	0.000	-0.059	-0.002	-1.400
0.559	0.000	-0.033	0.000	-0.059	0.000	-0.060	-0.000	-1.200
0.619	0.000	-0.034	0.000	-0.055	0.000	-0.055	0.000	-1.000
0.686	0.000	-0.033	0.000	-0.048	0.000	-0.048	0.000	-0.800
0.757	0.000	-0.029	0.000	-0.038	0.000	-0.038	0.000	-0.600
0.834	0.000	-0.022	0.000	-0.027	0.000	-0.027	0.000	-0.400
0.916	0.000	-0.013	0.000	-0.014	0.000	-0.014	0.000	-0.200
1.000	0.000	0.000	0.000	0.000	0.000	0262.400	0.000	-0.000
1.087	-0.006	0.015	0.000	0.014	0.000	0.015	0.000	0.200
1.182	-0.018	0.034	0.000	0.029	0.000	0.030	0.000	0.400
1.286	-0.034	0.055	0.000	0.043	0.001	0.046	0.000	0.600
1.399	-0.053	0.079	0.000	0.056	0.002	0.062	0.000	0.800
1.521	-0.074	0.105	0.000	0.069	0.003	0.079	0.000	1.000
1.653	-0.099	0.134	0.000	0.081	0.005	0.095	0.000	1.200
1.796	-0.126	0.164	0.000	0.091	0.006	0.113	0.000	1.400
1.950	-0.154	0.197	0.000	0.100	0.008	0.130	0.000	1.600
2.116	-0.185	0.230	0.000	0.108	0.009	0.147	0.000	1.800
2.293	-0.217	0.265	0.000	0.115	0.011	0.165	0.000	2.000
2.789	-0.299	0.354	0.000	0.126	0.013	0.210	0.000	2.500
3.367	-0.382	0.441	0.000	0.129	0.015	0.254	0.000	3.000
4.031	-0.457	0.518	0.000	0.127	0.014	0.299	0.000	3.500
4.785	-0.518	0.579	0.000	0.120	0.013	0.344	0.000	4.000
5.630	-0.556	0.615	0.000	0.108	0.011	0.388	0.000	4.500
6.570	-0.565	0.619	0.000	0.094	0.008	0.432	0.000	5.000
7.603	-0.536	0.582	0.000	0.076	0.005	0.476	0.000	5.500
8.731	-0.461	0.497	0.000	0.057	0.003	0.519	0.000	6.000
9.952	-0.332	0.357	0.000	0.036	0.001	0.561	0.000	6.500
11.265	-0.144	0.153	0.000	0.014	0.000	0.603	0.000	7.000
12.666	0.113	-0.120	0.000	-0.009	0.000	0.645	0.000	7.500
14.154	0.443	-0.470	0.000	-0.033	0.001	0.686	0.000	8.000
15.726	0.854	-0.903	0.000	-0.057	0.003	0.726	0.000	8.500
17.376	1.351	-1.424	0.000	-0.081	0.006	0.766	0.000	9.000
19.101	1.939	-2.039	0.000	-0.106	0.011	0.805	0.000	9.500
20.897	2.624	-2.752	0.000	-0.130	0.016	0.844	0.000	10.000

Real part matching.

matching equation but are not determined by them but are free to be set by some other requirement e.g. self-consistency. Also the symmetry points could be complex and this could be used to represent amplitudes with circular cuts etc.

3. Basic equations of Matching

$$A(\nu_{Fj}) = \frac{N(\nu_{Fj})}{D(\nu_{Fj})} \qquad j = 1 \ldots n_F$$

$$A_{\ell I}(\nu) = \frac{4}{\pi\nu}\int_0^\infty d\nu' \sum_{\ell' I'} \mathrm{Im}\, A_{\ell' I'}(\nu).(2\ell+1).\beta_{II'} P_{\ell'}\left[1 + \frac{2(\nu+1)}{\nu'}\right] Q_\ell\left[1 + \frac{2(\nu'+1)}{\nu}\right]$$

~ crossed amplitude - given.

by N and D, we mean the Balazs pole form

$$N(\nu) = (\nu - \nu_0) \sum_{i=1}^{n_\ell} \frac{F^i}{\nu - \nu^i}$$

where $\nu' = \nu_0$; $F^1 = A(\nu_0)$.

$$D(\nu) = 1 - \frac{(\nu - \nu_0)}{\pi} \sum_{i=1}^{n_\ell} F^i . I(\nu, \nu)$$

for far left and possibly some treatment of the near left.

(i). Real parts only

$$\mathrm{Re}\, A(\nu_{Fj}) = A^j = \frac{(\nu_{Fj} - \nu_0) \sum_i \frac{F^i}{\nu_{Fj} - \nu_i}}{1 - \frac{(\nu_{Fj} - \nu_0)}{\pi} \sum_i F^i . I(\nu_{Fj}, \nu_i)}$$

$$\therefore \quad \sum_i E^{ji} . F^i = A^j$$

$$E^{ji} = (\nu_{Fj} - \nu_0)\left[\frac{1}{(\nu_{Fj} - \nu_i)} + A^j . \frac{I(\nu_{Fj}, \nu_i)}{\pi}\right]$$

The region of real part matching can be extended. Note $\mathrm{Im}\, A(\nu_0) \neq 0$ if $\nu_0 < -1$.

(ii). Imaginary part matching, with just normalisation point restriction on real part ..

$$N(\nu) = A(\nu_0) + \frac{(\nu - \nu_0)}{\pi}\int_{-\infty}^{-1} \frac{\mathrm{Im}\, N(\nu')\, d\nu'}{(\nu' - \nu)(\nu' - \nu_0)}$$

$$\mathrm{Im}\, N(\nu') = \mathrm{Im}\, A(\nu') . D(\nu').$$

$$N(\nu) = (\nu - \nu_0) \sum_{i=1}^{n_\ell} \frac{F^i}{\nu - \nu^i} + \frac{(\nu - \nu_0)}{\pi}\int_{-\infty}^{-1} \frac{\mathrm{Im}\, N(\nu')\, d\nu'}{(\nu' - \nu)(\nu' - \nu_j)}$$

$$\nu' = \nu_o \quad , \quad F' = A(\nu_o)$$

Ignore far poles and put $\nu_o = o$ so $A(\nu_o) = o$ leaving only the near left singularities in $N(\nu)$. Now replace near integral by numerical integration

$$\sim \frac{(\nu - \nu_o)}{\pi} \sum_{i=1}^{nk} \frac{\text{Im } N(\nu_i) . W^i}{(\nu - \nu)(\nu_i - \nu)}$$

$$\text{Im } N(\nu_i) = \text{Im} A(\nu_i) . D(\nu_i).$$

$$\sim (\nu - \nu_o) \sum_{i=1}^{nk} \frac{F^i}{(\nu - \nu_i)}$$

$$F^i = \frac{\text{Im } N(\nu_i) . W^i}{\pi (\nu_i - \nu)}$$

$$F^i = - \frac{W^i}{\pi (\nu_i - \nu_o)} . \text{ Im } A(\nu_i) . \left[1 - \frac{(\nu_i - \nu_o)}{\pi} \sum_{j=1}^{nclink} F^j I^{ij} \right]$$

$$i = 1 \ldots nk$$

so $$\sum_{j=1}^{nk} \left[\delta^{ij} + \frac{(\nu_i - \nu_o)}{\pi} I^{ij} . A^i \right] . F^j . = + A^i$$

$$A^i = - \frac{W^i . \text{ Im } A(\nu^i)}{\pi (\nu_i - \nu_o)} .$$

or $$\sum_{j=1}^{nk} (\nu_i - \nu) . \left[\frac{\pi \delta^{ij}}{- W^i} + \frac{I^{ij}}{\pi} . B^i \right] . F^j = B^i$$

$$B^i = \text{Im } A(\nu_i).$$

(iii) Imaginary part matching with NFP real poles with real symmetry points not on cut.

$$N(\nu) = A(\nu_o) + \frac{(\nu - \nu_o)}{\pi} \int_{-\infty}^{-1} \frac{\text{Im } N(\nu') \, d\nu'}{(\nu' - \nu)(\nu' - \nu_o)} \qquad \text{(i)}$$

$$\text{Im } N(\nu') = \text{Im } A(\nu') . D(\nu') . \qquad \text{(ii)}$$

represent far left by N F P real poles

$$N(\nu) = A(\nu_1) + (\nu - \nu_o) \sum_j \frac{F^j}{(\nu - \nu_j)} + \frac{(\nu - \nu_o)}{\pi} . \int_{co}^{-1} \frac{\text{Im } N(\nu') \, d\nu'}{(\nu' - \nu)(\nu' - \nu_c)} \qquad \text{(iii)}$$

denote $\nu_o = \nu_1$ $\qquad A(\nu_o) = F^1_{NL}$ $\qquad$ (iv)

replace integral by $$\frac{(\nu - \nu_o)}{\pi} \sum_{J=NFP+1} \frac{\text{Im } N(\nu_j) .}{(\nu_j - \nu)(\nu_j - \nu_o)} W^j \qquad \text{(v)}$$

and further by $$(\nu - \nu_o) \sum_{J=NPP+1}^{NL} \frac{F^j}{\nu - \nu_j} \qquad \text{(vi)}$$

$$\text{where } F^j = -\frac{W^j \cdot \operatorname{Im} N(\nu_j)}{(\nu_j - \nu_o)} \qquad j = NFP+1 \,..\, NL \qquad \text{(vii)}$$

$$\text{so} \quad N(\nu) = (\nu - \nu_o) \sum_{j=1}^{NL} \frac{F_j}{\nu - \nu_j} \qquad \text{(viii)}$$

$$\text{and } D(\nu) = 1 - \frac{(\nu - \nu_o)}{\pi} \sum_j F^j I^i{}_j. \qquad \text{(ix)}$$

now match real parts at real sym. points ν_{Fi} $i = 1 \ldots NFP$

and imaginary parts . . . . $NFP+1 \,..\, NL$

to the crossed amplitude A^i (Re $A(\nu_{Fi})$ $i = 1 \,..\, NFP$

Im $A(\nu_{Fi})$ $i = NFP+1 \,..\, NL$)

$$\text{so} \quad \sum_j \beta^{ij} \cdot F^j = N^i = N(\nu_i) \qquad \text{(x)}$$

where for $i \leq NFP$

$$\beta^{ij} = \frac{\nu_{F_i} - \nu_o}{\nu_{Fi} - \nu_j} \qquad \text{(xi)}$$

$i > NFP$

$$\beta^{ij} = -\frac{\pi}{\omega^i} \cdot (\nu_{Fi} - \nu_o) \cdot \delta_{ij}. \qquad \text{(xii)}$$

$$\frac{\sum_j \beta^{ij} F^j}{1 - (\nu_i - \nu_o) \sum F_j I'_j} = A^i \qquad \text{(xiii)}$$

$$\sum_j E^{ij} F^j = A^i \qquad \text{(xiv)}$$

$$E^{ij} = \beta^{ij} + \frac{(\nu_{Fi} - \nu_o)}{\pi} \cdot A^i \cdot I^{ij} \qquad \text{(xv)}$$

$$\text{Thus } \frac{(\nu_{Fi} - \nu_o) \sum_{j=1}^{NFP} \frac{F_j}{\nu_i - \nu_j} + (\nu_{Fi} - \nu_o) \sum_{j=NFP+1}^{NL} \frac{F_j}{\nu_i - \nu_j} = \underset{(\operatorname{Re} A(\nu_i))}{A^i} \quad i = 1..NFP}{\left[1 - \frac{(\nu_i - \nu_o)}{\pi} \sum_j F^j I^{ji}\right]}$$

$$\frac{(\nu_i - \nu_o) \cdot \frac{-\pi}{W^i} F^i}{\left[1 - \frac{(\nu_i - \nu_o)}{\pi} \sum_j F^j I^{ji}\right]} = \underset{(\operatorname{Im} A(\nu_i))}{A^i} \qquad i = NFP+1 \,..\, NL$$

or more transparently

$$\frac{(\nu_i - \nu_o)\cdot F^i}{\left[1 - \frac{(\nu_i - \nu_o)}{\pi} \sum_j F^j I^{ji}\right]} = \frac{(\nu_i - \nu_o)}{\pi} \cdot \frac{\mathrm{Im}\, A^i}{(\nu_o - \nu_i)} \cdot W^i$$

$$\beta = \begin{matrix} \uparrow \\ i \\ \downarrow \end{matrix} \begin{matrix} \uparrow \\ \mathrm{NFP} \\ \downarrow \end{matrix} \left[\begin{matrix} \longleftarrow\ j\ \longrightarrow \\ \frac{\nu_i - \nu_o}{\nu_i - \nu_j} \\ \hline 0 \quad \Big| \quad -\pi\delta_{ij}\frac{(\nu_i - \nu_o)}{\omega^i} \end{matrix}\right]$$

Note that real poles influence imaginary ones only by their occurrence in the D function whereas imag. ones influence real ones by occurrence in N and D; this gives some insight into the relative roles of the real and imaginary parts of the crossed amplitude and hence a bearing on the near and far cut contributions.

To reconstruct $\{A^i\}$ given $\{F^j\}$

Matching equations are

$$\frac{(\nu_i - \nu_o) \sum_{j=1}^{NL} \frac{F_j}{\nu_i - \nu_j}}{D(\nu_i)} = A^i \qquad i = 1 \,..\, NFP$$
$$(\mathrm{Re}\ A(\nu_i))$$

$$\frac{(\nu_i - \nu_o) - \frac{\pi}{W^i} F^i}{D(\nu_i)} = A^i \qquad i = NFP + 1 \,..\, NL$$
$$(\mathrm{Im}\ A(\nu_i))$$

i.e. $$(\nu_i - \nu_o) \sum_{j=1}^{NL} \frac{F^j}{\nu_i - \nu_j} = N^i \qquad i = 1 \,..\, NFP$$
$$(\mathrm{Re}\ N(\nu_i))$$

$$(\nu_i - \nu_o)\cdot \frac{-\pi}{W^i} \cdot F^i = N^i \qquad i = NFP + 1 \,..\, NL$$
$$(\mathrm{Im}\ N(\nu_i))$$

$$D^i = 1 - \frac{(\nu_i - \nu_o)}{\pi} \sum_{j=1}^{NL} F^j I^{ji}$$

hence reconstruction.

(iv). Matching with real symmetry points on the cut.

Equations (i) .. (x), (xii) still hold, i.e. breakdown into poles and

matching of imaginary parts same but now the expression for contribution of near poles to real Symmetry points

$$(\nu_{Fi} - \nu_o) \sum_{j=1}^{NL} \frac{F_j}{\nu_{Fi} - \nu_j} \pm N_i$$

because the denominator vanishes when $\nu_{Fi} \simeq \nu_j$. Incidentally, the real Symmetry points on cut are taken to coincide with near pole positions so that Im $N(\nu_{Fi})$ is given by a simple combination of F's, in fact by (vii); otherwise an interpolated value would be necessary.

Going back to the integral form

$$N(\nu) = (\nu - \nu_o) \sum_{j=1}^{NFP} \frac{F_j}{\nu - \nu_j} + \frac{(\nu - \nu_o)}{\pi} \int_{co}^{-1} \frac{d\nu' \ \mathrm{Im}\, N(\nu')}{(\nu' - \nu)(\nu' - \nu_o)}$$

we see that, for a value of ν on the cut, this is best written

$$N(\nu) = (\nu - \nu_o) \sum_{j=1}^{NFP} \frac{F_j}{\nu - \nu_j} + \frac{(\nu - \nu_o)}{\pi} \int_{co}^{-1} \frac{d\nu' \left[\mathrm{ImN}(\nu') - \mathrm{ImN}(\nu)\right]}{(\nu' - \nu)(\nu' - \nu_o)}$$

$$+ \mathrm{Im}\, N(\nu) \cdot \frac{(\nu - \nu_o)}{\pi} \int_{co}^{-1} \frac{d\nu'}{(\nu' - \nu)(\nu' - \nu_o)}$$

where expression

$\left[\frac{\mathrm{ImN}(\nu') - \mathrm{ImN}(\nu)}{(\nu' - \nu)}\right]$ has value $\mathrm{ImN}'(\nu)$ when $\nu' = \nu$

Now, $(\nu - \nu_o) \int_{\infty}^{-1} \frac{d\nu'}{(\nu' - \nu)(\nu' - \nu_o)} = \left[\log \frac{\nu' - \nu}{\nu' - \nu_o}\right]_{co}^{-1}$

$$= \log \left| \frac{(1 + \nu)(co - \nu_o)}{(1 + \nu_o)(co - \nu)} \right|$$

So, $N(\nu) = (\nu - \nu_o) \sum_{j=1}^{NFP} \frac{Fj}{\nu - \nu j} + \frac{(\nu - \nu_o)}{\pi} \int_{co}^{-1} \frac{d\nu' \left[\mathrm{ImN}(\nu') - \mathrm{ImN}(\nu)\right]}{(\nu' - \nu)(\nu' - \nu_o)}$

$$+ \frac{\mathrm{ImN}(\nu)}{\pi} \cdot \log \left| \frac{(1 + \nu) \cdot (co - \nu_o)}{(1 + o) \cdot (co - \nu)} \right|$$

We now replace integral by poles, taking

$$\mathrm{ImN}'(\nu_j) = \left\{ \frac{\mathrm{ImN}(\nu_{j+1}) - \mathrm{ImN}(\nu_{j-1})}{\nu_{j+1} - \nu_{j-1}} \right\}$$

So,

$$N(\nu) = (\nu - \nu_o) \sum_{j=1}^{NFP} \frac{F_j}{\nu - \nu_j} + \frac{(\nu - \nu_o)}{\pi} \sum_{j=NFP+1}^{NL} \left[\frac{ImN(\nu_j) - ImN(\nu)}{(\nu_j - \nu)(\nu_j - \nu_o)} \right] . W^j$$

$$+ \frac{ImN(\nu)}{\pi} \cdot \log \left| \frac{(1+\nu)(co - vo)}{(1+\nu_o)(co - \nu)} \right|$$

This can be simply expressed in terms of $\{ F_j \}$ when

$$\nu = \nu_{Fi} = \nu_J \quad \text{say}$$

$$N(\nu) = (\nu - \nu_o) \sum_{J=1}^{NFP} \frac{F_j}{\nu_J - \nu_j} + (\nu_J - \nu_o) \sum_{\substack{j=NFP+1 \\ j \neq J}}^{NL}$$

$$\left[\frac{F_j - F^J \cdot \frac{W^j}{W^J} \frac{(\nu_J - \nu_o)}{(\nu_j - \nu_o)}}{\nu_J - \nu_j} \right]$$

$$- \frac{(\nu_J - \nu_o)}{W_J} \cdot F^J \cdot \log \left| \frac{(1 + \nu_J) \cdot (co - vo)}{(1 + \nu_o) \cdot (co - \nu_J)} \right|$$

$$+ \frac{ImN'(\nu_J) \cdot W^J}{\pi}$$

last term $\rightarrow$ $\frac{W^J}{\pi} \cdot \left[\frac{ImN(\nu_{J+1}) - ImN(\nu_{J-1})}{\nu_{J+1} - \nu_{J-1}} \right]$

$$= - W^J \left[\frac{(\nu_{J+1} - \nu_o) \cdot F^{J+1}}{W^{J+1}} - \frac{(\nu_{J-1} - \nu_o) \cdot F^{J-1}}{W^{J-1}} \right]$$

$$(\nu_{J+1} - \nu_{J-1})$$

So finally we have our expression for $N(\nu)$ at one of the pole positions, in terms of $\{ F_j \}$.

$$N(\nu_J) = (\nu_J - \nu_o) \sum_{j=1}^{NFP} \frac{F^j}{\nu_J - \nu_j} + (\nu_J - \nu_o) \sum_{\substack{j=NFP+1 \\ j \neq J}}^{N} \left[\frac{F^j - F^J \cdot \frac{W^j}{W_J} \frac{(\nu_J - \nu)}{(\nu_j - \nu_o)}}{(\nu_J - \nu_j)} \right]$$

$$- (\nu_J - \nu_o) \cdot \frac{F^J}{W^J} \cdot \log \left| \frac{(1 + \nu_J)(co - \nu_o)}{(1 + \nu_o)(co - \nu_J)} \right|$$

$$- \frac{\omega_J W^J}{(\nu_{J+1} - \nu_{J-1})} \left[\frac{(\nu_{J+1} - \nu_o) \cdot F^{J+1}}{W^{J+1}} - \frac{\nu_{J-1} - \nu_o) \cdot F^{J-1}}{W^{J-1}} \right] \quad (A)$$

This expression is used for matching to the crossed amplitude at symmetry points and for reconstructing the matched amplitude at other points on the cut, as well as at the symmetry points. Writing it as

$$\sum_{j=1}^{NL} B_{Jj} \cdot F^j = N_J \qquad J \sim \text{on cut}$$

clearly $B_{Jj} = \dfrac{\nu_J - \nu_o}{\nu_J - \nu_j} \qquad j \neq J-1, J, J+1 \qquad \text{(xi)}$

$$B_{Jj} = \frac{-(\nu_J - \nu_o)}{W^J} \cdot \log \frac{(1+\nu_J)\cdot(\infty - \nu_o)}{(1+\nu_o)\cdot(\infty - \nu_J)} + (\nu_J - \nu_o) \sum_{\substack{j=NFP+1 \\ j\neq J}}^{NL} \left[\frac{-W^j_j}{W^J} \cdot \frac{(\nu_J - \nu_o)}{(\nu_j - \nu_o)} \cdot \frac{1}{\nu_J - \nu_j} \right]$$

$$B_{Jj} = \frac{(\nu_J - \nu_o)}{\nu_J - \nu_j} - \frac{(\nu_{J\pm1} - \nu_o)\cdot W^J}{(\nu_{J+1} - \nu_{J-1})\cdot W^{J\pm1}} \qquad \begin{matrix} j \equiv J \\ j \equiv J \pm 1 \end{matrix}$$

One then obtains $E(i, j)$ using (xiii), (xiv), (xv). Note B has same structure as before.

$$B = \begin{matrix} \uparrow \\ i \\ \downarrow \end{matrix} \quad \begin{matrix} \uparrow \\ NFP \\ \downarrow \end{matrix} \quad \left[\begin{matrix} \longleftarrow j \longrightarrow \\ 0 \quad \sim \delta_{ij} \end{matrix} \right]$$

To reconstruct $\{N^i\}$ given $\{F_j\}$.

$$N^i = N(\nu_{Fi}) = N(\nu_i)$$

changing notation for simplicity.

We simply use equation (A) to define N^i.

$$\sum_{j=1}^{NL} B_{ij} F_j = N^i$$

$$B_{ij} = \frac{\nu_i - \nu_o}{\nu_i - \nu_j} \qquad \begin{matrix} i \sim \text{on cut} \\ j = 1 \ldots NL \\ j \neq i-1, i, i+1 \end{matrix}$$

$$B_{ij} = \frac{(\nu_i - \nu_o)}{(\nu_i - \nu_j)} - \frac{(\nu_{i \pm 1} - \nu_o)}{(\nu_{i+1} - \nu_{i-1})} W^{i \pm 1}$$

$i \sim$ on cut

$j = i \pm 1$

$$B_{ij} = -\frac{(\nu_i - \nu_o)}{W^i} \cdot \log \left| \frac{(1 + \nu_i)\ (\infty - \nu_o)}{(1 + \nu_o)\ (\infty - \nu_i)} \right| + \frac{(\nu_i - \nu_o)^2}{W^i} \sum_{\substack{j = NFP + 1 \\ j \neq 1}}^{NL} \frac{-W^j}{(\nu_j - \nu_o)\ (\nu_i - \nu_j)}$$

$i \sim$ on cut

$j \equiv i.$

Note that decoupling of real and imaginary matching occurs if we average out the D function, i.e. following Patil and Kane (3), we take

$$D(\nu) = 1 - \frac{(\nu - \nu_o)}{(\nu_R - \nu_o)}$$

thus $$F^i = \frac{-W^i}{\pi\ (\nu^i - \nu o)} \mathrm{Im}A(\nu_i) \cdot \left[1 - \frac{(\nu_i - \nu_o)}{(\nu_R - \nu_o)} \right]$$

$i = 1, nk.$

(For Imaginary but not Real part matching, the far pole residues are obtained from the real part matching equations.)

We can also easily match $N(\nu)$ to $C(\nu)$, instead of $\frac{N(\nu)}{D(\nu)}$ to $C(\nu)$, giving some sort of analogue of the Zachariasen ansatz but with different asymptotic behaviour of N. [illegible] or C( ).

Compatibility and Comparison of Real, Imaginary and Complex Matching

$$E^{ij} = B^{ij} + A^i \cdot (\nu_i - \nu_o)\ \frac{I^{ji}}{\pi}$$

(a) Real.. $$B^{ij} = \frac{\nu_i - \nu_o}{\nu_i - \nu_j}$$

(b) Imaginary..

$$B^{ij} = \frac{\pi \delta^{ij} \cdot (\nu^i - \nu^o)}{-W^i}$$

(c) Complex:

Imaginary. $\dfrac{-\pi . \delta^{ij}}{W^i} \quad (\nu^i - \nu^o)$

Real far $\left\{\dfrac{\nu_i - \nu_o}{\nu_i - \nu_j}\right\}$

Real near $\left\{\dfrac{\nu_i - \nu_o}{\nu_i - \nu_j}\right\}$ $\qquad j \neq i-1, i, i+1$

complicated expressions. $\qquad j = i-1, i, i+1.$

Incidentally, although the imaginary part matching is equivalent to numerical integration of the N/D equations, this is not true for real or complex matching. The location of poles and the choice of symmetry point region allows a certain amount of scope for intuition and allows one to see what is happening in geometrical terms.

4. Modification to introduce extra poles on left

To be able to simulate the Oades method (Chapter 5) and for general completeness reasons, it is desirable to be able to put in extra poles on the left to be either fixed or varied in self consistent calculations.

Oades simply puts in poles in the A function but we are working with an N/D form which is always unitary and it would be disastrous with many unknown consequences to simply add poles in A, making it nonunitary etc. Hence, we must add poles to the N function, automatically modifying D and leaving A unitary.

We should still like to be able to match at symmetry points, to determine the other poles, and this is seen to be possible, for

$$\frac{(\nu_j - \nu_o)\sum_{i=1}^{nl+nah} \dfrac{F^i}{j-i} = A^j}{\left\{1 - \dfrac{(\nu_j - \nu_o)}{\pi}\sum_{i=1}^{nl+nah} F^i I^{ij}\right\}} \qquad j = 1 \ldots 4\ell$$

nl ordinary poles
nah extra ("ad hoc") poles

$$(\nu_j - \nu_o)\sum_{i=1}^{nl+nah} F^i\left[\frac{1}{\nu_j - \nu_i} + \frac{1}{\pi} A^j I^{ij}\right] = A^j \qquad j = 1 \ldots nl$$

$$(\nu_j - \nu_o) \sum_{i=1}^{nl} F^i \left[\frac{1}{\nu_j - \nu_i} + \frac{1}{\pi} A^j I^{ij} \right]$$

$$= A^j - (\nu_j - \nu_o) \sum_{i=nl+1}^{nl+nah} F^i \left[\frac{1}{\nu_j - \nu_i} + \frac{1}{\pi} A^j I^{ij} \right] \qquad j = 1 \,..\, nl$$

F^i, ν_i. $i = nl + 1$, $nl + nah$ are data or determined otherwise, so we see that there is merely a correction to A^j leaving E^{ij} unchanged.

In a self consistency calculation, it is important that the parametrisation be (able to be) identical for input and output functions, so we should like to put the poles also in the input function automatically. This is easily accomplished by putting $nl \rightarrow nl + nah$ in calculating ReD, ReN, ImA for input function, thus no anomalies arise here.

An extra advantage is seen in that we can now look for solutions with various numbers of spare parameters and do not have to lean too hard on matching and self consistency to determine all the parameters, committing ourselves to a full bootstrap with no free parameters.

One might think that poles in input and output functions are equivalent to none, i.e. calcellation of effects. This is true in demanding self-consistency, but not at the matching stage, so they do have a non-trivial rôle.

5. Extension to cuts not on the real axis

This is trivial.

Imaginary parts.. $\dfrac{F^j}{D(\nu_j)} = F^{jl}$ $\qquad i = 1 \,..\, (n+1)$ poles outside.

Real parts..

$$\frac{(\nu_j - \nu_o) \sum \left\{ \dfrac{F^i}{\nu_j - \nu_i} + \dfrac{F^{i\,*}}{\nu_j - \nu_i{}^*} \right\}}{D(\nu_j)} = A(\nu_j) \qquad j = 1 \,..\, (n+1)$$

$\ldots$ is a complex quantity.

If ν_j on the real axis, then imaginary parts vanish.

For far poles on real axis we need only use ν_j on real axis. The usual

situation will be that the poles in complex plane will be determined by "imaginary part" matching and far poles will occur on the far real axis and will be determined by real part matching at real symmetry points.

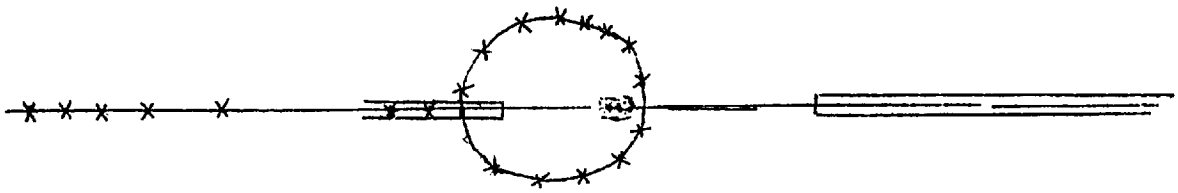

far region near region physical region

6. Results of improved matching

The result of imaginary part matching only is shown in Fig. 10 and tabulated in Table 10, proving that the near left discontinuity from the exchange of the ρ is small and has the wrong sign and that a nearby singularity approac is either wrong or else one needs a lot more left hand cut extending into the double spectral region. The effect of imaginary part matching in the case of δ function approximation to $C(\nu)$ is interesting since it shows that the near left discontinuity has a large effect and probably determines small scale structure of the real part on the near left.

The results for complex matching were erratic and disappointing. The amplitudes obtained were similar to those for real part matching only and were sensitive to $\{\nu_F\}$ and, tended to settle down as n increased, keeping ν_{Fi} fixed, to amplitudes with a zero in the physical region or else a vague rise of ReA in the physical region. Very few resonant amplitudes were obtained. The results are summarised in Table 11 and tabulated in Table 12 and shown for n = 9 in Fig. 11. The fit to real and imaginary parts on the near left was of course very good, and even the rapidly changing δ function form of $C(\nu)$ could be reproduced results for real, imaginary and complex matching are tabulated in Tables 13, 14, 15 and shown in Fig. 12. Using the "Zachariasen" matching, $N(\ )_{Fj} = C(\ )_{Fj}$ was found to be very similar to the Balazs matching A = C in the simple cases in which it was looked at.

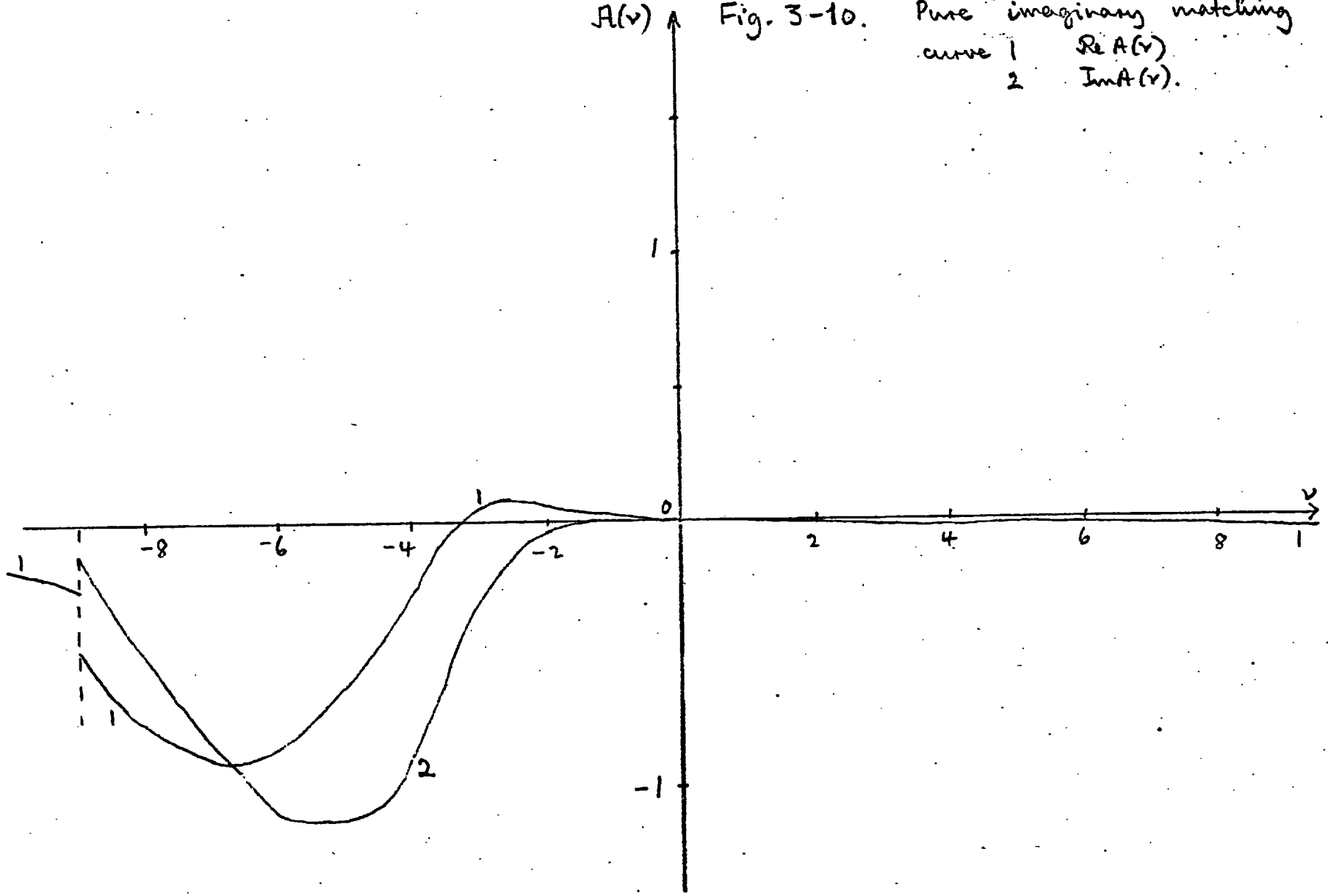

Fig. 3-10. Pure imaginary matching
curve 1 Re A(ν)
2 Im A(ν).

Table 3-10

ZED	THD	REN	THN	REM	THM	REC	THC	Y
0.972	0.000	-0.174	0.000	-0.179	0.000	-3.229	0.261	-10.000
0.973	0.000	-0.196	0.000	-0.201	0.000	-3.092	0.068	-9.500
—	—	—	—	—	—	-2.933	-0.135	-8.973
0.974	0.000	-0.514	-0.175	-0.528	-0.180	-2.894	-0.180	-8.856
0.974	0.000	-0.574	-0.253	-0.590	-0.259	-2.823	-0.259	-8.649
0.975	0.000	-0.656	-0.361	-0.673	-0.370	-2.721	-0.370	-8.356
0.976	0.000	-0.741	-0.496	-0.759	-0.508	-2.572	-0.508	-7.985
0.978	0.000	-0.814	-0.651	-0.833	-0.665	-2.385	-0.665	-7.544
0.980	0.000	-0.861	-0.814	-0.878	-0.831	-2.146	-0.831	-7.043
0.983	0.000	-0.865	-0.969	-0.880	-0.986	-1.833	-0.986	-6.495
0.985	0.000	-0.811	-1.090	-0.823	-1.106	-1.471	-1.106	-5.911
0.988	0.000	-0.687	-1.140	-0.695	-1.153	-1.059	-1.153	-5.306
0.990	0.000	-0.492	-1.073	-0.497	-1.084	-0.624	-1.084	-4.694
0.991	0.000	-0.257	-0.861	-0.259	-0.869	-0.227	-0.869	-4.089
0.990	0.000	-0.053	-0.546	-0.053	-0.552	0.016	-0.552	-3.505
0.989	0.000	0.054	-0.266	0.054	-0.269	0.053	-0.269	-2.957
0.989	0.000	0.075	-0.104	0.076	-0.106	0.014	-0.106	-2.456
0.989	0.000	0.062	-0.034	0.063	-0.034	-0.029	-0.034	-2.015
0.990	0.000	0.045	-0.008	0.045	-0.008	-0.052	-0.008	-1.644
0.991	0.000	0.032	-0.001	0.032	-0.001	-0.060	-0.001	-1.351
0.992	0.000	0.024	-0.000	0.025	-0.000	-0.059	-0.000	-1.144
—	—	—	—	—	—	-0.056	-0.000	-1.027
0.994	0.000	0.015	0.000	0.015	0.000	-0.048	0.000	-0.800
0.995	0.000	0.011	0.000	0.011	0.000	-0.038	0.000	-0.600
0.996	0.000	0.007	0.000	0.007	0.000	-0.027	0.000	-0.400
0.998	0.000	0.003	0.000	0.003	0.000	-0.014	0.000	-0.200
1.000	0.000	0.000	0.000	0.000	0.000	7447.680	0.000	-0.000
1.003	0.001	-0.003	0.000	-0.003	0.000	0.015	0.000	0.200
1.004	0.003	-0.006	0.000	-0.006	0.000	0.030	0.000	0.400
1.006	0.005	-0.008	0.000	-0.008	0.000	0.046	0.000	0.600
1.007	0.007	-0.010	0.000	-0.010	0.000	0.062	0.000	0.800
1.008	0.009	-0.012	0.000	-0.012	0.000	0.079	0.000	1.000
1.008	0.011	-0.014	0.000	-0.014	0.000	0.095	0.000	1.200
1.008	0.012	-0.016	0.000	-0.016	0.000	0.113	0.000	1.400
1.009	0.014	-0.018	0.000	-0.018	0.000	0.130	0.000	1.600
1.009	0.016	-0.019	0.000	-0.019	0.000	0.147	0.000	1.800
1.009	0.017	-0.021	0.000	-0.021	0.000	0.165	0.000	2.000
1.008	0.021	-0.024	0.000	-0.024	0.000	0.210	0.000	2.500
1.008	0.024	-0.027	0.000	-0.027	0.001	0.254	0.000	3.000
1.007	0.026	-0.030	0.000	-0.030	0.001	0.299	0.000	3.500
1.006	0.029	-0.032	0.000	-0.032	0.001	0.344	0.000	4.000
1.005	0.031	-0.034	0.000	-0.034	0.001	0.388	0.000	4.500
1.004	0.033	-0.036	0.000	-0.036	0.001	0.432	0.000	5.000
1.003	0.035	-0.038	0.000	-0.038	0.001	0.476	0.000	5.500
1.002	0.036	-0.039	0.000	-0.039	0.001	0.519	0.000	6.000
1.001	0.038	-0.041	0.000	-0.041	0.002	0.561	0.000	6.500
1.000	0.039	-0.042	0.000	-0.042	0.002	0.603	0.000	7.000
0.999	0.041	-0.043	0.000	-0.043	0.002	0.645	0.000	7.500
0.998	0.042	-0.044	0.000	-0.044	0.002	0.686	0.000	8.000
0.997	0.043	-0.045	0.000	-0.045	0.002	0.726	0.000	8.500
0.996	0.044	-0.046	0.000	-0.046	0.002	0.766	0.000	9.000
0.995	0.045	-0.047	0.000	-0.047	0.002	0.805	0.000	9.500
0.995	0.046	-0.048	0.000	-0.048	0.002	0.844	0.000	10.000

Imaginary part unbelong.

TABLES - 3-11

Static studies. complex matching. input (3.4, 2.6)

(a) Continuous C(ν)

NFP	NNP	matching region	comments
0	20	[0, -9]	ReA small and negative
1	20	[0, -9]	ReA rises to 0.44
2	20	[-0.8, 0]	ReA rises to 0.5 then falls
2	20	[-2.5, 0]	resonance - self consistent
3	20	[-4, 0]	ReA negative. Zero of ReD ~ -1.0
3	20	[-9, 0]	ReA negative.
4	20	[-4, 0]	ReA rises to .38 then falls.
5	20	"	Zero of ReN at 4.0
6	20	"	" 5.5
7	20	"	" 5.3
8	20	"	" 6.5 zero of ReD at 0.4
9	20	"	" 4.3
9	20	[-8, 0]	ReA rises to 0.2 then falls.
9	20	[-8. 0]	(Input experimental values) Zero of ReN at 6.6

(b) function approximation in C(ν)

0	20	[. .]	ReA small and negative.
2	20	[-0.8, 0]	ReA rises to 0.55 then falls.
2	20	[-2.5, 0]	self consistent resonance
9	20	[-8, 0]	ReA rises to 0.3 then falls.

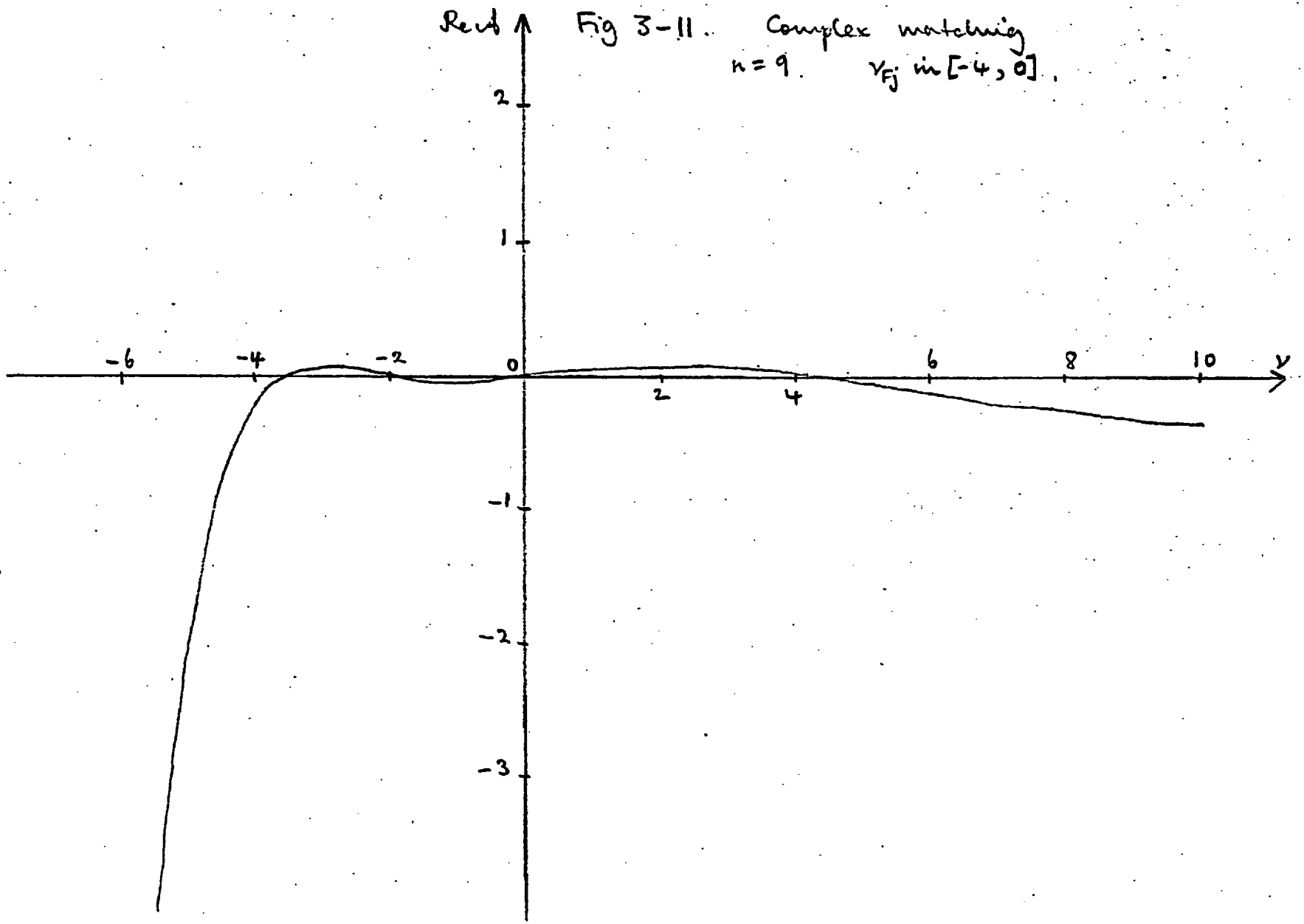

Fig 3-11. Complex matching
$n = 9$. ν_{Fj} in $[-4, 0]$.

Table 3-12.

RED	IMD	REN	IMN	REA	IMA	REC	IMC	Y
2.087	0.0000909	6.834	0.0000018	8.464	0.000	-3.229	0.261	-10.000
1.801	0.0008089	5.395	0.0004491	1.874	0.000	-3.092	0.068	-9.500
						-2.933	-0.135	-8.973
1.464	0.000	-367.709	-0.264	-251.232	-0.180	-2.894	-0.180	-8.856
1.363	0.000	-79.534	-0.354	-58.347	-0.259	-2.823	-0.259	-8.649
1.228	0.000	-12.691	-0.454	-10.339	-0.370	-2.721	-0.370	-8.356
1.066	0.000	-2.743	-0.542	-2.572	-0.508	-2.572	-0.508	-7.985
0.891	0.000	-1.918	-0.593	-2.152	-0.665	-2.385	-0.665	-7.544
0.714	0.000	-1.562	-0.593	-2.146	-0.831	-2.146	-0.831	-7.043
0.547	0.000	-1.018	-0.540	-1.860	-0.986	-1.833	-0.986	-6.495
0.402	0.000	-0.591	-0.444	-1.471	-1.106	-1.471	-1.106	-5.911
0.287	0.000	-0.304	-0.331	-1.059	-1.153	-1.059	-1.153	-5.306
0.209	0.000	-0.131	-0.227	-0.626	-1.084	-0.624	-1.084	-4.694
0.172	0.000	-0.039	-0.149	-0.227	-0.869	-0.227	-0.869	-4.089
0.174	0.000	0.001	-0.096	0.008	-0.552	0.016	-0.552	-3.505
0.212	0.000	0.011	-0.057	0.053	-0.269	0.053	-0.269	-2.957
0.276	0.000	0.004	-0.029	0.014	-0.106	0.014	-0.106	-2.456
0.357	0.000	-0.010	-0.012	-0.029	-0.034	-0.029	-0.034	-2.015
0.442	0.000	-0.023	-0.004	-0.052	-0.008	-0.052	-0.008	-1.644
0.521	0.000	-0.031	-0.001	-0.060	-0.001	-0.060	-0.001	-1.351
0.583	0.000	-0.034	-0.000	-0.059	-0.000	-0.059	-0.000	-1.144
						-0.056	-0.000	-1.027
0.696	0.000	-0.034	0.000	-0.049	0.000	-0.048	0.000	-0.800
0.767	0.000	-0.030	0.000	-0.039	0.000	-0.038	0.000	-0.600
0.842	0.000	-0.023	0.000	-0.028	0.000	-0.027	0.000	-0.400
0.921	0.000	-0.013	0.000	-0.015	0.000	-0.014	0.000	-0.200
1.000	0.000	0.000	0.000	0.000	0.000	7447.680	0.000	-0.000
1.080	-0.007	0.017	0.000	0.016	0.000	0.015	0.000	0.200
1.165	-0.020	0.037	0.000	0.032	0.001	0.030	0.000	0.400
1.258	-0.038	0.062	0.000	0.049	0.001	0.046	0.000	0.600
1.358	-0.060	0.090	0.000	0.066	0.003	0.062	0.000	0.800
1.465	-0.086	0.122	0.000	0.083	0.005	0.079	0.000	1.000
1.580	-0.116	0.157	0.000	0.099	0.007	0.095	0.000	1.200
1.704	-0.150	0.196	0.000	0.114	0.010	0.113	0.000	1.400
1.836	-0.188	0.239	0.000	0.129	0.013	0.130	0.000	1.600
1.978	-0.229	0.285	0.000	0.142	0.016	0.147	0.000	1.800
2.130	-0.273	0.335	0.000	0.155	0.020	0.165	0.000	2.000
2.556	-0.398	0.471	0.000	0.180	0.028	0.210	0.000	2.500
3.053	-0.539	0.622	0.000	0.198	0.035	0.254	0.000	3.000
3.628	-0.690	0.782	0.000	0.208	0.040	0.299	0.000	3.500
4.287	-0.847	0.947	0.000	0.213	0.042	0.344	0.000	4.000
5.034	-1.005	1.108	0.000	0.212	0.042	0.388	0.000	4.500
5.874	-1.150	1.260	0.000	0.207	0.040	0.432	0.000	5.000
6.809	-1.282	1.394	0.000	0.198	0.037	0.476	0.000	5.500
7.842	-1.391	1.502	0.000	0.186	0.033	0.519	0.000	6.000
8.975	-1.468	1.577	0.000	0.171	0.028	0.561	0.000	6.500
10.207	-1.508	1.612	0.000	0.155	0.023	0.603	0.000	7.000
11.539	-1.501	1.598	0.000	0.136	0.018	0.645	0.000	7.500
12.969	-1.440	1.527	0.000	0.116	0.013	0.686	0.000	8.000
14.497	-1.318	1.394	0.000	0.095	0.009	0.726	0.000	8.500
16.119	-1.128	1.189	0.000	0.073	0.005	0.766	0.000	9.000
17.834	-0.864	0.908	0.000	0.051	0.002	0.805	0.000	9.500
19.638	-0.519	0.544	0.000	0.028	0.001	0.844	0.000	10.000

Complex modeling.

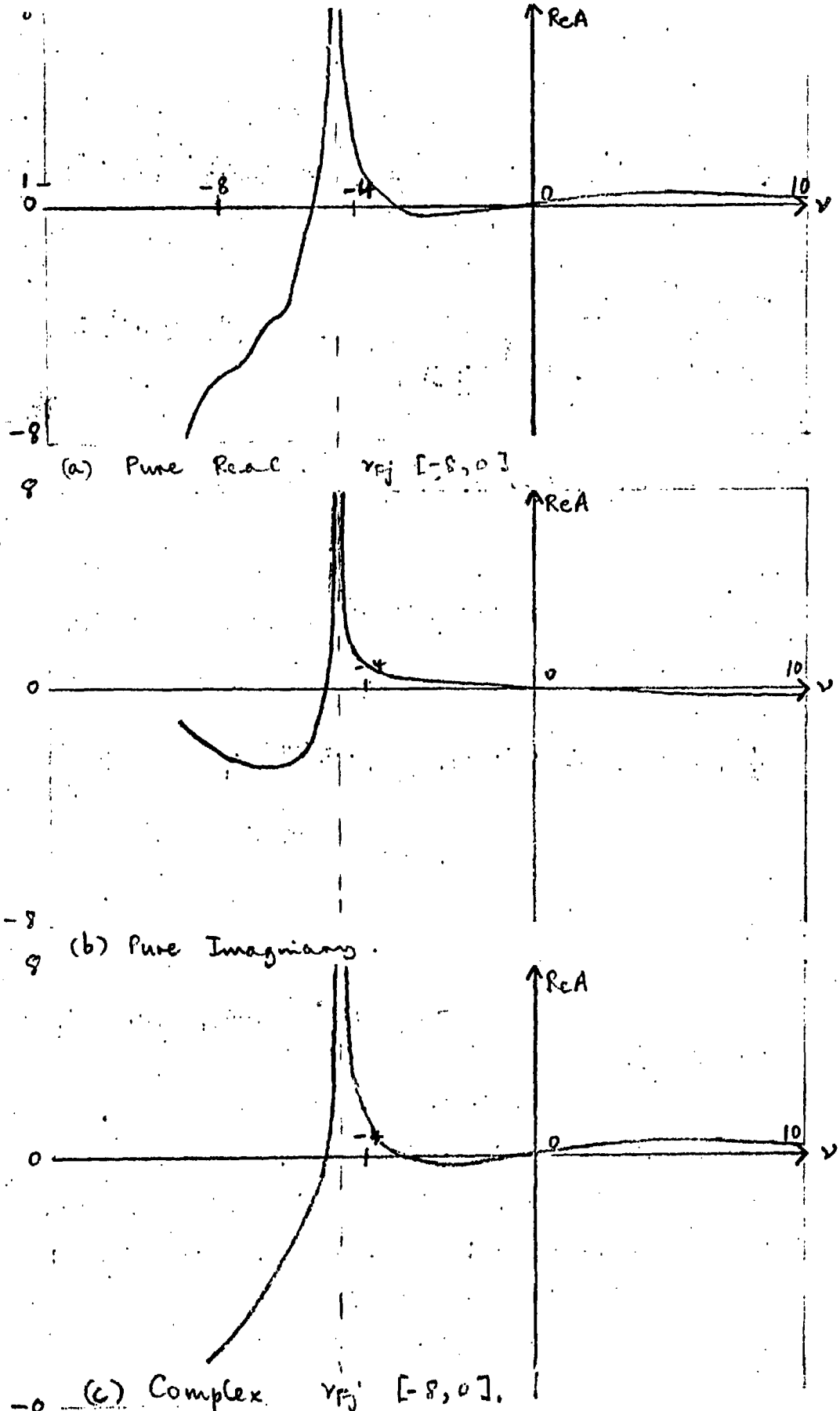

Fig 3-12. Matching to δ function approximation to $C(\gamma)$

Table 3-13 Real part matching with δ function approximation.

RED	IMD	REN	IMN	REA	IMA	ν
0.741	0.000	-960.295	0.000	1295.860	0.000	-9.000
0.580	0.000	-17.086	0.000	-29.478	0.000	-8.500
0.437	0.000	-2.631	0.000	-6.017	0.000	-8.000
0.314	0.000	-1.807	0.000	-5.752	0.000	-7.500
0.211	0.000	-1.110	0.000	-5.262	0.000	-7.000
0.128	0.000	-0.573	0.000	-4.477	0.000	-6.500
0.066	0.000	-0.254	0.000	-3.875	0.000	-6.000
0.024	0.000	-0.087	0.000	-3.572	0.000	-5.500
0.005	0.000	-0.005	0.000	-1.076	0.000	-5.000
0.007	0.000	0.031	0.000	4.745	0.000	-4.500
0.031	0.000	0.041	0.000	1.336	0.000	-4.000
0.077	0.000	0.034	0.000	0.435	0.000	-3.500
0.147	0.000	0.015	0.000	0.101	0.000	-3.000
0.239	0.000	-0.010	0.000	-0.042	0.000	-2.500
0.353	0.000	-0.034	0.000	-0.097	0.000	-2.000
0.405	0.000	-0.043	0.000	-0.105	0.000	-1.800
0.460	0.000	-0.049	0.000	-0.107	0.000	-1.600
0.519	0.000	-0.054	0.000	-0.104	0.000	-1.400
0.581	0.000	-0.056	0.000	-0.097	0.000	-1.200
0.646	0.000	-0.056	0.000	-0.086	0.000	-1.000
0.714	0.000	-0.052	0.000	-0.073	0.000	-0.800
0.784	0.000	-0.045	0.000	-0.058	0.000	-0.600
0.856	0.000	-0.034	0.000	-0.040	0.000	-0.400
0.929	0.000	-0.019	0.000	-0.021	0.000	-0.200
1.000	0.000	-0.000	0.000	-0.000	0.000	-0.000
1.067	-0.010	0.024	0.000	0.022	0.000	0.200
1.140	-0.028	0.052	0.000	0.046	0.001	0.400
1.219	-0.052	0.086	0.000	0.070	0.003	0.600
1.303	-0.083	0.124	0.000	0.095	0.006	0.800
1.394	-0.118	0.167	0.000	0.119	0.010	1.000
1.492	-0.159	0.215	0.000	0.143	0.015	1.200
1.597	-0.205	0.268	0.000	0.165	0.021	1.400
1.709	-0.256	0.326	0.000	0.187	0.028	1.600
1.830	-0.312	0.389	0.000	0.207	0.035	1.800
1.960	-0.373	0.456	0.000	0.225	0.043	2.000
2.326	-0.544	0.643	0.000	0.262	0.061	2.500
2.757	-0.740	0.854	0.000	0.289	0.078	3.000
3.260	-0.957	1.085	0.000	0.306	0.090	3.500
3.841	-1.189	1.329	0.000	0.316	0.098	4.000
4.505	-1.429	1.580	0.000	0.319	0.101	4.500
5.257	-1.672	1.832	0.000	0.316	0.101	5.000
6.101	-1.910	2.077	0.000	0.310	0.097	5.500
7.040	-2.136	2.307	0.000	0.300	0.091	6.000
8.074	-2.342	2.516	0.000	0.287	0.083	6.500
9.206	-2.521	2.695	0.000	0.272	0.075	7.000
10.435	-2.665	2.837	0.000	0.255	0.065	7.500
11.762	-2.766	2.934	0.000	0.236	0.056	8.000
13.185	-2.818	2.979	0.000	0.216	0.046	8.500
14.702	-2.814	2.966	0.000	0.195	0.037	9.000
16.311	-2.746	2.887	0.000	0.172	0.029	9.500
18.009	-2.609	2.737	0.000	0.149	0.022	10.000

Table 5-14

RED	IMD	REA	IMA	REA	IMA	REC	IMC	V
0.937	0.000	-0.422	0.000	-0.450	0.000	-6,592	1.284	-10.000
0.938	0.000	-0.464	0.000	-0.494	0.000	-6,524	0.783	-9.500
						-6,406	0.218	-8.973
0,940	0.000	-0.473	0.082	-0.503	0.087	-6,373	0.087	-8.856
0,941	0.000	-0.826	-0.140	-0.878	-0.149	-6,305	-0.149	-8.649
0.943	0.000	-1.212	-0.464	-1.285	-0.492	-6,191	-0.492	-8.356
0.946	0.000	-1.614	-0.896	-1.706	-0.947	-6,009	-0.947	-7.985
0,950	0.000	-2.012	-1.438	-2.117	-1.513	-5.729	-1.513	-7.544
0,956	0.000	-2.378	-2.093	-2.487	-2.189	-5,305	-2.189	-7.043
0,964	0.000	-2.671	-2.854	-2.770	-2.960	-4,668	-2.960	-6.495
0,974	0.000	-2.828	-3.701	-2.902	-3.798	-3,704	-3.798	-5.911
0,987	0.000	-2.744	-4.576	-2.779	-4.634	-2,198	-4.634	-5.306
1.002	0.000	-1.948	-5.345	-1.943	-5.333	0.628	-5.333	-4.694
0,961	0.000	0.860	0.000	0.895	0.000	1.680	0.000	-4.089
0,964	0.000	0.334	0.000	0.346	0.000	0.435	0.000	-3.505
0,968	0.000	0.210	0.000	0.217	0.000	0.083	0.000	-2.957
0,971	0.000	0.142	0.000	0.147	0.000	-0,049	0.000	-2.456
0,975	0.000	0.101	0.000	0.104	0.000	-0.097	0.000	-2.015
0,978	0.000	0.074	0.000	0.076	0.000	-0.107	0.000	-1.644
0,981	0.000	0.056	0.000	0.057	0.000	-0.103	0.000	-1.351
0,983	0.000	0.045	0.000	0.046	0.000	-0,094	0.000	-1.144
						-0.088.	0.000	-1.027
0,987	0.000	0.029	0.000	0.030	0.000	-0,073	0.000	-0.800
0,989	0.000	0.021	0.000	0.021	0.000	-0,058	0.000	-0.600
0,992	0.000	0.013	0.000	0.014	0.000	-0,040	0.000	-0.400
0,996	0.000	0.006	0.000	0.006	0.000	-0,021	0.000	-0.200
1.000	0.000	-0.000	0.000	-0.000	0.000	5712.000	0.000	-0.000
1,006	0.002	-0.006	0.000	-0.006	0.000	0.022	0.000	0,200
1,010	0.006	-0.012	0.000	-0.011	0.000	0,045	0.000	0.400
1,013	0.010	-0.017	0.000	-0.017	0.000	0,069	0.000	0.600
1,015	0.014	-0.022	0.000	-0.021	0.000	0.093	0.000	0.800
1,017	0.019	-0.026	0.000	-0.026	0.000	0.119	0.000	1.000
1,019	0.023	-0.031	0.000	-0.030	0.001	0,145	0.000	1.200
1,020	0.026	-0.035	0.000	-0.034	0.001	0.171	0.000	1.400
1,020	0.030	-0.038	0.000	-0.038	0.001	0.198	0.000	1.600
1,021	0.034	-0.042	0.000	-0.041	0.001	0.225	0.000	1.800
1,021	0.037	-0.046	0.000	-0.045	0.002	0.252	0.000	2.000
1,021	0.045	-0.053	0.000	-0.052	0.002	0.321	0.000	2.500
1,020	0.052	-0.060	0.000	-0.059	0.003	0.391	0.000	3.000
1,018	0.058	-0.066	0.000	-0.065	0.004	0.462	0.000	3.500
1.017	0.064	-0.072	0.000	-0.070	0.004	0.532	0.000	4.000
1.015	0.069	-0.077	0.000	-0.075	0.005	0.603	0.000	4.500
1,013	0.074	-0.081	0.000	-0.080	0.006	0,673	0.000	5.000
1,011	0.078	-0.085	0.000	-0.084	0.007	0.742	0.000	5.500
1,008	0.082	-0.089	0.000	-0.088	0.007	0.811	0.000	6.000
1,006	0.086	-0.092	0.000	-0.091	0.008	0,879	0.000	6.500
1,004	0.089	-0.095	0.000	-0.094	0.008	0,947	0.000	7.000
1.002	0.092	-0.098	0.000	-0.097	0.009	1.014	0.000	7.500
1.000	0.095	-0.101	0.000	-0.100	0.010	1,080	0.000	8.000
0,998	0.098	-0.104	0.000	-0.103	0.010	1.145	0.000	8.500
0,995	0.100	-0.106	0.000	-0.105	0.011	1,209	0.000	9.000
0,993	0.103	-0.108	0.000	-0.108	0.011	1,272	0.000	9.500
0,991	0.105	-0.110	0.000	-0.110	0.012	1.335	0.000	10.000

Imaginary part matching. δ function approximation.

Table 3-15. Complex matching. δ function approximation.

RED	IMD	REN	IMN	REA	IMA	REC	IMC	V
0.721	0.000	-136.661	0.063	-189.421	0.087	-6.373	0.087	-8.856
0.654	0.000	-27.663	-0.097	-42.307	-0.149	-6.305	-0.149	-8.649
0.564	0.000	-5.570	-0.278	-9.877	-0.492	-6.191	-0.492	-8.356
0.459	0.000	-2.760	-0.435	-6.009	-0.947	-6.009	-0.947	-7.985
0.349	0.000	-2.035	-0.528	-5.835	-1.513	-5.729	-1.513	-7.544
0.242	0.000	-1.282	-0.529	-5.305	-2.189	-5.305	-2.189	-7.043
0.147	0.000	-0.667	-0.435	-4.540	-2.960	-4.668	-2.960	-6.495
0.073	0.000	-0.271	-0.278	-3.704	-3.798	-3.704	-3.798	-5.911
0.027	0.000	-0.059	-0.124	-2.198	-4.634	-2.198	-4.634	-5.306
0.013	0.000	0.015	-0.068	1.141	-5.333	0.628	-5.333	-4.694
0.031	0.000	0.052	0.000	1.680	0.000	1.680	0.000	-4.089
0.081	0.000	0.036	0.000	0.439	0.000	0.435	0.000	-3.505
0.156	0.000	0.013	0.000	0.083	0.000	0.083	0.000	-2.957
0.249	0.000	-0.012	0.000	-0.049	0.000	-0.049	0.000	-2.456
0.349	0.000	-0.034	0.000	-0.097	0.000	-0.097	0.000	-2.015
0.447	0.000	-0.048	0.000	-0.107	0.000	-0.107	0.000	-1.644
0.533	0.000	-0.055	0.000	-0.103	0.000	-0.103	0.000	-1.351
0.597	0.000	-0.056	0.000	-0.094	0.000	-0.094	0.000	-1.144
0.712	0.000	-0.052	0.000	-0.073	0.000	-0.073	0.000	-0.800
0.783	0.000	-0.045	0.000	-0.057	0.000	-0.058	0.000	-0.600
0.855	0.000	-0.034	0.000	-0.040	0.000	-0.040	0.000	-0.400
0.929	0.000	-0.019	0.000	-0.021	0.000	-0.021	0.000	-0.200
1.000	0.000	0.000	0.000	0.000	0.000	5712.000	0.000	-0.000
1.068	-0.010	0.024	0.000	0.022	0.000	0.022	0.000	0.200
1.142	-0.028	0.052	0.000	0.045	0.001	0.045	0.000	0.400
1.222	-0.052	0.085	0.000	0.069	0.003	0.069	0.000	0.600
1.308	-0.082	0.123	0.000	0.093	0.006	0.093	0.000	0.800
1.400	-0.117	0.165	0.000	0.117	0.010	0.119	0.000	1.000
1.500	-0.157	0.212	0.000	0.140	0.015	0.145	0.000	1.200
1.607	-0.202	0.264	0.000	0.162	0.020	0.171	0.000	1.400
1.722	-0.252	0.321	0.000	0.183	0.027	0.198	0.000	1.600
1.845	-0.306	0.382	0.000	0.202	0.033	0.225	0.000	1.800
1.978	-0.366	0.448	0.000	0.219	0.040	0.252	0.000	2.000
2.351	-0.532	0.629	0.000	0.255	0.058	0.321	0.000	2.500
2.790	-0.721	0.833	0.000	0.280	0.072	0.391	0.000	3.000
3.302	-0.929	1.053	0.000	0.296	0.083	0.462	0.000	3.500
3.892	-1.149	1.284	0.000	0.304	0.090	0.532	0.000	4.000
4.567	-1.375	1.520	0.000	0.305	0.092	0.603	0.000	4.500
5.329	-1.601	1.754	0.000	0.302	0.091	0.673	0.000	5.000
6.182	-1.819	1.978	0.000	0.294	0.087	0.742	0.000	5.500
7.128	-2.022	2.184	0.000	0.284	0.080	0.811	0.000	6.000
8.170	-2.203	2.366	0.000	0.270	0.073	0.879	0.000	6.500
9.308	-2.353	2.515	0.000	0.254	0.064	0.947	0.000	7.000
10.541	-2.465	2.624	0.000	0.236	0.055	1.014	0.000	7.500
11.869	-2.532	2.686	0.000	0.216	0.046	1.080	0.000	8.000
13.291	-2.548	2.694	0.000	0.195	0.037	1.145	0.000	8.500
14.805	-2.505	2.640	0.000	0.173	0.029	1.209	0.000	9.000
16.409	-2.396	2.519	0.000	0.150	0.022	1.272	0.000	9.500
18.098	-2.217	2.325	0.000	0.127	0.015	1.335	0.000	10.000

To get a more realistic $C(\nu)$ function, the S and D waves were included in the crossed channel. The extra structure introduced, especially by the s waves, on the near left caused the output amplitude to become pathological with zeros of N and D on the left and right. See Table 16 and Fig. 13.

7. Experiments with self-consistency conditions

Taking the standard Balazs calculation with ν_{Fi} = -2.1, -1.9, 0.0 and 2 left hand poles at -6.0 and -50.0, we looked at the effect of different self-consistency criteria. In all previous work we used the rough self-consistency criteria of course i.e. demanding the value and gradient of ReA be the same at the resonance position for input and output. We now used ^{2} criteria of the types described in Chapter 2.

First we tried

$$\chi^2 = \sum_i \left[\mathrm{Im}A \text{ out } (\nu_i) - \mathrm{Im}A_{in}(\nu_i)\right]^2 . \; W_i$$

with the ν_i equally spaced in an interval $[o, co]$, and with the W_i constants, independent of the variable parameters. Ten sampling points were used throughout. $\mathrm{Im}A_{in}$ was a Breit Wigner formula with $\nu_R, \Gamma\nu_R$ as parameters and ImA out was the N/D form produced by crossing and matching from it.

The results were as follows:-

(i) Cut-off = 10. Dependence on weighting function evenly spaced points (20)

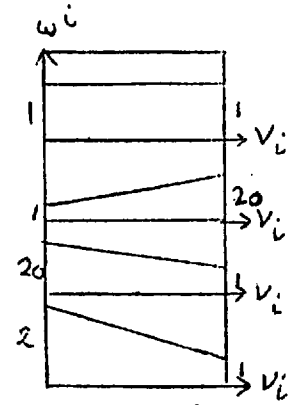

	ν_R	$\Gamma\nu_R$	Γ
	5.73	9.84	1.72
~	6.97	14.96	2.145
~	4.54	5.65	1.24
~	5.46	8.85	1.62

Thus both ν_R and Γ increase as weight swings to higher values

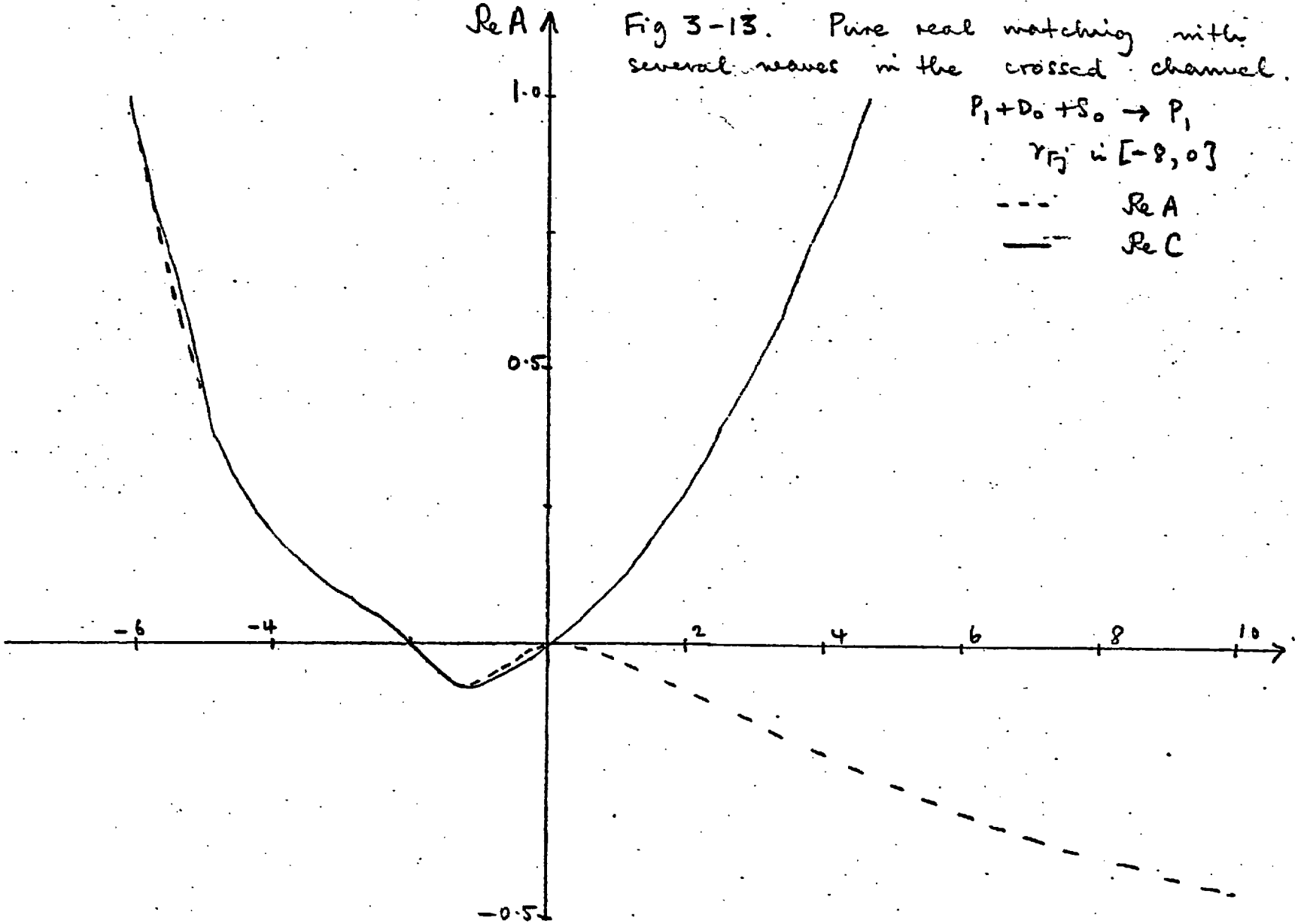

Fig 3-13. Pure real matching with several waves in the crossed channel.

$P_1 + D_0 + S_0 \rightarrow P_1$

r_{Fj} in $[-8, 0]$

--- Re A

—— Re C

TABLE 3-16

Several waves, real part matching, $n = 9$, ν_{Fd} in $[-8, 0)$

1. $P_1 + D_o + S_{o\,res} + S_2 \rightarrow P_1, D_o$

   P_1 zero of N at 0.8

   D_o " at 6.5

2. $P_1 + D_o + S_o \rightarrow P_1, D_o$

   P_1 negative

   D_o zeros of N and D near the origin . .

3. $P_1 + D_o + S_o \rightarrow P_1, D_o$

   P_1 zeros of ReD at -2.0 and + 1.2 ReA negative.

   D_o { zeros of ReD at -2.5 and at 0.0 -
   (zeros of ReN at +7.5 and at 0.0 -

4. $P_1 + D_o + S_o + S_2 \rightarrow P_1, D_o$

   P_1 ReA neg.

   D_o (ReD zeros at -2.5 and 0.0 -
   (ReN zeros at -2.5, -0.8, 0.0 -
   (ReA +ve.

swing 20- to 20+ gives factor 2 in Γ

and $1\frac{1}{2}$ in ν_R

swing mainly ingoing from 20- to evens for Γ

(ii). Dependence on cut-off, even weights.

	ν_R	$\Gamma\nu_R$	Γ
co = 10	5.73	9.84	1.72
20	10.6	37.2	3.51
5	3.92	3.87	0.988
40	22.33	148.22	6.62

Very strong dependence not linear

5 → 10 10 → 20 gives $5.73 \rightarrow 10.6$ $\lesssim \times 2$, ν_R

and $1.72 \rightarrow 3.51$ $\gtrsim \times 2$, Γ

5 → 10 gives $3.92 \rightarrow 5.73$ i.e. $\times 1.46$, ν_R

and $0.99 \rightarrow 1.72$ i.e. $\times 1.72$, Γ

10 → 20 ν_R $\times 1.85$ Γ $\times 2.04$

20 → 40 ν_R $\times 2.1$ Γ $\times 1.89$

Next we tried

$$\chi^2 = \sum_i \left[\frac{(\mathrm{Im}A_{out}(\nu_i) - \mathrm{Im}A_{in}(\nu_i))^{P1}}{(\mathrm{Im}A_{out}(\nu_i) + \mathrm{Im}A_{in}(\nu_i))^{P2}} \right]^2$$

This dynamical weighting allows the desired weighting to be applied in the same places relative to the resonant hump and will follow the resonance as it moves. This should remove any constraint introduced by having the rigid static weighting. However, the ν_i were again equally spaced in $[o,co]$ and not dynamic.

The results are

P1	P 2	ν_R	$\Gamma\nu_R$
1	1	4.07	4.76
1	0	5.73	9.84
1	2	4.71	9.64
1	-1	6.70	13.57

We also did

$$\chi^2 = \sum_i \left[\frac{(\mathrm{Im}A_{out}(\nu_i) - \mathrm{Im}A_{in}(\nu_i)^{P1}}{(\mathrm{Im}A_{out}(\nu_i)^{P1} + \mathrm{Im}A_{in}(\nu_i)^{P2}} \right]^2 \cdot W^i$$

with result, keeping $W^i = 1$ all i.

P1	P2	P3	P4	ν_R	$\Gamma\nu_R$
1	1	1	0	5.41	8.73
1	1	0	1	5.33	8.49

and combining functional and dynamic weighting:-

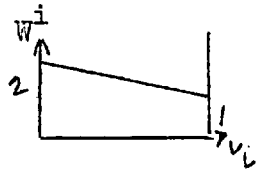

P1	P2	P3	P4	ν_R	$\Gamma\nu_R$
1	1	1	1	3.69	3.62

We also tried dynamical cut-offs described by an index P

P	sampling region
-1	$[\nu_R - \Gamma\nu_R, \nu_R \Gamma\nu_R]$
0	$[o, 2\nu_R]$
1	$[o, \infty]$

p = o gave (2.81, 1.86)

and we also tried sampling the input function i.e. cutting off the C (ν) integral in a dynamical way with results

P input	P output	ν_R	$\Gamma\nu_R$
0	1	3.13	3.13
0	0	2.51	1.62

These experiments merely serve to show that one can alter the result for positions and width independently by a factor of 2 , either way, by a suitable choice of χ^2 criterion and, as one has no *a priori* way of choosing such a criterion, one's results must remain indefinite to this extent. This applies to the comparison of Breit Wigner and N/D forms and will be different for other clashes of parametrisation. The values of χ^2 usually obtained were $\sim 10^{-2}$.

8. N/D parametrisation

We next tried using an N/D parametrisation in the crossed channel and it was felt desirable to take the same number of left hand poles in both crossed and direct channels, so that all χ^2 criteria would be identical and be equivalent to the paramtric self consistency criterion

$$\chi^2 = \sum_i \left[a_{i\,\text{in}} - a_{i\,\text{out}} \right]$$

where $\{ a_{i\,\text{in}} \}$ are the parameters (residues of poles) of the N/D form in crossed channel and $\{ a_{i\,\text{out}} \}$ are those in the direct channel. The $C(\nu)$ function using the residues appropriate to the Balazs self consistent solution in the case n = 2, was very similar to the previous one using the BW formula and the result of matching also similar. A self consistent calculation, which had to use a χ^2 criterion in the case of a parametrisation which does not automatically give a resonant form, was performed and gave a very small χ^2 and self consistent values

$$F^i = -0.0\,34, -1.54, 13.66 \quad (\text{This was with poles at } -6, -50$$
$$\nu_{Fj} = -2.1, 1.9, 0.0)$$

very close to the Balaz solution. The χ^2 obtained was $10,^{-4}$ but would probably have gone to a true zero if the numerical calculation had been allowed to continue.

The disadvantage of N/D parametrisation used with the matching process in its present form is that to reproduce the detail on the left one needs many poles in the direct channel and hence many poles in the crossed channel and hence many parameters to vary. For ten pole fits, one is having to search a (10 parameter space. Clearly we must decouple these two properties.

9. χ^2 approach to matching

The answer is to make n the number of poles and nF the number of symmetry points independent. We already have a sufficiently general matching

procedure at our disposal which allows extra poles to be present. Thus we can use N/D parametrisation and choose the number of poles to be used, say n. This will be the same in direct and crossed channels. We now choose the number of symmetry points usually larger, say NF. We automatically make the residues F^i be the same in both channels and we vary them to give proximity to crossing of real and imaginary parts on the left. The self consistency on the right is of course now automatically satisfied. We are thus minimising a χ^2 which can be obtained from the matching equations

$$\sum_{i=1}^{n} E^{ji} F^i = Q^j \qquad j = 1 \,..\, NF(=n).$$

become

$$\chi^2 = \sum_{j=1}^{NF} \left(\sum_{i=1}^{n} E^{ji} F^i - A^j \right)^2 .$$

This approach, in the author's opinion, is the ultimate in the generalisation of the Balazs idea. A programme was constructed to carry out such calculations but it was never completely debugged and has never been used. It was a difficult programme to follow and would have needed rewriting to debug. Also by this time, the inverse amplitude calculations (Chapter 6) had shown an easier way of obtaining the same requirements. Also it was found that the variational calculations (Chapter 5) could be easily modified to do this generalised Balaz calculation. This was done and will be described in Chapter 5; however no satisfactory solutions were obtained, although the number of attempts was quite small. We tried one search in each of the cases (n = 2, 3, 4, 5) (X) (nF = 10). The most acceptable solution was found in the case n = 3, which was close to the original Balazs solution.

FURTHER GENERALISATION TO SMOOTH FUNCTIONS

Instead of using pole forms, one might try to use the same matching idea using unitary functions with smooth left hand discontinuities. The difficulty of doing the D integral is then present; however this approach would allow $A(\nu)$

functions with different asymptotic behaviours to be explored. Such considerations are to a certain extent realised in the variational calculations in Chapter 5.

CHAPTER 4

THE ZACHARIASEN METHOD

Statement of the Method

First introduced by F. Zachariasen (1), this is a simple, elegant method for preliminary calculations. It has been used widely and a list of references to applications of the method to a variety of processes is to be found in Ch. 1.

The method is to make the ansatz

$$N(\ ) = C(\nu) \tag{i}$$

where $C(\nu)$ is the crossing function introduced in Chapter 2, and has always been taken as the simple pole form obtained by δ function approximation.

Then $D(\nu) = 1 - \left(\frac{\nu - \nu_0}{\pi}\right) \int_0^\infty \sqrt{\frac{\nu'}{\nu'+1}} \cdot \frac{C(\nu')\, d\nu'}{(\nu' - \nu)(\nu' - \nu_0)}$ (ii)

And $A(\nu) = \frac{N(\nu)}{D(\nu)}$

This amplitude has some desirable features. It obeys unitarity, has cuts $[0, \infty]$, $[-1, \infty]$, has correct threshold behaviour. The discontinuity on the left is not $\mathrm{Im}C(\nu)$ but $\frac{\mathrm{Im}C(\nu)}{D(\nu)}$ and hence is only correct when $D(\nu) = 1$ i.e. at ν_0. For this reason, Zachariasen specified that ν_0 should be always where $C(\nu)$ is largest and in the function case i.e. a simple pole exchange, this is at $\nu = \nu_R - 1$, hence

$$\nu_0 = -\nu_R - 1 \tag{iii}$$

So as we vary ν_R, Γ_{ν_R} looking for a solution, ν_0 also varies.

Γ_{ν_R}, ν_R are varied to obtain rough self consistency between the input function

$$\mathrm{Im}\, A_{in}(\nu') = \pi \Gamma_{\nu_R}^{-1} \cdot \delta(\nu' - \nu_R)$$

and the output function, $A_{out} = \frac{N}{D}$

by demanding the conditions

$$\text{Re } D_{out}(\nu_{Rin}) = 0.$$

$$(\Gamma^{l}_{\nu_R})_{out} = \frac{-N_{out}(\nu_{Rin})}{D_{out}(\nu_{Rin})} = (\Gamma^{l}_{\nu_R})_{in}$$

Discussion

Zachariasen actually introduced this method as being the 1st iteraction of a successive substitution procedure, in which the 1st stage was to put $D_1 = 1$, $N_1(\nu) = C(\nu)$. 2nd stage D_2 would be given by (ii) and $N_2(\nu) = C(\nu).D_2$ and so on. This iteration procedure diverges.

Notice also that Re $A(\nu) = \frac{\text{Re } C(\nu)}{D(\nu)}$, on the left, so that Re $A(\nu)$ and Im $A(\nu)$ differ by the same factor $D(\nu)$ from Re $C(\nu)$ and Im $C(\nu)$. So both the real and imaginary parts have similar forms to the estimated $C(\nu)$. The factor $D(\nu)$ however is very often ~ 3 or so on most of the near left.

Also note that $N(\nu) = C(\nu)$ everywhere, so that it has the same bad asymptotic behaviour as the Born term. The discontinuity $\frac{\text{Im } C(\nu)}{D(\nu)}$ holds on the whole of the left, not just the near left. It is this asymptotic behaviour which renders the method unreliable for quantitative prediction.

From Chapter 2

$$\text{Re } C_{ll'}(\nu) \to \nu^{l'-1} \log \nu$$

$$\text{Im } C_{ll'}(\nu) \quad \nu \to -\infty \quad \nu^{l'}$$

The behaviour of the integrand for $D(\nu)$ is

$$\nu'^{l'-3} \log \nu'$$

and so the integral diverges for $l' > 1$. We can only use the once subtracted form, on which the method is based since it puts the one subtraction constant =1 by crossing symmetry, for S and P waves. Indeed, because of subtraction in the fixed S dispersion relation required by the S-wave, the only wave in which we are safe is the P wave.

To estimate asymptotic behaviours, we use the results of Lanz & Prosperi

quoted in Chapter 1, for the asymptotic behaviour of the p. v. integral for $D(\nu)$.

$$D \sim \frac{(\nu-\nu_0)}{\pi} \int_{-\infty}^{\infty} \frac{\rho(\nu')}{\nu'-\nu}\, d\nu' = \frac{(\nu-\nu_0)}{\pi}.\ f(\nu)$$

$\rho(\nu') \sim \nu'^{\ell'-2}$ $\therefore \log \nu'$ $\nu' \to \infty$

$\therefore \rho(\nu') < \frac{1}{\nu'^{\,2-\ell'-\varepsilon}}$ $\qquad \alpha = 2-\ell'-\varepsilon$

$\rho'(\nu') = \nu'^{\ell'-3}.\ [1+(\ell'-2).\log\nu'] < \nu'^{\ell'-2}$

this is $\not< \frac{1}{\nu'^{\alpha+1}} = \frac{1}{\nu'^{\,3-\ell'-\varepsilon}}$, all ℓ'

For $\ell' = 0$ $\qquad \alpha = 2-\varepsilon > 1$

$|f(\nu)| < \frac{C_0}{|\nu|}$, $D \sim \lesssim$ constant $\nu \to \infty$

$\ell' = 1$ $\qquad \alpha = 1-\varepsilon < 1$

$$|f(\nu)| \lesssim \left[\frac{C_1 \log\nu.(1-\varepsilon)}{|\nu|^{1-\varepsilon}} + \frac{\text{constant}}{|\nu|^{1-\varepsilon}}\right]$$

$$< \frac{C_1}{|\nu|^{1-\varepsilon}} \quad \text{inside forward cone.}$$

$$|f(\nu)| < \frac{C_2}{|\nu|^{1-\varepsilon}} \quad \text{outside forward cone.}$$

$D \sim \lesssim |\nu|^{\varepsilon}$ $\qquad \ell' = 1$ $\qquad$ all finite ε.

which can probably be replaced in practice by

$$\to \lesssim \log^n \nu.$$

$\ell' = 2$ diverges.

$\therefore$ Re $D(\nu) \to <$ constant or $\lesssim C_3 \log^n \nu$; $\ell' = 0$ or 1.

Im $D(\nu) \to$ Re N $\sim \nu^{\ell'-1} \log\nu$

Re $N(\nu)$ $\sim \nu^{\ell'-1} \log\nu$.

$$\therefore \text{Re } A(\nu) = \frac{\text{Re N. Re D}}{|D|^2} \sim \frac{\nu^{\ell'-1}\log\nu\ .\ [< \text{Const. or} \lesssim C_3 \log^n\nu]}{\left|\nu^{\ell'-1}\ \frac{\max(n,1)}{\log\nu}\right|^2}$$

$$\sim < \text{constant} \quad \text{or} \quad \lesssim C_3$$

$$\text{Im } A(\nu) = \frac{\text{Re N. Im D}}{|D|^2} = \frac{\nu^{\ell'-1}\log\nu.\ \nu^{\ell'-1}\log\nu}{\left|\nu^{\ell'-1}\ \frac{\max(n,1)}{\log\nu}\right|^2}$$

$\longrightarrow$ constant.

$\therefore$ Pure imaginary or complex or pure real.

$$\frac{\text{Im } A(\nu)}{\text{Re } A(\nu)} = \frac{\text{Im } D}{\text{Re } D} = \frac{\nu^{\ell'-1} \log \nu}{\left\{ \begin{array}{l} \text{constant or} \\ \leq C_3 \log^n \nu \end{array} \right.}$$

for $\ell' = 1$ if $n = 1 \longrightarrow$ constant. complex

$2 \longrightarrow$ o puro real.

$\ell' = o$ if $\longrightarrow \log \nu$ pure imaginary.

If we use the rough rule of multiplication of the imaginary part by

$$\frac{\log \nu}{\nu},$$

we obtain $\text{Re } D(\nu) \longrightarrow \nu^{\ell'-1}, \log^2 \nu.$

$$\text{Im } D(\nu) \longrightarrow \nu^{\ell'-1} \log \nu$$

$$\text{Re } A(\nu) \longrightarrow \frac{1}{\log \nu}$$

$$\text{Im } A(\nu) \longrightarrow \frac{1}{\log^2 \nu}.$$

$A \longrightarrow o$ and purely real.

As $\nu \longrightarrow -\infty$

$$\text{Im } D = o$$

$$\text{Im } N = \text{Im } C \underset{\nu \to -\infty}{\longrightarrow} \nu^{\ell'}$$

$$\text{Re } N \underset{\nu \to -\infty}{\longrightarrow} \nu^{\ell'-1} \log \nu$$

$$\text{Re } D \longrightarrow \left\{ \begin{array}{l} \text{constant} \\ \text{or} \leq C_3 \log^n \nu, \quad \ell' = o \text{ or } 1. \\ \text{or } \nu^{\ell'-1} \cdot \log^2 \nu, \text{ by rough method.} \end{array} \right.$$

$$\therefore \text{Re } A(\nu) = \frac{\text{Re } N \text{ Re } D}{|D|^2}$$

$$= \frac{\text{Re } N}{\text{Re } D}$$

$$\underset{\ell' = o}{\longrightarrow} \frac{\log \nu}{\text{constant}} \longrightarrow \frac{\log \nu}{\nu}$$

$\nu \longrightarrow -\infty$ rough method $\log^2 \nu$.

$$\underset{\ell' = 1}{\longrightarrow} \frac{\log \nu}{C_3 \log^n \nu} \longrightarrow \log^{-n+1} \nu.$$

rough method. $\log^{-1}(\nu)$

$$\text{Im } A(\nu) = \frac{\text{Im } N}{\text{Re } D} =$$

$$\xrightarrow[\ell' = 0]{} \frac{1}{\text{Constant}} \longrightarrow \text{constant.}$$

$\nu \longrightarrow -\infty$, rough method, $\dfrac{1}{\log^{n}\nu} \longrightarrow \dfrac{\nu}{\log^{2}\nu}$

$$\xrightarrow[\ell' = 1]{} \frac{\nu}{\log^{n}\nu}$$

rough method $\nu / \log^{2}\nu$.

Threshold behaviour

$$\text{Re } N(\nu) \sim \nu^{\ell} \qquad \nu \to 0$$

Re $D(\nu)$ has behaviour dependent upon $\displaystyle\int_0 \frac{\sqrt{\nu'}\ \nu'^{\ell}}{\nu' - \nu}$

so for $\ell = 0$, D has 1st order cusp. i.e. discontinuous gradient.

$\ell = 1$, 2nd order etc.

$$\text{Im } D(\nu) \sim \sqrt{\nu} \cdot \text{Re } N \sim \sqrt{\nu}\cdot\nu^{\ell}$$

from this

A has finite value and 1st order cusp for $\ell = 0$

$\propto \nu$, 3rd order cusp for $\ell = 1$.

Contributions to Re D and the effect of a cut-off

$$D(\nu) = 1 - \frac{(\nu - \nu_0)}{\pi}\int_0^{\infty} \sqrt{\frac{\nu'}{\nu'+1}}\ \frac{\text{Re } C(\nu')\, d\nu'}{(\nu' - \nu)\ (\nu' - \nu_0)}$$

For ν fixed on the near right, the effect of the part of the integral above it has the same sign as Re $C(\nu')$. Thus for the $P_1 \to P_1$ case Re $C(\nu')$ is positive for $\nu' > 0$, so that the upper part of the range of integration gives a positive contribution and makes $D(\nu)$ tend to decrease from 1 and dip towards the axis i.e. tends to make it resonate. One might describe a montonically increasing Re $C(\nu)$ function thus as representing an attractive interaction. Certainly for $\nu < 0$, the whole of the integral contributes to this effect in

the same direction, but for ν on the cut it is less easy to see what will happen. As for numerical contributions, for the P_1 case the following numbers have been obtained

ν'	Re $C(\nu')$	$(\nu'-\nu)$ $(\nu'-\nu_o)$	$\mathrm{Re}C(\nu')/(\nu'-\nu)(\nu'-\nu_o)$
4.0	8.3	10	0.8
7.0	13.4	40	0.34
10.0	17.6	88	0.20

$$\nu = 2 \quad \nu_o = -1$$

contributed from $[4,7] \sim 3 \times 0.6 \sim 1.8$

$[7,10] \sim 3 \times 0.3 \sim 1.0$

The effect of a cut-off in such a case is to decrease the attractive effect, and similarly in other cases.

Self-consistency determination

We vary ν_R, $\Gamma\nu_R$ to satisfy the rough self-consistency conditions:

$$\mathrm{Re}\, D_{out}(\nu_{Rin}) = 0 \qquad \text{(i)}$$

$$-\frac{N_{out}(\nu_{R\,in})}{D'_{out}(\nu_{Rin})} = \Gamma_{in}\,\nu^{\ell}_{Rin} \qquad \text{(ii)}$$

We actually used $\mathrm{Re}\, A'_{out}(\nu_{Rin}) = \mathrm{Re}\, A'_{in}(\nu_{in})$ (iii)

Taking A_{in} to be the Breit Wigner formula with $\Gamma\nu_R, \nu_R$ as parameters, $\mathrm{Re}\, A'_{in}(\nu_{Rin}) = -1/\left[\Gamma.\nu_R^{\ell}\left(\frac{\nu_R}{\nu_R+1}\right)\right]$. Zachariasen and several other authors used a graphical method for determining $\Gamma\nu_R, \nu_R$ self-consistency namely from the intersection of the two curves given by (i) and (ii) in the $\Gamma\nu_R$, ν_R plane. We found it more convenient to use a minimising routine and iterated until equations (i) and (iii) were very close to being satisfied i.e. we searched the ν_R $\Gamma\nu_R$ plane to minimise

$$X^2 = \left[\mathrm{Re}\, D_{out}(\nu_{Rin})\right]^2 + \left[\mathrm{Re}\, A'_{out}(\nu_{Rin}) - \mathrm{Re}\, A'_{in}(\nu_{R\,in})\right]^2$$

or one can find ν_{Rout}, i.e. s.t. $\mathrm{Re}\, D_{out}(\nu_{R\,out}) = 0$ and use $(\nu_{Rout}-\nu_{Rin})^2$

For several coupled partial waves the graphical method loses its simplicity

Choice of ν_0

Zachariasen chose $\nu_0 = -\nu_R - 1$ as being the position of the singularity in the $C(\nu)$ function. However, this singularity is logarithmic and not so important as a pole would be. It is also the end of the left hand cut and where Im $C(\nu)$ is large, which is more reasonable. It is difficult to see how to treat the case of a continuous Im $A(\nu)$ in the crossed channel which do not produce these effects on the left. However, there is still structure, from the crossed channel, near $\nu = -\nu_R - 1$, which could motivate one to put ν_0 there. From the inverse amplitude approach, one might take ν_0 to be at the zero of the $C(\nu)$ function on the left.

The analysis of the original Zachariasen method

A programme was written to do the Zachariasen calculation and the method was systematically studied. Tables and graphs of N, D, Re A and Im A were obtained, Fig 1 and Table 1. The effects of ρ exchange in other waves using this method were obtained as graphs of Re A, Fig 3, and are summarised in Table 2, section 2. The effect of having a fixed ν_0 was found to be large. Also, following Din, we did the calculation for $\nu_0 = \alpha(-\nu_R - 1)$ for several different α's and found great sensitivity of the self consistent values to α. Static variation of ν_0 is shown in Fig. 2, self consistent values are given in Table 2 (5) [illegible] to . The effect of a cut off in the Re D integral was found to be not unreasonable. Two different self consistency criteria were tried, one following Zachariasen and the other following Balazs, the latter depends upon approximate linearity of D and was found to be not useful. The results of these investigations are found in Table 2.

Next, contour plots were obtained and an interesting effect was found. For ν_0 fixed, independent of parameters, the self consistent value lay in a narrow valley along the line $\Gamma = 1$. Fig. 4. For ν_0 dynamic and equal to

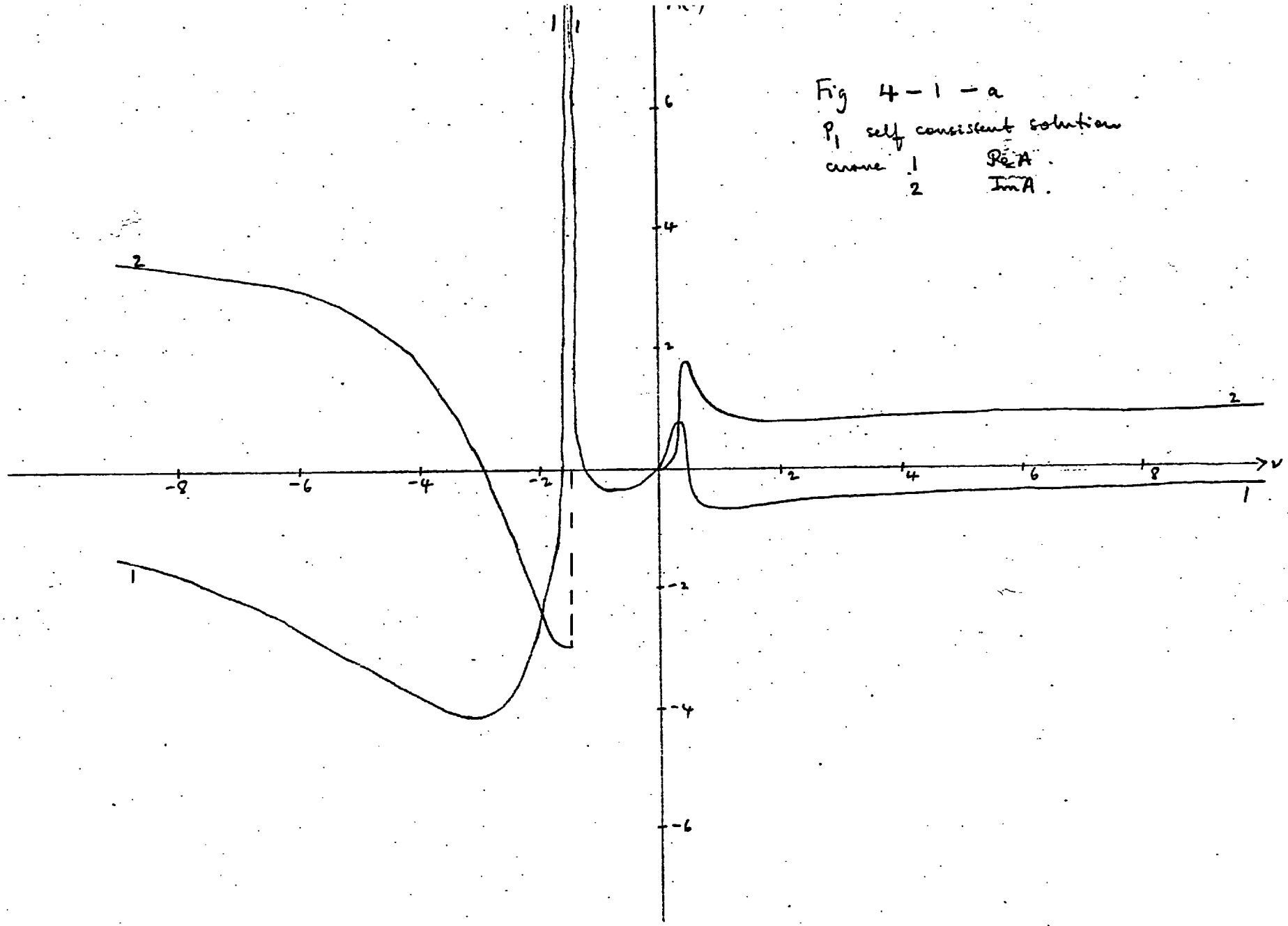

Fig 4 – 1 – a

P_1 self consistent solution

curve 1 $\mathrm{Re}\,A$.

2 $\mathrm{Im}\,A$.

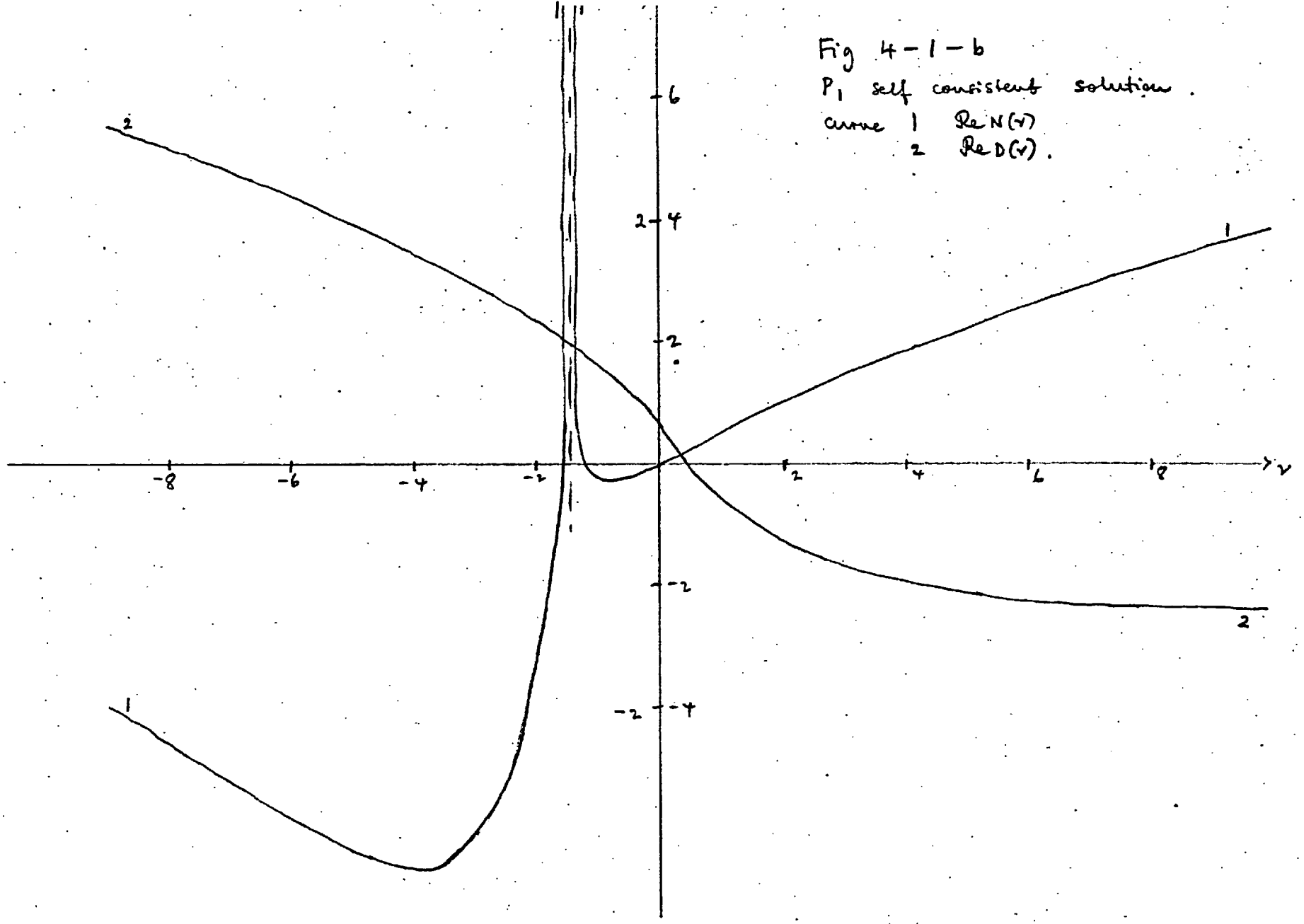

Fig 4-1-b
P_1 self consistent solution.
curve 1 Re N(ν)
2 Re D(ν).

Table 4-1. Self-consistent solution by Zacharias method.

RED	REN	IMN	REA	IMA	V
2.923	-3.441	10.043	-1.177	3.436	-10.000
2.840	-3.725	9.750	-1.312	3.433	-9.500
2.755	-4.017	9.428	-1.458	3.422	-9.000
2.668	-4.317	9.073	-1.618	3.400	-8.500
2.578	-4.623	8.679	-1.793	3.366	-8.000
2.486	-4.933	8.241	-1.984	3.315	-7.500
2.391	-5.245	7.750	-2.194	3.242	-7.000
2.292	-5.555	7.197	-2.424	3.140	-6.500
2.190	-5.856	6.570	-2.674	3.000	-6.000
2.084	-6.137	5.854	-2.945	2.809	-5.500
1.974	-6.381	5.031	-3.233	2.549	-5.000
1.858	-6.561	4.077	-3.530	2.194	-4.500
1.738	-6.632	2.967	-3.816	1.707	-4.000
1.611	-6.516	1.674	-4.046	1.039	-3.500
1.476	-6.077	0.184	-4.117	0.124	-3.000
1.333	-5.062	-1.453	-3.798	-1.090	-2.500
1.178	-2.998	-2.924	-2.544	-2.481	-2.000
1.113	-1.700	-3.231	-1.528	-2.903	-1.800
1.045	0.050	-3.102	0.048	-2.968	-1.600
0.975	0.811	0.	0.833	0.	-1.400
0.901	-0.070	0.	-0.077	0.	-1.200
0.823	-0.258	0.	-0.313	0.	-1.000
0.741	-0.286	0.	-0.386	0.	-0.800
0.653	-0.249	0.	-0.382	0.	-0.600
0.558	-0.181	0.	-0.324	0.	-0.400
0.453	-0.095	0.	-0.210	0.	-0.200
0.248	-0.050	0.	-0.200	0.012	0.100
0.176	0.100	0.	0.542	0.127	0.200
0.044	0.204	0.	0.647	1.611	0.400
-0.073	0.308	0.	-0.549	1.421	0.600
-0.177	0.412	0.	-0.683	1.061	0.800
-0.270	0.516	0.	-0.676	0.914	1.000
-0.353	0.618	0.	-0.655	0.847	1.200
-0.429	0.720	0.	-0.635	0.814	1.400
-0.498	0.820	0.	-0.617	0.797	1.600
-0.560	0.918	0.	-0.601	0.790	1.800
-0.617	1.014	0.	-0.587	0.788	2.000
-0.738	1.249	0.	-0.556	0.794	2.500
-0.836	1.473	0.	-0.529	0.807	3.000
-0.916	1.687	0.	-0.506	0.822	3.500
-0.980	1.891	0.	-0.485	0.837	4.000
-1.032	2.087	0.	-0.465	0.851	4.500
-1.074	2.275	0.	-0.447	0.864	5.000
-1.108	2.456	0.	-0.430	0.876	5.500
-1.135	2.629	0.	-0.414	0.887	6.000
-1.155	2.796	0.	-0.398	0.897	6.500
-1.170	2.958	0.	-0.384	0.907	7.000
-1.181	3.114	0.	-0.370	0.915	7.500
-1.188	3.264	0.	-0.356	0.923	8.000
-1.192	3.410	0.	-0.344	0.930	8.500
-1.192	3.551	0.	-0.332	0.937	9.000
-1.190	3.688	0.	-0.320	0.943	9.500
-1.186	3.821	0.	-0.309	0.948	10.000

TABLE 4 - 2

1. Static Dynamic ν_0

(a) Static at $\nu_0 = -1.000$

gives 1.423, - 1.004

tab $\rightarrow P_1, D_0, F_1$

gives 420, 480, 1060. Mev

X^2 contours give $\Gamma = 1$ valley.

(b) Dynamic at $\nu = -\nu_R - 1$

gives 0.547, 1.161

tab $\rightarrow p_1, D_0, F_1$

340, 400, 860. Mev

X^2 contours give $\Gamma = 1$ valley.

2. Effect of ρ on other channels

TABULATIONS $\rightarrow S_0, S_2, P_1, D_0, D_2, F_1$

S_0 $a_0 = -1.1$ Re A negative becomes V. small as ν increases.

S_2 $a_2 = -0.85$ Re A negative and slowly varying

P_1 s.c. resonance at $\nu_R = 0.47$

D_0 resonance at $\nu_R = 1.1$

D_2 negative, non resonant, small slowly varying

F_1 resonance at $\nu_R = 8.7$

3. Self consistency condition

Zachariasen type 0.547, -1.161

Balazs type 0.121, -0.936 $X^2 = 10^{-3}$

4. Dependence on cut off on right

ν_0 fixed 0.417, -0.563 $\sim$ 370 Mev

tab. $P_1 > D_0$, " F_1 " S_0

also

rising none none < 0

zero

ν_0 variable 0.351, -0.668 $\sim$ 346 Mev

5. Variation with ν_0, self consistent values

(1) static:

α	a_1	a_2	ν_R	Γ	$\Gamma\nu_R$
- 1.0	1.423	-1.004	1.417	0.996	1.411
- 0.5	3.831	-0.883	4.339	1.133	4.882
- 1.5	0.513	-1.170	0.439	0.850	0.375
- 2.0	0.074	-1.335	0.056	0.750	0.042

(2) dynamic

α	a_1	a_2	ν_R	Γ	$\Gamma\nu_R$
-1.0	0.547	-1.161	.472	0.861	.406
-0.8	0.740	-1.113	.665	0.898	.597
-1.2	0.402	-1.204	.334	0.831	.278
-1.5	0.236	-1.264	.186	0.79	.147
-0.7	0.862	-1.087	.79	0.92	.73

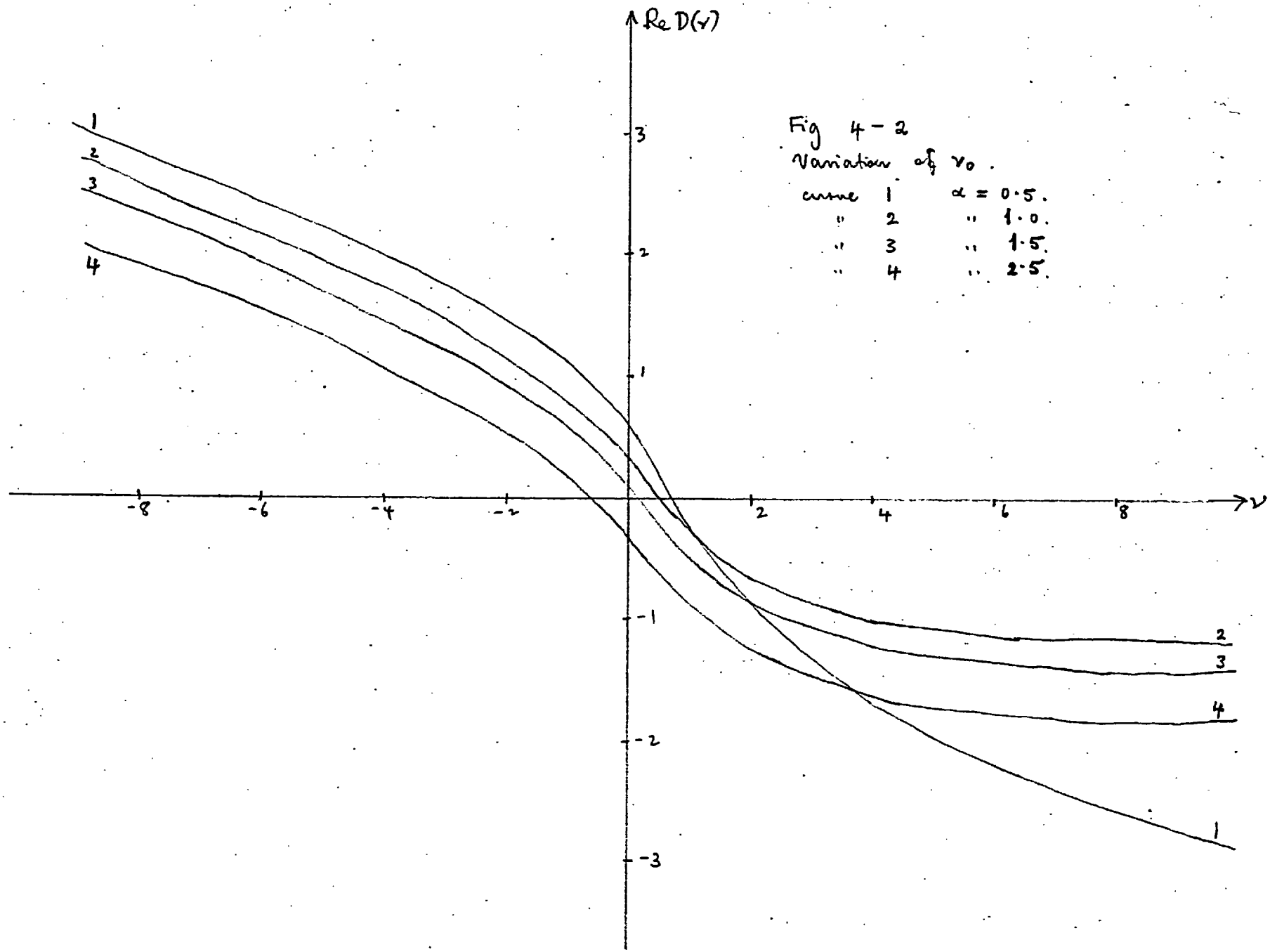

Fig 4 - 2
Variation of ν_0.
curve 1 $\alpha = 0.5$.
" 2 " 1.0.
" 3 " 1.5.
" 4 " 2.5.

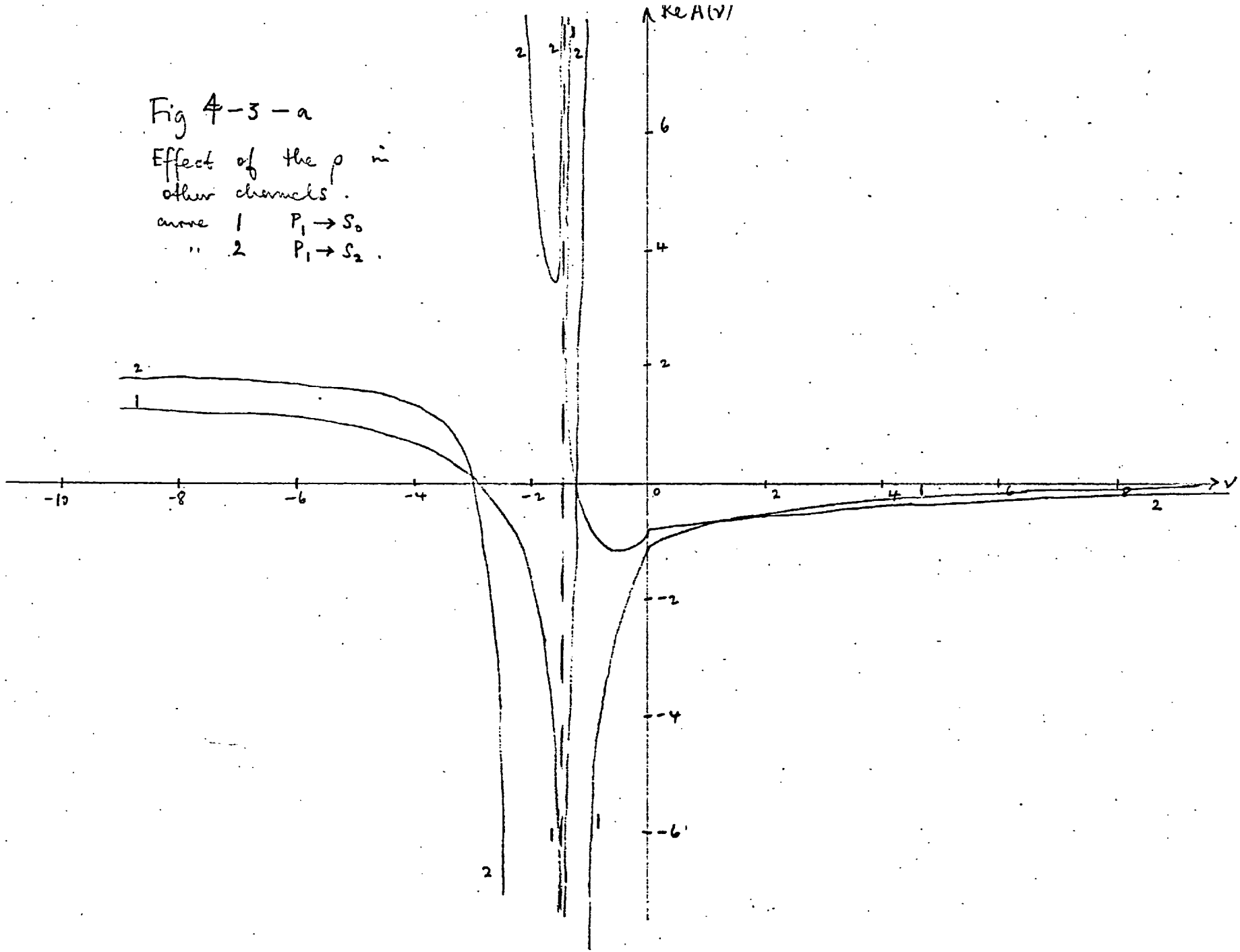

Fig 4-3-a

Effect of the ρ in other chemicals.

curve 1 $P_1 \rightarrow S_0$

" 2 $P_1 \rightarrow S_2$.

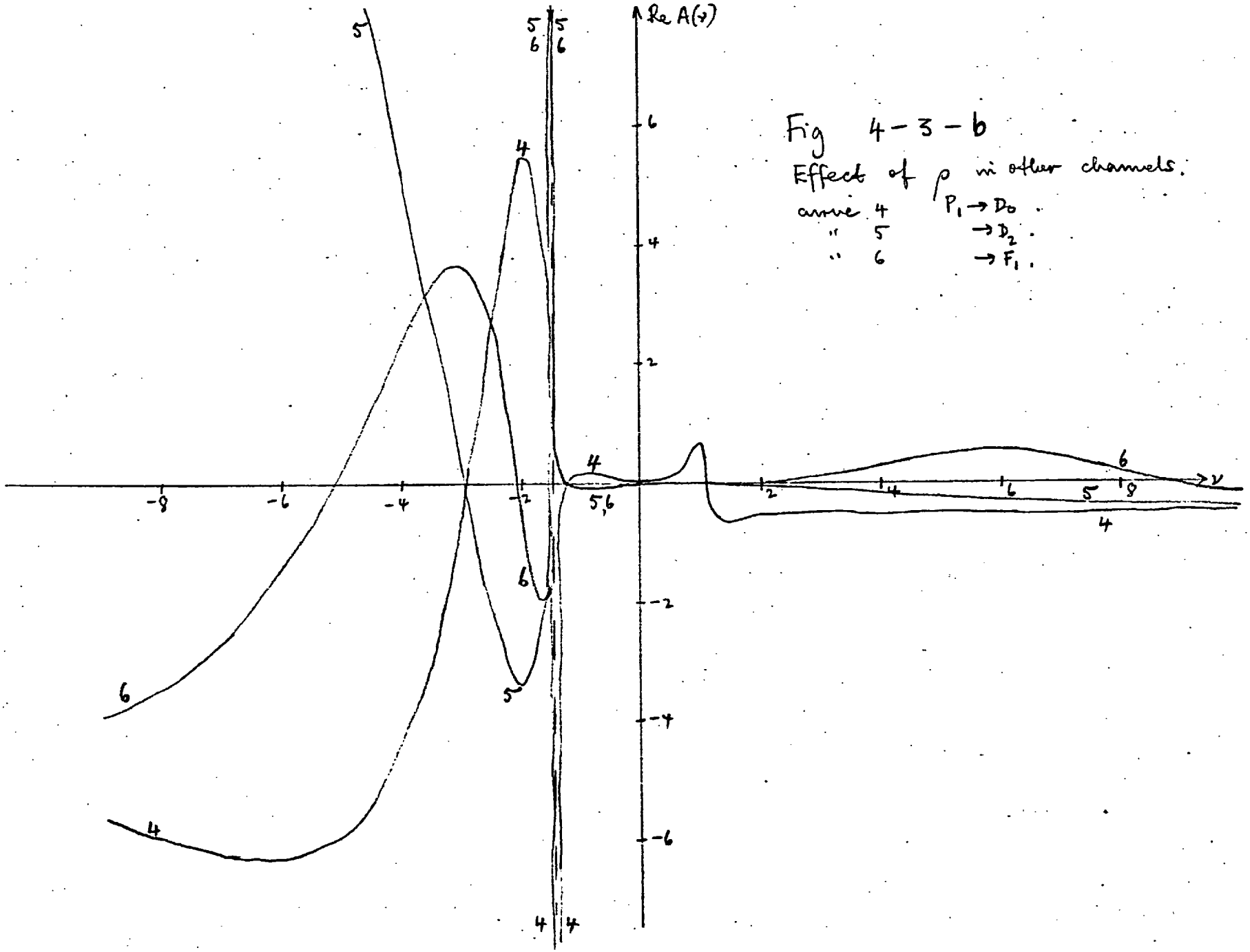

Fig 4-3-b

Effect of ρ in other channels.

arrow 4 $P_1 \to D_0$.

" 5 $\to D_2$.

" 6 $\to F_1$.

$-V_R - 1$, this was not so pronounced and the contours were more reasonable, however there still was a slight valley connecting the self consistent value with the trivial solution $V_R = 0$, Fig. 5. This valley is roughly along the line

$$-1 + 0.8\,\Gamma = -0.7\,V_R.$$

For comparison, we show the curves for the graphical method of solution in a diagram.

For the P wave only the graphical solution looks like this

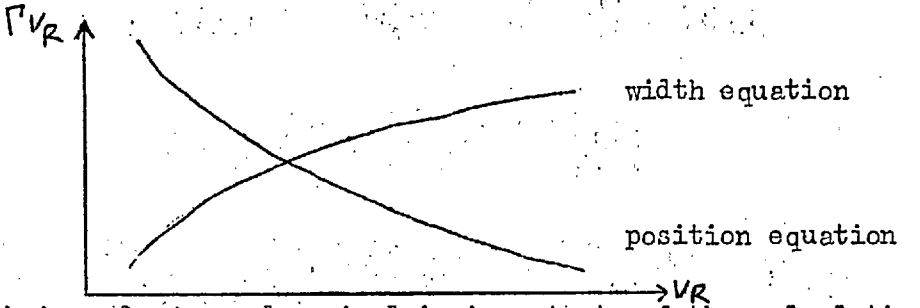

Thus, the choice of V_o as dynamical is important and the calculation is very sensitive to the actual dynamical choice. On the other hand, this choice of V_o is a structural part of the Zachariasen method and it is difficult to see how to modify it, to avoid this difficulty.

Other workers' analyses of the Zachariasen method

Zachariasen's result has been obtained by Martin (2), his result was

$m_\rho = 337$ Mev width 53 Mev

Also Dix (3) has analysed the method. He showed the α dependence by the following diagram

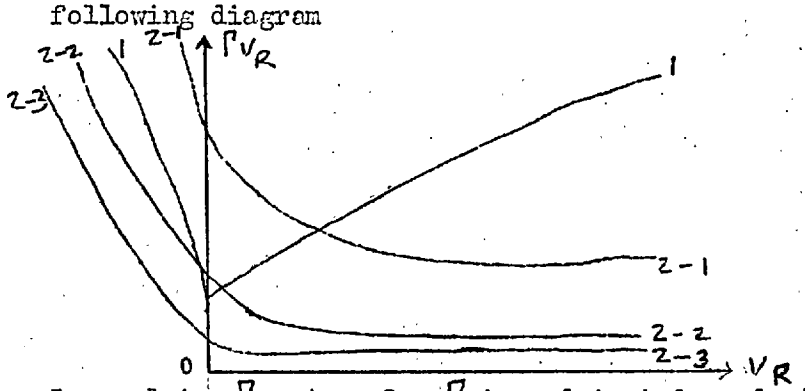

Curve 1 is Γ out vs Γ in and is independent of α, finite at $V_R = 0$ and $\to \infty$ as $V_R \to -1$.

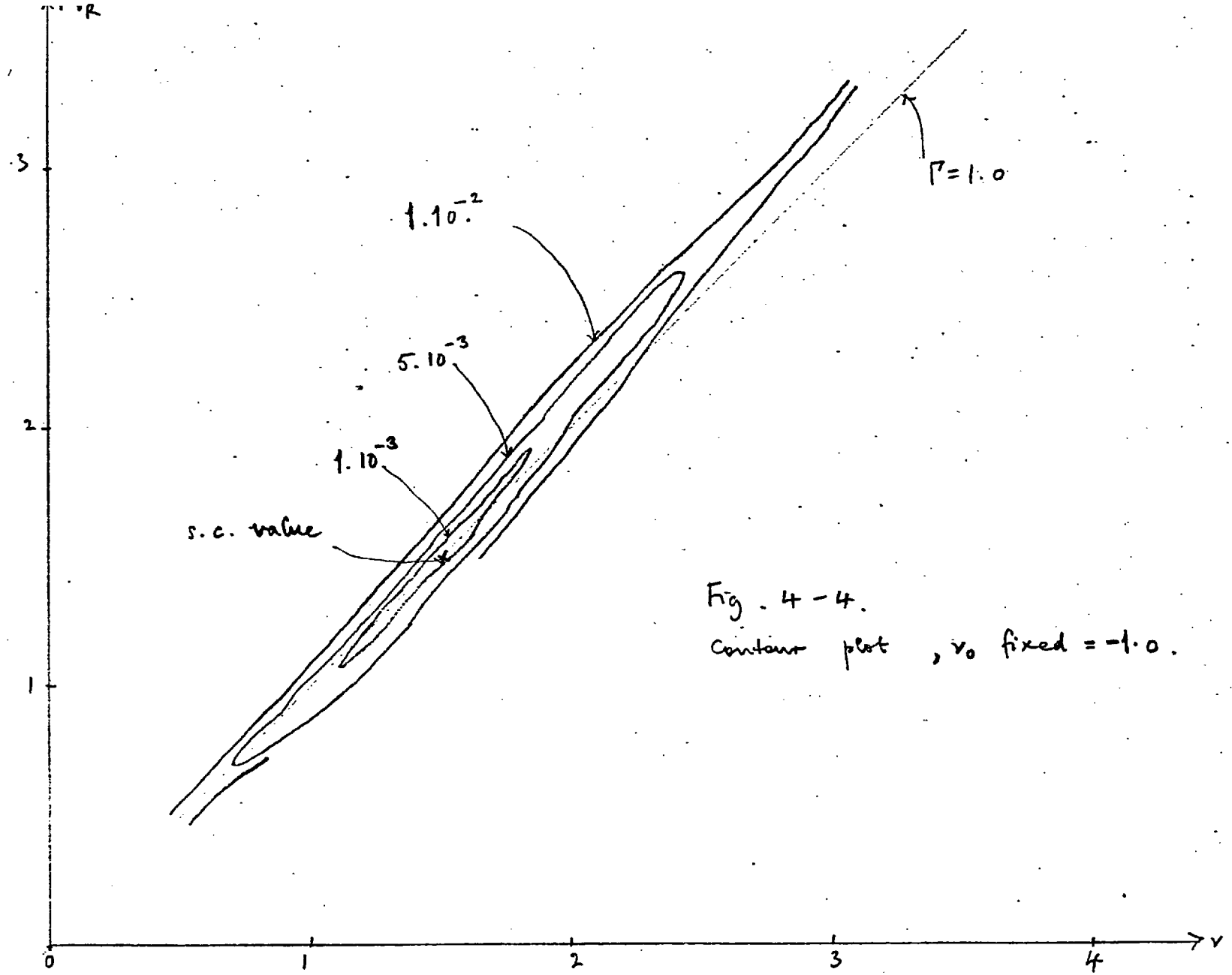

Fig. 4-4.
Contour plot, v_0 fixed $= -1.0$.

$\Gamma = 1.0$

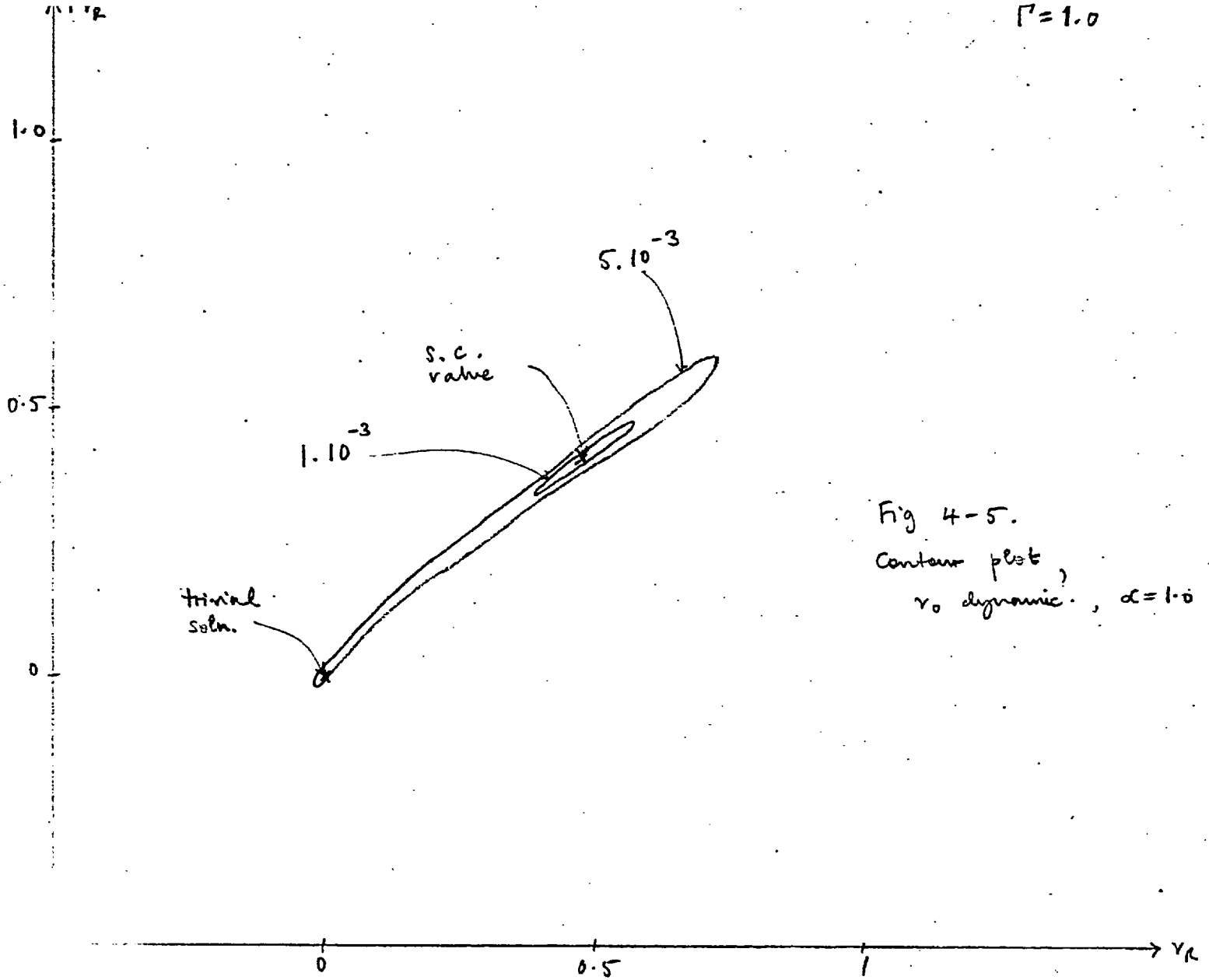

Fig 4-5.
Contour plot of v_0 dynamic, $\alpha = 1.0$

Curves 2 are ν_R out vs ν_R in for $\alpha = 1, 2, 3$ and show that there is no solution for $\alpha > 2$, this is supported by the author's calculations. Din's self-consistent values for $\alpha = 1$ were

m = 320 Mev width = 50 Mev.

Note that Γ is not the width, although Diu seems to be implying it is, but he also says that the width is 4 X too large. Martin is presumably also making a misinterpretation.

Gervais (4) has generalised the model to include the exchange of two-pions as well as the ρ pole, this gives a strong force, but no self consistent solution exists; the two curves, in the graphical solution, no longer meet.

In a further preprint, Abers and Zachariasen argued that the method would give two solutions in general and that bootstrap calculations in general would give two solutions for the ρ.

According to them, for every solution just above threshold there was one just below threshold. This was because N behaves like ν^{ℓ} and hence D has an $(\ell+1)^{th}$ order cusp at threshold. Thus ν_{Rin} vs. ν_{Rout} will have two solutions if N varies smoothly with ν_{Rin} and if Γ_{in} vs Γ_{out} is also slowly varying with ν_R [illegible] will be two solutions. They also used this argument to show how an S wave amplitude tends to avoid having solutions by Re D turning away from the axis at threshold.

Wong replied to this argument, saying that it only applies in the Zachariasen model and not in general.

The Zachariasen method in potential scattering for a Yukawa potential was studied by Luming (5).

The agreement with the exact solution was poor. In the S wave, too strong attraction, in the P wave, a spurious bound state. This was not present when the second born approximation was included, however the latter had a zero of N in the physical region which was not present in the exact solution.

Also no bound states at all were found in second order.

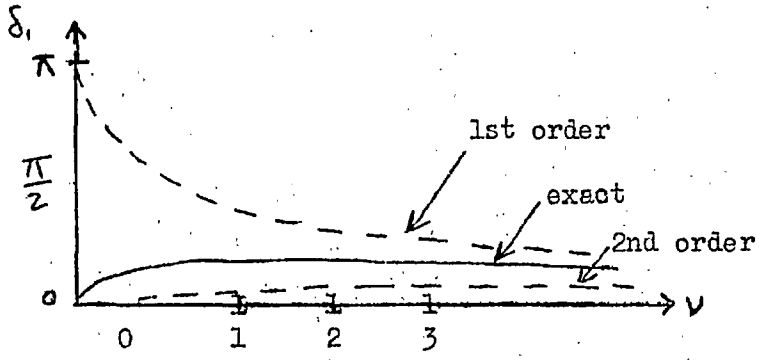

Luming showed that the D integral could be obtained in closed form in the potential scattering case which corresponds to S wave exchange, and has a simpler kinematic factor

$$\frac{1}{\sqrt{\nu'}} \quad \text{as opposed} \quad \sqrt{\frac{\nu'}{\nu'+1}}\,.$$

The author has been unable to find an analogous procedure in the relativistic case and the integrals are done numerically. The difference in kind is due to the integral being over $[0,\infty]$, which is the entire cut of $\frac{1}{\sqrt{\nu'}}$ but not of $\sqrt{\frac{\nu'}{\nu'+1}}$.

The author feel that the occurrence of a spurious P wave bound state in the potential case in the first Born approximation only may well be the answer to the stature of the P wave solution found by Zachariasen. That is to say, it may be an accidental solution of the same type.

Comparison of notation with that of other workers

We record here the notations of Din of Zachariasen & Zemach, and of Zachariasen at Edinburgh '62.

(a) D_{in} uses $S = 1 + \frac{4\pi i T}{q^2 + 1}$

so $\mathrm{Im}\, A^{-1} = -\frac{1}{2} \cdot \sqrt{\frac{\nu}{\nu+1}}$

$$N(\nu) = \frac{f\pi^2}{4\pi} \cdot \frac{1}{2} \cdot \frac{1}{4} \cdot \frac{2}{\nu} \left[2\nu + \nu_R + 2\right] \cdot 2 \cdot Q_1\left[1 + 2\left(\frac{\nu_R + 1}{\nu}\right)\right]$$

hence comparing with my equation

$$\frac{f\pi^2}{4\pi} = 12 \cdot \Gamma_{\nu_R \ell-1}$$

his self consistency condition for width is

$$\frac{f_\pi^2}{4\pi} = \frac{3}{\nu_R} - \frac{N}{\frac{\partial D}{\partial s}} = \frac{12}{\nu_R} \cdot \frac{N}{-\frac{\partial D}{\partial \nu}}$$

$$\text{i.e. } \frac{\nu_R}{12} \cdot \frac{f_\pi^2}{4\pi} = \frac{N}{-D'} = \Gamma_{\nu_R} \ell \cdot$$

he obtained $\frac{f_\pi^2}{4\pi} \simeq 10.$ expt value ~ 2.5

also $m_\rho = 320$ Mev.

He also said this $\sim$ 50 Mev, which can't be right.

(b) Z & Z used

$$\alpha = \frac{s}{4} = \nu_R + 1$$

$$\text{Im } t_L^{-1} = -1$$

$$\frac{N}{\frac{d \text{ Re } D}{d\alpha}} = \frac{1}{3} \cdot \frac{\gamma^2}{4\pi} \left(\frac{\alpha - 1}{\alpha}\right)^{3/2} \alpha$$

$$= \frac{1}{3} \cdot \frac{\gamma^2}{4\pi} \cdot \left(\frac{\nu_R}{\nu_R + 1}\right)^{3/2} \cdot (\nu_R + 1)$$

$$\frac{\gamma^2}{4\pi} = 12. \left(\frac{\nu_R + 1}{\nu_R}\right)^{3/2} \cdot \frac{\Gamma_{\nu_R}}{(\nu_R + 1)} = 12. \sqrt{\frac{\nu_R + 1}{\nu_R}} \cdot \Gamma_{\nu_R} \ell^{-1}$$

In Zachariasen's original letter $\gamma = \frac{1}{2}\gamma$

(They got for P_1 only
$m_\rho = 350$ Mev
$\frac{\gamma^2}{4\pi} = 0.6$)

(c) Zachariasen at Edinburgh '62

$$\text{Im } t^{-1} = \frac{-q}{\omega}$$

$$\frac{-N}{\frac{dRe\ D}{ds}} = -\frac{4}{3} \cdot \frac{\gamma^2}{4\pi} \cdot \left(\frac{\alpha - 1}{\alpha}\right)^{3/2} \cdot \alpha$$

$$\frac{\gamma^2}{4\pi} = 2.4. \sim \text{his s.c. value}$$

$$\frac{\gamma^2}{4\pi} = 1.9 \sim 250 \text{ Mev} \sim \text{Balazs's s. c. value}$$

same relation to my Γ as in (b).

Zachariasen's original letter (or rather its erratum) gave

$$m_\rho \sim 350 \text{ Mev}$$

and expt. value $m_\rho \sim 750$ Mev

$$\frac{\gamma^2}{4\pi} \simeq 1.$$

Further discussion

Several channels

For several channels, one chooses n channels and finds solutions of

$$\mathrm{Re}\, D_j \,\mathrm{out}\,(\nu_{Rjin}) = 0 = 1 - \left(\frac{\nu_{Rj} - \nu_{oj}}{\pi}\right) \sum_{K=1}^{n} \int_0^{\infty} \sqrt{\frac{\nu'}{\nu'+1}} \cdot \frac{C_{kj}(\nu', \nu_{Rk})}{(\nu' - \nu_{oj})\,(\nu' - \nu_{Rjn})}$$

$$\mathrm{Re}\, A\mathrm{out}'\,(\nu_{Rjin}) = \mathrm{Re}\, A_{in}'\,(\nu_{Rjin})$$

$$j = 1 \ldots n$$

However, it is not clear how to choose ν_o; for each kth of the crossed channels produces a different left hand cut in the jth direct channel, starting at $-\nu_{Rk} - 1$ respectively independent of j.

Divergence as we add more partial waves

If we are taking

$$N_{\ell}(\nu) = C_{\ell\ell'}(\nu)$$

as an estimate for

$$N_{\ell}(\nu) = \sum_{\ell'=0}^{\infty} C_{\ell\ell'}(\nu)$$

then, we are seriously wrong in principle, for this series diverges, in the physical region, where we are using our estimate of $N(\nu)$. Our estimate may still be a good one due to some unknown damping of higher waves or other obscure mechanism.

It may be possible to view the ansatz

$$N_{\ell}(\nu) = C_{\ell\ell'}(\nu)$$

in a different way, not as a truncated series but e.g. as a dominant diagram, i.e. leading term in a different, convergent, series.

Attempt at Extension of the Zachariasen method for arbitrary numbers of subtractions in D

Putting $N(\nu) = C(\nu) \longrightarrow \nu^{\ell'-1} \log \nu$

gives $\mathrm{Im}D(\nu) = - \frac{\nu}{\nu+1} \cdot \mathrm{Re}N(\nu) \longrightarrow \nu^{\ell'-1} \log \nu$

hence for $\ell' = 1$ we need one subtraction and in general for ℓ' wave exchange we need ℓ' subtractions to make the D integral converge. Taking them all at ν_0

$$D(\nu) = D(\nu_0) + (\nu - \nu_0)\, D'(\nu_0) + \cdots + (\ell - 1)^{-1} (\nu - \nu_0)^{\ell'-1} D^{\ell'-1}(\nu_0)$$

$$+ \frac{(\nu - \nu_0)^{\ell'}}{\pi} \int_0^\infty \frac{\mathrm{Im}D(\nu')\, d\nu'}{(\nu' - \nu)(\nu' - \nu_0)}$$

actually $\mathrm{Im}\, D(\nu')$ should be replaced by

$$\left[\mathrm{Im}\, D(\nu') - \mathrm{Im}\, D(\nu_0) \cdots - (\ell'-1)!^{-1} (\nu' - \nu_0)^{\ell'-1} \mathrm{Im}\, D^{\ell'-1}(\nu_0)\right]$$

but as we shall always take $\nu_0 \notin [0, \infty]$, these other terms will always be zero. The $D(\nu_0)$, $D'(\nu_0)$ . . . are arbitrary constants and cannot be determined from the Im D function, however there is always a multiplicative factor arbitrariness between N and D which allows us to choose $D(\nu_0) = 1$. If we make more than ℓ' subtractions, the further constants, e.g. $D^{\ell'}(\nu_0)$ are not arbitrary and can be calculated from ImD:-

$$D^n(\nu_0) = \frac{d^n}{d\nu^n} \cdot \left[\frac{(\nu - \nu_0)^{\ell'}}{\pi} \int_0^\infty \frac{\mathrm{Im}\, D(\nu')\, d\nu'}{(\nu' - \nu)(\nu' - \nu_0)} \right]$$

$$n \geq \ell'$$

We emphasize that ℓ' is the angular momentum of the exchanged particle, not of the partial wave we are considering.

In the spirit of the Zachariasen ansatz, which makes

$$A(\nu) \equiv \frac{N(\nu_0)}{D(\nu)} = C(\nu)\Big|_{\nu = \nu_0}$$

we can demand that

$$D^n(\nu_0) = 0 \qquad n = 1 \ldots \ell' - 1$$

satisfying crossing symmetry at ν_0 up to the nth derivative

which makes

$$A^n(\nu) = C^n(\nu)\Big|_{\nu = \nu_0}$$

This is obvious, and can be seen explicitly for the first two derivatives as follows:-

$$A' = \frac{N'D - D'N}{D^2} = \frac{N}{D}' = C'$$

$$A'' = \frac{N}{D}'' - \frac{N'D}{D^2} + \frac{ND'.2DD' - D^2ND'' - D^2N'D'}{D^4}$$

$$= \frac{N}{D}'' = C''.$$

etc.

The asymptotic behaviour can be estimated as follows:-

$$\text{Re } N \sim \nu^{\ell'-1} \log \nu'$$

$$\text{Re } D \sim \nu^{\ell'-1}$$

$$\text{Im } D \sim \nu^{\ell'-1} \log \nu$$

$$\text{Im } A = \frac{-\text{Im } D.N}{D^2} \sim \text{constant} = +1$$

$$\text{Re } A = \frac{\text{Re } D.N}{D^2} \sim \frac{1}{\log \nu} \longrightarrow 0.$$

A becomes purely imaginary as $\nu \to \infty$ and $\delta \to (2n+1)\pi/2$.

The threshold behaviour remains correct

$$A(\nu) \propto \nu^{\ell}.$$

This would not have been the case had we subtracted at the origin, which might have been desirable to obtain the same derivatives at the origin at $C(\nu)$. However in this case we have

$$\nu^{\ell'} \int_0^{\infty} \frac{1}{\nu'^{\ell'}} \cdot \frac{N(\nu') \cdot d}{(\nu' - \nu)} \cdot \sqrt{\frac{\nu'}{\nu'+1}}$$

a behaviour $\sqrt{\nu'}$ in the discontinuity gives a discontinuity in the 1st derivative, hence as $N(\nu) \propto \nu^{\ell}$, and we have a behaviour $\nu'^{(\ell-\ell')}.\sqrt{\nu'}$ we get a discontinuity in the $(\ell - \ell' + 1)$ st derivative. Indeed, for $\ell' > \ell$ the integral diverges because of behaviour of the integrand at the origin. Thus subtractions at the origin are unsatisfactory.

In the numerical determination of D, we evaluate by separation thus

$$\frac{(\nu-\nu_0)^{\ell'}}{\pi}\int_0^{\infty}\sqrt{\frac{\nu'}{\nu'+1}}\,\frac{\mathrm{Re}\,N(\nu')\,d\nu'}{(\nu'-\nu)\,(\nu'-\nu_0)^{\ell'}} = \frac{(\nu-\nu_0)^{\ell'}}{\pi}\int_0^{\infty}\frac{[\mathrm{Re}\,N(\nu')-\mathrm{Re}N(\nu)]\,d\nu'}{(\nu'-\nu)\,(\nu'-\nu_0)^{\ell'}}\sqrt{\frac{\nu'}{\nu'+1}}$$

$$+\,(\nu-\nu_0)^{\ell'}\cdot\frac{\mathrm{Re}N(\nu)}{\pi}\cdot\int_0^{\infty}\frac{d\nu'}{(\nu'-\nu)\,(\nu'-\nu_0)^{\ell'}}\sqrt{\frac{\nu'}{\nu'+1}}$$

To evaluate,

$$I^{\ell'}(\nu) = \frac{(\nu-\nu_0)^{\ell'}}{\pi}\int_0^{\infty}\sqrt{\frac{\nu'}{\nu'+1}}\cdot\frac{d\nu'}{(\nu'-\nu)\,(\nu'-\nu_0)}$$

given the value of

$$I(\nu) = \frac{(\nu-\nu_0)}{\pi}\int_0^{\infty}\sqrt{\frac{\nu'}{\nu'+1}}\cdot\frac{d\nu'}{(\nu'-\nu)\,(\nu'-\nu_0)}$$

We note that

$$I(\nu) = I(\nu_0) + (\nu-\nu_0)\cdot I(\nu_0) \cdots + (n')^{-1}(\nu-\nu_0)^n I^n(\nu_0)$$

$$+\,\frac{(\nu-\nu_0)^{n+1}}{\pi}\int_0^{\infty}\sqrt{\frac{\nu'}{\nu'+1}}\,\frac{d\nu'}{(\nu'-\nu)\,(\nu'-\nu_0)^{n+1}}$$

taking $I(\nu_\bullet) = 0$

Hence

$$I^{\ell'}(\nu) = I(\nu) - (\nu-\nu_0)\cdot I'(\nu_0) \cdots - \left((\ell'-1)!\right)^{-1}(\nu-\nu_0)^{\ell'-1}\cdot I^{\ell'-1}(\nu_0)$$

where the derivatives are obtained by differentiating the analytic expression for $I(\nu)$.

As shown in the appendix

$$I'(\nu) = -\frac{1}{(\nu+1)}\cdot\left[1+\frac{f(\nu)}{\nu}\right]$$

$$I''(\nu) = \frac{1}{2(\nu+1)^2\nu}\left[(2\nu-1)+\frac{f(\nu)}{\nu}\cdot(4\nu+1)\right]$$

etc.

where $f(\nu) = \sqrt{\frac{\nu}{\nu+1}}\cdot\log\left[\sqrt{\nu}+\sqrt{\nu+1}\,\right]$.

The logical conclusion of this approach is to look for convergence of the sequence of amplitudes obtained by taking more and more waves in the crossed channel and more and more subtractions in the direct channel.

$$N^L_{\ell}(\nu) = \sum_{\ell=0}^{L}\mathrm{Re}\,C_{\ell\ell'}(\nu)$$

$$D^L_{\ell}(\nu) = 1 - \frac{(\nu-\nu_0)^L}{\pi}\cdot\int_0^{\infty}d\nu'\sqrt{\frac{\nu'}{\nu'+1}}\cdot\frac{N^L_{\ell}(\nu')}{(\nu'-\nu)\,(\nu'-\nu_0)^L}$$

Does $\frac{N_\ell^L(\nu)}{D_\ell^L(\nu)}$ approach a limit as $L \to \infty$?

As L increases, D_ℓ becomes flatter and flatter on the left, so the amplitude might become independent of ν. It also approaches exact crossing closer and closer.

$$N_\ell^L(\nu) \xrightarrow[\nu \to \infty]{} \nu^{L-1}$$

$$D^L(\nu) \xrightarrow[\nu \to \infty]{} \nu^{L-1} \cdot \log \nu$$

so A_ℓ^L has asymptotic behaviour not strongly dependent on L. It has cuts in the right places and obeys unitarity. The author has not been able to prove that this sequence converges and suspects that it does not, for the following reason

$$A_\ell^{L-1}(\nu) = \frac{1}{\sum_{\ell'=0}^{L} \mathrm{Re}\, C_{\ell\ell'}(\nu)} \div \frac{(\nu-\nu_0)^L}{\pi} \cdot \int_0^\infty \sqrt{\frac{\nu'}{\nu'+1}}\, d\nu' \cdot \frac{\sum_{\ell=0}^{L} \mathrm{Re}\, C_{\ell\ell'}(\nu')}{\sum_{\ell=0} \mathrm{Re}\, C_{\ell\ell'}(\nu)} \cdot \frac{}{(\nu'-\nu)(\nu'-\nu_0)^L}$$

now $\sum \mathrm{Re}\, C$ diverges in $[0, \infty]$, and converges in $[0, -9]$. Hence the first term is either finite or zero and the second term must either diverge or vanish for in $[0, -9]$ or $[0, \infty]$, that is, at least one of these four possibilities must be true. This is very strange behaviour if one assumes that A_ℓ^{L-1} is going to converge to a sensible function.

With coupled channels one gets a slightly worrying effect. For example if we have a P wave in the crossed channel, we calculate the effect on the P, D etc. waves in the direct channel using one subtraction. Theeffect of a D wave on these would need two subtractions. If we now have P and D, so $C = C_p + D_D$, then we need two subtractions and the D integral has two parts, the D_p part subtracted twice and C_D part also subtracted twice. Thus the contribution to D from a given wave depends upon whether waves of higher ℓ' are being used as well. As we add more terms in the partial wave series we have to subtract more times. Thus as we add more waves, the effect on the direct channel is not just the additive one it appeared to be.

This is accentuated by our extended ansatz

$$D^n(\nu_0) = 0$$

If we had left in the subtraction terms, we could have calculated their values for the contributions from lower waves from integrals with less subtractions and merely put the incalculable part = 0. This gives a modified series, rather unrelated to our original aims, but having additivity of contributions to N (ν) from different ℓ' waves.

$$D_\ell(\nu) = 1 - \frac{1}{\pi}\int_0^\infty \sqrt{\frac{\nu'}{\nu'+1}} \cdot \frac{\mathrm{Re}C_{0\ell}(\nu')d\nu'}{\nu'-\nu} - \frac{(\nu-\nu_0)}{\pi}\int_0^\infty \sqrt{\frac{\nu'}{\nu'+1}} \cdot \frac{\mathrm{Re}C_{1,\ell}(\nu')\,d\nu'}{(\nu'-\nu)\,(\nu'-\nu_0)}$$

$$- \frac{(\nu-\nu_0)^2}{\pi}\cdot\int_0^\infty \sqrt{\frac{\nu'}{\nu'+1}} \cdot \frac{\mathrm{Re}\,C_{2\ell}(\nu')\,d\nu'}{(\nu'-\nu)\,(\nu'-\nu_0)^2} + \cdots$$

$$= 1 - \sum_{\ell'=0}^{L} \frac{(\nu-\nu_0)^{\ell'}}{\pi}\int_0^\infty \sqrt{\frac{\nu'}{\nu'+1}} \frac{\mathrm{Re}\,C_{\ell'\ell}(\nu')\,d\nu'}{(\nu'-\nu)\,(\nu'-\nu_0)^{\ell'}}$$

we no longer have $D^n(\nu_0) = 0 \qquad L > n \geq 1$

$$D(\nu_0) = 1$$

instead we have this property for all waves higher than nth for $D^n(\nu_0) = 0$. Thus the $\ell' = 0$ contribution violates $D(\nu_0) = 1$

and the $\ell' = 1$ contribution violates $D'(\nu_0) = 0$ but satisfies $D(\nu_0) = 1$

and so on.

Again, the convergence as $L \to \infty$ is an open question.

Further results

We looked at the effect of 0, 1, 2 and 3 subtractions for S, P, D, F exchange and obtained the tables and graphs shown. Table 3 and Fig. 6 show the effect of different numbers of subtractions for $P_1 \to P_1$, Table 4 for $S_0 \to P_1$; and Fig. 7 shows P + D ⟶ P for two subtractions and P + D + F → P for 3 subtractions. These amplitudes are not encouraging and show the damping of high energy behaviour as L increases. It was hoped to find a mechanism for the spurious nature of the P wave solution in the assignment of the

Table 4-3. Tables of ReD for different numbers of subtractions. $P_1 \to P_1$.

1 copy same as column 1, Table 4-1.

2 ICYN = 2	3 ICYN = 3	ν
-0.108	2.656	-10.000
-0.013	2.436	-9.500
0.080	2.233	-9.000
0.170	2.047	-8.500
0.258	1.878	-8.000
0.343	1.724	-7.500
0.426	1.587	-7.000
0.505	1.466	-6.500
0.580	1.360	-6.000
0.652	1.269	-5.500
0.720	1.193	-5.000
0.782	1.131	-4.500
0.839	1.082	-4.000
0.890	1.046	-3.500
0.933	1.022	-3.000
0.967	1.007	-2.500
0.990	1.001	-2.000
0.996	1.000	-1.800
0.999	1.000	-1.600
1.000	1.000	-1.400
0.997	1.000	-1.200
0.990	0.999	-1.000
0.979	0.997	-0.800
0.963	0.992	-0.600
0.939	0.983	-0.400
0.905	0.966	-0.200
0.814	0.889	0.100
0.784	0.848	0.200
0.743	0.770	0.400
0.728	0.712	0.600
0.742	0.684	0.800
0.785	0.702	1.000
0.859	0.779	1.200
0.964	0.929	1.400
1.100	1.169	1.600
1.269	1.512	1.800
1.470	1.973	2.000
2.115	3.739	2.500
2.961	6.566	3.000
4.007	10.681	3.500
5.248	16.306	4.000
6.682	23.657	4.500
8.303	32.946	5.000
10.108	44.378	5.500
12.093	58.155	6.000
14.253	74.471	6.500
16.583	93.516	7.000
19.081	115.476	7.500
21.742	140.532	8.000
24.564	168.858	8.500
27.541	200.629	9.000
30.671	236.011	9.500
33.951	275.168	10.000

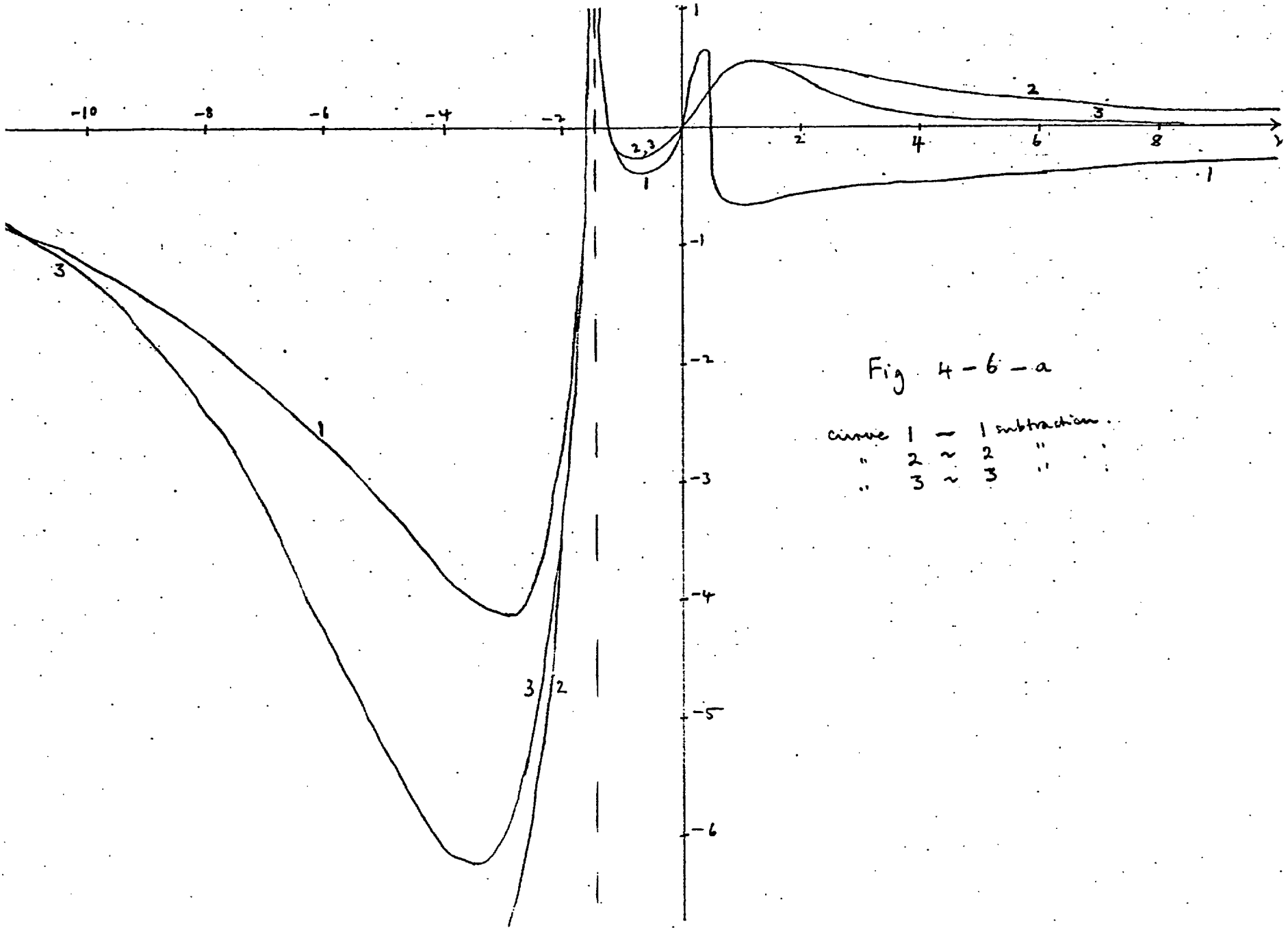

Fig 4-6-a

curve 1 — 1 subtraction.
" 2 ~ 2 "
" 3 ~ 3 "

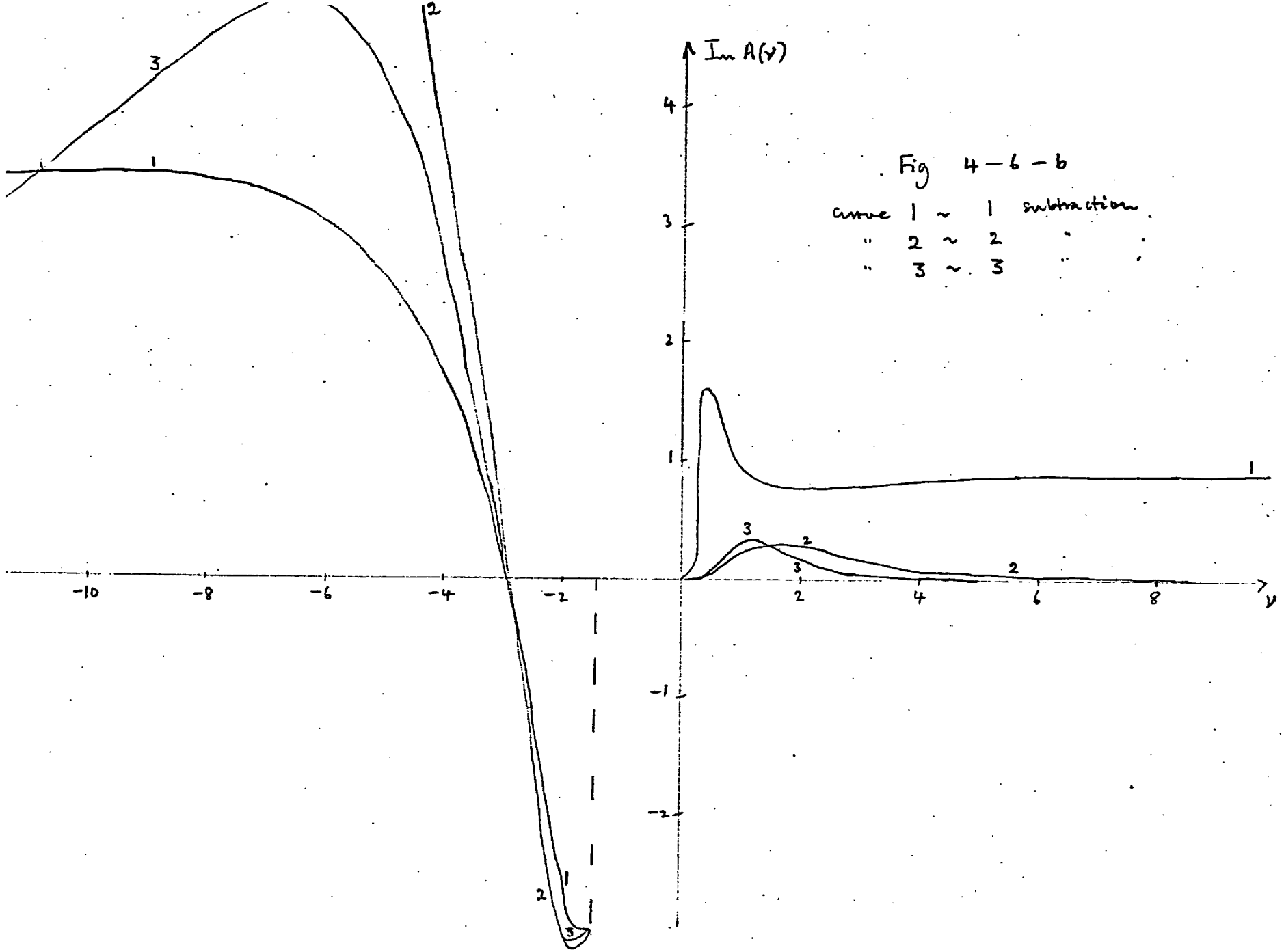

Fig 4-6-b

curve 1 ~ 1 subtraction

" 2 ~ 2 "

" 3 ~ 3 "

Table H-H. Tables of $Re_D(\nu)$ for 0, 1, 2, and 3 subtractions for $S_0 \to P_1$. also $Re_N(\nu)$.

0	1	2	3	REN	ν
-0.006	1.048	0.588	4.515	0.010	-10.000
-0.006	1.046	0.629	3.982	0.011	-9.500
-0.006	1.044	0.668	3.502	0.013	-9.000
-0.006	1.042	0.705	3.073	0.015	-8.500
-0.006	1.040	0.741	2.693	0.017	-8.000
-0.006	1.037	0.775	2.359	0.019	-7.500
-0.006	1.035	0.806	2.070	0.023	-7.000
-0.006	1.033	0.836	1.823	0.026	-6.500
-0.007	1.030	0.864	1.615	0.030	-6.000
-0.007	1.027	0.890	1.444	0.036	-5.500
-0.007	1.025	0.913	1.306	0.042	-5.000
-0.007	1.022	0.934	1.199	0.050	-4.500
-0.007	1.019	0.953	1.119	0.059	-4.000
-0.008	1.015	0.969	1.064	0.071	-3.500
-0.008	1.012	0.982	1.028	0.085	-3.000
-0.008	1.008	0.991	1.009	0.099	-2.500
-0.009	1.005	0.998	1.001	0.097	-2.000
-0.009	1.003	0.999	1.000	0.074	-1.800
-0.009	1.001	1.000	1.000	-0.004	-1.600
-0.009	0.999	1.000	1.000	-0.121	-1.400
-0.009	0.997	0.999	1.000	-0.048	-1.200
-0.010	0.996	0.998	0.999	-0.027	-1.000
-0.010	0.993	0.996	0.997	-0.016	-0.800
-0.010	0.991	0.992	0.993	-0.010	-0.600
-0.011	0.989	0.988	0.987	-0.005	-0.400
-0.011	0.986	0.982	0.977	-0.002	-0.200
-0.010	0.985	0.977	0.964	0.001	0.100
-0.008	0.987	0.980	0.967	0.002	0.200
-0.004	0.993	0.989	0.978	0.003	0.400
-0.001	0.998	1.000	0.998	0.004	0.600
0.002	1.004	1.014	1.027	0.005	0.800
0.004	1.009	1.029	1.067	0.006	1.000
0.005	1.015	1.047	1.118	0.006	1.200
0.007	1.020	1.067	1.182	0.007	1.400
0.008	1.025	1.088	1.259	0.007	1.600
0.009	1.031	1.112	1.350	0.007	1.800
0.010	1.036	1.137	1.456	0.008	2.000
0.012	1.048	1.207	1.791	0.008	2.500
0.013	1.060	1.286	2.236	0.009	3.000
0.014	1.071	1.373	2.799	0.009	3.500
0.015	1.081	1.468	3.491	0.009	4.000
0.015	1.091	1.570	4.319	0.009	4.500
0.016	1.101	1.679	5.291	0.009	5.000
0.016	1.110	1.794	6.415	0.009	5.500
0.016	1.118	1.915	7.696	0.009	6.000
0.016	1.126	2.042	9.141	0.009	6.500
0.016	1.134	2.174	10.755	0.009	7.000
0.016	1.142	2.310	12.545	0.009	7.500
0.016	1.149	2.452	14.515	0.009	8.000
0.016	1.156	2.598	16.670	0.009	8.500
0.016	1.163	2.748	19.015	0.009	9.000
0.015	1.169	2.902	21.554	0.008	9.500
0.015	1.175	3.060	24.291	0.008	10.000

Fig. 4-7. Increasing the number of waves and subtractions simultaneously.

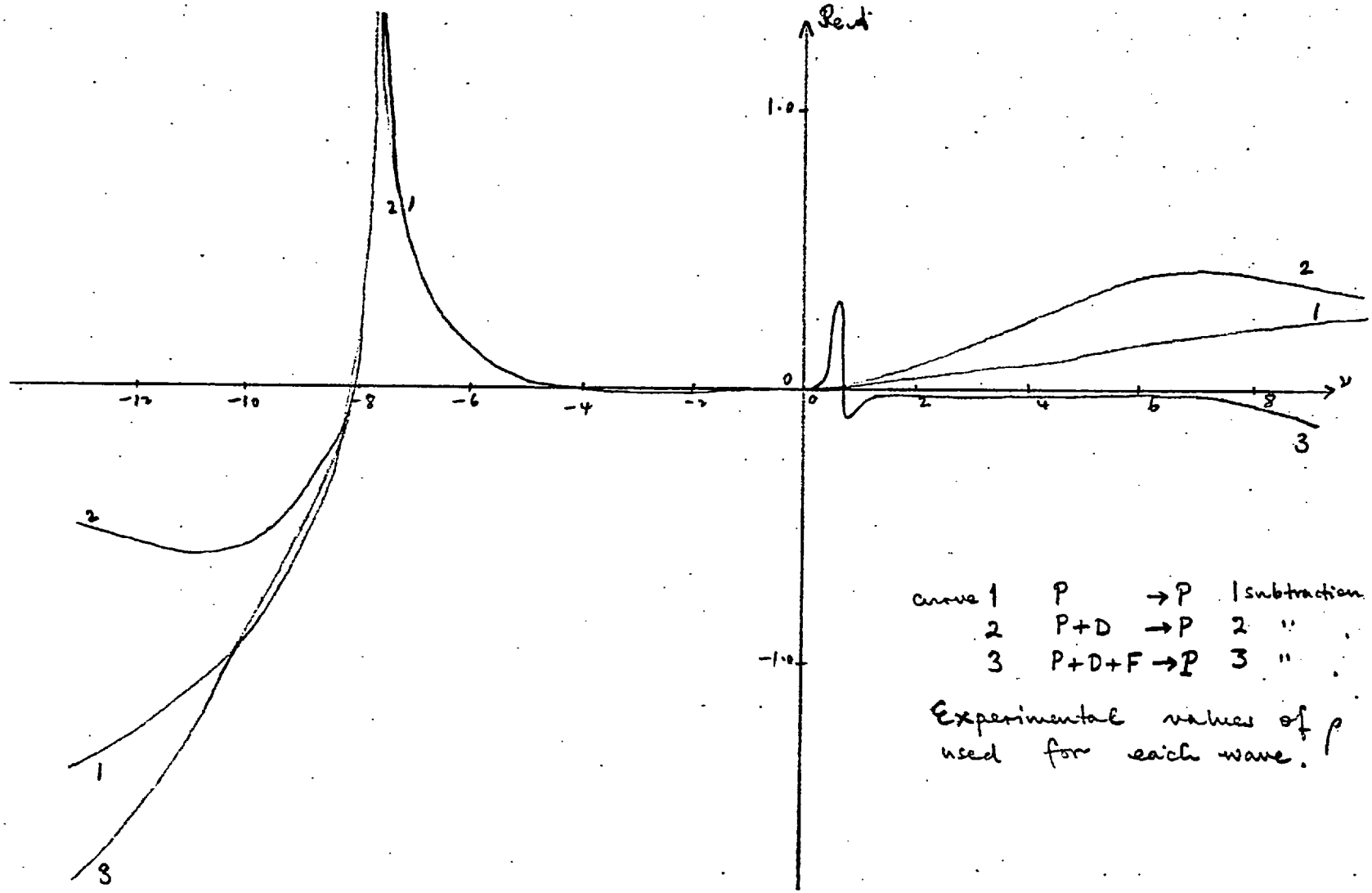

subtraction constant by crossing, but it is difficult to shed light on such an argument from the results obtained.

Possible further modifications

(a) Improved D function:

One might attribute several ills of the Zachariasen method to the choice $D(\nu) =$ on the left to get $N(\nu) = C(\nu)$. Initially we guess $D_1(\nu)$ Then take $\frac{N(\nu)}{D_1(\nu)} = C(\nu)$.

Then find $D_2(\nu) = \frac{-1}{\pi} \int_0^\infty \sqrt{\frac{\nu'}{\nu'+1}} \cdot \frac{C(\nu') \cdot D_1(\nu) \, d\nu'}{(\nu' - \nu)}$

If $D_2(\nu)$ is close to $D_1(\nu)$ then we will have better crossing symmetry on the near left.

One would like the form of $D_1(\nu)$ to be close to D_2, to have singularities only on the right, no poles except possibly on right, and to have reasonable asymptotic behaviour possibly the same as D_2, viz. $\nu^{L'-1}$ in subtracted form, however this would increase the asymptotic behaviour of $N(\nu)$ by this power and also that of D_2. The first idea is to follow Patil (6) and use

$$D_1(\nu) = \left(\frac{\nu - \nu_R}{\nu_0 - \nu_R}\right) = 1 - (\nu - \nu_0) \cdot \frac{1}{(\nu_R - \nu_0)}$$

This has reasonable linear form

$$D_1(\nu_0) = 1, \quad d_1(\nu_R) = 0$$

$$D_1(\nu) \xrightarrow[r \to \infty]{} \nu$$

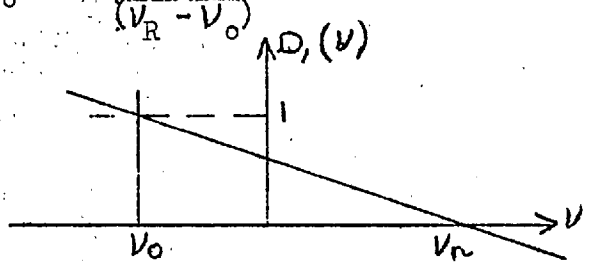

This was actually used by Patil to modify the Balaz method. To obtain $D_1(\nu) \xrightarrow[\nu \to \infty]{} \nu^2$, with a polynomial form, we can take

$$D_1(\nu) = \frac{(\nu - \nu_R)}{(\nu_0 - \nu_R)} \cdot \frac{(\nu - \nu_S)}{(\nu_0 - \nu_S)}$$

where ν_S is on the real axis and should be $> \nu_R$ to obtain $D_1'(\nu_R) < 0$.

ν_S is an arbitrary parameter of course, but could be adjusted to give good agreement between $D_1(\nu)$ and $D_2(\nu)$.

The second idea is to do two or more iterations. Thus

$$D_1(\nu) = 1$$

$$N_1(\nu) = C(\nu)$$

$$D_2(\nu) = \frac{-1}{\pi} \int \sqrt{\frac{\nu'}{\nu'+1}} \cdot \frac{C(\nu')}{\nu' - \nu} \, d\nu'$$

$$N_2(\nu) = C(\nu) \cdot D_2(\nu)$$

$$D_3(\nu) = \frac{-1}{\pi} \int \sqrt{\frac{\nu'}{\nu'+1}} \cdot \frac{C(\nu') \cdot D_2(\nu') \, d\nu'}{\nu' - \nu}$$

etc.

this is not a good idea. Apart from the large computing time required, this iteration procedure is a divergent one, for $\ell' > 1$, $D_2 \propto \nu^{\ell'-1}$, so if $\ell' > 1$, the $N(\nu)$ function gets a progresively worse asymptotic behaviour.

(b) More exact C function

One might try the exact $C(\nu)$ function rather than its function approximation.

$$C(\nu) = \frac{4}{\pi\nu} \int_0^\infty d\nu''. \operatorname{Im} A_{\ell'}(\nu''). (2\ell'+1). \beta_{II}'. P_{\ell'}\left[1 + 2\left(\frac{\nu+1}{\nu''}\right)\right]. Q_\ell\left[1 + 2\left(\frac{\nu''+1}{\nu}\right)\right].$$

In this case, for neatness and for minimisation of computation, one would interchange the orders of integration in

$$D(\nu) = 1 - \left(\frac{\nu - \nu_0}{\pi}\right)^{\ell'} \int_0^\infty d\nu' \sqrt{\frac{\nu'}{\nu'+1}} \cdot \frac{C\ell\ell'(\nu')}{(\nu'-\nu)(\nu'-\nu_0)}$$

This would involve the integrals

$$\int_0^\infty d\nu'. \sqrt{\frac{\nu'}{\nu'+1}} \cdot \frac{1}{(\nu'-\nu)(\nu'-\nu_0)^{\ell'}} \cdot \frac{1}{\nu'} \int_0^\infty d\nu''. \operatorname{Im} A_{\ell'}(\nu'').$$

$$P_{\ell'}\left[1 + 2\frac{(\nu'+1)}{\nu''}\right]. Q_\ell\left[1 + 2\left(\frac{\nu''+1}{\nu'}\right)\right]$$

$$= \int_0^\infty d\nu'' \operatorname{Im} A_{\ell'}(\nu''). \int_0^\infty d\nu' . \sqrt{\frac{\nu'}{\nu'+1}} \cdot \frac{1}{\nu'.(\nu'-\nu)(\nu'-\nu_0)}$$

$$. P_{\ell'}\left[1 + 2\frac{(\nu'+1)}{\nu''}\right]. Q_\ell\left[1 + 2\left(\frac{\nu''+1}{\nu'}\right)\right]$$

one might, hopefully, expect to evaluate the inner integral analytically.

(c) The use of an ansatz in other formalisms

We shall investigate in Chapter 5 the use of $C(\nu)$ as an ansatz for

$$B(\nu) \equiv \int_{-\infty}^{-1} \frac{\mathrm{Im}\, A(\nu')\, d\nu'}{\nu' - \nu}$$

in the variational method. It has also been used in a Uretsky $N/_D$ approach by D. Atkinson et. al as discussed in Chapter 1. In Chapter 6, we shall discuss $C^{-1}(\nu)$ as an ansatz for $\int_{-\infty}^{-1} \frac{\mathrm{Im}\, A^{-1}(\nu')\, d\nu'}{\nu' - \nu}$ in an inverse amplitude approach.

One difficulty with all these approaches except the last, is the threshold behaviour. For if $B(\nu) \underset{\nu \to 0}{\propto} \nu^{\ell}$ and $A(\nu) \underset{\nu \to 0}{\propto} \nu^{\ell}$ then it follows that the contribution from the right hand side $\int_0^{\infty} \frac{\mathrm{Im}\, A(\nu')\, d\nu'}{\nu' - \nu}$ must obey $\underset{\nu \to 0}{\propto} \nu^{\ell}$. The Zachariasen method and the inverse amplitude method do not suffer from this difficulty.

CHAPTER 5

THE VARIATIONAL METHOD

The idea of a variational method

Given the left hand discontinuity, the problem of constructing the amplitude so that it obeys unitarity can be attempted by the N/D method. This method has several disadvantages, the main one being the singularity of the integral equations obtained. From a practical point of view it is also more difficult to incorporate physically reasonable conjectures, about the rough form of the solution, or about the asymptotic behaviour, for example.

As an alternative approach, Hamilton, among others has proposed a variational method. The idea is to conjecture, usually by a parametric form, the discontinuities on the left, usually using crossing symmetry, and right, and then to vary the functions involved until unitarity is satisfied in the physical region. One way of looking at the method is that one is varying the left hand singularities to the consistent by continuation, through unitarity, with the second sheet singularities. If one has a parametrisation which is always unitary, then one is varying the contribution from the unphysical singularities of the parametric function to be close to the contribution from the unphysical singularities estimated from crossing.

The method of Donnachie and Hamilton

Donnachie and Hamilton (1) proposed a variational method and applied it to the π N system, in particular to (3, 3) resonance. Their method uses Gilbert dispersion relations (2), which we first discuss.

Gilbert Dispersion Relations

These are obtained by writing a dispersion relation for the function

$$G(\nu) = \frac{A(\nu)}{(\nu - \nu_0)^{\frac{1}{2}}}$$

we define $(\nu - \nu_0)^{\frac{1}{2}}$ to be cut along $[\nu_0, \infty]$, hence

$$(\nu + i\varepsilon - \nu_0)^{\frac{1}{2}} = \sqrt{(\nu - \nu_0)}\,(+ i\,O(\varepsilon)) \quad \nu > \nu_0 \text{ real}$$

$$(\nu - i\varepsilon - \nu_0)^{\frac{1}{2}} = -\sqrt{(\nu - \nu_0)}\,(+ i\,O(\varepsilon)) \quad \nu > \nu_0 \text{ real}$$

$$(\nu - \nu_0)^{1/2} = i\sqrt{\nu_0 - \nu} \quad \nu < \nu_0 \text{ real}$$

on the first sheet

Hence $G(\nu)$ has cuts $[-\infty, -1], [0, \infty]$, and

$$G(\nu + i\varepsilon) = \frac{\text{Re } A(\nu) + i \text{ Im } A(\nu)}{\sqrt{\nu - \nu_0}} \quad \nu > \nu_0 \text{ real}$$

$$G(\nu - i\varepsilon) = \frac{\text{Re } A(\nu) + i \text{ Im } A(\nu)}{-\sqrt{\nu - \nu_0}} \quad \nu > \nu_0 \text{ real}$$

$$G(\nu + i\varepsilon) = \frac{\text{Re } A(\nu) + i \text{ Im } A(\nu)}{i\sqrt{\nu_0 - \nu}} \quad \nu > \nu_0 \text{ real}$$

$$G(\nu - i\varepsilon) = \frac{\text{Re } A(\nu) - i \text{ Im } A(\nu)}{i\sqrt{\nu_0 - \nu}} \quad \nu > \nu_0 \text{ real}$$

hence the discontinuity on the right is

$$2\,\frac{\text{Re } A(\nu)}{\sqrt{\nu - \nu_0}}$$

and on the left is

$$2\,\frac{\text{Im } A(\nu)}{\sqrt{\nu_0 - \nu}}$$

Cauchy's theorem then gives the dispersion relation

$$\frac{A(\nu)}{\sqrt{\nu - \nu_0}} = \frac{1}{\pi i}\int_{\nu_0}^{\infty} \frac{\text{Re } A(\nu')\, d\nu'}{\sqrt{\nu' - \nu_0}\,(\nu' - \nu)} + \frac{1}{\pi i}\int_{-\infty}^{\nu_0} \frac{\text{Im } A(\nu')\, d\nu'}{\sqrt{\nu_0 - \nu'}\,(\nu' - \nu)}$$

According to where we take ν_0, we get different cuts and discontinuities. The situation is represented in a diagram. When $\nu_0 = 0$, as taken by Oades, we have

$$\frac{A(\nu)}{\sqrt{\nu}} = \frac{1}{\pi i}\int_0^{\infty} \frac{\text{Re } A(\nu')\, d\nu'}{\sqrt{\nu'}\,(\nu' - \nu)} + \frac{1}{\pi i}\int_{-\infty}^{-1} \frac{\text{Im } A(\nu')\, d\nu'}{\sqrt{-\nu'}\,(\nu' - \nu)}$$

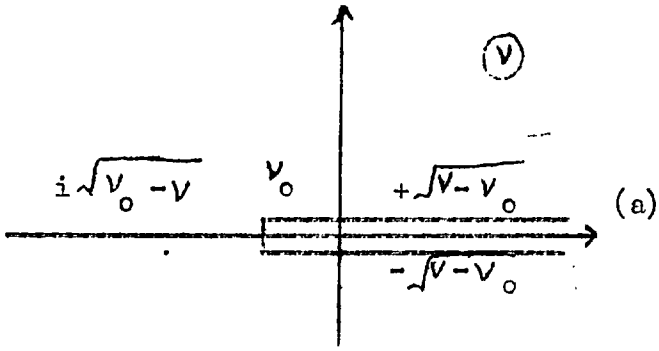

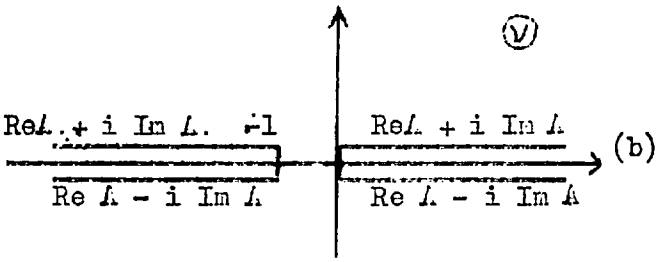

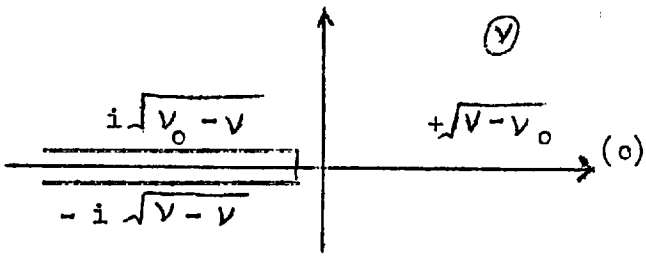

we thus have an unusual situation, with the discontinuity on the right being determined by the real part of the amplitude. Jackson (3) calls them "inverse dispersion relations" since they interchange the roles of real and imaginary parts.

When ν_0 is in $[0, \infty]$ or $[-1, -\infty]$, the two integrals overlap, e.g. if ν_0 is in $[\bullet, \infty]$

$$\frac{A(\nu)}{\sqrt{\nu}} = \frac{1}{\pi i}\int_{-\infty}^{-1} \frac{\mathrm{Im}A(\nu')\, d\nu'}{\sqrt{\nu_0 - \nu'}(\nu' - \nu)} + \frac{1}{\pi i}\int_{0}^{\infty} \frac{\mathrm{Re}\, A(\nu')\, d\nu'}{\sqrt{\nu' - \nu_0}(\nu' - \nu)}$$

$$+ \frac{1}{\pi i}\int_{-1}^{\nu_0} \frac{\mathrm{Re}\, A(\nu')\, d\nu'}{\sqrt{\nu' - \nu_0}(\nu' - \nu)}$$

$$G(\nu) = \frac{A(\nu)}{\sqrt{\nu - \nu_0}} \longrightarrow \frac{\mathrm{Re}\, A(\nu)}{\sqrt{\nu - \nu_0}} + \frac{i\, \mathrm{Im}\, A(\nu)}{\sqrt{\nu - \nu_\bullet}}$$

$$\nu \longrightarrow |\nu| \pm i\varepsilon \qquad |\nu| > \nu_0$$

dispersion integral

$$\longrightarrow \frac{1}{\pi i}\left[P\int_{\nu_0}^{\infty} \frac{\mathrm{Re}\, A(\nu')\, d\nu'}{\sqrt{\nu' - \nu_0}(\nu' - \nu)} + \frac{i\pi\, \mathrm{Re}A(\nu)}{\sqrt{\nu - \nu_0}}\right] + \frac{1}{\pi i}\int_{-\infty}^{\nu_0} \frac{\mathrm{Im}A(\nu')\, d\nu'}{\sqrt{\nu_0 - \nu'}(\nu' - \nu)}$$

$$\therefore \quad \frac{i\, \mathrm{Im}\, A(\nu)}{\sqrt{\nu - \nu_0}} = -\frac{1}{\pi} P\int_{\nu_0}^{\infty} \frac{\mathrm{Re}\, A(\nu')\, d\nu'}{\sqrt{\nu' - \nu_0}(\nu' - \nu)} \qquad -i\int_{-\infty}^{\nu_0} \text{ etc.}$$

$$\therefore \frac{\mathrm{Im}\Lambda(\nu)}{\sqrt{\nu-\nu_0}} = -\frac{1}{\pi} P\int_{\nu_0}^{\infty} \frac{\mathrm{Re}\,\Lambda(\nu')\,d\nu'}{\sqrt{\nu'-\nu_0}(\nu'-\nu)} - \frac{1}{\pi}\int_{-\infty}^{\nu_0} \frac{\mathrm{Im}\,\Lambda(\nu')\,d\nu'}{\sqrt{\nu'-\nu_0}(\nu'-\nu)}$$

$\nu_{\text{real}} > \nu_0$

as $\nu \to |\nu| + i\varepsilon$,

$\nu < \nu_0$.

$$G(\nu) \to \frac{\mathrm{Re}\,\Lambda(\nu) + i\,\mathrm{Im}\,\Lambda(\nu)}{i\sqrt{(\nu_0-\nu)}}$$

$$= -\frac{i\,\mathrm{Re}\,\Lambda(\nu)}{\sqrt{\nu_0-\nu}} + \frac{\mathrm{Im}\,\Lambda(\nu)}{\sqrt{\nu_0-\nu}}$$

dispersion integral

$$\to \frac{1}{\pi i}\left[P\int_{-\infty}^{\nu_0} \frac{\mathrm{Im}\,\Lambda(\nu')\,d\nu'}{\sqrt{\nu_0-\nu'}(\nu'-\nu)} - \frac{i}{\pi}\int_{\nu_0}^{\infty} \frac{\mathrm{Re}\,\Lambda(\nu')\,d\nu'}{(\nu'-\nu)\sqrt{\nu'-\nu_0}} + \frac{\mathrm{Im}\,\Lambda(\nu)}{\sqrt{\nu_0-\nu}}\right.$$

$$\therefore \frac{\mathrm{Re}\,\Lambda(\nu)}{\sqrt{\nu_0-\nu}} = P\int_{-\infty}^{\nu_0} \frac{\mathrm{Im}\,\Lambda(\nu')\,d\nu'}{\sqrt{\nu_0-\nu'}(\nu'-\nu)} + \frac{1}{\pi}\int_{\nu_0}^{\infty} \frac{\mathrm{Re}\,\Lambda(\nu')\,d\nu'}{(\nu'-\nu)\sqrt{\nu'-\nu_0}}$$

$\nu_{\text{real}} < \nu_0$

Thus the Gilbert dispersion relation gives integral expressions for the imaginary part on the right and the real part on the left.

We also remark that by taking the square root function to be cut along the negative real axis, we get a different type of relation.

$$(\nu-\nu_0)^{\frac{1}{2}} = \sqrt{\nu-\nu_0} \qquad \nu > \nu_0$$

$$(\nu+i\varepsilon-\nu_0)^{\frac{1}{2}} = +i\sqrt{\nu_0-\nu} \qquad \nu < \nu_0$$

$$(\nu-i\varepsilon-\nu_0)^{\frac{1}{2}} = -i\sqrt{\nu_0-\nu} \qquad \nu < \nu_0$$

$$G(\nu+i\varepsilon) = \frac{\mathrm{Re}\,\Lambda(\nu) + i\,\mathrm{Im}\,\Lambda(\nu)}{\sqrt{\nu-\nu_0}} \qquad \nu > \nu_0$$

$$G(\nu-i\varepsilon) = \frac{\mathrm{Re}\,\Lambda(\nu) - i\,\mathrm{Im}\,\Lambda(\nu)}{\sqrt{\nu-\nu_0}} \qquad \nu > \nu_0$$

$$G(\nu+i\varepsilon) = \frac{\mathrm{Re}\,\Lambda(\nu) + i\,\mathrm{Im}\,\Lambda(\nu)}{i\sqrt{\nu_0-\nu}} \qquad \nu < \nu_0$$

$$G(\nu-i\varepsilon) = \frac{\mathrm{Re}\,\Lambda(\nu) - i\,\mathrm{Im}\,\Lambda(\nu)}{-i\sqrt{\nu_0-\nu}} \qquad \nu < \nu_0$$

$$\therefore \frac{\Lambda(\nu)}{\sqrt{\nu-\nu_0}} = \frac{1}{\pi}\int_{\nu_0}^{\infty} \frac{\mathrm{Im}\,\Lambda(\nu')}{\sqrt{\nu'-\nu_0}(\nu'-\nu)}\,d\nu' - \frac{1}{\pi}\int_{-\infty}^{\nu_0} \frac{\mathrm{Re}\,\Lambda(\nu')}{\sqrt{\nu_0-\nu'}(\nu'-\nu)}\,d\nu'$$

so the discontinuity on the left comes from the real part on the left.

Also one can use $\sqrt{\frac{\nu}{\nu+1}}$ as a kinematic factor writing a dispersion relation for $A(\nu)\cdot\sqrt{\frac{\nu+1}{\nu}}$. The discontinuity is Re $A(\nu)\cdot\sqrt{\frac{\nu+1}{\nu}}$

$$\therefore \quad A(\nu)\cdot\sqrt{\frac{\nu+1}{\nu}} = \frac{-i}{\pi}\int \mathrm{Re}\,A(\nu')\cdot\sqrt{\frac{\nu'+1}{\nu'}}\cdot\frac{d\nu'}{\nu'-\nu}$$

just above the cut we have

left hand side $\rightarrow \left[\mathrm{Re}\,A(\nu) + i\,\mathrm{Im}\,A(\nu)\right]\cdot\sqrt{\frac{\nu+1}{\nu}}$

right hand side $\rightarrow \mathrm{Re}\,A(\nu)\cdot\sqrt{\frac{\nu+1}{\nu}} - \frac{i}{\pi}\int \mathrm{Re}\,A(\nu')\cdot\frac{d\nu'}{\nu'-\nu}\sqrt{\frac{\nu'+1}{\nu'}}$

$$\therefore \quad \mathrm{Im}\,A(\nu) = \frac{1}{\pi}\sqrt{\frac{\nu+1}{\nu}}\int \mathrm{Re}\,A(\nu')\cdot\sqrt{\frac{\nu'+1}{\nu'}}\cdot\frac{d\nu'}{\nu'-\nu}$$

It is clear that there are four types of kinematic function typified by 1, $\sqrt{\nu}$ cut $[0,\infty]$, $\sqrt{\nu+1}$ cut $[-1,-\infty]$, $\sqrt{\frac{\nu}{\nu+1}}$ cut $[-1,-\infty][0,\infty]$ for which the discontinuities are obtained from real and imaginary part as follows

	L	R
1	I	I
$\sqrt{\nu}$	I	R
$\sqrt{\nu+1}$	R	I
$\sqrt{\frac{\nu}{\nu+1}}$	R	R

Taking the limit onto the cut for the 2nd case

(1) if limit $\rightarrow$ point on right hand cut

left hand side $\rightarrow \quad \frac{\mathrm{Re}\,A(\nu) + i\,\mathrm{Im}\,A(\nu)}{i\sqrt{\nu}}$

right hand side $\rightarrow \quad \frac{\mathrm{Re}\,A(\nu)}{\sqrt{\nu}} + \int\frac{\mathrm{Re}\,A(\nu')\,d\nu'}{\sqrt{\nu'}\,(\nu'-\nu)}$

(2) If limit $\rightarrow$ point on left hand cut

left hand side $\rightarrow \quad \frac{\mathrm{Re}\,A(\nu) + i\,\mathrm{Im}\,A(\nu)}{\sqrt{\nu}}$

right hand side $\rightarrow \quad \frac{i\,\mathrm{Im}\,A(\nu)}{\sqrt{\nu}} + \int\frac{\mathrm{Im}\,A(\nu')\,d\nu'}{\sqrt{\nu'}\,(\nu'-\nu)}$

$\therefore$ we get a relation

$$\frac{\mathrm{Im}\,A(\nu)}{\sqrt{\nu}} = \frac{1}{\pi}\int_0^{\infty}\frac{\mathrm{Re}\,A(\nu')\,d\nu'}{\sqrt{\nu'}\,(\nu'-\nu)} + \frac{1}{\pi}\int_{-\infty}^{-1}\frac{\mathrm{Im}\,A(\nu')\,d\nu'}{\sqrt{\nu'}\,(\nu'-\nu)}$$

$\nu > 0$

for imaginary part on right

and a relation

$$\frac{\text{Re } A(\nu)}{\sqrt{\nu}} = \int_0^{\infty} \frac{\text{Re } A(\nu')\ d\nu'}{\sqrt{\nu'}\ (\nu' - \nu)} + \int_{-\infty}^{-1} \frac{\text{Im } A(\nu')\ d\nu'}{\sqrt{\nu'}\ (\nu' - \nu)}$$

$\nu < 0$

And similarly for the other types.

Subtractions

(a) $$\frac{\text{Im } A(\nu)}{\nu^{\frac{1}{2}}} = \frac{-1}{\pi}\int_0^{\infty} \frac{\text{Re } A(\nu')}{\sqrt{\nu'}} \cdot \frac{d\nu'}{(\nu' - \nu)} \quad \frac{-1}{\pi}\int_{-\infty}^{-1} \frac{\text{Im } A(\nu')}{\sqrt{-\nu'}} \cdot \frac{d\nu'}{(\nu' - \nu)}$$

at the origin

$$\text{Im } f(\nu') = \frac{\text{Re } A(\nu')}{\sqrt{\nu'}} \longrightarrow a_1\sqrt{\nu'}$$

integral converges, has 1st order cusp, but of course this is ironed out by the $\sqrt{\nu}$ factor.

(b) Subtracting once at the origin

$$\frac{\text{Im } A(\nu)}{\nu^{\frac{1}{2}}} = -\frac{\nu}{\pi} \cdot \int_0^{\infty} \frac{\text{Re } A(\nu')\ d\nu'}{\sqrt{\nu'}\cdot\nu'(\nu' - \nu)} - \frac{\nu}{\pi}\int_{-\infty}^{-1} \frac{\text{Im } A(\nu')\ d\nu'}{\sqrt{-\nu'}\ \nu'(\nu - \nu)}$$

now $\text{Im } f(\nu') = \dfrac{\text{Re}A(\nu')}{\nu'\sqrt{\nu'}} \longrightarrow \dfrac{a_1}{\sqrt{\nu'}}$ diverges
$\nu' \to 0$

but the integral converges. As a function of ν, the integral has a discontinuity at $\nu = 0$. A second subtraction would make it diverge.

(c) Write dispersion relation for

$$\frac{A(\nu) - a_1\nu}{\sqrt{\nu}}$$

so $$\text{Im } f(\nu') = \frac{\text{Re } A(\nu') - a_1\nu'}{\sqrt{\nu'}} \longrightarrow \frac{a_2\nu'^2 + 0(\nu'^3)}{\sqrt{\nu'}} \longrightarrow a_2\nu'^{3/2} + 0(\nu^{5/2})$$
$\nu' \to 0$

hence we can subtract once at the origin.

$$\frac{\text{Im } A(\nu)}{\sqrt{\nu}} = \frac{-\nu}{\pi}\int_0^{\infty} \frac{[\text{Re}A(\nu') - a_1\nu']d\nu'}{\sqrt{\nu'}\cdot\nu'\ (\nu' - \nu)} - \frac{\nu}{\pi}\int_{-\infty}^{-1} \frac{\text{Im}A(\nu')\cdot d\nu'}{\sqrt{-\nu'}\cdot\nu'(\nu' - \nu)}$$

subtracting twice

$$\frac{\text{Im } A(\nu)}{\sqrt{\nu}} = \frac{-\nu^2}{\pi}\int_0^{\infty} \left\{ \frac{[\text{Re } A(\nu') - a_1\nu'] - \nu' \cdot \frac{\partial}{\partial\nu'}[\text{Re } A(\nu') - a_1\nu']_{\nu'=0}}{\sqrt{\nu'}\ \cdot\ \nu'^2\ (\nu' - \nu)} \right\}$$

$$-\frac{\nu^2}{\pi}\int_{-\infty}^{-1} \frac{\text{Im } A(\nu') \; - \nu' \cdot \frac{\partial}{\partial \nu'}\left[\text{Im } A(\nu')\right]\Big|_{\nu'=0}}{\sqrt{-\nu'}\,.\,\nu'^2\,(\nu'-\nu)}$$

$$\frac{\partial}{\partial \nu'}\left[\text{Re } A(\nu') - a_1\nu'\right] \;\underset{\nu' \to 0}{=}\; \frac{3}{2}\, a_2\, \nu'^{\frac{1}{2}} + 0\left(\nu'^{3/2}\right) \underset{\nu' \to 0}{=} 0$$

$$\frac{\partial}{\partial \nu'}\left[\text{Im } A(\nu')\right] \underset{\nu' \to 0}{=} \frac{\partial}{\partial \nu'}\left[a_1 \nu'^{\,3/2}\right] \underset{\nu' \to 0}{=} 0$$

We obtain the equation

$$\frac{\text{Im } A(\nu)}{\sqrt{\nu}} = -\frac{\nu^2}{\pi}\int_0^{\infty} \frac{\left[\text{Re } A(\nu') - a_1\nu'\right] d\nu'}{\sqrt{\nu'}\,.\,\nu^2\,(\nu'-\nu)} - \frac{\nu^2}{\pi}\int_{-\infty}^{-1} \frac{\text{Im } A(\nu')\; d\nu'}{\sqrt{-\nu'}\,.\,\nu'^2.(\nu'-\nu)}$$

of course, we could have written a dispersion relation for $\frac{A(\nu') - \text{polynominal in } \nu'}{\sqrt{\nu'}}$ but there is no point and the extra terms would have cancelled under the integral sign, or cause the integral to diverge depending upon how many subtractions we take.

For general angular momentum we can take

$$f(\nu) = \frac{A(\nu)}{\nu^\ell}$$

so $$\frac{\text{Im } A(\nu)}{\nu^{\frac{1}{2}}.\,\nu^\ell} = -\frac{1}{\pi}\int_0^{\infty} \frac{\text{Re } A(\nu')\; d\nu'}{\nu'^{\frac{1}{2}}.\,\nu'^\ell(\nu'-\nu)} - \frac{1}{\pi}\int_{-\infty}^{-1} \frac{\text{Im } A(\nu')\; d\nu}{\nu'^{\frac{1}{2}}\,\nu'^\ell\,(\nu'-\nu)}$$

and one can subtract these if one likes, which transfers some high energy information to the subtraction constants and is therefore useful if one has accurate low energy information and poor high energy information.

The Hamilton variational method

We write a Gilbert dispersion relation and an ordinary dispersion relation for $\frac{A(\nu)}{\nu^\ell}$

$$\text{Re } A(\nu) = \frac{1}{\pi}.\nu^\ell \int \frac{\text{Im } A(\nu')\; d\nu'}{(\nu'-\nu)\,\nu'^\ell} + \frac{\nu^\ell}{\pi}\int_{-\infty} \frac{\text{Im } A(\nu')\; d\nu'}{(\nu'-\nu)\nu'^\ell} \qquad \text{(i)}$$

$$\underset{\nu > \nu_0}{\text{Im } A(\nu)} = -\frac{\nu^{\ell+\frac{1}{2}}}{\pi}\int_{\nu_0}^{\infty} \frac{\text{Re } A(\nu')\; d\nu'}{(\nu'-\nu)\nu'^{\ell+\frac{1}{2}}} - \frac{\nu^{\ell+\frac{1}{2}}}{\pi}\int_{-\infty}^{\nu} \frac{\text{Im } A(\nu')\; d\nu'}{(\nu-\nu')\;\nu'^{\ell+\frac{1}{2}}} \qquad \text{(ii)}$$

ν_0 is here the elastic threshold, ν_1 the start of left hand cut; ν_2 the inelastic threshold. We estimate the discontinuities on the cuts by using a trial

function $F(\nu)$. We use it directly on the right

$$\text{Im } A(\nu') \backsim \text{Im } F(\nu') \qquad \nu' > \nu_0 \qquad \text{(iii)}$$

$$\text{Re } A(\nu') \backsim \text{Re } F(\nu') \qquad \nu' > \nu_0 \qquad \text{(iv)}$$

and indirectly through crossingon the left. There may be other contributions also on the left, leading us to the estimate

$$\text{Im } A(\nu') = \rho(\nu') \qquad \nu' < \nu_1 \qquad \text{(v)}$$

Thus we define the function Aout by the equations

$$\text{Re } A \text{ out}(\nu) = \frac{1}{\pi} \nu^{\ell} \cdot \int_{\nu_0}^{\infty} \frac{\text{Im } F(\nu')\, d\nu'}{(\nu' - \nu)\nu'^{\ell}} + \frac{\nu^{\ell}}{\pi} \int_{-\infty}^{\nu_1} \frac{\rho(\nu')\, d\nu'}{(\nu' - \nu)\nu'^{\ell}} \qquad \text{(vi)}$$

$$\text{Im } A\text{out}(\nu) = -\frac{\nu^{\ell+\frac{1}{2}}}{\pi} \int_{\nu_0}^{\infty} \frac{\text{Re } F(\nu')\, d\nu'}{(\nu' - \nu)\nu'^{\ell+\frac{1}{2}}} - \frac{\nu^{\ell+\frac{1}{2}}}{\pi} \int_{-\infty}^{\nu_1} \frac{\rho(\nu')\, d\nu'}{(\nu' - \nu)\nu'^{\ell+\frac{1}{2}}} \qquad \text{(vii)}$$

In general, of course, A out(ν) is not a solution of the dispersion relations (i) and (ii), however it can be shown that Re Aout and ImA out as here defined, are the real and imaginary parts of an analytic function Aout which has cuts $[\nu_0, \infty]$, $[\nu_1, -\infty]$.

In general, Aout (ν) will not obey unitarity. We define the discrepancy from unitarity by

$$D(\nu) = 2 \cdot \left[\frac{\text{Re } A\text{out}^2 + \text{Im } A\text{out}^2 - \text{Im } A\text{out} \sqrt{\frac{\nu+1}{\nu}}}{\text{Re } A\text{out}^2 + \text{Im } A\text{out}^2 + \text{Im } A\text{out} \sqrt{\frac{\nu+1}{\nu}}} \right]$$

$$\Delta^2 = \frac{1}{\nu_2 - \nu_0} \int_{\nu_0}^{\nu_2} \left\{ D(\nu) \right\}^2 d\nu$$

i.e. Δ is the root mean square deviation from unitarity.

We vary the parameters to minimise Δ. If we find a very small value $\sim 3\%$, then we hope we have a function Aout satisfying our physical requirements.

Discussion of the Method

A thorough discussion of the method can be found in (1). D & H argue that the constraint of unitarity determines the otherwise arbitrary K function, i.e. function with right hand cut only, which satisfies homogeneous dispersion relations, i.e. with no left hand cut or force function. This,

they claim, can be viewed as an adjustment of the second sheet singularities of the K function. However, the present author regards this as a tricky point since the second sheet can only be reached when unitarity is satisfied exactly. A further argument in (1) is that when there is a pole on the 1st sheet there is often a pole nearby on the 2nd sheet. This is a little mystifying since it follows by the same analysis that there will be physical sheet poles corresponding to 2nd sheet resonance poles. They remark that the CDD ambiguity is avoided by choosing solutions not vanishing in $[s_o, \infty]$. The present author believes that the analogue of the CDD ambiguity found in the N/D method in the case of non N/D methods is to be found in the existence of arbitrary parameters and is not necessarily associated with zeros of $D(\nu)$.

D & H demanded unitarity be satisfied and did not ask for self consistency explicity in the X^2. However they showed that solutions would exist for which

$$B(\nu) \longrightarrow B_t(\nu)$$

where $B(\nu)$ is the force function from crossing and $B_t(\nu)$ is the left hand contribution to the unitary trial function. Further they regarded these as desirable solutions and excluded other types by demanding a further "consistency test" $\nabla_p \longrightarrow 0$ as $X^2 \rightarrow 0$

where $$\nabla_p{}^2 = \frac{1}{s_2 - s_o}\int_{s_o}^{s_2} ds' \left\{ \text{Re } A_{out}(s') - \text{Re } F(s') \right\}^2$$

D & H examine the analytic properties of $A_{out}(\nu)$ (not necessarily unitary) defined by the two dispersion relations. They suggest that, if trial function $F(\nu)$ is a poor approximation, then

$$G(\nu) = \tfrac{1}{2}\left\{ A_{out}(\nu) + F(\nu) \right\}$$

will automatically have correct singularities on the 1st sheet and will be a better approximation. They also give a general formulation in which the second sheet singularities can be directly parametrised.

THE OADES METHOD

G. C. Oades applied a similar variational method to the problem. The work was never published but appeared as a U.C. London preprint and was presented at the Sienna Conference 1962 and the Edinburgh Summer School 1962. Oades wrote down two equations, an ordinary dispersion relation and a twice subtracted Gilbert dispersion relation, for P wave $\pi\pi$.

$$\mathrm{Re}A(\nu) = \frac{\nu}{\pi}\int_0^{\infty} \frac{d\nu' \,\mathrm{Im}A(\nu')}{\nu'(\nu'-\nu)} + \frac{\nu}{\pi}\int_{-\infty}^{-1} \frac{d\nu' \,\mathrm{Im}A(\nu')}{\nu'(\nu'-\nu)}$$

$$\mathrm{Im}A(\nu) = \frac{-\nu^{5/2}}{\pi}\int_0^{\infty} d\nu' \cdot \frac{\left[\mathrm{Re}A(\nu') - a_1 \nu'\right]}{\nu'^{5/2}(\nu'-\nu)} - \frac{\nu^{5/2}}{\pi}\int_{-\infty}^{-1} \frac{d\nu' \,\mathrm{Im}A(\nu')}{\nu'^{5/2}(\nu'-\nu)}$$

a_1 being the P wave scattering length. He took a simple Breit Wigner trial function tion (our type 1) $F(\nu)$. He estimated the right hand cuts directly. For the left hand cut, he estimated the near part, up to a cut-off, from crossing

$$\mathrm{Im}A(\nu') = \frac{2}{\nu'}\int_0^{-\Lambda-1} d\nu'' \sum_{\ell=0}^{\infty} 2(\ell+1) \sum_{I'=0}^{2} \beta_{II'} \,\mathrm{Im}A_{\ell}^{I'}(\nu'')$$

$$\Lambda < \nu' < -1 \qquad \cdot P_{\ell}\left[1 + 2\left(\frac{\nu'+1}{\nu''}\right)\right] \cdot Pn\left[1 + 2\left(\frac{\nu''+1}{\nu'}\right)\right]$$

actually taking just the contributions from S_0, S_2, P_1 in the crossed channel. $\mathrm{Im}A_0^0$ and $\mathrm{Im}A_0^2$ in the crossed channel were put in from another calculation and held fixed. $\mathrm{Im}A_1^1$ in the crossed channel was estimated from the trial funotion

$$\mathrm{Im}A_1^1(\nu'') = \mathrm{Im}F(\nu'')$$

Usually Λ was = -9. The rest of the left hand cut was represented by a single pole giving contributions

$$\frac{\nu}{\nu_p} \cdot \frac{g_p}{\nu-\nu_p} \quad \text{and} \quad \frac{\nu^{5/2}}{\nu_p^{5/2}} \cdot \frac{g_p}{\nu-\nu_p}$$

to the real and imaginary parts respectively. In fact, in the solution obtained by Oades, $\nu_p = -7.3$, so it is quite near in. He inserted these estimates in the dispersion relations and evaluated the discrepancy from unitarity, to which he added the discrepancies from self consistency of the real and imaginary parts. The amplitude in physical region of the crossed channel is $F(\nu'')$, for the imaginary part was taken as $\mathrm{Im}F(\nu')$ and by unitarity the real part is $\mathrm{Re}F(\nu'')$ and self consistency between crossed and direct channels was the deviation

between $F(\nu)$ and Aout. Thus he took

$$\Delta = \left[\frac{1}{n}\sum_{j=1}^{n}(\Delta_1^2(\nu_j) + \Delta_2^2(\nu_j) + \Delta_3^2(\nu_j))\right]^{\frac{1}{2}} \times 100\%$$

$$\Delta_1(\nu) = 2.\left[\frac{\text{Re Aout}(\nu) - \text{ReF}(\nu)}{\text{Re Aout}(\nu) + \text{ReF}(\nu)}\right]$$

$$\Delta_2(\nu) = 2.\left[\frac{\text{Im Aout}(\nu) - \text{Im F}(\nu)}{\text{Im Aout}(\nu) + \text{Im F}(\nu)}\right]$$

$$\Delta_3(\nu) = 2.\left[\frac{\text{Re Aout}^2(\nu) + \text{ImAout}(\nu)^2 - \sqrt{\frac{\nu+1}{\nu}}\cdot \text{Im Aout}(\nu)}{\text{Re Aout}^2(\nu) + \text{Im Aout}(\nu)^2 + \sqrt{\frac{\nu+1}{\nu}}\cdot \text{Im Aout}(\nu)}\right]$$

the ν_j being sampling points. In fact, he took ten points, equally spaced in $[0, 10]$. He varied $[\nu_R, \nu_R\, g_p, \nu_p$ simultaneously and obtained a minimum of 0.3% at $\nu_R = 5.7, \Gamma\nu_R = 2.26$, i.e. 725 Mev, width 200 Mev, and $g_p = -1.32$, $\nu_p = -7.3$

The contribution to the right hand side of Rcout from the near left hand cut is

$$\frac{\nu}{\pi}\int_{-\infty}^{-1} \frac{d\nu'\ \text{Im Aout}(\nu')}{\nu'(\nu'-\nu)}$$

i.e. $$\frac{\nu}{\pi}\int_{\Lambda}^{\Lambda+1} \frac{d\nu'}{\nu'(\nu'-\nu)} \cdot \frac{2}{\nu'}\int_{0}^{-\nu'-1} d\nu'' \sum_{\ell=0}^{\infty}(2\ell+1)\sum_{I'=0}^{2}\beta_{II'}\ \text{Im } A_\ell^{I'}(\nu'')$$
$$\cdot P_\ell\left[1 + 2\frac{(\nu'+1)}{\nu''}\right] \cdot P_m\left[1 + 2\left(\frac{\nu''+1}{\nu'}\right)\right]$$

We can interchange the orders of integration (see diagram) to give

$$\frac{\nu}{\pi}\cdot\sum_{\ell=0}^{\infty}(2\ell+1)\cdot\sum_{I'=0}^{2}\beta_{II'}\int_{0}^{-\Lambda-1} d\nu''\cdot \text{Im } A_\ell^{I'}(\nu'')$$
$$\cdot\int_{\Lambda}^{-\nu''-1} d\nu'.\ P_m\left[1 + 2\left(\frac{\nu''+1}{\nu'}\right)\right] P_\ell\left[1 + 2\left(\frac{\nu'+1}{\nu''}\right)\right]$$

$$= \frac{\nu}{\pi}\cdot\sum_{\ell=0}^{\infty}(2\ell+1)\sum_{I'=0}^{2}\beta_{II'}\int_{0}^{-\Lambda-1} d\nu''\cdot \text{Im } A^{I}(\nu'')\ G_{\ell m}(\nu'',\nu)$$

where $$G_{\ell m}(\nu'',\nu) = \int_{\Lambda}^{-\nu''-1} \frac{d\nu'.\ Pm\left[1 + 2\left(\frac{\nu''+1}{\nu''}\right)\right].\ P_\ell\left[1 + 2\left(\frac{\nu'+1}{\nu''}\right)\right]}{\nu'^2\cdot(\nu'-\nu)}$$

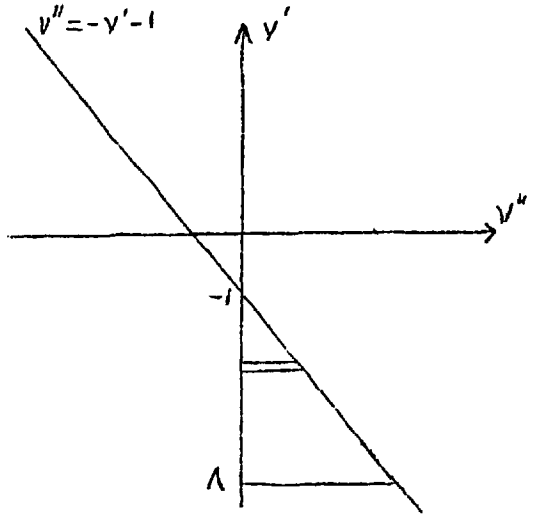

ν'' : $0 \to -\nu' - 1$

their ν' : $-1 \to \Lambda$

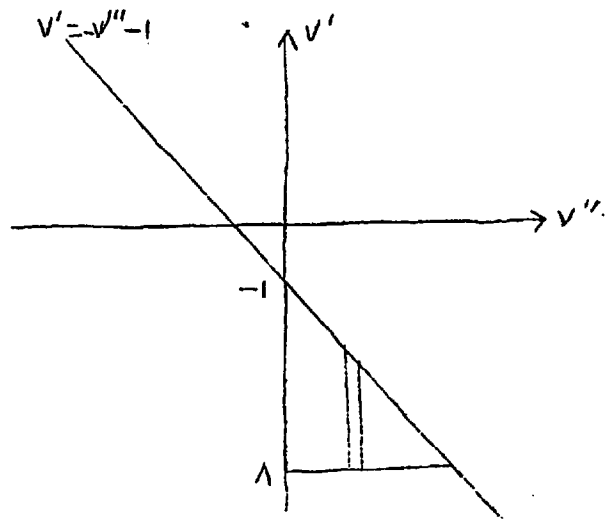

ν' : $-\nu'' - 1 \to \Lambda$

their ν'' : $0 \to -\Lambda - 1$.

Similarly the contribution to $\mathrm{Im}A_{out}(\nu)$ is

$$\frac{\nu^{5/2}}{\pi} \cdot \sum_{\ell=0}^{\infty} (2\ell+1) \cdot \sum_{I'=0}^{2} \beta_{II'} \cdot \int_{\Lambda}^{-\Lambda-1} \mathrm{Im}\, A_{\ell}^{I'}(\nu'') \cdot H_{\ell m}(\nu'',\nu)\, d\nu''$$

where $H_{\ell m}(\nu',\nu) = \int_{\Lambda}^{\rho} \frac{-\nu'-1}{(-\nu')^{7/2} \cdot (\nu'-\nu)} \cdot \mathrm{Pm}\left[1 + 2\left(\frac{\nu''+1}{\nu'}\right)\right] \cdot \mathrm{P}\left[1 + 2\left(\frac{\nu'+1}{\nu''}\right)\right]$

Oades gives closed expressions for Gem and Hem, for m = 1, = o, 1, in an Appendix to his thesis.

C. C. Oades U.C.L. thesis held in Senate House, London.

In practice, on a computer, it is quicker to use the previous form because one has to evaluate the integral over the left hand cut of the trial function, numerically.

If we choose Breit Wigner parametrisation, then after subtracting the dispersion relation for $F(\nu)$, we have

$$\mathrm{Re}A_{out}(\nu) - \mathrm{Re}F(\nu) = \frac{\nu}{\pi} \int_{-\infty}^{-1} \frac{[\mathrm{Im}A_{out}(\nu') - \mathrm{Im}F(\nu')]\, d\nu'}{\nu'(\nu'-\nu)}$$

$$\mathrm{Im}A_{out}(\nu) - \mathrm{Im}F(\nu) = -\frac{\nu^{5/2}}{\pi} \int_{-\infty}^{-1} \cdot \frac{[\mathrm{Im}A_{out}(\nu') - \mathrm{Im}F(\nu')]\, d\nu'}{\nu'^{5/2}(\nu'-\nu)}$$

The Breit Wigner formula, of course, has no poles on the physical sheet. We notice that when the cut off is introduced, we still have to evaluate the integral over ImF(ν) to infinity on the left.

In the twice subtracted form, we have taken a_1 to be the same as that in the dispersion relations for the Breit Wigner formula. We could leave it in as a separate parameter of course, giving an extra term to the second equation

$$-\frac{\nu^{5/2}}{\pi}\int_0^{\infty}\frac{\left[-a_1\nu' + a_{1t}\nu'\right]d\nu'}{\nu'^{5/2}\ (\nu'-\nu)}$$

a_{1t} being the scattering length of $F(\nu)$ and a_1 that of Aout. If we take $a_1 = a_{1t}$ then we see that we have a degeneracy as regards subtractions. For taking another subtraction would give a term $a_2\nu'^2$ under the integral which would be assumed the same as for $F(\nu)$ and therefore to cancel. Thus

$$\text{Im Aout} - \text{ImF}(\nu) = -\frac{\nu^{7/2}}{\pi}\int_{-\infty}^{-1}\frac{\left[\text{ImAout}(\nu') - \text{ImF}(\nu')\right]\ d\nu'}{\nu'^{7/2}\ (\nu-\nu)}$$

such a procedure can be continued indefinitely because even when the subtraction constants are nonvanishing they are equal for Aout(ν) and $F(\nu)$. This is clearly a bad thing but as s.c.is approached it presumably becomes more justified.

Investigation of the Oades Method

We constructed a programme to do the Oades calculation and to investigate its properties. We obtained slightly different values of self consistent parameters, the reason for which will be explained shortly. We put in the same S wave amplitudes in the crossed channel by fitting our parametrisation to his curves of $\delta_{\bullet}{}^2$ and $\delta_0{}^0$ in an auxiliary calculation. Our numerical integrations were more accurate. We first look at a breakdown of the solution shown in the figures. We see immediately that self consistency is obtained by the left hand pole having equal and opposite value to the contribution from

the near left. The contribution from the s waves is very small and from the left hand cut of the Breit Wigner formula also very small.

Next we investigated the effect of varying the cut off on the left and found that it had a very small effect. The left hand pole changed to compensate, by changing only its residue, its position remaining more or less fixed. See Table 1(a). We also varied the region over which self consistency was tested [α, L] say. We looked at the effect of taking a δ function approximation in the crossed channel and found only a small change. We looked at the effect of having the P wave only, in the crossed channel and found only a small change.

Next we looked at a contour plot against $\Gamma\nu_R$ and ν_R keeping g_p, ν_p fixed. The result is shown in the figure and is rather a shock, for there are "barriers" of high X^2 along lines ν_R =, constant, the constants being integers. The reason for this was soon discerned and depends upon three facts:

(a) sampling points for X^2 were at = 1, 2, 3 . . ;

(b) the % deviation formula is only valid if ReAout $\neq$ ReAin and this is not true when ReAin = 0;

(c) ReAin = 0 when $\nu = \nu_R$.

Thus, as ν_R varies and we calculate X^2, when it passes through a sampling point, the value of X^2 shoots up, from the contribution to X^2 from this point.

Normally, at a sampling point $\quad \mathrm{ReA}_{out} \neq \mathrm{ReA}_{in} \sim .2$

$$\mathrm{ReA}_{out} - \mathrm{ReA}_{in} \sim .001$$

$\therefore$ contribution from this point

$$= 4.\left(\frac{.001}{.4}\right)^2$$

when ν_R coincides with the sampling point, see diagram -

$$\mathrm{ReA}_{out} \neq .001$$

$$\mathrm{ReA}_{in} = 0$$

contribution

$$= 4.\left(\frac{.001}{.001}\right) = 4$$

larger by a factor of 160000.

Fig. 5-1. $A_{out}(\nu)$.
curve 1 $\mathrm{Re}\, A_{out}$.
2 $\mathrm{Im}\, A_{out}$.

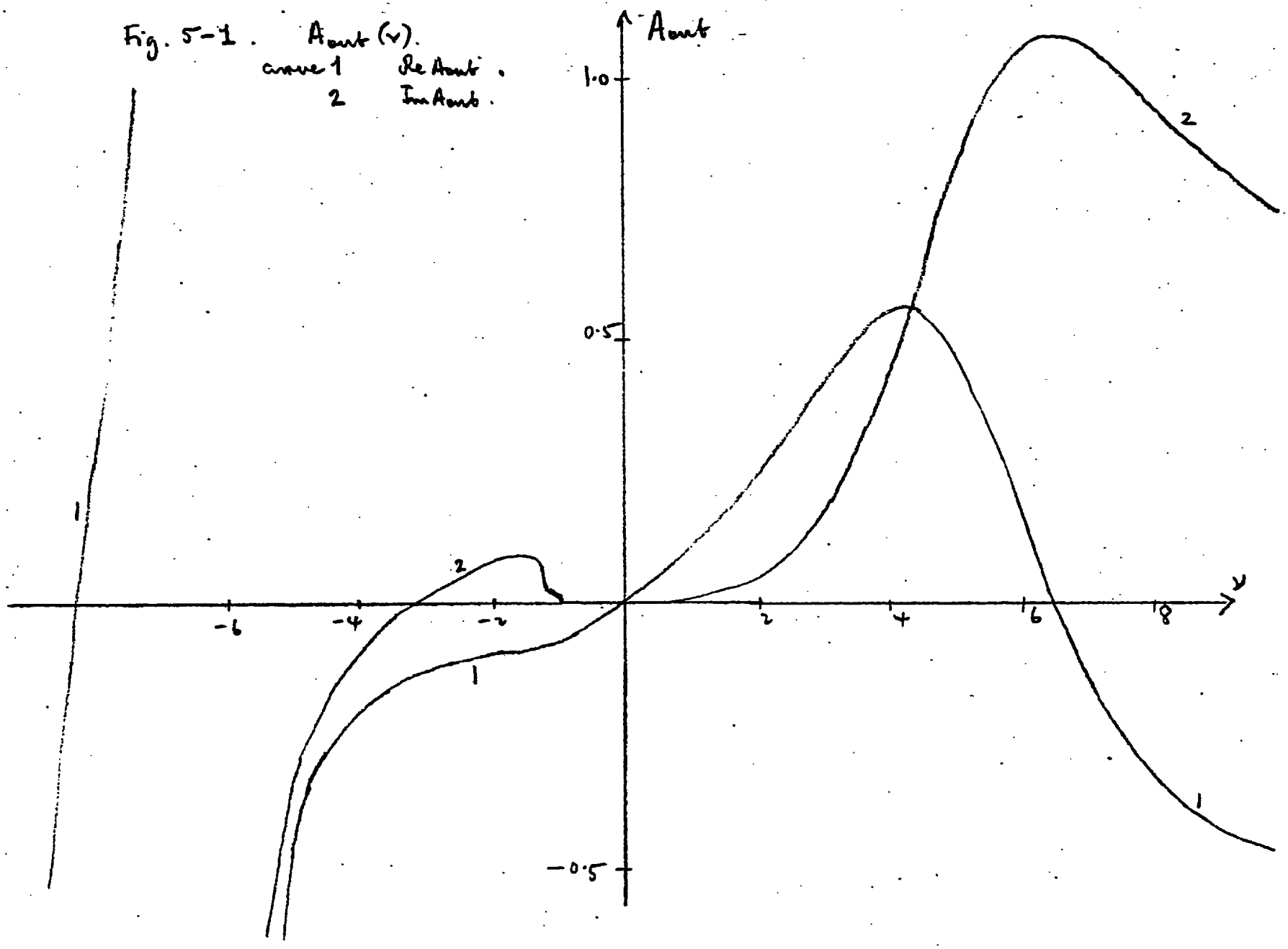

Table 5-2-a. $Re\,A(\nu)$ and contributions.

Pole	S Wigner	P Wigner	Δ	Breit Wigner	$Re\,A_{Inb}$	ν.
0.588	-0.004	-1.449	-0.865	-0.286	-1.152	-9.000
0.670	0.005	-0.782	-0.107	-0.281	-0.388	-8.500
0.795	0.009	-0.478	0.327	-0.275	0.051	-8.000
1.008	0.013	-0.233	0.788	-0.269	0.519	-7.500
1.455	0.016	-0.018	1.454	-0.262	1.191	-7.000
2.979	0.018	0.164	3.163	-0.255	2.908	-6.500
-13.423	0.021	0.299	-13.102	-0.247	-13.349	-6.000
-1.788	0.024	0.371	-1.391	-0.238	-1.629	-5.500
-0.876	0.027	0.383	-0.465	-0.228	-0.693	-5.000
-0.540	0.030	0.350	-0.158	-0.216	-0.375	-4.500
-0.365	0.033	0.297	-0.034	-0.204	-0.237	-4.000
-0.257	-0.035	0.240	0.018	-0.189	-0.171	-3.500
-0.185	0.034	0.187	0.038	-0.173	-0.135	-3.000
-0.132	0.030	0.141	0.040	-0.154	-0.114	-2.500
-0.093	0.017	0.103	0.028	-0.132	-0.104	-2.000
-0.080	0.008	0.089	0.019	-0.122	-0.104	-1.800
-0.068	-0.003	0.077	0.007	-0.112	-0.105	-1.600
-0.057	-0.016	0.065	-0.007	-0.100	-0.107	-1.400
-0.046	-0.028	0.055	-0.019	-0.087	-0.106	-1.200
-0.037	-0.021	0.079	0.021	-0.000	0.021	-1.000
-0.028	-0.010	0.040	0.002	-0.075	-0.073	-0.800
-0.020	-0.006	0.027	0.001	-0.054	-0.053	-0.600
-0.013	-0.003	0.016	0.001	-0.036	-0.035	-0.400
-0.006	-0.001	0.008	0.001	-0.018	-0.018	-0.200
0.000	0.000	-0.000	0.001	-0.000	0.001	-0.000
0.006	0.001	-0.008	0.001	0.019	0.020	0.200
0.012	0.002	-0.014	0.001	0.040	0.041	0.400
0.017	0.003	-0.020	0.001	0.063	0.063	0.600
0.022	0.003	-0.026	0.001	0.087	0.087	0.800
0.027	0.004	-0.031	0.001	0.113	0.114	1.000
0.032	0.004	-0.036	0.001	0.141	0.142	1.200
0.036	0.005	-0.041	0.000	0.172	0.172	1.400
0.040	0.005	-0.045	0.000	0.204	0.205	1.600
0.044	0.005	-0.049	0.000	0.239	0.240	1.800
0.047	0.005	-0.053	0.000	0.276	0.277	2.000
0.056	0.006	-0.062	0.000	0.377	0.377	2.500
0.063	0.006	-0.070	0.000	0.478	0.478	3.000
0.070	0.007	-0.077	0.000	0.551	0.551	3.500
0.076	0.007	-0.083	0.000	0.549	0.549	4.000
0.081	0.007	-0.089	-0.000	0.437	0.437	4.500
0.086	0.007	-0.094	-0.000	0.234	0.234	5.000
0.091	0.007	-0.099	-0.000	0.012	0.011	5.500
0.095	0.008	-0.103	-0.000	-0.173	-0.174	6.000
0.099	0.008	-0.107	-0.000	-0.305	-0.306	6.500
0.102	0.008	-0.111	-0.001	-0.392	-0.392	7.000
0.105	0.008	-0.115	-0.001	-0.447	-0.447	7.500
0.108	0.008	-0.118	-0.001	-0.480	-0.481	8.000
0.111	0.008	-0.121	-0.001	-0.501	-0.502	8.500
0.114	0.008	-0.124	-0.001	-0.513	-0.514	9.000
0.116	0.008	-0.126	-0.001	-0.519	-0.520	9.500
0.119	0.008	-0.129	-0.001	-0.522	-0.523	10.000

Table 5-2-b: $Im A_{amb}(\nu)$ with contributions.

Pole	S-wave	P-wave	Δ	Breit Wigner	$Im A_{amb}$	ν
1.058	0.180	0.533	1.770	0.097	1.867	-9.000
1.107	0.160	0.019	1.286	0.093	1.380	-8.500
1.199	0.147	-0.116	1.229	0.090	1.319	-8.000
1.381	0.134	-0.179	1.336	0.086	1.422	-7.500
1.796	0.123	-0.205	1.715	0.082	1.797	-7.000
3.290	0.113	-0.204	3.199	0.077	3.276	-6.500
-13.142	0.104	-0.186	-13.224	0.073	-13.151	-6.000
-1.536	0.096	-0.158	-1.598	0.068	-1.530	-5.500
-0.652	0.089	-0.131	-0.694	0.062	-0.632	-5.000
-0.343	0.085	-0.110	-0.368	0.057	-0.312	-4.500
-0.194	0.083	-0.096	-0.207	0.051	-0.156	-4.000
-0.112	0.085	-0.085	-0.112	0.045	-0.067	-3.500
-0.064	0.093	-0.076	-0.047	0.038	-0.009	-3.000
-0.035	0.108	-0.068	0.005	0.032	0.036	-2.500
-0.017	0.127	-0.062	0.048	0.026	0.074	-2.000
-0.013	0.134	-0.060	0.061	0.023	0.084	-1.800
-0.009	0.134	-0.060	0.065	0.021	0.086	-1.600
-0.006	0.119	-0.062	0.051	0.020	0.071	-1.400
-0.004	0.072	-0.073	-0.005	0.020	0.015	-1.200
-0.002	-0.013	0.036	0.020	0.000	0.020	-1.000
-0.001	-0.004	0.006	0.001	0.000	0.001	-0.800
-0.001	-0.001	0.002	0.000	0.000	0.000	-0.600
-0.000	-0.000	0.001	0.000	0.000	0.000	-0.400
-0.000	-0.000	0.000	0.000	0.000	0.000	-0.200
-0.000	-0.000	0.000	0.000	0.000	0.000	-0.000
-0.000	-0.000	0.000	0.000	0.000	0.000	0.200
-0.000	-0.000	0.000	0.000	0.001	0.001	0.400
-0.001	-0.001	0.001	0.000	0.002	0.002	0.600
-0.001	-0.001	0.002	0.000	0.005	0.005	0.800
-0.002	-0.002	0.004	0.000	0.009	0.009	1.000
-0.003	-0.003	0.006	0.000	0.015	0.015	1.200
-0.004	-0.004	0.008	0.000	0.023	0.023	1.400
-0.005	-0.005	0.011	0.000	0.034	0.034	1.600
-0.007	-0.006	0.014	0.000	0.048	0.048	1.800
-0.009	-0.008	0.017	0.000	0.066	0.066	2.000
-0.015	-0.012	0.027	0.000	0.135	0.136	2.500
-0.022	-0.017	0.039	0.001	0.253	0.253	3.000
-0.031	-0.022	0.053	0.001	0.432	0.432	3.500
-0.041	-0.028	0.070	0.001	0.663	0.663	4.000
-0.052	-0.035	0.087	0.001	0.891	0.892	4.500
-0.064	-0.042	0.107	0.001	1.043	1.044	5.000
-0.078	-0.049	0.128	0.001	1.087	1.088	5.500
-0.093	-0.057	0.151	0.001	1.052	1.053	6.000
-0.109	-0.065	0.176	0.001	0.979	0.980	6.500
-0.127	-0.074	0.202	0.001	0.898	0.899	7.000
-0.145	-0.083	0.229	0.001	0.822	0.823	7.500
-0.164	-0.093	0.258	0.002	0.755	0.757	8.000
-0.184	-0.102	0.288	0.002	0.698	0.700	8.500
-0.206	-0.113	0.320	0.002	0.649	0.651	9.000
-0.228	-0.123	0.353	0.002	0.608	0.610	9.500
-0.251	-0.134	0.387	0.002	0.573	0.575	10.000

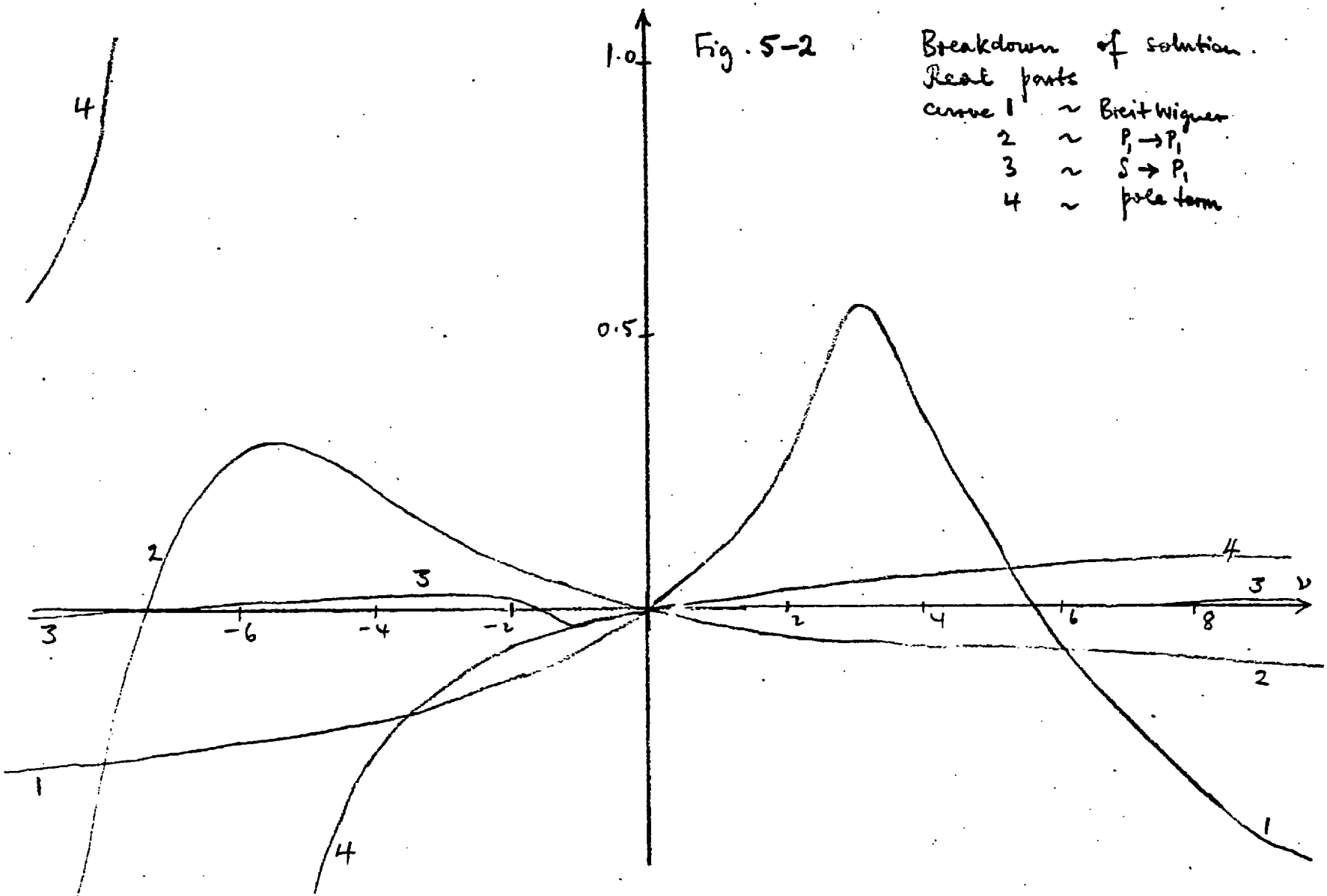
Fig. 5-2
Breakdown of solution.
Real parts
curve 1 ~ Breit Wigner
2 ~ $P_1 \to P_1$
3 ~ $S \to P_1$
4 ~ pole term
1.0
0.5
ν
-6
-4
-2
2
4
6
8

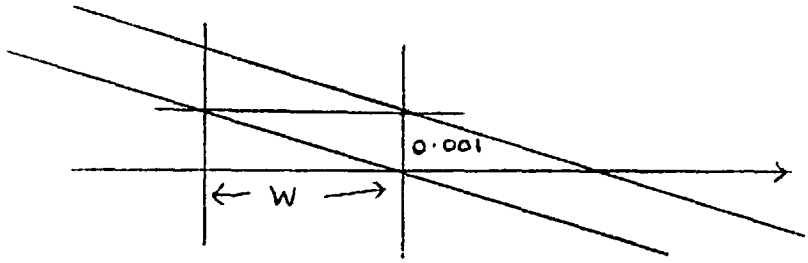

We plotted values of X^2 as V_R passed through a sampling point and obtained Figure 3(b). The barrier is very wide and completely invalidates the contour plot. It extends for 0.1 on either side of integer values. Thus the X^2 surface is divided into compartments and a search would get trapped very easily although it might walk over them initially if it were taking big strides. We estimated the width of the barrier from the diagram. Supposing ReAout to be slow moving, so all change is due to change in ReAin, we see that the barrier has disappeared when ReAin $\simeq$ ReAout. The gradient ReAin$'(V) \simeq \frac{.246}{.5}$ from the tabulation

Hence imagining the curve to move sideways with V_R, without deformity,

$$W \cdot \text{ReAin}' = .001$$

$$W = .002$$

This estimate is 50 X actual and this factor of 50 X must be due to ReAout following ReAin very closely as V_R varies. This is a consequency of the slow variation of contributions from the left to ReAout.

If the barriers were as narrow as.002, then they would be no problem in searching. Hence we redefined X^2 to be

$$\sum \left(\frac{\text{ReAout} - \text{ReAin}}{\text{ReA in}} \right)^2$$

The contour plot and the barriers are shown in Figs.4 The contour plots against g_p, V_p keeping V_R, ΓV_R fixed were also obtained and are shown in Figs. 4. We also used the definition $\sum (\text{ReAout} - \text{ReAin})^2$ i.e. simply numerical deviation and it was with this criterion that the results in Table 1 were obtained. The contour plots for this were also obtained, see Figs. 5.

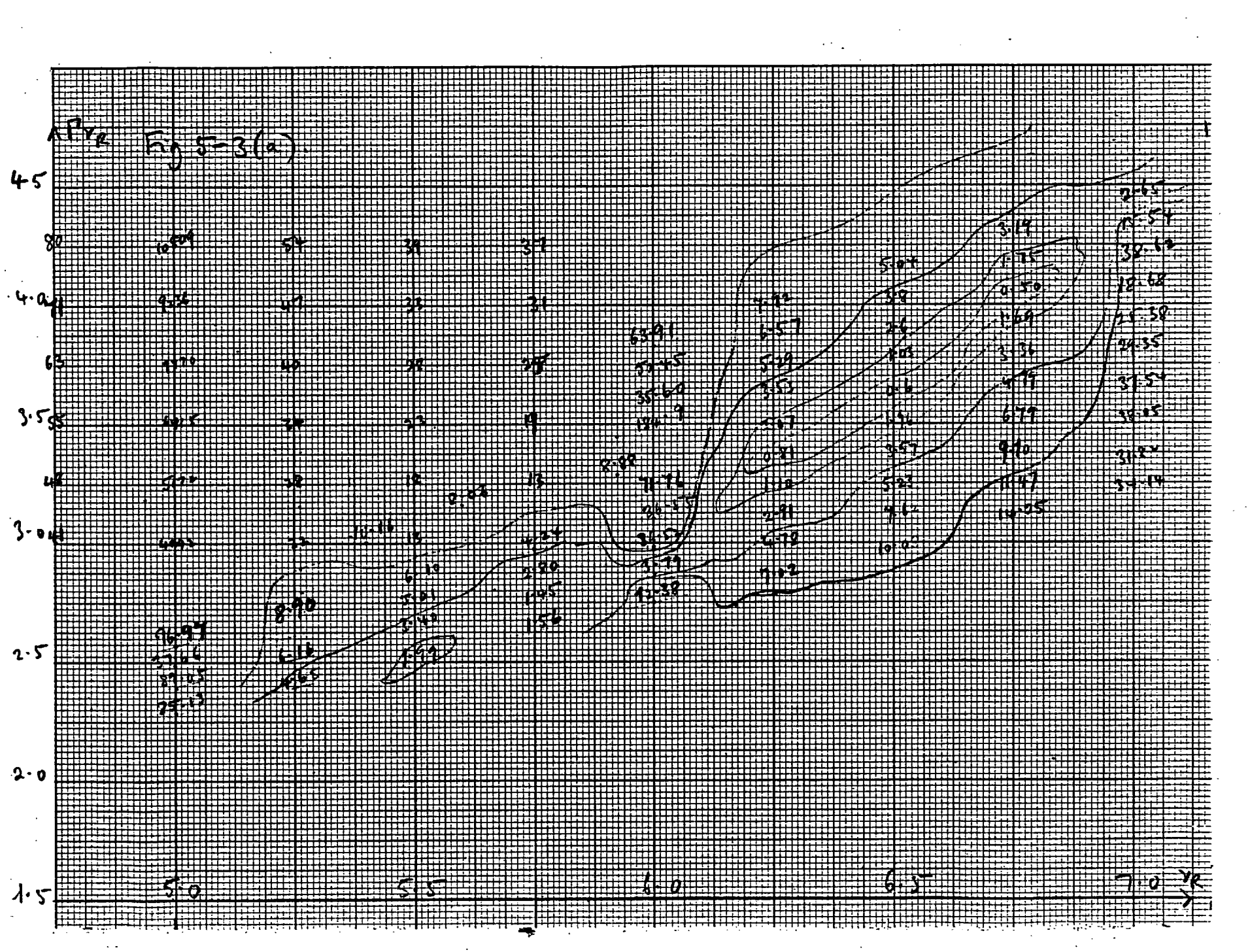
Fig 5-3(a)
P_{r_R}
γ_R
4.5
4.0
3.5
3.0
2.5
2.0
1.5
5.0
5.5
6.0
6.5
7.0

Fig 5-3(b)

Barrier profile width

% diminution

5·5 5·6 5·7 5·8 5·9 6·0 6·1 6·2 6·5

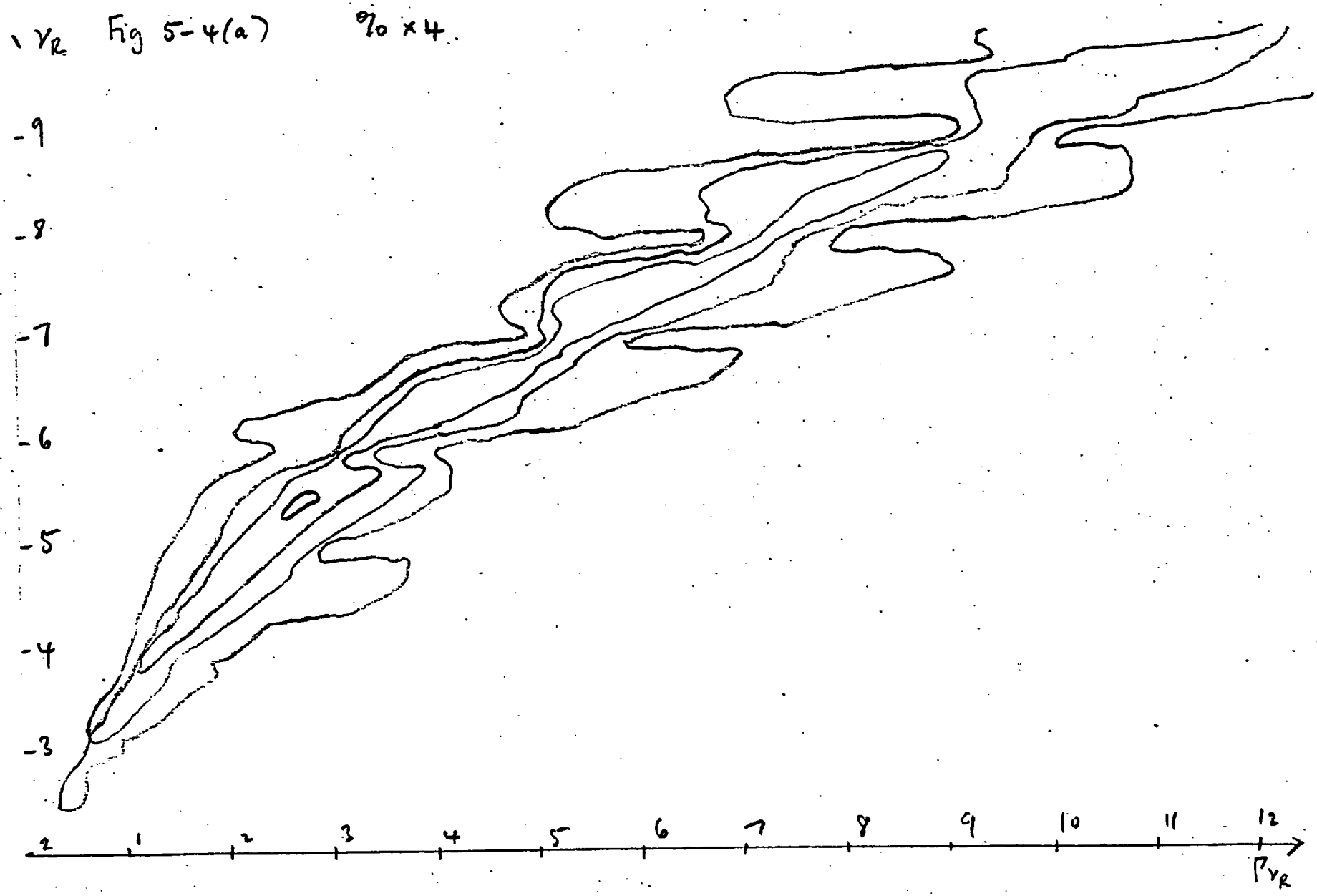

Fig 5-4(a) %0 x4.

Fig 5-4(b). $V_R = 5.45$, $\Gamma_{V_R} = 2.75$. % deviation.

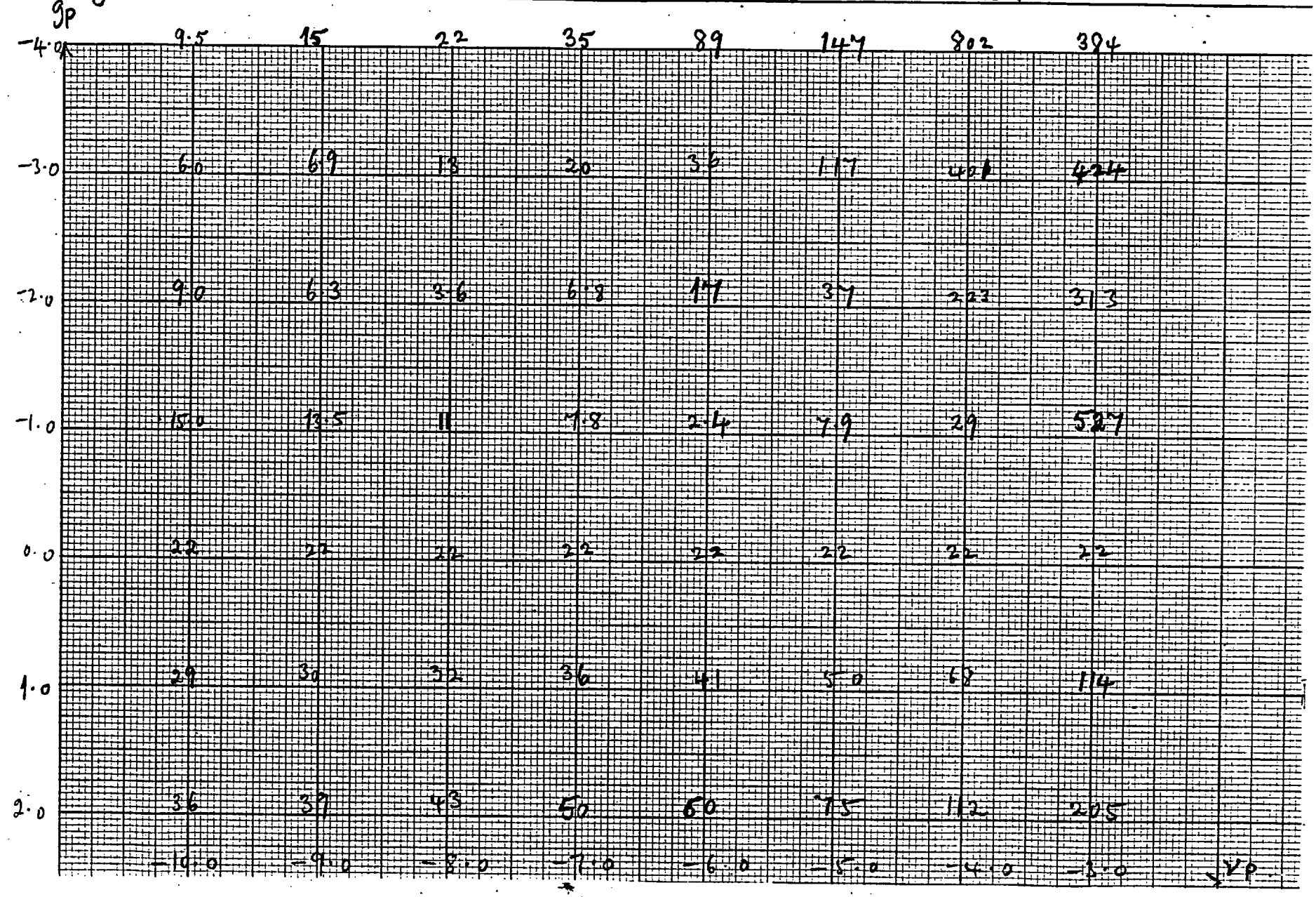

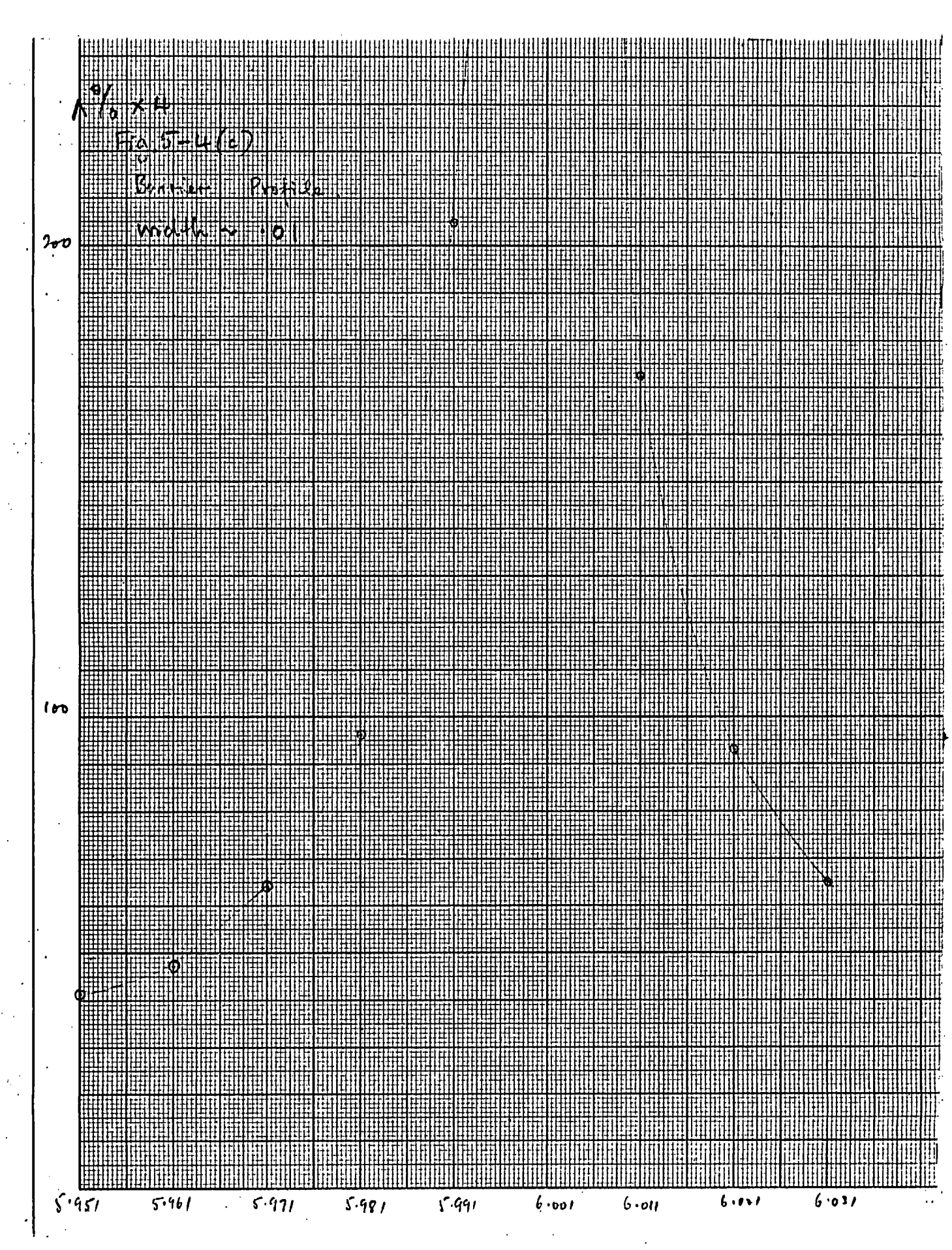
% × 4
Fig 5-4(c)
Burner Profile
width ~ .01
200
100
5.951
5.961
5.971
5.981
5.991
6.001
6.011
6.021
6.031

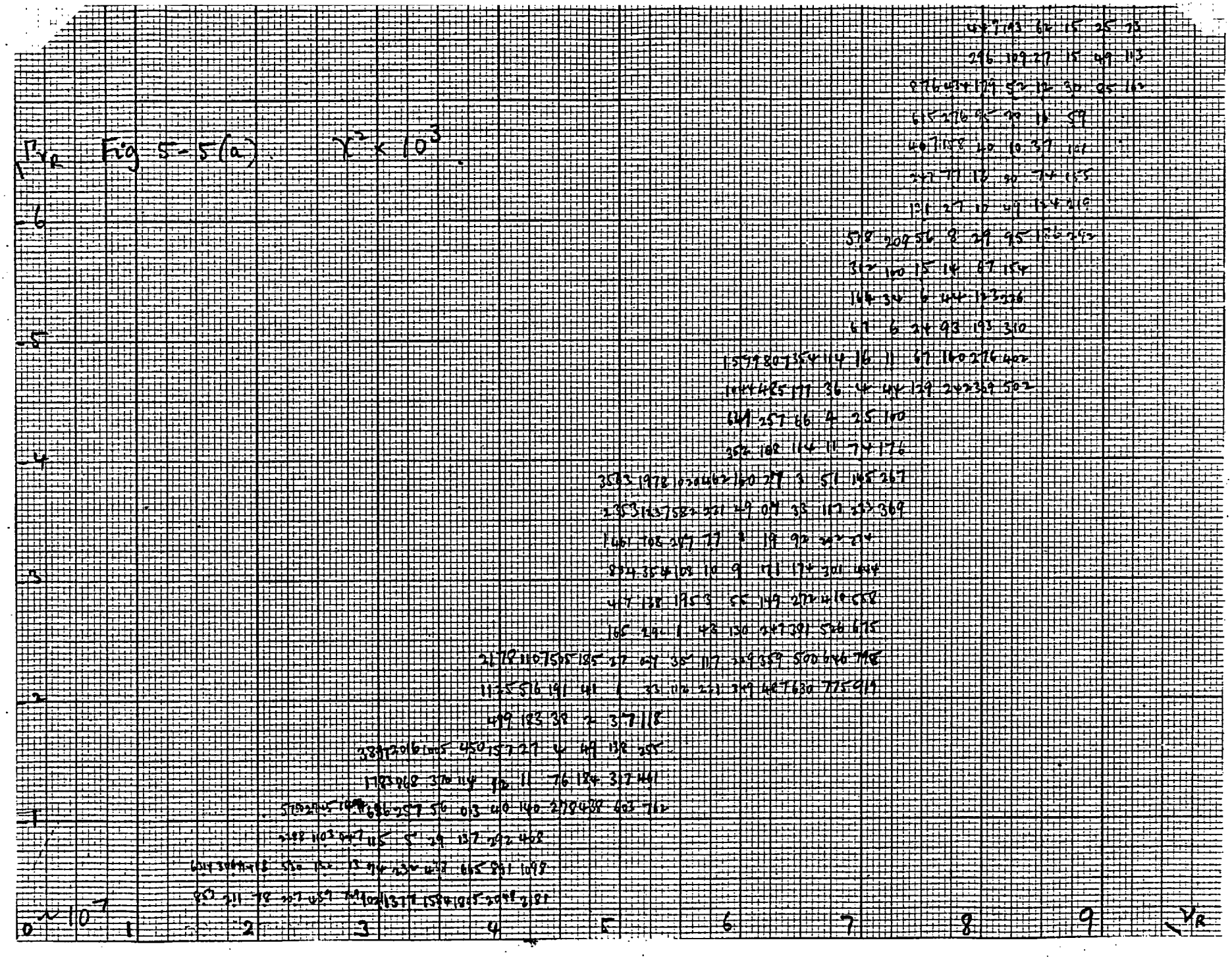
Fig 5-5(a)
$\chi^2 \times 10^3$
Γ_{VR}
-6
-5
-4
-3
-2
-1
0
$\sim 10^{-7}$
1
2
3
4
5
6
7
8
9
V_R

Fig 5-5(b) $\chi^2 \times 10^3$

η_p	-9.85	-8.25	-7.65	-7.05	-6.45	-5.85	-5.25	-4.65
-0.2								
-0.4		824	776	745	699	649	593	522	466	394	318	240
-0.6		630	573	521	465	406	342	276	209	149	86	47
-0.8		449	396	341	283	221	164	107	58	22	11	42
-1.0		309	256	202	148	97	52	19	2.0	16	77	212
-1.2		195	149	102	60	25	3.7	2.9	34	114	269	539
-1.4		115	75	40	14	3.0	13	56	147	308	576	1005
-1.6		60	32	13	9.6	25	72	172	333	590	989	1603
-1.8		31	18	20	43	96	192	368	629	953	1500	2328
-2.0		26	25	39	113	249	454	728	1108	1617	2370	3420

A further effect emerges, for we see that there is a long narrow valley in $\Gamma\nu_R$, ν_R along which the value of X^2 is very low and thus defining a continuous family of solutions. We tried to fit simple curves to the line of the valley but nothing simple was found. Perhaps the best was

$$\Gamma\nu_R = \frac{\nu_R^2}{12}$$

The result of this is that the calculation at most determines one parameter, namely the one going perpendicular to the valley and has a free parameter which runs along the valley. Hence in further investigations one should bear this in mind. If we had a reliable law like the above relation between position and width we could use it in a search. We could vary only ν_R and determine Γ_R using the relation. However tne author suspects that the ambiguity is more far reaching than this and that in fact there is a 4 region of which this valley is the intersection with a g_p, ν_p plane. In support of this idea, we consider the effect of using a rough self consistency condition, for the real parts only

$$\text{ReAout}(\nu_R \text{ in}) = 0 \qquad \text{(i)}$$

$$\text{ReAout}(\nu_R \text{ in}) = \text{ReA}'\text{in}(\nu_R \text{ in}) \qquad \text{(ii)}$$

$$\text{For a Breit Wigner formula } \text{ReA}'\text{in}(\nu_R) = \frac{-1}{\Gamma\nu_R\left[\frac{\nu_R}{\nu_R+1}\right]} \simeq \frac{-1}{\text{width}} \qquad \text{(iii)}$$

It can be seen that when these self consistency conditions are used, $\Gamma\nu_R$ and ν_R become completely arbitrary in calculations using a left hand pole correction term. For given a $\Gamma\nu_R$ and ν_R one can write down the self consistency equations and solve for g_p, ν_p. Clearly these equations have the form

$$\frac{\nu_R}{\nu_p} \cdot \frac{g_p}{\nu_R - \nu_p} = f_1(\Gamma\nu_R, \nu_R) \qquad \text{(iv)}$$

$$-\frac{g_p}{(\nu_R - \nu_p)^2} = f_2(\Gamma\nu_R, \nu_R) \qquad \text{(v)}$$

$$\therefore \text{(iv)}^2 \div \text{(v)} \quad -\frac{\nu_R^2}{\nu_p^2} \cdot g_p = \frac{f_1^2}{f^2}$$

substitute g_p in (iv)

$$\frac{\nu_R}{\nu_p} \cdot \frac{1}{\nu_R - \nu_p} \cdot - \frac{f_1^2}{f_2} \cdot \frac{\nu_p^2}{\nu_R^2} = f_1$$

$$\therefore \quad \frac{-\nu_R}{\nu_p} = \frac{f_2}{f_1} \cdot (\nu_R - \nu_p) = \frac{\nu_R f_2}{f_1} \left(1 - \frac{\nu_p}{\nu_R}\right)$$

$$\therefore \quad \nu_p = \frac{\nu_R^2 \cdot \frac{f_2}{f_1}}{\left(\frac{\nu_R f_2}{f_1} - 1\right)}$$

$$g_p = \frac{-f_1^2}{f_2} \cdot \frac{1}{\nu_R^2} \cdot \frac{\nu_R^4 \frac{f_2^2}{f_1^2}}{\left(\frac{\nu_R f_2}{f_1} - 1\right)^2}$$

$$= \frac{-\nu_R^2 \cdot f_2}{\left(\frac{\nu_R f_2}{f_1} - 1\right)^2}$$

Thus (g_p, ν_p) are determined uniquely and (i) and (ii) are exactly satisfied, for any (Γ_{x_R}, ν_R). A similar situation may obtain with the distributed s.c. condition i.e. for any (Γ_{ν_R}, ν_R) can we show that a (g_p, ν_p) can be found to make the deviation $\lesssim$ 10%, say. This was looked for: Table I(e)

There certainly exists a 2 subspace in the 4 parameter space $(\Gamma_{\nu_R}, \nu_R, g_p, \nu_p)$ on which (i) and (ii) are satisfied exactly. There may, of course, be addition arbitrariness from other sources, also. We could have taken rough s. c. condition for the unitarity condition, but it is more difficult to analyse and one feels it would lead to the same conclusions. This provides insight into the contour plots obtained, if we think it reasonable that the distributed s. c. condition will have a similar effect to the rough s. c. conditions (i) and (ii). The whole trouble really is that the left hand pole is completely arbitrary and adjusts itself to patch things up. It does not occur in the crossed channel, for there one takes the Breit Wigner formula alone. If the crossed channel could be made to include this left hand pole

so that it occurred in both channels, then it would not longer be arbitrary. If one takes the view that it represents effects of other channels, then a better procedure would be to estimate it by other means and then to keep it fixed.

TABLE 5 - 1 -- SYSTEMATIC INVESTIGATION OF ORIGINAL OADES METHOD

(a) Variation of left hand cut off, .

Λ	χ^2	ν_R	$\Gamma\nu_R$	g_p	ν_p
-4.5	10^{-3}	5.55	2.67	-0.206	-7.56
-9	10^{-5}	6.21	2.98	-1.128	-7.204
-18	10^{-5}	5.7	2.74	-1.806	-7.17

(b) Variation of self consistency region $[0, L]$

L	χ^2	ν_R	$\Gamma\nu_R$	g_p	ν_p
5	10^{-3}	2.46	1.30	-1.275	-4.407
10	10^{-5}	6.21	2.98	-1.128	-7.204
20	10^{-3}	4.6	2.65	-1.074	-4.566

(c) δ function approximation in crossed channel

χ^2	ν_R	$\Gamma\nu_R$	g_p	ν_p
10^{-3}	5.5	2.96	-3.113	-7.102

(d) P wave only in crossed channel

One solution out of presumed one parameter set

$\chi^2 = 10^{-4}$ ν_R 5.82 $\Gamma\nu_R$ 2.95

g_p -0.754 ν_p -4.673

(e) Other searches in (g_p, ν_p) at constant $(\Gamma\nu_R, \nu_R)$.

(1) $\nu_R = 5.35$, $\Gamma_R = 3.0$

g_p, ν_p = -1.033, -6.461 on plot χ^2 = 10.16

= -1.141, -5.563 after search 0.40

(2) $\nu_R = 12.15$, $\Gamma\nu_R = 15.4$

g_p, ν_p = -1.033, -6.461 on plot 4.76

= -0.608, -4.798 after search 0.76

TABLE 5 - 3 - Further Investigation

1. Different self consistency conditions.

$P_1 + (S_o + S_2)$ calculation

		ν_R	$\Gamma\nu_R$	g_p	ν_p	χ^2
(a)	$P_2 = 0$	6.21	2.98	-1.128	-7.204	2.10^{-5}
(b)	$P_2 = -1$	6.33	3.35	-1.065	-6.637	
(c)	Re parts only	5.7	2.9	-1.254	-6.707	0.3%
(d)	Imaginary parts only	2.93	0.942	-1.826	-5.874	3.10^{-4}

2. Two poles on left:
only same solution as for one pole found.

3. $P_1 + (D_o)$
Do very small give same as P_1 only.
(10.539, -1.923) -0.785 -4.458
$\nu_R = 5.46$ 2.62%

4. Parametrisation by Breit Wigner type 3 with 4 parameters,
solutions same as original

(a)	11.88 ,	-1.833	0.288 ,	0.051 ,	g_p -1.33	p -5.280
	$\nu_R = 6.5$			1.9%		
(b)	14.00 ,	-2.259	0.089 ,	-0.008 ,	p 0.67	p -5.0
	$_R = 6.2$			0.95%		

searches also done with Breit Wigner type 2 with 4 parameters, again giving similar solutions.

FURTHER DISCUSSION OF THE OADES METHOD

1. The effect of cut-offs

(a) Cut off on the left e.g. $\mathrm{Im}A_{\mathrm{cut}}(\ ) = [\text{etc}] + \frac{(\nu-\nu_0)^{5/2}}{\pi}\int_{-1}^{\infty} \frac{G(\nu')\ d\nu'}{\Lambda(\nu'-\nu_0)^{5/2}(\nu'-\nu)}$

$$\therefore\ \mathrm{Im}\,\Delta(\nu) = (\mathrm{Im}A_0 - \mathrm{Im}F_0) + [\text{pole terms}] + \frac{(\nu-\nu_0)^{5/2}}{\pi}\int_{\Lambda}^{\infty} \frac{\mathrm{Im}G(\nu') - \mathrm{Im}F(\nu')\ d\nu'}{(\nu'-\nu_0)^{5/2}(\nu'-\nu)}$$
$$- \frac{(\nu-\nu_0)^{5/2}}{\pi}\int_{-\infty}^{\Lambda} \frac{\mathrm{Im}F(\nu')\ d\nu'}{(\nu'-\nu_0)^{5/2}(\nu'-\nu)}$$

so if we cut off in the expression for $\mathrm{Im}A_{\mathrm{out}}$, we still have to subtract the entire left hand cut of the trial function from the cut off left hand cut of the contribution from crossing

(b) cut off on the right

e.g. $$\mathrm{Im}A_{\mathrm{out}}(\nu) = [\text{etc.}] + \frac{(\nu-\nu_0)^{5/2}}{\pi}\int_{0}^{\Lambda} \frac{[\mathrm{Re}F(\nu') - a_1\nu']\ d\nu'}{(\nu'-\nu_0)^{5/2}(\nu'-\nu)}$$

$$\mathrm{Im}\Delta(\nu) = \mathrm{Im}\Delta(\nu)_{\Lambda\to\infty} - \frac{(\nu-\nu_0)^{5/2}}{\pi}\int_{\Lambda}^{\infty} \frac{[\mathrm{Re}F(\nu') - a_1\nu']\ d\nu'}{(\nu'-\nu_0)^{5/2}(\nu'-\nu)}$$

Of course, if the parametrisation has been chosen to match the physical assumptions, these "extra terms will be small.

2. The once subtracted form for $\mathrm{Im}A_{\mathrm{out}}(\nu)$

$$\mathrm{Im}A_{\mathrm{out}}(\nu) = -\frac{\nu^{3/2}}{\pi}\,\mathrm{o}\,\frac{\mathrm{Re}F(\nu')\ d\nu'}{\nu'^{3/2}(\nu'-\nu)} - \frac{\nu^{3/2}}{\pi}\int_{-\infty}^{-1} \frac{\mathrm{Im}A_{\mathrm{out}}(\nu')\ d\nu'}{\nu'^{3/2}(\nu'-\nu)}$$

can be used.

3. Variation of subtraction point

One can write the same equations with different values of ν_0, but in general they will be more complicated than for $\nu_0 = 0$. They will have subtraction constants $\mathrm{Re}A_{\mathrm{out}}(\nu_0)$ and $\mathrm{Im}A_{\mathrm{out}}(\nu_0)$. Also as previously discussed, as ν_0 moves it pulls more cuts from underneath the existing ones. If it moves forwards negative values, we need to know $\mathrm{Re}A_{\mathrm{out}}(\nu')$ on the left to obtain the discontinuity on this cut.

4. Other workers who have looked at the Oades method include

R. G. Moorhouse, who tried to bootstrap the and failed because of minute left hand cut.

D. Morgan, who looked at it and wrote the preprint "Marginally Singular Forces" as a result.

H. C. Rae who tried to do D wave $\pi\pi$, given S = P waves. He could not find a suitable parametrisation and so used an inverse amplitude method.

D. H. Lyth did π N variation calculations - Birmingham preprint.

H. Burkhardt gave a talk at the informal meeting of British theorists at the Rutherford laboratory in 1965, but has not written anything yet.

5. As the left hand cut $\rightarrow$ 0, the output amplitude becomes indeterminate using the variational method, whereas the output amplitude $\rightarrow$ 0 when using N/D. The author feels that the latter behaviour is more bootstrap oriented.

6. Automatic bootstrap aspect

If we use only the real part dispersion relation in a variational method, then we have

$$\mathrm{ReA}(\nu) = \int_0^{\infty} \frac{\mathrm{ImA}(\nu')\, d\nu'}{(\nu' - \nu)} + \int_{-\infty}^{-1} \frac{\mathrm{ImA}(\nu')\, d\nu'}{(\nu' - \nu)}$$

if we now make assumptions like

$$\mathrm{ImA}(\nu') = \mathrm{ImF}(\nu'), \text{ a trial function} \qquad \nu' > 0$$

$$\mathrm{ImA}(\nu') = \frac{2}{\nu'} \int_0^{-\nu'-1} d\nu'\, \mathrm{ImF}(\nu'). \quad P\left\{\left[1 + 2\left(\frac{\nu''+1}{\nu}\right)\right]\right. \text{ . etc.}$$

or, as in my method (see later section)

$$\int_{-\infty}^{-1} \frac{\mathrm{ImA}(\nu')\, d\nu'}{\nu' - \nu} = C(\nu') = \frac{4}{\pi\nu} \int_0^{\infty} \mathrm{ImF}(\nu'')\ \text{P. Q. etc.}$$

then, we have automatically guaranteed that $\mathrm{ImA}(\nu)$, $\nu > 0$ is the same in the direct channel as in the crossed channel. We thus have automatically incorporated the bootstrap hypothesis, however we do not have automatic unitarity. We vary our bootstrapped amplitude until it satisfied unitarity.

On using both the real and imaginary part dispersion relations, the formulation is no longer so bootstrap oriented. The imaginary part on the right has different values according to whether we take one dispersion relation or the other. Admittedly if we had the exact analytic solution these would be the same, but when working with trial functions which can never be exactly correct, one may introduce impossible conditions and spurious effects by calculating a quantity in two different ways.

In the exact case, we can actually explicit by continuing the real part relation from the right hand c. to the left hand c. to obtain the left hand discontinuity and hence construct the imaginary part relation...

Hamilton & Damachie state that "it turns out in practice to be more convenient to use both dispersion relations."

7. Inelasticity

Oades also looked at the effect of inelasticity on his calculation. He used the function

$$R(\nu) = 1 + \vartheta(\nu - 3)\sqrt{1 - \frac{3}{\nu}} \cdot \left[1 - \frac{a}{\nu + b}\right]$$

to represent inelasticity. Its properties were discussed in Chapter 2. Its origin is a U.C. preprint '63 by N. Kronfli.

Inelasticity affects the calculation in two ways:

(i) the unitarity condition is modified to

$$\mathrm{Im}A_{out}(\nu) = R(\nu)\sqrt{\frac{\nu}{\nu+1}} \cdot \left[\mathrm{Im}A_{out}^2(\nu) + \mathrm{Re}A_{out}^2(\nu)\right] .$$

only affected for $\nu > 3$.

(ii) the discontinuity on the left is modified because of inelasticity in the crossed channel. It only affects ImAout for $\nu < -4$.

Increased inelasticity will increase the contribution from the left hand cut.

Oades found that inelasticity had very little effect up to $R(\nu_R) = 1.2$, at which the solution, with $\Delta = 0.2\%$ had values

$\nu_R = 6$, $\Gamma_{\nu_R} = 2.04$, i.e. 740 Mev, width 200 Mev,
$g_p = -1.2$, $\nu_p = -8.3$ values of a and b were
$a = 75$, $b = 100$. After this Δ increased rapidly e.g.
$\Delta = 1.4\%$ for $R(\nu_R) = 1.3$

We did not look at inelasticity.

8. Self consistency criterion

The criterion of a good fit in the physical region is seen to be a bad one, if the contribution from the left hand cuts of the parametric form and from crossing are small

$$\text{For } \% = \frac{B(\nu) - B_t(\nu)}{\text{R.H.}(\nu) + \text{R.H.}_t(\nu) + B(\nu) + B_t(\nu)}$$

which becomes small when $B(\nu), B_t(\nu) \ll \text{R.H.}(\nu), \text{R.H.}_t(\nu)$
one could instead take the function

$$\frac{B(\nu) - B_t(\nu)}{B(\nu) + B_t(\nu)}$$

i.e. % discrepancy in contributions from the left.

A more general atttitude is to look at the discrepancy on the left and right.

$$\sum_i \left[\frac{A_{out}(\nu) - A_{in}(\nu)}{A_{out}(\nu_i) + A_{in}(\nu_i)}\right]^2 \cdot w_i$$

sampled over say $[-9, +10]$. This would allow for very small right hand cuts as well.

A rough self consistency criterion can certainly be formulated

$$\text{ReAout}(\nu_R \text{ in}) = 0$$
$$\text{ReAout}(\nu_R \text{in}) = \text{ReAin}(\nu_{R\text{in}})$$

but will probably not be useful in the variational method. If a left hand pole is used, a solution would exist for all $\nu_R, \Gamma\nu_R$; also the criterion cannot b be used for N/D parametrisation, which includes non resonant amplitudes for which the criterion is meaningless.

IMPROVEMENTS TO THE OADES CALCULATIONS

(a) Gilbert dispersion relations

We then tried to obtain solutions not involving a left hand pole. For this we used only the imaginary parts and imaginary part self consistency conditions, i.e. we used Gilbert dispersion relations only. Two "solutions" are given in Table 4, for a simple Breit Wigner two parameter form. We also looked for solutions with 4 parameters and also with N/D pole form parametrisation, described in the next section, but were unable to find any. Contours for the solution are given in Figure 6, for X^2 and for %.

(b) N/D pole form parametrisation

We should like to explicitly demonstrate the parametrisation dependence of the Oades method and we did some calculations with N/D pole form parametrisation. Further, if Balazs is to be believed, the N/D pole form may be a good way of parametrising the amplitudes in the low-energy physical region. No solutions were found, the searches done are given in Table 4. The contributions from left to ReF(ν) itself are tabulated in Table 5 columns 1 and 4.

The Oades equations for N/D parametrisation are easy to set up

$$\text{e.g.} \quad \text{ImF}(\nu) = \left(\frac{\nu - \nu_0}{\pi}\right)^{5/2} \int_0^\infty \frac{[\text{ReF}(\nu') - a_1\nu']}{(\nu' - \nu_0)^{5/2}(\nu' - \nu)} \, d\nu'$$

$$+ \text{ImF}(\nu_0) + \frac{(\nu - \nu_0)^{5/2}}{(\nu_i - \nu_0)^{5/2}} \sum_{i=1}^{NL} \frac{G^i}{(\nu - \nu^i)}$$

TABLE 5 - 4

A) Gilbert dispersion relations

1. Solutions found.

(a) For $P_2 = 0$, $P_1 = 1$ and with S_o, S_2 amd D_o in the crossed channel

	ν_R	$\Gamma\nu_R$
$X^2 = 10^{-5}$	4.26	1.84

(b) $P_2 = -1$ $P_1 = 1$ S_o, S_2 only $L = 20.$

$X^2 = 10^{-5}$

ν_R	$\Gamma\nu_R$
6.8	0.874

2. Searches also done for

(a) with N/D parametrisation (q. v).

(b) with generalised Breit Wigner.

(c) with constraint on left (q. v).

B) N/D parametrisation

searches for

n = 2	1 pole	12% minimum
	pole	no solution found
	1 pole real parts only	16% minimum
n = 5	1 pole	no solution found.

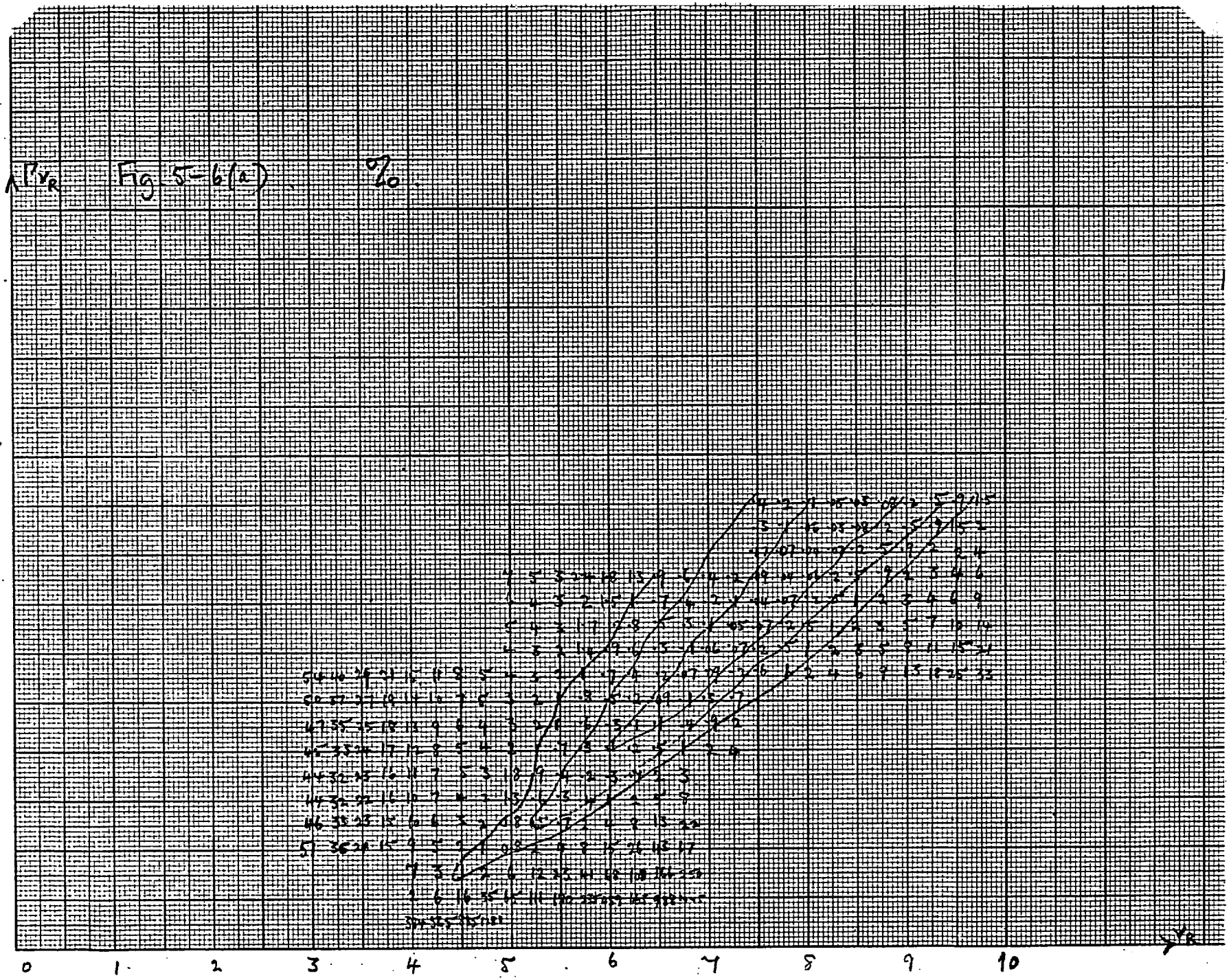
Γ_{V_R}
Fig 5-6(a)
%
γ_{V_R}
0
1
2
3
4
5
6
7
8
9
10

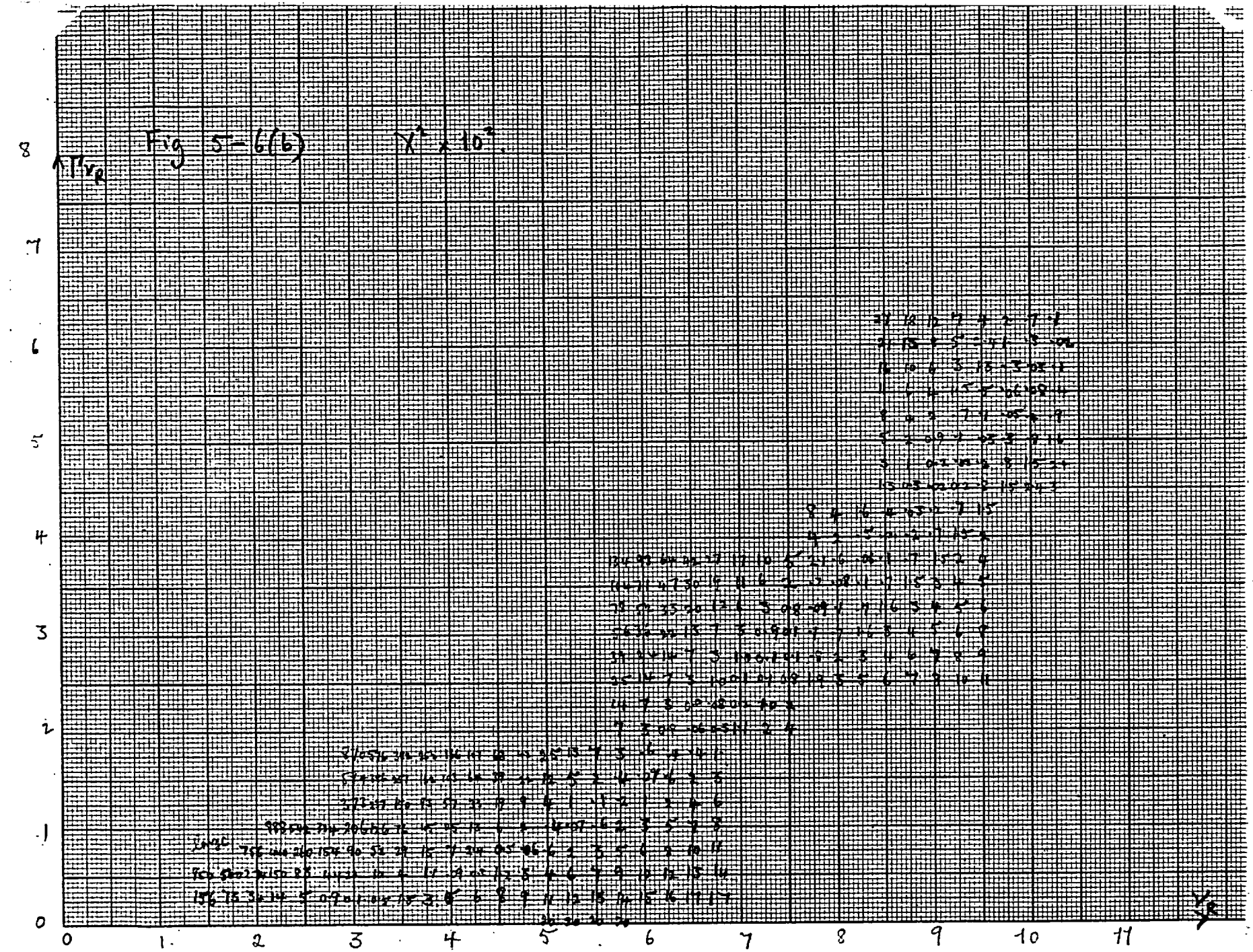
Fig 5-6(b) $\chi^2 \times 10^2$.
Γ_{V_R}
V_R
0
1
2
3
4
5
6
7
8
9
10
11

where $$G^i = \frac{F^i \cdot (\nu^i - \nu_c)}{1 - \frac{(\nu^i - \nu_o)}{\pi} \sum_i F^i I(\nu_i, \nu_i)}$$

so

$$\mathrm{Im}\,\Delta = (\mathrm{Im}A_o - \mathrm{Im}F_o)\ (\text{correcting pole}) + (\text{N/D poles})$$
$$+ \frac{(\nu - \nu_o)}{\pi}^{5/2} \int_{\Lambda}^{-1} \frac{\mathrm{Im}C(\nu')\ d\nu'}{(\nu' - \nu_o)^{5/2}(\nu' - \nu)}$$

Thus, in our equations for Δ, the correcting poles g_p, ν_p and the N/D poles G_i, ν_i occur in very similar roles in a sum of terms.

(c) Constraint on the left

Several searches were done with

(a) $\omega^i = 0.3,\ 0.3,\ 0.3$ ten parts on right, ten on left

(b) $\omega^i = 1,\ 0,\ 0$ " "

and "solutions" obtained. This was always achieved by a drastic narrowing of the resonance to give very small contribution from the left hand singularities. This was true with or without spare left hand poles and with or without static S waves. The best solution obtained is shown in Fig. 7. The left hand pole had negligble contribution and the agreement between real parts on the left was achieved by a narrowing of the resonance and consequent localisation of singularity into the nearby left integral causing this to be close to $C(\nu)$.

C(ν) ANSATZ MODEL

In the form proposed by Oades, only the near left discontinuity is used, and this, as shown in Chapter 3, cannot possibly be correct if MR + U is to describe the real world, since it gives a weak repulsive contribution where a strong attractive contribution is required to give a P wave resonance.

As an estimate for the force function $B(\nu)$, with marginally singular, i.e. asymptotically logarithmic, behaviour we used the Ansatz $B(\nu) = C(\nu)$, in a real part only calculation with real part self consistency conditions only.

Thus we take

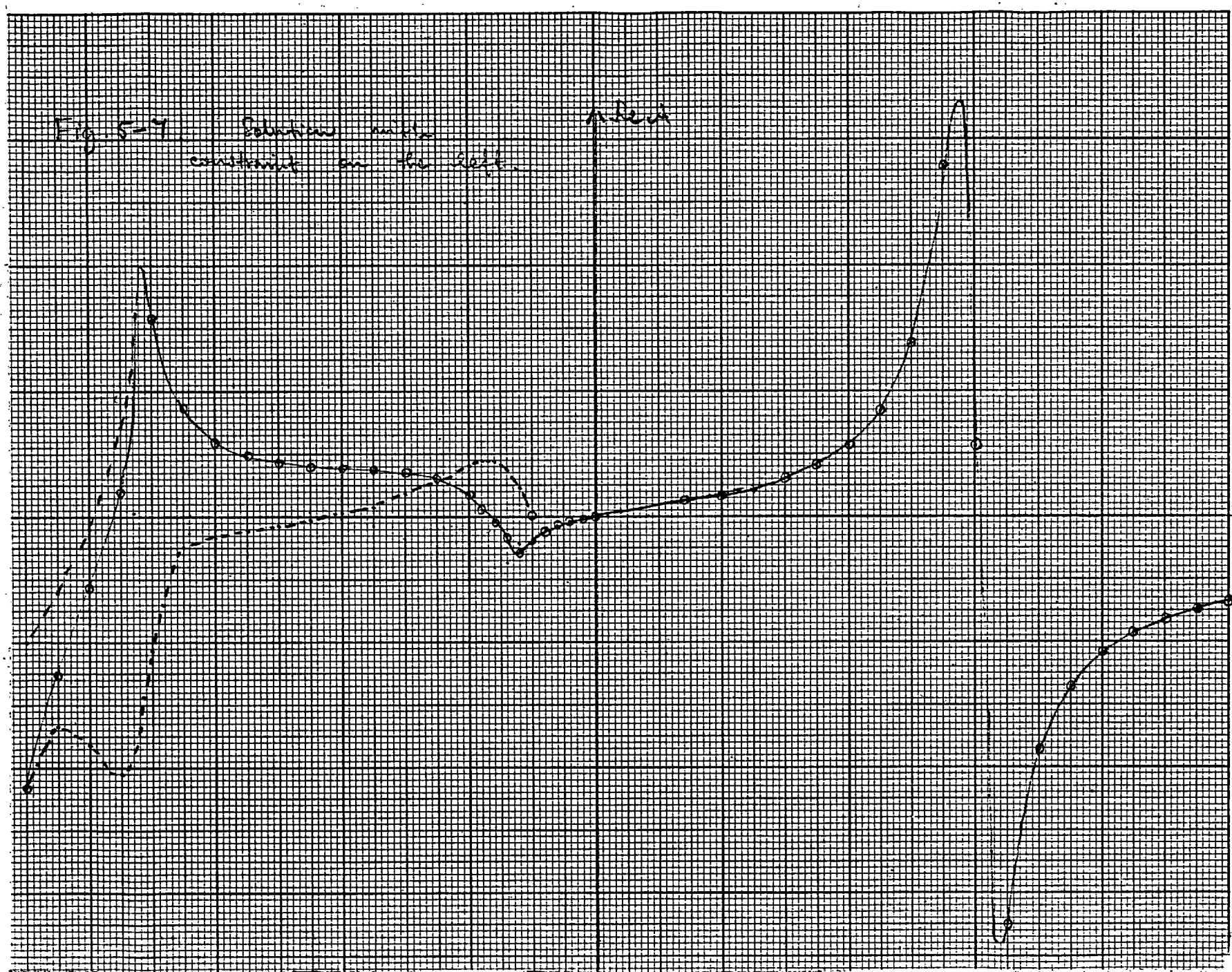
Fig. 5-7. Solution under constraint on the right.

$$\mathrm{ReA}_{out}(\nu) = \frac{(\nu-\nu_0)}{\pi}\int_0^{\infty} \frac{\mathrm{ImA}(\nu')\ d\nu'}{(\nu'-\nu)\ (\nu'-\nu_0)} + \mathrm{ReA}(\nu_0) + C(\nu)$$

$C(\nu)$ being determined from $\mathrm{ImA}(\nu)$ in the crossed channel as described in Chapter 2 and $\mathrm{ImA}(\nu)$ in the physical out dispersion integral being automatically the same as in the crossed channel. $\mathrm{ImA}(\nu)$ was obtained from a unitary parametrised form. The parameters were varied until $\mathrm{ReA}(\nu)$ obtained from this equation, was close to $\mathrm{ReA}(\nu)$ in the crossed channel, obtained from the real part of the parametric form. $\nu_0 = 0$ but threshold behaviour is incorrect except when amplitude is self consistent. The solution thus satisfies most of the desired requirements for the physical amplitude. As before, the solution is such that the contribution from the left hand cut of the parametrised form is equal to $C(\nu)$ on the right. We always parametrised with the N/D pole form. We also considered constraint on the left i.e. additional X^2 from the discrepancy between ReA_{out} and crossing on the near left. With N/D parametrisation, such a calculation is equivalent to a Balazs calculation with X^2 matching as described at the end of Chapter 3. Tabulation for original Balazs values of the parameters is in Table 5(a). The results obtained were as follows:-

$n = 2, 3$, searches with and without constraint on left, no solution found.

$n = 4, 5$, "solutions" found with $X^2 < 10^{-1}$.

$n = 4 \sim X^2 = 0.4, 10^{-2}$.

$F^i = 0.0, 5.859, -15.377, 19.579, 6.001$

resonance at $\nu = 6.25$

$n = 5 \sim X^2 = 6.10^{-2}$

$F^i = 0.0, 18.997, -33.272, 27.184, 0.086, 5.087$

resonance at $\nu = 2.0$

No real change could be produced by an additional left hand constraint, however the $n = 4$ solution had much better agreement with crossing in $[0,-2]$,

Table 5-5-a N/D parametrization and C(ν) model.

n = 2 F: -0.220 -1.397 14.058

N/D pole	C(ν)	Δ	V. P. f(ν)	R. Amt	ν
-3.764	-1.066	-4.705	-3.195	-7.900	-9.000
-4.076	-1.065	-5.017	-3.384	-8.400	-8.500
-4.591	-1.044	-5.511	-3.706	-9.217	-8.000
-5.526	-0.986	-6.388	-4.302	-10.689	-7.500
-7.574	-0.891	-8.341	-5.630	-13.970	-7.000
-14.908	-0.757	-15.541	-10.432	-25.974	-6.500
51.743	-0.583	51.284	33.409	84.694	-6.000
7.412	-0.367	7.169	4.285	11.455	-5.500
3.436	-0.111	3.449	1.695	5.144	-5.000
1.981	0.175	2.280	0.763	3.043	-4.500
1.246	0.458	1.828	0.307	2.135	-4.000
0.814	0.657	1.595	0.052	1.648	-3.500
0.538	0.631	1.294	-0.096	1.198	-3.000
0.353	0.420	0.898	-0.182	0.716	-2.500
0.226	0.241	0.591	-0.226	0.365	-2.000
0.186	0.194	0.504	-0.234	0.270	-1.800
0.151	0.159	0.434	-0.239	0.196	-1.600
0.121	0.132	0.378	-0.238	0.140	-1.400
0.095	0.111	0.331	-0.234	0.096	-1.200
0.073	0.087	0.284	-0.226	0.057	-1.000
0.053	0.064	0.241	-0.261	-0.019	-0.800
0.037	0.045	0.205	-0.206	-0.000	-0.600
0.022	0.028	0.174	-0.176	-0.002	-0.400
0.010	0.013	0.147	-0.150	-0.003	-0.200
-0.000	-0.001	0.123	-0.123	0.000	-0.000
-0.009	-0.013	0.102	-0.093	0.010	0.200
-0.016	-0.024	0.084	-0.052	0.032	0.400
-0.022	-0.035	0.068	0.002	0.070	0.600
-0.026	-0.044	0.054	0.073	0.127	0.800
-0.029	-0.053	0.042	0.164	0.205	1.000
-0.032	-0.062	0.031	0.277	0.308	1.200
-0.033	-0.069	0.022	0.406	0.428	1.400
-0.033	-0.077	0.014	0.532	0.546	1.600
-0.033	-0.084	0.008	0.611	0.619	1.800
-0.031	-0.090	0.003	0.597	0.599	2.000
-0.026	-0.105	-0.006	0.216	0.210	2.500
-0.017	-0.117	-0.010	-0.126	-0.136	3.000
-0.005	-0.128	-0.009	-0.291	-0.300	3.500
0.009	-0.138	-0.005	-0.366	-0.371	4.000
0.025	-0.147	0.002	-0.402	-0.400	4.500
0.043	-0.155	0.012	-0.420	-0.408	5.000
0.061	-0.162	0.023	-0.429	-0.405	5.500
0.081	-0.169	0.036	-0.432	-0.396	6.000
0.101	-0.175	0.051	-0.432	-0.381	6.500
0.122	-0.181	0.066	-0.430	-0.364	7.000
0.144	-0.186	0.083	-0.427	-0.345	7.500
0.166	-0.190	0.100	-0.424	-0.323	8.000
0.189	-0.195	0.118	-0.419	-0.301	8.500
0.211	-0.199	0.137	-0.414	-0.277	9.000
0.234	-0.202	0.156	-0.409	-0.253	9.500
0.257	-0.206	0.176	-0.404	-0.228	10.000

Table 5-5-b.

N/P Pole term	Re C(ν)	Re Δ(ν)	Re F(ν)	Re A_{out}(ν)	ν
-44.595	-1.406	-45.999	=45.599	-91.599	=9.000
-16.011	-0.857	-16.866	=16.434	-33.300	=8.500
-8.141	-0.612	-8.752	-8.436	-17.187	=8.000
-4.741	-0.412	-5.152	-4.995	-10.147	=7.500
-2.971	-0.228	-3.197	-3.213	-6.410	=7.000
-1.950	-0.054	-2.002	-2.188	-4.191	=6.500
-1.320	0.105	-1.214	-1.558	-2.772	=6.000
-0.915	0.241	-0.672	=1.151	-1.824	=5.500
-0.644	0.340	-0.303	=0.878	-1.180	=5.000
-0.459	0.391	-0.066	=0.687	-0.753	=4.500
-0.329	0.392	0.064	=0.550	-0.486	=4.000
-0.237	0.349	0.114	=0.446	-0.332	=3.500
-0.170	0.283	0.114	=0.365	-0.251	=3.000
-0.121	0.211	0.091	=0.297	-0.206	=2.500
-0.084	0.145	0.062	=0.238	-0.176	=2.000
-0.072	0.121	0.051	=0.215	-0.164	=1.800
-0.060	0.100	0.041	=0.193	-0.152	=1.600
-0.050	0.082	0.032	=0.171	-0.138	=1.400
-0.041	0.065	0.025	=0.149	-0.124	=1.200
-0.033	0.051	0.019	=0.126	-0.107	=1.000
-0.025	0.038	0.015	=0.113	-0.098	=0.800
-0.018	0.027	0.010	=0.080	-0.070	=0.600
-0.012	0.017	0.007	=0.054	-0.047	=0.400
-0.005	0.008	0.004	=0.028	-0.024	=0.200
0.000	-0.000	0.001	0.000	0.001	=0.000
0.006	-0.008	-0.001	0.031	0.030	0.200
0.011	-0.015	-0.003	0.066	0.063	0.400
0.016	-0.022	-0.005	0.104	0.099	0.600
0.020	-0.029	-0.007	0.146	0.139	0.800
0.025	-0.034	-0.008	0.191	0.183	1.000
0.029	-0.040	-0.009	0.238	0.229	1.200
0.034	-0.045	-0.010	0.288	0.278	1.400
0.038	-0.050	-0.011	0.340	0.328	1.600
0.042	-0.055	-0.012	0.391	0.379	1.800
0.046	-0.059	-0.012	0.440	0.427	2.000
0.055	-0.069	-0.013	0.539	0.526	2.500
0.065	-0.078	-0.012	0.577	0.564	3.000
0.075	-0.086	-0.011	0.538	0.528	3.500
0.084	-0.094	-0.008	0.441	0.433	4.000
0.094	-0.100	-0.005	0.320	0.315	4.500
0.104	-0.106	-0.001	0.203	0.202	5.000
0.114	-0.111	0.004	0.101	0.105	5.500
0.124	-0.116	0.009	0.020	0.028	6.000
0.134	-0.121	0.015	=0.045	-0.030	6.500
0.145	-0.125	0.021	=0.095	-0.074	7.000
0.155	-0.129	0.028	=0.134	-0.106	7.500
0.166	-0.132	0.035	=0.164	-0.129	8.000
0.177	-0.136	0.043	=0.187	-0.144	8.500
0.188	-0.139	0.051	=0.205	-0.155	9.000
0.199	-0.142	0.059	=0.220	-0.161	9.500
0.211	-0.145	0.068	=0.231	-0.163	10.000

than the n = 5. and one might call this a Balazs solution. It is tabulated in Table 5 (b). Searches were done with n = 6 but no solutions found. The n = 5 solution was obtained by optimising from the n = 4 solution, but, of course, when n changes the positions of all the left hand poles change, so there is no correspondence between residues.

THE SHIRKOV MODEL

1. The neutral Shirkov model

As an exercise in the solution of a soluble model by the variational method, the neutral Shirkov model was considered (see Chapter 1). From the Shirkov equations, the estimate of the left hand cut from crossing in the P wave only case is

$$\mathrm{Im}A_1(\nu) = \mathrm{Im}A_1(-\nu).$$

As shown by Shirkov etal, the resulting equations have families of resonant and non-resonant solutions. A tabulation of contributions to A_{out} is given in Table 6(b). We tried one search with N/D (n = 3) parametrisation and found no solution, however, the X^2 for the random starting values was quite low $\sim 10^{-1}$

2. The charged Shirkov model

We looked also at the charged Shirkov model, with a view to finding solutions of it by the variational method, since it appears impervious to analytical solution. A tabulation for P and S waves with a cut-off at -9, is given in Table 6(a). Here the X^2 is quite large. We did one search with P wave only and N/D (n = 2) parametrisation but found no solution, but as the soluble neutral model did not seem promising, we did not continue the search.

Table 5-6-a Skirkow charged model

S_{wave}	P_{wave}	Δ	Breit Wigner	Re Amt	ν
0.040	-0.259	-0.218	-0.150	-0.369	-9.000
0.045	-0.229	-0.184	-0.147	-0.331	-8.500
0.048	-0.156	-0.107	-0.143	-0.250	-8.000
0.052	-0.019	0.033	-0.139	-0.106	-7.500
0.055	0.152	0.208	-0.135	0.073	-7.000
0.058	0.263	0.322	-0.130	0.192	-6.500
0.061	0.280	0.342	-0.125	0.217	-6.000
0.065	0.247	0.312	-0.120	0.192	-5.500
0.068	0.202	0.270	-0.114	0.156	-5.000
0.071	0.160	0.232	-0.107	0.125	-4.500
0.074	0.126	0.201	-0.100	0.101	-4.000
0.077	0.098	0.175	-0.092	0.083	-3.500
0.077	0.076	0.153	-0.083	0.070	-3.000
0.073	0.057	0.130	-0.073	0.057	-2.500
0.057	0.042	0.099	-0.062	0.037	-2.000
0.044	0.036	0.081	-0.057	0.024	-1.800
0.025	0.031	0.057	-0.052	0.005	-1.600
-0.005	0.027	0.023	-0.047	-0.024	-1.400
-0.056	0.023	-0.033	-0.041	-0.074	-1.200
-0.134	0.023	-0.110	-0.000	-0.110	-1.000
-0.048	0.015	-0.032	-0.031	-0.063	-0.800
-0.026	0.011	-0.015	-0.023	-0.038	-0.600
-0.014	0.007	-0.007	-0.016	-0.022	-0.400
-0.006	0.003	-0.002	-0.008	-0.010	-0.200
0.000	-0.000	0.001	-0.000	0.001	-0.000
0.005	-0.003	0.002	0.008	0.011	0.200
0.008	-0.006	0.003	0.018	0.020	0.400
0.011	-0.009	0.003	0.027	0.030	0.600
0.014	-0.011	0.003	0.038	0.041	0.800
0.016	-0.014	0.003	0.049	0.052	1.000
0.018	-0.016	0.003	0.061	0.063	1.200
0.020	-0.018	0.002	0.073	0.075	1.400
0.021	-0.020	0.001	0.087	0.089	1.600
0.023	-0.022	0.001	0.102	0.103	1.800
0.024	-0.024	0.000	0.118	0.118	2.000
0.026	-0.028	-0.002	0.165	0.163	2.500
0.028	-0.032	-0.004	0.223	0.219	3.000
0.030	-0.036	-0.005	0.293	0.288	3.500
0.032	-0.039	-0.007	0.378	0.371	4.000
0.033	-0.042	-0.009	0.471	0.461	4.500
0.034	-0.045	-0.011	0.540	0.529	5.000
0.035	-0.048	-0.012	0.509	0.497	5.500
0.036	-0.050	-0.014	0.290	0.276	6.000
0.037	-0.052	-0.015	-0.048	-0.063	6.500
0.037	-0.054	-0.017	-0.318	-0.335	7.000
0.038	-0.056	-0.018	-0.460	-0.478	7.500
0.038	-0.058	-0.019	-0.516	-0.535	8.000
0.039	-0.060	-0.021	-0.528	-0.549	8.500
0.039	-0.062	-0.022	-0.523	-0.544	9.000
0.040	-0.063	-0.023	-0.510	-0.532	9.500
0.040	-0.065	-0.024	-0.494	-0.518	10.000

Table 5-6-b. Shkikov neutral model

N/D pole	P-wave	Δ	Re F(ν) (N/D)	Re Δ out	ν
-3.216	-0.329	-3.544	-3.351	-6.895	-9.000
-3.456	-0.280	-3.736	-3.601	-7.337	-8.500
-3.862	-0.223	-4.084	-4.015	-8.099	-8.000
-4.606	-0.156	-4.761	-4.767	-9.528	-7.500
-6.251	-0.074	-6.324	-6.421	-12.745	-7.000
-12.169	0.030	-12.139	-12.360	-24.499	-6.500
41.720	0.160	41.880	41.673	83.552	-6.000
5.894	0.317	6.211	5.749	11.961	-5.500
2.690	0.485	3.175	2.538	5.713	-5.000
1.524	0.616	2.140	1.370	3.511	-4.500
0.939	0.651	1.590	0.788	2.379	-4.000
0.599	0.580	1.180	0.454	1.634	-3.500
0.385	0.454	0.840	0.249	1.088	-3.000
0.244	0.327	0.572	0.119	0.691	-2.500
0.150	0.222	0.372	0.039	0.411	-2.000
0.121	0.187	0.309	0.017	0.326	-1.800
0.096	0.156	0.253	0.001	0.254	-1.600
0.076	0.129	0.205	-0.012	0.193	-1.400
0.058	0.105	0.163	-0.020	0.143	-1.200
0.043	0.083	0.126	-0.025	0.101	-1.000
0.030	0.063	0.094	-0.027	0.067	-0.800
0.020	0.045	0.066	-0.025	0.041	-0.600
0.012	0.029	0.041	-0.020	0.021	-0.400
0.005	0.014	0.019	-0.011	0.008	-0.200
-0.000	-0.001	-0.000	0.000	-0.000	-0.000
-0.004	-0.014	-0.017	0.015	-0.002	0.200
-0.007	-0.027	-0.033	0.034	0.002	0.400
-0.008	-0.038	-0.046	0.058	0.012	0.600
-0.009	-0.049	-0.057	0.086	0.028	0.800
-0.008	-0.060	-0.068	0.118	0.051	1.000
-0.007	-0.070	-0.076	0.156	0.080	1.200
-0.005	-0.080	-0.084	0.199	0.115	1.400
-0.002	-0.089	-0.090	0.247	0.156	1.600
0.001	-0.097	-0.096	0.298	0.203	1.800
0.005	-0.105	-0.100	0.353	0.253	2.000
0.017	-0.125	-0.107	0.487	0.380	2.500
0.031	-0.142	-0.110	0.568	0.458	3.000
0.048	-0.158	-0.109	0.546	0.437	3.500
0.066	-0.172	-0.105	0.430	0.325	4.000
0.085	-0.185	-0.099	0.280	0.181	4.500
0.106	-0.197	-0.090	0.141	0.051	5.000
0.128	-0.208	-0.080	0.032	-0.048	5.500
0.150	-0.219	-0.068	-0.050	-0.118	6.000
0.173	-0.229	-0.055	-0.109	-0.164	6.500
0.196	-0.238	-0.041	-0.152	-0.193	7.000
0.219	-0.246	-0.026	-0.183	-0.210	7.500
0.243	-0.254	-0.010	-0.206	-0.217	8.000
0.267	-0.262	0.006	-0.223	-0.217	8.500
0.291	-0.269	0.023	-0.235	-0.212	9.000
0.315	-0.275	0.040	-0.244	-0.203	9.500
0.339	-0.282	0.058	-0.250	-0.192	10.000

CHAPTER 6

"INVERSE AMPLITUDE METHODS"

Discussion of properties of the inverse amplitude

The idea of writing down and attempting to solve dispersion relations for the inverse amplitude suggests iself from the unitarity condition

$$\mathrm{Im}A_\ell^{-1}(\nu) = -\sqrt{\frac{\nu}{\nu+1}} \cdot R(\nu) \qquad \nu > 0 \qquad \text{(i)}$$

Methods have been proposed by Matthews and Salam (1) (2) and Moffat (3) (4) where refs 1, 3, 4 define separate different inverse amplitude procedures. If the amplitude $A_\ell(\nu)$ obeys the causal dispersion relation

$$A_\ell(\nu) = \frac{1}{\pi}\int_0^\infty \frac{d\nu'\ \mathrm{Im}A(\nu')}{\nu' - \nu} + \frac{1}{\pi}\int_{-\infty}^{-1} \frac{d\nu'\ \mathrm{Im}A(\nu')}{\nu' - \nu} \quad \text{p.s.} \qquad \text{(ii)}$$

then $A_\ell^{-1}(\nu)$ will have cuts in the same places $[0,\infty]$, $[-1, -\infty]$. In addition, because of the threshold behaviour

$$A_\ell(\nu) \underset{\nu \to 0}{\sim} \nu^\ell \qquad \text{(iii)}$$

$A_\ell^{-1}(\nu)$ will have an ℓth order pole at threshold and will have a term

$$\sum_{n=1}^{\ell} \frac{g_\ell^n}{\nu^n} \qquad \text{where } g_\ell^n = \frac{1}{2\pi i}\int \frac{A^{-1}(\omega)\ d\omega}{(\omega)^{n+1}} \qquad \text{(iv)}$$

in its dispersion relation, note there is no constant term. In addition, the only other singularities $A_\ell^{-1}(\nu)$ can have are isolated poles of any order and these can be anywhere, in the plane, where they must occur in conjugate pairs because A_ℓ^{-1} is real analytic, or on the real axis, except on the physical cut where $\mathrm{Im}A_\ell^{-1}$ cannot become infinite by unitarity. These poles introduce an apparent arbitrariness into the equations. There is no reason why they should not occur, and it is not clear that they all correspond to CDD

ambiguities and can be excluded by demanding a special form of Levinson's theorem hold. In the interests of simplicity, we shall assume there are no such poles.

We can now write the dispersion relation

$$A_\ell^{-1}(\nu) = \frac{1}{\pi}\int_0^\infty \frac{\mathrm{Im}A^{-1}(\nu')\,d\nu'}{\nu'-\nu} + \frac{1}{\pi}\int_{-\infty}^{-1} \frac{\mathrm{Im}A^{-1}(\nu')\,d\nu'}{\nu'-\nu} + \sum_{n=1}^{\ell-1} \frac{g_\ell^n}{\nu^n} \qquad \text{p.s.} \qquad (v)$$

We now see the big advantage of using the inverse amplitude. By substituting (1) into (v), we immediately obtain the contribution from the right hand cut and automatically have unitarity satisfied. We also have control over the threshold behaviour. On the other hand, we need to know $\mathrm{Im}A^{-1}$ on the left, and the Mandelstam representation can more easily give values of ImA. We thus need to know ReA on the left in order to construct $\mathrm{Im}A^{-1}$. Two procedures have been adopted, one can neglect the left hand cut or one can use the clever iteration procedure of Moffat which uses the value of ReA on the left from the previous iteration, starting the first iteration with $\mathrm{Im}A^{-1} = 0$ $\nu<-1$. If one assumes that ImA behaves like a polynominal at infinity, then the inverse amplitude will be a good method for in that case $\mathrm{Im}A^{-1} \to 0$, so we have good asymptotic behaviour. If, on the other hand, ImA has violent oscillations, then so will $\mathrm{Im}A^{-1}$. Most workers take one subtraction and that this is reasonable follows from discussions in Chapter 1. Then

$$A_\ell^{-1}(\nu) = A_\ell^{-1}(\nu_0) + \frac{(\nu-\nu_0)}{\pi}\int_0^\infty \frac{\mathrm{Im}A^{-1}(\nu')\,d\nu'}{(\nu'-\nu)(\nu'-\nu_0)} + \frac{(\nu-\nu_0)}{\pi}\int_{-\infty}^{-1} \frac{\mathrm{Im}A^{-1}(\nu')\,d\nu'}{(\nu'-\nu)(\nu'-\nu_0)} + (\nu-\nu_0)\sum_{n=1}^{\ell-1} \frac{g_\ell^n}{\nu^n}$$

Bransden and Moffat take $\nu_0 = -2/3$, the centre of the Δ. They write $A_\ell^{-1}(\nu_0) = \frac{1}{a_\ell}$ and care must be taken not to confuse these a_ℓ with the scattering lengths. The threshold residues, g_ℓ^n, have to be determined,

possibly by self consistency, as in Dr ansden and Moffat's work. The main disadvantages, as far as the author can see, are the pole ambiguity and general accountancy in numbers of parameters, and the need for the value of ReA on the left to which the calculation is very sensitive since ReA probably has zeros on the near left.

Zeros of A^{-1} will correspond to poles of A i.e. to particles. We thus have to constrain A^{-1} to the requirement of no complex zeros on the physical sheet. This is a difficult requirement to implement. One can obtain criteria for the certain nonexistence of zeros, but if these are not satisfied, one has to do a numerical search of the complex plane, or rather, the near part of it. The main disadvantages of using the inverse amplitude are thus:

(a) The pole ambiguity - there is no reason why one should not have complex poles of A^{-1}, and maybe the correct solution has them. There is general complication in accountancy of the number of parameters, which extends to the threshold residues. One can hope to remove these ambiguities by careful self consistent calculations.

(b) Zeros of A^{-1} - one has to check that one's solution has no complex zeros which is not a simple matter.

(c) One needs to know the value of ReA on the left to which the calculation is very sensitive since ReA probably has zeros on the near left.

One can write dispersion relations for $\nu^{l}.A_{l}^{-1}(\nu)$ to remove the threshold poles but this will probably cause bad asymptotic behaviour and so will not help. We remark that the nearby singularity assumption for A does not correspond to a nearby singularity assumption for A^{-1}, in fact in some ways the opposite. If A increases rapidly at infinity, then we can develop a nearby singularity method for A^{-1}, with impunity.

To complete the introduction, one might ask whether one ought, because of automatic unitarity, to reformulate dispersion theory using A^{-1}. However, it

does seem that A is a much better quantity. For poles in A correspond to particles in all known theories and the value of A is the probability of the process concerned happening. High values of A correspond to large numbers of events occurring. On the other hand, A^{-1} must be a measure of the absence of events. High values of A^{-1} correspond to very little taking place.

PREVIOUS WORK

In their first paper (1) Matthews and Salam proposed a T^{-1} matrix formalism for a finite number of two body channels and in their second (2) they applied it to K-p and scattering. Their main purpose was to set up a formalism to handle the KN and s systems, where unitarity is very complicated. They ignored poles of T^{-1}. They also supposed $T = B$ whenever the latter was infinite and that there was a point ν_B at which $B(\nu_B) = \infty$ This leads to the dispersion relation for T^{-1}. B

$$T^{-1}\ B = 1 - \frac{(\nu - \nu_B)}{\pi} \int_{\text{cuts}} \frac{\mathrm{Im} T^{-1} B \ . \ d\nu'}{(\nu' - \nu)\ (\nu' - \nu_B)}$$

The present author remarks that the estimate of a δ function approximate to $C(\nu)$ for $B(\nu)$ has such a singularity at $\nu_B = -\nu_R - 1$. They also generalised these equations to many two body channels. They then wrote down the $\pi\pi$ S wave solution in the case of no left hand cut, which is

$$\sqrt{\frac{\nu}{\nu+1}} \cot\delta_0 = \frac{1}{a} + \frac{(\nu - \nu_0)}{\pi} \cdot I(\nu, \nu_0)$$

In his first paper (3), Moffat introduced a very simple inverse amplitude method, which neglected the left hand cut and assumed $A^{-1} \longrightarrow (0)$. $\nu \longrightarrow -\infty$ He applied it to obtaining a resonance formula for N scattering. In his second paper (4) he proposed a new method in general, once subtracted, straightforward dispersion relation for $A^{-1}(\nu)$. He mentioned the arbitrariness in the poles of A^{-1} and neglected them. He proposed his iterative procedure for generating solutions, as follows:-

(1) Choose $\mathrm{Im} A^{-1}(\nu)\ \nu < _0 = 0$
(2) Calculate $\mathrm{Re} A(\nu) \nu < _0$ and $\mathrm{Im} A(\nu)\ \nu > _0$ from the inverse amplitude relation
(3) Calculate $\mathrm{Im} A(\nu) \nu < _0$, using $\mathrm{Im} A(\nu)\ \nu > _0$, and crossing on the near left
(4) Hence calculate a new value of $\mathrm{Im} A^{-1}(\nu)\ \nu < _0$, and cycle to convergence.

He used this method to find P wave only solutions. Starting from the previous solution, he found the left hand cut gave only a small contribution. He produced a criterion for no complex zeros and verified his solution satisfied it.

Bransden and Moffat (5) (6) applied a similar iteration procedure to an S-P calculation.

In this calculation, there were $(\ell + 1)$ constraints in each partial wave viz. $A^{-1}(\nu_n)$ and g_ℓ^n. Sufficient crossing conditions at the symmetry point $\nu_0 = -2/3$, were introduced to leave one free parameter, . They first expressed a_0^0 and a_0^2 in terms of λ, leaving 3 parameters λ, a_1 and g_1^1. They then varied the parameters a_1, g_1^1 systematically, keeping λ fixed at each stage during the iteration procedure and calculating the solution. When crossing was satisfied, this was taken as a solution for that value of λ. They also checked for consistency by looking at the next higher order derivative crossing conditions. For a range of values of λ, the iteration procedure diverged but for the rest they were able to give tables of solutions. Perhaps the most realistic is for $\lambda = -0.1$

$$a_1 = -0.005, \quad g_1^1 = +199.5$$

$$\nu_R = 5.25 \qquad 700 \text{ Mev}$$

$$\Gamma\nu_R = 0.2 \qquad 63 \text{ Mev}$$

$$\left.\begin{aligned} a_0^0 &= 0.67 \\ a_2^0 &= 0.2 \end{aligned}\right\} \text{ S wave scattering lengths}$$

Their solutions depended very strongly upon λ. We see that there is very strong cancellation between the two large terms $\frac{1}{a_1}$ and $(\nu - \nu_0)\ g_1^1$.

The S waves depended only weakly on the P waves and the P waves depended strongly upon the S waves. They also found the CMN small P wave solutions and showed they did not satisfy the higher derivative check. Their paper was criticised by Ball and Wong (7). who said that A^{-1} has a zero just beyond the left hand cut off and that this gives a strong distant singularity in A which is producing the resonance. However, they replied strongly (6) with numerical evidence for very small dependence on cut-off on left . They remark that the P wave resonance is determined mainly by a_1 and g_1^1 which in turn are determined by derivative matching conditions to the S waves at $\nu_0 = -2/3$.

PROPOSED NEW INVERSE AMPLITUDE METHOD

The Moffat iteration procedure gives exact solutions not involving trial functions, but seems very difficult to use. The iteration procedure is not always stable and becomes very complicated for large numbers of waves. The main objection is that one cannot see clearly what is going on. We therefore proposed a different approach using the real part on the left obtained from a fixed S dispersion relation considered in Chapter 2.

THE LEFT HAND CUT

We used trial functions in the crossed channel and by fixed s dispersion relations obtained $\mathrm{Re}A^{-1}(\nu)$ and $\mathrm{Im}A^{-1}(\nu)$ in $[0, -9]$. The form of the functions obtained is shown in the figures and one is immediately struck by the nearby singularity nature of the situation. For most waves, $\mathrm{Im}A^{-1}(\nu)$ has high values near the beginning of the left hand cut and becomes much smaller near $\nu = -9$. Thus we might hope that this would give a good approximation to the total contribution from the left hand cut. The solutions of Brarsden and Moffat show a similar behaviour.

THE LEFT HAND POLE

We see that the large value of $\mathrm{Im}A^{-1}(\nu)$ is often, but not always, associated with a zero of $\mathrm{Re}A(\nu)$ in a region where $\mathrm{Im}A(\nu)$ is very small (see diagram). In this case, the contribution can be represented by a pole. For, in the neighbourhood of the zero, ν_z, say

$$\mathrm{Re}A(\nu) = (\nu - \nu_z).A'(\nu_z) + 0\left((\nu - \nu_z)^2\right).$$

Taking ImA roughly constant = C, then

$$\mathrm{Im}A^{-1}(\nu) = -\frac{C}{(\nu - \nu_z)^2 . A'(\nu_z)^2 + C^2}$$

so

$$\mathrm{Im}A^{-1}(\nu_z + \epsilon) = \frac{C}{\frac{\epsilon^2}{g^2} + C^2}$$

Table 6-1.

$F(\nu) \equiv C(\nu)$ $P_1 \to P_1$ for $\nu < 0$
$F(\nu)$ = Breit Wigner for P_1 for $\nu > 0$
$C\delta = C(\nu)$ for δ function approx to $C(\nu)$.

REC δ	REC δ-1	REF	IMF	REF-1	IMF-1	ν
-1.760	-0.491	-0.551	-0.721	-0.669	0.875	-9.500
-1.633	-0.477	-0.418	-0.733	-0.587	1.029	-9.000
-1.473	-0.451	-0.274	-0.713	-0.470	1.222	-8.500
-1.270	-0.406	-0.130	-0.641	-0.303	1.498	-8.000
-1.006	-0.334	-0.002	-0.503	-0.010	1.988	-7.500
-0.651	-0.221	0.084	-0.328	0.732	2.865	-7.000
-0.127	-0.041	0.107	-0.188	2.295	4.018	-6.500
1.073	0.229	0.088	-0.105	4.700	5.605	-6.000
0.615	1.626	0.058	-0.059	8.406	8.579	-5.500
0.260	3.846	0.032	-0.034	14.537	15.581	-5.000
0.117	8.550	0.012	-0.020	22.343	36.833	-4.500
0.044	22.939	-0.002	-0.011	-14.941	85.929	-4.000
0.003	291.276	-0.011	-0.006	-69.075	38.683	-3.500
-0.018	-55.405	-0.016	-0.003	-59.708	11.523	-3.000
-0.028	-35.756	-0.018	-0.001	-54.691	4.077	-2.500
-0.030	-33.039	-0.018	-0.000	-56.211	1.366	-2.000
-0.030	-33.761	-0.017	-0.000	-58.679	0.790	-1.800
		-0.016	-0.000	-62.407	0.389	-1.600
-0.026	-38.086	-0.015	-0.000	-67.874	0.138	-1.400
-0.024	-42.180	-0.013	-0.000	-75.798	0.020	-1.200
-0.021	-48.368	-0.011	0.000	-87.566	0.000	-1.000
-0.017	-58.091	-0.009	0.000	-105.890	0.000	-0.800
-0.013	-74.761	-0.007	0.000	-137.090	0.000	-0.600
-0.009	-108.659	-0.005	0.000	-200.272	0.000	-0.400
-0.005	-211.263	-0.003	0.000	-391.094	0.000	-0.200
		0.003	0.000	338.120	-0.302	0.100
		0.006	0.000	166.385	-0.408	0.200
		0.012	0.000	80.518	-0.535	0.400
		0.019	0.000	51.895	-0.612	0.600
		0.027	0.000	37.584	-0.667	0.800
		0.034	0.001	28.997	-0.707	1.000
		0.043	0.001	23.273	-0.739	1.200
		0.052	0.002	19.184	-0.764	1.400
		0.062	0.003	16.117	-0.784	1.600
		0.073	0.004	13.732	-0.802	1.800
		0.084	0.006	11.824	-0.816	2.000
		0.118	0.012	8.389	-0.845	2.500
		0.161	0.023	6.099	-0.866	3.000
		0.216	0.043	4.463	-0.882	3.500
		0.287	0.079	3.237	-0.894	4.000
		0.379	0.150	2.283	-0.905	4.500
		0.484	0.291	1.519	-0.913	5.000
		0.543	0.559	0.895	-0.920	5.500
		0.375	0.928	0.374	-0.926	6.000
		-0.076	1.069	-0.066	-0.931	6.500
		-0.414	0.873	-0.443	-0.935	7.000
		-0.522	0.636	-0.770	-0.939	7.500
		-0.527	0.470	-1.057	-0.943	8.000
		-0.502	0.363	-1.309	-0.946	8.500
		-0.472	0.292	-1.534	-0.949	9.000
		-0.443	0.243	-1.735	-0.951	9.500
		-0.418	0.208	-1.915	-0.953	10.000

Fig. 6-1 $C^{-1}(\nu)$. $P_1 \to P_1$.

curve 1 $\mathrm{Re}\, C^{-1}$.
2 $\mathrm{Im}\, C^{-1}$.

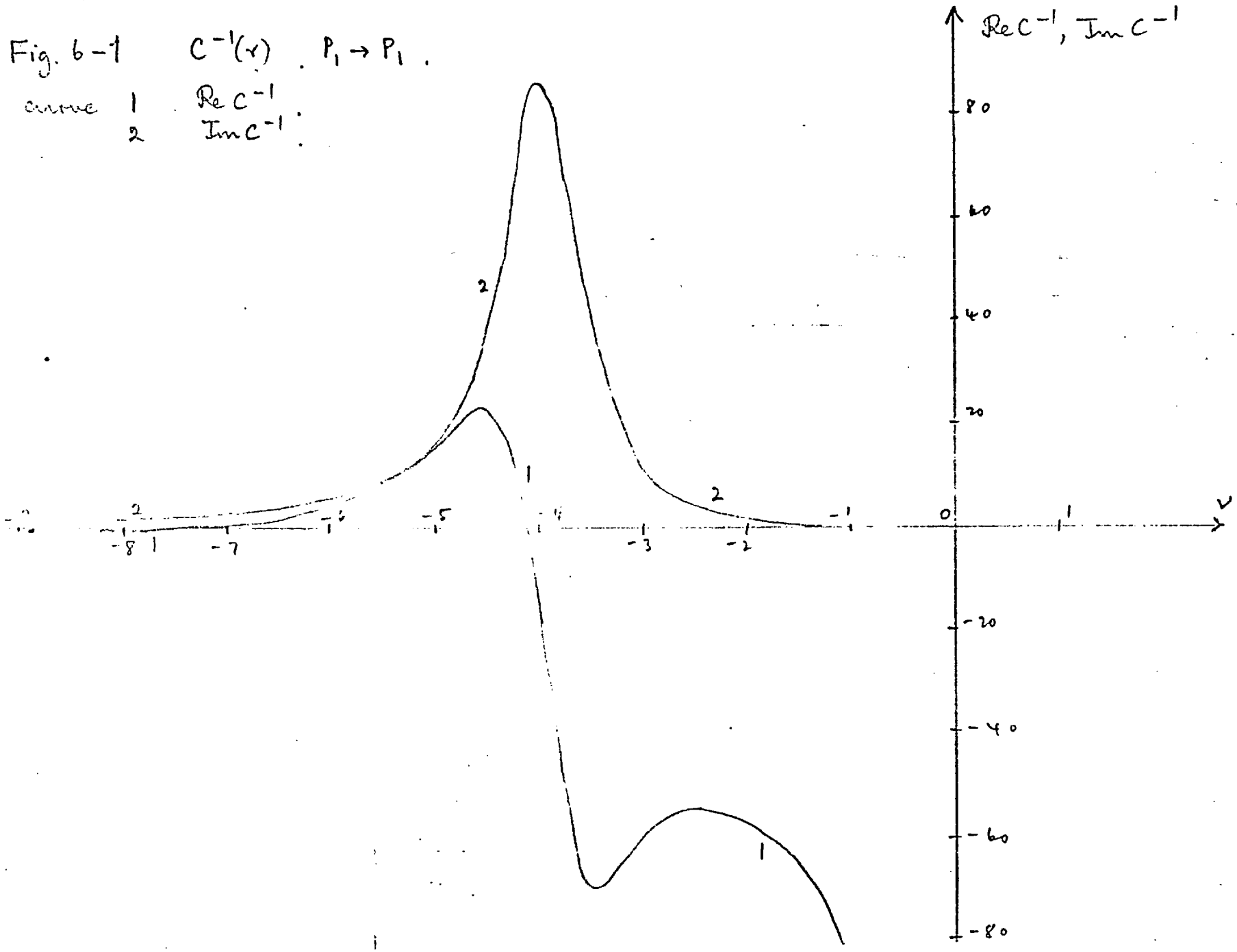

Re C(ν)

Fig. 6-2(a) Breakdown of Re C(ν), contributions to P_1.

1	S_0
2	S_2
3	P_1
4	D_0

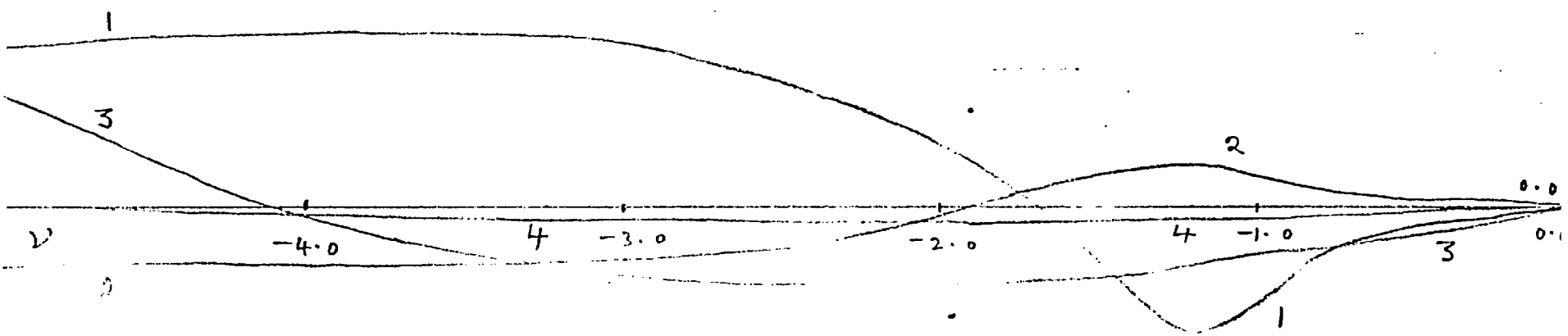

Fig. 6-2(b). Breakdown of contributions to ReC for D_0 wave.

curve 1 S_0
2 S_2
3 P_1

D_0 negligible.

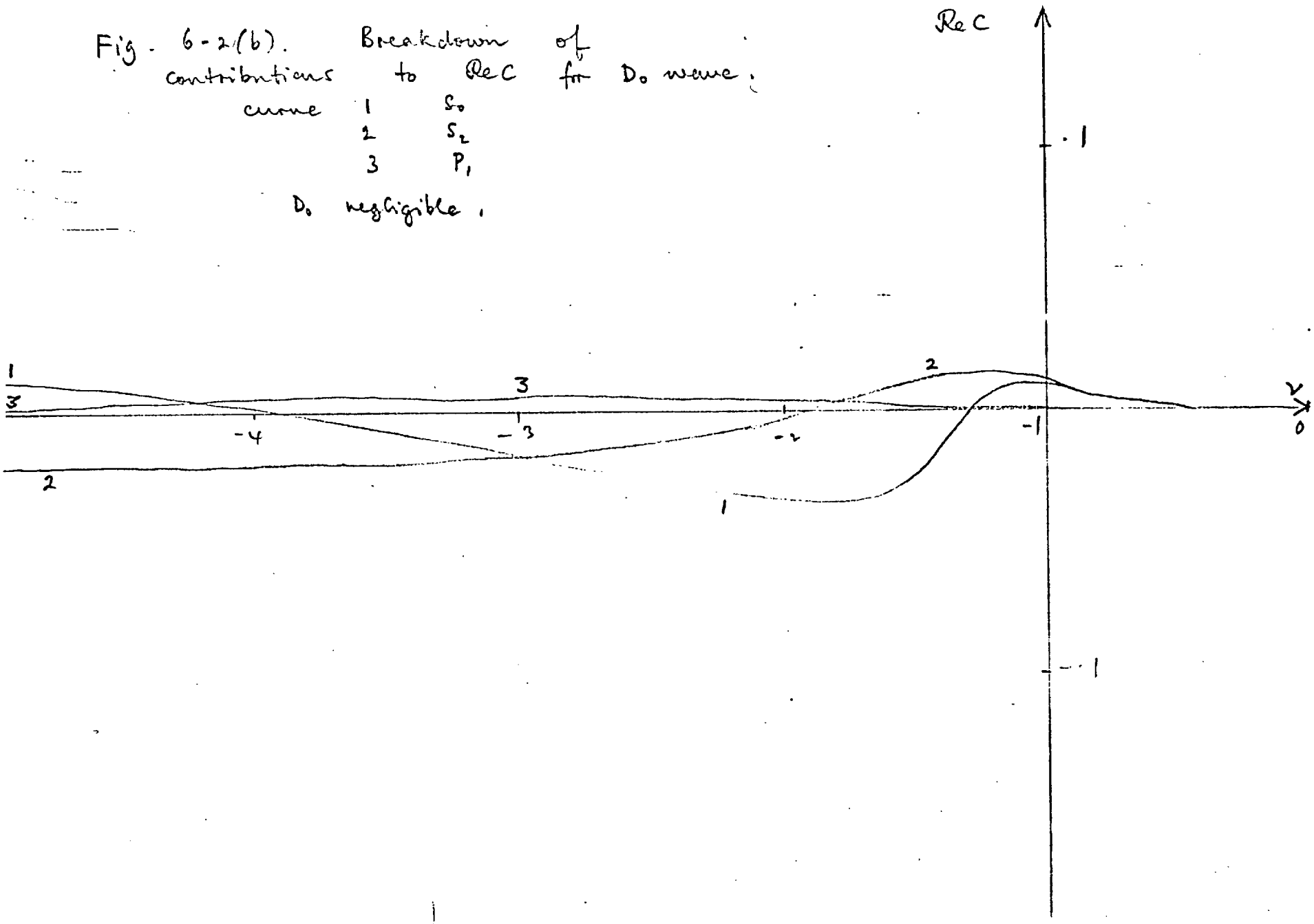

$$\frac{1}{\pi}\int_{\text{region of zero}} \frac{\mathrm{Im}A^{-1}(\nu')\,d\nu'}{\nu'-\nu} \;-\; \frac{1}{\pi}\int \frac{C}{\frac{x^2}{g^2}+c^2}\cdot\frac{d\nu'}{\nu'-\nu}$$

As $C \to 0$ $\mathrm{Im}A^{-1}(\nu_z + x) \longrightarrow -\pi\,\delta\left(\frac{x}{g}\right) = -\pi g\,\delta(x)$

so contribution $\longrightarrow -g\cdot\frac{1}{(\nu_z-\nu)}$

This involves the reasonable assumption that $\frac{1}{\nu'-\nu}$ is slowly varying in the region of the bump, which is clearly true for ν on the right hand side.

Hence for small c, we expect this region of the cut to be representable by a pole with residue

$$-1/\mathrm{Re}A'(\nu_z).$$

If this is the maincontribution from the whole of the cut, then we have a one pole approximation. A difficult point arises when we realise that, for small +ve c, $g = -1/\mathrm{Re}A'(\nu_z)$, but for small -vec, $g = +1/\mathrm{Re}A(\nu_z)$. As ImA changes from +ve to -ve, $\mathrm{Im}A^{-1}$ flips from a large -ve peak to large +ve peak. This sign change will normally be under the control of the S waves in the crossed channel since the zero usually occurs on the near left where the S waves dominate, in the truncated sum at least. Thus the effect of the exchange of higher waves can be reversed in sign according to the value of the S waves. This is a very strange circumstance, though not necessarily incorrect.

δ FUNCTION APPROXIMATION IN THE CROSSED CHANNEL

In this case, the cut starts at $-\nu_R - 1$ and is very small and one might suspect that there had been a dramatic change in going from the distributed case to the δ function case. However, $\mathrm{Re}C(\nu)$ has a zero in $[0, -\nu_R - 1]$ and so we have a pole there and it has residue $-1/\mathrm{Re}C'(\nu_z)$. It seems it will be a good approximation to neglect the rest of the left hand cut. See diagram and compare with distributed form.

Whether to take a +ve or -ve sign must be decided with reference to more exact forms.

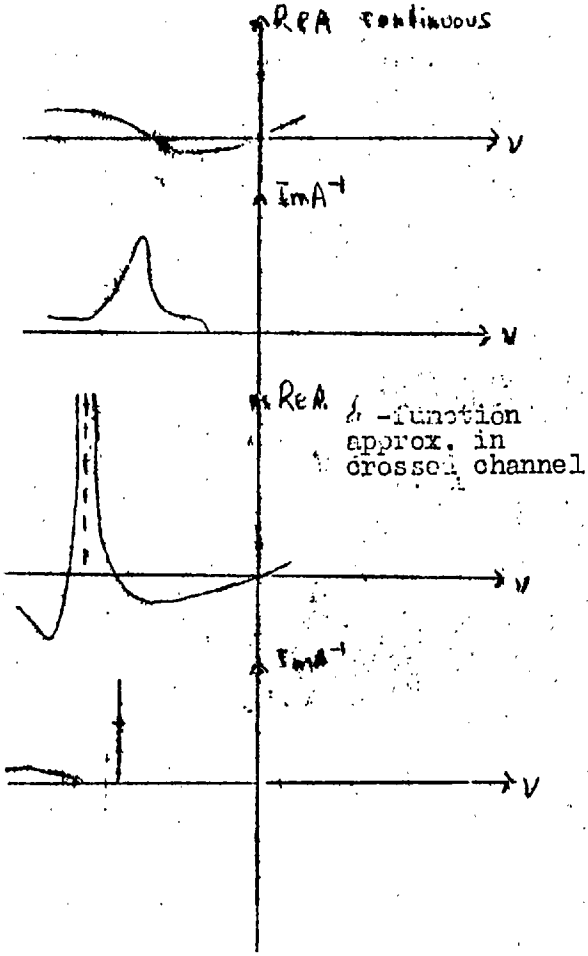

VALUE OF SUBTRACTION CONSTANT

We propose to either treat this as a parameter or to estimate it from $C(\nu)$.

$$A^{-1}(\nu_o) = C^{-1}(\nu_o) \qquad \nu_o \text{ in } [-9, 0] .$$

THRESHOLD RESIDUES

We propose to either treat these as parameters to be determined self consistently or to estimate them from $C(\nu)$. This we do as follows:-

We take the same residues as the C^{-1} function

$$C^{I-1}_{\ell}(\nu) = \sum_{n=1}^{\ell} \frac{d_n}{\nu^n} .$$

To evaluate them, we first evaluate the expansion of $C^I_\ell(\nu) = \sum_{k=1}^{\infty} C^I_k \cdot \nu^{\ell+k-1}$

so $$\frac{C^I_\ell(\nu)}{\nu^\ell} = \sum_{k=1}^{\infty} C^I_k \cdot \nu^{k-1} .$$

The $\{ C^I_k \}$ can be obtained from the derivatives evaluated at the origin, but it was found to be much easier to evaluate the expansions about the origin of

$$P_{\ell'}\left[1 + 2\left(\frac{\nu+1}{\nu'}\right)\right] = \sum_{j=0}^{\ell'} b_j \cdot \nu^j$$

and

$$\frac{Q_{\ell'}\left[1 + 2\left(\frac{\nu'+1}{\nu}\right)\right]}{\nu^{\ell}} = \sum_{i=1}^{\infty} a_i \cdot \nu^i$$

then

$$C^I_{\ell k} = \frac{4}{\pi}\int_0^\infty d\nu' \sum_{\ell'=0}^{\infty} (2\ell'+1) \sum_{i=0}^{\ell'} \left(\beta_{II}, \mathrm{Im}A^I_{\ell'}(\nu')\right) \cdot C'^I_{k\ell'}(\nu')$$

where

$$C'_1 = a_1 \cdot b_o$$
$$C'_2 = a_2 b_o + a_1 b_1$$
$$C'_3 = a_3 b_o + a_2 b_1 + a_1 b_2 \quad \text{etc.}$$

i.e. $C'_k = \sum_{i=1}^{k} a_i \cdot b_{k-i}$.

The values of the coefficients $\{a_i\}, \{b_j\}$ which depend on ν' in general are displayed below:-

$$\frac{Q_{\ell'}\left[1 + 2\left(\frac{\nu'+1}{\nu}\right)\right]}{\nu'^{\ell'}} = \sum_{i=1}^{\infty} e_i \cdot \nu^i$$

ℓ' \ i	1	2	3
0	$\frac{1}{2}\cdot\left(\frac{1}{\nu'+1}\right)$	$-\frac{1}{4}\frac{1}{(\nu'+1)^2}$	$+\frac{1}{6}\frac{1}{(\nu'+1)^3}$
1	$\frac{1}{12}\cdot\frac{1}{(\nu'+1)^2}$	etc.	
2	$\frac{1}{60}\cdot\frac{1}{(\nu'+1)^3}$	$\frac{-1}{40}\frac{1}{(\nu'+1)^4}$	etc.
3	$\frac{1}{280}\cdot\frac{1}{(\nu'+1)^4}$	$-\frac{1}{140}(\nu'+1)^5$	$\frac{1}{560}(\nu'+1)^6$ etc.

$$P_{\ell'}\left[1 + 2\left(\frac{\nu+1}{\nu'}\right)\right] = \sum_{j=0}^{\ell'} b_j \nu^j$$

ℓ' \ j	0	1	2	3
0	1			
1	$1 + \frac{2}{\nu'}$	$\frac{2}{\nu'}$		
2	$1 + \frac{6}{\nu'} + \frac{6}{\nu'^2}$	$\frac{6}{\nu'} + \frac{12}{\nu'^2}$	$\frac{6}{\nu'^2}$	

Having obtained the C_k we can evaluate the d_n by binomial expansion:-

$$C^{-1}(\nu) \cdot \nu^{\ell'} = \frac{1}{\sum_{k=1} C_k \cdot \nu^{k-1}}$$

$$C^{-1}(\nu) = \frac{1}{\nu^{\ell'}} \cdot \left\{ \frac{1}{C_1 \cdot \left[1 + \frac{C_2}{C_1}\nu + \frac{C_3}{C_1}\nu^2 \cdots\right]} \right\}$$

$$= \left(\frac{1/a_1}{\nu^{t-1}}\right) + \left(\frac{-c_2/c_1^2}{\nu^{t-1}}\right) + \left(\frac{-a_3/a_1^2 + a_2^2/a_1^3}{\nu^{t-2}}\right) + \cdots\cdots$$

i.e. $d_1 = \frac{1}{c_1}$

$d_2 = \frac{-c_2}{c_1^2}$

$d_3 = \frac{-a_3}{a_1^2} + \frac{a_2^2}{a_1^3}$ etc.

These formulae are probably not valid for the P wave, since one probably needs two subtractions in the fixed s dispersion relation for ν in $[-1, 0]$ leaving the P wave undetermined. This difficulty is not present for the D and higher waves, however there still remains the problem of the accumulation of higher partial waves in the crossed channel diffraction peak for ν in $[-1, 0]$. The partial wave series in the crossed channel diverges for $\nu = 0$, however this does not necessarily mean that our formulae are incorrect since they converge right up to $\nu = 0$ and each term in $\mathrm{Re}C(\nu) \underset{\nu \to 0}{\propto} \nu^t$. It could still be true that we have a reasonable estimate.

MODELS 1 AND 2

We can now define two "models".

(a) Model 1

Integrate the near left hand cut exactly.

(b) Model 2

Replace the left hand cut by a pole, whose residue $= \frac{-1}{\mathrm{Re}C'(\nu_z)}$ . . .

In either of these models, we either calculate from $C(\nu)$ or take as free the term $A^{-1}(\nu_0)$ and the threshold residues. The right hand cut is taken to be

elastic, initially.

$C(\nu)$ can either be taken in a distributed or δ - function form, but the δ - function form is not meaningful for Model 1.

To integrate the left hand cut accurately, we usually use 40 points in the interval $[-1, -8]$.

Different procedures were needed according to whether ν_0 was on or off the cut, see Appendix 3.

To evaluate the left hand pole position and residue, we used an auxiliary search routine which minimised $[\mathrm{ReC}(\nu_z)]^2$ and having found the minimum value to be zero, calculated $\mathrm{ReC}'(\nu)$ at that point. To evaluate the threshold residues from the expression given above, we simply integrated numerically, the integral is well behaved.

The effect of P waves only in the crossed channel is shown in the figures. They show that the Model 2 is a good one in this case and that taking a δ - function approximation in the crossed channel is a reasonable thing to do (and highly desirable for conserving computer time). We show further that these Models are independent of ν_0, even when ν_0 moves through the highly singular near left region where $A^{-1}(\nu_0)$ varies wildly in value and sign over a numerical range 0.3 to 200.

Model 2 also defines a parametrisation, which we discussed in Chapter 2

$$F(\nu) = \frac{1}{\dfrac{(\nu-\nu_0)}{(\nu_p-\nu_0)}\dfrac{g_p}{(\nu-\nu_p)} + a + \dfrac{(\nu-\nu_0)}{\pi} \cdot I(\nu, \nu_0) + T_1(\nu)}$$

Using this parametrisation in the crossed channel in a Model 2 calculation enables one to have the same parametrisation in both channels, which is a desirable feature in self consistent calculations.

We note that the right hand cut gives a very small contribution in Models 1 and 2 and that, as we can choose ν_0 far on the left, where we expect

Table 6-2. The Right hand cut.

Elastic RHCUT	Elastic $ImA^{-1}(\nu)$	Inelastic RHCUT	Inelastic $ImA^{-1}(\nu)$	ν
0.015		0.020		-9.500
-0.000		-0.000		-9.000
-0.016		-0.021		-8.500
-0.033		-0.043		-8.000
-0.051		-0.066		-7.500
-0.071		-0.090		-7.000
-0.091		-0.116		-6.500
-0.113		-0.144		-6.000
-0.137		-0.173		-5.500
-0.163		-0.205		-5.000
-0.191		-0.239		-4.500
-0.222		-0.277		-4.000
-0.257		-0.319		-3.500
-0.297		-0.365		-3.000
-0.342		-0.419		-2.500
-0.397		-0.481		-2.000
-0.422		-0.510		-1.800
-0.480		-0.575		-1.400
-0.514		-0.613		-1.200
-0.554		-0.656		-1.000
				-0.800
				-0.600
				-0.400
				-0.200
-1.131		-1.170		0.
-1.078	-0.408	-1.106	-0.408	0.200
-0.987	-0.535	-1.054	-0.535	0.400
-0.912	-0.612	-1.012	-0.612	0.600
-0.849	-0.667	-0.975	-0.667	0.800
-0.794	-0.707	-0.944	-0.707	1.000
-0.745	-0.739	-0.917	-0.739	1.200
-0.702	-0.764	-0.893	-0.764	1.400
-0.662	-0.784	-0.871	-0.784	1.600
-0.627	-0.802	-0.852	-0.802	1.800
-0.594	-0.816	-0.834	-0.816	2.000
-0.524	-0.845	-0.796	-0.845	2.500
-0.464	-0.866	-0.765	-0.866	3.000
-0.413	-0.882	-0.699	-0.974	3.500
-0.368	-0.894	-0.642	-1.019	4.000
-0.328	-0.905	-0.591	-1.052	4.500
-0.293	-0.913	-0.545	-1.078	5.000
-0.260	-0.920	-0.504	-1.099	5.500
-0.231	-0.926	-0.467	-1.117	6.000
-0.203	-0.931	-0.433	-1.133	6.500
-0.178	-0.935	-0.401	-1.147	7.000
-0.154	-0.939	-0.372	-1.159	7.500
-0.132	-0.943	-0.344	-1.171	8.000
-0.112	-0.946	-0.319	-1.181	8.500
-0.092	-0.949	-0.294	-1.190	9.000
-0.074	-0.951	-0.272	-1.199	9.500
	-0.953		-1.207	10.000

Table 6-3. Model 1. $P_1 \rightarrow P_1$.

$\nu_R = 5.0$ $\Gamma\nu_R = 1.25$

REA	IMA	REA-1	IMA-1	LHCUT	THPOLE	ν
-0.715	-0.187	-1.308	0.343	-8.417	4.639	-9.500
-0.689	-0.230	-1.305	0.436	-6.113	4.353	-9.000
-0.663	-0.284	-1.274	0.546	-7.745	4.033	-8.500
-0.631	-0.360	-1.196	0.682	-7.290	3.672	-8.000
-0.582	-0.470	-1.039	0.840	-6.707	3.264	-7.500
-0.461	-0.641	-0.739	1.029	-5.921	2.798	-7.000
-0.067	-0.771	-0.112	1.287	-4.736	2.250	-6.500
0.295	-0.404	1.179	1.616	-2.795	1.632	-6.000
0.206	-0.358	1.209	2.099	-1.999	0.890	-5.500
0.147	-0.206	2.292	3.217	0.	-0.000	-5.000
0.089	-0.104	4.823	5.036	3.648	-1.080	-4.500
0.050	-0.055	9.048	10.009	9.264	-2.449	-4.000
0.013	-0.026	15.365	31.484	17.365	-4.197	-3.500
-0.007	-0.011	-40.561	61.987	-36.191	-6.529	-3.000
-0.018	-0.005	-51.015	12.776	-43.334	-9.793	-2.500
-0.023	-0.001	-43.786	2.660	-31.154	-14.690	-2.000
-0.023	-0.001	-43.541	1.362	-28.154	-17.410	-1.800
-0.021	-0.000	-47.173	0.200	-23.962	-25.183	-1.400
-0.019	-0.000	-51.536	-0.027	-22.465	-31.012	-1.200
-0.017	0.	-60.111	0.	-22.840	-39.173	-1.000
-0.014	0.	-69.157	0.	-20.412	-51.414	-0.800
-0.011	0.	-89.548	0.	-19.686	-71.817	-0.600
-0.008	0.	-130.061	0.	-19.079	-112.622	-0.400
-0.004	0.	-252.188	0.	-18.563	-235.038	-0.200
-0.039	0.	-16.853	0.	-18.117	0.	0.
0.004	0.000	238.273	-0.408	-17.728	254.624	0.200
0.009	0.000	116.291	-0.535	-17.385	132.209	0.400
0.013	0.000	75.866	-0.612	-17.080	91.404	0.600
0.018	0.000	55.800	-0.667	-16.807	71.001	0.800
0.023	0.000	43.859	-0.707	-16.561	58.759	1.000
0.028	0.001	35.970	-0.739	-16.339	50.598	1.200
0.033	0.001	30.368	-0.764	-16.136	44.769	1.400
0.038	0.001	26.239	-0.784	-15.951	40.397	1.600
0.043	0.002	23.044	-0.802	-15.780	36.997	1.800
0.049	0.002	20.513	-0.816	-15.624	34.276	2.000
0.062	0.003	16.030	-0.845	-15.251	29.320	2.500
0.076	0.005	13.111	-0.866	-14.995	26.115	3.000
0.090	0.007	11.074	-0.882	-14.751	23.784	3.500
0.103	0.010	9.573	-0.894	-14.542	22.035	4.000
0.117	0.013	8.441	-0.905	-14.360	20.675	4.500
0.131	0.016	7.548	-0.913	-14.201	19.586	5.000
0.144	0.019	6.831	-0.920	-14.060	18.696	5.500
0.157	0.023	6.249	-0.926	-13.934	17.954	6.000
0.169	0.027	5.757	-0.931	-13.821	17.326	6.500
0.182	0.032	5.346	-0.935	-13.720	16.788	7.000
0.193	0.036	4.995	-0.939	-13.628	16.322	7.500
0.205	0.041	4.693	-0.943	-13.544	15.914	8.000
0.216	0.046	4.430	-0.946	-13.467	15.554	8.500
0.227	0.051	4.200	-0.949	-13.396	15.234	9.000
0.237	0.056	3.997	-0.951	-13.332	14.948	9.500
0.247	0.062	3.817	-0.953	-13.272	14.690	10.000

Fig 6-3(a) Re A, Im A

Model 1. $P_1 \rightarrow P_1$

(5·0, 1·25) ~ Table 6-3.

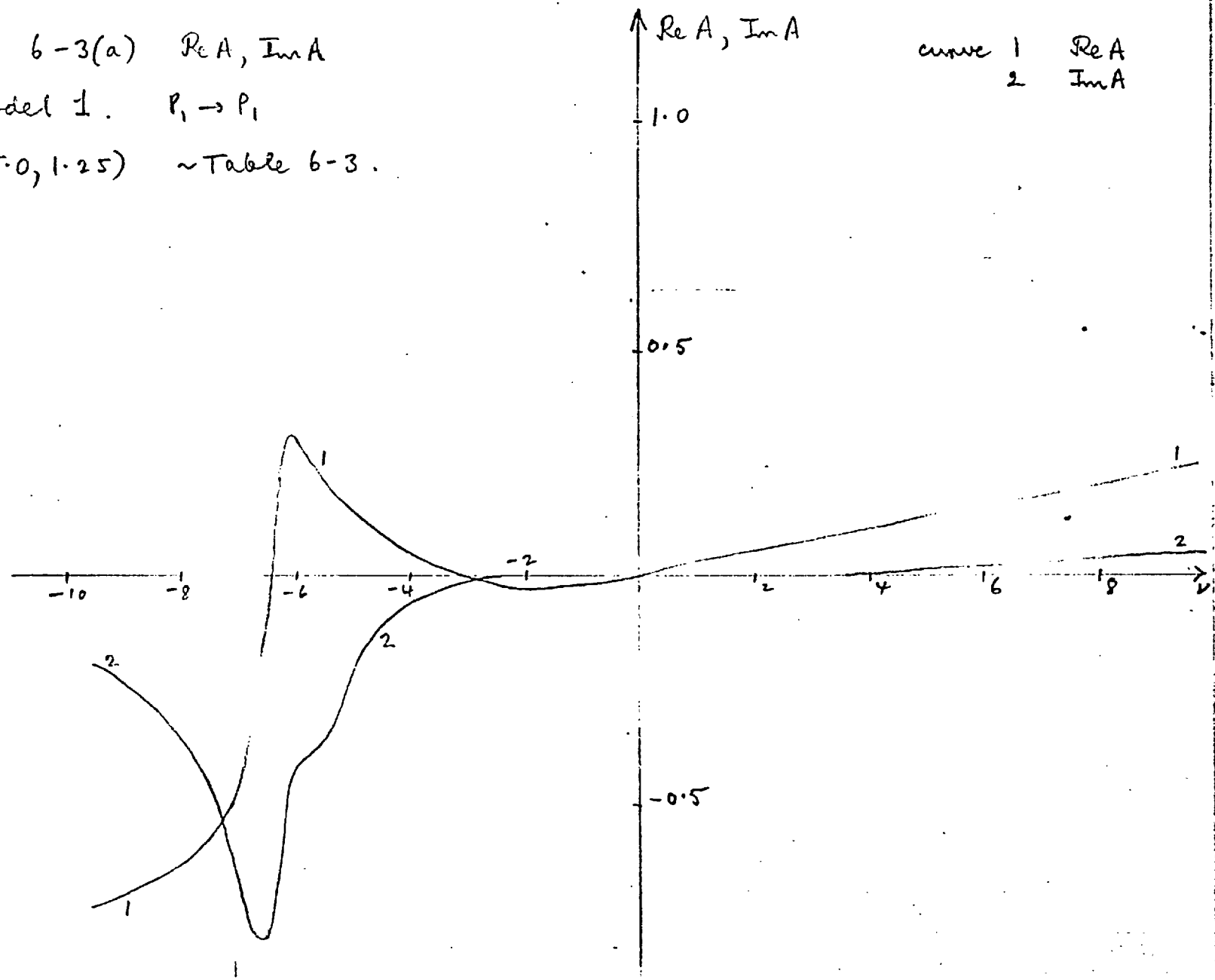

Fig 6-3(c)
Breakdown of contributions to $\mathrm{Re}\,A^{-1}$.

curve 1 left-hand cut.
2 Threshold pole
3 corresponding left-hand pole
4 Right-hand cut

$\nu_0 = -5$

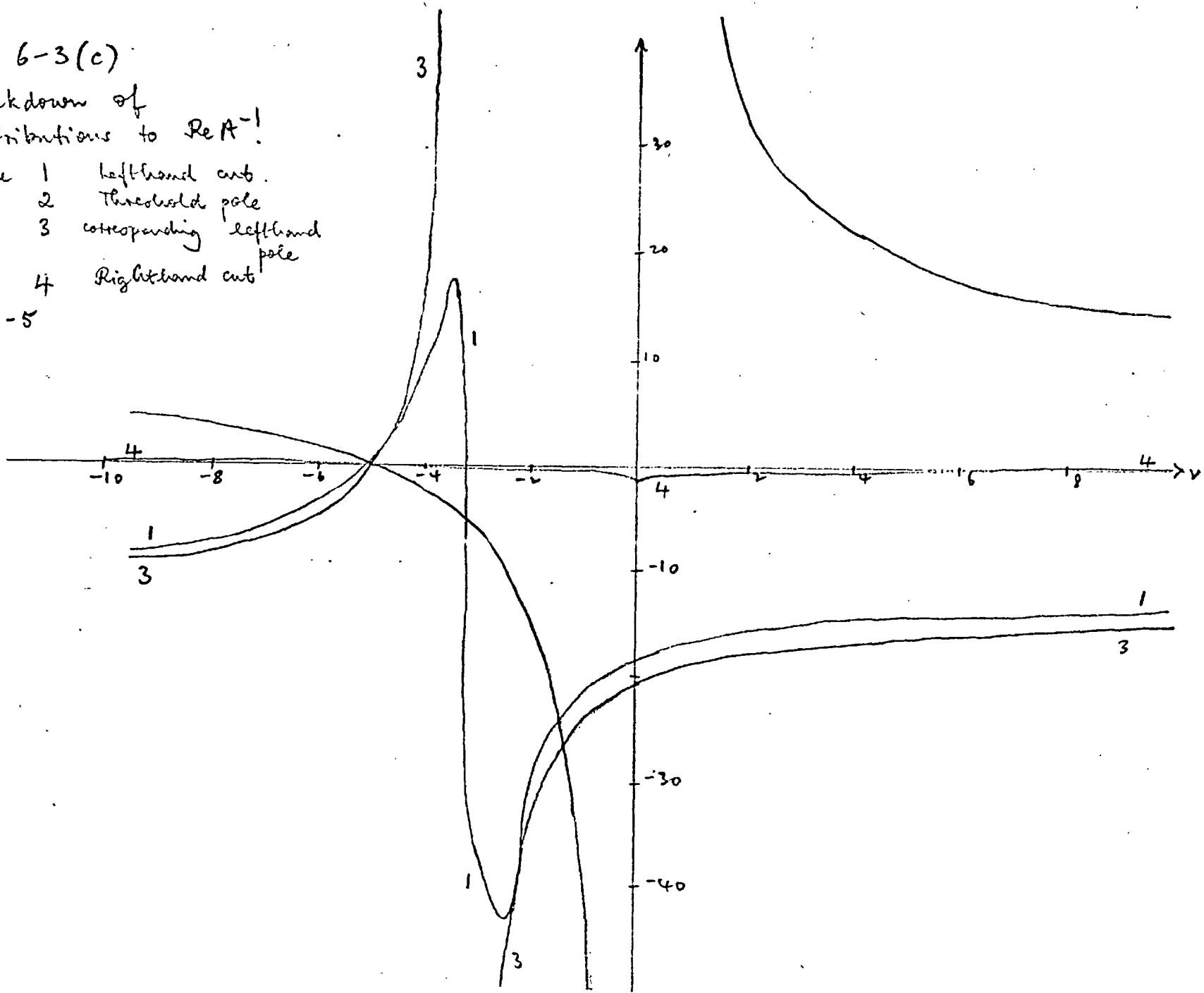

Table 6-5. Model 2. $P_1 \rightarrow P_1$. S function $C(v)$.

$v_R = 6.0$ $\Gamma_{v_R} = 1.5$

REA	IMA	REA-1	REC	IMC	REC-1	V
-1.354	-1.184	-0.418	-1.355	-1.194	-0.415	-9.500
-1.149	-1.355	-0.364	-1.149	-1.355	-0.364	-9.000
-0.846	-1.582	-0.263	-0.887	-1.515	-0.288	-8.500
-0.303	-1.793	-0.092	-0.540	-1.670	-0.175	-8.000
0.558	-1.621	0.190	-0.032	-1.813	-0.010	-7.500
1.126	-0.682	0.650	1.083	-1.934	0.220	-7.000
0.706	0.	1.416	0.745	0.	1.341	-6.500
0.364	0.	2.747	0.342	0.	2.927	-6.000
0.190	0.	5.250	0.176	0.	5.683	-5.500
0.093	0.	10.707	0.087	0.	11.486	-5.000
0.037	0.	27.217	0.035	0.	28.710	-4.500
0.004	0.	285.282	0.003	0.	295.672	-4.000
-0.015	0.	-65.545	-0.015	0.	-66.371	-3.500
-0.025	0.	-40.544	-0.025	0.	-40.254	-3.000
-0.028	0.	-35.936	-0.029	0.	-35.008	-2.500
-0.027	0.	-37.425	-0.028	0.	-35.815	-2.000
-0.025	0.	-39.388	-0.027	0.	-37.440	-1.800
-0.024	0.	-42.288	-0.025	0.	-39.935	-1.600
-0.022	0.	-46.403	-0.023	0.	-43.547	-1.400
-0.019	0.	-52.241	-0.021	0.	-48.731	-1.200
-0.016	0.	-60.744	-0.018	0.	-56.340	-1.000
-0.014	0.	-73.012	-0.015	0.	-68.108	-0.800
-0.010	0.	-95.839	-0.011	0.	-88.110	-0.600
-0.007	0.	-140.860	-0.008	0.	-128.595	-0.400
-0.004	0.	-275.910	-0.004	0.	-250.862	-0.200
0.002	0.000	535.483	0.004	0.000		0.100
0.004	0.000	265.319	0.009	0.000		0.200
0.008	0.000	130.480	0.018	0.000		0.400
0.012	0.000	85.720	0.028	0.000		0.600
0.016	0.000	63.459	0.039	0.001		0.800
0.020	0.000	50.184	0.050	0.002		1.000
0.024	0.000	41.394	0.063	0.003		1.200
0.028	0.001	35.160	0.076	0.004		1.400
0.033	0.001	30.520	0.091	0.007		1.600
0.037	0.001	26.939	0.107	0.009		1.800
0.041	0.001	24.096	0.125	0.013		2.000
0.052	0.002	19.046	0.178	0.027		2.500
0.063	0.003	15.746	0.244	0.054		3.000
0.074	0.005	13.435	0.329	0.105		3.500
0.085	0.006	11.734	0.431	0.203		4.000
0.095	0.008	10.436	0.527	0.387		4.500
0.105	0.010	9.415	0.529	0.690		5.000
0.115	0.012	8.594	0.288	1.005		5.500
0.125	0.015	7.921	-0.115	1.068		6.000
0.134	0.017	7.361	-0.395	0.901		6.500
0.143	0.019	6.888	-0.506	0.706		7.000
0.151	0.022	6.484	-0.532	0.555		7.500
0.159	0.024	6.136	-0.524	0.449		8.000
0.167	0.027	5.832	-0.506	0.375		8.500
0.175	0.030	5.566	-0.485	0.321		9.000
0.182	0.032	5.332	-0.465	0.281		9.500
0.189	0.035	5.123	-0.447	0.251		10.000

Fig 6-3 (b) $\mathrm{Re}A^{-1}$ and $\mathrm{Im}A^{-1}$ for Model 1. $P_1 \to P_1$ (5.0, 1.25) ~ Table 6-3.

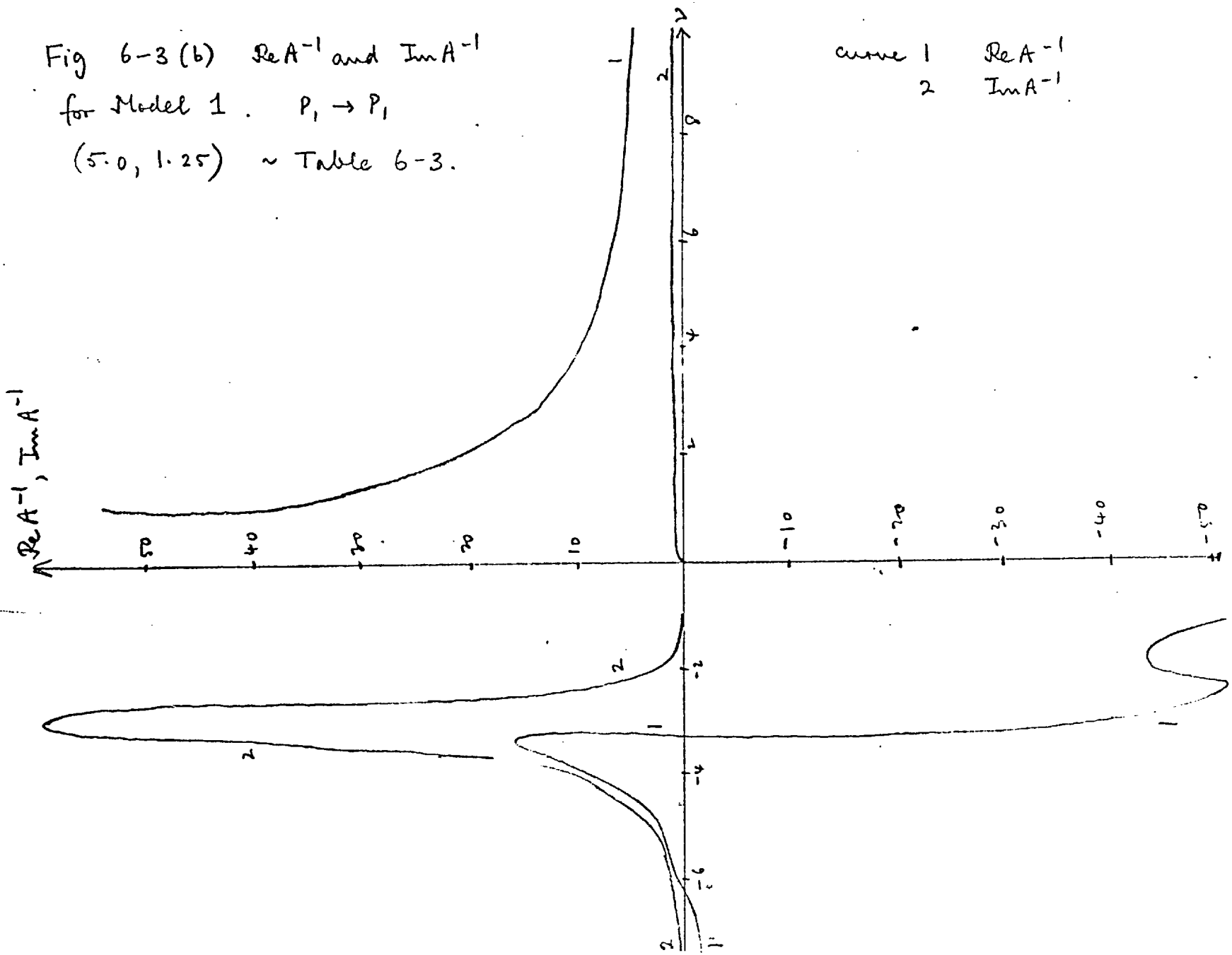

Table 6-4. Model 2. $P_1 \rightarrow P_1$. continuous $C(\nu)$.

$\nu_R = 5.0$ $\Gamma_{\nu_R} = 1.25$

REA	IMA	REA-1	IMA-1	LHPOLE	THPOLE	ν
-0.427	-0.064	-2.293	0.343	-9.402	4.639	-9.500
-0.425	-0.082	-2.269	0.436	-9.077	4.353	-9.000
-0.425	-0.105	-2.219	0.546	-8.690	4.033	-8.500
-0.426	-0.136	-2.130	0.682	-8.224	3.672	-8.000
-0.428	-0.181	-1.981	0.840	-7.649	3.264	-7.500
-0.426	-0.252	-1.740	1.028	-6.923	2.798	-7.000
-0.388	-0.369	-1.353	1.287	-5.977	2.260	-6.500
-0.230	-0.516	-0.721	1.616	-4.695	1.632	-6.000
0.078	-0.463	0.352	2.099	-2.856	0.890	-5.500
0.147	-0.206	2.292	3.217	0.000	-0.000	-5.000
0.097	-0.079	6.217	5.036	5.042	-1.088	-4.500
0.045	-0.028	16.116	10.009	16.332	-2.448	-4.000
0.013	-0.006	62.419	31.484	64.419	-4.197	-3.500
-0.006	-0.003	-140.790	61.987	-136.420	-6.529	-3.000
-0.017	-0.004	-55.203	12.776	-47.523	-9.793	-2.500
-0.022	-0.001	-45.762	2.660	-33.130	-14.690	-2.000
-0.022	-0.001	-45.643	1.362	-30.266	-17.410	-1.800
-0.020	-0.000	-49.661	0.200	-26.454	-25.183	-1.400
-0.018	-0.000	-54.193	0.027	-25.121	-31.012	-1.200
-0.016	0.	-61.304	0.	-24.032	-39.173	-1.000
-0.014	0.	-71.865	0.	-23.125	-51.414	-0.800
-0.011	0.	-92.219	0.	-22.358	-71.817	-0.600
-0.008	0.	-132.702	0.	-21.700	-112.622	-0.400
-0.004	0.	-254.756	0.	-21.131	-235.038	-0.200
-0.052	0.	-19.368	0.	-20.633	0.	0.
0.004	0.000	235.808	-0.408	-20.193	254.624	0.200
0.009	0.000	113.874	-0.535	-19.803	132.209	0.400
0.014	0.000	73.493	-0.612	-19.453	91.404	0.600
0.019	0.000	53.468	-0.667	-19.139	71.001	0.800
0.024	0.000	41.566	-0.707	-18.854	58.759	1.000
0.030	0.001	33.712	-0.739	-18.596	50.598	1.200
0.035	0.001	28.162	-0.764	-18.360	44.769	1.400
0.042	0.001	24.046	-0.784	-18.144	40.397	1.600
0.048	0.002	20.880	-0.802	-17.945	36.997	1.800
0.054	0.002	18.375	-0.816	-17.761	34.276	2.000
0.071	0.004	13.952	-0.845	-17.359	29.380	2.500
0.090	0.007	11.085	-0.866	-17.021	26.115	3.000
0.109	0.011	9.092	-0.882	-16.734	23.784	3.500
0.129	0.015	7.635	-0.894	-16.486	22.035	4.000
0.150	0.021	6.530	-0.905	-16.271	20.675	4.500
0.172	0.028	5.666	-0.913	-16.083	19.586	5.000
0.194	0.036	4.975	-0.920	-15.915	18.696	5.500
0.217	0.046	4.412	-0.926	-15.766	17.954	6.000
0.240	0.057	3.945	-0.931	-15.633	17.326	6.500
0.263	0.069	3.553	-0.935	-15.512	16.788	7.000
0.286	0.084	3.219	-0.939	-15.403	16.322	7.500
0.309	0.099	2.933	-0.943	-15.304	15.914	8.000
0.331	0.117	2.684	-0.946	-15.213	15.554	8.500
0.353	0.136	2.467	-0.949	-15.129	15.234	9.000
0.374	0.156	2.276	-0.951	-15.052	14.948	9.500
0.354	0.178	2.107	-0.953	-14.981	14.690	10.000

$A^{-1}(\nu_0) \neq 0$, the main terms are the threshold poles and the left hand cut (pole). The existence of resonances must be due to these terms alone. For a single left hand pole in the P_1 wave a resonance can only arise by cancellation of the left hand pole and the threshold term . Because the threshold pole term is important and its estimation by the fixed S dispersion relation is not very accurate, it is probably better to treat the threshold residues as parameters to be determined by self consistency requirements.

MODEL 3

It was also realised that one can use $C^{-1}(\nu)$ itself to represent the left hand singularities and this defines "Model 3."

In a once subtracted form

$$A_l^{-1}(\nu) = [C_l^{-1}(\nu) - C_l^{-1}(\nu_0)] + A^{-1}(\nu_0) + \frac{(\nu-\nu_0)}{\pi} \cdot I(\nu, \nu_0)$$

This has $\mathrm{Im}A_l^{-1}(\nu) = -\sqrt{\frac{\nu}{\nu+1}}$ ν in $[0,\infty]$

$= \mathrm{Im}C_l^{-1}(\nu)$ ν in $[-1, -\infty]$

Note $\mathrm{Im}A_l(\nu) \neq \mathrm{Im}C_l(\nu)$. $\nu < -1$.

Also A_l^{-1} has threshold poles of orders 1, . . (l-1) with residues the same as those of $C_l^{-1}(\nu)$. It has the near left hand cut exactly integrated, but has the (very small) far left hand cut of $C^{-1}(\nu)$ also added.

If $C^{-1}(\nu)$ is taken with δ-function approximation in the crossed channel, then it will have the correct left hand pole.

Tabulations in the P_1 only case are shown and are close to those for Models 1 and 2. This confirms the accuracy of the integrations in Model 1 and also indicates that Model 3 does not have any complex poles, since Model 1 only has the contribution from the cut and neglects contributions from any complex poles.

This model is parallel to the Ansatz procedures for the Zachariasen

Table 6-6 $P_1 \rightarrow P_1$ Model 3.

Re A	Im A	Re A-1	Im A-1	Re C	Im C	Re C-1	ν
-1.567	-0.826	-0.499	0.263	-1.262	-0.480	-0.592	-10.000
-1.343	-0.890	-0.517	0.343	-1.157	-0.570	-0.695	-9.500
-1.127	-0.933	-0.526	0.436	-1.036	-0.656	-0.689	-9.000
-0.914	-0.956	-0.523	0.546	-0.897	-0.732	-0.669	-8.500
-0.699	-0.956	-0.498	0.682	-0.731	-0.794	-0.628	-8.000
-0.490	-0.934	-0.441	0.840	-0.547	-0.832	-0.552	-7.500
-0.286	-0.879	-0.335	1.028	-0.344	-0.830	-0.427	-7.000
-0.060	-0.773	-0.100	1.287	-0.102	-0.764	-0.171	-6.500
0.099	-0.603	0.265	1.616	0.081	-0.608	0.216	-6.000
0.188	-0.385	1.026	2.099	0.185	-0.388	1.000	-5.500
0.147	-0.206	2.292	3.217	0.147	-0.206	2.292	-5.000
0.099	-0.104	4.822	5.036	0.099	-0.103	4.850	-4.500
0.050	-0.051	9.723	10.009	0.050	-0.051	9.783	-4.000
0.013	-0.025	16.425	31.484	0.013	-0.025	16.520	-3.500
-0.007	-0.011	-39.680	61.987	-0.007	-0.011	-39.546	-3.000
-0.018	-0.005	-51.136	12.776	-0.018	-0.005	-50.957	-2.500
-0.023	-0.001	-43.909	2.660	-0.023	-0.001	-43.675	-2.000
-0.023	-0.001	-43.658	1.362	-0.023	-0.001	-43.399	-1.800
-0.021	-0.000	-47.234	0.200	-0.021	-0.000	-46.917	-1.600
-0.019	-0.000	-51.566	0.027	-0.020	-0.000	-51.214	-1.400
-0.017	0.	-58.586	0.	-0.017	0.	-58.195	-1.200
-0.014	0.	-69.136	0.	-0.014	0.	-69.518	-1.000
-0.011	0.	-89.500	0.	-0.011	0.	-89.163	-0.800
-0.008	0.	-129.984	0.	-0.008	0.	-129.313	-0.600
-0.004	0.	-251.966	0.	-0.004	0.	-251.066	-0.400
-0.973	0	-1.028	0.			-0.001	-0.200
0.002	0.000	482.399	-0.302			483.365	0.
0.004	0.000	238.044	-0.408			238.959	0.100
0.009	0.000	116.185	-0.535			117.010	0.200
0.013	0.000	75.805	-0.612			76.555	0.400
0.018	0.000	55.764	-0.667			56.450	0.600
0.023	0.000	43.840	-0.707			44.471	0.800
0.028	0.001	35.963	-0.739			36.545	1.000
0.033	0.001	30.389	-0.764			30.928	1.200
0.038	0.001	26.250	-0.784			26.749	1.400
0.043	0.002	23.061	-0.802			23.526	1.600
0.049	0.002	20.536	-0.816			20.968	1.800
0.062	0.003	16.065	-0.845			16.426	2.000
0.076	0.005	13.156	-0.866			13.457	2.500
0.089	0.007	11.126	-0.882			11.376	3.000
0.103	0.010	9.637	-0.894			9.843	3.500
0.116	0.012	8.503	-0.905			8.669	4.000
0.129	0.016	7.615	-0.913			7.745	4.500
0.142	0.019	6.901	-0.920			6.999	5.000
0.155	0.023	6.318	-0.926			6.386	5.500
0.167	0.027	5.833	-0.931			5.873	6.000
0.179	0.031	5.424	-0.935			5.439	6.500
0.191	0.035	5.075	-0.939			5.067	7.000
0.202	0.040	4.775	-0.943			4.744	7.500
0.212	0.044	4.513	-0.946			4.462	8.000
0.222	0.049	4.284	-0.949			4.214	8.500
0.232	0.054	4.082	-0.951			3.993	9.000
0.242	0.059	3.903	-0.953			3.796	9.500
							10.000

method and the variational method, but here we have automatic unitarity and automatically correct threshold behaviour.

The unsubtracted version is

$$A^{-1}(\nu) = C^{-1}(\nu) + \frac{2}{\pi}\sqrt{\frac{\nu}{\nu+1}} \cdot \log\left[\sqrt{\nu} + \sqrt{\nu+1}\right]$$

One can see that Model 3 is unlikely to produce resonances since $C^{-1}(\nu)$ usually has a single sign for $\nu > 0$ for one or two exchanged particles, and is much larger than the second term. For a resonance, we need $A^{-1}(\nu_R) = 0$. A difference between Model 3 and Models 1 and 2 is their asymptotic behaviour, which we now discuss in general.

ASYMPTOTIC BEHAVIOUR

A. Behaviour of right hand cut, threshold term and constant term

Right hand cut $I(\kappa, \nu_0) \cdot (\nu - \nu_0)$ $\quad \mathrm{Re}A^{-1}(\nu_0) \longrightarrow_{\nu \to \pm\infty}$ const.

$\mathrm{Re}(\mathrm{RHC}(\nu)) \longrightarrow_{\nu \to \pm\infty} -\log \nu$ $\quad (\nu - \nu_0)\sum_{n=1}^{l-1} \frac{g_l^n}{\nu^n} \longrightarrow_{\nu \to \pm\infty} g_1^1$

$\mathrm{Im}(\mathrm{RHC}(\nu)) = \sqrt{\frac{\nu}{\nu+1}} \cdot R(\nu) \longrightarrow_{\nu \to +\infty} R(\infty)$, probably finite.

B. Behaviour of $C^{-1}(\nu)$

as discussed in Chapter 2.

$$\mathrm{ImC}_{lm}(\nu) \longrightarrow_{\nu \to -\infty} \nu^{l}$$

$$\mathrm{ReC}_{lm}(\nu) \longrightarrow_{\nu \to \pm\infty} \nu^{l-1}\log\nu$$

$$\therefore \frac{\mathrm{ImC}_{lm}}{\mathrm{ReC}_{lm}} \longrightarrow_{\nu \to -\infty} \frac{\nu}{\log\nu} \longrightarrow_{\nu \to +\infty} 0$$

$$\therefore \mathrm{ImC}^{-1}_{lm} \longrightarrow_{\nu \to -\infty} \frac{1}{\pi \mathrm{ImC}_m} \longrightarrow \nu^{-l}.$$

$$\mathrm{ReC}^{-1}_{lm} = \frac{\mathrm{ReC}_{lm}}{\mathrm{Re}^2 + \mathrm{Im}^2}$$

$$\longrightarrow_{\nu \to -\infty} \nu^{l-1}\log\nu = \nu^{-l-1}\log\nu$$

$$\longrightarrow_{\nu \to +\infty} \frac{\nu^{1-l}}{\log\nu}$$

C. MODEL 3

$$A^{-1} = C^{-1} + \text{RHC}$$

for $\ell \geq 1$ RHC dominates as $\nu \longrightarrow +\infty$

and $A^{-1} \underset{\nu \to +\infty}{\longrightarrow} 0(\log \nu) + i R(\infty)$

for $\ell = 0$ C^{-1} dominates

so $A_0^{-1} \longrightarrow 0(\nu / \log \nu) + i R(\infty)$.

As $\nu \longrightarrow -\infty$ RHC dominates for all ℓ

$A^{-1} \longrightarrow 0(\log \nu) + i R(\infty)$.

D. MODELS 1 and 2

Models 1 and 2 LHC $\underset{\nu \to \pm\infty}{\longrightarrow} 0\left(\frac{1}{\nu}\right) + i.0$

$\therefore$ RHC dominates as $\longrightarrow \pm\infty$

$A^{-1} \underset{\nu \to \pm\infty}{\longrightarrow} C(\log \nu) + i R(\infty)$

E. MARGINAL SINGULARITY AND PURE ABSORPTION

In these models, we see that the amplitude becomes purely real as $\nu \longrightarrow +\infty$. If we want it to become purely imaginary, assuming $R(\infty)$ stays finite, then since $\text{Im}A = -\text{Im}A^{-1} / |A^{-1}|^2$, and $\text{Re}A = \text{Re}A^{-1} / |A^{-1}|$ and we want $\frac{\text{Re}A}{\text{Im}A} \longrightarrow 0$ we need $\frac{\text{Re}A^{-1}}{\text{Im}A^{-1}} \longrightarrow 0$.

$$\text{Re}A^{-1}(\nu_0) \underset{\nu \to \infty}{\longrightarrow} \text{const. real}$$

$$(\nu - \nu_0) \sum_{n=1}^{\ell-1} \frac{g_n}{\nu^n} \underset{\nu \to \infty}{\longrightarrow} g_1, \text{ real}$$

$$\text{RHC} \underset{\nu \to +\infty}{\longrightarrow} 0(\log \nu). + i.R(\infty)$$

$\therefore$ it follows that Re LHC $\underset{\nu \to +\infty}{\longrightarrow} \log \nu$

in order to cancel this and further that the real constant terms cancel out each other, so $A^{-1} \longrightarrow i R(\infty)$.

Thus, if we assume this behaviour, we only need 1 subtraction of our partial wave dispersion relation.

If we assume $\mathrm{Im}A \longrightarrow$ constant, $\mathrm{Re}A \longrightarrow 0$, then $\mathrm{Im}A^{-1} \longrightarrow$ constant $\mathrm{Re}A^{-1} \longrightarrow 0$.

Also since RHC $(A^{-1}) \longrightarrow$ log

then LHC $(A^{-1}) \longrightarrow$ log (independent of [ )

and if we take $\mathrm{Im}B^{-1} \longrightarrow$ constant

$\mathrm{Im}B \longrightarrow$ constant

then it follows that $\mathrm{Re}B \longrightarrow 0$.

(note here $B^{-1} = \int_{-\infty}^{-1} \frac{\mathrm{Im}A^{-1}(\nu')\, d\nu'}{\nu' - \nu}$ * $\frac{1}{B}$).

The condition LHC $\longrightarrow \log \nu$ is not satisfied by any of our models, which all give purely real behaviour at infinity. Of course, if we are pursuing a purely elastic model, these considerations are less relevant.

MODEL 3 RESULTS AND DISCUSSION

Lu ing has defined a similar approximation in potential scattering which he calls a "unitarised Born approximation."

Since $A^{-1} = B^{-1} + K$. a pole of B is not a pole of A but a zero of A. A pole of A is obtained by $BK + 1 = 0$ and will be near a pole of B if Kg_p is small w.r.t. $(\nu - \nu_p)$ where g_p, ν_p are its residue and position. In the multi-channel case, A^{-1} is the K^{-1} matrix and Dalitz has defined a particle to be a pole of K not of T. These are not always the same and there is sometimes (9) no nearly associated pole of the T matrix. Model 3 is not independent of ν_c, unless we take

$$A^{-1}(\nu) = A^{-1}(\nu_o) + \left[C^{-1}(\nu) - C^{-1}(\nu_o)\right] + \frac{(\nu - \nu_o)}{\pi} \cdot I(\nu, \nu_o)$$

If we take

$$A^{-1}(\nu) = C^{-1}(\nu) + \frac{(\nu - \nu_o)}{\pi} \cdot I(\nu, \nu_o)$$

the second term varies logarithmically with ν_o. We showed the Model to be fairly insensitive in the near region. Tables 6 and 7 - C show $P_1 \longrightarrow P_1$

Table 6-7-a $P_1 \rightarrow S_0$ Model 3.

ReA	ImA	ReA-1	ImA-1	ReC-1	ν
0.428	6.080	0.012	-0.164	-0.018	-10.000
-0.370	5.983	-0.010	-0.167	-0.026	-9.500
-1.144	5.681	-0.034	-0.169	-0.034	-9.000
-1.825	5.195	-0.060	-0.171	-0.044	-8.500
-2.364	4.571	-0.089	-0.173	-0.056	-8.000
-2.743	3.871	-0.122	-0.172	-0.070	-7.500
-2.985	3.144	-0.159	-0.167	-0.088	-7.000
-3.155	2.406	-0.200	-0.153	-0.109	-6.500
-3.562	1.513	-0.238	-0.101	-0.125	-6.000
-2.131	0.	-0.469	0.	-0.332	-5.500
-1.354	0.	-0.738	0.	-0.576	-5.000
-0.840	0.	-1.190	0.	-0.999	-4.500
-0.424	0.	-2.357	0.	-2.135	-4.000
-0.046	0.	-21.929	0.	-21.672	-3.500
0.336	0.	2.973	0.	3.269	-3.000
0.769	0.	1.300	0.	1.642	-2.500
1.342	0.	0.745	0.	1.142	-2.000
1.654	0.	0.604	0.	1.026	-1.800
2.615	0.	0.382	0.	0.862	-1.400
3.476	0.	0.288	0.	0.802	-1.200
5.062	0.	0.198	0.	0.751	-1.000
1.078	0.	0.927	0.	0.708	-0.800
5.839	0.	0.171	0.	0.671	-0.600
-5.095	0.	-0.196	0.	0.638	-0.400
-2.308	0.	-0.433	0.	0.609	-0.200
-1.649	0.	-0.606	0.	0.584	0.
-1.192	0.942	-0.516	-0.408	0.561	0.200
-0.920	1.102	-0.447	-0.535	0.541	0.400
-0.740	1.161	-0.390	-0.612	0.522	0.600
-0.611	1.185	-0.343	-0.667	0.505	0.800
-0.513	1.194	-0.304	-0.707	0.490	1.000
-0.436	1.195	-0.269	-0.739	0.476	1.200
-0.373	1.193	-0.239	-0.764	0.463	1.400
-0.321	1.188	-0.212	-0.784	0.451	1.600
-0.277	1.183	-0.188	-0.802	0.439	1.800
-0.238	1.176	-0.165	-0.816	0.429	2.000
-0.162	1.161	-0.118	-0.845	0.406	2.500
-0.103	1.145	-0.078	-0.866	0.386	3.000
-0.057	1.131	-0.044	-0.882	0.369	3.500
-0.018	1.118	-0.014	-0.894	0.354	4.000
0.015	1.105	0.012	-0.905	0.341	4.500
0.043	1.094	0.036	-0.913	0.329	5.000
0.068	1.083	0.058	-0.920	0.318	5.500
0.091	1.072	0.078	-0.926	0.309	6.000
0.111	1.063	0.097	-0.931	0.300	6.500
0.129	1.053	0.114	-0.935	0.292	7.000
0.145	1.044	0.131	-0.939	0.285	7.500
0.160	1.036	0.146	-0.943	0.278	8.000
0.174	1.028	0.160	-0.946	0.272	8.500
0.187	1.020	0.174	-0.949	0.266	9.000
0.199	1.012	0.187	-0.951	0.261	9.500
0.211	1.005	0.200	-0.953	0.256	10.000

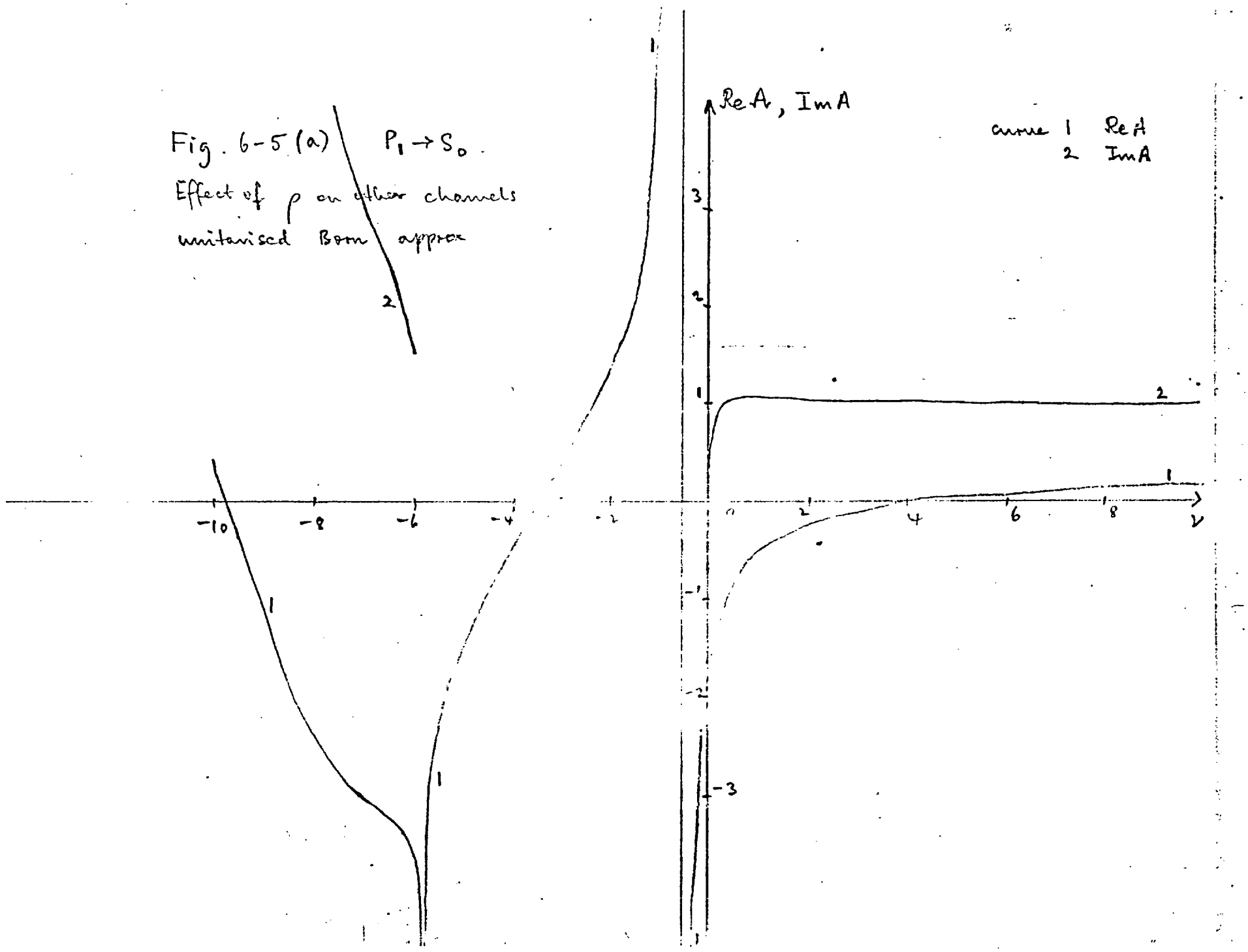
Fig. 6-5 (a)
$P_1 \to S_0$
Effect of ρ on other channels
unitarised Born approx
2
1
Re A, Im A
curve 1 Re A
2 Im A
3
2
1
2
1
-1
-2
-3
-10
-8
-6
-4
-2
0
2
4
6
8
ν
1
1

Table 6-7-b $P_1 \rightarrow S_2$ Model 3.

ReA	ImA	ReA-1	ImA-1	ReC-1	Y
0.600	-2.932	0.067	0.327	0.037	-10.000
0.578	-2.887	0.067	0.333	0.051	-9.500
0.572	-2.841	0.068	0.338	0.068	-9.000
0.586	-2.795	0.072	0.343	0.088	-8.500
0.628	-2.754	0.079	0.345	0.112	-8.000
0.709	-2.723	0.090	0.344	0.141	-7.500
0.859	-2.717	0.106	0.335	0.176	-7.000
1.162	-2.788	0.127	0.306	0.219	-6.500
2.293	-3.404	0.136	0.202	0.249	-6.000
1.855	0.	0.528	0.	0.665	-5.500
1.012	0.	0.988	0.	1.151	-5.000
0.553	0.	1.807	0.	1.998	-4.500
0.247	0.	4.048	0.	4.270	-4.000
0.025	0.	43.086	0.	43.343	-3.500
-0.146	0.	-6.835	0.	-6.539	-3.000
-0.276	0.	-3.627	0.	-3.284	-2.500
-0.373	0.	-2.680	0.	-2.284	-2.000
-0.404	0.	-2.474	0.	-2.053	-1.800
-0.454	0.	-2.205	0.	-1.725	-1.400
-0.472	0.	-2.118	0.	-1.604	-1.200
-0.486	0.	-2.056	0.	-1.502	-1.000
-0.836	0.	-1.197	0.	-1.416	-0.800
-0.543	0.	-1.841	0.	-1.341	-0.600
-0.474	0.	-2.111	0.	-1.276	-0.400
-0.442	0.	-2.262	0.	-1.219	-0.200
-0.424	0.	-2.358	0.	-1.168	0.
-0.432	0.057	-2.275	-0.302	-1.145	0.100
-0.439	0.082	-2.200	-0.408	-1.122	0.200
-0.453	0.117	-2.069	-0.535	-1.081	0.400
-0.465	0.146	-1.957	-0.612	-1.044	0.600
-0.477	0.171	-1.859	-0.667	-1.011	0.800
-0.487	0.194	-1.773	-0.707	-0.980	1.000
-0.496	0.216	-1.696	-0.739	-0.951	1.200
-0.504	0.236	-1.627	-0.764	-0.925	1.400
-0.511	0.256	-1.564	-0.784	-0.901	1.600
-0.517	0.275	-1.506	-0.802	-0.879	1.800
-0.523	0.294	-1.452	-0.816	-0.858	2.000
-0.535	0.338	-1.335	-0.845	-0.812	2.500
-0.543	0.380	-1.236	-0.866	-0.772	3.000
-0.547	0.420	-1.151	-0.882	-0.738	3.500
-0.550	0.457	-1.076	-0.894	-0.708	4.000
-0.549	0.492	-1.010	-0.905	-0.681	4.500
-0.547	0.526	-0.950	-0.913	-0.658	5.000
-0.543	0.557	-0.897	-0.920	-0.637	5.500
-0.538	0.587	-0.848	-0.926	-0.617	6.000
-0.531	0.616	-0.803	-0.931	-0.600	6.500
-0.523	0.643	-0.762	-0.935	-0.584	7.000
-0.515	0.668	-0.724	-0.939	-0.570	7.500
-0.505	0.692	-0.689	-0.943	-0.556	8.000
-0.495	0.714	-0.655	-0.946	-0.544	8.500
-0.484	0.735	-0.624	-0.949	-0.532	9.000
-0.473	0.755	-0.595	-0.951	-0.522	9.500
-0.461	0.774	-0.568	-0.953	-0.512	10.000

Table 6-4-c $P_1 \to P_1$ Model 3. $\nu_0 = -9$.

$\mathcal{A}(\nu_0) = -0.477$. $\nu_R = 5.0$, $\Gamma\nu_R = 1.25$.

ReA	ImA	ReA-1	ImA-1	RHI	ReC-1	ν
-1.036	-0.155	-0.944	0.142	0.030	-0.497	-10.000
-1.008	-0.206	-0.953	0.194	0.015	-0.491	-9.500
-0.979	-0.261	-0.954	0.254	-0.000	-0.477	-9.000
-0.950	-0.323	-0.944	0.321	-0.016	-0.451	-8.500
-0.921	-0.396	-0.916	0.394	-0.033	-0.406	-8.000
-0.894	-0.487	-0.863	0.470	-0.051	-0.334	-7.500
-0.872	-0.612	-0.768	0.539	-0.071	-0.221	-7.000
-0.878	-0.819	-0.609	0.568	-0.091	-0.041	-6.500
-1.240	-1.375	-0.362	0.401	-0.113	0.229	-6.000
0.988	0.	1.013	0.	-0.137	1.626	-5.500
0.312	0.	3.207	0.	-0.163	3.646	-5.000
0.127	0.	7.882	0.	-0.191	8.550	-4.500
0.045	0.	22.240	0.	-0.222	22.939	-4.000
0.003	0.	290.542	0.	-0.257	291.276	-3.500
-0.018	0.	-56.178	0.	-0.297	-55.405	-3.000
-0.027	0.	-36.576	0.	-0.342	-35.756	-2.500
-0.029	0.	-33.913	0.	-0.397	-33.039	-2.000
-0.029	0.	-34.659	0.	-0.422	-33.761	-1.800
-0.028	0.	-36.321	0.	-0.449	-35.394	-1.600
-0.026	0.	-39.043	0.	-0.480	-38.086	-1.400
-0.023	0.	-43.171	0.	-0.514	-42.180	-1.200
-0.020	0.	-49.398	0.	-0.554	-48.368	-1.000
-0.017	0.	-58.349	0.	0.219	-58.091	-0.800
-0.013	0.	-75.737	0.	-0.499	-74.761	-0.600
-0.009	0.	-109.970	0.	-0.834	-108.659	-0.400
-0.005	0.	-212.783	0.	-1.043	-211.263	-0.200
0.002	0.000	405.495	-0.302	-1.131	407.102	0.100
0.005	0.000	199.732	-0.408	-1.078	201.287	0.200
0.010	0.000	97.107	-0.535	-0.987	98.571	0.400
0.016	0.000	63.093	-0.612	-0.912	64.483	0.600
0.022	0.000	46.210	-0.667	-0.849	47.535	0.800
0.028	0.001	36.164	-0.707	-0.794	37.434	1.000
0.034	0.001	29.526	-0.739	-0.745	30.748	1.200
0.040	0.001	24.831	-0.764	-0.702	26.009	1.400
0.047	0.002	21.344	-0.784	-0.662	22.483	1.600
0.053	0.002	18.659	-0.802	-0.627	19.763	1.800
0.060	0.003	16.532	-0.816	-0.594	17.604	2.000
0.078	0.005	12.770	-0.845	-0.524	13.771	2.500
0.096	0.008	10.325	-0.866	-0.464	11.266	3.000
0.115	0.012	8.621	-0.882	-0.413	9.511	3.500
0.134	0.016	7.373	-0.894	-0.368	8.218	4.000
0.153	0.021	6.425	-0.905	-0.328	7.230	4.500
0.172	0.028	5.682	-0.913	-0.293	6.452	5.000
0.190	0.034	5.088	-0.920	-0.260	5.825	5.500
0.209	0.042	4.602	-0.926	-0.231	5.310	6.000
0.227	0.050	4.199	-0.931	-0.203	4.879	6.500
0.245	0.059	3.860	-0.935	-0.178	4.515	7.000
0.262	0.069	3.572	-0.939	-0.154	4.203	7.500
0.278	0.079	3.324	-0.943	-0.132	3.933	8.000
0.294	0.090	3.108	-0.946	-0.112	3.697	8.500
0.310	0.101	2.920	-0.949	-0.092	3.489	9.000
0.324	0.112	2.754	-0.951	-0.074	3.305	9.500
0.338	0.124	2.607	-0.953	-0.056	3.140	10.000

Table 6-7-d $P_1 \to D_0$ Model 3.

Re A	Im A	Re A-1	Im A-1	Re C-1	V
1.469	-2.517	0.173	0.296	0.143	-10.000
1.747	-2.311	0.208	0.275	0.193	-9.500
2.073	-2.042	0.245	0.241	0.245	-9.000
2.450	-1.657	0.280	0.189	0.296	-8.500
2.858	-1.066	0.307	0.115	0.340	-8.000
3.178	-0.114	0.314	0.011	0.366	-7.500
3.022	1.333	0.277	-0.122	0.348	-7.000
1.578	2.866	0.147	-0.268	0.239	-6.500
-1.580	2.638	-0.167	-0.279	-0.054	-6.000
-0.549	0.	-1.822	0.	-1.635	-5.500
-0.180	0.	-5.561	0.	-5.399	-5.000
-0.064	0.	-15.510	0.	-15.319	-4.500
-0.019	0.	-51.720	0.	-51.498	-4.000
-0.001	0.	-817.429	0.	-817.171	-3.500
0.005	0.	195.545	0.	195.842	-3.000
0.006	0.	161.976	0.	162.318	-2.500
0.005	0.	198.862	0.	199.259	-2.000
0.004	0.	231.019	0.	231.440	-1.800
0.004	0.	278.583	0.	279.032	-1.600
0.003	0.	350.022	0.	350.502	-1.400
0.002	0.	461.746	0.	462.261	-1.200
0.002	0.	648.309	0.	648.863	-1.000
0.001	0.	993.309	0.	993.089	-0.800
0.001	0.	1735.794	0.	1736.293	-0.600
0.000	0.	3854.167	0.	3855.001	-0.400
0.000	0.	15268.664	0.	++++++++	-0.200
0.000	0.000	50565.622	-0.302	++++++++	0.100
0.000	0.000	15141.728	-0.408	++++++++	0.200
0.000	0.000	3742.565	-0.535	3743.553	0.400
0.001	0.000	1658.026	-0.612	1658.939	0.600
0.001	0.000	930.763	-0.667	931.611	0.800
0.002	0.000	595.153	-0.707	595.947	1.000
0.002	0.000	413.314	-0.739	414.059	1.200
0.003	0.000	303.924	-0.764	304.626	1.400
0.004	0.000	233.067	-0.784	233.729	1.600
0.005	0.000	184.569	-0.802	185.196	1.800
0.007	0.000	149.928	-0.816	150.523	2.000
0.010	0.000	96.851	-0.845	97.375	2.500
0.015	0.000	68.059	-0.866	68.523	3.000
0.020	0.000	50.697	-0.882	51.110	3.500
0.025	0.001	39.415	-0.894	39.783	4.000
0.032	0.001	31.603	-0.905	31.932	4.500
0.038	0.001	26.102	-0.913	26.394	5.000
0.045	0.002	21.972	-0.920	22.232	5.500
0.053	0.003	18.817	-0.926	19.047	6.000
0.061	0.003	16.350	-0.931	16.553	6.500
0.069	0.005	14.362	-0.935	14.560	7.000
0.078	0.006	12.786	-0.939	12.941	7.500
0.087	0.007	11.473	-0.943	11.605	8.000
0.096	0.009	10.377	-0.946	10.489	8.500
0.105	0.011	9.454	-0.949	9.546	9.000
0.114	0.013	8.667	-0.951	8.741	9.500
0.123	0.015	7.991	-0.953	8.047	10.000

Table 6-4-e $P_1 \rightarrow D_2$ Model -

Re A	Im A	Re A-1	Im A-1	Re C-1	ν
-0.614	1.422	-0.256	-0.593	-0.286	-10.000
-0.841	1.251	-0.370	-0.551	-0.386	-9.500
-1.036	1.021	-0.490	-0.482	-0.490	-9.000
-1.184	0.737	-0.609	-0.379	-0.592	-8.500
-1.269	0.407	-0.714	-0.229	-0.681	-8.000
-1.277	0.037	-0.783	-0.023	-0.731	-7.500
-1.185	-0.378	-0.766	0.244	-0.695	-7.000
-0.932	-0.878	-0.568	0.535	-0.477	-6.500
-0.017	-1.792	-0.005	0.558	0.108	-6.000
0.309	0.	3.234	0.	3.371	-5.500
0.094	0.	10.635	0.	10.737	-5.000
0.033	0.	30.448	0.	30.639	-4.500
0.010	0.	102.773	0.	102.995	-4.000
0.001	0.	1634.086	0.	1634.343	-3.500
-0.003	0.	-391.980	0.	-391.683	-3.000
-0.003	0.	-324.979	0.	-324.636	-2.500
-0.003	0.	-398.914	0.	-398.517	-2.000
-0.002	0.	-463.303	0.	-462.881	-1.800
-0.001	0.	-701.483	0.	-701.003	-1.400
-0.001	0.	-925.035	0.	-924.521	-1.200
-0.001	0.	-1298.279	0.	--------	-1.000
-0.001	0.	-1985.959	0.	--------	-0.800
-0.000	0.	-3473.085	0.	--------	-0.600
-0.000	0.	-7710.837	0.	--------	-0.400
-0.000	0.	-30540.457	0.	--------	-0.200
-0.840	0.	-1.190	0.	0.000	0.
-0.000	0.000	----------	-0.302	--------	0.100
-0.000	0.000	-30286.688	-0.408	--------	0.200
-0.000	0.000	-7488.093	-0.535	--------	0.400
-0.000	0.000	-3318.790	-0.612	--------	0.600
-0.001	0.000	-1864.071	-0.667	--------	0.800
-0.001	0.000	-1192.687	-0.707	--------	1.000
-0.001	0.000	-828.864	-0.739	-828.119	1.200
-0.002	0.000	-609.953	-0.764	-609.251	1.400
-0.002	0.000	-468.120	-0.784	-467.458	1.600
-0.003	0.000	-371.019	-0.802	-370.392	1.800
-0.003	0.000	-301.640	-0.816	-301.045	2.000
-0.005	0.000	-195.274	-0.845	-194.750	2.500
-0.007	0.000	-137.510	-0.866	-137.046	3.000
-0.010	0.000	-102.633	-0.882	-102.220	3.500
-0.013	0.000	-79.935	-0.894	-79.567	4.000
-0.016	0.000	-64.312	-0.905	-63.984	4.500
-0.019	0.000	-53.082	-0.913	-52.789	5.000
-0.022	0.000	-44.724	-0.920	-44.464	5.500
-0.026	0.001	-38.325	-0.926	-38.095	6.000
-0.030	0.001	-33.309	-0.931	-33.106	6.500
-0.034	0.001	-29.298	-0.935	-29.120	7.000
-0.038	0.001	-26.035	-0.939	-25.881	7.500
-0.043	0.002	-23.342	-0.943	-23.210	8.000
-0.047	0.002	-21.089	-0.946	-20.977	8.500
-0.052	0.003	-19.183	-0.949	-19.091	9.000
-0.057	0.003	-17.555	-0.951	-17.462	9.500
-0.062	0.004	-16.151	-0.953	-16.095	10.000

Table 6-7-f $P_1 \rightarrow F_1$ Model 3.

Re A	Im A	Re A-1	Im A-1	Re C-1	ν
1.031	0.708	0.659	-0.453	0.629	-10.000
0.838	0.923	0.539	-0.594	0.524	-9.500
0.560	1.101	0.367	-0.722	0.367	-9.000
0.155	1.196	0.133	-0.814	0.149	-8.500
-0.229	1.152	-0.166	-0.835	-0.133	-8.000
-0.647	0.920	-0.512	-0.727	-0.460	-7.500
-0.965	0.478	-0.832	-0.412	-0.762	-7.000
-1.057	-0.193	-0.915	0.167	-0.824	-6.500
-0.413	-1.408	-0.192	0.654	-0.079	-6.000
0.156	0.	6.420	0.	6.556	-5.500
0.035	0.	28.204	0.	28.367	-5.000
0.010	0.	102.448	0.	102.639	-4.500
0.002	0.	431.836	0.	432.058	-4.000
0.000	0.	8564.157	0.	8564.414	-3.500
-0.000	0.	-2585.742	0.	--------	-3.000
-0.000	0.	-2781.931	0.	--------	-2.500
-0.000	0.	-4487.426	0.	--------	-2.000
-0.000	0.	-5924.380	0.	--------	-1.800
-0.000	0.	-8213.442	0.	--------	-1.600
-0.000	0.	-12043.911	0.	--------	-1.400
-0.000	0.	-18915.256	0.	--------	-1.200
-0.000	0.	-32487.235	0.	--------	-1.000
-0.000	0.	-63331.977	0.	--------	-0.800
-0.000	0.	----------	0.	--------	-0.600
-0.000	0.	----------	0.	--------	-0.400
0.000	0.	353945.997	0.	++++++++	-0.200
0.000	0.000	3113.708	-0.302	3114.839	0.100
-0.000	0.000	-42006.589	-0.408	--------	0.200
0.000	0.000	597256.533	-0.535	++++++++	0.400
0.000	0.000	166150.261	-0.612	++++++++	0.600
0.000	0.000	67479.791	-0.667	++++++++	0.800
0.000	0.000	35464.260	-0.707	++++++++	1.000
0.000	0.000	20805.658	-0.739	++++++++	1.200
0.000	0.000	13319.050	-0.764	++++++++	1.400
0.000	0.000	9070.444	-0.784	9071.106	1.600
0.000	0.000	6478.488	-0.802	6479.114	1.800
0.000	0.000	4804.729	-0.816	4805.324	2.000
0.000	0.000	2570.349	-0.845	2570.873	2.500
0.001	0.000	1555.714	-0.866	1556.179	3.000
0.001	0.000	1025.155	-0.882	1025.568	3.500
0.001	0.000	718.763	-0.894	719.131	4.000
0.002	0.000	528.287	-0.905	528.616	4.500
0.002	0.000	402.937	-0.913	403.229	5.000
0.003	0.000	316.623	-0.920	316.883	5.500
0.004	0.000	254.957	-0.926	255.187	6.000
0.005	0.000	209.533	-0.931	209.736	6.500
0.006	0.000	175.200	-0.935	175.377	7.000
0.007	0.000	148.673	-0.939	148.827	7.500
0.008	0.000	127.784	-0.943	127.917	8.000
0.009	0.000	111.062	-0.946	111.174	8.500
0.010	0.000	97.479	-0.949	97.571	9.000
0.012	0.000	86.303	-0.951	86.377	9.500
0.013	0.000	77.002	-0.953	77.068	10.000

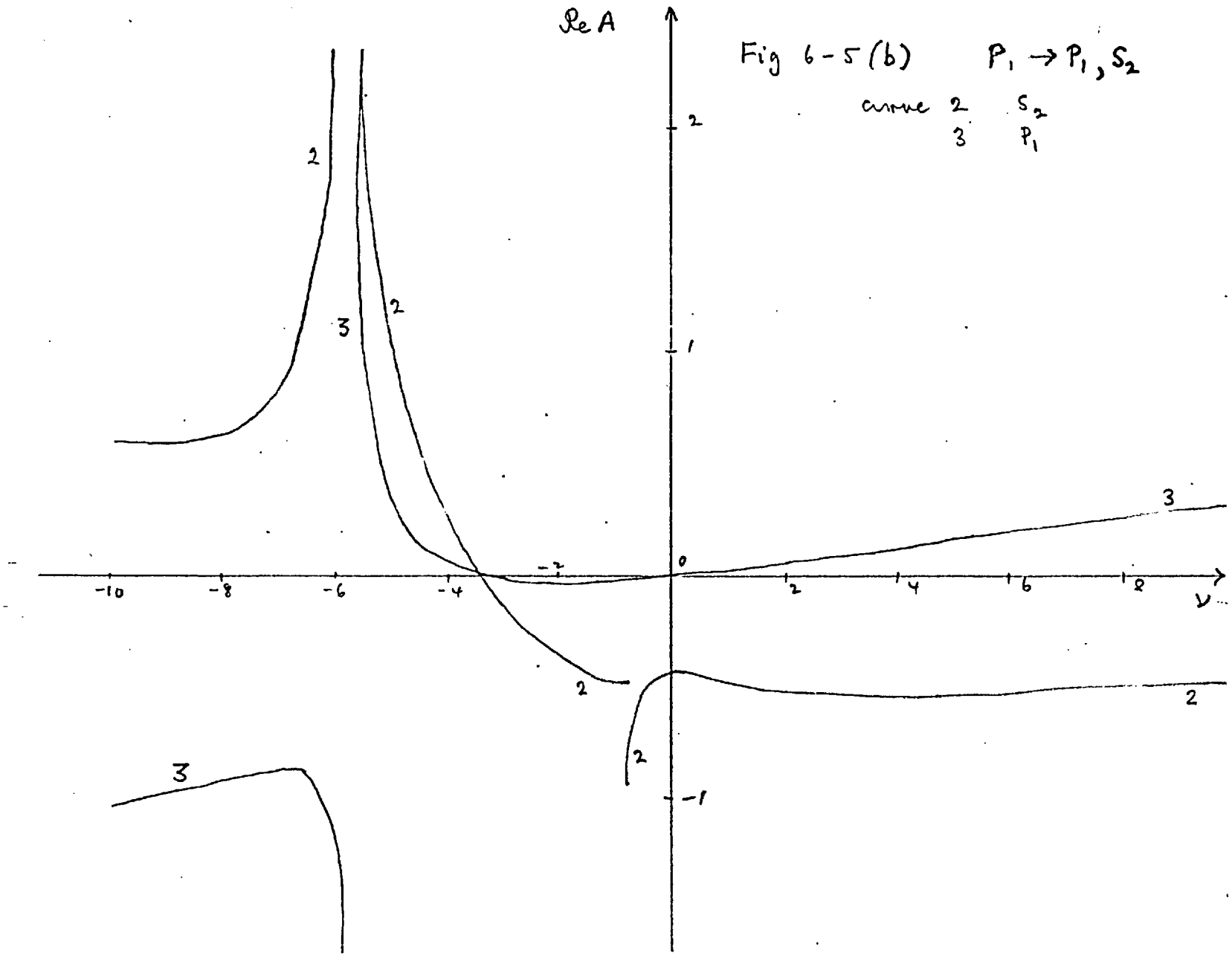

Fig 6-5 (b) $P_1 \rightarrow P_1, S_2$

curve 2 S_2

3 P_1

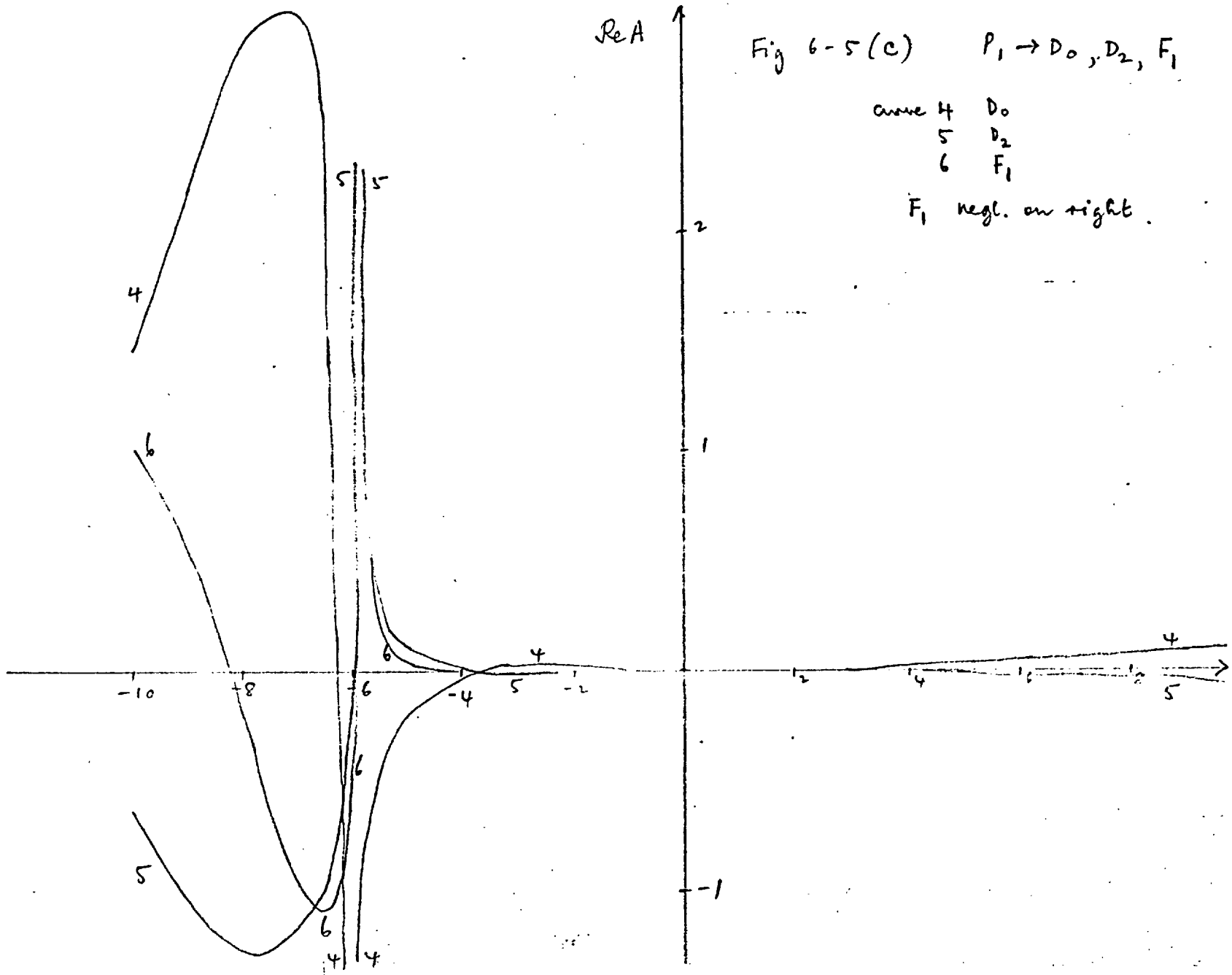
ReA
Fig 6-5(c) $P_1 \rightarrow D_0, D_2, F_1$
curve 4 D_0
5 D_2
6 F_1
F_1 negl. on right.
2
1
-1
-10
-8
-6
-4
-2
4
5
6

for $\nu_R = 5.0, \Gamma\nu_R = 1.25$ and show reasonable agreement with crossing of real and imaginary parts. Tables 7 and Figures 5 show estimates of effect of ρ in channels S_0, S_2, P_1, D_0, D_2, F_1, using Model 3. We did various searches with various types of parametrisation and self consistency condition but were unable to find any self consistent values.

MODELS 1 and 2 RESULTS AND DISCUSSION

The fact that a cut off dispersion integral for C^{-1} agreed with the exact value of C^{-1} shows the nearby singularity nature of the $P_1 \rightarrow P_1$ case. Further, the close approximation obtained by a single pole justifies the use of Model 2 in this case. Such a situation (i) affords a simple parametrisation of the P wave amplitude and (ii) gives a physical picture of a single "force pole", given by the pole of $C^{-1}(\nu)$. Searches were attempted using the same parametrisation in the crossed channel, using the exact form of $C^{-1}(\nu)$, extracting the pole term to give the direct channel amplitude. Thus we have a bootstrap calculation with the same parametrisation in both channels, a desirable circumstance, as discussed in Chapter 2. However, we were unable to find any self consistent solutions.

Model 2 can be used with a δ function approximation in $C^{-1}(\nu)$, but this cannot have the same parametrisation in both channels. In more complicated situations, with several waves, the number of zeros of ReC on the left increases and Model 2 becomes inapplicable in many cases. One can estimate the number of zeros from the δ function form

$$C(\nu) \propto \frac{1}{\nu} \cdot P_\ell \cdot \left[1 + 2\left(\frac{\nu+1}{\nu_R}\right)\right] \cdot Q_\ell \left[1 + 2\left(\frac{\nu_R+1}{\nu}\right)\right] .$$

Number of zeros $= \ell \times \ell$, but some of these zeros are at $\nu = -1$ or $\nu = -\infty$ on the far left.

However, the force pole in the $P_1 \rightarrow P_1$ case at least, actually comes from the zero associated with the singularity at $-\nu_R - 1$. This singularity has

a zero on each side of it, and the one not on the cut has a much smaller gradient and this gives the dominant force pole in A^{-1}. In pursuit of the force pole idea, one would like each exchanged particle to produce one or a set of force poles. This can happen under certain conditions. If the positions of the narrow resonances in the crossed channel are widely separated, then the $C(\nu)$ function is the sum of those due to individual waves in the crossed channel and, if we use a δ function approximation in $C(\nu)$, there will be a region near $-\nu_{Rj}-1$ where the jth resonance will dorinate due to its singularity. It will give two zeros of $C(\nu)$, and if it is like the $P_1 \rightarrow P_1$ case we have looked at, one of these has a much smaller gradient than the other and will be the force pole due to the exchange of the jth resonance. If the resonances are widely separated, the contribution to $C(\nu)$ from the other waves will be slowly varying in this region and will merely displace the zeros slightly and hardly alter the gradient at the zero. Thus the left hand singularities of $A^{-1}(\nu)$ will simply be a sum of force poles, possibly one from each exchanged particle. This force pole picture does not seem to apply in the more realistic cases we looked at. Indeed, in many cases, the main structure of the left hand discontinuity was not associated with zeros of $ReC(\nu)$. We showed Models 1 and 2 to be independent of and to agree with each other.

Table 3 shows a Model 1 amplitude for $P_1 \rightarrow P_1$. Tables 4 and 5 show Model 2 amplitudes for $P_1 \rightarrow P_1$, using the continuous $C(\nu)$ function and its δ function approximation respectively. We see that the amplitude produced agrees well with crossing on the near left, probably better than the other methods discussed in other chapters. Comparing Model 2 with the Balazs method, we obtain a very good fit to $C(\nu)$ on the near left by just using the single pole, i.e. with two parameters, compared to the many parameter fits using the Balazs method. We tried searches but found no solutions. We searched with the threshold parameters (a) fixed, (b) deduced from $C^{-1}(\nu)$, (c) as variable

parameters. However it is obvious that resonant solutions can be obtained for by choosing g_1^1 say in the P wave the amplitude can be made to have a zero at ν_R say. In the D wave $g^1{}_2$, g_2^2 allow both position and gradient to be chosen arbitrarily. We can generate a P wave resonance at the position of the by choosing $g_1^1 = 50.35$, for ρ exchange Model 2, function in crossed channel. However the width is then $2\frac{1}{2}$ x too small. We can generate the f_o by choosing $g_2^2 = -145.0$, $g_2^1 = 275.0$ where we neglect the left hand cut and obtain the resonance by cancellation of the two threshold terms. We display a resonant P wave in Table 8 and Figure 6. In the P wave case, this leads to a simple possible explanation of description of the one parameter ambiguities "disoovered" by the contour plots of previous methods.

EXPLANATION (OR PARAMETRISATION) OF ONE PARAMETER AMBIGUITY BY THRESHOLD POL RESIDUE

Assume that P wave does not influence itself very sensitively to ν_R. i.e. for all ν_R get

vaguely

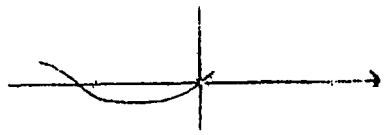

Fix S waves. Then varying threshold pole in crossed channel won't affect ReC(P→P) very much as S wave dominates on near left? Varying it in direct channel varies ν_R strongly but with correlated $\Gamma\nu_R$. If the terms other than threshold give a negative increasing function $f(\nu)$, which we take to be

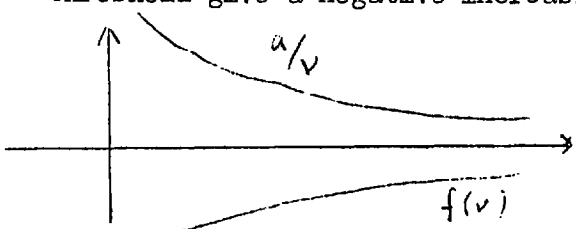

independent of ($\Gamma\nu_R$, ν_R),

fixed

and the threshold term gives $\frac{a}{\nu}$. Then ν_R is such that $\frac{a}{\nu_R} = -f(\nu_R)$

$$1/\Gamma\nu_R \propto \mathrm{Re}A^{-1} \quad (\nu_R)$$

$$= f'(\nu_R) - \frac{a}{\nu_R{}^2}$$

$$= f'(\nu_R) + \frac{1}{\nu_R} f(\nu_R)$$

Table 6-8. $S_0 + S_2 + P_1 \rightarrow P_1$ with threshold residue put in by hand at value 4.2.
$\Delta(\nu_0) = -0.446$ $\nu_0 = -9.$

REA	IMA	REA-1	IMA-1	LHI	TP	V
-0.673	-0.382	-1.124	0.637	-1.175	0.467	-10.000
-0.662	-0.604	-0.825	0.752	-0.640	0.246	-9.500
-0.461	-0.906	-0.446	0.877	0.000	-0.000	-9.000
0.046	-0.957	0.050	1.043	0.786	-0.275	-8.500
0.354	-0.597	0.736	1.239	1.798	-0.583	-8.000
0.324	-0.271	1.816	1.519	3.247	-0.933	-7.500
0.214	-0.113	3.663	1.929	5.513	-1.333	-7.000
0.185	-0.123	3.756	2.491	6.088	-1.795	-6.500
0.136	-0.095	4.921	3.446	7.814	-2.333	-6.000
0.101	-0.077	6.253	4.779	9.805	-2.970	-5.500
0.067	-0.061	8.186	7.404	12.528	-3.733	-5.000
0.045	-0.050	9.863	10.944	15.166	-4.667	-4.500
0.028	-0.042	10.795	16.564	17.297	-5.833	-4.000
0.017	-0.035	11.219	23.257	19.256	-7.333	-3.500
0.010	-0.027	11.420	32.349	21.496	-9.333	-3.000
0.005	-0.019	13.366	49.417	26.287	-12.133	-2.500
0.002	-0.009	19.876	109.775	37.052	-16.333	-2.000
0.000	-0.005	11.711	218.439	31.245	-18.667	-1.800
-0.002	-0.000	-490.927	28.057	-468.449	-21.583	-1.600
-0.004	0.005	-91.530	-115.192	-65.271	-25.333	-1.400
-0.011	0.009	-54.722	-43.913	-23.429	-30.333	-1.200
-0.017	0.000	-57.240	0.000	-18.907	-37.333	-1.000
-0.013	0.000	-76.479	0.000	-28.420	-47.833	-0.800
-0.011	0.000	-94.704	0.000	-28.426	-65.333	-0.600
-0.008	0.000	-128.908	0.000	-27.294	-100.333	-0.400
-0.004	0.000	-232.814	0.000	-25.992	-205.333	-0.200
0.003	0.000	398.923	-0.302	-24.167	424.667	0.100
0.005	0.000	189.526	-0.408	-23.617	214.667	0.200
0.012	0.000	85.628	-0.535	-22.606	109.667	0.400
0.019	0.000	51.604	-0.612	-21.705	74.667	0.600
0.029	0.001	34.971	-0.667	-20.901	57.167	0.800
0.040	0.001	25.246	-0.707	-20.182	46.667	1.000
0.053	0.002	18.941	-0.739	-19.535	39.667	1.200
0.068	0.004	14.568	-0.764	-18.951	34.667	1.400
0.087	0.006	11.386	-0.784	-18.422	30.917	1.600
0.110	0.010	8.986	-0.802	-17.941	28.000	1.800
0.139	0.016	7.126	-0.816	-17.501	25.667	2.000
0.242	0.052	3.946	-0.845	-16.551	21.467	2.500
0.423	0.184	1.987	-0.866	-15.770	18.667	3.000
0.550	0.703	0.691	-0.882	-15.117	16.667	3.500
-0.249	1.059	-0.210	-0.894	-14.563	15.167	4.000
-0.552	0.580	-0.861	-0.905	-14.087	14.000	4.500
-0.509	0.346	-1.345	-0.913	-13.673	13.067	5.000
-0.453	0.243	-1.713	-0.920	-13.310	12.303	5.500
-0.412	0.191	-1.999	-0.926	-12.990	11.667	6.000
-0.382	0.160	-2.225	-0.931	-12.704	11.128	6.500
-0.361	0.140	-2.405	-0.935	-12.448	10.667	7.000
-0.345	0.127	-2.551	-0.939	-12.218	10.267	7.500
-0.333	0.118	-2.670	-0.943	-12.009	9.917	8.000
-0.324	0.111	-2.768	-0.946	-11.818	9.608	8.500
-0.316	0.105	-2.849	-0.949	-11.645	9.333	9.000
-0.310	0.101	-2.917	-0.951	-11.485	9.088	9.500
-0.305	0.098	-2.973	-0.953	-11.338	8.867	10.000

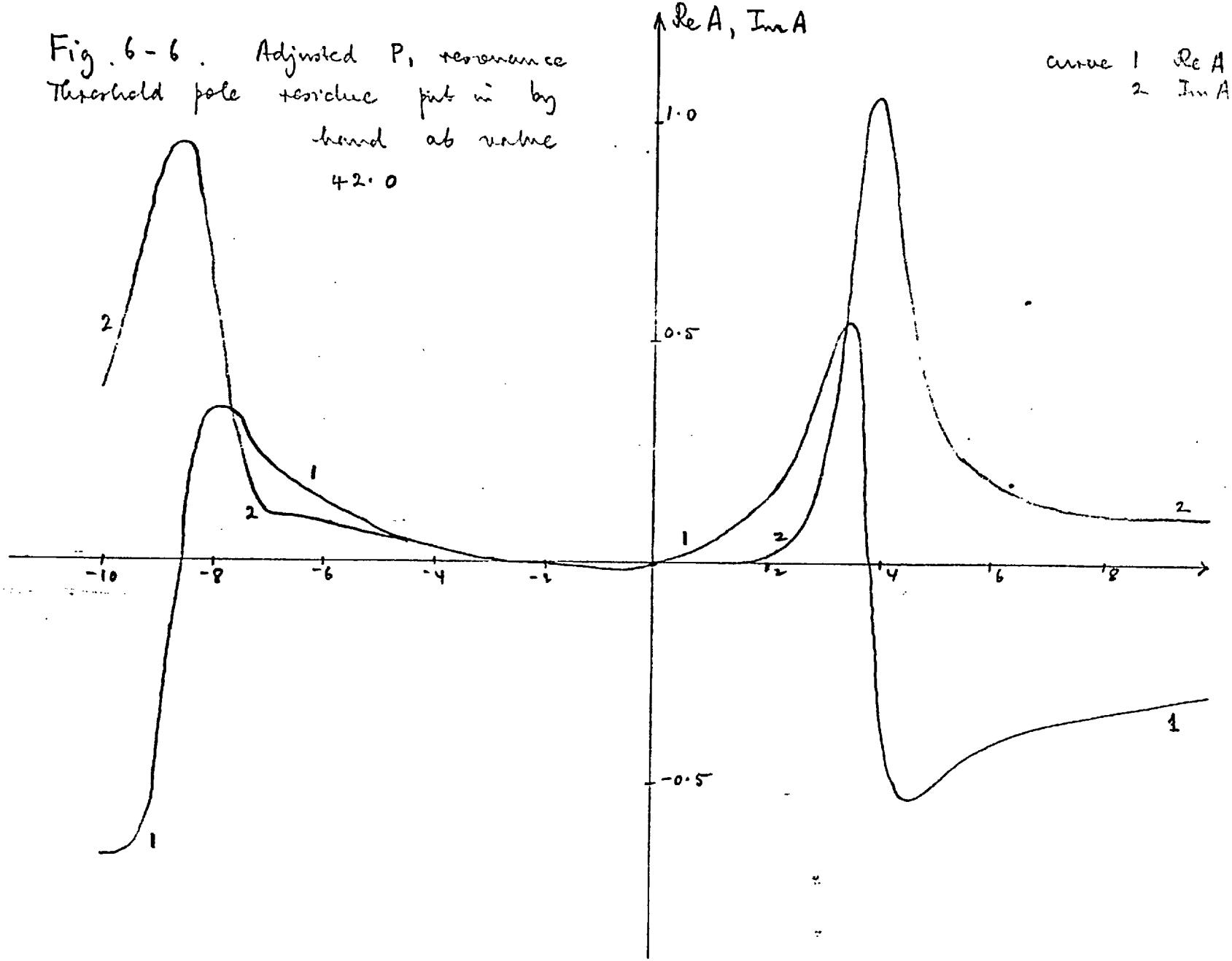

Fig. 6-6. Adjusted P, resonance
Threshold pole residue put in by
hand ab value
42·0

In the case of a Model 2 amplitude, with force pole residue relatively insensitive to (Γ_{ν_R}, ν_R)

$$A^{-1}(\nu) = \frac{g}{\nu - \nu_p} + \frac{a}{\nu}$$

$$A^{-1}(\nu_R) = 0 = \frac{g}{\nu_R - \nu_p} + \frac{a}{\nu_R} \qquad \text{(i)}$$

$$\frac{1}{\Gamma_{\nu_R}} = A^{-1\,\prime}(\nu_R) = \frac{-g}{(\nu_R - \nu_p)^2} - \frac{a}{(\nu_R)^2} \qquad \text{(ii)}$$

parametrised by a

$$a = -\frac{g\,\nu_R}{(\nu_R - \nu_p)}$$

$$\frac{1}{\Gamma_{\nu_R}} = \frac{-g}{(\nu_R - \nu_p)^2} + \frac{(g\,\nu_R)}{(\nu_R - \nu_p)} \cdot \frac{1}{(\nu_R)^2}$$

$$= \frac{g}{\nu_R(\nu_R - \nu_p)^2} \cdot \left[-\nu_R + (\nu_R - \nu_p) \right]$$

$$\therefore \Gamma_{\nu_R} \propto \frac{\nu_R \cdot (\nu_R - \nu_p)^2}{-g \cdot \nu_p}$$

Thus if we vary the threshold pole in the crossed and direct channels, we can maintain self consistency provided Γ_{ν_R} and ν_R are related by the above relation. Thus, a the threshold residue, provides a parametrisation of the arbitrariness in determination of Γ_{ν_R} and ν_R. We can also deal with a one parameter ambiguity by choosing $\nu_o = \nu_{R\,in}$, $\mathrm{Re}A^{-1}(\nu_o) = 0$.

Turning our attention to the requirement of a resonant P wave, we took a careful look at C^{-1} and its contributions from various waves in the crossed channel. The effects of the P wave was always small and the main structure came from the zero of ReC which was supplied mainly by the P wave and the small imaginary part supplied by the S wave. The values of $\mathrm{Im}C^{-1}$ for three different choices of S waves are given in Table 9 and Figure 4. We see that $\mathrm{Im}C^{-1}$ is very sensitive to the S waves although $\int \frac{\mathrm{Im}C^{-1}(\nu')}{\nu' - \nu} d\nu'$ is not so sensitive. Further a change in sign of the total B^{-1} can be effected by variation of the

Table 6-9. Sensitivity of Pwave to Swave. see Fig. 6-4.

$S_0 + S_2 + P_1 \nu \rightarrow P_1$

$S_2 = 2.84, 0.434, 0.239$ | $S_2 = 1.48, 0.516, -0.059$

LHI	THPOLE	IHC-1	LHI	THPOLE	IHC-1	ν
-0.041	0.265	0.758	-0.640	0.490	0.752	=9.500
0.000	=0.000	0.893	0.000	=0.000	0.877	=9.000
0.087	=0.296	1.074	0.786	=0.548	1.043	=8.500
0.269	=0.630	1.285	1.798	=1.164	1.239	=8.000
0.721	=1.008	1.580	3.247	=1.862	1.519	=7.500
1.759	=1.439	2.000	5.513	=2.660	1.929	=7.000
0.664	=1.938	2.560	6.088	=3.581	2.491	=6.500
0.279	=2.519	3.382	7.814	=4.655	3.446	=6.000
-0.613	=3.206	4.388	9.805	=5.925	4.779	=5.500
-1.765	=4.030	6.395	12.528	=7.449	7.404	=5.000
-4.757	=5.038	8.468	15.166	=9.311	10.944	=4.500
=11.919	=6.297	11.378	17.297	=11.638	16.564	=4.000
-26.114	=7.917	6.940	19.256	=14.631	23.257	=3.500
=32.556	=10.076	=19.989	21.496	=18.621	32.349	=3.000
-6.098	=13.098	=33.484	26.287	=24.208	49.417	=2.500
8.651	=17.632	=25.904	37.052	=32.587	109.775	=2.000
12.229	=20.151	=22.534	31.245	=37.243	218.439	=1.800
15.027	=23.300	=18.604	=468.449	=43.062	28.057	=1.600
17.631	=27.348	=15.016	=65.271	=50.544	=115.192	=1.400
19.910	=32.746	=9.472	-23.429	=60.519	-43.913	=1.200
17.475	=40.303	0.000	=18.907	=74.485	0.000	=1.000
12.029	=51.638	0.000	=28.420	=95.434	0.000	=0.800
9.774	=70.530	0.000	=28.426	=130.349	0.000	=0.600
8.334	=108.313	0.000	=27.294	=200.179	0.000	=0.400
7.304	=221.664	0.000	=25.992	=409.669	0.000	=0.200
6.195	458.442		=24.167	847.270		0.100
5.903	231.740		=23.617	428.290		0.200
5.401	118.389		=22.606	218.801		0.400
4.985	80.605		=21.705	148.971		0.600
4.634	61.713		=20.901	114.056		0.800
4.333	50.378		=20.182	93.107		1.000
4.073	42.822		=19.535	79.141		1.200
3.846	37.424		=18.951	69.165		1.400
3.646	33.376		=18.422	61.683		1.600
3.469	30.227		=17.941	55.864		1.800
3.310	27.708		=17.501	51.209		2.000
2.979	23.174		=16.551	42.829		2.500
2.718	20.151		=15.770	37.243		3.000
2.507	17.992		=15.117	33.252		3.500
2.334	16.373		=14.563	30.260		4.000
2.188	15.113		=14.087	27.932		4.500
2.065	14.106		=13.673	26.070		5.000
1.959	13.282		=13.310	24.546		5.500
1.867	12.595		=12.990	23.277		6.000
1.786	12.013		=12.704	22.202		6.500
1.715	11.515		=12.448	21.282		7.000
1.652	11.083		=12.218	20.483		7.500
1.595	10.705		=12.009	19.785		8.000
1.544	10.372		=11.818	19.169		8.500
1.498	10.076		=11.645	18.621		9.000
1.457	9.811		=11.485	18.131		9.500
1.419	9.572		=11.338	17.690		10.000

Fig 6-4. Sensitivity of $S+P \to P$ to S wave.

S_0 ~ 0.822, 0.363, 0.123, −0.014

P_1 ~ 24.3, −3.78

S_2 ~ 1.48, 0.516, −0.059 ~ curve 1

2.84, 0.434, 0.239, −0.022 ~ curve 2.

Parametrisation ~ polynomial BW.

See Table 6-9.

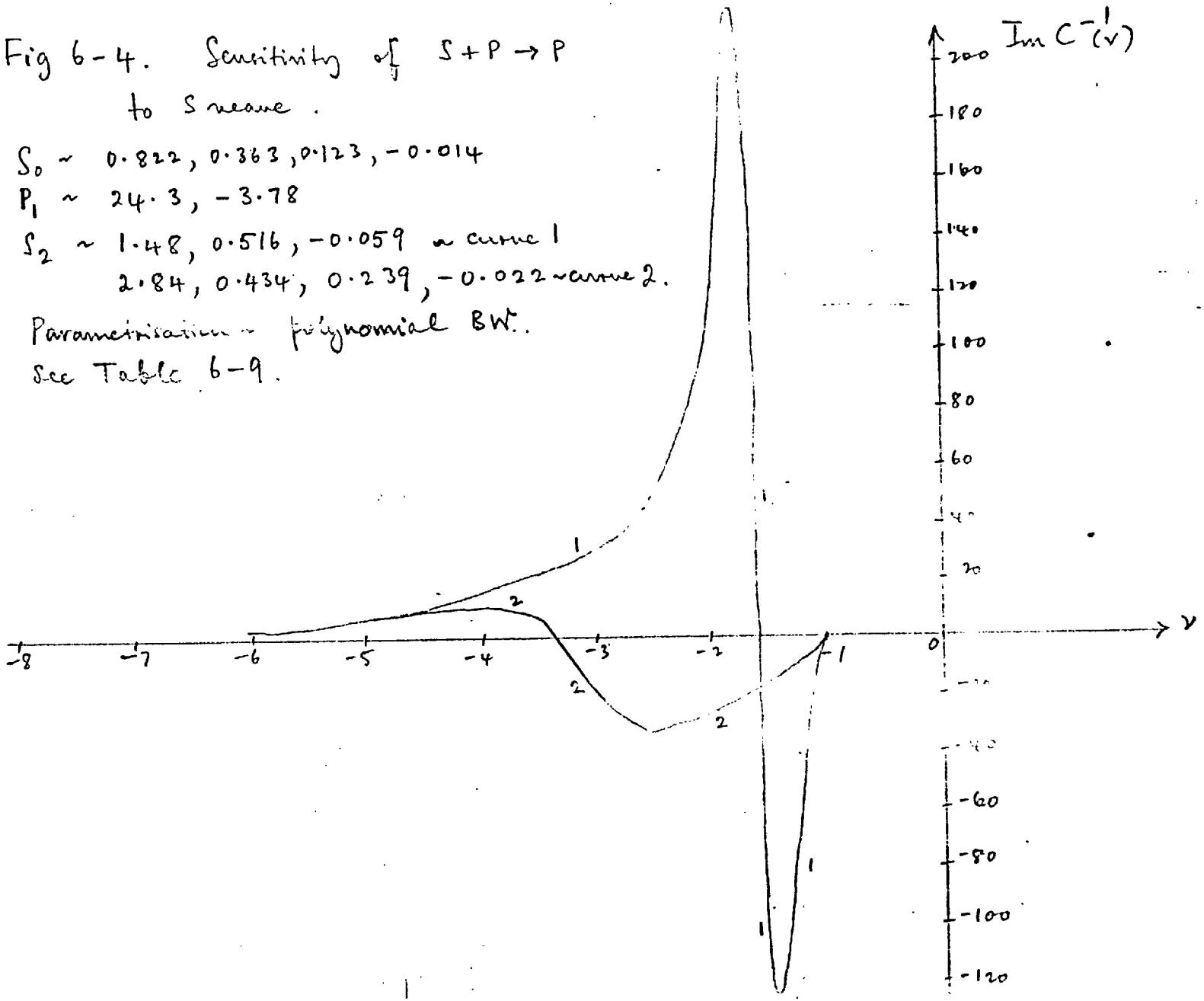

S waves. Thus physically the force is determined in magnitude principally by the P wave exchange, and in sign by the S waves; one might picture exchanged resonating P wave particles in an atmosphere of S waves causing their effect to be completely altered in sign. In practice, it was found very difficult for sensible S waves to get a repulsive force, however it was also difficult to get a very strong attractive force and a resonance could not be obtained except by choosing the threshold residues appropriately.

FURTHER DISCUSSION

Inelasticity

Effect small, putting Oades inelasticity function with parameters at his values, the right hand cut term became more negative, see Table 2, tending towards the production of a resonance, but not by a large amount numerically.

AN ATTEMPT TO MEET MARGINAL SINGULARITY IN AN INVERSE AMPLITUDE MODEL

One might try a model in which the near singularities are given by crossing and the far ones by the condition of pure absorption and marginal singularity.

Thus we take

$$A^{-1}(\nu) = \frac{(\nu-\nu_0)}{\pi} I(\nu,\nu_0) + A^{-1}(\nu_0) + T(\nu) + L(\nu,\nu_0)$$

where

$$L(\nu,\nu_0) = \frac{(\nu-\nu_0)}{\pi}\int_{\Lambda}^{\infty} \frac{\mathrm{Im}A^{-1}(\nu')\, d\nu'}{(\nu'-\nu)(\nu'-\nu_0)} + F L(\nu,\nu_0)$$

now all we know about $FL(\nu, \nu_0)$ is that it is cut $[\Lambda, -\infty]$ and must $\longrightarrow_{\nu\to+\infty} C.\log\nu$, C independent of ν_0. There are many functions satisfying these conditions, but one might choose the simplest, viz.

$$\left[\log(\nu-\Lambda) - \log(\nu_0-\Lambda)\right]$$

One can also take $\frac{(\nu-\nu_0)}{\pi} . I(\Lambda-\nu, \nu_0)$

This defines a purely absorptive model, but of course the far left hand term is

is large and unknown, one can add any term cut $[\Lambda, -\infty]$ and $\longrightarrow 0$ to it. $\nu \to \infty$
As it happens a term $-\log(\nu + 9)$ has value, at $\nu = +5$, of $-\log(14) = -2.3$ which would tend to produce a resonance in the P wave.

THE CASE FOR THE PHYSICAL SIGNIFICANCE OF THE LEFT HAND CUT OF THE INVERSE AMPLITUDE

For an exponential potential, the left hand cut is replaced by poles. If the potential is repulsive, the residues of neighbouring poles have the same sign; if attractive, opposite signs. Hence the singularities of the inverse amplitude in this case are as follows:-

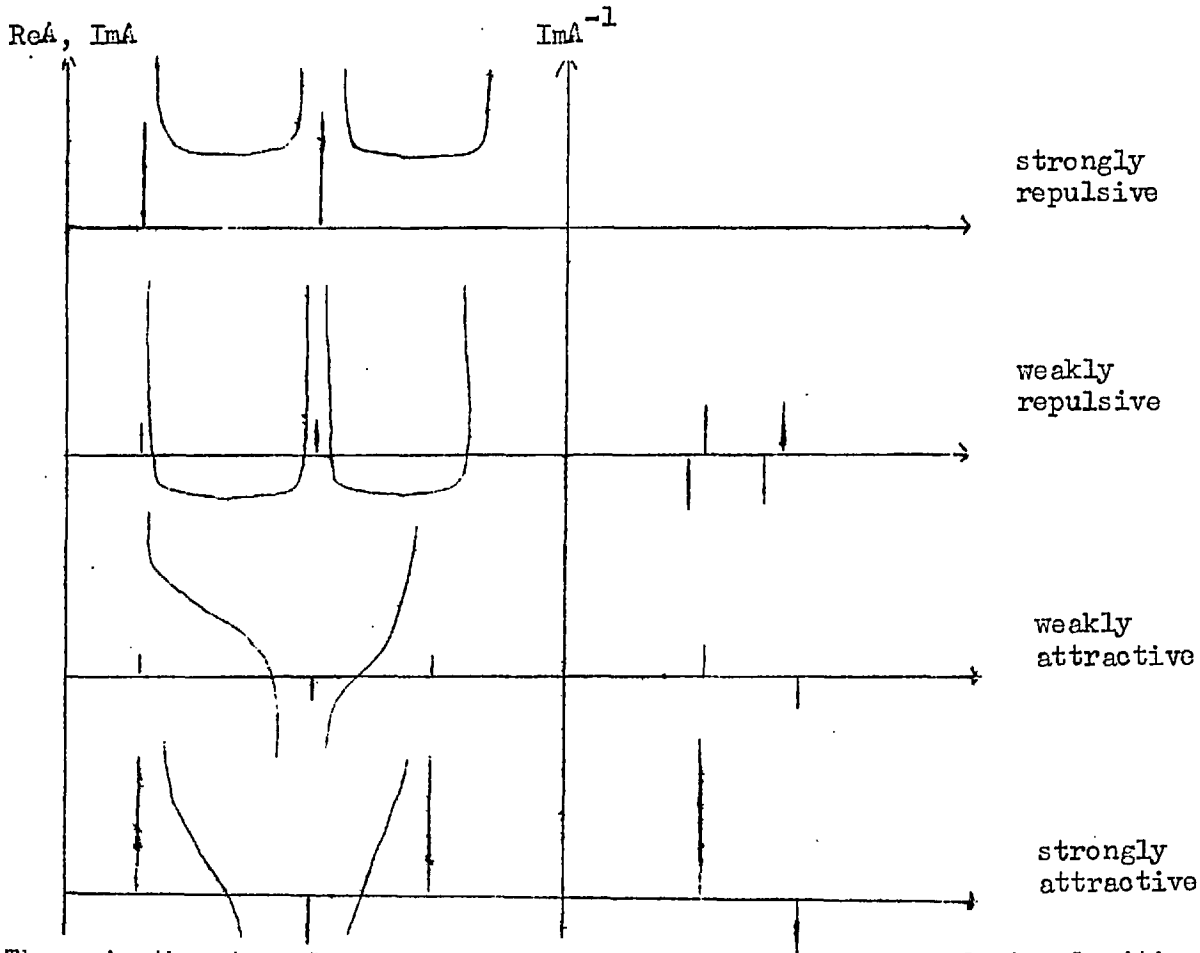

Thus, in the strongly repulsive case, there are no left hand singularities in the inverse amplitude, and when there is attraction there are singularities. However, this is a very naive argument, since we disregard the irrelevance of potential theory and the inapplicability of the concepts of overall attractive or overall repulsive interaction.

Finally notice that, in some sense, whereas unitarity exerts some restriction upon $\mathrm{Im}A$, it has not so direct a constraint on $\mathrm{Im}A^{-1}$. Of course, $\mathrm{Im}A^{-1}$ is no longer a sum of contributions from partial waves in the crossed channel, but in this highly nonlinear problem, this is not necessarily wrong in principle. However, it does make it more difficult to use a partial wave expansion in the crossed channel.

ATTEMPS TO SOLVE INVERSE AMPLITUDE DISPERSION RELATIONS ANALYTICALLY

If we are given $\mathrm{Im}A^{-1}$ on the left and the threshold residues, the whole amplitude follows immediately. If on the other hand we are given $\mathrm{Im}A$ on the left and the threshold residues, is it possible to obtain the amplitude using an inverse amplitude dispersion relation?

Well $$A^{-1}_{(\nu)} = B^{-1}(\nu) + I(\nu) + T(\nu)$$

where I, the right hand cut contribution and T, the threshold contribution are known functions.

Then consider the function

$$f(\nu) \equiv B^{-1}(\nu) = U + iV$$

it is real analytic real in $[-1, +\infty]$, cut $[-1, -\infty]$

$$\mathrm{Im}A = \frac{-V}{[(I+T)+U]^2 + V^2}$$

so $$U^2 + V^2 + 2U.(I+T) + (I+T)^2 = -\frac{V}{\mathrm{Im}A}$$

$\therefore$ f( ) satisfies a non-linear condition on its boundary, of the type

$$U^2 + V^2 + aV + b = 0$$

functions satisfying the same conditions as f except that they obey a linear relation, with given coefficients, on the boundary considered can be found by standard methods (this is the Rieman-Hilbert problem (10)). However, non-linear problems seem to be intractable.

INVERSE AMPLITUDE WITH COMPLEX ℓ

Looking at Model 3, we have

$$A_\ell^{-1}(\nu) = B_\ell^{-1}(\nu) + \frac{(\nu - \nu_0)}{\pi} \cdot I(\nu, \nu_0)$$

The right hand cut is independent of ℓ in the elastic case.

$$B_\ell^{-1}(\nu) = \frac{1}{\frac{4}{\pi\nu} \cdot (2\ell'+1) \cdot \beta_{II'} \cdot P_{\ell'}\left[1 + 2\left(\frac{\nu+1}{\nu_R}\right)\right] \cdot Q_\ell\left[1 + 2\left(\frac{\nu_R+1}{\nu}\right)\right]}$$

Thus the amplitude has a continuation in ℓ (and ℓ'). Now Q_ℓ is meromorphic with poles at the negative integers for all values of its argument. Regge poles will occur for those values of (ℓ, ν) for which $A^{-1}(\nu)$ is zero.

GILBERT DISPERSION RELATIONS

It is possible to write Gilbert dispersion relations for the inverse amplitude

e.g. $\nu > -1$

$$\mathrm{Re}A^{-1}(\nu) = \frac{\sqrt{\nu+1}}{\pi} \int_c^\infty \frac{d\nu' \sqrt{\nu'}}{(\nu'+1)(\nu'-\nu)} + \frac{\sqrt{\nu+1}}{\pi} \int_{-\infty}^{-1} \frac{\mathrm{Re}A^{-1}(\nu') \, d\nu'}{(\nu'-\nu) \cdot \sqrt{\nu'+1}}$$

THE PROBLEM OF ZEROS IN THE COMPLEX PLANE

As we have already discussed, there may be zeros in the complex plane for the amplitudes in our models and for the exact (unknown) amplitudes.

We obtain expressions for the real and imaginary parts at a complex point (ν_R, ν_I) by substituting

$$\nu = \nu_R + i\nu_I$$

then $$\frac{1}{\nu' - \nu} = \frac{1}{\nu' - \nu_R - i\nu_I} = \frac{(\nu - \nu_R) + i\nu_I}{(\nu - \nu_R)^2 + \nu_I^2}$$

$$\nu - \nu_0 = (\nu_R - \nu_0) + i\nu_I$$

$$\frac{\nu - \nu_0}{\nu' - \nu} = \frac{\{(\nu_R - \nu_0)(\nu' - \nu_R) - \nu_I^2\} + i\nu_I(\nu' - \nu_0)}{[(\nu' - \nu_R)^2 + \nu_I^2]}$$

$$\mathrm{Im}\left\{ \frac{(\nu - \nu_0)}{} \int \frac{\mathrm{Im}A^{-1}(\nu')\, d\nu'}{(\nu' - \nu_0)(\nu' - \nu)} \right\}$$

$$= \frac{\nu_I}{\pi} \cdot \int \frac{\mathrm{Im}A^{-1}(\ ')\ .\ d\ '}{\left[(\nu' - \nu_R)^2 + \nu_I^2\right]}$$

We see that, for a zero, $\mathrm{Im}A^{-1}(\ ')$ must at least change sign in the region of integration. Hence for an elastic amplitude with no left hand cut there are n zeros in the plane. For a Model 2 elastic amplitude with one pole whose resid has the same sign as $\mathrm{Im}A^{-1}$ on the physical cut, again there will be no zeros. In more complicated cases, the integrals will have to be done numerically. Criteria of this type have been used by Moffat and by Chew and Mandelstam.

One can search for zeros in the complex plane by minimising $\left[(\text{Real part})^2 + (\text{Imaginary part})^2\right]$.

COMPARISON

We can view all the calculations in Chapters 3, 4, 5 and 6 as stemming from the projection of a fixed s dispersion relation into the s channel. In the author's opinion, of these the only ones likely to succeed are

(i) the marginally singular $B(\nu)$ solved by Uretsky N/D, mentioned in Chapter 1;

(ii) the nearby singularity calculations for the inverse amplitude in Chapter 6. The difficulty here is in the estimation of the threshold pole residues from crossing or self consistency.

CHAPTER 7

"FURTHER THEORETICAL IDEAS"

In this chapter, we consider three ideas relating to the solution of MR + U for the $\pi\pi$ system. We have not done any numerical work on these ideas.

1. The Projection of the fixed s dispersion relation into the channel, to give an expression for B (ν) in the low energy physical region, in terms of physical region amplitudes in the crossed channel, and without using uniformity.

2. "Consistency checks". A consistency constraint on the simultaneous confirmation from the t and u channels to the same region.

3. The transformation of variables, from (s,t) to curvilinear coordinates, enabling a family of single dispersion relations to be written, covering the entire s-, t- and u- physical regions, but avoiding the double spectral regions. This leads to the idea of a physical region dynamical scheme.

I. PROJECTION OF THE FIXED s DISPERSION RELATION INTO THE t CHANNEL.

This is a fixed momentum transfer dispersion relation and may be thought of as a fixed t relation as opposed to the previous fixed energy treatment in Chapter 2 which is fixed s, however we are here going to use again a fixed s dispersion relation but use the t channel as the physical channel we are considering.

Starting from

$$A^I(s,t,u) = \frac{1}{\pi}\int_4^\infty A_t^I(s,t')\cdot\left[\frac{1}{t'-t} + \frac{(-1)^I}{t'-u}\right]dt' \qquad (1)$$

$I = 0, 1, 2$ possibly subtracted

we first re-express these equations as relations between $A^I(s,t,u)$ the amplitudes for isospin eigenchannels in the t channel. Labelling them s and t for emphasis,

$$A^{sI} = \sum_{I''=0}^{2} \beta_{II''} A^{tI''}$$

but

$$\sum_{I''=0}^{2} \beta_{I'I} \beta_{II''} A^{tI''} \quad \therefore \sum_{I=0}^{2} \beta_{I'I} \cdot A^{sI} = A^{tI'}$$

If we take these combinations of equations (i), the absorptive parts combine as follows

$$\sum_{I=0}^{2} \beta_{I'I} \cdot A_t^{sI} = A_t^{tI'}$$

$$\sum_{I=0}^{2} \beta_{I'I} (-1)^I A_t^{sI} = \sum_{I=0}^{2} \beta_{I'I} (-1)^I \sum_{I''=0}^{2} \beta_{II''} A_t^{tI''}$$

$$= \sum_{I''=0}^{2} \beta'_{I'I''} A_t^{tI''}$$

where

$$\beta'_{I'I''} = \sum_{I=0}^{2} \beta_{I'I} (-1)^I \beta_{II''}$$

$$= (-1)^{I'+I''}$$

Hence

$$A^{tI'}(s,t,u) = \frac{1}{\pi} \int_{4}^{\infty} dt' \cdot \left[\frac{A_t^{tI'}(s,t')}{t'-t} + \sum_{I''=0}^{2} \frac{\beta_{I'I''} A_t^{tI''}(s,t')}{t'-u} \right] \qquad \text{(ii)}$$

possibly subtracted.

Making the asymptotic possible for $A_t(s,t')$, that

$$A_t^{I'}(s,t') \underset{t' \to \infty}{\propto} t'^{\alpha_{I'}(s)} \qquad \text{(iii)}$$

where $\mathrm{Re}\,\alpha_{I'}(s) < 1$ for $s < 0$

we need one subtraction at some point to, at which point $u = u_0 = 4 - s - t$, giving

$$A^{I'}(s,t,u) = A^{I'}(s,t_0,u_0) + \frac{(t-t_0)}{\pi}\int_{4}^{\infty}\frac{dt'}{(t'-t_0)}\left[\frac{A_t^{I'}(s,t')}{t'-t} + \sum_{I''=0}^{2}\frac{\beta_{I'I''}A_t^{I''}(s,t')}{t'-u}\right] \quad (iv)$$

We can now project this equation into partial waves in the t channel.

$$A_\ell^{I'}(t) = \frac{1}{2}\int_{-1}^{+1} P_\ell(\cos\theta')\, d(\cos\theta')\, A^{I'}(s,t,u)$$

$$\cos\theta' = 1 + \frac{2s'}{t-4}$$

$$A_\ell^{I'}(t) = \frac{1}{t-4}\cdot\int_{4-t}^{?} ds'\, P_\ell\left[1+\frac{2s'}{t-4}\right]\cdot A^{I'}(s',t,u) \quad (v$$

for $d(\cos\theta')\Big|_t = \frac{2\,ds'}{t-4}$ and $\cos\theta' = 1 \sim s' = 0$

" $-1 \quad 4-t$

the integration is at constant t and runs along a line of constant t between the lines $\cos\theta' = \pm 1$ which border the t physical region. s' is the running coordinate and $u = 4 - t - s'$., see Fig. 1 . Applying this to (iv) and taking t_0, the subtraction point in the fixed s dispersion relation, as the same for all s, we obtain

$$A_\ell^{I'}(t) = A_\ell^{I'}(t_0) + \frac{(t-t_0)}{\pi}\int_{4-t}^{0}\frac{ds'}{t-4}\int_{4}^{\infty}\frac{dt'}{t'-t_0}\cdot\Bigg\{ \quad (vi$$

$$P_\ell\left[1+\frac{2s'}{t-4}\right]\cdot\left[\frac{A_t^{I'}(s',t')}{t'-t} + \sum_{I''=0}^{2}\frac{\beta_{I'I''}A_t^{I''}(s',t')}{t'-u}\right]\Bigg\}$$

The imaginary part is given by

$$\mathrm{Im}\, A_\ell^{I'}(t) = \int_{4-t}^{0}\frac{ds'}{t-4}\cdot P_\ell\left[1+\frac{2s'}{t-4}\right]\cdot A_t^{I'}(s',t) \quad (vi$$

Referring to the figure, (1) -- the fixed s dispersion relation runs along CD and EF giving the value at some point P as an integral over the absorptive parts along CD and EF from the b and u channels respectively. Such a relation can be written for all points on

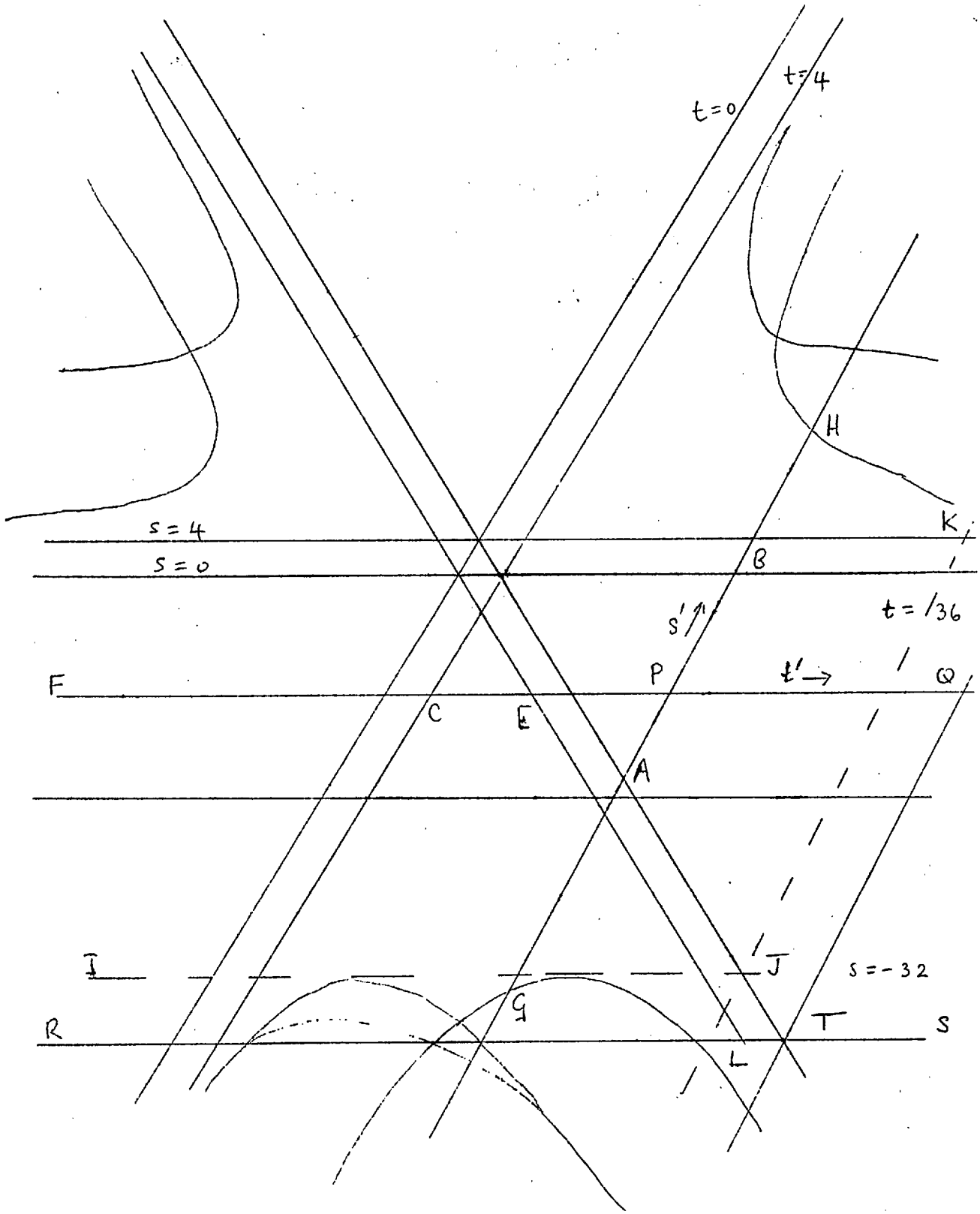

Fig. 7 - 1. Mandelstam diagram for projection of fixed s dispersion relation into t channel.

the segment AB, a line of constant t, and by integrating along AB weighted by a Legendre polynomial we obtain the partial wave amplitude at t.

The real and imaginary parts of (vi) should be related by the unitary condition

$$\mathrm{Im}\, A_\ell(t) = \sqrt{\frac{t-4}{t}}\; N_\ell(t) \left[\mathrm{Im}\, A_\ell(t)^2 - \mathrm{Re}\, A_\ell(t)^2 \right] \quad \text{(viii)}$$

One can now take to $\to 4$ giving

$$A_\ell^{I'}(t) = A_\ell^{I'}(4) + \frac{1}{\pi} \int_{4t}^{\infty} ds' \int_4^{\infty} \frac{dt'}{t'-4} \cdot \{ \quad \} \quad \text{(ix)}$$

and use the fact that

$$A_\ell^{I}(4) = a^{I'} \cdot \delta_{\ell 0}. \quad \text{(x)}$$

$a^{I'}$ being the s wave scattering lengths.

For to = 4, the dt′ integral appears to diverge at its lower limit, however

$$A_t^{I'}(s',t') \underset{t' \to 4+}{\sim} (t'-4)^{\frac{1}{2}}$$

since $A_t^{I'}(s',t') = \sum_{\ell'=0}^{\infty} (2\ell'+1)\, \mathrm{Im}\, A_{\ell'}(t')\, P_{\ell'}\left[1 + \frac{2s'}{t'-4}\right]$ (xi)

$$\mathrm{Im}\, A_{\ell'}(t') \sim (t'-4)^{2\ell'+\frac{1}{2}}$$

$$P_\ell\left[1 + \frac{2s'}{t'-4}\right] \sim \left(\frac{1}{t'-4}\right)^{\ell'}$$

$\therefore$ each term $\longrightarrow (t'-4)^{\ell'+\frac{1}{2}}$

Hence the integral converges, however $A_\ell^{I'}(t)$ appears to have a discontinuous first derivative. One hopes this is not a real effect and will be cancelled by something else, once the equations are independent of to and Re A_ℓ(to) should be continuous up to the ℓth derivative at to = 4.

in fact Re $A_\ell(t_0) \propto (t_0-4)^\ell$ $\quad t_0 \to 4$

To estimate $A_t^I(s', t')$, one can use the partial wave series (xi) provided $s' > -32$, which restricts its usefulness in (ix) to $t' < 36$, i.e. $\nu' < 8$.

Referring to the figure, in order to obtain the partial wave amplitude for the value of t at P, we need values for the whole of AB. For the value of t at Q we need values for whole of LM. In the latter case one needs for example the value at T and hence the values of the absorptive part along RS, some of which lies in the double spectral region. Thus when using a partial wave series estimate for the absorptive part, one is restricted to values of t below the line JK, which has $t = 36 \sim \nu' = 8$.

However, note that $P_\ell(z)$

is either even or odd

$$\therefore \quad A_\ell(\nu') = \tfrac{1}{2} \int_{-1}^{+1} P_\ell(z) \cdot A(\nu', z)\, dz$$

Now, A^I if I = 1 only contains odd waves

$\therefore A^I(\nu', z)$ is odd in Z.

$$\therefore A_\ell(\nu') = 0 \text{ for } \ell \text{ even}$$
$$= \tfrac{1}{2} \int_{-1}^{+1} P_\ell(z) \cdot A(\nu', z)$$

$$A_\ell^{-1}(\nu') = \int_0^{+1} P_\ell(z) \cdot A(\nu', z)$$

for $I = 0, \quad 2$ only even waves

$$\therefore A_\ell^I(\nu') = \int_0^1 P_\ell(z) \cdot A(\nu', z)$$

Apart from providing a consistency constraint, this enables us to obtain $A_\ell(\nu)$ for higher values of t. For, we can now go to that value of ν' such that the fixed s dispersion relation passing through $Z = 0$, just to-

the double spectral region.

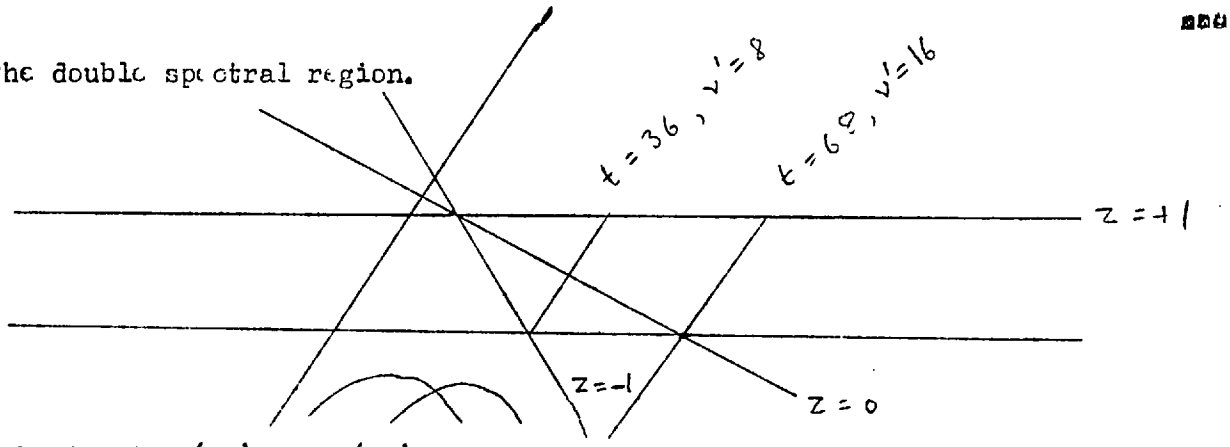

Substituting (xi) into (ix),

$$A_\ell^{I'}(t) = A_\ell^{I'}(4) + \frac{1}{\pi}\int_{4-t}^{0} ds' \int_{4}^{\infty} \frac{dt'}{t'-4} \left\{ \frac{\left[\sum_{\ell'=0}^{\infty} (2\ell'+1)\, \mathrm{Im} A_{\ell'}^{I'}(t')\, P_{\ell'}\left[1+\frac{2s'}{t'-4}\right]\right]}{t'-t} \right.$$

$$\left. + \sum_{I''=0}^{2} \beta_{I'I''} \frac{\sum_{\ell'=0}^{\infty} (2\ell'+1)\, \mathrm{Im} A_{\ell'}^{I''}(t')\, P_{\ell'}\left[1+\frac{2s'}{16-4}\right]}{t'-u} \cdot P_\ell\left[1+\frac{2s}{t-4}\right] \right\}$$

interchanging orders of summation and integration, the first term gives

$$\sum_{\ell'=0}^{\infty} (2\ell'+1) \cdot \frac{1}{\pi} \cdot \int_4^\infty \frac{dt' \cdot \mathrm{Im} A_{\ell'}(t')}{(t'-4)(t'-t)} \cdot \int_{4-t}^{0} ds' P_{\ell'}\left[1+\frac{2s'}{t'-4}\right] \cdot P_\ell\left[1+\frac{2s'}{t-4}\right]$$

and the second term gives

$$\sum_{\ell'=0}^{\infty} (2\ell'+1) \cdot \sum_{I''=0}^{2} \beta_{I'I''} \cdot \frac{1}{\pi} \int_4^\infty \frac{dt' \mathrm{Im} A_{\ell'}(t')}{t'-4} \int_{4-t}^{0} \frac{ds' P_{\ell'}\left[1+\frac{2s'}{t'-4}\right] \cdot P_\ell\left[1+\frac{2s'}{t-4}\right]}{\left[t' - (4 - s' - t)\right]}$$

where we leave isolated the part that could be done analytically.

Hence,

$$A_\ell^{I'}(t) = \frac{1}{\pi} \sum_{\ell'=0}^{\infty} (2\ell'+1) \int_4^\infty \frac{dt'}{(t'-4)} \cdot \left[\mathrm{Im} A_{\ell'}^{I'}(t') \cdot X_{\ell'\ell}(t',t) + \sum_{I''=0}^{2} \beta_{I'I''} \cdot \mathrm{Im} A_{\ell'}^{I''}(t') \cdot Y_{\ell'\ell}(t',t) \right] + a^{I'} \cdot \delta_{\ell 0} \qquad \text{—(xii)}$$

where

$$X_{\ell'\ell}(t',t) = \frac{1}{t'-t} \cdot \int_{4-t}^{0} ds' \cdot P_{\ell'}\left[1+\frac{2s'}{t'-4}\right] \cdot P_\ell\left[1+\frac{2s'}{t-4}\right] \qquad \text{(a)}$$

$$Y_{\ell'\ell}(t',t) = \int_{4-t}^{0} ds' \cdot P_{\ell'}\left[1+\frac{2s'}{t'-4}\right] \cdot P_\ell\left[1+\frac{2s'}{t-4}\right] \qquad \text{—(b)}$$

(xiii)

One can now postulate equations (viii), (xii), (xiii) as a basis for a dynamical calculation.

DISCUSSION

The main advantage of the method is that we do not need to know the asymptotic behaviour in the double spectral region.

The integrals lie in the physical regions for the t and n channels, and we can make reasonable asymptotic assumptions here like $A_t(s,t') \to$ constant or better. $t' \to \infty \qquad s < 0$

However, using a partial wave series one cannot calculate $\mathrm{Re}\, A_\ell(t)$ for $t > 4$ so that the method is not complete in this case, in the sense that not all the input material can be compared with and determined by the output material. One can assume that the $\mathrm{Im} A_\ell(t) \to$ constant smoothly. The integral is damped by the denominators $\frac{1}{(t'-4)(t'-t)}$

One might hope to get the ρ meson at $\nu' = 6$, $t = 28$, but possibly not the f_0 meson at $\nu' = 19$, $t = 80$. On the other hand, the method neither uses determines the values of the partial wave amplitudes on the left i.e. for $t < 4$. This is an example of how the Mandelstain representation can give relations between limited parts of the complete description.

Crossing is well represented. The n channel explicitly appears and the equations express the relation between crossed channels as given by the Mandelstam representations i.e. analytical correctedness. We get automatically the same amplitude and same parametrisation in all (three) channels and uniformity in all three channels.

The main drawbacks are, first the difficulty in determining the

amplitude for large t' already mentioned. Second, the experience of the Oades variational method indicates that the contribution from the t channel absorptive part to the amplitude in the t channel physical region may be much larger than the contribution from the u channel. This would lead to poor determination of the parameters and to sensitivity to choice of parametrisation.

Thirdly, there may be sensitivity to errors in continuation off the physical region.

The equations can be used to determine waves. The constants $\alpha^{I'}$ may or may not be arbitrary, if arbitrary they can be put in from other analyses from which they are accurately determined, if not arbitrary they can be determined by self consistency. One can tell whether or not they are arbitrary by trying the latter and seeing how well determined they are.

The method is only applicable in its partial wave series from to process with double spectral regions sufficiently set back to draw lines like FD through. The method can be considered to be an extension of treatments using just the forward dispersion relation, which is a fixed s dispersion relation with s = o.

Increasing the number of terms in the ℓ' sumation should improve the method, and the formulae converge satisfactorily as $\ell' \to \infty$

The method will not take much computing time. Since the X and Y functions can be evaluated analytically and expressed in terms of elementary functions, one has simply to evaluate two numerical integrals per partial wave per self consistency point t_i.

The first term only is singular for $t > 4.$, it is out from $t = 4 \to \infty$ and has the correct imaginary part

$$\mathrm{Im}\, A_\ell(t) = \frac{1}{(t-4)} \sum_{\ell'=0}^{\infty} (2\ell'+1)\, \mathrm{Im} A_{\ell'}^{I'}(+1) \cdot \delta(\ell'-\ell) \cdot \int_{4-t}^{0} ds'\, P_\ell\left[1+\frac{2s'}{t-4}\right] \cdot P_{\ell'}\left[1+\frac{2s'}{t'-4}\right]$$

The second term appears to be singular from $n = 4 \longrightarrow \infty$

The denominator is $z' -$

$$t' - (4 - s' - t)$$

vanishes when $t' = 4 - t - s'$

when $s' = 4 - t$, $t' = 0$ $\notin [4, \infty]$.

when $s' = 0$, $t' = 4 - t$

and for $t > 4$ $t' \notin [4, \infty]$

Thus the second term is actually cut in t for $t = 0 \longrightarrow -\infty$. i.e. $v' = -1 \longrightarrow -\infty$, Of course, the expression for $A_\ell(t)$ is not continuable to $t < 4$ since the partial wave series has not been proved to converge there, and in fact probably diverges. The above analytic structure holds even if the partial wave series is truncated.

Thus, using fixed s dispersion relations, from a knowledge of

$$\{ \mathrm{Im} A_\ell(t) \} \quad \ell = 0, 1, 2 \ldots \quad t \text{ in } [4, \infty],$$

one can obtain

(1) $\mathrm{Im} A_\ell(t)$ $\ell = 0, 1, 2 \ldots$ t in $[0, -32]$

(2) $\mathrm{Re} A_\ell(t)$ t in $[4, -32]$ actually a complex region including this

(3) $\mathrm{Re} A_\ell(t)$ t in $[4, 68]$ " "

This is illustrated on the diagrams

A (s, t) known completely in region:-

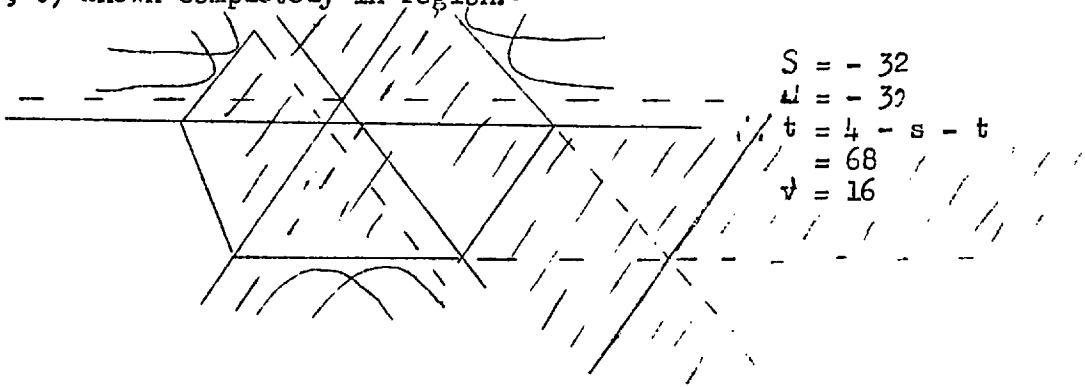

$A_t(t)$ known completely in

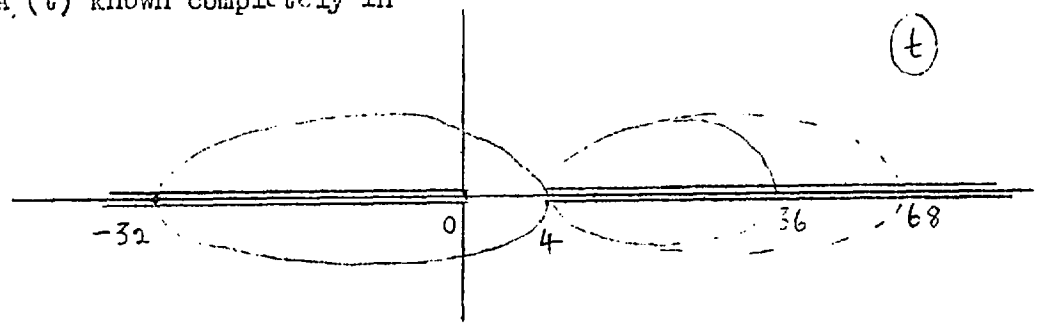

$A_t(s,t)$ known in this region:-

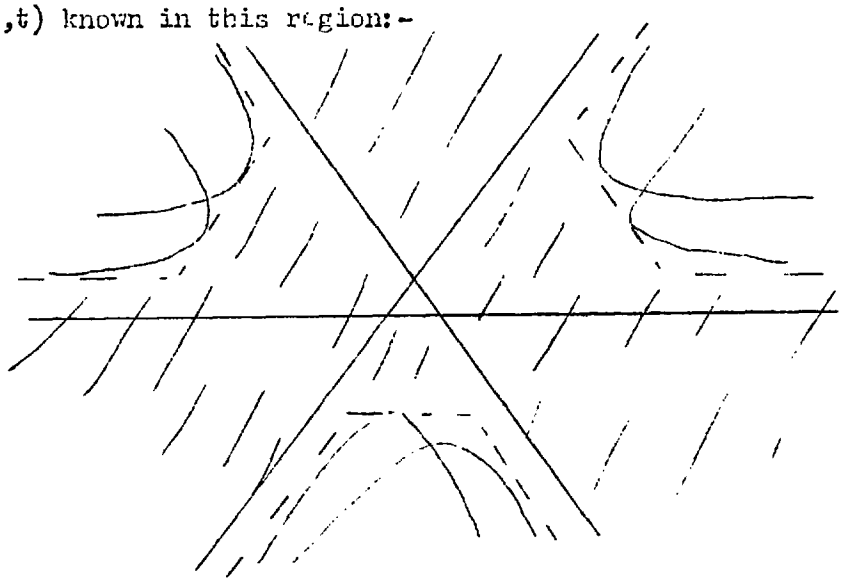

All from a knowledge of $A_t(s,t)$ in

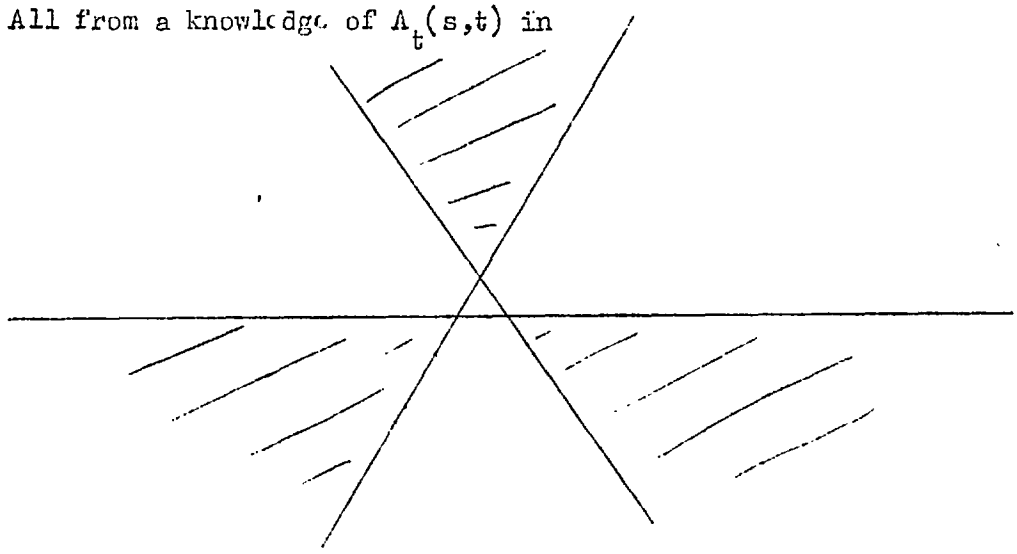

using fixed s dispersion relations only.

Unfortunately, for a closed dynamical scheme one needs

$$\text{Re } A_1(t) \text{ for } t \text{ in } [4, \infty]$$

If one had this, then one would have an exact set of equations for A(s,t) in the physical region without needing a knowledge of the double spectral function.

A(s,t) is also known in the diffraction strips using fixed s dispersion relations

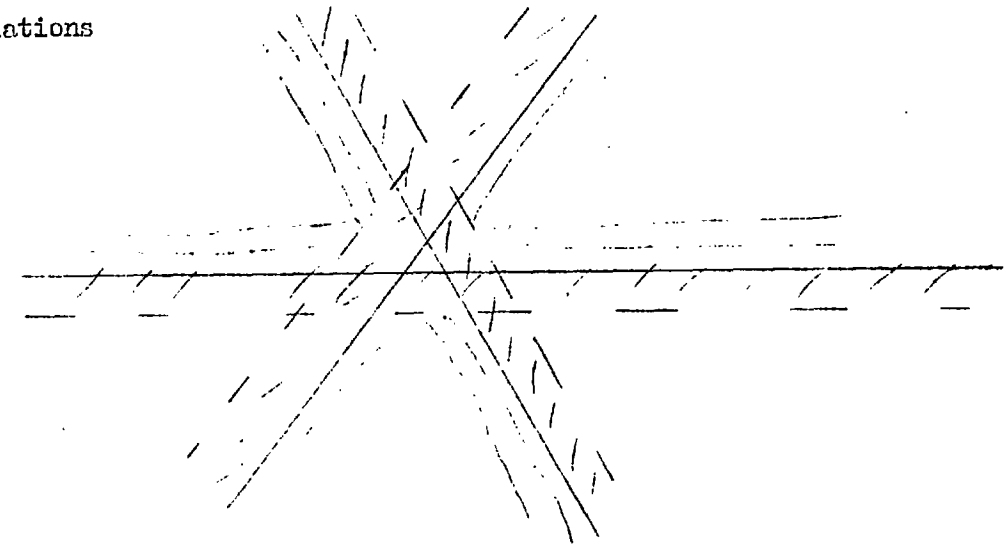

One also has consistency checks, see Section 2.

One can write down various "models":

1. P-WAVE DOMINANT EQUATIONS

$$A_\ell(t) = \frac{1}{\pi}\int_4^\infty \frac{\text{Im } A_\ell(t')\,dt'}{t'-t} + \frac{1}{\pi}(2u'+1)\cdot\beta'\int_4^\infty dt'\,\text{Im } A_{\ell'}(t')\cdot \int_{4-t}^{0} ds'\cdot \frac{P_{\ell'}\left[1+\frac{2s'}{t'-4}\right]P_\ell\left[1+\frac{2s'}{t-4}\right]}{[s'-(4-t'-t)]}$$

compare C-M P dominant, n no cut-off after interchanging integrations (see Chapter 5):

$$B_\ell(t) = \frac{1}{\pi}(2u'+1)\cdot\beta\int_0^\infty dt'\,\text{Im } A_{\ell'}(t')\int_{-\infty}^{4-t'} \frac{P_{\ell'}\left[1+\frac{2t'}{u'-4}\right]P_\ell\left[1+\frac{2u'}{t-4}\right]}{u'-t}$$

2. FUNCTION APPROXIMATION

$$B(\nu) = (2\ell'+1)\cdot\beta'\cdot\Gamma\nu_R\int_{4-t}^{0}\frac{ds'\;P_{\ell'}\left[1+\frac{2s'}{t_R-4}\right]P_\ell\left[1+\frac{2s'}{t-4}\right]}{\left[s'-(4-t_R-t)\right]}$$

$\ell'=0$ gives

$$B \sim \int_{4-t}^{0}\frac{ds'\cdot P_\ell\left[1+\frac{2s'}{t-4}\right]}{\left[s'-(4-t_R-t)\right]}$$

$$z = 1+\frac{2s'}{t-4} \qquad dz = \frac{2ds'}{t-4}$$

$$B \sim \int_{-1}^{+1}\frac{dz\cdot P_\ell(z)}{\left[\frac{2s'}{t-4}+1+\frac{2t_R}{t-4}\right]}$$

$$= \int_{-1}^{+1}\frac{dz\;P_\ell(z)}{\left(z+\frac{2t_R}{t-4}\right)}$$

$$= -2\cdot Q_\ell\left(-\frac{2t_R}{t-4}\right)$$

$$\xrightarrow[t\to+\infty]{} \sim \log(t-4)$$

$\ell'=1$ gives

$$\int_{-1}^{+1}\frac{dz\cdot P_\ell(z)}{\left(z+\frac{2t_R}{t-4}\right)}\cdot\left[1+\frac{1}{t_R-4}\cdot(z-1)(t-4)\right]$$

$$[\text{etc.}] = \left\{1 + \left(\frac{t-4}{t_R-4}\right)\right\} + 2\cdot\left(\frac{t-4}{t_R-4}\right)^2$$

$$= a_0 P_0(z) + a_1 P_1(z)$$

$$\therefore B \sim 2a_0\left[-Q_1\left(-\frac{2t_R}{t-4}\right)\right] + 2a_1 P_1\left(-\frac{2t_R}{t-4}\right)\cdot\left[+Q_1\left(-\frac{2t_R}{t-4}\right)\right]$$

i.e. technique is to use

$$P_{\ell'}\left[1 + \frac{2s'}{t_R-4}\right] = \sum_n a_{n\ell''}(t)\cdot P_{\ell''}\left[1 + \frac{2s'}{t-4}\right]$$

and

$$\frac{1}{2}\int_{-1}^{+1} \frac{P_\ell(z)\, P_{\ell'}(z)\, dz}{\omega - z} = P_{\ell'}(\omega) Q_\ell(\omega) \qquad \ell' \leq \ell .$$

3. COMPLEX 1.

APPLICATION TO OTHER PROCESSES

The application to other processes is less likely to succeed because the double spectral regions are comparatively nearer in. General Mandelstam diagrams have been given by Kibble.

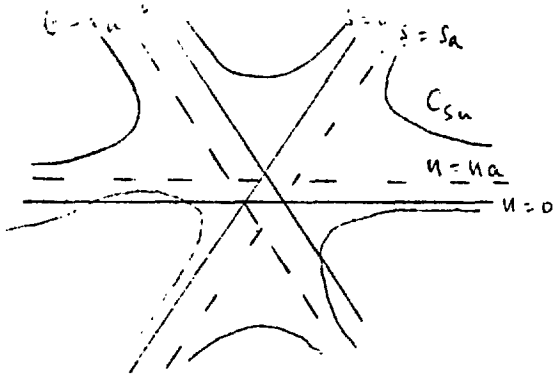

Physical regions

asymptotic to $u = 0$, $s = 0$, $t = 0$

$u = u_b$ ~ pole terms, if any

s_a, t_a, u_a ~ masses of lowest two particle intermediate states.

The π N case is well known (1)

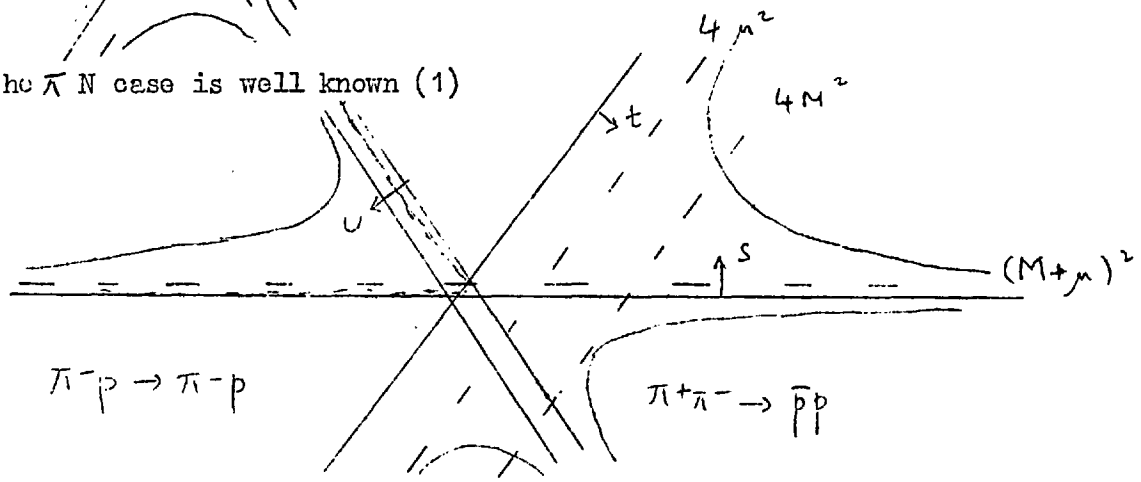

For π p, there are no intermediate states with lower mass. There is a pole term p. For $\pi^+ \pi^- \to \bar{p}\, p$, there is $\pi\pi$ intermediate state, hence cut lower than threshold. What matters for our equations is the location of line just touching the double spectral regions. Given π^- p $\to$ π^- p in the strip, one can obtain the low energy force function for $\pi^+ \pi^- \to p\, \bar{p}$ etc.

DYNAMICAL CALCULATIONS

Given $B(\nu)$ in low energy region only one can define various approximate solutions for $A(\nu)$.

(1) unitarity variational method. A possible procedure using a variational method is as follows:

(a) Choose trial functions, $\{ \mathrm{Im}A_1(t') \}$, with parameters $\{ a_{jl} \}$, for a finite set of waves, supposed to dominate. It would be best if they were automatically consistent with unitarity

e.g. $\mathrm{Im}A_1(t') \leq \sqrt{\dfrac{t'}{t' - 4}}$ all t' and all values of other params.

(b) Using (xii) and (xiii), calculate $\mathrm{Re}A_1(t)$, for all the chosen waves.

(c) Calculate the discrepancy from unitarity

$$\Delta(t) = \mathrm{Re}A_1(t)^2 + \mathrm{Im}A_1(t)^2 - \sqrt{\frac{t}{t-4}} \cdot \mathrm{Im}A_1(t) \qquad t = t_i$$

on a set of points t_i in $[0, 36]$

(d) Vary the parameters $\{ a_{jl} \}$, to minimise

$$\chi^2 = \sum_i \Delta (t_i)^2$$

Depending on how low a value of χ^2 was obtained and how well determined the $\{ a_{jl} \}$ were, one would then have a variational solution to the problem.

(2) Uretsky N/D. To suppress high energies, one must cut off, possibly after making some subtractions

$$N(\nu) = B(\nu) + \frac{1}{\pi}\int_0^{\Lambda} \frac{B(\nu') - B(\nu)}{\nu' - \nu} \cdot N(\nu') \cdot (\nu') \cdot d\nu'.$$

$$D(\nu) = \int_0^{\Lambda} \mathcal{P} \frac{(\nu') \cdot N(\nu')\, d\nu'}{\nu' - \nu}$$

To include diffraction peak in crossed channel

$$\frac{1}{\pi} \cdot \sum_{l'} (2l' + 1) \cdot \beta' \int_4^{\infty} dt' \int_{4-t}^{0} ds' \cdot P_{l'} \left[1 + \frac{2s'}{l'-4} \right] \cdot \mathrm{Im}A_{l'}(t') \cdot \frac{P_l \left[1 + \frac{2s'}{t-4} \right]}{\left[s' - (4 - t' - t) \right]}$$

O.K. to truncate for low t'. For high t', put in an explicit exponential par

$$\frac{1}{\pi} \int_{\Lambda}^{\infty} dt' \int_{4-t}^{0} ds' \cdot \frac{P_l \left[1 + \frac{2s'}{t-4} \right] \cdot A_t^I(s', t')}{\left[s' - (4 - t' - t) \right]}$$

$$A_t^I(s', t') \sim b \cdot \exp.(-as').$$

change $\int_{4-t}^{0}$ to $\int_{\gamma}^{0}$

being width of diff. peak.

So we have 4 parameters Λ, γ, b, a. For high energy contribution. Note that because of fixed width γ, the asymptotic behaviour as $t \to +\infty$, is smaller by fact or ; t ; but asymptotic behaviours are irrelevant anyway.

COMPARISON WITH METHODS BASED ON PROJECTION INTO THE S CHANNEL

The projection of fixed dispersion relations into the t channel gives a different class of calculations entirely, from the calculations in Chapters 3, 4, 5 and 6. The equations are not the same as the Shirkov equations (see Chapter 1) being convergent in a much larger region. We remark that statement like "the dominant force for the P_1 wave comes from the P_1 wave in the crossed channel" depend upon the approximation scheme used, and it is conceivable that waves important in projection into the s channel could be unimportant in projection into the t channel, and vice-versa, even though each calculation converged to the same solution.

2. CONSISTENCY CHECKS

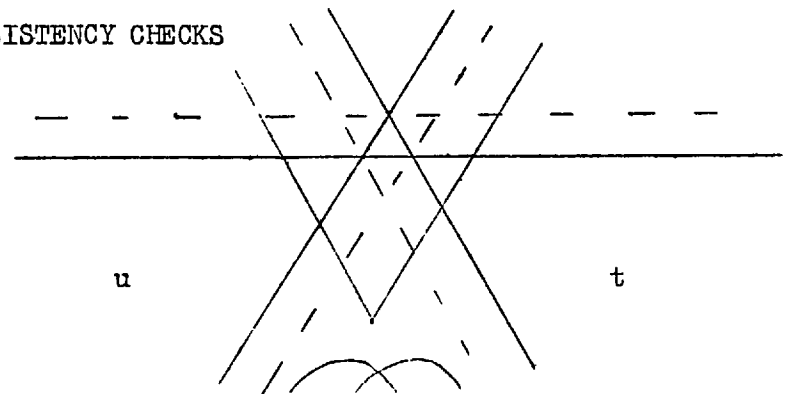

The absorptive parts in the t and u channels are related by crossing symmetry. Each can be expressed as a partial wave series in its own physical region. Now these expansions are convergent out to the double spectral region and there is thus (see diagram) a region in which both converge, this is ($t > 4$, $u > 4$; $\rho_{tu} = 0$). Over this region, the two expansions must agree and this provides a consistency constraint upon the absorptive parts. The two expansions must "dovetail" together. This is a generalisation of the symmetry point ideas of Chew and Mandelstam. The requirement is non-trivial since the t, say, variatio in one expansion is the angular variable and, in the other expansion, the energy variable. Thus we get a correlation of energy and angle in the low energy region. In order to use the requirement, we truncate the two series and estimate over what region, we expect the truncated series to be a good

approximation. Then we demand

$$\sum_{l=0}^{L}(2l+1)\,\mathrm{Im}A_l^{I}(t)\cdot P_l\left[1+\frac{2s}{t-4}\right]=\sum_{l'=0}^{L}(2l'+1)\sum_{I'=0}^{2}\beta_{II'}^{l'}\,\mathrm{Im}A_{l'}^{I'}(t)\cdot P_{l'}\left[1+\frac{2s}{t-4}\right]$$

$$I=0,\ 1,\ 2$$

over the region. This could be achieved numerically either (i) by using trial functions for the $\mathrm{Im}A_l$ and varying parameters to minimise χ^2 over the region or (ii) by using a mesh of values of $\mathrm{Im}A_l$ and varying them to minimise χ^2.

To get an idea of the mechanism, we consider the case of P wave dominance Even in this simple case, we get a difficult functional equation to solve analytically

$$\mathrm{Im}A_1(4-3-u)=\frac{\beta_{11}'\cdot\ \mathrm{Im}A_1(u)\cdot P_1\left[1+\frac{2s}{t-4}\right]}{P_1\left[1+\frac{2s}{-s-4}\right]}$$

The equation cannot be satisfied over a whole region but we can take it on a line. Suppose we take the line $u=8$, define $z=-s-4$, then

$$\mathrm{Im}A_1(z)=\frac{\beta_{11}'\cdot\ \mathrm{Im}A_1(8)\cdot\ \left(-1-\frac{2z}{4}\right)}{-\frac{(z+12)}{(z-4)}}$$

$$=\tfrac{1}{2}\cdot\mathrm{Im}A_1(8)\cdot\ \frac{(4+2z)}{4}\ \cdot\ \frac{(z-4)}{z+12}$$

This has a vaguely rising form with a zero at threshold. Note $(z-4)$ not $(z-4)^{5/2}$ as $z\to 4$ required by unitarity.

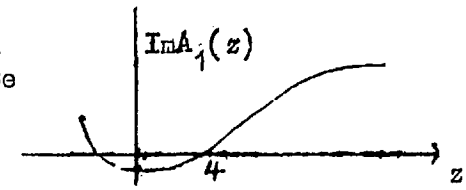

One could deduce from this that a P_1 wave resonance in the u channel would demand a rising P_1 wave in the s channel, however a detailed calculation must be done to produce a reliable prediction.

3. TRANSFORMATION OF VARIABLES

An attempt to extend the scope of fixed s relations. The divergence of both forms, obtained from the fixed s dispersion relation, so far discussed, is due to the necessity for values of the amplitude in the double spectral regions

where the partial wave series diverges. We attempt to circumvent this difficulty by changing variables. A fixed s dispersion relation is obtained by viewing A(s, t) as a function of t, whilst s remains fixed. Can one define new variables

$$x = x(s, t)$$
$$y = y(s, t)$$

and consider A(s(x,y), t(x,y)) as a function of x with y fixed, so as to give more useful equations? One might be able to arrange the curve y = constant to avoid the double spectral region but penetrate the physical regions. Of course one needs A(x) to satisfy a dispersion relation in (x) and this limits one's choice of transformation. For example, orthogonal coordinates

$$s + t - 4 = d \cos h\, x \cos y$$
$$s - t = d \sin h\, x \sin y$$

with x closely related to arc length and y a label for the family give curves

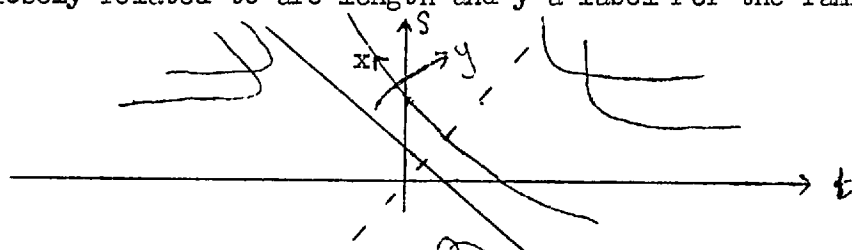

which can be constrained to go through (s ≥ t, t = o) and (s = o, t = 4 by

$$d = \pm 4\sqrt{\sec^2 y - \operatorname{cosec}^2 y}\ .$$

However, the extra kinematic singularities generated by this transformation may make it difficult to use. Fixed angle dispersion relations are along curves of constant z

$$z = 1 + \frac{2t}{(s - 4)}$$

for $\pi\pi$ are certainly straight lines. for 太 N,

$$t = -2q^2 (1 - z)$$
$$q^2 = \tfrac{1}{4} \left\{ s - 2(M^2 + \mu^2) + \frac{(M^2 - \mu^2)^2}{s} \right\}$$
$$z = 1 + \frac{t}{2q^2}$$
$$= 1 + \frac{t}{2} \cdot \frac{4}{\left[s - 2(M^2 + \mu^2) + \frac{(M^2 - \mu^2)^2}{s} \right]}$$

$$= 1 + \frac{2st}{\left[s^2 - 2s(M^2 + \mu^2) + (M^2 - \mu^2)^2 \right]}$$

clearly a curve (which bounds physical region for $z = \pm 1$, see diagram in section 1). Hence, for fixed angle dispersion relations (3), we have curves in the (s, t) plane. We shall use [2] Mandelstam diagram (Fig. 2)

Now,

$$A(s, t, u) = \int\int_C \frac{ds'}{(s' - s)} \cdot \frac{dt'}{(t' - t)} \cdot \rho(s', t')$$

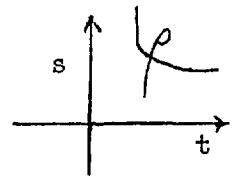

has singularities for complex s real t
complex t real s
real s real t
but not complex s complex t

For z real

$$z = 1 + \frac{2t}{s - 4}$$

then if t is complex, so is s. Hence no singularities. Cannot have one complex without the other. Hence only singularities are to be found in the real (s,t) plane.

Suppose we choose to fix some other variable

$$x = as^2 + bst + ct^2 + dt + es + f$$

Then fix x real. Then singularities will occur for s and t real and not for s and t complex. However for s complex, it may be possible that t is real, for certain choices of s, giving singularities as a function of so with x fixed In general, there will exist some complex points of s for which this is true. For fix x real and fix t real in its spectral region. Then s must be the solution of

$$as^2 + s(bt + e) + (ct^2 + dt + f - x) = 0.$$

which will sometimes be real, if

$$(bt + e)^2 - 4a(ct^2 + dt + f - x) > 0$$

and sometimes complex if < 0.

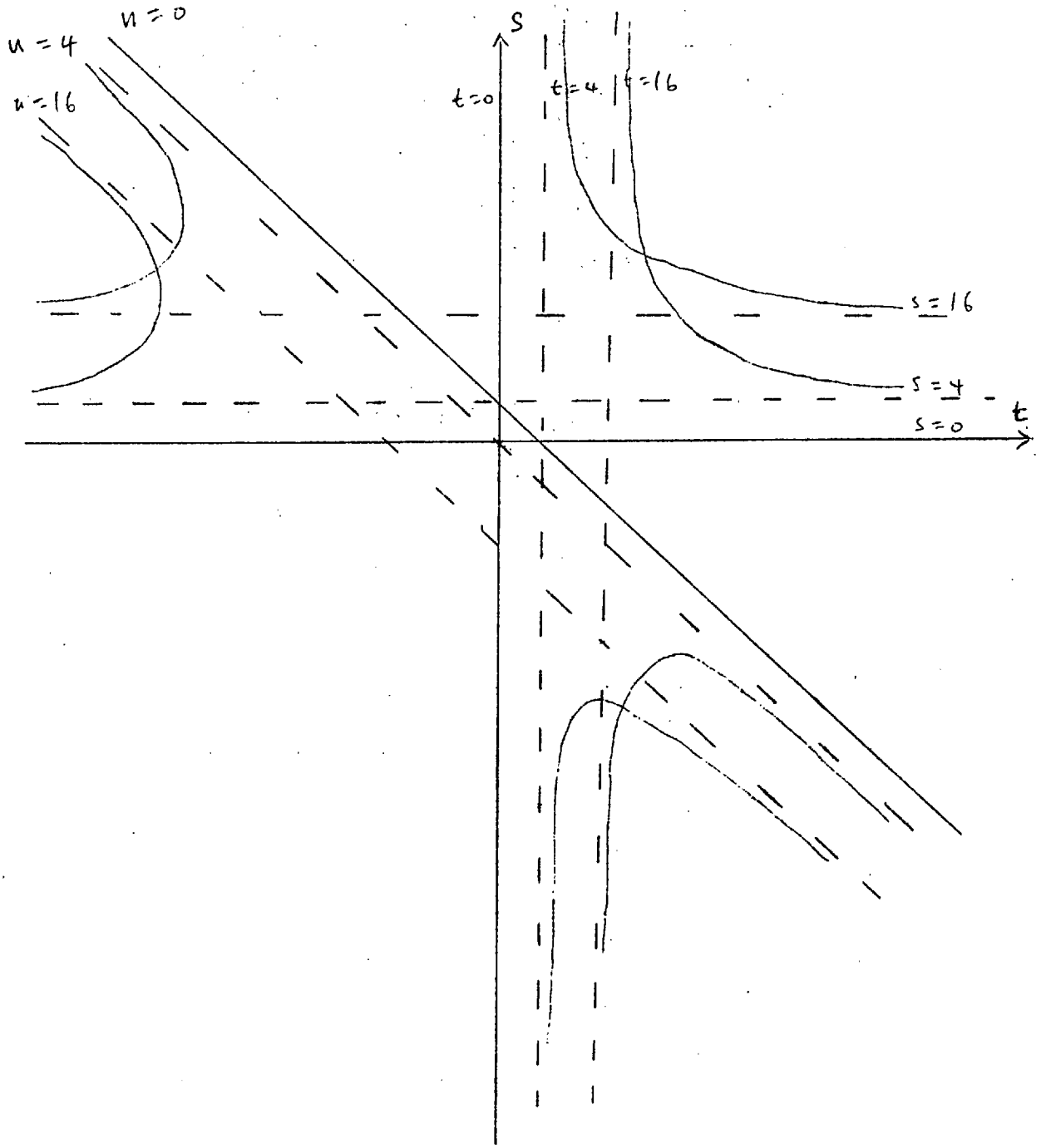

Fig. 7 - 2. Mandolstam diagram in ordinary (s, t) coordinates.

Hence for these values of s and t there will be singularities, giving complex cuts in the s plane.

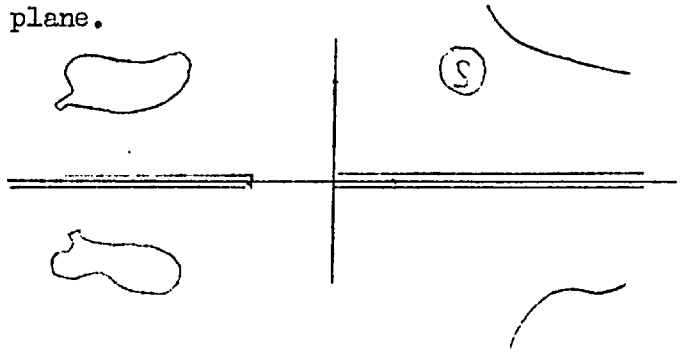

What we want is that for this fixed x, then A(s, t) have simple analytic properties as a function of so, so a dispersion relation can be written. Note that for a = o it is always true, i.e. For real s and real t there will be singularities, for real and complex t there will be complex's and real t there cannot be singularities provided b and c are real. Complex s complex t none. Hence all cuts on real axis of s plane.

Fix x real and s real, then t is the solution of a quadratic

$$c^{?} + (bs + d)\,t + (es^{*} f - x) = 0$$

and is either real or complex:

$$\text{real if } (bs + d)^2 = c.(es + f - x) > 0$$

Hence, really we want t. to be either real or complex and inside Lehman ellipse for this particular value of s. If this is a line on the (s,t) diagram then there is a real t satisfying the equation. We have already ensured cuts only on real s axis by making a = o. Hence by ensuring that it is quadratic relatio so that all (both in this case) values of t are either both real or both comple and by ensuring that

$$x = bst + ct^2 + dt + es + f$$

is a curve in the (s,t) plane we have ensured that for each real s there are only real values of t satisfying this equation. Further, the imaginary part is just given by its value on the diagram. This is thus the most general curve fo

which this can be done.

Further requirement is of course that we remain off the double spectral region. With a t^2 term we have a double valued function of s leading presumably to two sheets, s channel on sheet 1, t channel on sheet 2. We can ensure that t is real for s real, giving discontinuities from physical region values, and also make s single valued on the curve x = const, by dropping the t^2 term. Thus we are lead to the hyperbolae $(s - a) \cdot (t - b) = c^2$.

Dropping the t^2 term means that we have curves asymptotic to s = const. or t = const., we now have

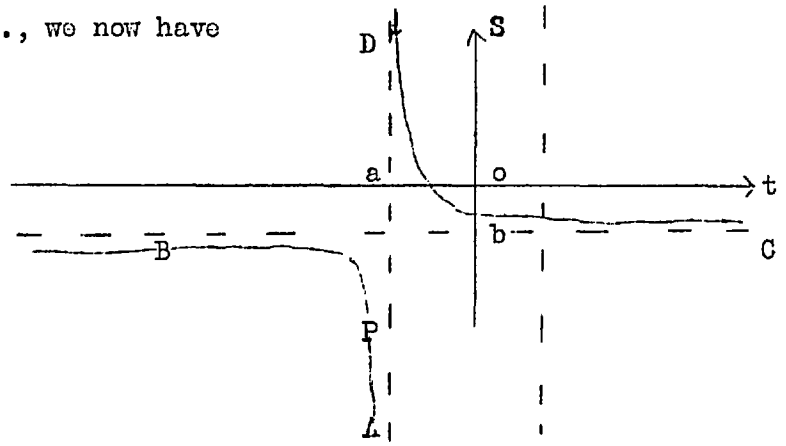

These curves lie entirely in physical regions. As a function of s, with x fixed, $A(s,t)$ is analytic in a cut plane cuts $[o, -\infty]$, $[4,\infty]$.

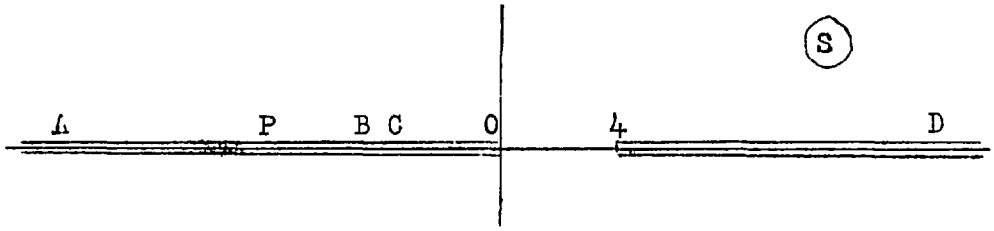

It is real in $[0,4]$, (s,t) being in the central triangle and the discontinuity on the cuts is twice the imaginary part. The imaginary part is the $\mathrm{Im}A(s,t)$ in the physical region and can be represented by the appropriate partial wave series. The problem remaining is the nature of the behaviour at B and C. . Now, as s approaches B from below the point (s,t) in the (s,t) plane moves off to $t = -\infty$ and remerges at $t = +\infty$. As it does so, $\mathrm{Im}A$ certainly has a continuous value by the Phragman-Lindelöf theorem (see Ch. 1

but its higher derivatives may be discontinuous. Also if we look at the phase of $(s - a)$, for c^2 real, we always have phase of $(t - b)$ = - phase $(s - a)$.

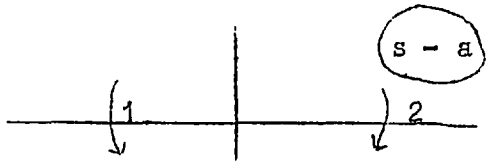

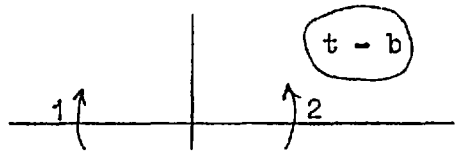

so, referring to the diagram, as $(s - a)$ moves across its real axis on either side of zero, $(t - b)$ moves the opposite way. This should not invalidate a dispersion relation in s, of the form

$$A(s) = \frac{1}{\pi}\int_4^\infty \frac{\mathrm{Im}A(s')}{s' - s}\,ds' + \frac{1}{\pi}\int_{-\infty}^0 \frac{\mathrm{Im}A(s')\,ds'}{s' - s}$$

We now have a family of hyperbolae with 3 parameters a, b, c and can make a curve go through any point in the plane.

Can we define family

$$(s - a).(t - a) = c^2$$

which covers entire physical region and avoids the double spectral region?

(i) Suppose we want it to go through $s = 0$, $t = 4$ and $t = 0$, $s = 4$

then $-a.(4 - a) = c^2$

$a^2 - 4a - c^2 = 0$ 2 solutions

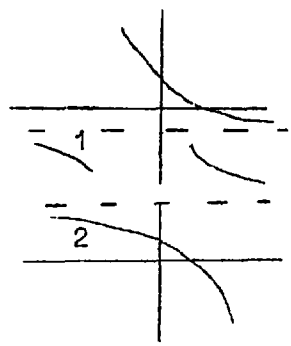

we take the smaller a

$$a = \frac{4 \pm \sqrt{16 + 4c^2}}{2}$$

$$= 2 \pm \sqrt{4 + c^2}$$

i.e. take $a = 2 - \sqrt{4 + c^2}$

Then different values of c^2 define the family. Can we span physical region?

as $a \to 0$. $c \to 0$

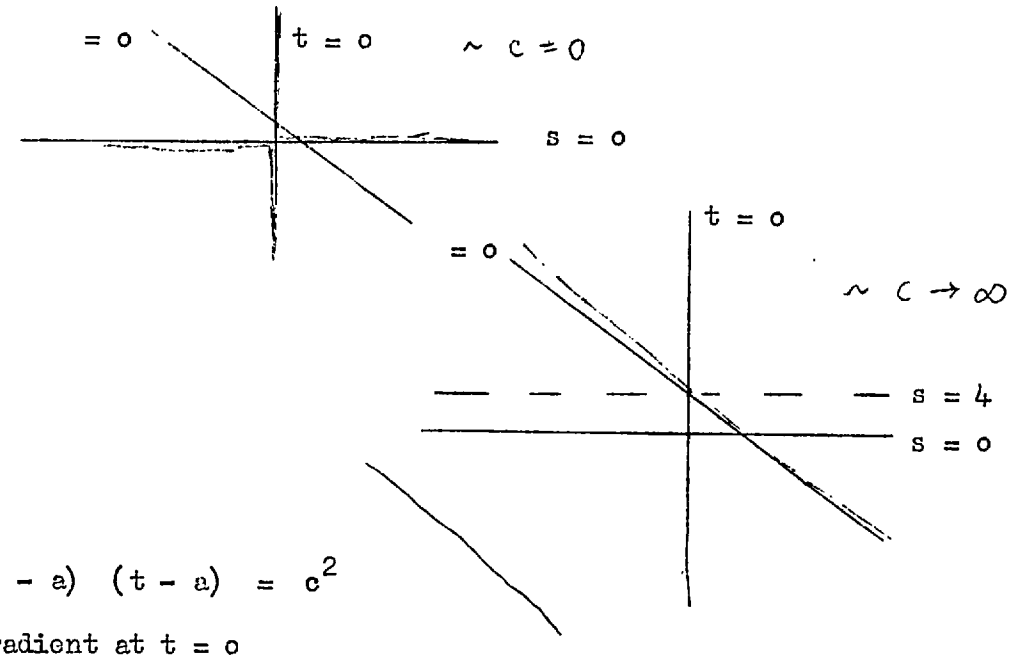

$(s - a)\ (t - a) = c^2$

gradient at $t = o$

$(s - a) = \dfrac{c^2}{t - a}$

$\dfrac{ds}{dt} = \dfrac{-c^2}{(t - a)^2}\Bigg|_{t = o} = \dfrac{-c^2}{(-a)^2} = -\dfrac{c^2}{a^2}$

for $\rightarrow -1$ need $c^2 \rightarrow a^2$

but $a = 2 - \sqrt{4 + c^2}$

clearly c and a $\rightarrow \infty$

The u branch retreats to infinity and the s, t branch lies along $u = o$.

Thus the family

$$(s - a)\ (t - a) = c^2 \ : \quad a = 2 - \sqrt{4 + c^2}$$

is a one parameter family, exactly covering once all the physical regions.

Every member through $s = 4$, $t = o$ and $s = o$, $t = 4$ and the central Δ, which is covered once

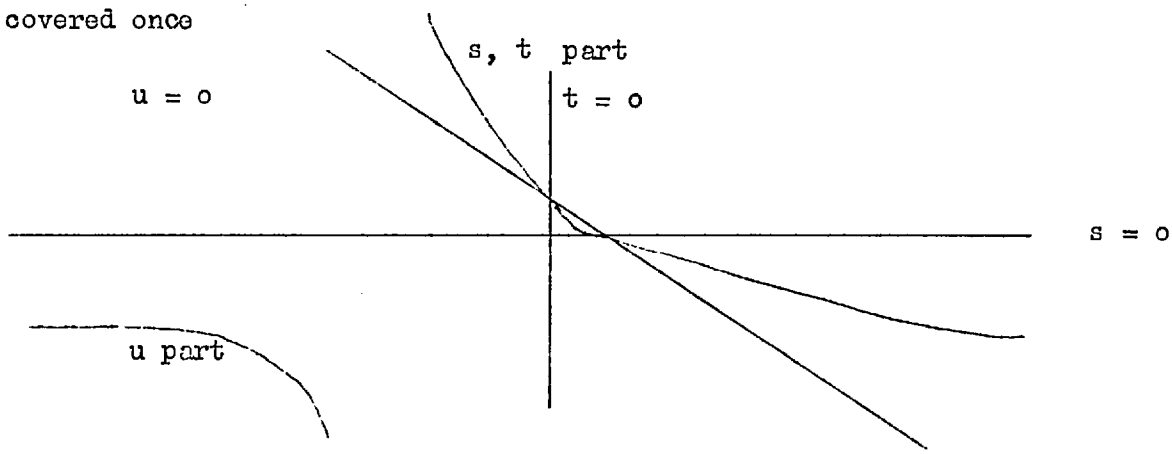

PROJECTION INTO PARTIAL WAVES

Suppose now we wish to project out the partial wave amplitude in the t channel

$$\text{Then } A(t, c^2) = \frac{1}{\pi} \int_{R(c^2)} \frac{\mathrm{Im}A(t'c^2)}{t' - t}\, dt'$$

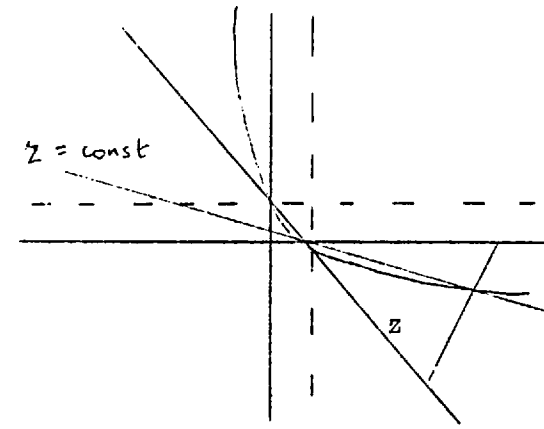

The value of z is $1 + \frac{2s}{t - 4}$

$$z = 1 + 2\,\frac{\left[\frac{c^2}{t - c} + a\right]}{t - 4}$$

We can make z replace c as the variable now by solving w.r.t. t

$$(z - 1) \cdot (t - 4) = 2 \cdot \left[\frac{c^2}{t - a} + a\right]$$

will have two roots for t. Take the one > 4. Now we want to integrate w.r.t. z at constant t, so c^2 will vary; hence we must eliminate c^2 in favour of z leaving:

$$A(t, z) = \frac{1}{\pi} \int_R \frac{\mathrm{Im}A(t', z)\, dt'}{t' - t}$$

$$A_1(t) = \tfrac{1}{2} \int_{-1}^{+1} P_1(z) \cdot A(t, z)\, dz.$$

Thus we obtain $A_1(t)$ in the entire physical region expressed in terms of integrals over the three physical regions. From the point of view of dynamics the main thing we want is $B_1(t)$ in terms of integrals over the two crossed regions (s and u channels). From this we could solve for $A_1(t)$ using unitarit However, the 3 physical regions all contribute to each other in a form not easily separable into left hand cut and right hand cut. A dynamical calculation based on the equations would have to be an overall mesh scheme.

NOTE TWO CORRESPONDENCES BETWEEN HYPERBOLAE AND EXPERIMENT

(1) behaviour as $t \longrightarrow \infty$ becomes s independent.

(2) as one branch retreats to wide angle asymptotic region, it becomes unimportant.

THE IDEA OF A PHYSICAL REGION DYNAMICAL SCHEME

Thus using the hyperbolic and other coordinates we can write down dynamical equations which enable us to obtain an expression for $B_1(t)$ for all

t in $[4, \infty]$ i.e. all physical region and all l waves, given only the amplitude in the crossed physical regions. This is a very happy state of affairs since

(i) the behaviour of the amplitude in the double spectral region is very bad possibly not even polynomially bounded. In this case M.R. breaks down, but our equations do not, being based upon a more general analyticity postulate which is more easily provable rigorously.

(ii) the behaviour in the physical region is good and reasonable estimates of asymptotic behaviour are available from experiment. We can use experimental data directly in the crossed channel if we like.

(iii) the double spectral region can be explored from analytically solved models based upon the equations.

If we can obtain a set of equations based only upon analyticity properties in the three physical regions (s-, t-, u-) and reality in the central triangle, then we can consider the possibility of using this set as a dynamical scheme in its own right, independent of MR. MR would then be a special case. The unitarity condition would still be applicable. The advantages of abandoning the double spectral regions are several. We avoid the bad behaviour in these highly unphysical regions, but we retain the essential attractive analyticity postulates of Mandelstam and the idea of crossing symmetry. Philosophically, we concern ourselves more with physical regions, where the physics takes place.

The difficulties are in tractability. Such a scheme may well be very complicated and not easily projected into partial waves and not easily approximated. The whole attitude to solution is different, depending more on the idea of setting up approximations, which allow <u>continuation</u> to other regions, than upon the direct <u>parametrisation</u> of singularities. The bad behaviour in the double spectral region may be difficult to parametrise.

Many questions remain:

(i) Can we find more suitable transformations of coordinates?

(ii) Can we make the equations more obviously crossing symmetric?

(iii) What is the exact region of analyticity in s and t, implied by the equations?

(iv) Can we write approximate schemes and will these give a natural breakdown of the amplitude into individual terms, each of which has the full analyticity properties? Each term would then be a natural physical object or concept.

SUMMARY

In Chapter 2, we studied fixed s dispersion relations.

$$A^I(s,t) = \frac{1}{\pi}\int_4^\infty dt'\, A_t^I(s,t')\left[\frac{1}{t'-t} + \frac{(-1)^I}{t'-u}\right] \qquad \text{p. s.}$$

I relates to an isospin decomposition in the s channel. We considered asymptotic behaviour and noted that we need at most one substraction for $s<0$, two for $0<s<4$. The Phragmen - Lindelhöf theorem gives the result

$$A_t^I(s,t') \underset{\substack{t'\to\infty \\ s \text{ fixed.}}}{\longrightarrow} 0 \quad \text{, for I odd}$$

We looked at the projection into partial waves in the s channel, obtaining a convergent expression for the real and imaginary parts of the partial wave amplitude, for ν in $[-9,0]$

$$C_\ell^I(\nu) = \frac{4}{\pi\nu}\int_0^\infty d\nu'\, \mathcal{A}_t^I(\nu',\nu)\, Q_\ell\left[1 + 2\left(\frac{\nu'+1}{\nu}\right)\right]$$

$-9<\nu<0$

Putting in

$$\mathcal{A}_t^I(\nu',\nu) = \sum_{I'=0}^{2} \beta_{II'} \sum_{\ell'=0}^{L} (2\ell'+1)\, \mathrm{Im}\, A_{\ell'}^{I'}(\nu')\, P_{\ell'}\left[1 + 2\left(\frac{\nu+1}{\nu'}\right)\right]$$

we found the complex domain of convergence in ν, which includes $[-9,0]$, of course.

We evaluated numerically contributions to $C_\ell^I(\nu)$ from the first few partial waves in the t channel, using the expected experimental forms, and concluded that, for S_0, S_2, P_f, D_0 in the t channel, we probably had reliable values in $[-6,-1]$.

We went on to discuss approximations in dispersion theory from a numerical analytic view-point and discussed Streater's attitude that arbitrary parameters, occurring in analytical solutions, could and should be detected and isolated in the corresponding approximate calculations.

In Chapter 3, we systematically studied the original Balazs method numerically. The method is to take a unitary parametric form $F(\nu,\{\alpha_i\})$ for the amplitude, and

to determine the parameters by equating (or 'matching') the real part on the near left to the real part obtained from the crossed channel, using a fixed s dispersion relation. He used an N/D pole form with parameters the residues of the poles. The positions of the poles were determined in an auxiliary calculation. In the auxiliary calculation a separable approximation is made to the kernel in the dispersion relation for N.

$$K_{exact}(x',\nu) = \frac{1}{1+x'\nu} \approx \sum_{i=1}^{\tilde{n}} \frac{g_i(x')}{1+x_i} = K_{approx}(x',\nu). \qquad x' = -1/\nu$$

The positionsof the poles areobtained by optimsing the fit of Kexact to Kapprox. Thus it is asserted that these pole positions are the best ones for any reasonable discontinuity of N. We studied this approximation and concluded that

(1) it is valid if and only if the dispersion relation converges.

(2) the asymptotic behaviour of the approximated integral is not necessarily $O\left(\frac{1}{\nu}\right)$.

(3) the Balazs contention, that it was still a good approximation for oscillating functions, was correct for the actual approximate forms found by this procedure.

(4) the positionsof the poles are close to those obtained by an orthodox numerical integration procedure.

We studied the Balazs method, as used by Balazs, and found that

(1) it is independent of normalisation point ν_0. An analytical proof is given.

(2) it is very sensitive to the matching region. In an n = 2 calculation, for symmetry points at -2.5, -2.3, o.o, the self-consistent resonance had position and width (3.82, 3.13) and at -1.5, -1.0, 0.0 had (1.88, 1.19).

(3) on increasing the number of poles, n, the solution disappears.

(4) there was a one parameter ambiguity, the width, Γ_{ν_k}, being determined by the calculation and the position, ν_k, being a free parameter.

(5) we looked at other partial waves and found some self-consistent solutions for certain values of n, and not for others. This consolidated the conclusion that the solutions are spurious.

We attempted to modify and generalise the Balazs method, to use the idea of crossing on the left, but to remove the difficulties found for Balazs original method. We took a smooth trial function in the crossed channel, instead of a δ- function and generalised the matching equations to match the real and imaginary parts in detail on the near left. We found

(1) that, by this procedure, we could get very good fits on the left, but the 'output' amplitude on the right was still sensitive to details of matching. For a fixed matching region, the solution settled down, as n increased, to a non-resonant output for resonant input.

(2) the contribution from the near left discontinuity was small and repulsive.

(3) the structure of the real part on the left wasrelated in detail to the discontinuity on the near left. This structure could be reproduced, but was irrelevant to the right hand side.

We tried minimisation of χ^2 deviation from crossing to determine the parameters rather than matching. Using this method, the only solutions found were similar to that of Balazs for n = 2..

We looked at different self-consistency conditions and found that the width and position of the self-consistent resonance could be varied by a factor of 2 either way by a suitable choice of self-consistency condition.

We also found that an uncertainty γ, in the crossed amplitude, produced the

same uncertainty γ in the width and position of the self-consistent resonance.

In Chapter 4, we looked at the Zachariasen method and found results similar to that of other workers. The Zachariasen method consists of an ansatz for continuation from left to right

$$N(\nu) = C(\nu)$$
$$D(\nu) = 1 - \left(\frac{\nu-\nu_0}{\pi}\right)\int_0^\infty \sqrt{\frac{\nu'}{\nu'+1}}\,\frac{C(\nu')\,d\nu'}{(\nu'-\nu)(\nu'-\nu_0)}$$
$$\nu_0 = -\nu_R - 1$$

We found that, taking $\nu_0 = \alpha(-\nu_R-1)$, the resonant solution was very sensitive to α, as α changed from 0.8 to 1.5, ν_R changed from .665 to .186 and Γ_{ν_R} from .597 to .147. With a fixed ν_0, independent of (ν_R, Γ_{ν_R}), there was a definite one parameter ambiguity with $\Gamma = 1, \nu_R$ free. For dynamic $\nu_0 = -\nu_R - 1$, this was not so marked. We extended the model to exchange of higher waves by further subtractions at ν_0, putting the subtraction terms = 0 to get agreement of higher derivatives of $C(\nu)$ ~~and~~ at $\nu = \nu_0$. Using this, we looked at the effect of higher waves in the t channel upon various waves in the s channel. This was inconclusive.

In Chapter 5, we investigated the variational method of Hamilton. This method estimates directly the contributions from left and right using a trial function $F(\nu)$, and crossing, and then directs us to vary $F(\nu)$ until unitarity is closely satisfied in the physical region. The right hand cut is taken to be the same as for the trial function. Two dispersion relations are used, one for the real part and a Gilbert dispersion relation for the imaginary part.

$$\mathrm{Re}\,A_{out}(\nu) = \left(\frac{\nu-\nu_0}{\pi}\right)\int_{\nu_0}^{\infty}\frac{\mathrm{Im}\,F(\nu')\,d\nu'}{(\nu'-\nu)(\nu'-\nu_0)} + \left(\frac{\nu-\nu_0}{\pi}\right)\int_{\Lambda}^{-1}\frac{\mathrm{Im}\,C(\nu')\,d\nu'}{(\nu'-\nu)(\nu'-\nu_0)} + \mathrm{Re}\,A_{out}(\nu_0)$$

$$\mathrm{Im}\,A_{out}(\nu) = -\left(\frac{\nu-\nu_0}{\pi}\right)^{3/2}\int_{\nu_0}^{\infty}\frac{\mathrm{Re}\,F(\nu')\,d\nu'}{(\nu'-\nu)(\nu'-\nu_0)^{3/2}} - \left(\frac{\nu-\nu_0}{\pi}\right)^{3/2}\int_{\Lambda}^{-1}\frac{\mathrm{Im}\,C(\nu')\,d\nu'}{(\nu'-\nu)(\nu'-\nu_0)^{3/2}} + \mathrm{Im}\,A_{out}(\nu_0)$$

p. s.

It is immediately obvious that the method is sensitive to choice of parameterisation, by writing similar dispersion relations for the unitary trial function (in fact, Breit-Wigner) used.

$$\mathrm{Re}\,F(\nu) = \left(\frac{\nu-\nu_0}{\pi}\right)\int_0^\infty \frac{\mathrm{Im}\,F(\nu')\,d\nu'}{(\nu'-\nu)(\nu'-\nu_0)} + \left(\frac{\nu-\nu_0}{\pi}\right)\int_{-\infty}^{-1}\frac{\mathrm{Im}\,F(\nu')\,d\nu'}{(\nu'-\nu)(\nu'-\nu_0)} + \mathrm{Re}\,F(\nu_0).$$

Thus, the 'solution' is that which minimises the difference between the contributions from the left and cuts. If we choose Breit-Wigner parametrisation, it has an extremely small left hand cut and we need a small contribution from crossing. If we choose N/D parametrisation, this gives a large left hand cut contribution. However, each parametrisation gives a believable resonant form on the right. When unitarity is attained, we get a very small % error ~ .3% but this ismerely an indication of the smallnessof the contribution from crossing. Further, we found a marked one parameter ambiguity from contours in the (ν_R, Γ_{ν_R}) plane.

Oades used the method for the $\pi\pi$ problem with a correcting pole on the left to represent contributionsfrom higher waves. Our investigation shows the solutions are spurious. We tried to define sensible variational calculations.

(1) using N/D parametrisation, no left hand correcting pole, Gilbert dispersion relation only.

(2) representing the left hand contribution by the ansatz $C(\nu)$.

(3) using a crossing constraint on the real part on the left.

We did obtain various solution, but believe them all to be spurious.

We looked at the solution of the Shirkov equations, which are known to have families of resonant solutions, by the variational method, but found no solutions.

In Chapter 6, we used the real and imaginary partson the left to obtain $\mathrm{Im}A^{-1}(\nu)$, giving an immdiate utiary solution by inverse amplitude dispersion relations, provided one can calculate the threshold residues. $\mathrm{Im}A^{-1}(\nu)$ was estimated from the first few partial waves in the t channel, with experimental values and was found to be massed in the near left, i.e. there was the possibility of a nearby singularity approximation. Indeed, in some cases,

the left hand side was well represented by a single pole. Using threshold residues estimated from $C(\nu)$, we could not get any self-consistent solutions, however the threshold term is such a large one that a slight variation in it could produce a resonant P wave. The corresponding P wave scattering length was not unreasonable. We also looked at a unitarised Born approximation.

$$A^{-1}(\nu) = C^{-1}(\nu) + 2\sqrt{\frac{\nu}{\nu+1}} \cdot \log\left[\sqrt{\nu} + \sqrt{\nu+1}\right] \qquad \text{p.s.}$$

which yielded no self-consistent solutions. We remark that uncertainty in the threshold residue gives a one parameter ambiguity similar to those found for the methods in Chapters 3, 4 and 5.

One can compare the preductions for the effect of the on S_0, S_2, P_1, D_0, D_2, F_1, Born approximation by looking at Figures 3-8, 4-3, and 6-5.

Our overall conclusion is that none of the methods is suitable for bootstrap calculations and that any 'solutions' obtained are spurious. Some methods might be reliable for low energies up to $\nu \approx 3$, at the most.

As alternatives, we proposed, in Chapter 7, three ideas.

(1) 'consistency checks' - a consistency contraint on the simultaneous continuation from the t and u channels to the same region. This could be used for low energy work.

(2) the projection of the fixed s dispersion relation into the t channel.

$$A_\ell^{I'}(t) = \frac{1}{\pi}\sum_{\ell'=0}^{\infty}(2\ell'+1)\int_4^\infty \frac{dt'}{(t'-4)}\cdot\left[\mathrm{Im}\,A_{\ell'}^{I'}(t')\cdot X_{\ell'\ell}(t',t) + \sum_{I''=0}^{2}\beta_{I'I''}\,\mathrm{Im}\,A_{\ell'}^{I''}(t')\cdot Y_{\ell'\ell}(t',t)\right] + a^{I'}\cdot\delta_{\ell 0}$$

where

$$X_{\ell'\ell}(t',t) = \frac{1}{t'-t}\int_{4-t}^{0} ds'\, P_{\ell'}\left[1+\frac{2s'}{t'-4}\right] P_\ell\left[1+\frac{2s'}{t-4}\right]$$

$$Y_{\ell'\ell}(t',t) = \int_{4-t}^{0} \frac{ds'\cdot P_{\ell'}\left[1+\frac{2s'}{t'-4}\right] P_\ell\left[1+\frac{2s'}{t-4}\right]}{t'-u'}$$

This gives an expression $B(\nu)$, in the low to medium energy physical region,

given partial waves in the crossed channel. The series diverges at $\nu = 16$, so it should be reliable out to $\nu = 8$, but this may not be sufficient for bootstrap calculation. It has the advantage of not needing to be continued (like the Born term for example) from the left but being a direct physical region estimate.

(3) by transforming variables, we outline how it is possible to arrive at a complete dynamical scheme, based only upon values of the amplitude in the three physical regions.

APPENDIX 1. LEGENDRE POLYNOMIALS

(i) General references (1)

Some useful standard results (for ℓ integral).

a. $$\frac{1}{t - z} = \sum_{n=0}^{\infty} (2n + 1)\, P_n(z)\, Q_n(t)$$

b. If $\rho \geq 1$ is radius of convergence of $\sum c_n z^n$ then $\sum c_n P_n(z)$ converges in ellipse semi axes $\frac{1}{2}\left(\rho + \frac{1}{\rho}\right), \frac{1}{2}\left(\rho - \frac{1}{\rho}\right)$; with foci -1, $+1$.

c. $P_n(z)$ have forms

$P_0(z) = 1$, $P_1(z) = z$, $P_2(z) = \frac{1}{2}(3z^2 - 1)$

$P_3(z) = \frac{1}{2}(5z^3 - 3z)$

$P_n(z)$ is entire function

$\longrightarrow z^n$

$|z| \longrightarrow \infty$

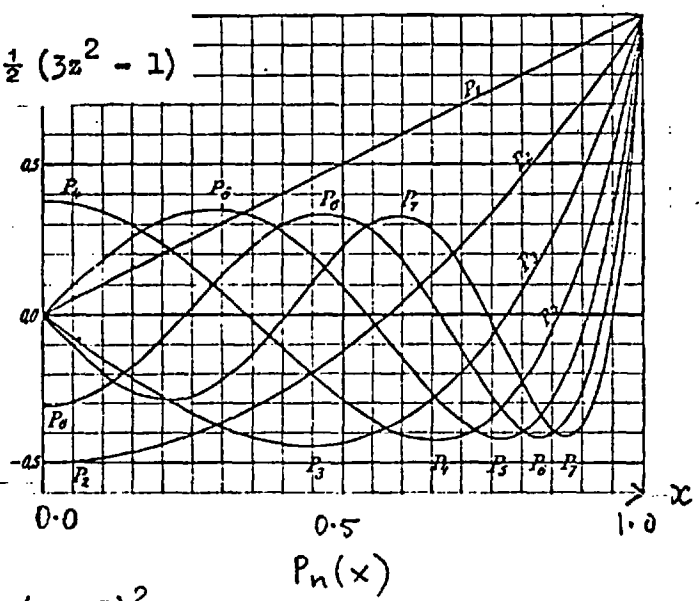

$P_n(x)$

d. $$Q_n(z) = P_n(z) \cdot \left[Q_0(z) - R_n(z) \right]$$

where

$$Q_0(z) = \frac{1}{2} \log \frac{z + 1}{z - 1}$$

$$R_n(z) = \frac{1}{2} + \frac{1^2}{3z} + \frac{2^2}{5z} \cdot \cdot \cdot + \frac{(n - 1)^2}{(2n - 1)^2}$$

So Q_n is out $[-1, +1]$

with discontinuity $-P_n(z)$

$$Q_n(z) = \frac{1}{2}\int_{-1}^{+1} \frac{P_n(w)\, dw}{z - w}$$

$$Q_n(z) \longrightarrow z^{-\ell-1}$$

$|z| \longrightarrow \infty$

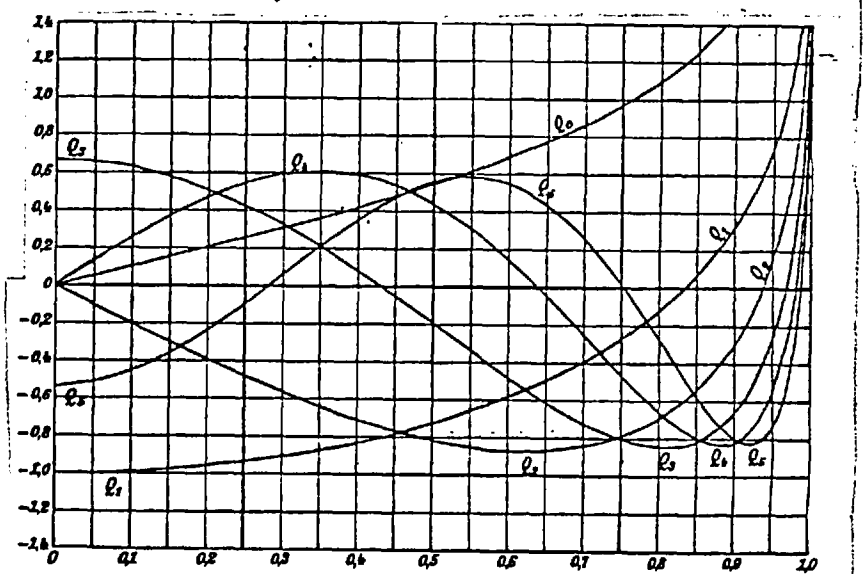

$Q_n(x)$

(ii) Derivatives of C(ν) functions

$$z = 1 + \frac{2(\nu' + 1)}{\nu}$$

$$y = 1 + 2\left(\frac{\nu + 1}{\nu'}\right)$$

$$\frac{dz}{d\nu} = -2\left(\frac{\nu' + 1}{\nu^2}\right)$$

$$\frac{dy}{d\nu} = \frac{2}{\nu'}$$

$$\frac{dP_\ell(y)}{dy} = \begin{cases} 0.0 & \ell = 0 \\ 1.0 & 1 \\ 3y & 2 \\ \frac{15}{2}y^2 - \frac{3}{2} & 3 \end{cases}$$

$$\frac{dQ_m(z)}{dz} = \begin{cases} \frac{-1.0}{z^2 - 1} & m = 0 \\ Q_0(z) - \frac{z}{z^2 - 1} & 1 \\ 3.z.Q_0 - \frac{1}{2}\left(\frac{3z^2 - 1}{z^2 - 1}\right) - \frac{3}{2} & 2 \\ \frac{1}{2}(15z^2 - 3).Q_0 - \frac{1}{2}.\left(\frac{15z^3 - 13z}{z^2 - 1}\right) & 3 \end{cases}$$

$$\mathrm{Re}\,\frac{dC_{\ell m}(\nu)}{d\nu} = \frac{4.(2\ell + 1)}{\nu}.\left(-\frac{Q_m.P_\ell}{\nu} + \frac{dQ_m}{dz}.\frac{dz}{d\nu}.P_\ell + Q_m.\frac{dP_\ell}{dy}\frac{dy}{d\nu}\right)$$

$$\mathrm{Im}\,\frac{dC_{\ell m}(\nu)}{d\nu} = \frac{2\pi}{\nu}.(2\ell + 1).\left(-\frac{Q_m.P_\ell}{\nu} + \frac{dP_\ell}{dy}.\frac{dy}{d\nu}.P_m + \frac{dP_m}{dz}.\frac{dz}{d\nu}.P_\ell\right)$$

(iii) The Evaluation of $\int^x Q_\ell(x)dx$

$$Q_0(x) = \tfrac{1}{2} \log \frac{x+1}{x-1}$$

$$Q_1(x) = \frac{x}{2} \log \frac{x+1}{x-1} - 1$$

$$Q_2(x) = \frac{(3x^2 - 1)}{4} \cdot \log \frac{x+1}{x-1} - \frac{3x}{2}$$

$$Q_3(x) = \frac{(5x^3 - 3x)}{4} \cdot \log \frac{x+1}{x-1} - \frac{5x^2}{2} + \frac{2}{3}$$

$$\int \log \frac{x+1}{x-1}\, dx + (x+1) \log (x+1) - (x+1) - (x-1) \log (x-1) - (x-1)$$

$$= x \log \frac{x+1}{x-1} - 2 + \log (x^2 - 1)$$

$$\therefore \int \log \frac{x+1}{x-1}\, dx = \int d\left(\frac{x^2}{2}\right) \log \frac{x+1}{x-1}$$

$$= \frac{x^2}{2} \cdot \log \frac{x+1}{x-1} - \frac{x^2}{2} \cdot \frac{-2}{x^2-1}\, dx$$

(since $\frac{d}{dx} \cdot \log \frac{x+1}{x-1} = \frac{1}{x+1} - \frac{1}{x-1} = \frac{-2}{x^2-1}$

$$= \frac{x^2}{2} \log \frac{x+1}{x-1} + \frac{x^2 - 1 + 1}{x^2 - 1}\, dx$$

$$= \frac{x^2}{2} \log \frac{x+1}{x-1} + x - \tfrac{1}{2} \int \left(\frac{1}{x+1} - \frac{1}{x-1}\right) dx$$

$$= \frac{(x^2 - 1)}{2} \log \frac{x+1}{x-1} + x$$

$$\int x^2 \log \frac{x+1}{x-1}\, dx = \int d\left(\frac{x^3}{3}\right) \log \frac{x+1}{x-1}$$

$$= \frac{x^3}{3} \cdot \log \frac{x+1}{x-1} - \int \frac{x^3}{3} \cdot \frac{-2}{x^2-1}\, dx$$

$$= \frac{x^3}{3} \log \frac{x+1}{x-1} + \frac{2}{3} \int \left(\frac{x(x^2 - 1) + x}{x^2 - 1}\right) dx$$

$$= \frac{x^3}{3} \cdot \log \frac{x+1}{x-1} + \frac{2}{3} \cdot \frac{x^2}{2} + \frac{2}{3} \cdot \log (x^2 - 1).$$

$$\int x^3 \log \frac{x+1}{x-1}\, dx$$

$$= \frac{x^4}{4} \cdot \log \frac{x+1}{x-1} - \int \frac{x^4}{4} \cdot \frac{-2}{x^2-1}\, dx$$

$$= \frac{x^4}{4} \log \frac{x+1}{x-1} + \frac{2}{4}\int \frac{(x^2(x^2-1) + (x^2-1) + 1)}{x^2-1}\, dx$$

$$= \frac{x^4}{4} \log \frac{x+1}{x-1} + \frac{1}{2}\left(\frac{x^3}{3} + x\right) + \frac{1}{2}\int \frac{dx}{x^2-1}\, dx$$

$$= \frac{x^4}{4} \log \frac{x+1}{x-1} + \frac{1}{2}\left(\frac{x^3}{3} + x\right) - \frac{1}{4} \log \frac{x+1}{x-1}$$

$$= \left(\frac{x^4-1}{4}\right) \log \frac{x+1}{x-1} + \frac{x^3}{6} + \frac{x}{2}$$

$$\therefore \int Q_0(x)\, dx = \frac{x}{2} \log \frac{x+1}{x-1} + \frac{1}{2} \log (x^2-1) \quad (+ \text{const.})$$

$$\int Q_1(x)\, dx = \left(\frac{x^2-1}{4}\right) \log \frac{x+1}{x-1} - \frac{x}{2} \cdot$$

$$\int Q_2(x)\, dx = \frac{3}{4}\left[\frac{x^3}{3} \log \frac{x+1}{x-1} + \frac{x^2}{3} + \frac{1}{3} \log (x^2-1)\right]$$

$$- \frac{1}{4} x \log \frac{x+1}{x-1} + \log (x^2-1)^{-\frac{3}{2}} \cdot \frac{x^2}{2}$$

$$= x\left(\frac{x^2-1}{4}\right) \log \frac{x+1}{x-1} - \left(\frac{x^2-1}{2}\right)$$

$$\int Q_3(x)\, dx = \frac{5}{4}\left[\left(\frac{x^4-1}{4}\right) \log \frac{x+1}{x-1} + \frac{x^3}{6} + \frac{x}{2}\right]$$

$$- \frac{3}{4}\left[\left(\frac{x^2-1}{2}\right) \log \frac{x+1}{x-1} + x\right]$$

$$- \frac{5}{2} \cdot \frac{x^3}{3} + \frac{2x}{3}$$

$$= \left(\frac{5x^4 - 5 - 5x^2 + 6}{16}\right) \log \frac{x+1}{x-1}$$

$$+ \frac{5x^3}{6}\left(\frac{1}{4} - 1\right) + x\left(\frac{5}{8} - \frac{3}{4} + \frac{2}{3}\right)$$

$$= \left(\frac{5x^4 - 6x^2 + 1}{16}\right) \log \frac{x+1}{x-1} - \frac{5}{8} x^3 + \frac{13}{24} \cdot x \cdot$$

APPENDIX 2. N/D POLE FORMS

Here we consider the evaluation and properties of the integrals occurring in N/D pole forms, sometimes known as kernel functions.

$$I_1(\nu) = \int_0^L \sqrt{\frac{\nu'}{\nu'+1}} \cdot \frac{d\nu'}{(\nu'-\nu)(\nu'+\nu_0)}$$

$$I_2(\nu) = \int_0^L \sqrt{\frac{\nu'}{\nu'+1}} \cdot \frac{d\nu' \cdot R(\nu')}{(\nu'-\nu)(\nu'-\nu_0)}$$

We also want to know the values of these integrals with infinite upper limit.

If we write

$$I_2(\nu) = \int_0^L \sqrt{\frac{\nu'}{\nu'+1}} \cdot \frac{R(\nu')\, d\nu'}{(\nu'-\nu_0)} \cdot \left[\frac{1}{\nu'-\nu} - \frac{1}{\nu'-\nu_0}\right]$$

we see that we need to investigate

$$I_3(\nu) = \int_0^L d\nu' \cdot \sqrt{\frac{\nu'}{\nu'+1}} \cdot \frac{R(\nu')}{\nu'-\nu}\,; \quad I_4(\nu) = \int_0^L \sqrt{\frac{\nu'}{\nu'+1}} \cdot \frac{d\nu'}{\nu'-\nu}$$

where one choice of $R(\nu')$ is $R(\nu') = 1$. We might want to use a parametric form for $R(\nu')$

$$R(\nu') = 1 + \theta(\nu'-3) \cdot \sqrt{\frac{\nu'-3}{\nu'}} \cdot \left[1 - \frac{e}{\nu'-f}\right]$$

So,

$$I_3(\nu) = \int_0^L \sqrt{\frac{\nu'}{\nu'+1}} \cdot \frac{d\nu'}{\nu'-\nu} + \int_3^L \sqrt{\frac{\nu'-3}{\nu'+1}} \cdot \frac{d\nu'}{\nu'-\nu} \cdot \left[1 - \frac{e}{\nu'-f}\right]$$

$$= I_4(\nu) + I_5(\nu, 1, 3, L) - \frac{e}{\nu-f}\left[I_5(\nu, 1, 3, L) - I_5(f, 1, 3, L)\right]$$

since, $\int_0^L \sqrt{\frac{\nu'-3}{\nu'+1}} \frac{d\nu'}{(\nu'-\nu)(\nu'-f)} = \int_0^L \sqrt{\frac{\nu'-3}{\nu'+1}} \cdot \frac{d\nu'}{(\nu-f)}\left[\frac{1}{\nu'-\nu} - \frac{1}{\nu'-f}\right]$

also, $I_4(\nu) = \int_0^L \sqrt{\frac{\nu'}{\nu'+1}} \cdot \frac{d\nu'}{\nu'-\nu} = I_5(\nu, 1, 0, L)$

where

$$I_5(a, b, c, L) = \int_0^L \sqrt{\frac{\nu'-c}{\nu'+b}} \cdot \frac{d\nu'}{\nu'-a}$$

$b > 0 \qquad c > 0$

Note also

$$I_1(\nu) = \frac{1}{(\nu-\nu_0)} \cdot \left[I_4(\nu) - I_4(\nu_0)\right]$$

$$I_2(\nu) = \frac{1}{(\nu-\nu_0)} \cdot \left[I_3(\nu) - I_3(\nu_0)\right]$$

If we take

$$R(\nu) = 1 + \theta(\nu-3)\sqrt{\frac{\nu-3}{\nu}} \cdot \left[1 - \sum_i \frac{e_i}{\nu - f_i}\right]$$

then

$$I_3(\nu) = I_4(\nu) + I_5(\nu, 1, 3, L) - \sum_i \frac{e_i}{\nu - f_i}\left[I_5(\nu, 1, 3, L) - I_5(f_i, 1, 3, L)\right].$$

we could also consider the forms

$$R(\nu) = 1 + \theta(\nu-3)\cdot\sqrt{\nu-3}\cdot\left[1 - \sum_i \frac{e_i}{\nu - f_i}\right]$$

and

$$R(\nu) = 1 + \theta(\nu-3)\cdot\sqrt{\frac{\nu+1}{\nu}}\cdot\left[1 - \sum_i \frac{e_i}{\nu - f_i}\right]$$

We need only consider I_4:

$$I_4(a, b, c, L) = \int_c^L \sqrt{\frac{\nu'-c}{\nu'+b}} \cdot \frac{d\nu'}{(\nu'-a)}.$$

put $z^2 = \frac{\nu'-c}{\nu'+b}$. $\qquad \nu' = -b + \frac{(b+c)}{1-z^2}$

$$d\nu' = \frac{(b+c)\cdot 2z\,dz}{(1-z^2)^2}$$

$\nu' = c \quad \sim z = 0$

$\nu' = L \quad \sim z = z_L = \sqrt{\frac{L-c}{L+b}}$

$$\int_0^{z_L} \frac{2z\,dz\,(b+c)}{(1-z^2)^2} \cdot z \cdot \frac{1}{\left[\left(\frac{bz^2+c}{1-z^2}\right) - a\right]}$$

$$= \int_0^{z_L} 2\left(\frac{b+c}{a+b}\right) \cdot \frac{z^2\,dz}{(1-z^2)\left[z^2 + k\right]}$$

$$k = \frac{c-a}{a+b} \qquad k > 0 \text{ if } a \in [-b, c]$$
$$< 0 \quad " \quad \notin \quad "$$

$$= \int_0^{z_L} 2\cdot\left(\frac{b+c}{a+b}\right)\cdot\frac{dz}{1+k}\cdot\left\{\frac{1}{1-z^2} - \frac{k}{z^2+k}\right\}$$

$$\int \frac{dz}{1-z^2} = \int \frac{dz}{2}\left[\frac{1}{1-z} + \frac{1}{1+z}\right] = \frac{1}{2}\log\frac{1+z}{1-z}$$

$$I_6(k) = \int \frac{dz}{z^2+k} = \frac{1}{\sqrt{k}}\cdot\tan^{-1}\left[\frac{z}{\sqrt{k}}\right], \text{ if } k > 0.$$

if $K<0, = -\ell$

$$\int \frac{dz}{z^2-\ell} = \int \frac{dz}{2\sqrt{\ell}} \cdot \left[\frac{1}{(z-\sqrt{\ell})} - \frac{1}{(z+\sqrt{\ell})}\right] = \frac{1}{2\sqrt{\ell}} \cdot \log\left[\frac{z+\sqrt{\ell}}{z-\sqrt{\ell}}\right]$$

L

$I_5(\nu, b, c, L)$

$$= 2.\left\{\frac{1}{2}\log\left(\frac{1+z}{1-z}\right) - \left(\frac{c-\nu}{\nu+b}\right)\cdot\sqrt{\frac{\nu+b}{c-\nu}}\ \tan^{-1}\left[\sqrt{\frac{\nu'-c}{\nu'+b}}\Big/\sqrt{\frac{c-\nu}{\nu+b}}\right]\right\}$$

$k>0$ i.e. ν in $[-b, c]$

$$= 2.\left\{\frac{1}{2}\log\left(\frac{1+z}{1-z}\right) - \left(\frac{c-\nu}{\nu+b}\right)\cdot\frac{1}{2}\cdot\frac{1}{\sqrt{\frac{\nu-c}{\nu+b}}}\cdot\log\left|\frac{\sqrt{\frac{\nu'-c}{\nu'+b}}+\sqrt{\frac{\nu-c}{\nu+b}}}{\sqrt{\frac{\nu'-c}{\nu'+b}}-\sqrt{\frac{\nu-c}{\nu+b}}}\right|\right.$$

$k<0$ i.e. ν not in $[-b, c]$

Now we need not consider the 1st term since it does not depend upon ν and we shall never be using I_5 by itself but always in combinations like $[I_5(\nu_1) - I_5(\nu_2)]$ so that the 1st term goes out. It is in fact the divergent part as $L \longrightarrow \infty$

$$\text{1st term} = \log\left(\frac{1+\sqrt{\frac{L-c}{L+b}}}{1-\sqrt{\frac{L-c}{L+b}}}\right)$$

$$\xrightarrow[L\to\infty]{} - \log\left(1-\sqrt{\frac{L+b-(b+c)}{L+b}}\right)$$

$$\longrightarrow \quad -\log\left(1 - \sqrt{1 - \frac{(b+c)}{(L+b)}}\right)$$

$$\longrightarrow \quad -\log\left(+\tfrac{1}{2}\,\frac{(b+c)}{(L+b)}\right)$$

$$\longrightarrow \quad -\log L.$$

so 2nd term finite.

hence I_5, ν fixed $\quad L \to \infty, \quad \longrightarrow \log L.$

Putting in the limits c, L, we consider the function

$$I_7(\nu) = -2\sqrt{\frac{c-\nu}{\nu+b}}\cdot \tan^{-1}\left[\sqrt{\frac{L-c}{L+b}}\cdot\sqrt{\frac{\nu+1}{-\nu}}\right] \qquad \nu \text{ in } [-b, c]$$

$$= \sqrt{\frac{\nu-c}{\nu+b}}\ \log\left|\frac{\sqrt{\frac{b-c}{L+b}} + \sqrt{\frac{\nu-c}{\nu+b}}}{\sqrt{\frac{L-c}{L+b}} - \sqrt{\frac{\nu-c}{\nu+b}}}\right| \qquad \nu \text{ not in } [-b, c]$$

and, since

$$\operatorname{Im} I_5(\nu) = \pi\cdot\sqrt{\frac{\nu-c}{\nu+b}} \qquad \nu \quad [c, L]$$

$$= 0 \qquad \nu_{real} \notin [c, L]$$

we see that the continuation of

$$I_7(\nu) = \int_0^L \sqrt{\frac{\nu'-c}{\nu'+b}}\ \frac{d\nu'}{\nu'-\nu} - \log\left(\frac{1+\sqrt{\frac{L-c}{L+b}}}{1-\sqrt{\frac{L-c}{L+b}}}\right)$$

to complex values of ν is

$$I_7(\nu) = \sqrt{\frac{\nu-c}{\nu+b}}\cdot\log\left[\frac{\sqrt{\frac{L-c}{L+b}} + \sqrt{\frac{\nu-c}{\nu+b}}}{-\sqrt{\frac{L-c}{L+b}} + \sqrt{\frac{\nu-c}{\nu+b}}}\right]$$

$$= \sqrt{\frac{\nu-c}{\nu+b}}\cdot\log\omega$$

$$\omega = \frac{1+z}{-1+z}$$

$$z = \sqrt{\frac{\nu-c}{\nu+b}}\cdot\sqrt{\frac{L+b}{L-c}}$$

$$\sqrt{\frac{\nu-c}{\nu+b}} = \begin{cases} \nu < -b & \sqrt{\dfrac{\nu-c}{\nu+b}} \\ -b < \nu < c & -\dfrac{1}{i}\sqrt{\dfrac{c-\nu}{\nu+b}} \\ c < \nu & \sqrt{\dfrac{\nu-c}{\nu+b}} \end{cases}$$

	$\nu < -b$	$-b < \nu < c$	$c < \nu < L$	$L < \nu$
z	real > 1	pure imag.	$0 <$ real < 1	real > 1
ω	> 1	$\left[\dfrac{1 + i\sqrt{\frac{c-\nu}{\nu+b}}\sqrt{\frac{L+b}{L-c}}}{-1 + i\sqrt{\frac{c-\nu}{\nu+b}}\sqrt{\frac{L+b}{L-c}}}\right]$ real < -1		> 1

$$\text{phase} = -2\tan^{-1}\left[\sqrt{\frac{c-\nu}{\nu+b}}\cdot\sqrt{\frac{L+b}{L-c}}\right]$$

$$\text{modulus} = 1.$$

$$\therefore I_7(\nu) = \sqrt{\frac{\nu-c}{\nu+b}}\cdot\log\omega$$

$$\log\omega = -\log|\omega| + i\phi$$

$\nu < -b$

$$I_7(\nu) = \sqrt{\frac{\nu-c}{\nu+b}}\cdot\log\left|\frac{\sqrt{\frac{L-c}{L+b}} + \sqrt{\frac{\nu-c}{\nu+b}}}{\sqrt{\frac{L-c}{L+b}} - \sqrt{\frac{\nu-c}{\nu+b}}}\right| + i\cdot 0$$

$-b < \nu < c$

$$I_7(\nu) = i\sqrt{\frac{c-\nu}{\nu+b}} - 2i\tan^{-1}\left[\sqrt{\frac{c-\nu}{\nu+b}}\cdot\sqrt{\frac{L+b}{L-c}}\right]$$

$$= 2\sqrt{\frac{c-\nu}{\nu+b}}\cdot\tan^{-1}\left[\sqrt{\frac{c-\nu}{\nu+b}}\cdot\sqrt{\frac{L+b}{L-c}}\right] + i\cdot 0$$

$c < \nu < L$

$$I_7(\nu) = \sqrt{\frac{\nu-c}{\nu+b}}\cdot\log\left|\frac{\sqrt{\frac{L-c}{L+b}} + \sqrt{\frac{\nu-c}{\nu+b}}}{\sqrt{\frac{L-c}{L+b}} - \sqrt{\frac{\nu-c}{\nu+b}}}\right| + i\cdot\pi\cdot\sqrt{\frac{\nu-c}{\nu+b}}$$

$L < \nu$

$$I_7(\nu) = \sqrt{\frac{\nu-c}{\nu+b}}\cdot\log\left|\frac{\sqrt{\frac{L-c}{L+b}} + \sqrt{\frac{\nu-c}{\nu+b}}}{\sqrt{\frac{L-c}{L+b}} - \sqrt{\frac{\nu-c}{\nu+b}}}\right|.$$

explicitly showing the cut

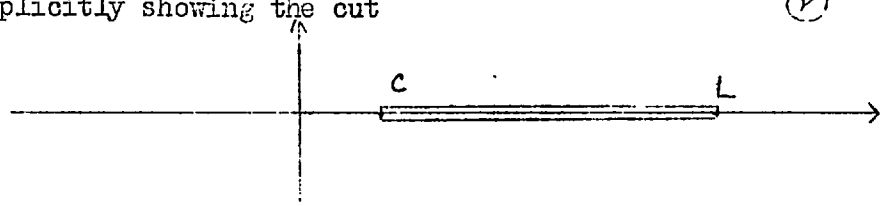

L fixed $\nu \to \infty$

$$\to \log \left| \frac{\sqrt{\frac{L-c}{L+b}} + 1}{\sqrt{\frac{L-c}{L+b}} - 1} \right| + i\pi$$

$$\longrightarrow - \log \left| \sqrt{\frac{\nu-c}{\nu+b}} - 1 \right| + i\pi$$

$$\longrightarrow \log \nu + i\pi$$

In the special case $L = \infty$, $c = 0$, $b = +1$, the usual kernel function,

$$I_{\nu}(\nu) = \sqrt{\frac{\nu}{\nu+1}} \cdot \log \left[\frac{1 + \sqrt{\nu/(\nu+1)}}{1 - \sqrt{\nu/(\nu+1)}} \right]$$

in this case it can be written as

$$2 \cdot \sqrt{\frac{\nu}{\nu+1}} \cdot \log \left[\sqrt{\nu} \pm \sqrt{-\nu-1} \right]$$

since $\sqrt{-\nu} + \sqrt{-\nu-1} = \dfrac{1}{\sqrt{-\nu} - \sqrt{-\nu-1}}$, identically for all complex ν.

Derivatives of $I(\nu, \nu_0)$

$$I(\nu, \nu_0) = (\nu - \nu_0) \int_0^{\infty} \sqrt{\frac{\nu'}{\nu'+1}} \cdot \frac{d\nu'}{(\nu'-\nu)(\nu'-\nu_0)}$$

$$= -2 \cdot [\, f(\nu) - f(\nu_0)]$$

$$f(\nu) = \sqrt{\frac{\nu}{\nu+1}} \cdot \log \left[\sqrt{\nu} + \sqrt{\nu+1} \right]$$

$$\frac{d}{d\nu} f(\nu) = \log \left[\sqrt{\nu} + \sqrt{\nu+1} \right] \cdot \left\{ \frac{1}{2} \cdot \sqrt{\frac{\nu+1}{\nu}} \cdot \frac{1}{(\nu+1)^2} \right\}$$

$$+ \sqrt{\frac{\nu}{\nu+1}} \cdot \frac{1}{\left[\sqrt{\nu} + \sqrt{\nu+1}\right]} \cdot \left[\frac{1}{2\sqrt{\nu}} + \frac{1}{2\sqrt{\nu+1}} \right] \cdot$$

$$= \frac{1}{2} \cdot \frac{1}{(\nu+1)} \cdot \left[1 + \frac{1}{\nu} \cdot \sqrt{\frac{\nu}{\nu+1}} \cdot \log \left[\sqrt{\nu} + \sqrt{\nu+1} \right] \right]$$

$$\therefore f'(\nu) = \frac{1}{2(\nu+1)} \cdot \left[1 + f(\nu)/\nu \right]$$

$$I'(\nu) = \frac{-1}{(\nu+1)} \cdot \left[1 + f(\nu)/\nu \right]$$

$$\therefore I''(\nu) = \frac{1}{(\nu+1)^2} + \left[\frac{1}{\nu(\nu+1)^2} + \frac{1}{\nu^2(\nu+1)} \right] \cdot \left(-\frac{1}{2} I \right) + \frac{1}{2\nu(\nu+1)} \cdot I'$$

$$= \frac{1}{2(\nu+1)^2 \nu} \cdot \left\{ (2\nu - 1) + \frac{(4\nu+1)}{\nu} \cdot f(\nu) \right\}$$

APPENDIX 3. NUMERICAL METHODS AND PROGRAMMING

Numerical Methods.

1. Integrations.

These were discussed in Chapter 2. We used a fast 20 point gaussian routine which we wrote ourselves and checked the accuracy using a library routine QA02A.

Infinite integrals were performed by transforming to a finite range, integrating, and transforming back again, using in the case $\int_a^\infty dx$, the transformation $z = \frac{x-a}{x}$.

Principal value and other singular integrals were performed by subtracting out the singularity, e.g.

$$\int \frac{f(x)\,dx}{x-z} = \int \left[\frac{f(x)-f(z)}{x-z}\right] dx + f(z)\cdot\int \frac{dx}{x-z}$$

Another method has been given by Longman (1).

To evaluate

$$(\nu-\nu_0)\int_a^b \frac{f(\nu')\,d\nu'}{(\nu'-\nu)(\nu'-\nu_0)} \qquad \text{(i)}$$

in the 4 cases ν on cut. (i) ν_0 on cut (ii) ν_0 off cut.
ν off cut. (iii) ν_0 on cut (iv) ν_0 off cut.

(iv) ν_0 off ν off nonsingular evaluate

$$(\nu-\nu_0)\int_a^b \frac{f(\nu')\,d\nu'}{(\nu'-\nu)(\nu'-\nu_0)} \qquad \text{(ii)}$$

(iii) ν_0 on ν off

$$(\nu-\nu_0)\int \left[\frac{f(\nu')-f(\nu_0)}{(\nu'-\nu)(\nu'-\nu_0)}\right] d\nu' + (\nu-\nu_0)\cdot f(\nu_0)\cdot\int \frac{d\nu'}{(\nu'-\nu)(\nu'-\nu_0)}$$

$$= (\nu-\nu_0)\int_a^b \left[\frac{f(\nu')-f(\nu_0)}{(\nu'-\nu)(\nu'-\nu_0)}\right] d\nu' + f(\nu_0)\cdot\left[\log\left|\frac{\nu'-\nu}{\nu'-\nu_0}\right|\right]_a^b \qquad \text{(iii)}$$

(ii) ν on ν_0 off

$$= (\nu-\nu_0)\int_a^b \left[\frac{f(\nu')-f(\nu_0)}{(\nu'-\nu)(\nu'-\nu_0)}\right] d\nu' + f(\nu)\cdot\left[\log\left|\frac{\nu'-\nu}{\nu'-\nu_0}\right|\right]_a^b \qquad \text{(iv)}$$

(i) ν on ν_0 on $\nu \neq \nu_0$

$$= \int_a^b f(\nu')\,d\nu'\cdot\left[\frac{1}{(\nu'-\nu)} - \frac{1}{\nu'-\nu_0}\right]$$

$$= \int_a^b \left\{\left[\frac{f(\nu')-f(\nu)}{\nu'-\nu}\right] - \left[\frac{f(\nu')-f(\nu_0)}{\nu'-\nu_0}\right]\right\} d\nu' + f(\nu)\int_a^b \frac{d\nu'}{\nu'-\nu}$$

$$-f(\nu_0)\Big|^b \; d\nu'/\nu'-\nu_0$$

$$= \int_a^b \left\{ \left[\frac{f(\nu')-f(\nu)}{\nu'-\nu} \right] - \left[\frac{f(\nu')-f(\nu_0)}{\nu'-\nu_0} \right] \right\} d\nu' + \left[f(\nu).\log|\nu'-\nu| - f(\nu_0).\log|\nu'-\nu_0| \right]_a^b \quad (v)$$

If range infinite and these integrals do not converge, then

$$\int \left\{ \left[\frac{f(\nu').\nu' - f(\nu).\nu}{(\nu'-\nu).\nu'} \right] - \left[\frac{f(\nu').\nu' - f(\nu_0).\nu_0}{(\nu'-\nu_0).\nu'} \right] \right\} d\nu'$$

$$+ f(\nu).\nu \int \frac{d\nu'}{(\nu'-\nu).\nu'} - f(\nu_0).\nu_0 \int \frac{d\nu'}{(\nu'-\nu_0).\nu'}$$

$$= \int_a^b \left\{ \left[\frac{f(\nu').\nu' - f(\nu).\nu}{(\nu'-\nu).\nu'} \right] - \left[\frac{f(\nu').\nu' - f(\nu_0).\nu_0}{(\nu'-\nu_0).\nu'} \right] \right\} d\nu'$$

$$+ \left[f(\nu).\log\frac{\nu'-\nu}{\nu'} - f(\nu_0').\log\frac{\nu-\nu_0}{\nu'} \right]_a^b \quad (vi)$$

One might remark that, when ν_0 is on the cut, a large importance is given to the region near $\nu' = \nu_0$ only if $f(\nu')$ is changing rapidly here, in which case the real part of the integral will also have a large value and thus so will the subtraction constant.

Note that gradient of density function is also required for evaluating contribution from singular part neighbourhood.

A bibliography on numerical integration has been given by Stroud (2). The integration of oscillatory functions over an infinite range is treated in (3).

2. Matrix inversions.

These were done using a standard routine MA02A.

3. Iteration.

We looked at three standard routines, VA01A, VA02A and VA04A and decided to use VA02A. The numerical analysis has been published by M.J.D. Powell in Computer Journal. The assumptions on the behaviour of the χ^2 function are that it is a sum of squares and that, in the expression

$$\frac{\partial^2 F}{\partial x_k \partial x_j} = \sum_i 2 \cdot \left(\frac{\partial f_i}{\partial x_j} \cdot \frac{\partial f_i}{\partial x_k} + f_i \frac{\partial^2 f_i}{\partial x_k \partial x_j} \right)$$

where $F\ (\equiv \chi^2) \equiv \sum_i f_i^2(\{x_j\})$.

i.e, the second term is much smaller than the first, allowing an estimation of the curvature from the gradients.

PROGRAMMING

All programmes were written in FORTRAN which uses subroutine structure. Details of the programmes can be obtained from the author. The computers used were the I.C.T. ORION and ATLAS at Chilton, Berkshire and the computation was carried out under the auspices of the Rutherford Laboratory.

The use of subroutines allowed the same sub-computations to be used in different programmes, for example one subroutine calculated the Breit Wigner function and was used as part of several different programmes.

The layout of a typical programme was as follows:

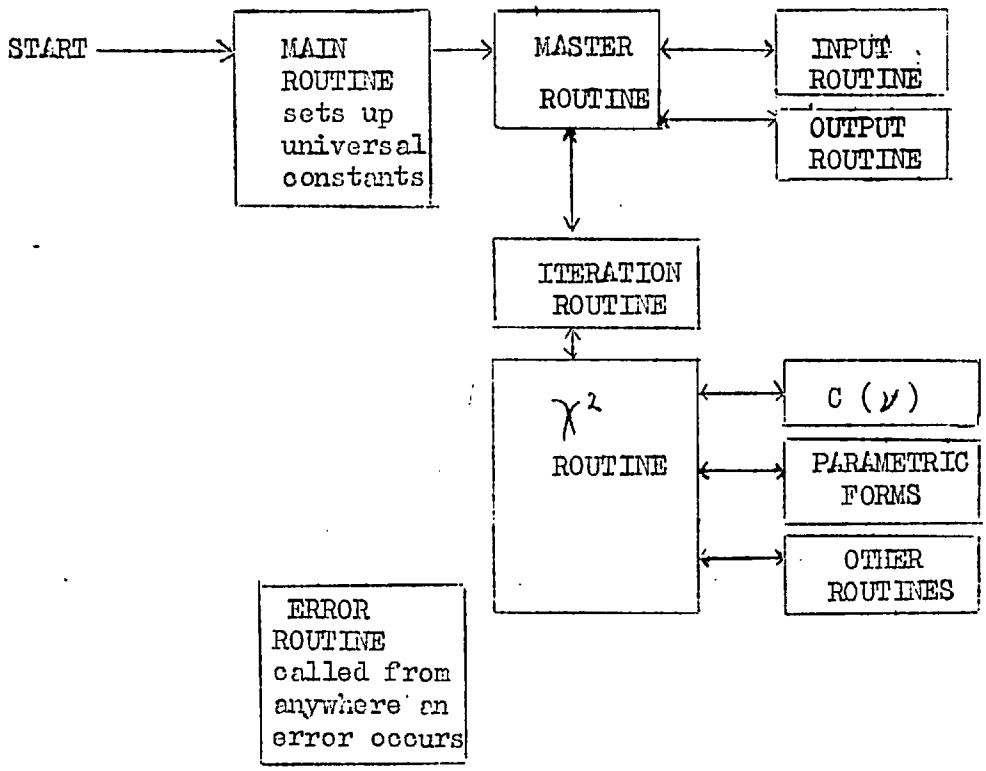

Typically there were about 30 routines in one programme. Each programme could handle all aspects of one method as well as some modifications. One could automatically tabulate any functions in the method, or print χ^2 or iterate for any given subset of variables, then test the value of χ^2, then finally tabulate all relevant functions. A typical time on Atlas for a 30 step search (adequate for 2 variables) followed by a complete tabulation was 30 seconds.

ABBREVIATIONS USED IN THE REFERENCES

P.R.	Physical Review
P.R.L.	Physical Review letters
N.C.	Il Nuovo Cimento
N.C.S.	Il Nuovo Cimento Supplemento
A.P.	Annals of Physics
N.P.	Nuclear Physics
P.L.	Physics Letters
P.T.P.	Progress in Theoretical Physics
J.E.T.P.	Soviet Physics J.E.T.P.
J.M.P.	Journal of Mathematical Physics
A.T.P.	Advances in Theoretical Physics
M.T.A.C.	Mathematical Tables and Aids to Computation
M. Comp.	Mathematics of Computation
C. Phil. Soc.	Proceedings of the Cambridge Philosophical Society
P.	Physics
Z.S.f.P.	Zeitschrift für Physik

Conferences and Summer Schools:

e.g. Oxford, '65

REFERENCES

CHAPTER I

1. Tables by Rosenfeld. Oxford '65.
2. see Schweber textbook.
3. see Jauch and Rohrlich textbook.
4. see R. F. Streater and A. S. Wightman textbook.
5. Matthews. Brandeis '60.
6. see, for example, A. Hendry. RHEL/R 102 1965.
7. S. Mandelstam. P.R. 112. 1344 '58
   E. J. Squires. Edinburgh '63.
8. see J. Hilgevoord "Dispersion relations and Causal Description" NHPC 1960.
9. V. Glaser. Oxford '65.
10. Blankenbecler, Goldberger, Khuri and Treiman. A.P. 10 62 '60.
11. J. Bros. Trieste '65.
12. J. Bros., H. Epstein and V. Glaser to be put in C.M.P.
    V. Glaser. Oxford '65.
12. Newton. J.M.P. 1 '60.
13. Bargman. RMP 21 488 '49.
14. Martin N.C. 14 403 '59.
    Jost H.P.A. 20 256 '47.
    Regge N.C. 8 671 858.
    R. E. Peierls P.R.S. A253 16, '59.
15. Martin N.C. 15 99 '60.
16. A. Martin CERN 63 - 26.
    BGKT (ref. 10).
    Goldberger & Watson, textbook.
    Fubini. Trieste '62 348.
    M. Luming. P.R. 136 V1120. '64.
    Jost and Pais. P.R. 82 840 '51.
    Morse and Feshbach textbook. P.1082.
17. A. Martin. seminar.
    P. Noyes and D. Y. Wong. PRL 3 191 '59.
18. W. Ramsey and M. Luming. P.R. 137 B134 '65.
19. M. Froissart. P.R. 123 1053 '61.
20. A. Martin P.R.L. 9 410 11/62.
21. A. Martin. Edinburgh '63.
    A. Martin. CERN TH.637 12/65.
22. S. Mandelstam. N.C. 15 658 '60.
23. A. Martin. P.R. 129 1432 '63.
    Y.S. Jin and A. Martin. P.R. 135 B1375 '64.
    A. Martin. CERN TH 606.
24. L. Lukaszuk. N.C. 41 67 '66.
    B. N. Geshkenbein and B. L. Joffe. JETP 17 820 '64.
    S. D. Drell etal. P.R. 136 B1439.
    Meiman. JETP 17 830 64, '63.
    A. Martin. Preprint.
    Müller. N.C. 42 185.
25. J. G. Taylor. N.C.S. P.R. 136 B1134 '64.
26. J. R. Taylor. P.R. 140 B187 '65.
27. H. P. Stapp. Matscience report, 26.

CHAPTER I (CONTD.)

28. H. P. Stapp. RMP 34 390 '62.
G. F. Chew. P. 1 77 '64.
H. P. Stapp. P.R. 125 B745 '64.
D. Olive. P.R. 135 B745 '64.

29. Amati, Fubin and Stanghellini. N.C. 26 896 '62. ("multiperpheral model").
Van Hove. R.M.P. 36 655 '64. ("statistical model").

30. J. Hamilton. Edinburgh '63.

31. T. Regge. N.C. 14 951 '59.

32. N. N. Khuri. P.R. 130 429 '63.
PRL 10 420 '63.
PR 132 913 '63.

33. G. F. Chew. PR 129 2363 '63.
130 1264 '63.

34. G. F. Chew and Jones. P.R. 135 208 '64.

35. R. J. Eden. PR 132 912 10/63.
N.C. 31 998 3/64.

36. M. Kretzchmar. N.C. 39 835 10/65.
W. J. Abbe etal. P.R. 140 B.1595 12/65.
H. Cheng and T. T. Wu. Harvard report (unpublished).

37. S. J. Lindenbaum. Dubna '64.

38. J. L. Orear. P.L. 13 190 '64.
P.R.L. 12 112 '64.

39. N. E. Booth and A. Abashian. P.R. 132 2314 '63.
B. H. Bransden etal. N.C. 30 207 '63.
A. H. Rosenfeld. UCRL - 8030 9/65.
Oxford '65.

40. A. Abashian, N. E. Booth and K. M. Crowe.
1 P.R.L. 5 258 '60.
2 P.R.L. 7 35 '61.
3 R.M.P. 33 393 '61.
4 P.R. 132 2314 '63.

R. J. Kurz. UCRL - 10564 '62.
J. Schwarz etal. UCRL - 10676 '63.

41. N. N. Khuri and S. B. Treiman. PR 119 1115 '60.
M. A. B. Beg and P. C. Decelles. PRL 8 46 '62.

42. Chew and Low. P.R. 113 1640 '59.
G. Goebel. PRL. 1 337 '58.
A. R. Erwin etal. P.R.L. 6 628 '61.
C. Ceolin - R. Stroffolini. N.C. 23 437 '61.
J. Kirz, J. Schwarz and R. D. Tripp. PR 126 763 '62.
S.O.B.B. N.C. 25 365 '62.
N.C. 29 515 '63.
N.C. 35 1 '65.
N.C. 35 713 '65.
F. Ferrari and F. Selleri P.R.L. 7 387 '61.
F. Selleri. P.L. 3 76 '62.
J.D. Jackson etal. P.R. 139 B428 '65.
C. J. Goebel and H. J. Schnitzer P.R. 123 1021 '61.

43. H. J. Schnitzer P.R. 125 1059 '62.

44. A. Anselm and V. N. Gribov. JETP 10 354 '60.
Y. A. Batusov etal. Rochester '60. p.79.

45. B. Budini and L. Fonda. P.R.L. 6 419 '61.
46. Ishida etal. P.T.P. 23 731 '60.
Efremov etal. J.E.T.P. 12 308 '60.
HMOV P.R. 128 1881 '62.
D. Atkinson. P.R. 128 1908 '62.
47. P. Cziffra etal. P.R. 114 880 '59.
Scotti and Wong. P.R.L. '65.
48. L. Durand III, Y.T. Chin P.R.L. 14 329 '65.
errat. P.R.L. 14 680 4/65.
K. Gottfried and J. D. Jackson. N.C. 34 735 '64.
V. Hagopian etal. P.R.L. 14 1077 '65.
49. G. F. Chew. P.R.L. 16 60 '66.
50. A. O. Barut and W.S. Au. P.R.L. 13 165 '64.
N. P. Samios etal. P.R.L. 9 139 '62
J. Kirz etal. P.R. 130 2481 '63.
C. Richardson etal. CERN '62.
I. Aitcheson. P.R. '66.
51. Rosenfeld. Oxford '65.
52. Oxford group. RPP/H/7 5/65.
53. A. O. Barut. P.R. 123 1873 '62.
54. D. Atkinson preprint.
55. G. Wolf. P.L. 19 328 '65.
56. See references in 57.
57. A. Martin. N.C. 29 704 '65.
58. R. J. Eden. P.R.L. 16 39 '66 and Maryland lecture notes.
59. A. Martin. CERN 553 4/65.
60. Tin and Martin. P.R. 135 B1375 '64.
61. R. J. Eden, Seminar Rutherford '66.
62. Hamilton Edinburgh '63.
63. L. Lanz and G. M. Prosperi. N.C. 33 201 '64.
G. Frye and R. L. Warnock. P.R. 130 478 '63.
64. R. Omnès. UCRL 11008 '63.
65. Chew and Mandelstam. P.R. 119 467 '60.
R. Omnès. N.C. 8 316 '58.
66. Squires. Edinburgh '63.
67. Hamilton. Edinburgh '63.
68. J. L. Uretsky. P.R. 123 1459 '61.
69. Frye and Warnock. P.R. 130 478 '63.
70. L. Castillejo, R. H. Dalitz and J. Dyson. P.R. 101 453 '56.
71. Gell-Mann and Zachariesen. P.R. 124 953 '61.
72. F. Zachariesen. Trieste '65.
73. N. Levinson. D.V.S. N-f, M. 25 No. 9 '49.
74. V. Bargmen. R.M.P. 21 488 '49.
75. Titchmarsh "Theory of Functions" P.115.
76. Chew. P.R.L. 16 60 '66.
77. R. L. Warnock. P.R. 131 1320 '63.
78. J. M. Charap. N.C. 36 419 '65.
79. J. R. Choudbury. N.C. 38 419 '65.
80. C. R. Hagen. N.C. 43 597 '66.
81. M. Bander, P.W. Coulter and G. L. Shaw. P.R.L. 14 270 '65.
82. D. Atkinson, K. Dietz and D. Morgan. CERN TH. 564 '65.
CERN TH. 531 '65.
83. E. J. Squires. N.C. 34 1751 '64.
E. J. Squires and P. J. S. Watson. RUL - R 476 N.C. 42 77 '66

84. J. B. Hartle and C. E. Jones. 2 Princeton preprints '65.
J. Finkelstein. UCRL 16091 '65.
D. Atkinson etal. CERN preprint '65.
85. H. Munczek. P.L. 13 92 11/64.
86. G. F. Chew and S. Mandelstam. P.R. 119 467 '60.
N.C. 19 752 '61.
Chew, Mandelstam and Noyes. P.R. 119.
87. J. W. Moffat. P.R. 121 926 '61.
N.C. 21 505 '61.
P.R. 128 859 '62.
88. H. Ding-Chang etal. JETP 39 1668 '60.
A. V. Efremov etal. JINR - E - 545.
NP. 22 202 '60.
C. Lovelace - N.C. 21 305 '61.
22 102 '61.
Serebryakov and D. V. Shirkov JETP 15 610 '62.
Efremor etal. JINR D - 757.
JETP 14 603.
JINR D - 697.
D. V. Shirkov. Trieste '65.
89. C. Lovelace. N.C. 21 305 '61.
90. N. B. Pivarcna JEPT 17 262 '63.
91. F. Zachariesen. PRL 7 112 '61.
errat. 7 268 '61.
92. R. Feynman. Aix-en - Provence '61.
93. F. E. Low. N.C. 25 678 '62.
94. A. Salam. N.C. 25 224 '62.
95. Gell-Mann etal. P.R. 133 145 '64.
96. S. Mandelstam. P.R. 137 949 '65.
97. F. Zachariesen. Edinburgh '63.
P. G. O. Freund. Chicago preprint.
D. C. Teplitz and V. L. Teplitz. P.R. 137 142 '65.
M. Bander and G. L. Shaw P.R. 134 B267 '64.
D. Y. Wong. P.R. 126 1220 '62.
J. D. Arrand and G. C. Joshin. N.C. 38 1588 '65.
98. Bransden etal. N.C. 30 207 '63.
99. P. Burko etal. CERN '62.
100. Collins and Teplitz. P.R. 140 663 '65.
P.D.B. Collins. P.R. 142 1156 '66.
101. P. D. B. Collins, P.R. 142 1162 '66.
102. J. D. Bjórken. P.R.L. 4 473 '60.
J. D. Bjórken and M. Nauenberg. P.R. 121 1250 '61.
103. F. Zachariasen and C. Zemach. P.R. 128 849 '62.
A. W. Martin and K. C. Wali. P.R. 130 2455 '62.
104. G. L. Shaw. P.R.L. 12 345 '64.
105. F. Zachariasen. Edinburgh '63.
R. H. Capps. P.R.L. 10 312 '63.
E. Abers etal. P.R. 132 1831 '63.
J. R. Fulco and D. Y. Wong. P.R. 136 198 '64.
106. R. E. Cutkosky. P.R. 131 1888 '63.
107. R. C. Hwa and S. H. Patil. P.R. 140 B1486 '65.
R. F. Dashen and S. C. Frautschi. P.R. 140 B698 '65.

CHAPTER I (CONTD.)

108. Dalitz. Oxford '65. A. N. Mitra P.R. 142 1119 '66
A. N. Mitra P.R. 142 1119 '66.
A. Hendry Rutherford preprint.
Morpergo P 2
also models by Squires and by N. Evans.
109. V. Massidda and A. Pignotti P.L. 20 437 '66.
110. G. F. Chew P.R.L. 9 233 '62.
F. E. Low P.R.L. 9 277 '62.
111. B. Diu N.C. 37 1749.
112. Squires N.C. 1965.
113. Huang and Low P.R.L. 13 596 '65
JMP '65.
114. J. D. Bjørken and A. Goldberg N.C. 16 539 '60.
115. M. Luming P.R. 136 B1120 '64.
116. D. Morgan CERN. TH. 463.
A. Bastaietal N.C. 30 1512 '63.
R. Oehme N.C. 25 183 '62.
117. G. F. Chew P.R. 130 1264 '63.
C. E. Jones UCRL - 11125 '63.
UCRL - 11167 '63.
118. Dietz and Domokos P.L. 11 91 '64.
Domokos thesis '63 Dubua (unpublished).
119. Atkinson and Contogouris CERN TH. 534
and TH. 541 '65.
120. D. H. Lyth Birm. preprint '65.
121. Van Hove CERN 65 - 22.
122. D. H. Lyth Brin preprint '65.
123. Schweber. textbook p. 705.
S. Mandelstan P.R.S. A233 '55.
P. Rowe thesis I.C.
124. Schweber ibid p. 566.
125. W. Zimmermann N.C. 10 597 '58.
126. R. Haag P.R. 112 669 '58.
K. Nishijima P.T.P. 17 765 57
P.R. 111 995 58.
T. G. Taylor N.C.S. '65.
127. A. Salam N.C. 25 224 '62.
P.R. 130 1287 '63.
128. I. S. Gerstein and N. G. Despanude P.R. 140 B1643 '65.
T. Yoshimura N.C. 40 495 '65.
M. A. Braun JETP 19 460 '64.
Y. Ataka PTP 25 369 '61.
ibid 27 211 '62.
J. S. Dowker and J. E. Paton NC 30 450 '63.
R. M. Rockmore PR 132 878 '63.
D. Luriè and A. J. MacFarlane PR 136 816 '64.
C. R. Hagen AP 31 185 '65
W. Güttinger NC 36 968 '65.
P. A. Cook Manchester preprint '65
(bootstraps parity conservation).
129. M. T. Vaughan, R. Aaron and R. D. Amado
P.R. 124 1258 '61.
130. J. C. Houard and B. Jouvet N.C. 18 466 '60.

131. B. Jouvet N.C. 5 1 '57.
132. Fonda etal P.R. 133 196 '64
Joseph and Wada N.C. 28 7 '63
Wada N.C. 24 508 '62
B. Di[illegible] N.C. 28 834 '63.
133. F. E. Low N.C. 25 678 '62.
134. Lardner and Woo N.C. 28 210 '63.
135. E. G. P. Rowe N.P. 45 593 '63
thesis I.C.
136. F. Zachariasen P.R. 121 1851 '61
Thirring T[illegible]este '62
P.R. 126 1209 '62
N.C. 23 1064 '62
Gell-Mann and Zachariasen P.R. 124 953 '61
Gell-Mann Rochester '56.
137. J. S. Dowker N.C. 25 1135 '62.
138. R. Acharya N.C. 24 870 '62
139. M. L. Whipp[illegible]n and I. S. Gerstein preprint.
140. W. Thirring P.R. 126 1209 '62.
141. E. G. P. Rowe N.C. 32 1422 '64.
142. J. S. Dowker N.C. 33 110 '64.
143. B. W. Lee etal A.P. 28 466 '64.
144. R. L. Zimmermann P.R. 141 1554 '66.
145. S. Weinberg Brandeis '64.

CHAPTER II

1. G. F. Chew and S. C. Frautschi P.R.L. 7 394 '61
P.R.L. 8 41 '62
2. H. Ding-Chang, Ho Tsu-Hsin, W. Zöllner JETP 39 1668 '60.
3. A. V. Efre[illegible], V. A. Meschcryakov, D. V. Shirkov, H. Y. Tzu.
N.P. 22 202 '61.
4. L. Balazs BV.
5. V. Singh and B. M. Udgaokar P.R. 130 1177 5/63.
6. G. Barton " Dispersion Theory". Benjamin.
7. Ser[illegible]ar Imperial College.
8. J. L. Walsh. "Interpolation and Approximation by Rational Functions in the Complex Demain".
9. G. A. Baker, Jr. A.T.P. 1 1 '65.
10. J. S. R. Chisholm J.M.P. 7 39 1/66.
11. J. L. Gauvel and F. A. McDonald P.R. 142 1245 2/66.
J.S.R. Chisholm J.M.P. 4 1506 '63.
S. T[illegible] P.R. 139 1011 '65.
12. M. Baudo[illegible] J.M.P. 5 1427 10/64.
13. G. E. Lo[illegible]s, "Methods in Computational Physics"
4 '65 Ed. B. Adler etal.
14. A.P. Balach[illegible]dran J.M.P. 5 614 '64.
15. A.P. Balach[illegible]dran A.P. 30 476 '64.
16. Lawson N.C. 20 1207 '61.
[illegible]achie z Hamilton See Ch. 5.
17. L. A. P. Bal[illegible]s P.R. 129 872 1/63.
18. G. C. Cades. Thesis. (University of Londo[illegible])
19. Ross and Shaw A.P. 9 391 '60.
and A.P. 13 147 '61.
Dalitz's book.
20. L. D. Roper UCRL - 14193.

CHAPTER 3

1. Balazs I. P.R. 128 1935 10/62
   II. P.R. 128 1939 10/62
   III. P.R. 129 872 1/63
   IV. P.R.L. 10 171 3/63
   II and III reprinted in "Complex Angular Momenta and Particle Physics", E. J. Squires - Benjamin 1963.
2. Mehta and Srivastava. P.R. 137 423 1/65
3. S. K. Bose and M. Dersarkissian
   N.C. 30 878 1963 D in NN
   N.C. 30 894 1963 scattering
   J. C. Pati P.R. 134 387 4/64 $\equiv^*$ in $\bar{K}$
   G. L. Kane P.R. 135 843 8/64 $^-$ in $\bar{K}$ $\equiv$
   S. P. Chaudhury and L. K. Pande
   P.R. 135 1027 8/64 $^-$ in $\bar{K}$ $\equiv$
   V. Singh and B. M. Udgaonkar
   P.R. 128 1820 11/62
   Nuclear form factor.
   P.R. 130 1177 5/63 n^* in N
4. Kanki and Tubis. P.R.136 723 11/64
   D. Singh P.R. 136 804 '64
   V. L. Pande and P. Narayanaswamy
   P.R. 136 1760 '64
   E. Golowich P.R. 139 158 7/65
5. Zachariasen. P.R.L. 7 112 1961.
6. See, for example, Z. Kopal, Numerical Analysis, 2nd ed. Chapman and Hall. P.349 et. seq.

CHAPTER 4

1. F. Zachariasen P.R.L. 7 112 8/61 errat ibid p.268
2. A. Martin Argonne preprint.
3. B. Diu. ORSAY TH. 32
4. Gervais. ORSAY preprint.
5. M. Luming. P.R. 136 1120 11/64
6. J. C. Patil. P.R. 134 B387 4/64.

CHAPTER 5

1. A Donnachie and J. Hamilton P.R. 133 B1053 2/64
2. W. Gilbert P.R. 108 1078 '57.
3. Jackson Edinburgh '60.

CHAPTER 6

1. P. T. Matthews and A. Salam N.C. 13 381 '59
2. G. Feldman, P.T. Matthews and A. Salam. N.C. 16 549 '60.
3. J. Moffat. N.P. 18 75 '60.
4. J. Moffat. P.R. 121 926 2/61.
5. B. Bransden and J. Moffat. N.C. 21 505 8/61.
6. B. Bransden and J. Moffat. P.R.L. 8 145 2/62.
7. J. S. Ball and D. Y. Wong. P.R.L. 7 390 11/61.
8. H.C. Rae.
9. A. T. Davies (private communication).
10. Muskhelishvili "Singular Integral Equations." p.99.

CHAPTER 7

1. Jacob and Chew. book. Benjamin.
2. Chew and Mandelstam. P.R. 119 '60.
3. CGLN method see Hamilton. Edinburgh '63.
   Modification - Höhler and Dietz. CERN '62 and ZSfP 160 453.
   See also Hamilton and Woolcock. RMP 35 737 '63.

APPENDIX 1

1. H. Bateman "Higher Transcendental Functions" Vol. I.
   Whittaker and Watson.
   Morse and Feshbach. Vols. I and II.

APPENDIX 3

1. I. M. Longman MTAC 12 205 '58
2. A. H. Stroud / M. Comp 15 '52.
3. I. M. Longman C. Phil. Soc. 52 764 '56.
   P. J. Davis "On Numerical Approximation" R. E. Langer. Ed.

LIST OF FIGURES AND TABLES

CHAPTER 1

CHAPTER 2

Figures

12 Breit Wigner formula

13 N/D contributions from l.h. and r.h.

14 A^{-1} parametrisation.

15 "Experimental" curves used.

16 Effects of inelasticity on resonant amplitude.

17 " " on (a) ReC (b) ImC

Tables

2 - 1 Total and Breakdown Re and Im. → P_1, D_0, D_2, E_1.

2 "Experimental" curves.

CHAPTER 3

Figures

1 "Two pole fit to the kernel"

(a) The exact and approximate kernels plotted against x, for a series of values of ν.

(b) Plotted against ν, for a series of values of X.

(c) $K_{exact}(\nu, \nu') - K_{approx.}(\nu,\nu')$ vs. ν with typical ν'.

2 "The Functions of the Balazs Approximation."
Graphs of (1) ReD(ν)
(2) ReN(ν)
(3) ReA(ν)
(4) ImA(ν)
(5) ReC(ν)

showing how matching between ReA(ν) and ReC(ν) occurs and the functions it produces.

3 Contour plot for the two-pole P_1 calculation.

4 "Static Studies."
$\nu_R = 3.4$, $\Gamma\nu_R = 2.6$
(a) Derivative matching. n = 1. 2. 3. 4. 6. 7.
(b) Distributed matching. n = 2. 3. 4. 5.
(c) " n = 6(1), 6(2), 7.
(d) Different sets of symmetry points
(1) -2.1 -1.9 0.0
(2) -2.5 -2.3 0.0
(3) -1.5 -1.0 0.0
(4) -2.1 -1.0 0.0
(5) -0.8 -0.5 0.0

5 "S wave self-consistent solution."
Two pole S_0 single channel.

6 "The P_1 - D_0 calculations."
(a) Reflections into the P wave
(1) ReA P + D → P
(2) ReC P + D → P
(3) ReA D → P

(4) ReC $D \rightarrow P$
(5) ReA $P \rightarrow P$
(6) ReC $P \rightarrow P$

(b) Reflections into the D wave

(1) ReA $P + D \rightarrow D$
(2) ReC $P + D \rightarrow D$
(3) ReA $D \rightarrow D$
(4) ReC $D \rightarrow D$
(5) ReA $P \rightarrow D$
(6) ReC $P \rightarrow D$

7 "Variation of n for $D_o \rightarrow P_1$."

(1) ReC
(2) n = 2
(3) n = 3
(4) n = 4

8 "Effect of the f on the other channels."

$\nu_R = 3.4$, $\Gamma\nu_R = 2.6$

(a) $P_1 \rightarrow S_o$
(b) $\rightarrow S_2$
(c) $\rightarrow D_o$
(d) $\rightarrow D_2$

In (a), (b), (c), c')

(1) ReC
(2) n = 2
(3) n = 3
(4) n = 4

9 Pure real matching. n = 8, ν_{Fj} in $[-4, o]$.

Zero of ReD at -2.5
Zeros of ReN at -3.5, -2.5_-, -2.5_+

10. Pure imaginary matching.

11. Complex matching, n = 9, $[-4, o]$.

12. Matching to δ function approximation to $C(\nu)$.

(a) Pure real
(b) Pure Imaginary
(c) Complex

13. Pure real matching with several waves in crossed channel.
$P_1 + D_o + S_o \rightarrow P_1$ $\quad \nu_{Fj}$ in $[-8, 0]$

Tables

1 Balazs Pole positions.

(1) Basic result
(2) variation with ν_L
(3) variation with p^L
(4) variation with n

(5) variation with ν.
(6) χ^2 approximation.

2 (a) Gaussian pole positions.
(b) Evenly spaced pole positions
(c) Balazs pole positions.

3 (a) Dynamic studies.
(1) variation with $\{\nu_{Fj}\}$
(2) " " ν_o
(3) " n

(b) Tabulation of Functions.
(c) Matching equations.

4 Self-consistent values.

5 Single channel searches.

6 $P_1 - D_o$ Self-consistent values.

7 Dynamic studies with real part matching.

8 Static studies. " " "

9 Tabulation of functions with " " "

$n = 9 \qquad \nu_R = 3.36 \qquad \Gamma\nu_R = 2.56$

$\nu_{li} = -0.001, \quad -9.137, \quad -9.783, \quad -11.180, \quad -13.637$
$-18.0, \quad -26.622, \quad -46.512, \quad -109.757, \quad -566.046$

$\nu_{Fj} = 0.0, \quad -8.0, -7.0, -6.0, -5.0, -4.0, -3.0, -2.5, -1.4, -?$

10 Tabulation for imaginary part matching

$\nu_R = 3.36, \ \Gamma\nu_R = 2.56$
20 poles at Gaussian points in $[-1, -9]$
$_o = -0.001.$

11 Static studies for complex matching.

12 Tabulation for complex matching.
$n = 9$, 20 near poles in $[-1, -9]$.
9 far poles in $[-9, -\infty]$.
$\nu_o = -0.001.$
$\nu_R = 3.36, \Gamma\nu_R = 2.56$
ν_{Fj} = near pole positions and also
0.0, -7.985, -7.044, -5.911, -5.306
-4.09, -2.957, -2.456, -2.015, -1.351

13 Tabulation for real part matching with δ function approximation.
$n = 9$ in $[-9, -\infty]$. $\nu_{Fj} = -8, -7, -6, -5, -4, -3, -2.5,$
$-1.4, -0.8, 0.0$ as in Table 9.

14 Tabulation with imaginary part matching and δ function approximation
$n = 9$, 20 near poles all as in Table 10.

15 Tabulation with complex matching and δ function approximation, as in Table 12.

16 Static studies with several waves.

CHAPTER 4

Figures

1. P_1 self consistent solution
   (a) ReA(ν), ImA(ν)
   (b) ReN(ν), ReD(ν).
2. Variation of ν_o.
3. Effect of ρ in other channels
   (a) $P_1 \rightarrow S_o, S_2$
   (b) $P_1 \rightarrow D_o, D_2, D_1$.
4. Contour plot, ν_o fixed.
5. Contour plot, ν_o dynamic.
6. Variation of number of subtractions
   $P_1 \rightarrow P_1$ (a) ReA(ν) (b) ImA(ν)
7. Increasing the number of waves and subtractions simultaneousl

Tables

1. P_1 self consistent solution tabulation.
2. Results of systematic investigation of the Zachariasen method
3. Table of ReD(ν) $P_1 \rightarrow P_1$ for different numbers of subtractions.
4. Table of ReD(ν) for $S_o \rightarrow P_1$ for different numbers of subtractions. Also ReN(ν).

CHAPTER 5

Figures

1. Typical solution.
   $\nu_R = 6.5$, $\Gamma = 0.56$, $g_p = -1.03$, $\nu_I = 6.46$.
2. Breakdown of real part.
3. (a) Contours with original s.c. condition. $\Gamma\nu_R$, ν_R.
   (b) barrier profile.
4. Contours with new % s.c. condition.
   (a) $\Gamma\nu_R$, ν_R
   (b) g_p, ν_p
   (c) barrier profile.
5. Contours with absolute χ^2.
   (a) $\Gamma\nu_R$, ν_R
   (b) g_p, ν_p.
6. Contours for solution of Gilbert dispersion relation.
   (a) % deviation
   (b) absolute χ^2.
7. Solution with constraint on left.
   Maximum deviation in $[-7, 10] \lesssim 0.002$.

Tables

1. Systematic investigation of original Oades method.
   (a) Variation of left hand cut off.
   (b) Variation of self consistency region [0, L].
   (c) δ function approximation in crossed channel.
   (d) P wave only in crossed channel.
   (e) Other searches in (g_p, ν_p) with constant $(\nu_R, \Gamma\nu_R)$

2. Standard tabulation
   (a) real parts
   (b) imaginary parts. Pole at -1.157, -6.085; .274%
   $\nu_R = 5.52 \quad \Gamma\nu_R = 2.85.$

3. Further investigation of the Oades method.
   (1) different self consistency conditions.
   (2) Two poles on the left.
   (3) P and D wave in crossed channel.
   (4) Parametrisation by Generalised Breit Wigner.

4. Gilbert dispersion relation calculations.

5. N/D parametrisation, tabulation of real parts, in $C(\nu)$ Ansatz model.
   (a) Balazs values, $\nu_{Li} = 0.220, -1.309, 14.058$
   $\nu_i = -2.0, -6.0, -50.0$
   (b) n = 4 Balazs type solution.

6. Shirkov soluble model. Tabulation of real parts.
   (a) charged pions. Breit Wigner param. including S waves.
   (b) Neutral pions, N/D param. P wave only.
   S, P wave $\sim$ experimental values. Left hand cut-off = -9.

CHAPTER 6

Figures

1. $\mathrm{Re}C^{-1}$, $\mathrm{Im}C^{-1}$ for $P_1 \rightarrow P_1$ and all $\rightarrow P_1, D_0$ for δ function $P_1 \rightarrow P_1$.

2. ReC, ImC — P_1, D_0 breakdown.

3. Breakdown of terms.

4. Three different s waves $s + P_1 \rightarrow P_1$. $\mathrm{Im}C^{-1}$ left hand.

5. $P_1 \rightarrow$ all Model 3. ReC and ReA.

6. Adjusted ρ amplitude. ReA and ImA.

Tables

1. $\mathrm{Re}C^{-1}$ $\mathrm{Im}C^{-1}$, ImC for $P_1 \rightarrow P_1$, NR=20, and NR = 1.

2. Right hand cut contribution [illegible] elastic and inelastic.

3.	Model 1 $P_1 \rightarrow P_1$ for NR = 20	breakdown and comparison
4.	Model 2 $P_1 \rightarrow P_1$, $R = 1.25$, $R = 5$, NR = 20	
5.	Model 2 " NR = 1	
6.	Model 3 " NR = 20	
7.	Model 3 $P_1 \rightarrow$ all inc. P_1 NR = 1	
8.	Adjusted ρ amplitude.	
9.	The ImC^{-1} ( ) for the three S waves.	

CHAPTER 7

Figures

7 - 1	Mandelstam diagram for projection of fixed s dispersion relation into t channel.
7 - 2	Mandelstam diagram in 2 dimensions.

ACKNOWLEDGMENTS

The author would like to thank all the many people who have helped him throughout the work.

He would like to thank Professor Matthews for hospitality in the theoretical group at Imperial College; Dr. R. F. Streater for his continual support and interest; Dr. C. Lovelace for suggesting the initial problem.

Most the work was done whilst the author was a university visitor at the Rutherford Laboratory, Chilton. The author would like to thank Mr. W. Walkinshaw very much for his hospitality at the Rutherford and for permission to use the excellent computing facilities. He would like to thank the theoretical group at the Rutherford, in particular Dr. R. G. Moorhouse and A. T. Davies. He would like to acknowledge stimulating discussions with many people, including D. Morgan and M. Andrews.

He acknowledges a D.S.I.R. research Studentship for the period 1961-64 and would like to warmly thank Mr. E. B. Bein for financial support during 1965-66.

He thanks Miss J. E. Robertson for moral support during this time.

Finally, he would like to thank Mrs. E. Bond for making such a good job of typing the thesis.